LA--11964-C

DE91 000511

Proceedings of the Workshop on the Science of Intense Radioactive Ion Beams

April 10-12, 1990

Compiled by
John B. McClelland
David J. Vieira

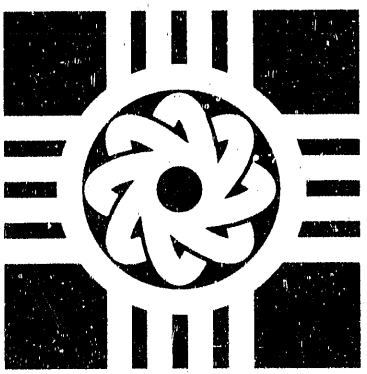

Los Alamos
NATIONAL LABORATORY
Los Alamos, New Mexico 87545

PROCEEDINGS OF THE WORKSHOP ON THE SCIENCE OF INTENSE RADIOACTIVE ION BEAMS
April 10-12, 1990

ABSTRACT

by

John B. McClelland and David J. Vieira

This report contains the proceedings of a 2 1/2 day workshop on the Science of Intense Radioactive Ion Beams which was held at the Los Alamos National Laboratory on April 10-12, 1990. The workshop was attended by 105 people, representing 30 institutions from 10 countries. The thrust of the workshop was to develop the scientific opportunities which become possible with a new generation intense Radioactive Ion Beam (RIB) facility, currently being discussed within North America. The workshop was organized around five primary topics: (1) reaction physics; (2) nuclei far from stability/nuclear structure; (3) nuclear astrophysics; (4) atomic physics, material science, and applied research; and (5) facilities. Overview talks were presented on each of these topics, followed by 1 1/2 days of intense parallel working group sessions. The final half day of the workshop was devoted to the presentation and discussion of the working group summary reports, closing remarks and a discussion of future plans for this effort.

Preface

This report contains the proceedings of a 2 1/2 day workshop on the Science of Intense Radioactive Ion Beams which was held at the Los Alamos National Laboratory on April 10-12, 1990. The workshop was attended by 105 people, representing 30 institutions from 10 countries. The thrust of the workshop was to develop the scientific opportunities which become possible with a new generation intense Radioactive Ion Beam (RIB) facility, currently being discussed within North America. The workshop was organized around five primary topics: (1) reaction physics; (2) nuclei far from stability/nuclear structure; (3) nuclear astrophysics; (4) atomic physics, material science, and applied research; and (5) facilities. Overview talks were presented on each of these topics, followed by 1 1/2 days of intense parallel working group sessions. The final half day of the workshop was devoted to the presentation and discussion of the working group summary reports, closing remarks and a discussion of future plans for this effort.

This workshop came about as a result of the recent Nuclear Science Advisory Committee (NSAC) Long Range Planning (LRP) activity during 1989. Town Meetings sponsored by the Division of Nuclear Physics of the American Physical Society were held in preparation for the LRP. The communities of nuclear scientists studying nuclei far from stability and those using low-energy beams as nuclear probes both strongly endorsed establishing a RIB facility within the next ten years. The case for such a facility was presented to the full NSAC Long Range Plan Working Group during its meeting in Boulder, Colorado on August 6-11, 1989, in which priorities for the field were discussed and recommendations formulated for the DOE and NSF. The scientific case for a RIB facility was well received by that group and several references to these scientific opportunities discussed can now be found in various sections of the Long Range Plan.

At this workshop we have concentrated our attention on outlining the scientific program that would be made possible by the development of such beams. We did not restrict our discussions to a particular production scheme or facility. As such, this workshop represents only our initial steps in preparing the case for such a facility -- further work will be needed to develop the scientific issues and to better define the type of radioactive beam facility which would best meet these new challenges.

The success of this workshop represents the hard work of many individuals. Of special note are the working group chairmen: Wolfgang Bauer, Rick Casten, John D'Auria, Jerry Garrett, Stan Hanna, Michael Howard, and Bob Stokstad, who took on the bulk of this undertaking by organizing the working groups and in preparing the summary reports; the invited overview speakers: Grant Mathews,

Mike Nitschke, Ingemar Ragnarsson, Jerzy Sawicki, and John Schiffer, who set the stage for our discussions and prepared manuscripts for these proceedings; the International Advisory Committee (listed below) for their help in preparing the workshop program and by encouraging more international participation at the workshop; and our fellow members of the Local Organizing Committee (also listed below) whose combined efforts were essential in the preparation and organization of the workshop. Moreover, we extend our thanks for a job well done to the conference secretary, Kathy Garduno; the LANL Protocol Office coordinators, Jan Hull and Mildred Saxman, for organizing the Study Center meetings; and Xiao-Lin Tu, Xiao-Gang Zhou, and Hardy Seifert for audio-visual and general assistance during the conference.

John B. McClelland

David J. Vieira

International Advisory Committee:

G. Bertsch (Michigan State)
R. F. Casten (Brookhaven)
J. M. D'Auria (Simon Fraser)
C. N. Davids (Argonne)
C. Detraz (GANIL)
W. Haxton (Washington)
W. Henning (GSI)
D. J. Horen (Oak Ridge)
S. E. Koonin (Caltech)
K.-L. Kratz (Mainz)
G. J. Mathews (Livermore)
J. M. Nitschke (Berkeley)
J. R. Nix (Los Alamos)
C. Rolfs (Munster)
B. M. Sherrill (Michigan State)
F. S. Stephens (Berkeley)
B. H. Wildenthal (New Mexico)
H. Wollnik (Giessen)
T. Yamazaki (INS)

Local Organizing Committee:

T. S. Bhatia
P. E. Koehler
C. J. Maggiore
J. B. McClelland, Co-Chairman
P. Möller
J. R. Nix
D. D. Strottman
W. L. Talbert
R. D. Taylor
D. J. Vieira, Co-Chairman

CONTENTS

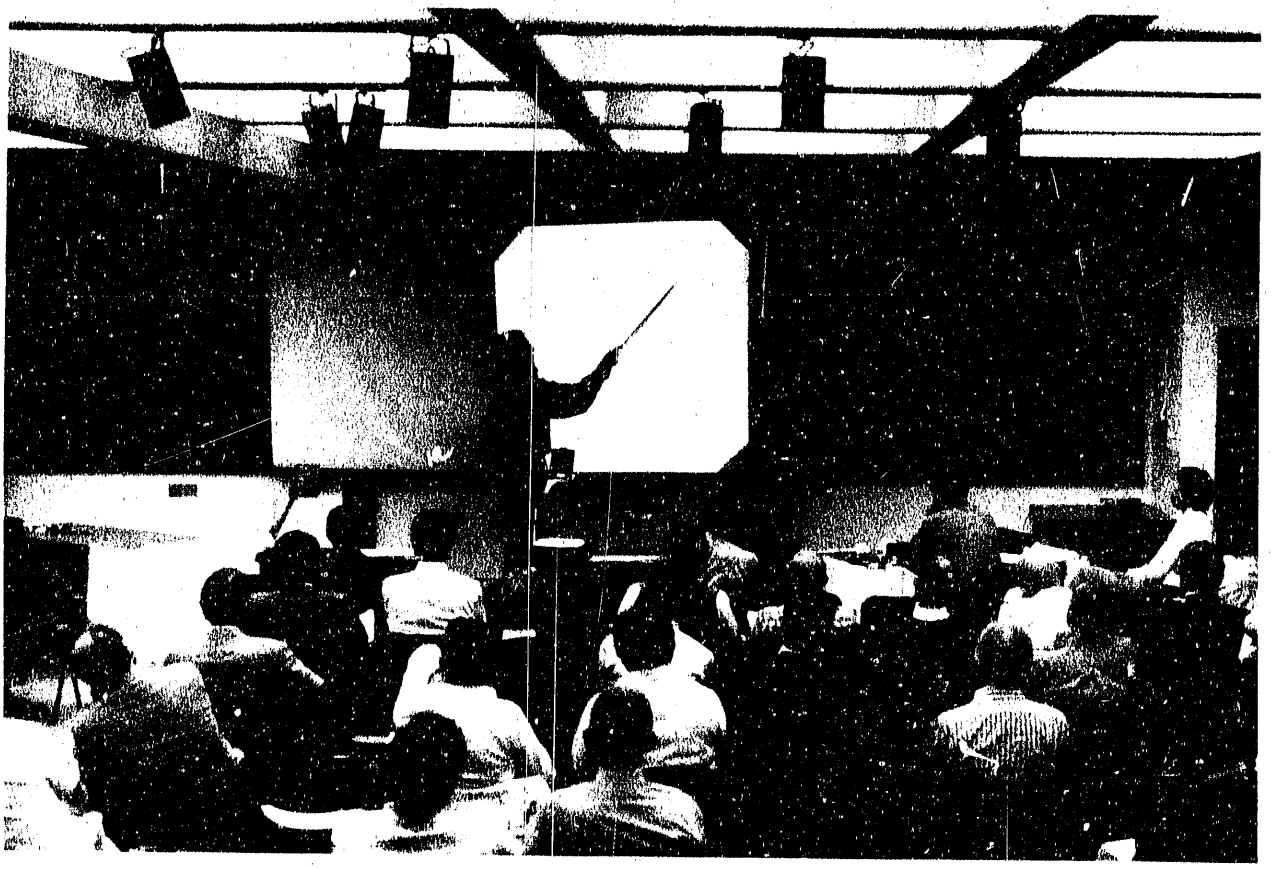

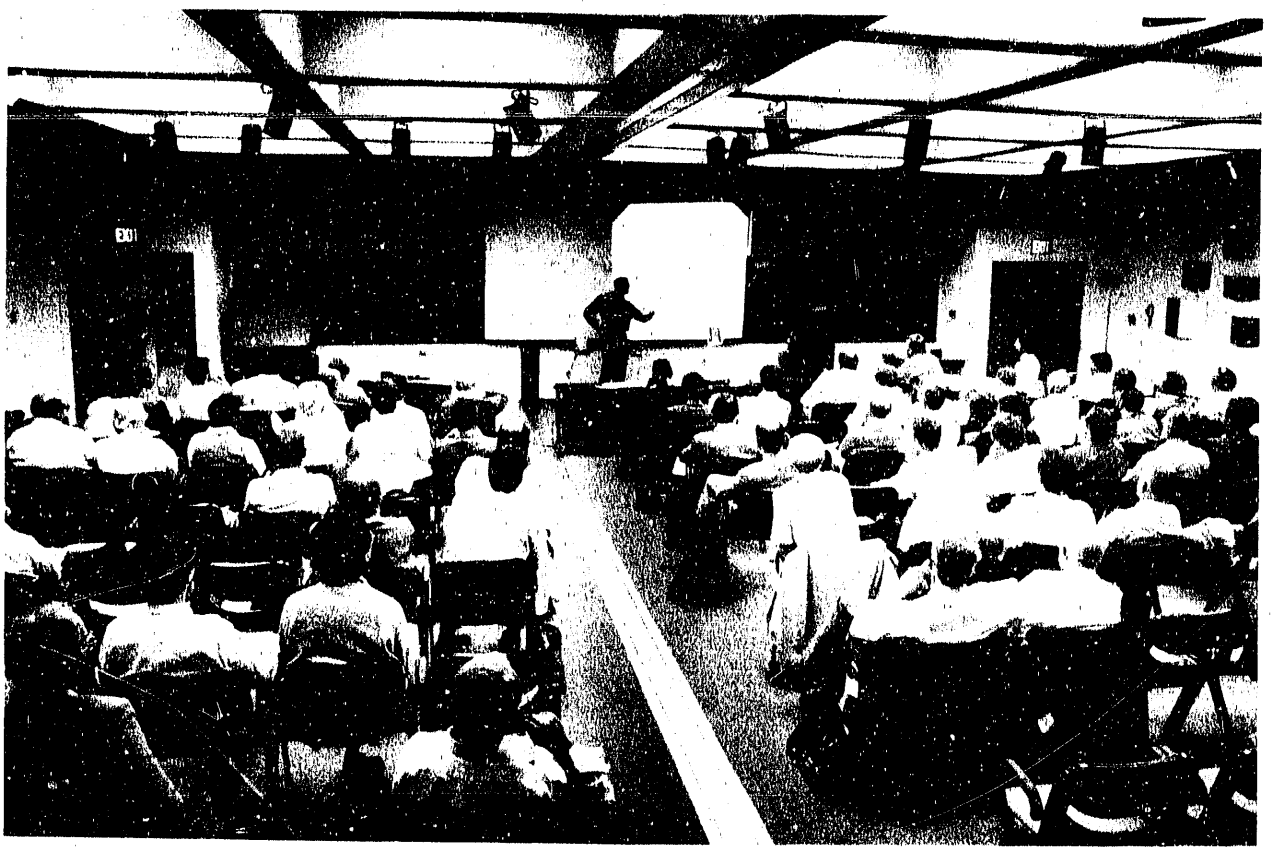
EXIT
EXIT


EXIT

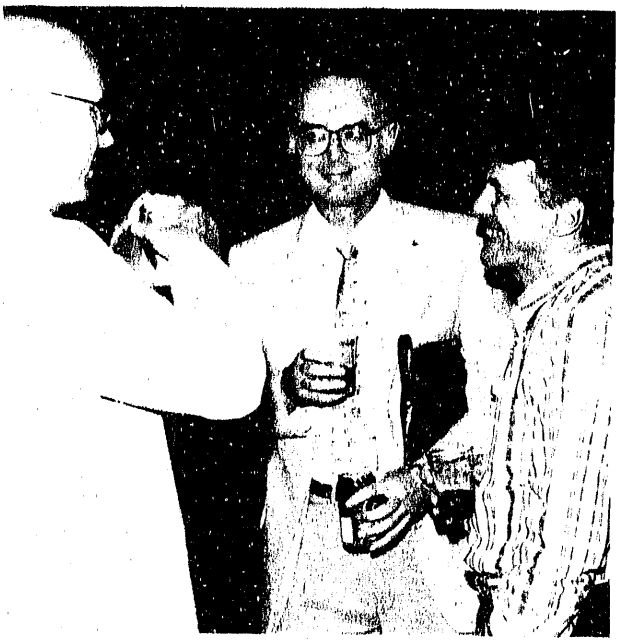


SMOKING
PROHIBITED

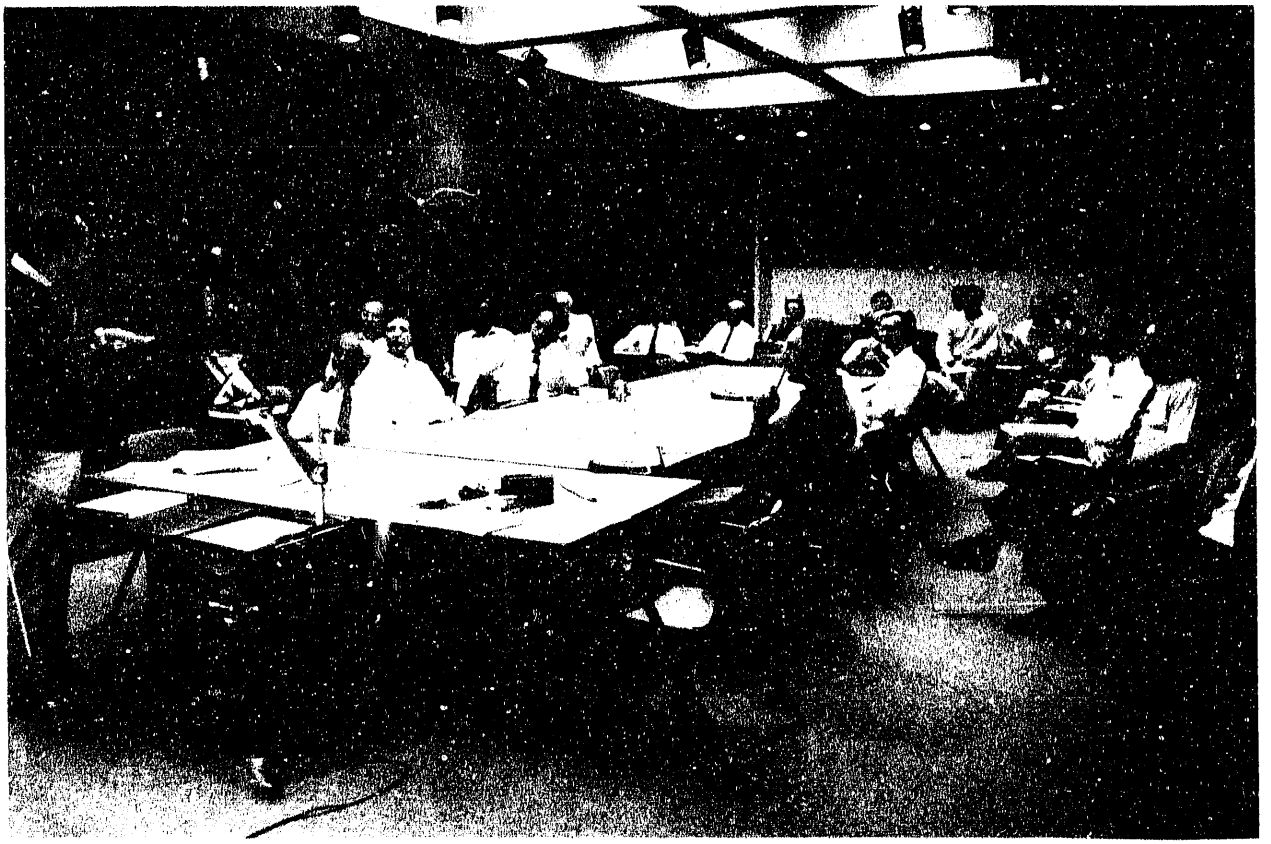

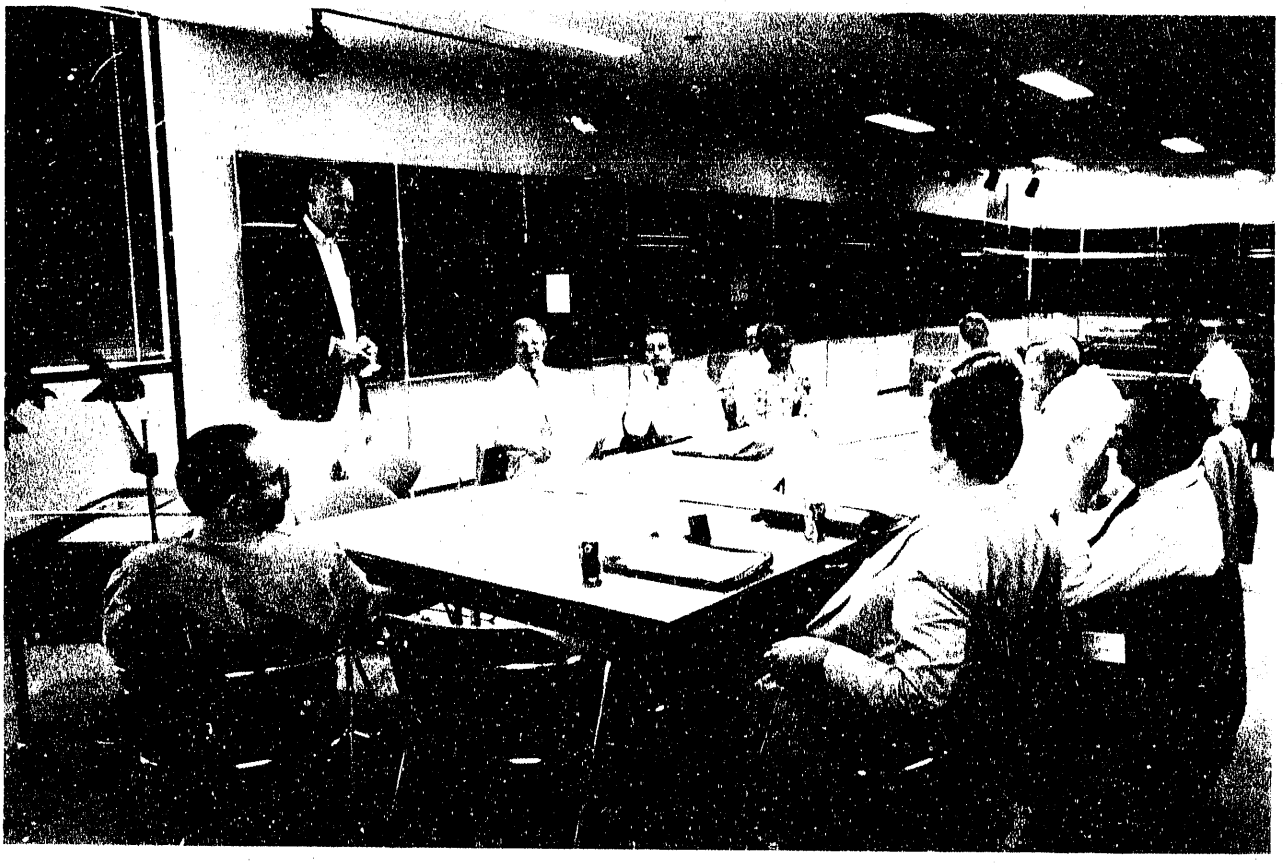

POSITION PAPER OF WORKING GROUP 1 ON REACTION PHYSICS

R. G. Stokstad, Chairman
D. D. Strottman and J. R. Nix, Coordinators

Contributions by F. Ajzenberg-Selove, W. W. Bauer, F. D. Becchetti, D. DiGregorio, C. D. Goodman, R. C. Haight, A. C. Hayes, D. J. Horen, H. J. Kim, S. Kubono, D. G. Madland, K. W. McVoy, P. Möller, D. M. Moltz, W. D. Myers, J. R. Nix, J. O. Rasmussen, J. P. Schiffer, B. M. Sherrill, E. R. Siciliano, K. P. Snover, R. G. Stokstad, D. D. Strottman, R. E. Tribble, D. J. Vieira, A. C. C. Villari, W. B. Walters, H. R. Weller, and J. B. Wilhelmy

1. Introduction

The limits of nuclear matter will be reached through nuclear reactions, just as much of what we know about nuclear structure has come from reaction studies. For studying the limits of nuclear matter, radioactive ion beams will both open up new vistas in several important dimensions and offer a fresh look at more familiar terrain. These will include extremes in the neutron-to-proton ratio (isospin), energy transfer, excitation energy, angular momentum, polarization, and nuclear shape.

We have divided the many reactions with radioactive ion beams that were suggested in our working group into four main categories. The first category involves nuclear matter in motion, or multidimensional reaction dynamics, and is discussed in sect. 2 of this position paper. The second category is concerned with the paths to neutron matter, which include neutron halos, or the physics of loosely bound nuclei, as well as the determination of the neutron drip line. Because of the intrinsic importance of this subject and its relation to both reaction physics and nuclear structure, it is included as a separate position paper. Section 3 continues with our third category, reactions that serve as probes of nuclear structure. Section 4 treats our fourth category, isomeric radioactive ion beams, where the projectile nuclei are in excited states.

It will be apparent in the following discussion that there is a wide range of difficulty in the suggested experiments. Some reactions will be extremely difficult, having small cross sections and even involving radioactive targets as well as radioactive beams, whereas others could be studied with existing instrumentation today, were the radioactive beams available. Furthermore, the experiments discussed below are only examples representing classes or categories of experiments. The requirements placed by the experiments on the radioactive beams—mass, energy, energy resolution, and other characteristics—are not dealt with systematically or in detail. But it will be

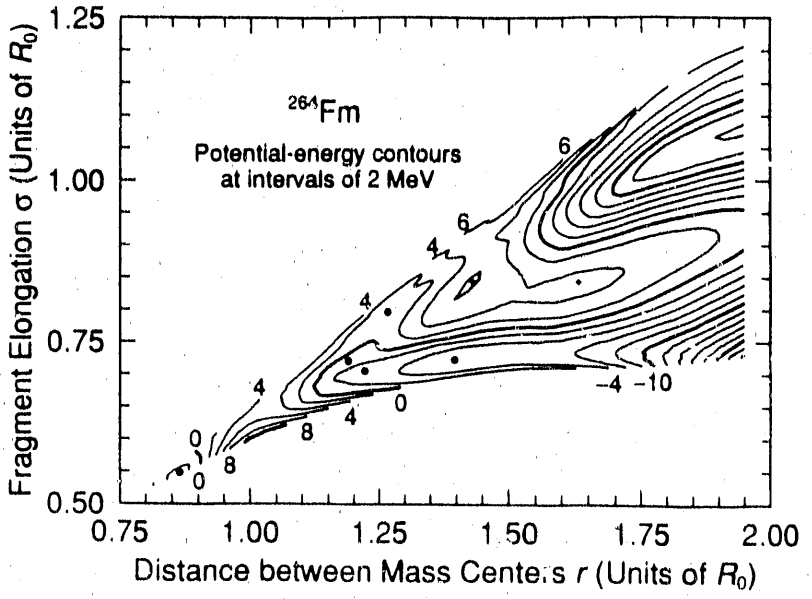

Figure 1: Calculated potential-energy surface for ^{264}Fm.

apparent that, just as with stable beams, more than one production method (e.g., ISOL or Fragmentation) is required if one is going to be able to perform the wide range of experiments illustrated below.

2. Nuclear matter in motion: multidimensional reaction dynamics

The opportunity afforded by radioactive ion beams to reach new regions of nuclei will help resolve many issues concerning collective nuclear motion. These include such diverse items as the effect of single-particle shell structure on the multidimensional nuclear potential energy of deformation, the flow and transfer of neutrons in subbarrier fusion, and isospin mixing at high excitation energies. New data provided by radioactive ion beams will assist in our quest for a fully microscopic understanding of nuclear collectivity.

2.1. PATHWAYS TO VERY HEAVY NUCLEI

Recent fission experiments [1,2]) have shown astonishingly abrupt transitions at ^{258}Fm in three separate properties: fission-fragment mass distributions, fission-fragment kinetic-energy distributions, and spontaneous-fission half-lives. All three of these phenomena are explained by the discovery of a new fission valley [3,4]) in ^{258}Fm and nuclei beyond. The calculated valley for ^{264}Fm is illustrated in fig. 1, which shows the potential energy as a function of the distance between mass centers r and fragment elongation σ of the two nascent fragments [3]). The lower left-hand corner of the diagram corresponds to the ground state of ^{264}Fm, and the lower right-hand corner corresponds to the configuration of two nearly spherical doubly magic

^{132}Sn nuclei. The long, narrow valley connecting these two configurations is separated from the traditional fission valley in the upper right-hand corner by a complicated topology involving saddle points, mountain tops (indicated by plus signs), and a high ridge. The solid circles in the diagram correspond to local minima.

Radioactive ion beams will provide important pathways to this region, through both very asymmetric transfer reactions and nearly symmetric fusion reactions. Examples of the former are ^{254}Es(^{11}Li,^{3}He)^{262}Fm and ^{254}Es(^{9}Li,^{3}He)^{260}Fm, involving ^{11}Li and ^{9}Li projectiles, with half-lives of 8.7 ms and 177 ms, respectively, incident on a ^{254}Es target, with half-life 276 d. An example of the latter is ^{132}Sn + ^{126}Sn $\rightarrow$ ^{258}Fm, involving a ^{132}Sn projectile, with half-life 40 s, incident on a ^{126}Sn target, with half-life 10^5 y. The reaction ^{132}Sn + ^{132}Sn $\rightarrow$ ^{264}Fm might ultimately be possible through the use of rapid-deposition target-production techniques.

These are only four examples of many reactions with radioactive ion beams that lead to especially large single-particle effects on the multidimensional nuclear potential energy of deformation. The resulting multiple minima and valleys separated by saddle points and ridges will significantly affect the reaction dynamics, especially at subbarrier energies. By increasing the bombarding energy, one will also be able to study the disappearance of single-particle effects with increasing excitation energy.

Just as the peculiar structure of ^{132}Sn is thought to influence the fission of the heaviest Fm isotopes, other aspects of nuclear structure may be at work in determining the mass distribution associated with fission. Robertson and Walters [5]) have suggested that a softness against octupole deformation for nuclei in the Cs-Ba mass-145 region might be responsible for the interesting phenomenon that the heavy partner in an asymmetric mass split is always a nucleus of about this mass, with the mass of the lighter fission fragment increasing or decreasing as the mass of the parent fissioning nuclide changes. Their argument is that an octupole deformation resembles the shapes fission fragments must acquire as they approach scission. Nuclei that can be easily deformed to an octupole shape will then be favored in fission. If this argument is correct, and if the Cs-Ba mass-145 nuclei have ground states that either have or are easily induced to acquire an octupole component, then the barrier for fusion might be lowered [6]) for heavy radioactive isotopes of Cs and Ba bombarding neutron-rich but stable targets around mass 100 to 120. Performing such a reaction would be similar to bombarding ^{126}Sn with ^{132}Sn—one would be working back up a fission valley in this multidemensional space toward a very heavy compound nucleus, taking advantage of the same nuclear-structure effects that cause the valley and the trajectory along it in the fission process.

2.2. FISSION IN THE PRE-ACTINIDE REGION

A real possibility exists to take advantage of reverse kinematics with radioactive beams in the Z = 84–94 region. There has been a lot of effort in the Fm region to exploit the rapid changes in fission properties. These changes are also present in the pre-actinide area as well. If we could have beams of neutron-deficient isotopes of these pre-actinides then we could do simple direct reactions with reverse kinematics

and measure the fission de-excitation channels. The reverse kinematics focuses the reaction products in the lab and therefore gives high geometric coverage and, since the decay products will have near beam velocities, they are much easier identified with counter techniques.

Another of these reverse reactions would be to study fission shape isomerism. In the light Th and Ra regions, the inner fission barrier should be around 3 MeV above the isomeric level, while the outer barrier is substantially above this value. This should be a condition which allows sufficient population of an isomeric state and also permits it to have a reasonable half-life (> ns). These isomers should decay by gamma branching back to the ground state. Cross sections will be small (on the order of microbarns) but one could take advantage of the reverse kinematics to move the products out of the reaction zone (i.e., recoil shadowing) and possibly see some of these decays.

2.3. NEUTRON TRANSFER IN SUBBARRIER FUSION

The transfer of nucleons among colliding nuclei on the path to fusion is one of several dimensions (deformation, vibration, and neck formation) that can influence the probability of fusion. At energies above the barrier a single dimension, the radial degree of freedom defining the separation of the two nuclei, is sufficient to describe the fusion of light to medium-mass nuclei. Particularly at subbarrier energies, though, the extra dimensions mentioned above can be very important in determining the cross section. Radioactive beams will give us a unique tool to study the importance of the ground-state Q-value for neutron transfer on the cross section for subbarrier fusion.

Just to give an example, systems like $^{15}O + ^{143}Nd$ and $^{14}O + ^{144}Nd$ possess very large ground-state Q-values (see table 1) for 1-neutron pickup (+9.5 MeV) and for 2-neutron pickup (+14.5 MeV), respectively. For comparison, the existing transfer data [7-10]) are for Q-values less than +2 MeV and +6.6 MeV for the 1n- and 2n-pickup reactions, respectively. The effect of the positive ground-state Q-value on the fusion at subbarrier energies can be illustrated by a simplified coupled-channel calculation [11]) for the fusion cross sections in the systems $^{15}O + ^{143}Nd$ and $^{14}O + ^{144}Nd$. These calculations, presented in fig. 2, show a large enhancement at low energies that has a different energy dependence than, for example, the coupling to a series of low-lying rotational states.

TABLE 1
Ground-state Q-values for one- and two-nucleon transfer reactions
(+ means pickup, − means stripping)

System	Neutrons				Protons			
	−1	−2	+1	+2	−1	−2	+1	+2
$^{15}O + ^{143}Nd$	−22.8	−5.4	+9.5	+3.9	−3.6	−2.6	−8.1	−12.2
$^{14}O + ^{144}Nd$	−26.9	−17.4	+5.4	+14.5	+5.3	+0.2	−10.3	−15.3

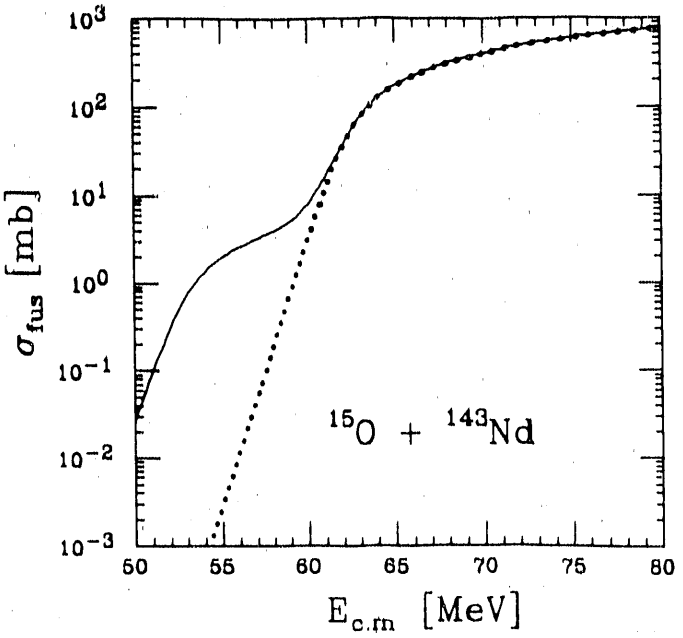

Figure 2: Cross sections for subbarrier fusion of ^{15}O + ^{143}Nd calculated with the coupled-channels code of Dasso and Landowne [11]). The dotted line is the result for no coupling in the entrance channel. The effect of the coupling of a neutron-transfer channel is shown by the full line. The large enhancement predicted below the barrier arises from the large positive Q-value for neutron transfer from ^{143}Nd to ^{15}O. While a useful guide for developing experiments, this estimate has been made with the simplified code CCFUS, which may overestimate the size of the effect compared to that predicted by a more refined calculation.

To study the correlation of positive Q-values with the enhancement of the subbarrier fusion as well as the relative effect of the different transfer channels, it would be interesting to make an experimental investigation of the fusion and transfer reactions in ^{15}O + ^{143}Nd and ^{14}O + ^{144}Nd. The measurements of the fusion cross sections as functions of bombarding energy can be achieved by detecting the evaporation residues with two low-pressure multiwire proportional counters. The identification of the evaporation residues will be made by their time of flight and the energy loss in any of the counters. This technique has already been used to measure the fusion cross sections for ^{12}C + ^{128}Te at different bombarding energies. It is worth noting [12]) that beam intensities required for these experiments are very modest (less than 10^7 particles/s). The transfer-reaction measurements can be made by detecting and identifying the reaction products at backward angles in a silicon surface-barrier ΔE-E telescope with a thin ΔE detector and good timing resolution, which provides mass resolution through time of flight and nuclear-charge resolution via energy losss. This technique has been succesfully used in $^{16,18}O$ + Sn transfer studies performed by Henning et al. [7]). Another technique will be to tag the various transfer channels through the observation of discrete-line gamma rays by an array of Compton-suppressed Ge detectors.

2.4. NEUTRON FLOW IN SUBBARRIER FUSION

A large body of data points to the beginning phase of heavy-ion fusion as proceeding through doorway processes such as those mentioned in the preceding section. The doorway provides extra degrees of freedom that enhance fusion cross sections at subbarrier energies. A process related to the effect of neutron transfer channels discussed above and that gives a good account of some of the observed fusion enhancements is the recently suggested free-flow of neutrons [13]). In this proposed process the transfer of a valence neutron, which proceeds via tunnelling at large internuclear separations, becomes a free-flow process once the colliding nuclei approach each other sufficiently close for the neutron barrier to disappear (due to overlapping tails of nuclear potentials). The internuclear distance where the neutron flow commences is intimately related to the binding energy of the least-bound neutron of the system and systematically lies outside (by about 2 fm for $40 < A < 100$) the corresponding distance where strong absorption occurs [13,14]). This neutron flow in turn precipitates the formation of a neck connecting the nuclei, e.g., via liquid-drop effects [15,16]). Coalescence of the neck leads to fusion, and re-separation leads to energy-damped multinucleon transfers. For the case of the ^{50}Ti + ^{93}Nb system [17]), the scission of the neck preferentially populates channels that involve transfers of up to four nucleons from the heavy to the light collision partner, i.e., the system tends toward symmetric partition, very reminiscent of familiar spontaneous fission.

Neutron flow is the key to this subbarrier process, and as the binding of the valence neutron weakens, the internuclear distance where the free flow commences becomes larger. Accordingly, radioactive beams of nuclides near the neutron drip line, where the neutron is weakly bound by less than about 1 MeV, would open an exciting new vista to explore this interesting subbarrier process.

2.5. ISOSPIN MIXING IN GIANT-DIPOLE DECAY OF COMPOUND NUCLEI

Compound nuclear isospin mixing at high excitation energies (50 MeV and higher) can be studied [18]) in light $N = Z$ nuclei by looking at GDR gamma-emission in heavy-ion fusion-evaporation in reactions with $T = 0$ entrance channels, e.g., ^{16}O + ^{12}C $\rightarrow$ ^{28}Si*. In such reactions, (isovector) GDR gamma-decay is strongly hindered for states of pure isospin, due to the low level density of $T = 1$ final states. There is a surprising result, viz., that very large mixing widths of 1 MeV or greater for the mixing of $T = 1$ states with $T = 0$ states are necessary to explain the data [18]). However, it is necessary to "calibrate" the statistical model by studying neighboring $N = Z$ compound nuclei. A much better calibration would be to look at the same $N = Z$ compound nuclei formed in a $T \neq 0$ entrance channel, for which GDR gamma-decay would not be hindered. This is not possible with stable heavy ions, for which one always has $N \geq Z$. With radioactive beams, proton-rich projectiles are possible that permit such reactions. For example, ^{28}Si* could be formed in the reactions ^{15}O + ^{13}C and ^{14}O + ^{14}C. Other $N = Z$ nuclei could be studied in a similar fashion.

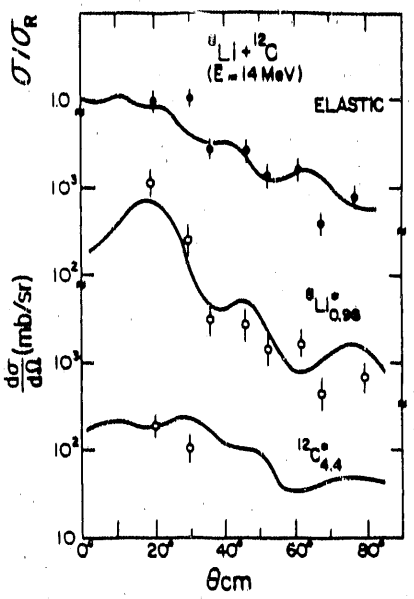

Figure 3: Differential cross sections measured for a beam of ^{8}Li scattered by a ^{12}C target [23]).

3. Reactions as probes of nuclear structure

3.1. TOTAL REACTION CROSS SECTION

The total reaction cross section or, closely related to it, the interaction cross section σ_I, is related to the most basic structural feature of the nucleus, its size. Some of the first measurements to be made with secondary beams of radioactive nuclei were the interaction cross sections [19]). These measurements at high energies (typically 800 MeV/A) revealed a remarkable change in interaction radius with changing isopspin. Measurements at lower energies and for a wide variety of radioactive nuclei also reveal interesting changes in the mean-square radius with isospin [20–22]). These results are considered in the section on neutron halos in a separate position paper.

3.2. ELASTIC SCATTERING

Like the total reaction cross section, the differential cross sections for elastic scattering are one of the most basic and important reaction quantities in nuclear physics. And because the cross sections can be large, they will also be among the first quantities to be measured when a new radioactive beam facility is developed. Figure 3 shows the cross sections [23]) for the elastic scattering of ^{8}Li by ^{12}C at an energy of 14 MeV. The full curves give the results of DWBA calculations using a deformed optical model form factor. The inelastic excitation for the projectile is significant and can be attributed to the peculiar properties of ^{8}Li (weakly bound, T, and J^{π}).

Another reason for the special role of elastic scattering is the degree to which this process is understood theoretically, particularly for elementary projectiles, where

extensive studies using optical-potential models have provided a data base from which microscopic information has been obtained.

Radioactive ion beams would allow us to test and extend the optical-potential models for elastic scattering into new extremes of spin and isospin. The types of projectiles that could be used for these new studies would include neutron-rich and proton-rich ground states, as well as excited (isomeric) states of these nuclei. Here we mention some of the new possibilities that would be provided by the elastic scattering of proton-rich ground states. The new opportunities that would be provided by the elastic scattering of neutron-rich ground states and of isomeric states are given in other sections.

With a RIB facility, one may have available light, $J^\pi = 0$ projectiles such as ^{10}C, ^{14}O, ^{18}Ne, and ^{22}Mg. Elastic-scattering experiments using these projectiles from a proton target would provide us with the opportunity to study the single-particle matter distributions for relatively simple cases where $N < Z$. In the case of ^{10}C and ^{14}O, the nuclei ^{11}N and ^{15}F that would be produced in compound-nucleus reactions lie beyond the proton drip line! We also may be able to test our understanding of the optical-potential models by comparing these results to the corresponding scattering from neutron-rich isotopes such as ^{14}C, ^{18}O, ^{20}Ne, and ^{26}Mg, in which case the Coulomb interaction would be fixed while the isospin part of the strong interaction would change from $T_z = -1$ to $T_z = 1$. Of course, the use of a polarized proton target would extend these studies to include the spin-isospin part of the interaction. Along the same lines as those mentioned above for *p*- and *sd*-shell nuclei, one may also consider the very interesting possibilities of studying the *d*-shell isotopes $^{36-39}$Ca.

3.3. INELASTIC SCATTERING

The inelastic scattering of radioactive beams affords the possibility of measuring transition matrix elements in nuclei that have heretofore been inaccessible. One example is shown in fig. 3 for the first excited state of ^{8}Li. Substituting a gold target for a carbon target should substitute electromagnetic excitation for nuclear excitation and determine the B(E2) value connecting the ground and first excited state [24]. Inelastic scattering of heavier beams from light targets, including hydrogen, could extend significantly our quantitative knowledge of collective transition strengths.

The assumption of time-reversal invariance imposes a reciprocity relationship for the unpolarized inverse reaction cross sections obtained at the same center-of-mass energy and scattering angle. Previously, this reciprocity relation has been studied by use of inverse transfer reactions such as ^{24}Mg(α,p)^{27}Al, and found to be accurate to within a fraction of a percent. The simultaneous availability of nuclear ground and excited states from a RIB facility would allow the reciprocity relation to be studied within the same nuclear environment, and possibly lead to a more stringent test. For example, inverse transitions such as ^{18}F(p,p$'$)^{18}F* could be used to study time-reversal invariance.

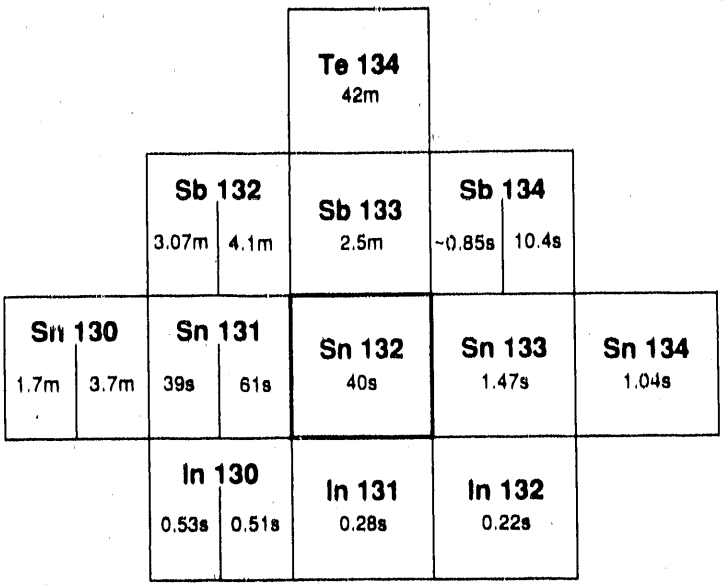

Figure 4: The doubly magic nucleus ^{132}Sn and its neighbors. The measurement of single- and few-nucleon transfer reactions in this region will map out the interaction energies among the single-particle orbitals [25]).

3.4. TRANSFER REACTIONS

The same measurements yielding elastic and inelastic scattering information from light targets (p, d, ^{3}He, and ^{4}He) would also provide a rich source of new information on single-particle motion. By observing the scattered target nucleus or target-like reaction product, the same kind of spectroscopic information can be obtained as has been gleaned from reactions such as (d,^{3}He), (d,t), (d,p), (p,d), and (^{3}He,d) using beams of hydrogen and helium isotopes. Indeed, measurements of this type are approved [25]) for the experimental storage ring, ESR, at GSI's new synchrotron, SIS-18. Here it will be of particular interest to map out the effective interaction among single-particle orbitals in the region of the double shell closure at ^{132}Sn. Figure 4 charts the region of the nuclides around ^{132}Sn. A beam of ^{132}Sn projectiles and targets of p, d, ^{3}He, and ^{4}He would enable the full arsenal of one- and two-nucleon transfer reactions to be applied to the mapping of particle and hole states in this region. This type of nuclear structure information in the vicinity of the doubly closed shell at ^{56}Ni shows a beautiful systematic behavior that is not well understood. Being able to obtain comparable information in the region of a different double shell closure may bring the clue for the solution of the problem in the Ni region, or it may raise new and unexpected questions.

The properties of single-particle orbitals in nuclei far from closed shells and in the regions of strong deformation are also of interest for study with radioactive beams in conjunction with multiple-high-resolution-gamma-detector arrays. Indeed, the latter have made possible a promising new class of nuclear reactions. Spherical actinide nuclei have produced neutron-transfer products at high spin. On the incoming path,

Coulomb excitation pumps the deformed partner to spins as high as 14, and one or more neutrons are transferred, giving rise to deformed transfer products, which are further excited to higher spins by Coulomb excitation on the outward path. These high-spin states reveal themselves through the de-exciting gamma-ray cascades. For example, the knowledge of the ground-state rotational bands in ^{160}Dy, ^{234}U, and ^{238}Pu has been extended to considerably higher spins.

At present a fundamental limitation on this powerful new spectroscopic tool in the actinides is that no stable, high-Z projectiles are available with neutron separation energies below those of the actinides, so that one can only extract neutrons but not add them to the actinides.

The addition of a neutron to a heavy target like ^{248}Cm at high spin could give unique information on Nilsson orbitals lying in the region of the possible superheavy island of stability. Learning the location of the $h_{11/2}$ or $k_{17/2}$ neutron levels would refine the half-life estimates of the superheavy elements. The experimental search would be similar to the experiments performed by Garrett and co-workers in locating the $i_{13/2}$ proton levels in the rare earths [26].

The best candidates seem to be ^{17}O and ^{210}Bi, although ^{137}Xe and ^{138}Cs may provide interesting possibilities. A beam of ^{17}O, because it does not excite ^{248}Cm to very high spins, would map the lower-spin orbitals while the heavier radioactive beams would reach the more interesting high-spin orbitals. And in addition to the spectroscopic goal of locating the nucleon orbitals, a study of the reaction mechanism—Coulomb excitation combined with neutron transfer—and further development of the calculational tools present important challenges.

3.5. CHARGE EXCHANGE

3.5.1. *General considerations.* Radioactive beams also provide unique opportunities for studing the charge-exchange reactions, again using reverse kinematics. Transitions induced by both the isospin and spin-isospin operators will yield information pertaining to $L = 0$ isospin transitions (Fermi) and spin-isospin transitions (GT) as well as higher-L transfer transitions. In a notation indicating reverse kinematics, the reaction on a hydrogen target is written p($_Z A_N$,$_{Z+1} A_{N-1}$)n, with the proton target being in the form of a plastic for a single pass beam or a gas if a circulation beam in a storage ring is used. A spectrometer (perhaps in conjunction with the magnetic elements of a storage ring) with particle identification will be required to measure the heavy-ion reaction product. In some cases, detection of the coincident neutron will be required.

Some advantages of using reverse kinematics for these particular experiments are: (1) The detector efficiency for the heavy fragment is close to unity. (2) The energy resolution of the heavy fragment could be much better than could be obtained from neutron time of flight. (3) One can measure the complete angular distribution with either one or a few angular settings of the spectrograph Crude calculations of counting rates indicate that such experiments will be feasible with particle fluxes expected from a RIB facility.

Measurements of isobaric transitions are expected to extend the data on Coulomb displacement energies and provide sensitive tests for isobaric mass formulas. Measurements of GT-strength distributions can be of value to both astrophysics and nuclear physics. Some other questions to be addressed are the distributions of $L = 1$, $S = 0$, and $S = 1$ strengths as functions of incident energy, as well as measurements of isospin splitting.

3.5.2. *Anomalies in Fermi and Gamow-Teller strengths.* It has been shown experimentally that cross sections for (p,n) reactions are proportional to beta-decay transition rates for initial and final states that are connected by allowed Fermi or Gamow-Teller transitions. In fact, when these transitions can be observed in (p,n) reactions at low momentum transfer, as, for example, at zero degrees and proton energy above 100 MeV, essentially the entire structure dependence of the cross section is contained in the beta-decay matrix element [27]). This fact is expected theoretically also. This simple structure dependence has been exploited not only in nuclear-structure studies, but also has been applied to determining neutrino detection cross sections for solar-neutrino detectors.

The (p,n) cross section also depends on kinematic factors that are easily calculated and on the nuclear mass A in a way that has so far defied calculation. Let us define the specific cross section as the (p,n) cross section per unit Fermi or Gamow-Teller transition probability, whichever is applicable to the transition in question. We also assume that correction has been made for kinematics and momentum transfer. Then we expect the specific cross section to have a smooth mass dependence. However, measured specific cross sections show large variations between adjacent A values. For example, the specific cross sections for $A = 13$ and $A = 15$ are nearly 1.5 times larger [28]) than those for $A = 12$ and $A = 14$. What is more puzzling is that the anomaly has not been observed in (n,p) reactions for the transition from ^{13}C to ^{13}B. The cross-section normalization for (p,n) reactions is done with isospin-related transitions but not exactly isospin-mirror transitions.

If one could bombard a proton target (it could be a plastic target) with a ^{13}N beam, for example, one could measure in reverse kinematics the (p,n) cross section for the transition between the ground state of ^{13}N and the ground state of ^{13}O, which is the isospin mirror of the measured beta-decay transition from ^{13}B to ^{13}C that was used to determine the GT matrix element to calibrate the specific cross section. This one measurement alone should be interesting because it addresses a case where a large anomaly is seen in the (p,n) cross section. Figure 5 illustrates the measurements needed for the $A = 13$ system.

In general, the availability of radioactive beams removes the severe restriction that GT and Fermi transitions can be studied with (p,n) reactions only for cases originating on nuclei that happen to be stable. The cross sections are typically large, a few millibarns per steradian. The energy should be about 100 MeV/A to get good selectability for F and GT transitions.

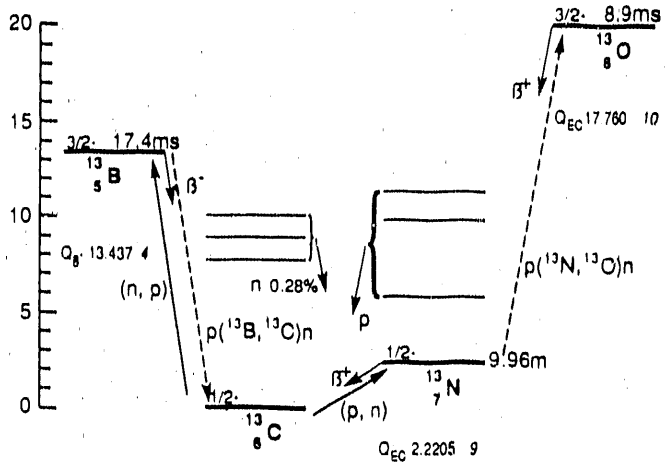

Figure 5: The mass-13 isobaric system. The ^{13}C(p,n)^{13}N reaction is anomalous with respect to the Gamow-Teller transitions in the $A = 12$ and $A = 14$ systems. The dashed arrows show the transitions that could be studied with radioactive beams.

3.5.3. *Double-beta decay.* Considerable theoretical and experimental effort has been invested in attempts to determine lifetimes of nuclei that double-beta decay. From this work one hopes to learn about extensions to the Standard Model. Thus far, there is only one laboratory measurement, that of ^{82}Se decaying to ^{82}Kr. For this case the theoretical predictions differ from the experimental data by factors of four to ten.

Double-beta decay can proceed with either zero or two neutrinos appearing in the final state; appearance of the former would signal lepton-number violation. The observed decay of ^{82}Se presumably is a two-neutrino decay. The dominant mechanism for the two-neutrino decay is the Gamow-Teller mechanism, with the transition proceeding through 1^+ states of the intermediate odd-odd nucleus. However, states of other spins may contribute, particularly in the case of zero-neutrino decay.

To understand the discrepancy between theory and experiment, and to provide additional tests of the nuclear wave functions, (p,n) and (n,p) reactions are being used to map out the Gamow-Teller strength. Additional constraints will result by using a radioactive beam composed of the intermediate nucleus. Such information is particularly important if one is able to measure double-beta decay to the 2^+ levels of the granddaughter nucleus. There are theoretical suggestions that such transitions are sensitive to extensions of the Standard Model such as right-handed currents.

Three of the most actively studied double-beta decaying nuclei are ^{76}Ge, ^{82}Se, and ^{100}Mo. The ground-state spins of the intermediate odd-odd nuclei are 2^- (^{76}As), 5^- (^{82}Br), and 1^+ (^{100}Tc), although there is a 6-minute isomer in ^{82}Br at 46 keV having angular momentum 2^-. Beams of either ^{76}As or ^{82m}Br would allow the measurements of transitions to states in neighboring nuclei, which would provide useful constraints

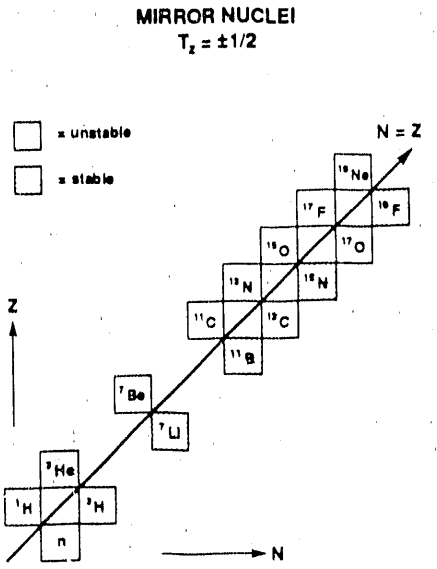

Figure 6: The $T_z = \pm 1/2$ mirror nuclei. Radioactive beams would enable the study of charge-exchange reactions among several mirror pairs and the contribution of this process to elastic scattering.

not otherwise attainable.

Particularly useful would be beams of ^{100}Tc since transitions induced by the (p,n) reaction from the ^{100}Tc 1^+ ground state to excited states of ^{100}Ru would provide information useful for calculating double-beta branching ratios that is not available from the beta decay of ^{100}Tc itself. This would in turn provide constraints on right-handed currents and massive neutrinos.

3.5.4. *Charge-exchange reactions between mirror nuclei.* Charge-exchange reactions between a stable projectile and a stable target are well established spectroscopic tools for studies of nuclear structure. If one could instead employ in a general way $T_z = \pm 1/2$ mirror nuclei for the projectile and target with the resulting interference between direct and exchange terms, a new type of charge-exchange reaction would become possible that could, in principle, probe unique parts of both ground-state and excited-state wave functions [29]). Utilizing mirror nuclei also has the property that the reaction Q-value ≈ 0, which enhances the possibility of observing non-perturbative effects (resonances). The basic idea behind such resonances is that two nucleon-equivalent cores elastically scatter off of each other and that the unpaired proton and neutron might resonantly interact via pion exchange terms between only these valence nucleons. The cross section for this process can be approximated by utilizing that for the elastic scattering of the two cores.

The only stable nucleus that has more protons than neutrons is ^{3}He. All other nuclei with $T_z = -1/2$ are unstable. Figure 6 illustrates this and points out the large number of such nuclei that become available with a radioactive beam facility. The only case of charge exchange among mirror nuclei studied to date is the ^{3}He–^{3}H(12 y) system [30,31]); an experiment to search for the effects predicted by

Vary and Nagarajan [29]) in the ^{7}Be(53 d)–^{7}Li system is underway [32]). The reactions ^{11}C(20 m) + ^{11}B and ^{13}N(10 m) + ^{13}C require radioactive beams because of the short half-lives of the $T_z = -1/2$ members.

In addition to the charge-exchange effects mentioned above, which are studied by the elastic scattering of a radioactive beam by its mirror nuclear target, there exists a specific comparison between mirror nuclear wave functions that could be uniquely investigated by utilizing an inelastic scattering process in reactions of mirror nuclei. Many years ago the Thomas-Ehrman effect was postulated [33,34]) to explain the energy difference between the $1/2^+$ first-excited states in ^{13}C and ^{13}N. The s-wave proton in the excited state of ^{13}N is unbound by about 0.4 MeV. The loosely bound proton experiences a lower Coulomb energy. This effect is most dramatic when an s-state is involved, and it has been invoked to explain the sudden extra stability of nuclei at the proton drip line [35]). By performing a mutual-excitation scattering measurement of ^{13}N on ^{13}C, it should be possible to identify changes in the mirror wave function. Furthermore, the technique can be calibrated by studying a case where the Thomas-Ehrman effect is not present, but which is otherwise similar. The ^{11}C–^{11}B system is such a case. Study of the elastic scattering of the $A = 11$ mirror nuclear system will also permit us to explore unresolved theoretical issues that are expected to arise from the presently incomplete theory [29]). The extension of these considerations to $T_z = -1$ nuclei, also available as radioactive beams, is clear.

The large cross sections expected for these reactions make this general type of experiment feasible with the beam intensities that would be initially available at a radioactive beam facility. The 590-keV energy difference between the $1/2^+$ and $3/2^-$ states in ^{13}C demands a beam with a well-defined energy.

4. Isomeric radioactive ion beams

4.1. PROJECTILES EXISTING IN HIGH-SPIN ISOMERIC STATES

Consider first a beam of ^{178}Hf ions existing in the $J^\pi, K, E^* = 16^+, 16$, 2.447-MeV state. Performing Coulomb-excitation experiments could lead to population of the excited members of a rotational band built upon this state. This would be the first observation of a rotational band built upon such a high-spin isomer. Questions of shape (moment of inertia), band termination, and influence of the large value of K would be addressed.

Consider next a beam of ^{18}F* existing in the 5^+, 1.119-MeV state. The production of this isomer in a primary nuclear reaction can lead directly to an aligned and even polarized 5^+ isomeric-state beam. Such a beam would allow exploration of polarization phenomena with very high projectile spin [36]).

Excited-state scattering studies lead to the possibility of energy-gaining transitions in competition with elastic scattering, implying changes in the reactive content of the optical-model potential [37]). Relatively simple total reaction cross-section measurements would shed light on this question. The high-spin isomeric state also leads to a re-examination of the question of the presence of a spin-spin term of the form

$\mathbf{J_t \cdot J_m}$ in the optical-model potential, where the subscripts t and m refer to target and isomeric state, respectively. A good example for studying changes in the reactive content of the optical-model potential may be the 16^+, 2.905-MeV state in ^{212}Po, which is a member of the ground-state rotational band that has a half-life of 45 s.

For the excitation of the giant-dipole resonance one may speculate on the exotic spectroscopy that becomes possible. Brink showed many years ago that a giant resonance can be built upon any state, not just the ground state. It would be extremely interesting to observe through, e.g., in-beam spectroscopy, the giant resonance built upon a high-spin isomeric state, and the splitting of the resonance for large values of K.

References

1. E. K. Hulet, J. F. Wild, R. J. Dougan, R. W. Lougheed, J. H. Landrum, A. D. Dougan, M. Schädel, R. L. Hahn, P. A. Baisden, C. M. Henderson, R. J. Dupzyk, K. Sümmerer, and G. R. Bethune, Phys. Rev. Lett. **56** (1986) 313

2. D. C. Hoffman and L. P. Somerville, Particle emission from nuclei, vol. **III** (CRC, Boca Raton, 1988) p. 1

3. P. Möller, J. R. Nix, and W. J. Swiatecki, Nucl. Phys. **A492** (1989) 349

4. J. R. Nix, Nucl. Phys. **A502** (1989) 609c

5. J. D. Robertson and W. B. Walters, Proc. Symp. on exotic nuclei, 198th American Chemical Society National Meeting, Miami Beach, Florida, 1989, to be published

6. F. Catara, C. H. Dasso, and A. Vitturi, J. Phys. G: Nucl. Phys. **15** (1989) L191

7. W. Henning, F. L. H. Wolfs, J. P. Schiffer, and K. E. Rehm, Phys. Rev. Lett. **58** (1987) 318

8. G. Montagnoli et al., Proc. Symp. on the many facets of heavy-ion fusion reactions, Argonne, Illinois, 1986, Argonne National Laboratory Report ANL-PHY-86-1 (1986) p. 555

9. K. E. Rehm, Proc. XII Workshop on nuclear physics, Iguazu Falls, Argentina, 1989 (World Scientific, Singapore) to be published.

10. Heavy ion interactions around the coulomb barrier, edited by C. Signorini et al., Lecture notes in physics, vol. **317** (Springer-Verlag, Berlin, 1988)

11. C. H. Dasso and S. Landowne, Phys. Lett. **183B** (1987) 141

12. D. DiGregorio and R.G. Stokstad, private comunication

13. P. H. Stelson, Phys. Lett. **205B** (1988) 190

14. P. H. Stelson, H. J. Kim, M. Beckerman, D. Shapira, and R. L. Robinson, Phys. Rev. **C41** (1990) 1584

15. C. E. Aguiar, V. C. Barbosa, L. F. Canto, and R. Donangelo, Nucl. Phys. **A472** (1987) 571

16. A. Iwamoto and K. Harada, Z. Phys. **A326** (1987) 201

17. H. J. Kim, private communication

18. M. N. Harakeh, D. H. Dowell, G. Feldman, E. F. Garman, R. Loveman, J. L. Osborne, and K. A. Snover, Phys. Lett. **176B** (1986) 297

19. I. Tanihata, T. Kobayashi, O. Yamakawa, S. Shimoura, K. Ekuni, K. Sugimoto, N. Takahashi, T. Shimoda, and H. Sato, Phys. Lett. **206B** (1988) 592

20. W. Mittig, J. M. Chouvel, W. L. Zhan, L. Bianchi, A. Cunsolo, B. Fernandez, A. Foti, J. Gastebois, A. Gillibert, C. Gregoire, Y. Schultz, and C. Stephan, Phys. Rev. Lett. **59** (1987) 1889

21. A. C. C. Villari et al., Proc. XXVII Int. Winter Meeting on Nuclear Physics, Bormio, Italy, 1989, University of Milan Report (1989) p. 74

22. M. G. Saint-Laurent, R. Anne, D. Bazin, D. Guillemaud-Mueller, U. Jahnke, J. G. Ming, A. C. Mueller, J. F. Braundet, F. Glasser, S. Kox, E. Liatard, T. U. Chan, G. J. Costa, C. Heitz, Y. El-Masri, F. Hanappe, R. Bimbot, E. Arnold, and R. Neugart, Z. Phys. **332A** (1989) 457

23. J. Brown, F. D. Becchetti, W. Z. Liu, J. W. Jänecke, D. A. Roberts, J. J. Kolata, A. Morsad, and R. E. Warner, Proc. First Int. Conf. on radioactive nuclear beams, Berkeley, California, 1989 (World Scientific, Singapore, 1990) p. 372

24. F. D. Becchetti, J. Brown, J. W. Jänecke, W. Z. Liu, D. A. Roberts, J. J. Kolata, R. Smith, K. Lamkin, A. Morsad, and R. E. Warner, Proc. First Int. Conf. on radioactive nuclear beams, Berkeley, California, 1989 (World Scientific, Singapore, 1990) p. 305

25. J. P. Schiffer, these Proceedings

26. C. X. Yang, J. Kownacki, J. D. Garrett, G. B. Hagemann, B. Herskind, J. C. Bacelar, J. R. Leslie, R. Chapman, J. C. Lisle, J. N. Mo, A. Simcock, J. C. Wilmott, W. Walus, L. Carlén, S. Jönsson, J. Lyttkens, H. Ryde, P. O. Tjøm, and P. M. Walker, Phys. Lett. **133B** (1983) 39

27. C. D. Goodman, C. A. Goulding, M. B. Greenfield, J. Rapaport, D. E. Bainum, C. C. Foster, W. G. Love, and F. Petrovich, Phys. Rev. Lett. **44** (1980) 1755

28. T. N. Taddeucci, C. A. Goulding, T. A. Carey, R. C. Byrd, C. D. Goodman, C. Gaarde, J. Larsen, D. Horen, J. Rapaport, and E. Sugarbaker, Nucl. Phys. **A469** (1987) 125

29. J. P. Vary and M. A. Nagarajan, Proc. Workshop on radioactive nuclear beams, Washington, D.C., 1984, Lawrence Berkeley Laboratory Report LBL-18187 (1984) p. 113

30. A. D. Bacher, R. J. Spiger, and T. A. Tombrello, Nucl. Phys. **A119** (1968) 481

31. R. F. Haglund, G. G. Ohlsen, R. A. Hardekopf, N. Jarmie, R. E. Brown, and P. A. Schmelzbach, Phys. Rev. **C15** (1977) 1613

32. R. N. Boyd, M. S. Islam, J. Kolnicki, M. Farrell, T. F. Wang, K. E. Sale, and G. J. Mathews, Proc. First Int. Conf. on radioactive nuclear beams, Berkeley, California, 1989 (World Scientific, Singapore, 1990) p. 311

33. R. G. Thomas, Phys. Rev. **80** (1950) 136; **88** (1952) 1109

34. J. B. Ehrman, Phys. Rev. **81** (1951) 412

35. E. Comay, I. Kelson, and A. Zidon, Phys. Lett. **210B** (1988) 31

36. F. D. Becchetti, private communication

37. D. G. Madland, private communication

NUCLEAR STRUCTURE/NUCLEI FAR FROM STABILITY

Report of Working Group II

Co-chairmen: R. F. Casten [1] and J. D. Garrett [2]

Local Coordinator: P. Moller

Members: W. W. Bauer, D. S. Brenner, G. W. Butler, J. E. Crawford, C. N. Davids, P. L. Dyer, K. Gregorich, E. G. Hagbert, W. D. Hamilton, S. Harar, P. E. Haustein, A. C. Hayes, D. C. Hoffman, H. H. Hsu, D. G. Madland, W. D. Myers, H. T. Penttila, I. Ragnarsson, P. L. Reeder, G. H. Robertson, N. Rowley, F. Schreiber, H. L. Seifert, B. M. Sherrill, E. R. Siciliano, G. D. Sprouse, F. S. Stephens, K. Subotic, W. Talbert, K. S. Toth, X. L. Tu, D. J. Vieira, A. C. C. Villari, W. B. Walters, B. H. Wildenthal, J. B. Wilhelmy, J. A. Winger, F. K. Wohn, J. M. Wouters, X. G. Zhou, and Z. Y. Zhou

1 Introduction

Our current knowledge of nuclear structure is confined to nuclei produced with projectiles and targets that have equilibrated for a significant fraction of the lifetime of the universe. Such a long equilibration (a few billion years) must evade many of the most exotic nuclear configurations, which due to their special properties, decrease the stability of the nucleus. The present basis of nuclear structure is phenomenlogical, that is, it is not derivable from a simple set of master equations. Not only is the structure of the nucleus sensitive to bulk properties, such as its mass and charge, but it also is strongly dependent on the details of the independent-particle quantal states that the protons and neutrons occupy and how these states interact with each other and modify the bulk nuclear properties. Far from stability the various possible combinations of exotic single-particle states make the problem

even more complicated. Therefore, it is not possible simply to extend the present knowledge theoretically to such exotic situations not accessible to experimental study. Thus the use of Radioactive Ion Beams (RIBs) should provide unique opportunities, not only to answer critical issues concerning some of the most fundamental current nuclear structure themes, but it also will allow the study of entirely new phenomena unavailable with current techniques and not derivable from our present knowledge of nuclear theory.

It is useful to highlight a few such possibilities in these introductory remarks in anticipation of the more detailed discussions given below: (i) The long-predicted island of superheavy stability may be established. Not only is this of interest as a long-standing, elusive, historic goal, but it also is perhaps the ultimate test of the predictive power of current nuclear models and, therefore, of our understanding of the interplay of independent-particle and macroscopic structure in nuclei. (ii) The nuclear equation of state will be refined and the enticing hints of the possible binding of pure neutron matter can be probed by mass measurements and the associated definition of the drip lines. (iii) New information in neutron-rich nuclei may finally provide sufficient detailed information to pin down the site, environment, and mechanism of r-process nucleosynthesis. (iv) Detailed measurements of the properties of predicted closed-shell nuclei, such as ^{78}Ni, ^{100}Sn, and ^{132}Sn, will offer a stringent test of the microscopic independent-particle quantum structure forming the foundation of the nuclear shell model itself. (v) New data and analyses of the spectrum of single-particle states will provide detailed new information on the fundamental single-particle structure of nuclei and on the residual interactions that modify that structure. (vi) New manifestations of collectivity, such as the long-sought stable triaxial nuclei, may be found and a better understanding of others (for example reflection asymmetric shapes, which only now are beginning to be probed) should be in the offing. (vii) The study of neutron halos, or skins, representing nearly-pure, low-density neutron matter is a most intriguing and exciting venture. (viii) Complete spectroscopy near stability will allow the first comprehensive connections between low- and high-spin physics to be forged making possible uniquely-sensitive tests of modern nuclear structure models. The exciting concept of quantal chaos in nuclei can be more readily studied in such nuclei and in others that can be formed with extremely-high beta-decay energies. (ix) In the realm of high spin, the increased fission barriers in newly accessible neutron-rich nuclei may allow the discovery of hyperdeformed nuclear shapes with a 3:1 ratio of major to minor nuclear axes. (x) Access to exotic hig-h-j, low-Ω configurations and the associated magnified Coriolis effects

should open unique new vistas in which the single-particle effects are dominated by rotation.

In the following pages we briefly outline some of these and other topics. It should be recognized that it is impossible to do justice to such a broad field in these few pages. Since this work represents the collective viewpoints of a diverse Working Group, and since it is not clear which of the topics discussed will in fact turn out to be the most interesting in an operating facility a number of years hence, we have resisted the temptation to discuss only a couple of topics in detail and rather try to present as broad a coverage as possible. At the other extreme we try to avoid making this report a mere listing of an even larger number of topics by attempting to present sufficient material to indicate an interest in each case. That is, in each subarea we try to identify the main themes, undercurrents, and motivations, and to identify a few experimentally-accesible examples. Finally, since this is the collective report of a Working Group discussing scientific applications, and is neither a complete nor a review paper, we have dispensed with a complete set of references. The field covered by this report is so vast and active that, to have done otherwise, would have highlighted a miniscule segment of the literature at the expense of numerous equally deserving accomplishments. A few "typical" references, however, are included to assist the nonexpert. For additional information the reader is referred to one of several recent reviews and/or conferences on this subject [3,4,5,6].

Although the scientific justification for further studies of nuclei far from stability with RIBs should be amply demonstrated below, and elsewhere in this report, it is interesting to reflect for a moment on the history of such studies. A few examples that come to mind include that of ^{146}Gd and the discovery that, for certain neutron numbers, Z = 64 acts as a closed shell [7]. This was one of the earliest additions to the traditional complement of magic numbers. Similarly, recent studies of deformation near ^{31}Na and ^{80}Zr show that N = 20 and Z = 40 does not ensure a spherical nuclear shape [8,9]. The discovery, in the early 1970's, of an abrupt spherical-deformed phase or shape transition region at N=60 near A=100 [10] and within a few mass units of a significant neutron subshell closure at N = 56,58 [11] hinted at the need for a more detailed understanding of the onset of collectivity in nuclei and led, several years later, to the Federman-Pittel mechanism [12] in which the valence p–n interaction modifies the underlying single-particle structure of one type of particle as a function of the number of nucleons of the other type. The discovery of beta-delayed nucleon, or few-nucleon, radioactivity (β–p,β–2p,β–n,β–2n,...), often near the drip lines [4], revealed

the spectroscopic richness of regions with high-decay energies and offered new insights into the structure and stability of nuclei at the extremes of isospin. Nearer stability, the discovery, in recent years, of examples of multiparticle radioactivity in which intact ^{14}C or even ^{24}Ne or ^{34}Si nuclei are emitted [13] pointed to the amazing complexities of the nuclear potential-energy surface and to the possibility of exotic-cluster formation near the nuclear surface. The discovery of symmetric fission in the heaviest known actinides [14] demonstrated the key role played by structure (extra binding) in the fission fragments. Finally, the discovery of superdeformation in rapidly-rotating neutron-deficient heavy nuclei [15] has opened up wholly new high-spin phenomena that continue to reveal remarkable discoveries, such as essentially identical rotational sequences in neighboring isotopes and isotones [16]. Together, these and other studies have led to new ideas on shell effects (e.g., Strutinsky shell corrections) and residual interactions, to the discovery of dynamical symmetries in nuclei, to the development of new generations of more sophisticated macroscopic-microscopic models, and to a more profound understanding of pairing and collectivity in nuclei.

2 Masses, Stability, Beta Decay, and the Heaviest Elements

Under this rubric gross nuclear properties are stressed. These properties reflect, in a sense, the most obvious and global characteristics of each nucleus and are, therefore, the net result of the single-particle motion, collective correlations, and interactions that are active. The motivation for studying such properties is, of course, to elucidate these facets but also, more specifically, to understand such important concepts as the nuclear equation of state, in particular its compressibility and charge distribution. Studies in this area are also of paramount importance to eradicating the nuclear uncertainties in the r-process of stellar nucleosynthesis. Finally, work here is also directed toward discovering and studying the heaviest elements and, possibly, a superheavy island of stability. Even work on nuclei far removed from this island is important, since it leads to improved modelling of nuclear masses and lifetimes and therefore to more sophisticated extrapolations to unknown nuclei.

2.1 Fission/Heaviest Elements

As noted, a prime interest is the creation and study of nuclei in the predicted superheavy island of stability [17]. This is a long sought goal of nuclear physics, which has often been thought to be unattainable. However, recent improvements in macroscopic-microscopic models offer greater confidence in predicting the existence and properties of superheavy nuclei [18] Such models are quite sophisticated and are capable of handling complex potential energy surfaces with multiple minima and saddle points. Moreover, they take into account the structure not only of the fissioning system, but also that of the daughter products, since this is the barrier to that fission which determines the stability of a given nuclear species. It is only with RIBs that any realistic chance exists to reach the superheavy island, thereby discovering the heaviest nuclei, and testing the ultimate single-particle bases for all nuclear structure. Aside from the general issue of producing superheavy nuclei there are other associated goals. The fission of excited nuclei in the lead region is symmetric, that is, the fission product masses are nearly equal. The spontaneous fission of most of the actinide nuclei, on the other hand, is highly asymmetric. Therefore, the identificaton of the onset of asymmetric fission near A = 220--230 is critical to the understanding of the fission process and an understanding of the competition among fission modes as a function of Z, N, excitation energy and angular momentum of the fissioning system in terms of both macroscopic, droplet behavior and modulations due to the underlying shell structure. Studies might center on the light Ra isotopes. A second area concerns heavy actinides with N > 160. Figure 1 shows a calculation of the fission barriers near A = 264 [19]. There is a fascinating competition between asymmetric and symmetric fission with very high kinetic energy associated with the fission of nuclei such as $^{264}No_{162}$, $^{264}Md_{163}$, and $^{264}Es_{165}$. In these nuclei the barrier to symmetric fission can be offset by the extra binding of the symmetric, doubly-magic, daughter nuclei $^{132}Sn_{82}$. (Incidentally, since fission probabilities depend not only on the structure of the parent but also on that of the daughter, this is yet another motivation for the study of nuclei in the vicinity of ^{132}Sn.) About 12 MeV of energy is gained for each Sn fragment, thereby opening a symmetric fission path characterized by an anomalously-high kinetic energy of the fission fragments. Conversely it is noted that the inverse process, the fusion of two nuclei in the vicinity of the ^{132}Sn closed shell, should have an enhanced cross section and might, indeed, be a method of synthesising some of the heaviest elements. Less complicated transfer reactions, using RIBs, to produce nuclei

with A $\approx$ 264 include $^{264}Es_{155} + {}^{96}Rb_{59} \rightarrow {}^{264}Fm_{164}$, $^{264}Md_{163}$, $^{264}No_{162}$, and $^{264}Lr_{161}$.

2.2 Drip Lines

The study of both proton and neutron drip lines is important in indicating the limits of particle stability of nuclei in general, in further testing of macroscopic-microscopic models and (see below) in gaining access to nuclei with extremely high decay energies which offer the possibility of exotic decay modes. The neutron drip line is a particularly-important regime which is of critical interest to the study of neutron halos and skins. The discovery of nuclei with halo properties such as ^{11}Li [20,21] hints that pure or nearly-pure neutron matter may even be bound under certain circumstances. Recent nuclear matter calculations directed toward this issue [22], therefore, take on renewed interest. They are parameterized in terms of a constant that can be fixed empirically by the precise location of the neutron drip line. (Additional information on neutron halos is contained in subsecton 3.2.1 and in a separate chapter in this report.) Finally, the locus of the proton and neutron drip lines is of interest in limiting possible nucleosynthesis scenarios.

2.3 Masses

The mass is a fundamental nuclear property. Since masses give binding energies and, therefore, neutron and proton separation energies, they are essential to the understanding and the modelling of the r-process for nucleosynthesis (discussed below). They also give indirect information on the nuclear equation of state, provide crucial tests of macroscopic-microscopic models, and yield information on the structure of the nuclear ground state.

Masses are particularly useful in delineating the nuclear equation of state. The concept of nuclear compressibility plays a key role here, determining, for example, the energy of giant monopole resonances and the "skin" properties of nuclei. Since the compressibility essentially reflects the restoring force against oscillations of the outermost nucleons, its determination relies on the empirical knowledge of nuclear masses. RIB studies will enable many new and critical mass determinations.

An interesting concept which has arisen in connection with nuclear halos as well as in other contexts is that of Coulomb redistribution, or the suppression of the proton density in the nuclear interior due to a combination of Coulomb repulsion and an associated in-filling of neutrons. This effect

has been empirically detected in electron-scattering experiments [24] and also appears in some Hartree-Fock calculations [25]. Liquid-drop models do not incorporate such proton-deficient cores, but droplet models, which agree better with the masses of the heaviest elements, do. Therefore, additional masses of heavy nuclei will aid the delineation of such models and refine the understanding of proton core suppression.

Certain double differences of nuclear masses can be used to extract empirical proton-neutron two-body residual matrix elements [26]. It has become increasingly evident recently that these matrix elements, representing a T=0 residual interaction, are of critical importance in understanding the evolution of nuclear shell structure as a function of particle number, isospin, and angular momentum and, therefore, of the onset and development of collectivity and phase transitions in nuclei. Such interactions will be considered in greater detail in the following section, but suffice it to say here that new mass determinations in certain critical regions would go far toward reducing the uncertainty in two-body residual interaction matrix elements.

Aside from specific theoretical reasons for measuring the masses of selected nuclei, there are several mass regions where no empirical data exists in which the various theories exhibit large deviations. Clearly, the measurement of even a few masses in these regions would help distinguish between the models and, inevitably, refine them. In particular, neutron rich nuclei with Z = 10–20, the Z = 28–36 nuclei with N > 50, and the Z = 44–50 nuclei with N $\approx$ Z are such examples.

A particularly enigmatic region occurs near ^{34}Na. Here, not only do significant deviations exist between theoretical and experimental masses, but the measured Na masses themselves have a different isotopic trend relative to the neighboring isotones. Some of these masses have sizable experimental uncertainties. Recently an "island of inversion" has been proposed for these nuclei [27] in which $0\hbar\omega$ and $2\hbar\omega$ excitations cross, leading to the sudden onset of deformation at N = 20, a neutron number previously considered as a classic magic number. Improved masses for the neutron-rich Na isotopes and new results for neighboring isotones would test these ideas and help to solidify our understanding of how and where nuclear deformation arises in terms of the detailed spectrum of single-particle states.

2.4 Beta Decay and Lifetimes

Beta decay is valuable for a variety of reasons: a measure of Gamov-Teller (G–T) matrix elements as a test of weak interaction theory, a source of

nuclear lifetimes, or as a means of access to interesting nuclear structure questions. In the present section we focus on the first two points leaving the discussion of the last topic with regard to the study of nuclei far from stability for the following section.

One of the interesting beta-decay puzzles is the apparent empirical quenching of G–T strength. G–T matrix elements are often substantially smaller than predicted, even in nuclei near closed shells where both parent and daughter configurations are simple and, presumably, well known [28]. Before the question can be fully addressed, though, it is necessary to determine that the full empirical strength has been found. Strength can be missed either if it is fragmented (by the mixing of states in the daughter nucleus) into too fine a structure to be observed or (again due to mixing) if some of it is pushed to excitation energies above the effective threshold for significant beta feeding. Both sources of error are minimized for nuclei with high beta-decay energies. More levels in the daughter nucleus are available for population; therefore, a more complete and reliable level scheme can be constructed and the range of excitation energies in which to search for the beta-decay strength is also increased. The use of RIBs to populate beta-decaying nuclei extremely far from stability with their associated higher beta-decay energies thus offers an opportunity to more thoroughly address the long-standing G–T quenching problem. Likewise access to neutron-rich nuclei just below the Pb closed shell using RIBs will allow the first measurement of beta-decay matrix elements connecting states differing by two major shells.

Beta decay far from stability with high Q_β values also can lead to particle-unstable daughter nuclei. A number of cases of such beta-delayed particle (β-p, β-2p, ...) emission have been discussed [4]. They are interesting because they provide structure information for the daughter nucleus, information on the position, strength, and distribution of the G–T giant resonance, and a study of super-allowed beta-decay matrix elements. Moreover, β^+ decay populates isobaric analogue states and, especially in light nuclei, or medium nuclei with N $\approx$ Z, allows a determination of the isotopic-spin purity. An example of the advantage of RIBs for populating exotic nuclei where such questions can be addressed is given by a comparison of fusion-evaporation calculations for various reactions leading to ^{51}Co. The ^{40}Ca(^{16}O,xp,yn) reaction at 170 MeV has a cross section of 0.004 mb. In contrast, the corresponding ^{14}O reaction, ^{40}Ca(^{14}O,xp,yn), at the more convenient lower energy of only 70 MeV has a cross section, 0.17 mb, over 40 times larger. The lower required beam energy helps to compensate for the

difficulty of providing ^{14}O beams.

The use of RIBs to make beta-unstable nuclei, either by reactions or as fission products of heavy actinides, allows the study of many new nuclei along the r-process path [29]. A critical issue in supernova r-process nucleosynthesis is the time scale ("cycle" time) needed for the production by neutron capture and beta decay, of the actinides from "seed region" nuclei near ^{56}Fe. This time scale is dominated by the half lives of the so-called waiting-point nuclei where the r-process abundance peaks cross a neutron magic number. At such points the r-process halts until these nuclei can beta decay. It is, therefore, crucial to determine the lifetimes and binding energies of nuclei in these waiting-point regions so as to determine, or set limits on, the required duration of the intense supernova explosion. Recently, some of these nuclei have been studied for the first time, but more information is needed on all three waiting point regions near ^{80}Zn, ^{130}Cd, and especially ^{195}Tm, where no experimental information exists. It may be possible to study such species either through reactions with RIBs or through the beta decay following the fission of heavy, very neutron rich actinides produced with RIBs.

In modern "network" r-process calculations [29], the waiting-point approximation (of ignoring all but the lifetimes of the waiting point nuclei) is bypassed by incorporating the properties ($T_{1/2}$, binding energies, etc.) of all nuclei along the r-process path into these complex calculations. Therefore, these data are needed so that a larger fraction of the information inserted into these calculations is empirical. This is especially important because, even though recent models are greatly improved over their predecessors, the discrepancies between measured and predicted lifetimes even near stability average at least a factor of 2–3 (in both directions) and can exceed an order of magnitude in selected cases. This constitutes a significant impediment to determining the site and environment (neutron flux, duration, and temperature) of the r-process.

2.5 Cluster Decay

A fascinating phenomenon, now known in several cases, is heavy-ion radioactivity, in which an unstable nucleus decays by emitting a massive chunk, such as ^{14}C, or even ^{25}Ne or ^{34}Si [13]. This process is clearly a major challenge to nuclear theory, since it requires an understanding of both the formation amplitudes of such fragments near the nuclear surface, as well as the probability of their emission through a complicated barrier. Though this decay

mode was actually predicted before its observation, it is still far from well understood and new empirical examples, and their systematics, would be valuable. There is the intriguing possibility that this decay mode may be even more prominent farther from stability in nuclei accessible with RIBs.

2.6 Laser Spectroscopy

The access to nuclei with extremes of isospin also introduces exciting possibilities for using laser-spectroscopic methods. Many of the most fundamental properties of a nuclear state, e.g. the mean-square radius $< r^2 >$, the magnetic moment μ, the magnitude and **sign** of the quadrupole moment Q, and in some cases the spin, can be measured using techniques based on lasers [30].

Laser techniques generally involve exciting ions resonantly and mapping out the isotope shifts and hyperfine structure by scanning the laser wavelengths. The use of radioactive beams circumvents the usual problem of producing and transporting short-lived nuclei to the laser beam. The exotic nuclei could be obtained either as a direct beam or as the residue of a reaction based on RIBs. Laser methods well matched to both production methods are available: e.g., the collinear method [31] for direct beams and recoil into gas [32] for less intense production by reactions.

Nuclear phenomena that can be studied include unusual distributions of nuclear matter, shape changes, and high-spin effects including superdeformation. Several of these possibilities are discussed in more detail in the following paragraphs:

Local deviations of the neutron to proton density ratio. Nuclei with a large deficit or excess of neutrons may minimize their energy by local variations in the properties of nuclear matter, e.g. the neutron "skins" or "halo" and Coulomb redistribution discussed elsewhere in this article. Indeed at the extremes of isospin, accessible with RIBs, even more extreme variations in the N/Z density ratio, e.g. a local "precipitation" may occur. Such effects could be studied by comparing results of laser spectroscopy, which measures properties of the proton distribution, and hadronic probes, that determine the matter distribution. Deviations of $< r^2 >$ from an $A^{1/3}$ dependence alone, can yield an indication of a separation of the neutrons from the protons.

Specific properties of exotic states. Measurements of $< r^2 >$, μ, and in some cases Q can be made using laser techniques for special nuclear states, such as the superdeformed and other exotically-deformed states described

elsewhere in this report.

Transitional nuclei. The most definitive signature of a nuclear shape transition is a sudden change in $< r^2 >$ and an associated change in the sign of Q. An example is that observed using laser techniques in the Pt, Au, Hg, and Tl isotopes [30,33]. The use of RIBs will allow an extension of measurements in this mass region to lighter nuclei and for similar measurement in the region of the more exotic shape transitions discussed elsewhere in this report.

Radii of closed-shell nuclei far from stability. Measurements of $< r^2 >$ would be a test of the proposed double-shell closure in, e.g. ^{100}Sn and ^{132}Sn. The charge radii for the tin chain studied thus far ^{108,125}Sn [34] show a smooth parabolic variation. Measurements and extrapolations indicate smaller values than calculated from microscopic theories for $^{118-132}$Sn.

3 Nuclear Shell Structure, Shapes, Collectivity, and Shape/Phase Transitions

Neglecting effects, such as quark degrees of freedom, coupling to baryon excitations (e.g., delta resonances), which appear to be superfluous for low-energy (say < 100 MeV/A) phenomena, the Fermion Shell Model is the most fundamental model of nuclear structure. This model is based on a mean field (mostly due to a central potential) leading to quantal single-particle states, and residual interactions that contribute in a many-body environment. Where calculations are practical, it is the paradigm. In general, it is the rationalization and microscopic justification for other models, models which are themselves generally simplifications or truncations of the Shell Model designed to avoid its calculational complexities and to focus on simple, often collective, excitation modes, symmetries and the like. In view of this theoretical hierarchy, tests of the fundamental properties of shell structure are vital to a profound understanding of nuclear physics and, ultimately, to providing the input for the development of a realistic nuclear theory which remains elusive. Nuclei in the new frontiers far from stability offer wholly new vistas leading toward this goal. In addition, access to new combinations of N and Z, the exploitation of high decay energies, and of opportunities for "complete spectroscopy" will reveal new manifestations of collective many-body behavior, symmetries, and afford a qualitative leap in our appreciation of the interplay of the single-particle and collective facets of nuclear structure.

3.1 Single-Particle Structure

The underlying microscopic basis for all nuclear structure is the Shell Model whose most important characteristic is a set of single-particle eigenstates and eigenvalues. This is fundamental to all other manifestations of single-particle and collective behavior. As alluded to earlier, however, the single-particle energies of nuclei do not constitute an immutable substructure. Rather, due to gross changes (e.g., radius) in the mean field and to the effects of residual interactions, the single-particle structure, and its attendant patterns of major and minor gaps, is an evolving, dynamic concept, which is dependent, separately and in concert, on the numbers of protons and neutrons and, in particular, on the numbers of valence particles of each type. Even the magic numbers are not sacrosanct in that some nuclei with N = 20 or Z = 40 (e.g., ^{31}Na and ^{80}Zr) are well deformed and nucleon numbers such as Z = 64 can provide strong inducements to spherical shapes. Thus one of the most important roles of RIBs in nuclear structure will be the study of such as yet unreachable doubly-magic nuclei as ^{78}Ni, ^{100}Sn, and ^{132}Sn and the mapping of single-particle structure in the neighboring odd-proton and odd-neutron nuclei. This can be done only by exploiting reverse kinematic stripping and pickup reactions using RIBs. Nickel-78, ^{100}Sn, and ^{132}Sn all are expected to be doubly closed-shell nuclei with properties similar to ^{208}Pb. If these expectations should turn out to be false, it would be a devastating assault on our most basic concepts of nuclear structure and, just as clearly, a challenge and mandate for a deeper understanding of the shell structure of nuclei, which results from the interplay of fundamental quantum degeneracies in central potentials and the critical residual interactions which modulate that shell structure.

The two most obvious and predominant components of these residual interactions are nucleon pairing and the valence p–n interaction. Though the former has been rather thoroughly studied, recent work suggests new features such as a possible dependence of pairing on neutron excess, (N–Z)/A. Whether such effects are due to a fundamental neutron-excess dependence of the pairing interaction or whether they arise from macroscopic effects or p–n interactions is an open, and basic, question. RIBs will make possible the production and study of new nuclei spanning extended isotopic or isotonic chains. One case where such chains have recently provided intriguing data is the set of neutron rich V–Fe isotopes where no isospin effects are observed [35].

The valence p–n interaction affects nuclear structure in several ways

[36]. It appears in two forms, as a T=1 interaction identical to the nuclear p–p and n–n forces, and, more importantly, as a T=0 force that leads to single-nucleon configuration mixing and hence, perforce, to collectivity and deformed nuclear shapes. The T=0 interaction appears, predominantly, in two guises, a monopole and a quadrupole component. The latter, which is dependent on the angular orientation of the respective proton and neutron orbits plays a key role in the evolution of collective behavior in deformed regions and contributes to the saturation of collectivity near midshell (where individual quadrupole p–n matrix elements vanish). The monopole component is, perhaps, even more crucial, and certainly less well known: depending on radial overlaps, it varies with the (nlj) single-particle quantum numbers of the interacting orbits and contributes effective shifts to their single-particle energies. These shifts can eradicate shell and subshell gaps, both for spherical and deformed shapes, and therefore, vitally affect the evolution of nuclear structure. An example is the A = 100 and 150 phase-transitional nuclei where the dynamics of the Z = 38 or 40 and Z = 64 gaps contributes to the sudden onset of deformation at N = 60 and to that at N = 90. This effect is particularly dramatic for the Sr isotopes where the onset of deformation is gradual below N = 50 but virtually instantaneous on the neutron-rich side at N = 60 [37]. Another example is the structure of the heavy N = Z nucleus ^{80}Zr which, despite having nucleon numbers of 40, is deformed rather than spherical in its ground state.

Unfortunately, the monopole p–n interaction matrix elements are not well known and it is not yet possible to account quantitatively for the known shifts of single-particle energies (e.g., the inversion of the neutron $2d_{5/2}$ and $1g_{7/2}$ orbits between Zr and Sn). Excellent empirical sets of two-body matrix elements are available for the 2s-1d shell in light nuclei but the reliability of such empirical sets falls off rapidly beyond the $1f_{7/2}$ shell. Partly, this is due to the lack of accessible nuclei where the appropriate combinations of proton and neutron single-particle states are available. As a specific example, the proton Z = 50–82 and neutron N = 82–126 shells have five and six orbits, respectively, and hence 30 two-body p–n T=0 matrix elements. However, since these shells tend to fill together near stability, empirical information is only available on the matrix elements between orbits occupying similar positions in each shell. Thus, for example, one can estimate the $\pi(2d_{5/2})$–$\nu(2f_{7/2})$ interaction, but not the $\pi(2d_{5/2})$–$\nu(3p_{1/2})$ or the $\pi(2d_{3/2})$–$\nu(2f_{7/2})$ interactions. Determination of the latter two interactions requires binding energies of the 0^+ ground states of even-even nuclei and single-particle energies in odd-mass nuclei that have, for example, two valence nucleons of one

type and many of the other (e.g., the neutron-rich Te, Z = 52, isotopes or the proton-rich N = 84 isotones). Such studies can revolutionize our knowledge of residual interactions. Combined with the capabilities of modern computers, this offers the hope that realistic *ab initio* microscopic nuclear-structure calculations in heavy nuclei may become possible for the first time.

Empirical p–n interactions of the last proton and last neutron may be estimated from double differences of binding energies of neighboring nuclei [26]. Figure 2 shows such empirical interactions for the ground states of even-even nuclei. The microstructure (see inset) reflects primarily the complementary contributions of the monopole and quadrupole components. In deformed nuclei, the behavior of the latter is usually understandable (at least qualitatively) in terms of the angular orientations of the respective Nilsson orbits. This gives the hope of another approach to extracting the monopole part. This is easiest in regions (near midshell) where the quadrupole component is small. However, to do this requires new data (binding energies) on such nuclei as ^{240}Cf, ^{244}Fm, ^{250}No, and ^{254}104, beyond point "A" in Fig. 2. A similar region may exist in the rare-earth region near N = 100, but it is less obvious empirically (region "B" in Fig. 2). Precise binding energies for such nuclei as ^{156,158}Er, $^{160-164}$Yb, ^{164,166}Hf, and ^{168}W, which should be accessible using RIBs, would be enormously useful. Indeed, measurement of these eight masses would immediately give p–n interactions in fourteen additional nuclei. Dysprosia–168,170 would fill in critical *lacunae* as well.

Lastly, it is known that T=0 p–n interactions in light N = Z nuclei are anomalously large (indeed, they appear as singularities in region "C" of Fig. 2), and also that they decrease in magnitude with increasing N or A. Shell-model calculations with realistic interactions reproduce this effect, as a consequence of the enhanced T = 0 matrix element in orbit combinations having high spatial symmetry that occur for N = Z. It will be especially interesting to extend such data (requiring sets of four adjacent masses) to still heavier N = Z regions where one might expect the spatial symmetry to be reduced due to the effects of the Coulomb force in altering the proton single-particle energies. Studies between Z = 40 and 50 would be particularly intriguing since ^{80}Zr has recently, and surprisingly (N,Z = 40 are often considered magic numbers), been discovered to be deformed [9] and ^{100}Sn is expected to be a good doubly-magic nucleus such as ^{208}Pb. With RIBs one can expect to form the entire N = Z sequence from ^{80}Zr to ^{100}Sn and perhaps beyond.

The overriding goal, which is now barely on the verge of achievement even in the phenomenological sense, is to achieve a truly unified macroscopic and

microscopic understanding of nuclear structure, collectivity, phase transitions, and deformation.

3.2 Access to New N,Z Combinations

Much of the discussion in the preceeding subsection, of course, relies on access to new regions of N and Z in the sense that the T = 1 and 0 residual interactions are dependent on the proton and neutron orbits; hence new effects and new information, often crucial not just incremental, can be obtained by extending the ranges of N and Z. Here we focus on different aspects of this, in particular on the interplay of single-particle and collective effects that may give rise, in uncharted nuclei, to new types of collective motion or shapes or to new examples of known types that will aid in an improved understanding of their structure and microscopic origins.

3.2.1 Neutron Halos and Skins

One of the most interesting and exotic new nuclear phenomena involves the concept of neutron skins or halos in extremely neutron-rich nuclei, such as ^{11}Li or ^{14}Be. Greatly-enhanced nuclear radii are observed for these cases [20,21] see Figure 3, where the last pair of neutrons is only barely bound. The opportunities for future studies here are many, ranging from the structure of the halos themselves to the exploitation of the loose binding and beta-decay lifetime of these nuclei in reactions, where such phenomena as neutron flow, large isospin transfer, and the like can be studied. The halo regions may be conceived of as an extremely low-density form of (neutron) nuclear matter. As such they are intermediate between free nucleons and normal-nuclear matter and one might think that they could provide a third regime in which to study nuclear interactions and medium modifications (e.g., EMC type effects). Clearly such experiments on halo nuclei will be extremely difficult at best, but measurements of, for example, the neutron magnetic moment in odd-neutron halo nuclei by laser spectroscopy, could be fascinating. The entire subject of neutron halos and skins is treated in greater detail in a separate chapter of this report [22].

3.2.2 New Collective Modes

Collective shapes are favored microscopically when single-particle orbits with that specific shape are occupied. Collective modes appear when orbits are occupied that have large matrix elements of the particular mode creation

operator with another nearby orbit. Therefore, access to new more exotic N,Z combinations affords the possibility to observe even more exotic shapes and collective excitations. Some of these, such as super and hyperdeformed shapes, which depend on large angular momentum for stability will be discussed in the next section.

Despite years of use of models of triaxial nuclei, there is essentially no firm evidence that nuclei exist with stable rigidly-asymmetric shapes [38]. Indeed, it is difficult to distinguish between stable triaxial shapes and fluctuations with respect to the triaxial (gamma) degree of freedom. Similarly, nuclei with oblate ground-state shapes are very few (e.g., some Pt and Au nuclei) and in those it also is likely that one is observing a gamma-soft configuration with a slightly oblate rms shape rather than a static oblate deformation.

Triaxial nuclei are likely to occur when the protons are filling prolate orbits and the neutrons oblate orbits or vice versa. In a Nilsson context these are, respectively, the downsloping and upsloping orbits that occur at the bottom or the top of a shell. In heavy nuclei examples of such "schizophrenic" nuclei are, therefore, to be sought in extremely neutron-poor or -rich species such as, isotopes of Hf – Pt nuclei with N $\approx$ 90 which could be produced with neutron deficient RIBs.

Oblate shapes occur when both protons and neutrons have nearly full shells. The Fermi surface then lies near highly oblate-driving orbits that cancel the normal prolate-driving preference that has been accumulated by the filled orbits. The oblate-prolate competition can often lead to two minima in the potential energy surface, one of each shape, and the nuclear ground state is then determined by rather subtle details. Coexistence is possible, as evidenced, for example, by nuclei with A $\approx$ 130 [39], as is gamma-softness (e.g., Pt, Au), if there is a path between the minima through the gamma plane. Interesting searches for oblate nuclei in the neutron deficient Se, Kr region, the light (N $<$ 82) Ba nuclei, and the light Au nuclei will again be facilitated by the use of fusion-evaporation reactions with neutron-deficient RIBs.

Of course, nuclear shape coexistence, just alluded to, is now known to be a widespread phenomena. Indeed the classic example is ^{152}Dy in which slightly-deformed oblate, "normally-deformed" prolate and superdeformed prolate states coexist at the same angular momentum [15,40]. Other beautiful examples of shape coexistence have been mapped out in the Pb, Tl, Hg region, down to neutron midshell (e.g., $^{182}Hg_{102}$ [41]) [see Figure 4]. The energy systematics of the intruding configuration shows a parabolic drop to-

wards midshell against N. This is consistent with the most popular interpretation of such states which predicts an energy minimum near midshell where the enhanced proton-neutron interaction in the intruder (particle-hole) excitation is a maximum. The Cd nuclei, known on both sides of neutron midshell, indeed suggest that the intruder energies rise roughly symmetrically about midshell. However, the absolute intruder excitation energies depend on the strength of the residual interaction relative to the energy gap that must be overcome and, in Cd, these energies happen to lie very close to the vibrational two-phonon states. While this gives a possibility to study the mixing of normal and intruder configurations, it also obscures the behavior of the latter. Therefore, a better testing ground would be even more neutron deficient-nuclei in the Hg region than can currently be populated. RIBs are crucial to further study of this issue. Another fascinating region centers on the N = 60 isotones near ^{100}Zr where the lowest known excited 0^+ states of any deformed nucleus have been discovered. The physics of intruder states is intimately linked with mechanisms for the onset of deformation and provides a unique view of those mechanisms.

In the last few years many examples of reflection-asymmetric nuclei [42] have been identified, usually by their signatures of parity-doublet rotational bands (0^+, 1^-, 2^+, 3^-, ... sequences, usually slightly displaced from each other), relatively enhanced E1 transitions and, in odd-mass nuclei, anomalous decoupling parameters. (An example [43] is shown in Figure 5.) Nevertheless, it remains an open question to what extent such fundamental shapes, which break an important spatial symmetry, are static or dynamic. Octupole shapes are expected in regions where both valence neutrons and protons filling the orbits of a "$\Delta l = 3$" pair (e.g., $\pi(2d_{5/2}$-$1h_{11/2})$ and $\nu(2f_{7/2}$-$1i_{13/2})$ in the rare earths). These orbits are strongly connected by the Y_3 operator. Octupole collective nuclei are known in the light Rn-Th region and in the rare earths near ^{146}Ba. With RIBs, other examples, in lighter nuclei, such as ^{90}Se and ^{94}Kr or their odd-mass neighbors, could be sought. Also, in many neutron-deficient nuclei formed in heavy-ion fusion-evaporation reactions, the low-j (especially the 3^-) states are not observed and therefore the octupole collectivity remains poorly established. Access to these nuclei by "softer" reactions using RIBs is an intriguing possibility. The light ($A \approx 120$) Xe, Te region would be especially interesting for such studies.

Higher moments in the nuclear shape, such as hexadecapole deformations, are also well established, especially in the stable W nuclei where diagonal Y_4 matrix elements among high-j, unique-parity, orbits are large. Hexadecapole vibrations are also a likely component of low-lying ($\approx$ 1 MeV)

K = 4 bands in Os. A positive ϵ_4 (barrel shape) is naturally expected when the configurations with the largest radii are filling mid-K Nilsson orbits. These orbits are oriented $\approx 45°$ relative to the nuclear equator and thus favor an infilling of nuclear matter in the "corners". Such shapes also should appear in lighter nuclei, for example, heavy Pd nuclei ($^{116-120}$Pd) which could be produced with very neutron rich RIBs or by fission of the heaviest actinides.

Finally, there are sporadic hints of even higher moments (e.g., β_5 and β_6 deformations [44]). Five-minus levels are often considered as rotational excitations built on lower-lying 3^- states. However, near the top of each shell in heavy nuclei, there is the possibility of a direct $\Delta l = 5$, two-quasiparticle, excitation, such as an $h_{11/2} \otimes s_{1/2}$, in the 50–82 shell. Indeed, the Te–Ba nuclei with N $\approx$ 70 have anomalously low 5^- states (relative to the 3^- states). In some cases even $E_x(5^-) < E_x(3^-)$. It is interesting to speculate whether the analogous $\Delta l = 5$ excitations in heavier nuclei, namely $i_{13/2} \otimes p_{3/2}$ and $j_{15/2} \otimes d_{5/2}$ in the 82–126 and 126–184 shells have sufficient degeneracy to allow the development of collective 5^- correlations. However, the present knowledge of 5^- states in the rare earth and actinide nuclei is limited, e.g. to Dy isotopes with A < 158, Ra with A $\leq$ 158, and Th with A $\leq$ 232, where the $i_{13/2}$ or $j_{15/2}$ are barely occupied. If substantially more neutron-rich Dy, Er, Ra, or Th nuclei could be studied using RIBs, this new collective mode might be disclosed.

The possibility of observing new collective modes or symmetries implies as well the likelihood of discovering new shape/phase transitional regions, or of extending existing ones. This is an attractive opportunity since, historically, more has probably been learned about (collective) nuclear structure, its manifestations and dynamics, from such regions than in any others. Recent work in the very neutron-deficient rare earth nuclei, especially the light Ce and Nd isotopes with A = 120–130, has provided evidence [45] for a new, gradual, spnerical to soft shape transition that has the earmarks of becoming stably-deformed for slightly-smaller neutron number. This region has only begun to be mapped out; the largest $E_x(4^+)/E_x(2^+)$ ratios in the region are still only $\approx$ 3.0, and the vibrational modes are as yet virtually unstudied). This region is interesting because its smooth evolution is in contrast with the sharp onset of deformation in the A = 100 and 150 mass regions. A thorough study, using proton-rich RIBs, will be helpful in understanding the mechanism for deformation and the interplay of the dynamics of the underlying single-particle structure and the collective correlations that develop.

Of course, one of the most exciting new regions centers on the heaviest known N = Z nuclei (discussed earlier in a different but related context). Zirconium-80 has recently been found [9] to be deformed despite having 40 protons and 40 neutrons (see Figure 6). Neighboring nuclei as well as the heavier N = Z species approaching ^{100}Sn will provide perhaps the most exciting opportunity yet to observe the evolution and coexistence of shapes and the persistence of magic numbers, since it is widely expected that the so far elusive ^{100}Sn will be doubly magic. Where, along the N = Z path, does the spherical configuration become the ground state? How stable are the 40 and 50 magic numbers? These are key questions at the heart of our understanding of shell and collective structure. Experimentally, these nuclei might be reachable with reactions on unstable, long-lived targets, such as ^{40}Ca + ^{56}Ni $\rightarrow$ ^{96}Cd* or ^{40}Ca + ^{44}Ti $\rightarrow$ ^{84}Mo*, or with neutron-deficient RIBs.

3.2.3 Other Issues

The Fermion Dynamical Symmetry Model [46] suggests sudden "breaks" in nuclear systematics (e.g., in the actinides when the normal-parity neutron shell is 1/3 filled) due to special Pauli effects. In simple terms, the filling of certain classes of states ultimately blocks some collective modes, causing others (in this scheme) to suddenly become the ground state. Concomitant effects in transition rates should accompany this phenomenon. The use of RIBs to establish either the existence, or the nonexistence, of such effects, for example in the neutron-rich actinides, could be a litmus test for these models.

Finally, other models, currently nearing the stage of practical calculations, attempt, for the first time, to encompass multi-$\hbar\omega$ spaces and to incorporate the collectivity of giant resonances and low-lying structures into a single unified framework, without effective charges [47]. The study of higher-spin states of stable nuclei (e.g., ^{168}Er), which is accessible with RIBs (see below), would provide the critical tests of these models.

3.3 Complete Spectroscopy and Chaos

The access to high decay energies far from stability allows numerous opportunities for extending spectroscopic studies as a function of N, Z, and E_x. Several of these possibilities have already been mentioned, e.g. the study of beta-delayed particle instability, cluster emission, and G-T quenching. How-

ever, one aspect of high decay energies remains to be considered: namely the possibility for "complete" spectroscopic studies [48]. This term refers to the experimental establishment of sets of levels, in certain ranges of excitation energy and spin, that are known to be essentially complete, and the further delineation of as many of their properties, e.g. decay routes, moments, lifetimes, etc., as possible. Such complete data not only provide the most strigent tests of nuclear models, they also provide a very detailed information base for a specific quantum system that can be utilized for understanding even more general physical ideas and for technical applications. A currently-fashionable example is analyses to determine whether nuclear levels are "ordered" or "chaotic."

3.3.1 Complete Spectroscopic Measurements

The classic tool for ensuring that the set of states populated is complete, only usable along the stability line, is the (n,γ) reaction, especially in the Average Resonance Capture (ARC) mode. However, other reactions, which feed the nucleus at suffiently-high excitations energies (temperatures) and which deexcitate statistically, also offer a virtual guarantee of completeness in the appropriate cases. One can cite, for example, the (n,n'γ) reaction for low-spin states, the ($\alpha, xn\gamma$) or (light heavy-ion,xnγ) reactions for intermediate spin states and (heavier heavy-ion,xnγ) reactions for still higher spins, as well as, to a lesser degree, beta-decay with extremely large Q_β values.

There are two conceptually-distinct areas of work here. One is the study of low-spin states very far from stability (primarily by beta decay), providing the first tests of nuclear models of, for example, collective modes, in such new N,Z regions. Perhaps even more intriguing is the opportunity to use neutron-rich RIBs to study high-spin states of stable or near-stable nuclei, in order to complement already existing, complete, low-spin data, and thereby, forging the first comprehensive links between high- and low-spin nuclear structure. Perhaps the best heavy case for this is ^{168}Er which is known, for I = 0–6, in an essentially complete form up to about 2 MeV. Here, the use of reactions, such as ^{130}Te(^{42}S,4n)^{168}Er, and/or ^{154}Sm(^{18}C,4n)^{168}Er, would provide a comparable completeness for high-spin levels and offer perhaps the only nucleus where the full panoply of nuclear structure models could be simultaneously tested. In general, low-spin data is abundant in rare earth nuclei near stability. Figure 7 shows the loci of nuclei that could be produced at high spin using RIBs with 6 neutrons beyond stability. Today's models aim at being more and more comprehensive but require correspondingly-

thorough data for their testing. This is not a program to be carried out on every possible nucleus, but as history has shown, such studies in isolated, well chosen, cases can be extremely valuable. Another example, this time an odd-mass nucleus, might be ^{109}Pd in which a nearly full set of unique-parity favored and unfavored anti-aligned states based on the $\nu(h_{11/2})$ orbit is known and where disclosure of the complementary aligned states would permit the best test to date of particle-rotor models.

3.3.2 Average Nuclear Properties

Complete spectroscopic data will provide a means of establishing average nuclear properties and thereby distinguishing these average properties from the "truely-novel" exceptions. For example, neither the low-lying collective states (the subject of much of the past two decades of low-spin experimental studies) nor the highly-aligned near-yrast high-spin states (likewise the main subject of the past two-decades of high-spin studies - see the following section) are representative of the average nuclear states. Both are strongly-populated in statistical reactions, hence available for study, because their special properties (correlations and the Coriolis force respectively) cause them to occur at low excitation energies. More complete data, however, will establish average quantities (e.g. level densities, transition rates, decay widths, ...) as a function of the experimentally accesible quantities N, Z, I, π, and E_x. Such information would be of considerable importance for a variety of applications.

3.3.3 Is the Nuclear Spectrum of States Ordered or Chaotic?

Finally, complete spectroscopy will provide a greatly-expanded opportunity to investigate seriously the issue of quantum chaos in nuclei [49]. Sufficient data exists to indicate that the spacing of nuclear states at the neutron and proton thresholds is describable by random-matrix theory [50], i.e. nuclei under these conditions are "chaotic." Yet special states (such as isobaric analogue states, molecular resonances, superdeformed states, very high-K states, ...) at the same excitation energy seem to remain "pure." They apparently do not mix with the background of strongly-mixed, "chaotic" states. Attempts at extending such analyses to lower excitation energies to study the temperature and angular-momentum dependence of the transition from ordered to chaotic systems have not been conclusive [51] because of the lack of complete nuclear data.

The description of the nuclear quantum system in terms of the currently-fashionable concept of "order" and/or "chaos" is by no means complete. Fundamental questions, such as: how the nuclear quantum system evolves from ordered to chaotic behavior, the coexistence of ordered and chaotic states, transition rates in chaotic systems, the role of symmetries in preserving order, more efficient (i.e. simpler) descriptions of chaotic quantal systems, and the relation between a chaotic nucleus and other chaotic quantal systems, remain to be answered. Detailed studies of nuclei like ^{26}Al [52] have already set the stage; however, complete data for selected nuclei sampling the variety of phenomena described in the previous sections are needed to answer the questions posed by this new approach to nuclear physics.

4 High-Spin Studies with Radioactive Ion Beams

The use of radioactive ion beams, not only will allow high-spin studies similar to those in vogue today (see e.g. [53,54]) to be extended to a wider range of nuclei testing our current understanding of rapidly-rotating nuclei, it also will allow new physical concepts to be studied. Some of these ideas are summarized in this section.

4.1 Exotic Nuclear Shapes at High Spin

The exotic equilibrium shapes, such as superdeformed (2:1 ratio of major to minor axis), octupole (pear-shaped), and triaxial that nuclei can assume in the extreme condition of rapid rotation are an excellent illustration of the intimate connection between independent-particle and collective degrees of freedom. Since these shapes depend on the details of the spectrum of single-particle quantum states, the greater variety of such states that nuclei at the limits of isospin will provide is desirable. The condition of minimum energy and the strong, attractive, short-ranged nuclear interactions tend to select "conventional" equilibrium shapes. By enlarging the variety of single-particle states by forming nuclei at the extremes of both isospin and angular momentum more exotic shapes become feasible. For example:

Superdeformed states occur [15] when large gaps (providing negative single-particle energy contributions) develop in the spectra of single-proton and single-neutron states for a 2:1 ratio of the major to minor axis. Calculations [55] indicate that such gaps occur in prolate nuclei for $Z \approx$14–17, 34, 39–42, 65–69, and 82–94 and $N \approx$ 30–47, 63–67, 78–92, 104–112, and 138–158. Superdeformed shapes already have been observed for (Z, N) =

(65–69,78–92), (82–94,104–112), and (82–94,138–158) corresponding to the ^{152}Dy region, the ^{192}Hg region, and the fission isomers, respectively [54]. The use of radioactive beams should provide other mass regions where both proton and neutron single-particle spectra favor superdeformed shapes, for example, (Z, N) = (65–69,63–67), (39–42,63–67), and (39–42,30–47), and extend the possible superdeformed studies in other regions only partly accessible to stable targets and beams.

Shell corrections also should occur for oblate superdeformed shapes (2:1 ratio of major to minor axis, but with two major axes *versus* one major axis for prolate superdeformed systems). As yet no oblate superdeformed nuclei have been identified. The nucleus ^{148}Sm, which is not accessible at high spin with (heavy-ion, xn) reactions using stable beams and targets, is predicted to be one of the most favorable cases for superdeformed oblate collective shapes.

Hyperdeformed equilibrium shapes (3:1 ratio of major to minor axes) also have been predicted, but not yet observed. The most favorable predicted [56] cases for experimental studies, rapidly-rotating nuclei near ^{166}Er, can only be populated at maximum angular momentum with radioactive ion beams. The increased neutron excess of this isotope relative to those accessible with the fusion-evaporation reaction using stable heavy-ion beams also increases the angular momentum that the compound system can accomodate and survive fission. Such an angular momentum increase is crucial for observing hyperdeformed states. The nucleus requires a great deal of angular momentum to stablize such enlongated nuclear shapes. Indeed the added angular momentum associated with the radioactive beams may be the difference between observing and not observing hyperdeformation.

4.2 Exotic Configurations Dominated by the Coriolis Force

Many of the current topics of high-spin physics (e.g. band crossings ("backbends"), loss of collectivity at high spin, and signature dependent energies and transition rates) are associated with high-j, low-Ω configurations that have a large projection of the intrinsic angular momentum, j_x, on the rotational axis. These phenomena are the result of modifications of the spectrum of single-particle states by the Coriolis plus centrifugal interaction leading to a term in the independent-particle hamiltonian equal to $-\omega j_x$. Configurations always exist in the next higher shell with even larger values of j_x. For prolate deformations these "exotic" configurations lie low in the higher shell. (For superdeformed and hyperdeformed systems they intrude into the

lower shell and are important components in producing the deformed shell gaps that lead to stability.) In a rapidly rotating system such orbits also can intrude into the lower shell for normal deformations. Anomalous moments of inertia [57] and band crossings [58] are associated with the few cases where such high-j_x intruders presently are observed in near transitional nuclei. Using neutron-rich radioactive beams, it should be possible to populate such configurations in stably-deformed nuclei testing whether the observed anomalies are associated with these orbits or the stability of the nuclear shape.

In the actinides such high-j_x intruders correspond to shell-model states from above the superheavy shell gaps, e.g. the $j_{15/2}$ proton state and the $k_{17/2}$ neutron state. The low-ω components of these configurations, which are predicted [59] to lie just above the Fermi level for the heaviest possible actinide targets (e.g. ^{248}Cm and ^{252}Cf), should become yrast at moderate spins, I =20–30. Because of Q-value considerations (see below) radioactive beams probably are necessary for the population of such states in Coulomb excitation plus transfer reactions.

4.3 Residual Proton–Neutron Interactions at High Spin

The major modifications of the single-particle quantal states at large angular momentum described in the preceeding paragraphs also will change the overlaps of the nucleonic orbitals thereby modifying the residual nucleon-nucleon interactions. Not only are the high–j, low–Ω orbitals most-strongly affected by the Coriolis and centrifugal forces, but they also are the most localized [60], and therefore, the most sensitive to residual interactions. Interesting attempts at extracting empirical estimates of such interactions are described in [60,61,62]. The possibility of studying even higher–j, low–Ω intruder orbitals using RIBs, as described in the preceeding subsection, should allow even more exotic nucleon-nucleon interactions to be studied as a function of rotation.

In the limit of very large angular momentum, where the single-particle structure of the nucleus is dominated by Coriolis and centrifugal forces, the occupation of configurations associated with nucleons moving in equatorial orbitals in the direction of the nuclear rotation is increased [60]. Such orbitals have large spatial overlap. This is a necessary, though not sufficient, condition for a new type of correlation that might be termed "Coriolis correlations." The increased localization associated with the various substates of the even higher-j "intruder" orbitals that should be available in selected

nuclei that can be populated with RIBs (see the preceeding paragraph) will enhance this possible new type of collectivity.

Residual p–n interactions also can affect the alignment of angular momenta with the rotational axis, and hence band crossings [63]. As with all residual p–n interactions such phenomena are largest where the protons and neutrons are filling, not only the same shell, but also similar orbits of the same shell. Therefore, these effects, which to date have been largely negelected will be largest in those neutron-defficient, deformed nuclei with $N \approx Z$ that can be studied using neutron-deficient RIBs.

4.4 Transfer Reactions

Many of the possibilities of using heavy-ion transfer reactions, for example, to populate neutron-rich nuclei or the high-spin states based on intruder orbits originating from above the superheavy shell, as described in the preceeding subsections, are limited by the reaction mechanism. Heavy-ion induced transfer reaction cross sections are strongly Q–value dependent. Positive Q values enhance such cross sections. This is especially true for proton transfer reactions. Unfortunately the decrease in the binding energy curve for $A > 56$ leads to negative relative binding in the target for stripping reactions and hence requires projectiles with very weakly-bound protons or neutrons to compensate. For example, heavy-ion beams with a single proton or neutron outside a doubly-closed shell are desirable for single-proton and single-neutron transfer reactions. However, except for light heavy ions, such as ^{17}O (and ^{209}Bi in which the proton remains quite strongly-bound) these nuclides are not stable. ^{37}S and ^{49}Ca seem ideal for single-neutron transfer, and ^{38}S and ^{50}Ca are interesting beams for two-neutron stripping. Likewise, ^{41}Sc and ^{57}Cu beams are optimal for single-proton stripping as is ^{42}Ti for two-proton stripping. It is emphasized that transfer reactions and Coulomb excitation are the most efficient methods of populating the actinides at high spin, since the dominant decay of the highly-excited actinide residues of the heavy-ion fusion reaction is fission.

4.5 Coulomb Excitation of Exotic Radioactive Beams

It would be possible to determine the magnitude of the quadrupole moment of any RIB nuclei by Coulomb exciting the beam nuclei using, for example, a ^{208}Pb target. This technique would be important in exploring the new shell closures, transitional nuclei, and regions of deformation described elsewhere

in this report. It also would allow the first comparison of transition rates obtained from Coulomb excitation and Doppler-shift lifetime measurement based on (heavy-ion,xn) reactions.

5 Summary

This report outlines some of the nuclear structure topics discussed at the Los Alamos Workshop on the Science of Intense Radioactive Ion Beams. In it we also have tried to convey some of the excitment of the participants for utilizing RIBs in their future research. The introduction of radioactive beams promises to be a major milestone for nuclear structure perhaps even more important than the last such advance in beams based on the advent of heavy-ion accelerators in the 1960's. RIBs not only will allow a vast number of new nuclei to be studied at the extremes of isospin, but the variety of combinations of exotic proton and neutron configurations should lead to entirely new phenomena. A number of these intriguing new studies and the profound consequences that they promise for understanding the structure of the atomic nucleus, nature's only many-body, strongly-inteacting quantum system, are discussed in the preceeding sections. However, as with any scientific frontier, the most interesting phenomena probably will be those that are not anticipated—they will be truly new.

References

[1] Brookhaven National Laboratory, Upton, N.Y. Brookhaven National Laboratory is operated by the Associated Universities for the U.S. Department of Energy. Work supported under Contract No. DE-AC02-76CH00016.

[2] Oak Ridge National Laboratory, Oak Ridge, TN. Oak Ridge National Laboratory is operated by Martin Marietta Energy Systems Inc. for the U.S. Department of Energy under Contract No. DE-AC05-850R21400.

[3] Treatise on Heavy-Ion Science, Volume VIII — Nuclei Far From Stability, ed. D.A. Bromley (Plenum, 1989, New York).

[4] C. Detraz and D. Vieria, Ann. Rev. Nucl. Sci. 39 (1989) 407.

[5] Proceedings of Fifth International Conference on Nuclei far From Stability, AIP Conf. Series Number 164, ed. I.S. Towner (AIP, 1988, New York).

[6] Proceeding of the First International Conference on Radioactive Nuclear Beams (World Scientific, 1990, Singapore).

[7] M. Ogawa, *et al.*, Phys. Rev. Lett. 41 (1978) 289.

[8] C. Thibault, *et al.*, Phys. Rev. C12 (1975) 644; X. Campi, et al., Nucl. Phys. A251 (1975) 193; and C. Detraz, in Proc. Fourth Int'l. Conf. on Nuclei Far from Stability, Helsingor, 1981, eds. P.G. Hansen and O.B. Nielsen,CERN Rep. 81-09 (CERN, 1981, Geneve) p.361.

[9] C.J. Lister, *et al.*, Phys. Rev. Lett. 59 (1987) 1270.

[10] E. Cheifetz, R.C. Jared, S.G. Thompson and J.B. Wilhelmy, Phys. Rev. Lett. 25 (1970) 38.

[11] S.W. Yates and R.A. Meyer, Phys. Rev. C33 (1986) 1843.

[12] P. Federman and S. Pittel, Phys. Lett. 69B (1977) 385; and 77B (1978) 29.

[13] H.J. Rose and G.A. Jones, Nature 307 (1984) 245; D.V. Alexandrov, *et al.*, Zh. Exp. Theo. Fiz. 40 (1984) 152, JETP Lett. 40 (1984) 909; S. Gales, *et al.*, Phys. Rev. Lett. 53 (1984) 759; P.B. Price, *et al.*, Phys. Rev. Lett. 54 (1985) 297; W. Kutschera, *et al.*, Phys. Rev. C32 (1985) 2036; Barwick, *et al.*, Phys. Rev. C31 (1985) 1984; and M. Paul, *et al.*, Phys. Rev. C34 (1986) 1980.

[14] J.P. Balagna, *et al.*, Phys. Rev. Lett. 26 (1971) 145; see also D.C. Hoffman, *et al.*, Phys. Rev. C 21 (1980) 972; and E.K. Hulet, *et al.*, Phys. Rev. Lett. 56 (1986) 313.

[15] P.J. Twin, *et al.*, Phys. Rev. Lett., 57 (1986) 811.

[16] T. Byrski, *et al.*, Phys. Rev. Lett., 64 (1990) 1650; and W. Nazarewicz, P.J. Twin, P. Fallon, and J.D. Garrett, *ibid.* pg. 1654.

[17] S.G. Nilsson, *et al.*, Nucl. Phys. A131 (1969) 1.

[18] P. Möller, G.A. Leander, and J.R. Nix, Z. Phys A323 (1986) 41; and K. Böning, Z. Patyk, A. Sobiczewski, and S. Cwiok, Z. Phys. A325 (1986) 479.

[19] P. Möller, J.R. Nix, and W.J. Swiatecki, Nucl. Phys. A492 (1989) 349.

[20] I. Tanihata, *et al.*, Phys. Letts, 160B (1985) 380; Phys. Rev. Lett. 55 (1985) 2676; and Phys. Lett. 206B (1988) 592.

[21] I. Tanihata, in Proc. of Conf. on Nuclear Structure in the Nineties, ed. N.R. Johnson, Nucl. Phys. A, in press.

[22] See W. Bauer, Cont. in these Proceedings; and refs. therein.

[23] W. Myers, in Proc. of First Int'l. Conf. on Radioactive Nuclear Beams (World Scientific, 1990, Singapore), in press.

[24] See, e.g., B. Frois, in Nuclear Structure 1985, ed., R. Broglia, G. Hagemann, B. Herskind (North Holland, 1985, Amsterdam) p.25.

[25] J. Decharge and D. Gogny, Phys. Rev. C21 (1980) 1568; and J.W. Negele, Rev. Mod. Phys. 54 (1982) 913.

[26] D.S. Brenner, C. Wesselborg, R.F. Casten, D.D. Warner, and J.-Y. Zhang, Phys. Lett. B, in press.

[27] E.K. Warburton, J.A. Becker, and B.A. Brown, Phys. Rev. C41 (1990) 1147; C. Thibault, *et al.*, Phys. Rev. C12 (1975) 644; and C. Detraz, *et al.*, Nucl. Phys. A394 (1983) 378.

[28] I.S. Towner, in Nuclei Far from Stability, ed. I.S. Towner, AIP Conf. Proc. 164 (AIP, 1988, New York) p. 593.

[29] V. Trimble, Rev. Mod. Phys. 47 (1975) 877; and G.J. Mathews and R.A. Ward, Rep. Prog. Phys. 48 (1985) 1371.

[30] E.W. Otten, in Treatise on Heavy-Ion Science, ed D.A. Bromley (Plenum, 1989, New York) vol VIII, p. 515.

[31] K.-R. Anton, *et al.*, Phys. Rev. Lett. 40 (1978) 642.

[32] G.D. Sprouse, *et al.*, Phys. Rev. Lett. 53 (1989) 1463.

[33] J.A. Bounds, *et al.*, Phys. Rev C36 (1987) 2560; G. Ulm, *et al.*, Z. Phys. A325 (1986) 247; U. Krönert, *et al.*, Z. Phys. A331 (1988) 521; J.K.P. Lee, *et al.*, Phys. Rev. C38 (1988) 2985; H.T. Duong, *et al.*, Phys. Lett. B217 (1989) 401; and Th. Hilberath, *et al.*, Z. Phys. A332 (1989) 107.

[34] G. Huber, in The Variety of Nuclear Shapes, ed. J.D. Garrett, *et al.*. (World Scientific, 1988, Singapore).

[35] X.L. Tu, X.G. Zhou, D.J. Vieira, J.M. Wouthers, Z.Y. Zhou, M.L. Seifert, and V.G. Lind, Z. Phys. A, in press.

[36] I. Talmi, Rev. Mod. Phys. 34 (1962) 704; and K. Heyde, Int. J. Mod. Phys. A4 (1989) 2063.

[37] F. Wohn, *et al.*, to be published.

[38] I. Hamamoto, in Microscopic Model in Nuclear Structure Physics, ed. M.W. Guidry, *et al.*(World Scientific, 1989, Singapore) p. 173.

[39] E.S. Paul, *et al.*, Phys. Rev. Lett 58 (1987) 984; and M.J. Godfrey, *et al.*, J. Phys. G 15 (1989) 671.

[40] B.M. Nyako, *et al.*, Phys. Rev. Lett. 56 (1986) 2680.

[41] P. Van Duppen, E. Coenen, K. Deneffe, M. Huyse, and J.L. Wood, Phys. Lett. 154B (1985) 354.

[42] G.A. Leander and Y.S. Chen, Phys. Rev. C37 (1988) 2744.

[43] M. Dahlinger, *et al.*, Nucl. Phys. A484 (1988) 337.

[44] P.D. Cottle, *et al.*, Phys. Rev. C, in press.

[45] B.J. Varley, *et al.*, in Capture Gamma-Ray Spectroscopy and Related Topics- 1989, ed. S. Raman, AIP Conf. Proc. 125 (AIP, 1984, New York) p. 709.

[46] C.L. Wu, *et al.*, Phys. Lett. 168B (1986) 213; and M. Guidry in Proc. of the Sym. on Exotic Spectroscopy, ed. W. McHarris (American Chemical Society, 1990), in press.

[47] O. Castanos and J.P. Draayer, Nucl. Phys. A491 (1989) 349.

[48] R.F. Casten, D.D. Warner, M.L. Stelts, and W.F. Davidson, Phys. Rev. Lett. 45 (1980) 1077; and J.D. Garrett, in Proc. Workshop on Nucl. Struct. in the Era of New Spectroscopy, Part B—The Nucleus at High Spin (Niels Bohr Inst., 1989, Copenhagen) pg. 159.

[49] O. Bohigas and H.A. Weidenmuller, Ann. Rev. Nucl. Part. Sci. 38 (1988) 421; and W.J. Swiatecki, Nucl. Phys. A488 (1988) 375c.

[50] R.V. Haq, A. Pandey, and O. Bohigas, Phys. Rev. Lett. 48 (1982) 1986.

[51] T. von Egidy, H.H. Schmidt, and A.N. Behkami, Nucl. Phys. A481 (1988) 189; and J.D. Garrett and J.M. Espino, in Nuclear Structure in the Nineties, ed. N.R. Johnson (ORNL, 1990, Oak Ridge) pg. 126.

[52] G.E. Mitchell, *et al.*, Phys. Rev. Lett. 61 (1988) 1473; and J.F. Shriner, Jr., *et al.*, Phys. Rev. C, in press.

[53] GAMMASPHERE Proposal, eds. M.A. Deleplanque and R.M. Diamond, (1988).

[54] Proceedings of the Conference on Nuclear Stucture in the Nineties, ed. N.R. Johnson, Nucl. Phys. A, in press.

[55] T. Bengtsson, M.E. Faber, G. Leander, P. Möller, M. Ploszajczak, I. Ragnarsson, and S. Åberg, Physica Scripta 24 (1981) 200.

[56] J. Dudek, T. Warner, and L.L. Riedinger, Phys. Lett. B211 (1988) 252.

[57] B. Cederwall, *et al.*, Phys. Lett. B, in press.

[58] See e.g., C.-H. Yu, *et al.*, Nucl. Phys. A511 (1990) 157.

[59] J.B. Wilhelmy, R.R. Chasman, A.M. Friedman, and I. Ahmad, in Opportunities

[60] J.D. Garrett, J. Nyberg, C.Y. Yu, J.M. Espino, and M.J. Godfrey, in Contemporary Topics in Nuclear Structure Physics, ed. R. Casten, *et al.*(World Scientific, 1988, Singapore) p. 699.

[61] S. Frauendorf, *et al.*, Nucl. Phys. A431 (1984) 511.

[62] J. Y. Zhang, *et al.*, in Proc. of the Conf. on Nuclear Structure in the Nineties, ed. N.R. Johnson, Nucl. Phys. A (1990), in press.

[63] J.A. Sheikh, N. Rowley, and M.A. Nagarajan, Phys. Lett. B240 (1990) 11; and Phys. Rev. Lett., in press.

Figure Captions:

Figure 1. Potential energy contours as a function of r, the distance between the mass centers, and σ, the fragment elongation, for $^{252}Cf_{154}$, middle portion, and $^{258}Fm_{158}$, lower portion. The family of shapes considered are shown as a function of r and σ in the upper portion of the figure. The two fission paths are illustrated by the arrows superimposed in the lower-portion of the figure. For further details see [19].

Figure 2. The empirical residual interactions, δV_{pn}, extracted from double differences of the ground-state binding energies in neighboring even-even isotopes and isotones, see [26], are shown as a function of the number of neutrons. The inset gives an expanded view for N = 40–160. The portions of the curve labelled "A", "B", and "C" are discussed explicitly in the text.

Figure 3. Measured interaction radii, R_I, of neutron-rich isotopes of He, Li, Be, B, and C as a function of A. Note the striking deviation of r_I from 1.18 $A^{1/3}$ for ^{11}Li, ^{11,12,14}Be, and perhaps ^{17}B. See ref. [21], the source of this figure, for reference to the original data.

Figure 4. Plot of the excitation energy of the intruding coexisting deformed states in the isotopes of Tl, Pb, and Bi. See ref. [41], the source of this figure, for reference to the original data.

Figure 5. Partial level scheme for the nucleus $^{223}Th_{133}$ [43] showing two "parity-doublet" rotational sequences, connected by enhanced E1 transitions, characteristic of stable octupole deformations.

Figure 6. Low-lying level schemes [9] of self-conjugate nuclei $^{76}Sr_{38}$ and $^{80}Zr_{40}$, indicating the rotational behavior of these nuclei, $E_x(4^+)/E_x(2^+) \approx 2.85$ for both nuclei.

Figure 7. Comparison of stable nuclei (circles) and all the nuclei (squares) that can be populated as compound nuclei using heavy-ion fusion reactions on stable targets and with beams of $Z \geq 13$ and six neutrons beyond the heaviest stable isotope. Note that even allowing for the emission of 4-5 neutrons in the (H.I., xn) reaction, it is possible to overlap low-spin studies near stabil ty and high-spin studies populated using (H.I.,xn) in the same nuclei.

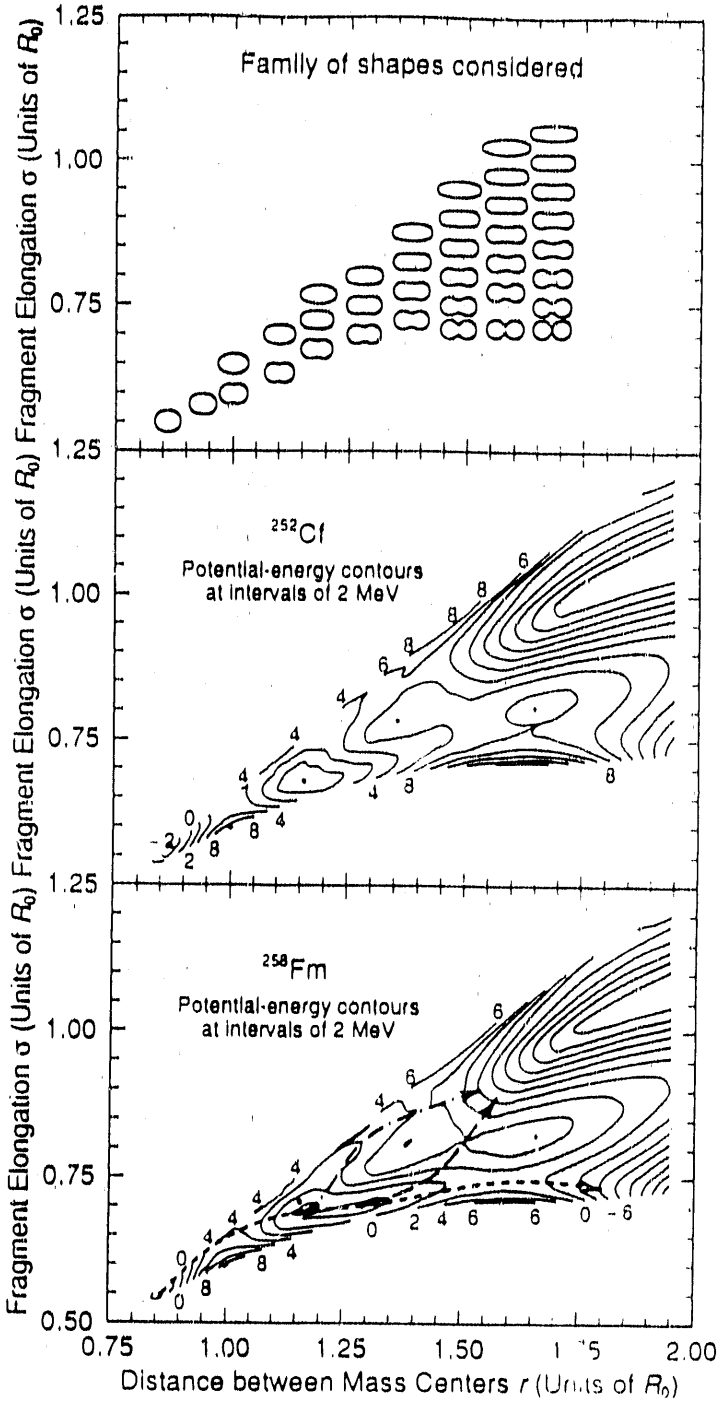
Family of shapes considered
^{252}Cf
Potential-energy contours
at intervals of 2 MeV
^{258}Fm
Potential-energy contours
at intervals of 2 MeV
Fragment Elongation σ (Units of R_0)
Distance between Mass Centers r (Units of R_0)
1.25
1.00
0.75
0.50
0.75
1.00
1.25
1.50
2.00

FIGURE 1

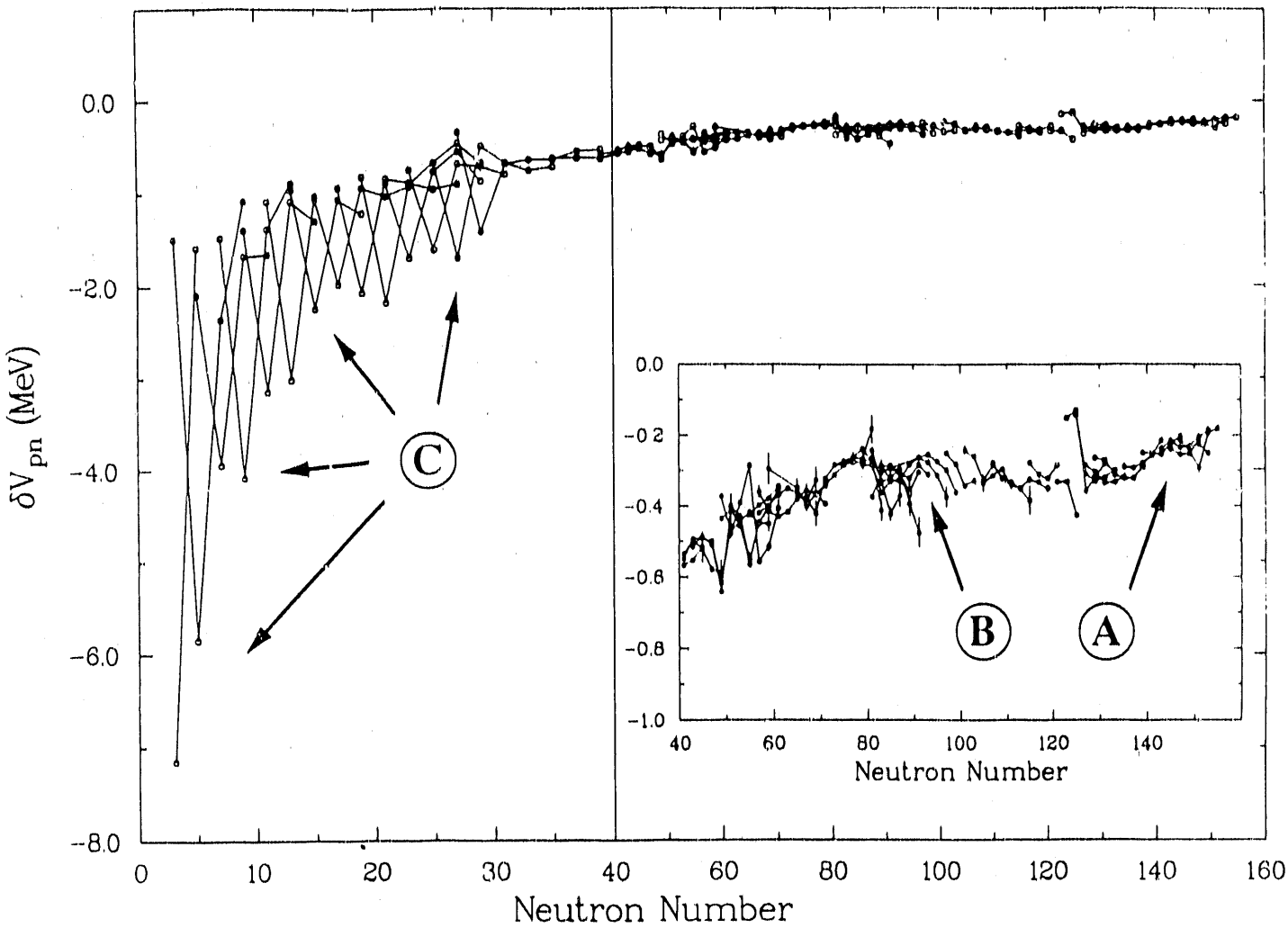
0.0
-2.0
-4.0
-6.0
-8.0
δV_{pn} (MeV)
0
10
20
30
40
60
80
100
120
140
160
Neutron Number
C
0.0
-0.2
-0.4
-0.6
-0.8
-1.0
40
60
80
100
120
140
Neutron Number
B
A

FIGURE 2

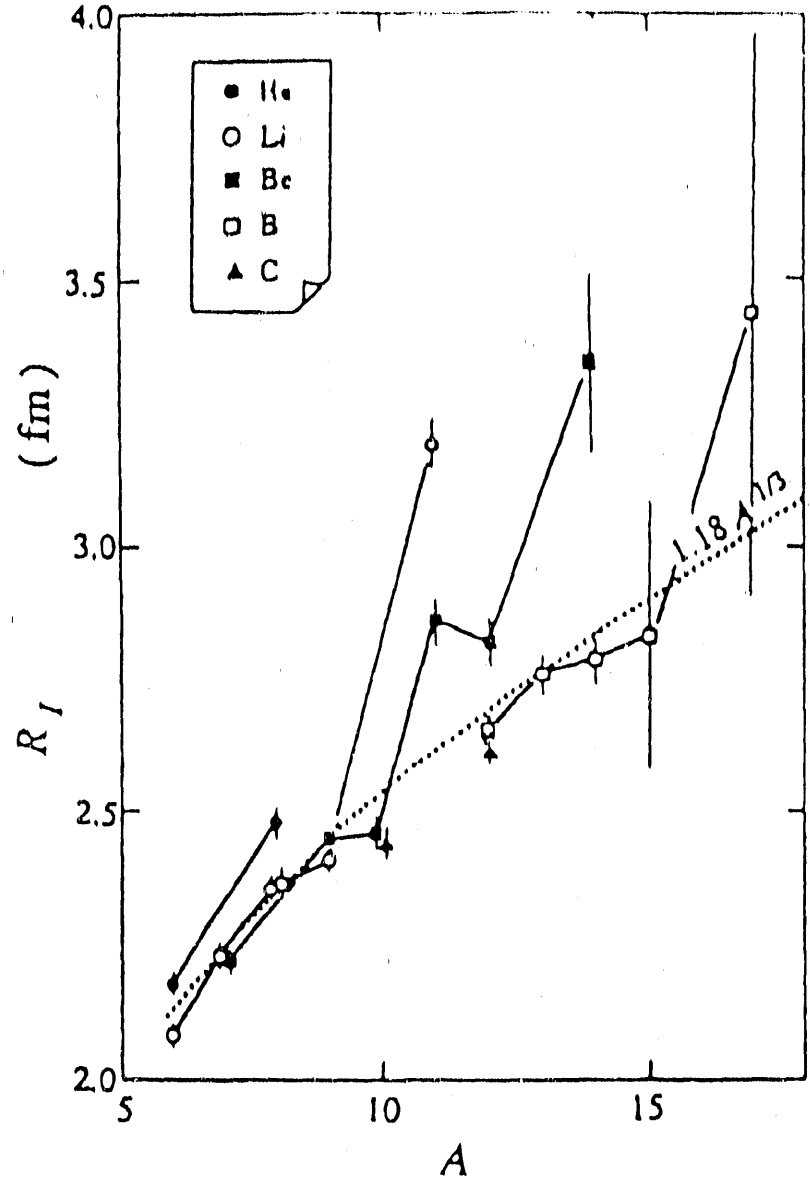

FIGURE 3

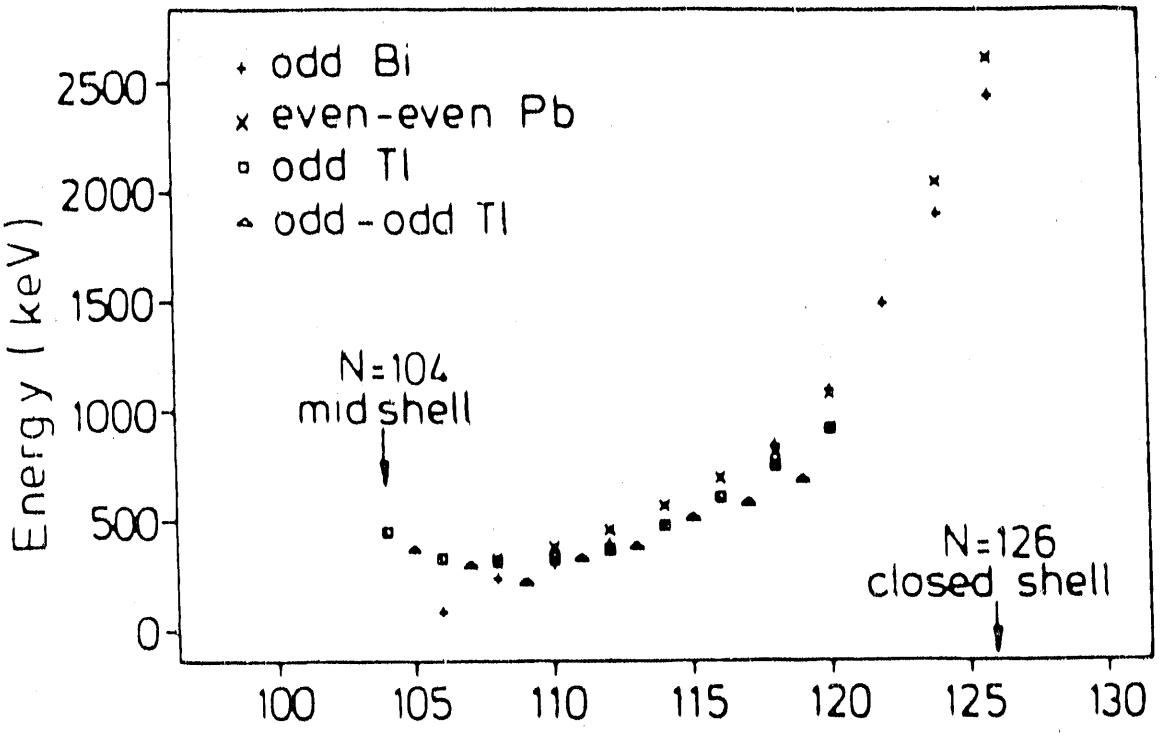
odd Bi
even-even Pb
odd Tl
odd-odd Tl
Energy (keV)
2500
2000
1500
1000
500
0
N=104
mid shell
N=126
closed shell
100
105
110
115
120
125
130

FIGURE 4

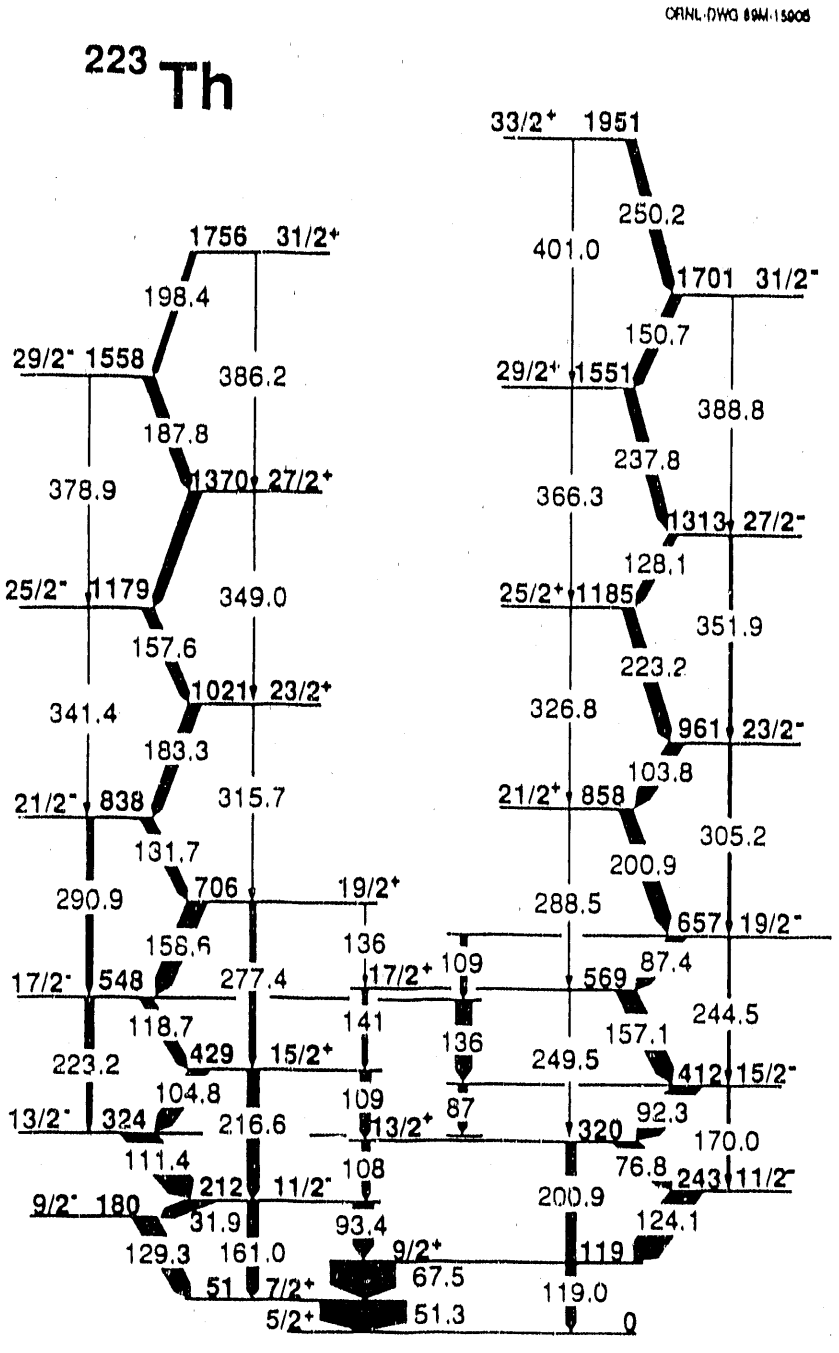
ORNL-DWG 89M-15905
223 Th
33/2+ 1951
250.2
401.0
1701 31/2-
150.7
29/2+ 1551
388.8
237.8
366.3
1313 27/2-
128.1
25/2+ 1185
351.9
223.2
326.8
961 23/2-
103.8
21/2+ 858
305.2
200.9
288.5
657 19/2-
87.4
569
244.5
157.1
249.5
412 15/2-
92.3
320
170.0
76.8
243 11/2-
200.9
124.1
119
119.0
0
1756 31/2+
198.4
29/2- 1558
386.2
187.8
378.9
1370 27/2+
349.0
25/2- 1179
157.6
341.4
1021 23/2+
183.3
21/2- 838
315.7
131.7
290.9
706 19/2+
158.6
136
17/2- 548
277.4
17/2+
109
118.7
141
136
223.2
429 15/2+
104.8
109
87
13/2- 324
216.6
13/2+
111.4
108
9/2- 180
212 11/2-
31.9
93.4
129.3
161.0
9/2+
67.5
51
7/2+
5/2+
51.3

FIGURE 5

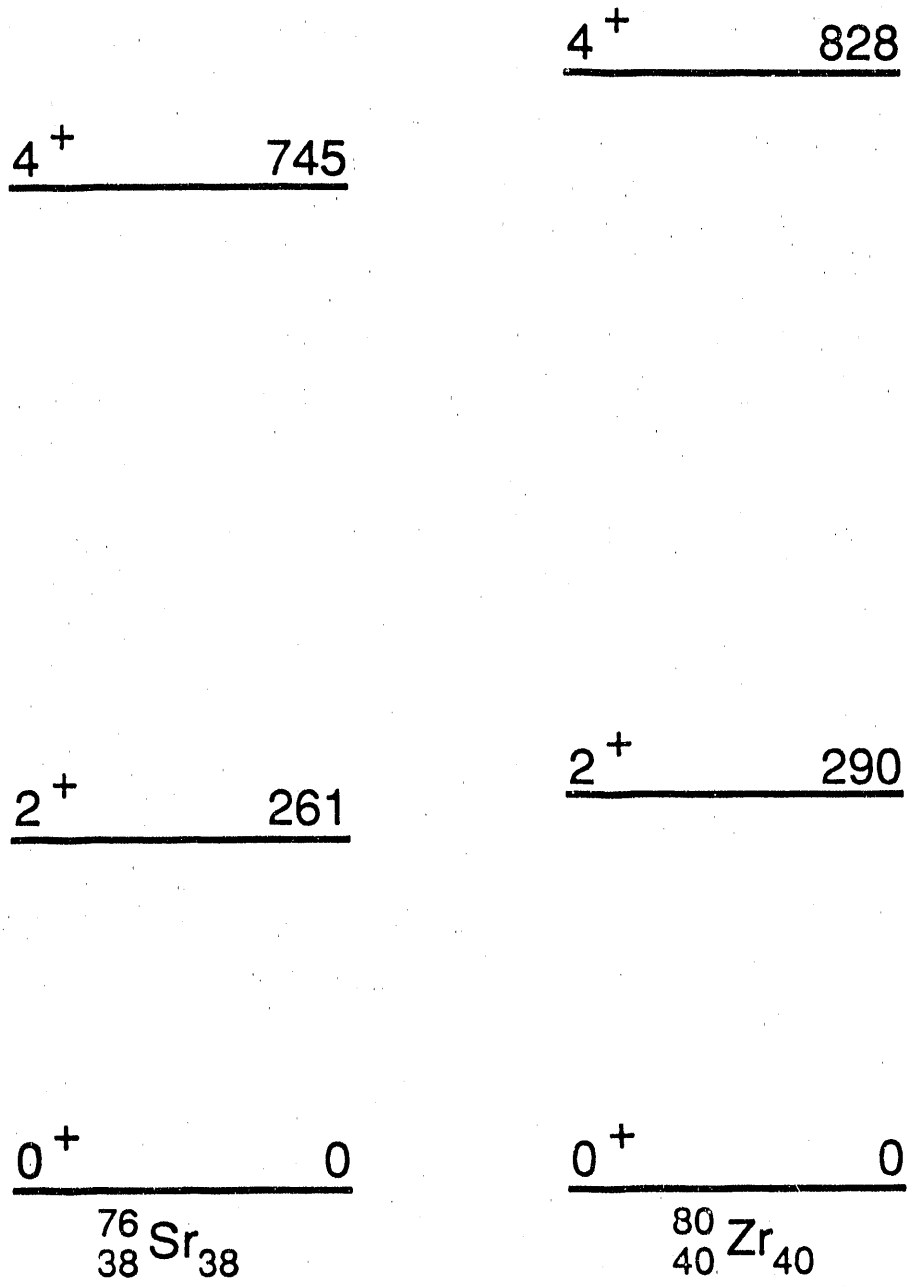

FIGURE 6

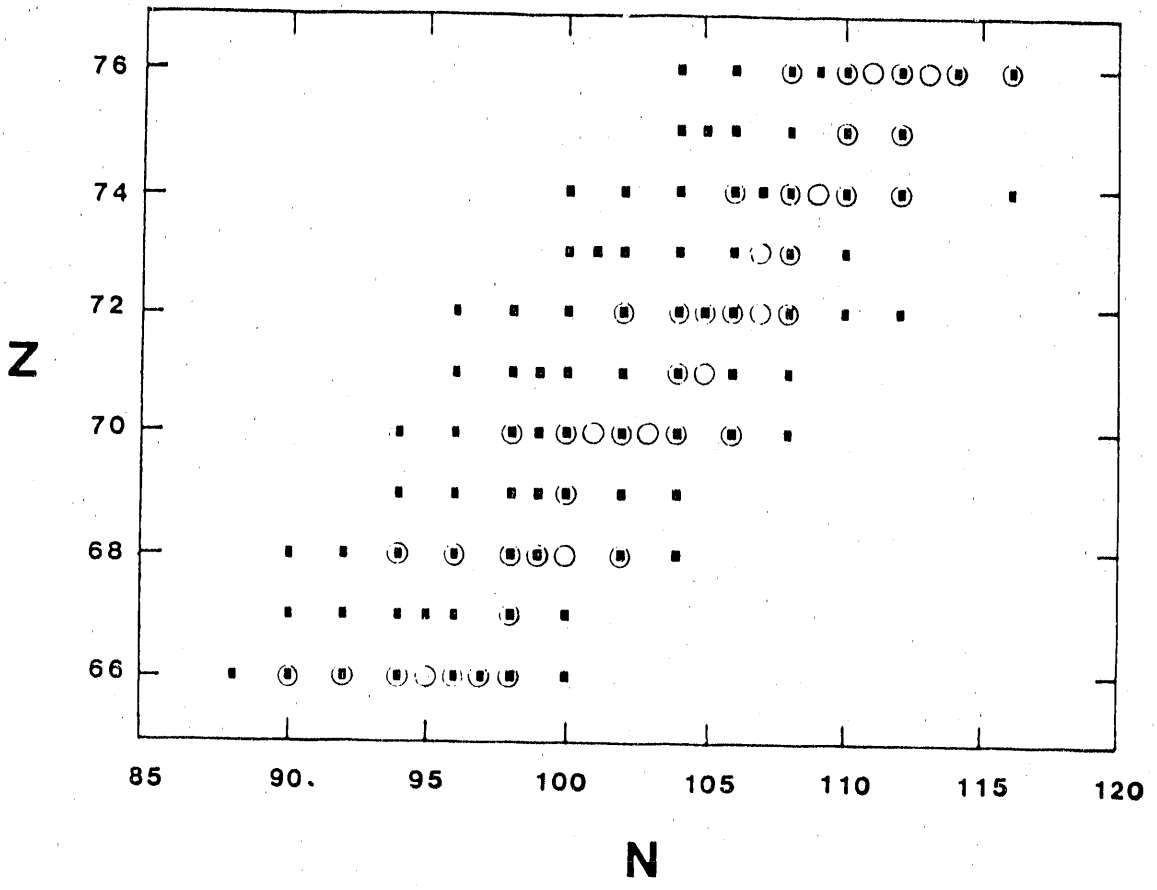

FIGURE 7

Position Paper on Neutron Halos and Drip Line Exotica

"At the Edge of Neutron Matter"

(Note: At the time of this workshop, it was felt that this paper should be written to combine material discussed in both Working Groups 1 and 2 to highlight this important aspect of a radioactive beam facility.)

W. Bauer[1], Chairman
D.J. Vieira[2], Coordinator

Contributions by: W. Bauer, G.F. Bertsch, F. Becchetti, B.A. Brown, A.C. Hayes, W.D. Myers, J.R. Nix, P.L. Reeder, D.D. Strottman, R.G. Stokstad, A. Sustich, D.J. Vieira, C.C. Villari

1. Introduction

Neutron matter exists in the cosmos in the form of neutron stars. It is kept stable by the interplay between the attractive gravitational interaction and the repulsive electromagnetic interaction which allows only very small proton admixtures. The minimum mass required for the gravitational interaction to become comparable to the nuclear interaction is approximately 1/10 of the mass of the sun. Therefore we cannot reproduce this state of matter in any laboratory on earth.

However, we can approach the edge of neutron matter by studying the properties of nuclear matter at the limits of neutron-stable nuclei. These nuclei are the last particle- stable nuclides and are located at the neutron "drip-line" - beyond which additional neutrons instantly break away. The large neutron excesses available in these nuclei will enable us to extrapolate to the neutron matter limit by studying their properties.

Radioactive ion beam facilities allow studies of these nuclei with the highest ratios of neutrons to protons achievable in the laboratory and thus

[1]NSCL, Michigan State University, East Lansing, MI 48824-1321
[2]LAMPF, Los Alamos National Laboratory, Los Alamos, NM 87545

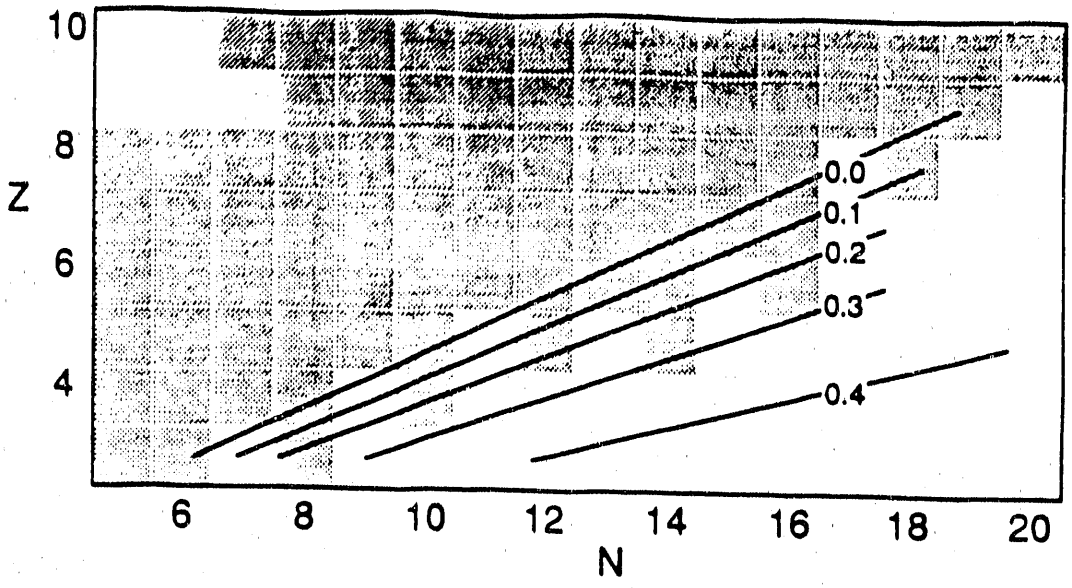

Figure 1: A portion of the nuclide chart showing as grey squares nuclei that are known to be stable against particle emission. The solid lines correspond to the predicted limits of stability for different values of a parameter r which determines by how much nuclear matter is unbound (taken from [1]).

provide the best data for extrapolations to the properties of neutron matter. In addition, neutron-rich nuclides near the drip line have unique structure and decay modes which extend our understanding of more normal nuclear matter.

2. Binding Energy of Neutron Matter

If neutron matter were bound, nuclear physics would be enriched by amazing structures. These structures, with life times limited only by beta decay, would include neutron balls of arbitrary size. Since the neutrons have no electrostatic repulsion from each other, the fission and alpha decay

channels would be closed to these neutron balls. Thus, their lifetime would not be limited by these strong processes, which proceed on a relatively fast time scale, and which constitute the main limitations on the life times of heavy chunks of normal nuclear matter.

These neutron balls might contain clusters of protons, with topologies not necessarily those of a single sphere, e.g. two or more fragments held apart by their Coulomb repulsion, or a hollow proton bubble filled with neutrons.

Since all searches for small bound clusters of neutrons have turned out negative thus far, we presently have to conclude that neutron matter is unbound in the absence of sizeable contributions of the gravitational interaction to the binding. However, it has to be stressed that we do not know exactly by how much neutron matter is unbound. This is, because we have no strict limits on the minimum size of neutron matter clusters from direct experimental observations. All of our knowledge is based on theoretical extrapolations from bound finite nuclei.

If neutron matter is only slightly unbound, we might expect to see precursors of such exotic neutron matter effects in phenomena that are observable at the neutron drip lines. The best way to proceed is to study nuclei with the largest possible neutron excess, both light and heavy nuclei, since even if bulk neutron matter were bound, small neutron balls would tend to be destabilized by their surface energy. Neutron matter is unbound and the maximum neutron excess for a given Z is limited by neutron drip. The actual location of the limit of stability is determined by the stiffness of the neutron matter equation of state [1] (compare Fig. 1).

One also expects the energy of the Giant Dipole Resonance to drop off at the limit of stability because the restoring force which comes mainly from the surface, will be affected by the neutron excess. It should also be mentioned that both the location of the limit of stability and the Giant Resonance energies are expected to depend on the overall excitation of the nucleus. Consequently, it may be possible to determine some of the temperature dependence of the nuclear equation of state.

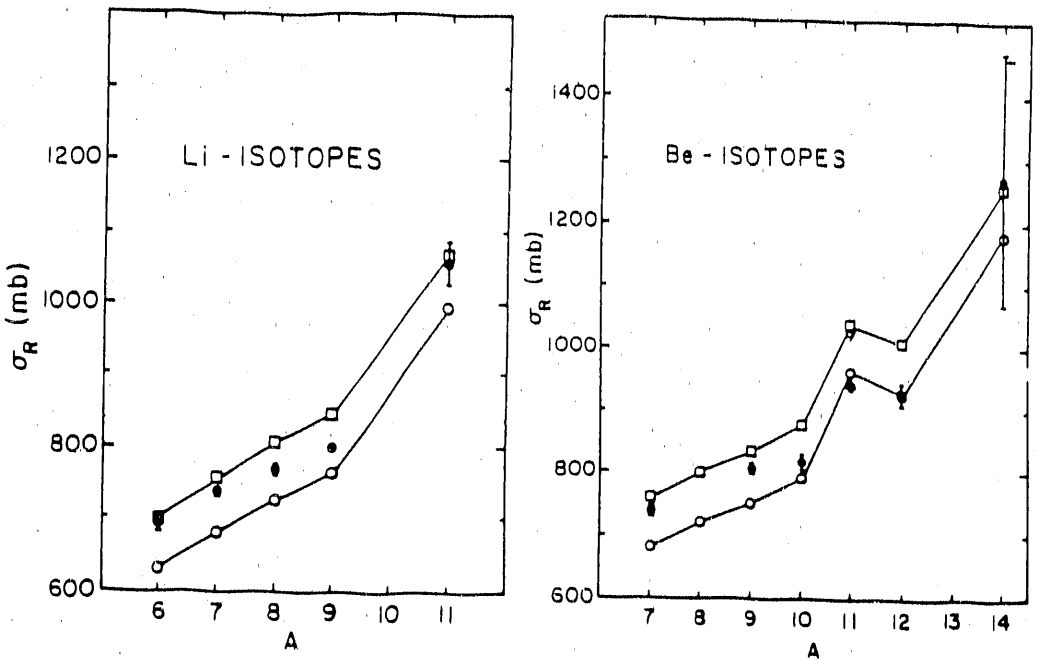

Figure 2: Reaction cross sections for Li and Be isotopes on a ^{12}C target. Filled symbols are the data (taken from [2]), and the solid lines and open squares (circles) are the results of calculations with finite (zero) range interactions (taken from [6]).

3. Microscopic Nuclear Properties: Neutron Halos

Beyond these macroscopic considerations there are significant opportunities for advancing our understanding of microscopic nuclear properties that also occur at the drip lines. The very last member of each isotopic sequence as we reach the limit of stability will be weakly bound. Due to this small binding energy and the Heisenberg uncertainty principle, the tail of the wave function is expected to extend far out beyond the normal nuclear matter radius obtained from an $A^{1/3}$ parametrization. This effect has already been seen in ^{11}Li and ^{14}Be [2,3,4] (see Fig. 2).

While there is nothing surprising in the increased reaction cross sections these nuclei have associated with their larger spatial extend, what is surprising is the fact that all Shell Model and Hartree-Fock calculations have

so far not quite succeeded to describe the properties of these nuclei. As a testing ground for established calculational approaches this has to be one of the best.

The effect of large neutron excess can most easily be seen among low Z elements. For example, modifications of the neutron density distributions can be observed by looking at elastic and inelastic scattering of all the Li isotopes from ^{8}Li to ^{11}Li. Our present understanding of ^{11}Li is that of a ^{9}Li core with 2 neutrons located predominantly in an extended surface region. These two neutrons are in essence responsible for the very large reaction cross section experimentally observed for ^{11}Li.

Similar neutron density trends can be studied by scattering experiments on boron isotopes from mass 8 to 19.

4. Nuclear Structure Physics with Neutron Halos

Because of this configuration of two neutrons interacting with each other and with the core, there exists the possibility of studying 3-body correlations in nuclear matter in an unusually clean manner.

Elastic and inelastic reactions at high beam energies can be used to establish the diffuseness of the neutron skin.

With radioactive ion beams, one can study neutron halos via sub-barrier transfer reactions such as (^{11}Li, ^{9}Li), (^{11}Li, ^{10}Li), etc. Important information will come from measurements of double differential cross sections as a function of beam energy and scattering angle. Such measurements also investigate the quantum mechanical nature of the neutrons in the halo, e.g. the important single particle configurations in the tail. One also can study a few excited states in these drip-line nuclides.

By using beams of these exotic nuclides, one can induce reactions to produce other unbound exotic nuclei such as (^{11}Li, ^{10}He), (^{11}Li, ^{10}Li), etc.

These exotic nuclides with neutron halos may lead to very cold fusion reactions via sub-barrier fusion. The neutron tails will give an assist to such reactions, because the neutrons in the halo are not subject to the

Coulomb interaction which is the major limiting factor in obtaining cold fusion reactions with normal nuclei.

The structure of ^{11}Li is of particular interest because of its unusually large ratio of neutrons to protons (8/3=2.67) and because of its unusually small binding energy. Existing measurements of the total reaction cross section for ^{11}Li and other neutron-rich light-mass nuclei have given the evidence for large matter radii [2]. No Hartree-Fock type calculation currently can explain the large radii [5]. One could expect Shell Model calculations to work better, but these calculations also fail. The only way in which theories are at present able to reproduce the reaction cross sections of light nuclei close to the drip line is by using densities which are artificially constrained to fit the empirical binding energies [6]. But it has to be stressed that self-consistent calculations have failed so far in this task. This may turn out to be not a failure in principle but only evidence for the finite accuracy of calculations for this type, because binding energies can rarely be predicted to an accuracy of less than one MeV. However, future studies from a theoretical as well as from an experimental standpoint are needed.

This raises a number of additional questions concerning the nature of such a halo.

1. Are nuclides such as ^{11}Li, ^{19}B, and/or other nuclei near mass 40 deformed or even superdeformed? It is possible that the huge neutron excess forces the neutrons to occupy high angular momentum states causing the nucleus to be deformed. This effect might be expected by examining the Nilsson model and observing the existence of intruder states from outer shells whose energy is lowered with increasing deformation. We estimate that a deformation of β=0.6 in ^{11}Li could have an effect of approximately 30% on the root mean square radius. A Shell Model calculation of the magnetic moment of ^{11}Li yields 2.997 μ_N for the superdeformed case and 3.793 μ_N for the closed neutron shell case [7]. From a comparison to the experimental data, which yield 3.6673(25) μ_N for the magnetic moment of ^{11}Li [8], a large deformation for this nucleus seems unlikely. However, a measurement of the quadrupole moment of this nucleus via in-beam laser spectroscopy should yield a more definitive answer.

2. Can beta decay life times be calculated from theory? In the case

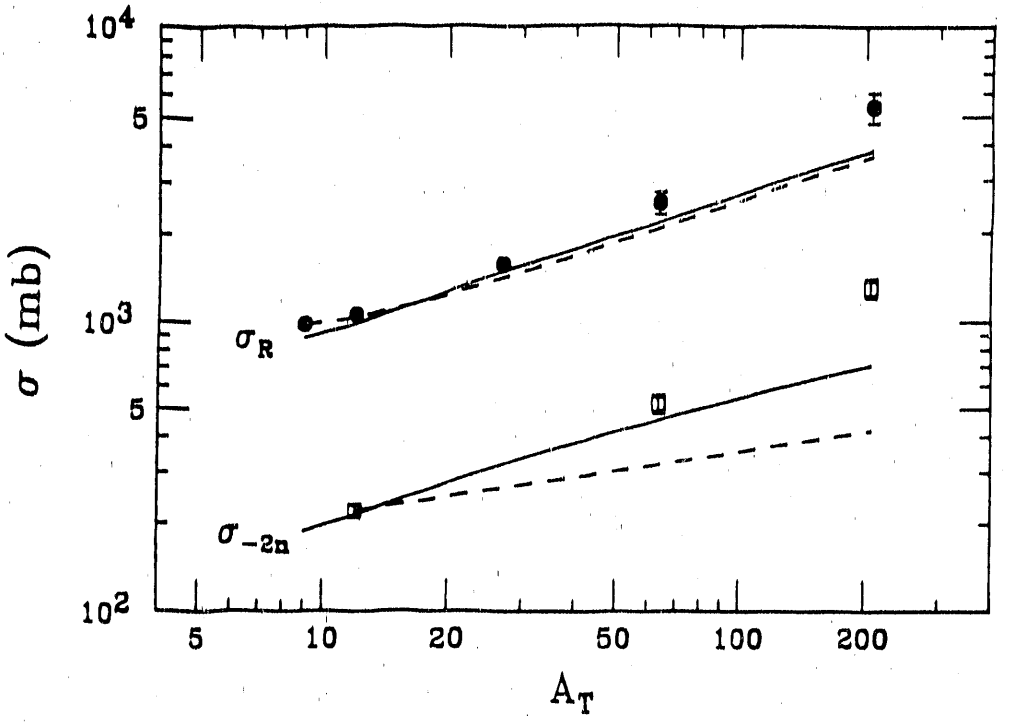

Figure 3: Reaction cross section for ^{11}Li as a function of target mass. Lines: Predicted nuclear contributions to the reaction cross section, using different models (taken from [10]).

of ^{11}Li, there is almost a factor of three discrepancy between the best Shell Model calculation and experiment [9]. It is important to perform measurements of decays to specific states with high Gamow-Teller transition probabilities, B(GT). This is because all low lying states in ^{11}Be with large branching ratios have only small B(GT) values for which small adjustments in the theory parameters have large consequences. By performing exclusive decay experiments to states with large B(GT) values, which cannot be freely adjusted by choice of the theoretical interaction parameters, a much more stringent test of existing theories can be performed. Because of the small branching ratios associated with these states, however, high radioactive beam currents are needed. Complementary information could be obtained by performing the ^{11}Li(p,n)^{11}Be reaction in reverse kinematics at sufficiently high beam energy ($\sim$ 100 MeV/nucleon). It seems also worthwhile to extend measurements and calculations to other exotic nuclides.

3. Can theory predict the electromagnetic dissociation cross sections?

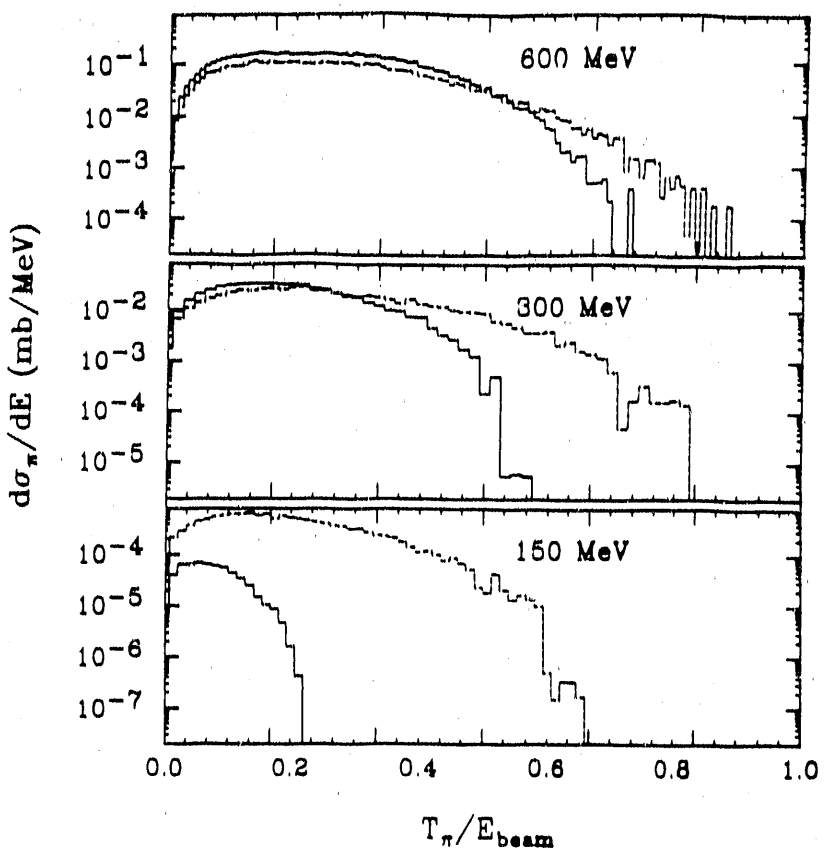

Figure 4: Predicted pion (π^+) energy distributions from one core (dashed histograms) and one halo neutron (solid histograms) of a ^{11}Li colliding with a proton from a ^{12}C target [13].

These can be measured by difference methods. However, these difference methods are model dependent, because one has to subtract the nuclear contribution from the total dissociation cross section in order to obtain the electromagnetic part. It turns out that a simple Glauber type approximation to the nuclear dissociation cross section is not sufficient. A better approach is the use of an eikonal approximation [10]. The inferred Coulomb cross section by using this method is **600** $\pm$ 100 mb for the reaction 790 MeV/nucleon ^{11}Li on ^{208}Pb (see **Fig. 3**).

This result has to be compared to a theoretical calculation using the Random Phase Approximation [11]. This theory predicts a softening of the dipole mode ("soft E1 resonances") as expected, and the response is sufficiently enhanced to explain the experimental data.

However, other theoretical investigations indicate a high sensitivity of the predicted E1 strength to the specific wave functions used [12]. Therefore the question if theory and experiment agree for the Coulomb dissociation cross section may still be open.

4. What is the momentum distribution of the halo neutrons? There are several methods which could be used to measure this distribution. One is to measure the ^{9}Li transverse momentum distribution from the reaction $^{11}\mathrm{Li} \rightarrow {}^{9}\mathrm{Li} + 2\mathrm{n}$. This yields two Gaussian components with different widths, 95 ± 12 and 23 ± 5 mb, respectively [4]. The smaller of the two is being attributed to the halo neutrons.

   Another way of obtaining similar information would be to measure pion momentum distributions from the reaction of a high energy beam of ^{11}Li on a ^{12}C target or on a ^{1}H target. The different neutron momentum distributions of core and halo neutrons in ^{11}Li would then show up as contributions to the pion energy distributions with different slopes (see Fig. 4). We estimate that a beam of 10^{5} ^{11}Li per second at a beam energy of 300 MeV/nucleon would produce about 10^{4} pions per second. With this production rate, a high quality experiment using a pion spectrometer could be performed. Alternatively, one can measure 2-neutron angular correlations at small angles by means of ^{11}Li stripping reactions.

Two other questions are related to the occurrence of soft E1 resonances for the neutron rich nuclei:

1. Are there soft E1 resonances for proton-rich nuclei? In proton-rich nuclei, there can be no proton "halo" due to the Coulomb barrier.

2. Is there a neutron halo in the presence of a low 1-neutron binding energy but a high 2-neutron binding energy? A first candidate for this effect appears to be the isotope ^{11}Be, but further studies are in order.

Both of these questions can be answered by studies near the particle drip-lines made accessible by radioactive ion beam facilities.

Another topic of great interest is how the nuclear surface (skin) changes as one approaches the drip-line either on the proton-rich or neutron-rich side of the valley of stability. This can be studied with the techniques of on-line laser spectroscopy discussed elsewhere in these proceedings.

As one approaches the neutron drip-line, the radioactive decay mode of beta-delayed two-neutron emission becomes more probable. The study of the two-neutron energy and angular correlation from such decays will provide information on the mechanism of two-neutron emission. The question is whether the neutrons come out sequentially or do they leave the nucleus as a di-neutron and break apart outside the nucleus?

Finally, studies at the neutron drip-line offer the possibility of discovering a postulated decay mode known as ground state two-neutron emission. This occurs when a given nuclide is stable with respect to one-neutron emission but is unstable with respect to two-neutron emission. This is analogous to the ground state two-proton emission being sought on the opposite side of the valley of stability. The protons feel a Coulomb barrier which retards the emission of the two protons and leads to predicted half-lives in the micro-second to milli-second range. However, neutrons do not have this barrier; so measurable life times will occur only if there is very low neutron energy available, there is an angular momentum barrier, and/or there are unfavorable transition matrix elements. By definition, ground state two neutron emission occurs only at the neutron drip line and thus requires the capabilities of a radioactive ion beam facility to produce such nuclides.

5. Conclusions

The topics listed above can only be viewed as a very preliminary glance at the amazing range of new possibilities for nuclear structure studies with radioactive beams. The phenomenon of the occurrence of neutron halos seems firmly established. Present and future suitable radioactive beam facilities will open new avenues for this kind of research and permit a detailed investigation of the edge of neutron matter.

References:

1. W. D. Myers, Proc. of the 1st Int. Conf. on Radioactive Nuclear Beams, 16-18 Oct. 1989, Berkeley, CA, World Scientific.
2. I. Tanihata et al., Phys. Lett. 160B, 380 (1985).
3. I. Tanihata et al., Phys. Rev. Lett. 55, 2676 (1985).
4. T. Kobayashi et al., Phys. Rev. Lett. 60, 2599 (1988).
5. H. Sato and Y. Okuhara, Phys. Lett. 162B, 217 (1987).
6. G.F. Bertsch et al., Phys. Rev. C 39, 1154 (1989).
7. B.A. Brown, unpublished.
8. E. Arnold et al., Phys. Lett. 197B, 311 (1987).
9. M.S. Curtin et al., Phys. Rev. Lett. 56, 34 (1986).
10. G.F. Bertsch et al., MSU preprint (1990).
11. G.F. Bertsch and J. Foxwell, Phys. Rev. C 41, 1300 (1990).
12. A.C. Hayes and D. Strottman, Los Alamos preprint (1990).
13. W. Bauer, work in preparation.

Report From Working Group 3: Nuclear Astrophysics

Chairman:
W. Michael Howard
Lawrence Livermore National Laboratory

Coordinator:
Paul Koehler
Los Alamos National Laboratory

Contributors:
M. Arnould, Institut d'Astronomie and d'Astrophysique
ULB, Bruxelles, Belgium
R. E. Azuma, CalTech, Pasadena
L. Buchmann, TRIUMF, Vancouver, B.C.
A. Champagne, Princeton University
G. M. Fuller, University of California, San Diego
S. Kubono, Institute for Nuclear Study, University of Tokyo
P. J. Leleux, University of Louvain, Belgium
M. Loiselet, Louvaine-La-Nueve, Belgium
G. J. Mathews, Lawrence Livermore National Laboratory
B. S. Meyer, Lawrence Livermore National Laboratory
P. Möller, Los Alamos National Laboratory
E. B. Norman, Lawrence Berkeley Laboratory
F.-K. Thielemann, Department of Astronomy, Harvard University
J. W. Truran, University of Illinois, Urbana
M. Wiescher, Department of Physics, University of Notre Dame
S. E. Woosley, University of California, Santa Cruz
J. M. Wouters, Los Alamos National Laboratory

The study of nuclear astrophysics involves the interaction of nuclei throughout the periodic table, both on the proton-rich and neutron-rich side of the valley of beta stability, over a range of energies from far below the Coulomb barrier to near the Coulomb barrier. In addition to nuclear reaction rates, nuclear astrophysicists need to know nuclear binding energies, fission properties and weak interactions rates of some very exotic nuclei. Calculation of these quantities imply detailed knowledge of nuclear levels and the nuclear level density, detailed nuclear structure information related to fission properties, and the statistical behavior of reaction rates for both neutron and charged-particle capture. To follow nature's evolution of the abundance of chemical elements requires knowledge of these nuclear properties for literally thousands of nuclei. Many important processes involve stable nuclei for which nuclear reaction rates can be measured. However, many more important processes involve radioactive nuclei which either are not easily produced in the laboratory, or up until now were impossible to produce. In this report we will make the case for a few selected examples for which an intense radioactive beam facility can be used to measure specific reactions and other nuclear properties of prime importance in astrophysics.

However, we will also make the case for the need to study the global properties of nuclei, both on the proton and neutron-rich sides of the valley of beta stability. Several processes in nuclear astrophysics, i.e. the p-process[1], the r-process[2] and the rp-process[3] depend on nuclear reaction rates, beta-decay rates, and nuclear masses for thousands of nuclei far from the valley of beta-stability. We need experiments to validate the statistical models of nuclear reactions and nuclear structure that are used for these calculations of nucleosynthesis. Of particular importance are Gamow-Teller strengths for neutron-rich isotopes in the mass range of A = 56 to 70[4] region and nuclear masses and beta decay rates for neutron-rich isotopes beyond the N = 50 neutron closed shell.[2]

This report draws contributions from various astrophysics groups. Included in the discussion are some of the nuclear physics needs for the astrophysical r-process, hydrogen burning[5] and the hot CNO cycle[3,6-8], the rp-process[3], and inhomogeneous big bang nucleosynthesis[9-15]. Also included is some discussion of intermediate mass nucleosynthesis, including the production of the radioactive nuclei ^{22}Na and ^{26}Al[7,16], as well as problems in supernovae calculations related to uncertainties in electron-capture rates[4]. The discussion is broad, but not comprehensive, and sometimes general rather than specific. The point of including the various discussions is to give a flavor for the wide range of problems that can be addressed for applications of radioactive ion beams to nuclear astrophysics. Although there are sometimes specific nuclear reactions that need to be measured, it would be a mistake to concentrate on a few light mass reactions, for example, when considering the design of a intense radioactive ion beam facility. Specifically, the rp-process and the r-process, as well as the p-process, are nucleosynthetic processes that require global nuclear structure and nuclear reaction rates for nuclei on both the proton and neutron-rich sides of the valley of beta stability. One break through with a radioactive ion beam facility for nuclear astrophysics would be the study of heavy neutron-rich nuclei that would be impossible to produce by other means. Although the study of individual nuclear reactions is always very important for nuclear astrophysics, we feel that more emphasis should be placed on the production of both proton-rich and neutron-rich heavy elements. This conclusion affirms the conclusion of Working Group 2 on Nuclei Far From Stability.

We will conclude the report with an analysis of the facilities required to meet the various experimental needs for nuclear astrophysics. This report also includes in an Appendix a description of radioactive ion beam experiments relevant for astrophysics presently underway in Japan and Belgium.

With the launch of the Hubble Space Telescope (HST), and the launch of the Gamma Ray Observatory (GRO) later this year, the science of nuclear astrophysics will become more exciting and more demanding in this decade. Nuclear physics learned from experiments with an intense radioactive ion beam facility could play an important part in pursuing our increased understanding of the nuclear reactions in the cosmos.

I. HYDROGEN BURNING AND THE HOT CNO CYCLE

An example of a particular reaction of importance involving a radioactive nucleus for the proton cycle in the Sun is $^{7}Be(p,\gamma)^{8}B$. This reaction governs the rate of ^{8}B neutrinos from the Sun, the ones measured by Dr. Ray Davis and his colleagues using a 100 000 gallon tank of C_2Cl_4 located at the bottom of the Homestake gold mine in South Dakota. The observed flux of neutrinos is about only one-third of the predicted flux. There appears to be a discrepancy outside the formal errors, with no agreed solution to the problem. Either the nuclear physics could be in error or the astrophysics associated with the determination of the physical conditions in the core of the Sun could be wrong. Although other neutrino experiments are planned that will detect neutrinos from the main p-p chain reactions, a new measurement of this reaction rate would be very important. Discordant measurements of this rate by different groups needs to be resolved.

As discussed in many places,[3,8] a major change in the classical CNO cycle occurs when the rate for $^{13}N(p,\gamma)^{14}O$ becomes more rapid than the ^{13}N beta-decay. Other proton capture rates on unstable species are involved in the hot CNO cycle are: $^{14}O(\alpha,p)^{17}F$, $^{17}F(p,\gamma)^{18}Ne$[17], $^{18}F(p,\gamma)^{19}Ne$, $^{18}F(p,\alpha)^{15}O$ and $^{19}Ne(p,\gamma)^{20}Na$.[18] The hot CNO cycle transforms into the rp-process when the rates for $^{15}O(\alpha,\gamma)^{19}Ne$ and $^{14}O(\alpha,p)^{17}F$ become more rapid than the corresponding beta-decays. In such a case the reaction $^{19}Ne(p,\gamma)^{20}Na$ may provide a breakout from the hot CNO cycle towards heavier elements. For the case of the study of hydrogen burning it is of prime importance to know detailed reaction rates for light-mass radioactive nuclei. These reaction rates are best studied in the energy range 0.2 to 1.0 Mev/nucleon. See the references for additional light reactions of importance. The reaction rates for many of these light reactions can also be determined by looking at inverse reactions, measuring spectroscopic factors or studying analog structures of mirror nuclei. However, these methods have various drawbacks, in determining the stellar rates, so that direct measurement with a radioactive ion beam may still be highly preferable.

II. INHOMOGENEOUS BIG BANG NUCLEOSYNTHESIS

Recently there has been considerable interest in baryon inhomogeneous cosmologies. Several processes such as a first order QCD phase transition, evaporating quark nuggets, or superconducting cosmic strings could have given rise to macroscopic baryon number fluctuations in the early universe. At later times, after weak decoupling, neutrons diffuse more readily out of high baryon density regions than do protons. In this way relatively neutron-rich and proton-rich regions could have formed prior to nucleosynthesis. The resulting light element yields from nucleosynthesis would then be different from those in a homogeneous universe.

One possible difference between homogeneous and inhomogeneous nucleosynthesis is that some elements with $A \geq 9$ could have been made in fairly substantial amounts in an inhomogeneous universe. This is to be contrasted with the homogeneous universe in which little production of elements with $A \geq 9$ occurs due to the lack of stable nuclei at mass five

and eight. Therefore, should relatively large quantities of A ≥ 9 nuclei be observed in extreme Population II stars, we would have good evidence for baryon inhomogeneity in the universe at the time of nucleosynthesis.

The formation of A ≥ 9 nuclei predominately occurs in neutron-rich regions in inhomogeneous universes. The important reaction sequence is $^{1}H(n,\gamma)\ ^{2}H(n,\gamma)\ ^{3}H(d,n)\ ^{4}He(t,\gamma)\ ^{7}Li(n,\gamma)\ ^{8}Li$. The nucleus ^{9}Be may be made by $^{8}Li\ (n,\gamma)\ ^{9}Li(\beta^{-})^{9}Be$ and $^{8}Li(d,n)^{9}Be$ (as well as by $^{7}Li\ (t,n)\ ^{9}Be$). Observations of the abundance of ^{9}Be in extreme Population II stars could provide constraints on inhomogeneous cosmologies. The chain leading to the intermediate mass elements is $^{8}Li\ (\alpha,n)\ ^{11}B(n,\gamma)\ ^{12}B(\beta-)\ ^{12}C(n,\gamma)\ ^{13}C$. Clearly, reactions on ^{8}Li are extremely important for formation of elements with A ≥ 9, and accurate ^{8}Li cross sections are necessary for reliable predictions of the nucleosynthesis of these nuclei. Subsequent evolution to higher mass is shown in Figure 1. As may be seen, one requires nuclear cross sections and nuclear masses for many neutron-rich light isotopes.

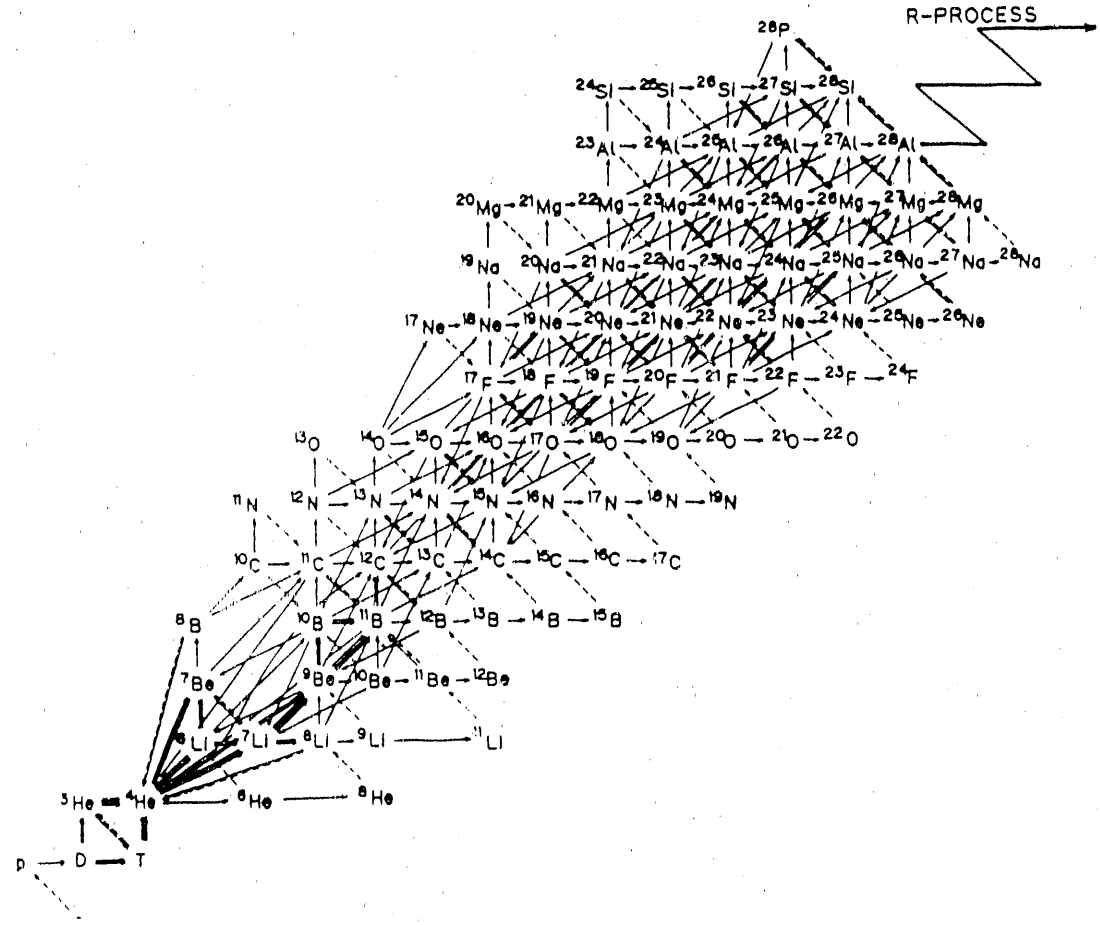

Fig. 1. A typical nuclear reaction network used in calculations of inhomogeneous big bang nucleosynthesis. From Ref. 15).

Aside from the possibility of formation of intermediate and heavy mass nuclei in the big bang, baryon inhomogeneous cosmologies may relax constraints on the present ratio of the baryon density to the closure density. Homogeneous nucleosynthesis provides the constraint $\Omega_b \lesssim 0.15$. Since inflation suggests $\Omega = 1$, the implication is that some 90% of the mass energy in the universe is in a form other than baryons (e.g. massive neutrinos, axions, etc.). In baryon inhomogeneous universes, Ω_b may be as large as 0.8, but only if the ^{7}Li constraint is relaxed. The nucleus ^{7}Li is overproduced in baryon inhomogeneous universes since it is made as ^{7}Li in the neutron-rich regions and as ^{7}Be in the proton-rich regions (^{1}H(n,γ)^{2}H(^{2}H,γ) ^{4}He(^{3}He, γ) ^{7}Be(β^+) ^{7}Li). It turns out, however, that late-time hydrodynamic dissipation of the density fluctuations during nucleosynthesis may have an important effect on ^{7}Li yields. In such a dissipation event, the high density, proton-rich region may be rapidly mixed with the lower-density, neutron-rich material. Destruction of ^{7}Be occurs via ^{7}Be (n,p) ^{7}Li (p, α) ^{4}He. When the mixing is instantaneous, the final ^{7}Li yield may be reduced by as much as two orders of magnitude. Also contributing to the destruction of ^{7}Li are the reactions ^{7}Li (t, α) ^{6}He and ^{7}Li(t,n) ^{9}Be$^* \rightarrow$ n + 2 ^{4}He. It would therefore be of great interest to have accurate cross sections for tritium capture reactions on ^{7}Li for energies in the range 10- 100 keV, as well as accurate reaction rates for the destruction of ^{8}Li.

III. GAMOW-TELLER STRENGTHS FOR INTERMEDIATE MASS NUCLEI

The extent of electron capture during the pre-supernova core collapse determines the resulting iron core and neutron star mass[19,20]. The more electron capture or neutronization, the smaller the value of Y_e, the number of electrons per nucleon, and the smaller the resulting core mass of the pre-supernova star. The dense core of the pre-supernova star tends to have a mass corresponding to a Chandrasakar mass. Most of the nuclei in the core are iron group nuclei in a range of mass $56 \lesssim A \lesssim 70$. High energy (n,p) reactions for neutron-rich nuclei in this mass region to deduce Gamow-Teller strength distributions would make a significant contribution towards understanding pre-supernova stellar evolution and also understanding the supernova explosion mechanism itself. A recent study[21] has determined that for pre-supernovae core evolution the most important electron captures are on ^{56}Ni,^{55,59,60}Co and ^{55}Fe, ^{52}V and ^{67,68}Cu, and the most important beta decays are for ^{56}Co, ^{55,57}Mn, ^{57,58}Cr and ^{67,69}Ni.

IV. ASTROPHYSICAL r-PROCESS

Although the mechanism of the astrophysical r-process has been studied for more than thirty years, we are still not sure of its site in nature.[1,22] Part of the reason for this is the complexity of the nuclear physics required to calculate the r-process, and the lack of experimental information. Recent years has seen great progress in the sophistication of the nuclear models used in the calculations. Except for a very few cases, we must rely on theoretical modelling for all of the necessary nuclear quantities that are used in the calculations. These quantities include, nuclear masses, nuclear partition functions, neutron

capture rates (including the effects of excited states), and beta decay rates (also including the effects of excited states). Of prime importance is the location of the neutron-drip line in the N-Z plane. Figure 2 shows a typical r-process path in the N-Z plane. Stable nuclei are included in black, while unstable nuclei which experimental mass determinations are shaded in grey. As one can observe from studying this figure, a radioactive ion beam facility that was capable of producing critical heavy neutron-rich nuclei could go a long way in providing information for the astrophysical r-process.

Current r-process calculations use macroscopic-microscopic models, such as the diffuse surface folded-Yukawa model of Möller and Nix[23,24] to consistently predict nuclear binding energies, fission and neutron emission probabilities,[25] and along with Gamow-Teller interactions,[26,27] and beta decay rates for neutron-rich heavy elements.[28] Experiments with radioactive ion beams to confirm or improve such models would be an important benefit to nuclear astrophysics.

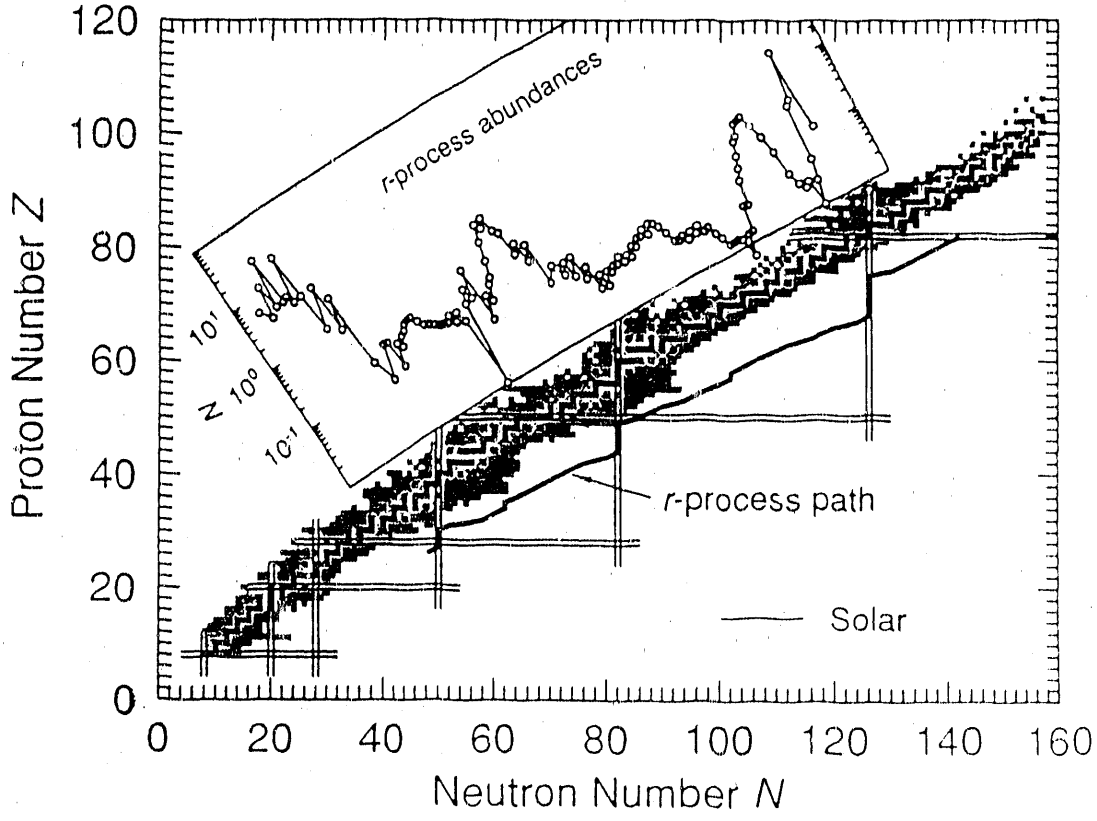

Fig. 2. Plot of the r-process path in the N-Z plane. Stable nuclei are shown in black, and unstable nuclei with experimental mass determinations are shown in grey. Also included is the abundance distribution of r-process nuclei as a function of A. (Figure due to P. Möller).

Of particular interest are the properties of nuclei near the r-process waiting points, or the neutron closed shells. Some r-process nuclei near the N = 82 closed shell are already studied. However, present heavy ion reactions are a long ways from producing r-process nuclei near the N = 126 closed shell. It is radioactive ion beams that could make an important impact in this region

The role of neutron-induced or beta-induced fission is important in terminating the r-process near the N = 184 closed neutron shell. The fragments from fission at the termination of the r-process may be responsible for the peak in the r-process distribution of isotopes in the rare-earth region. Beta-delayed fission and beta-delayed neutron emission rates for nuclei as they decay from the r-process path to the valley of beta stability in the mass region $232 \leq A \leq 260$ are important for studies of nuclear cosmochronolgy[25,29-31]. Such rates may influence the U/Th production ratios, which, in turn, coupled with models of Galactic evolution, help determine the age of the Galaxy.

It is not possible to measure neutron capture cross sections directly in radioactive ion beam facilities. Another method can, however, be applied which is presently widely used to predict proton capture reactions on unstable proton-rich nuclei. Reactions like (d,p) would produce the same compound nucleus as an (n,γ) reaction and allow one to investigate resonance energies and other properties (parity, partial widths) which then can be employed for an indirect calculation of the neutron capture cross sections. Independent of the individual cross section, such an investigation would also result in a systematic analysis of level densities in neutron-rich nuclei and their dependence on the distance from stability. A high nuclear level density is a prerequisite for the validity of statistical model calculations.[32,33] The (d,p) experiments should be performed at energies of about 20 MeV/nucleon.

V. INTERMEDIATE MASS NUCLEI -- AN EXAMPLE: ^{22}Na, ^{26}Al and ^{44}Ti

Classical novae explosions are known to provide an environment in which hydrogen-burning reactions proceed on carbon, nitrogen, and oxygen (CNO) nuclei, and heavier nuclei, at high temperatures and densities on a dynamical timescale. Weiss and Truran[16] recently suggested that for such conditions, the production of potentially interesting and detectable abundance levels of the radioactive isotopes ^{22}Na and ^{26}Al may occur. They conclude that novae may represent an important source of ^{26}Al in the Galaxy and that some nearby novae may be expected to produce detectable flux levels of ^{22}Na decay gamma rays. The detection of ^{22}Na in novae would provide critical constraints, both on their temperature and envelope convection histories and on their initial envelope composition. If one knows from early observations both that a nova is at a distance of less than one kiloparsec and that its envelope is significantly enriched in neon and magnesium, the Gamma Ray Observatory (GRO) to be launched late this year may have a chance to detect the gamma ray lines from the decay of ^{22}Na.[16]

The destruction rates of ^{22}Na and ^{26}Al, particularly the rate of the reactions $^{22}Na(p,\gamma)^{23}Mg$, $^{26}Al(p,\gamma)^{27}Si$ and $^{26m}Al(p,\gamma)^{27}Si$ are very important in determining how much ^{26}Al is produced in such novae explosions. Observations of ^{22}Na and ^{26}Al gamma ray lines from novae explosions could set constraints on the hydrodynamics, convection and initial compositions of such explosions. This is but one example, in light to intermediate mass nucleosynthesis, where the determination of a key reaction rates on radioactive nuclei can have important consequences. For nucleosynthesis of ^{44}Ca and γ-ray astronomy, the production and destruction rates for ^{44}Ti are important, as well as a measurement of its rather uncertain halflife.

VI. THE rp-PROCESS

The rp-process is the transmutation of CNO nuclei into iron group nuclei and beyond in hot ($0.3 < T_9 < 5.0$) proton-rich environments.[3] The reactions proceed through proton capture on light nuclei and alpha-particle capture on intermediate mass radioactive nuclei. At high temperature and density conditions, the reaction path will be close to the proton drip line. The result is that both nuclear binding energies and charged particle reaction rates on very proton-rich nuclei in the mass region $20 \leq A \leq 66$ will be necessary to accurately calculate this process. Such a process may have important consequences for nucleosynthesis, as well as being an important energy generation mechanism in novae explosions. As mentioned previously, the reaction $^{19}Ne(p,\gamma)^{20}Na$ is thought to govern the transition from CNO nuclei to intermediate nuclei.

Other important breakout reactions for the rp-process may include $^{27}Si(p,\gamma)^{28}P$, $^{31}Si(p,\gamma)^{32}Cl$, and $^{39}Ca(p,\gamma)^{40}Sc$.[34] These key reactions are mainly proton capture reactions on proton-rich radioactive nuclei with low Q values. In that case the cross sections and reaction rates are determined by single resonances and the direct capture process only and cannot be calculated by statistical methods (Hauser-Feshbach). The influence of the single resonances and the direct reaction contribution must be measured directly. In contrast, proton capture reactions on radioactive nuclei with $A > 26$ near the line of stability have typically rather high Q values and can therefore be estimated by Hauser Feshbach calculations.

The termination point of the rp-process depends crucially on whether the proton separation energy of ^{65}As is more than about 250 keV. If it is less than this value, the process halts at ^{64}Ge, if it is greater, the process continues up to approximately $A = 80$. The nucleus ^{65}As is so proton-rich that in order to produce it and have a charged-particle in the exit channel to detect, it is necessary to use a radioactive beam or target.

VII. REQUIRED FACILITIES

Experiments in nuclear astrophysics using radioactive ion beams will be among the most challenging in nuclear physics, because of the demand for either very proton-rich or

neutron-rich nuclei and the very small cross sections involved in the reactions. In the previous sections we have identified various astrophysical process and specific reactions of prime importance where the nuclear needs can be addressed with a radioactive ion beam facility. Regarding the required facility to meet these nuclear needs we define four major areas:

a) Nuclear capture reactions involving stellar processes.

b) Production of exotic nuclei for r-process or rp-process modelling.

c) Nuclear transfer reactions for simulating specific neutron, proton or alpha capture reactions.

d) Determination of Gamow-Teller strengths via (d,p) or (n,p) reactions on isotopes within the iron group.

The facility demands for these reactions are summarized in Table I. The processes a) and b) are quite distinct in intensity and energy from processes c) and d). The first two processes will require the highest intensities possible, as the cross sections involved are in general (for case a)) of order of microbarns. For target thicknesses of 10^{18} cm^{-2} and beams of order 10^{10} sec^{-1}, the resulting event rate for low-energy capture will be of order 10 hr^{-1}. Producing exotic nuclei will allow somewhat thicker targets, but the production cross section for the exotic nuclei will certainly be very small.

TABLE I. Facility Requirements

	a) Nucleon Capture	b)Exotic Nuclei	c) Nucleon Transfer	d) G. T.
Energy Range:	0.2-2 MeV/u	4-8 MeV/u	10-20 MeV/u	100-300 MeV/u
Intensity	$>10^9$ sec^{-1}	$>10^{10}$ sec^{-1}	$\geq 10^6$ sec^{-1}	$\geq 10^6$ sec^{-1}
Masses (Projectile):	7-200 (80)	40-100	7-200	40-70
Energy Spread:	< 1%	< 10%	< 10%	< 1%

The second class of experiments c) and d) will require more moderate beam intensities, but considerably high energies. Given the range and scope of proposed and existing

facilities, the first two reactions classes will require the highest intensities available at moderate energies, which requires an Isotope Separator On-Line (ISOL) facility. The second class of reactions seems to be well suited for heavy-ion fragmentation, especially when coupled to a storage ring. All experiments will require extensive detector development with high efficiency and high discriminatory capabilities. More attention should be given to the development of the required detectors for these proposed facilities.

VIII. CONCLUSIONS

We have outlined some of the needs of nuclear astrophysics that could be met with a radioactive ion beam facility. The nuclear needs cover the entire range of proposed facilities. We would like to emphasize the global natures of the nuclear needs for astrophysics. While individual reactions are always of prime importance in nuclear astrophysics, it is the reliability of the statistical and macroscopic-microscopic models that are used that provi understanding of the origin of the elements in nature. We would also like to point out t nuclear physics plays an important role not only in understanding the origin of the elements in nature, but also in processes like how supernovae or novae explode, or in putting constraints on cosmological models. With the launch of the Hubble Space Telescope (HST), and the launch of the Gamma Ray Observatory (GRO) late this year, many astronomical surprises await us in the next decade. Nuclear physics will undoubtly play an important role in understanding these phenomena. The understanding of the nuclear structure of a broad range of nuclei across the periodic table helps us understand the universe now and back to the big bang. A radioactive ion beam facility that will delineate this nuclear structure will play a key role in future astrophysical developments.

NUCLEAR ASTROPHYSICS EXPERIMENTS AT INS, TOKYO

S. Kubono
Institute For Nuclear Study, University of Tokyo

This is a brief description of the programs under way or in near future.

1. There are some experimental works under way at INS using two-body charged particle spectroscopy. These include the study of ^{21}Mg for the ^{20}Na(p,γ) ^{21}Mg stellar reaction rate.

2. There are three nuclear astrophysical experiments going on with using the projectile fragment separator RIPS at RIKEN.

   a. Measurement of the gamma width of the 2.637 MeV 1^+ state (the first excited state above the proton threshold in ^{20}Na), which is the critical physical parameter for the breakout problem from the hot-CNO cycle. So far, the ^{20}Mg yield was measured.

   b. Study of the reaction rate of ^{26m}Al(p,γ).

   c. Measurement of the gamma width of the 1^- state in ^{14}O is scheduled next month (May, 1990) by using Coulomb dissociation of ^{14}O which are collected by the RIPS.

STATUS REPORT ON THE RADIOACTIVE ION BEAM PROJECT AT LOUVAIN-LA-NEUVE

P. Leleux, M. Loiselet

Catholic University at Louvain
Chemin du Cyclotron, 2, B-1348 Louvain-la-Neuve, Belgium

The general layout of the Radioactive Ion Beam Project at Louvain-la-Neuve has been described elsewhere.[1,2] Recent advances have led to the acceleration of a $^{13}N^{1+}$ beam at 8 MeV with an intensity of 1.5×10^8 particles per second, i.e. 25 particles pA. This has been achieved through the following improvements: use of a ^{13}C target, bombarded with 100 μA, 30-MeV protons, with an efficiency for the release of the ^{13}N activity thereby produced of 10%; optimization of the efficiency of the ECR source for ionizing ^{13}N into the 1^+ Ionic state, raised to 5%; increase of the efficiency of the CYCLONE cyclotron for accelerating $^{13}N^{1+}$ ions, through an improvement of the vacuum and of other parameters, up to 4%. The next steps will be the lowering of the ^{13}C contamination in the ^{13}N beam, and a further increase of the accelerated intensity. The first reaction of astrophysical interest which will be studied is $^{13}N(p,\gamma)^{14}O$. The necessary apparatus has been built, and an overall test of its performances has been carried through a remeasurement of the cross section for the $^{13}C(p,\gamma)\ ^{14}N$ reaction at the 0.552-MeV resonance.

The coworkers are: Th. Delbar, W. Galster, I. Licot, E. Lienard, P. Lipnik, G. Ryckewaert, J. Vervier (University of Louvain-la-Neuve), P. Decrock, M. Huyse, P. Van Duppen (University of Leuven) J. Vanhorenbeeck (University of Brussels).

1. Th. Delbar, M. Huyse and J. Vanhorenbeeck, editors, The Radioactive Ion Beam Project at Louvain-la-Neuve, RIB-1988-01, Internal Report (1988).

2. Proc. First International Conference on Radioactive Nuclear Beams, Berkeley, USA, October 16-18,1989.

REFERENCES

1. S. E. Woosley and W. M. Howard, Astrophys. J. Suppl., 36, 285 (1978).

2. G. J. Mathews and R. A. Ward, Rep. Prog. Phys., 48, 1371 (1985).

3. R. K. Wallace and S. E. Woosley, Astrophys. J. Suppl. 45, 389 (1981).

4. M. B. Aufderheide, G. E. Brown, T. T. S. Kuo, D. B. Stout, and P. Vogel, Astrophys. J., in press (1990).

5. C. E. Rolfs and W. S. Rodney, Cauldrons in the Cosmos, (University of Chicago Press: Chicago, 1988).

6. W. A. Fowler, Rev. Mod. Phys., 56,149 (1984).

7. W. Hillebrandt and F.-K. Thielemann, Astrophys. J., 255, 617 (1982).

8. M. Arnould and W. Beelen, Astron. Astrophys. 33, 215 (1974).

9. R. A. Malaney, in Workshop on Primordial Nucleosynthesis, (ed. W. J. Thompson, B. W. Carney, H. J. K rwowski, World Scientific: Singapore, 1990).

10. R. A. Malaney and W. A. Fowler, in The Origin and Distributions of the Elements, (ed. G. J. Mathews, World Scientific: Singapore, 1987).

11. J. H. Applegate, C. J. Hogan, and R. J. Scherrer, Astrophys. J., 329, 572 (1988).

12. F.-K. Thielemann and M. Wiescher, in Workshop on Primordial Nucleosynthesis, (ed. W. J. Thompson, B. W. Carney, H. J. Karwowski, World Scientific: Singapore, 1990).

13. G. J. Mathews, B. S. Meyer, C. R. Alcock and G. M. Fuller, Astrophys. J., in press (1990).

14. H. Kuri-Suomio and R. Matzner, Phys. Rev. D, 39,1046 (1989).

15. T. Kajino, G. J. Mathews and G. M. Fuller, Astrophys. J., in press (1990).

16. A. Weiss and J. W. Truran, Astrophys. J., submitted, (1990).

17. M. Wiescher, J. Görres and F.-K. Thielemann, Astrophys. J., 326, 384 (1988).

18. S. Kubono, H. Orihara, S. Kato and T. Kajino, Astrophys. J., 344, 460 (1989).

19. G. E. Brown, ed.Theory of Supernovae, Phys. Rep. 163,1-203 (1988).

20. N. Strawmann, Particle Physics and Astrophysics, (Springer-Verlag: Berlin, 1988).

21. I. Fushiki, M. Aufderheide, S. E. Woosley and D. Hartmann, private communication, (1990).

22. G. J. Mathews and J. J. Cowan, Nature, submitted (1990).

23. P. Möller and J. R. Nix, At. Data Nucl. Data Tables 26, 165 (1981).

24. P. Möller and J. R. Nix, Nucl. Phys., A361, 117 (1981).

25. B. S. Meyer, W. M. Howard, G. J. Mathews, K. Takahashi, P. Moller, and G. A. Leander, Phys. Rev. C, 39,1876 (1989).

26. J. Krumlinde and P. Möller, Nucl. Phys., A417, 419 (1984).

27. K-I Kratz, J. Krumlinde, G. A. Leander, and P. Möller in Recent Advances in the Study of Nuclei Off the Line of Stability, (ed. R. Meyer and D. Brenner, American Chemical Society, Washington, 1985).

28. P. Möller and J. Randrup, Nucl. Phys., in press (1990).

29. F.-K. Thielemann, J. Metzinger, and H. V. Klapdor, Astron. Astrophys. 123, 162 (1983).

30. B. S. Meyer, P. Möller, W. M. Howard, and G. J. Mathews, in Proceedings of the 50 years with Nuclear Fission, (American Nuclear Society: Illinois, 1989).

31. F.-K. Thielemann, A. G. W. Cameron, and John J. Cowan in Proceedings of the 50 Years With Nuclear Fission (American Nuclear Society: Illinois, 1989).

32. F.-K. Thielemann, M. Arnould, and J. W. Truran, in Advances in Nuclear Astrophysics, (eds. E. Vangroni-Flam et al., editions frontures: Gifsur Yvette).

33. S. E. Woosley, W. A. Fowler, J. A. Holmes, B. A. Zimmerman, At. Data Nucl. Data Tables, 22, 371(1979).

34. M. Wiescher and J. Görres, Astrophys. J. 346, 1041 (1989).

THE BORDER REGIONS OF MEDICINE, CONDENSED MATTER, ATOMIC AND NUCLEAR PHYSICS

Report of Working Group IV

Chairman: S. S. Hanna

Local Coordinator: R. D. Taylor

Members: E. D. Arthur, J. E. Crawford, P. L. Dyer, W. D. Hamilton, S. S. Hanna, C. J. Maggiore, H. A. O'Brien, D. R. Phillips, J. Sample, J. A. Sawicki, G. D. Sprouse, R. D. Taylor, J. R. Tesmer, B. H. Wildenthal

1. Introduction

One of the great strengths of nuclear physics lies in the important contributions it has made to other fields such as medicine, biology, chemistry, atomic physics, and condensed matter physics. These contributions have come through (1) nuclear radiations and (2) interactions with the nuclear environment.

(1) Nuclear radiations such as the classical α, β, and γ radiations, fast and slow neutrons, and more recently the newer particles such as pions and muons have provided an incredibly rich and variable array of probes which have been adapted to diverse phenomena ranging from medical diagnosis and therapy to uncovering art forgeries. The richness of these probes has been due in large measure to the great number of available isotopes, each providing its own characteristic spectrum of particles and energies at isotopic lifetimes ranging between effectively zero and infinity. It is clear that the advent of a dedicated radioactive ion beam (RIB) facility would greatly enlarge the number of available isotopes and expand the richness and diversity of their isotopic properties.

(2) From a scientific standpoint the interaction of the nuclear moments with the electromagnetic fields of the nuclear environment - the hyperfine interaction - has provided a powerful tool, often inviting skill and ingenuity, for measuring these moments and fields. From a knowledge of the moments one can sometimes deduce the nuclear spins. The use of an RIB facility will greatly expand the scope of these measurements and could lead to

LA--11964-C

DE91 000511

Proceedings of the Workshop on the Science of Intense Radioactive Ion Beams

April 10-12, 1990

Compiled by
John B. McClelland
David J. Vieira

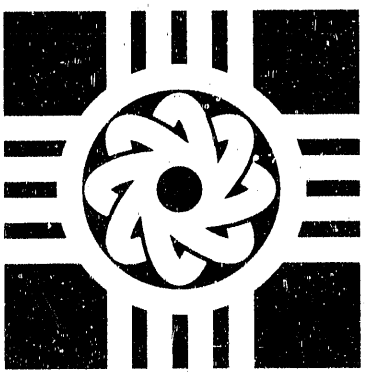

Los Alamos
NATIONAL LABORATORY
Los Alamos, New Mexico 87545

PROCEEDINGS OF THE WORKSHOP ON THE SCIENCE OF INTENSE RADIOACTIVE ION BEAMS
April 10-12, 1990

ABSTRACT

by

John B. McClelland and David J. Vieira

This report contains the proceedings of a 2 1/2 day workshop on the Science of Intense Radioactive Ion Beams which was held at the Los Alamos National Laboratory on April 10-12, 1990. The workshop was attended by 105 people, representing 30 institutions from 10 countries. The thrust of the workshop was to develop the scientific opportunities which become possible with a new generation intense Radioactive Ion Beam (RIB) facility, currently being discussed within North America. The workshop was organized around five primary topics: (1) reaction physics; (2) nuclei far from stability/nuclear structure; (3) nuclear astrophysics; (4) atomic physics, material science, and applied research; and (5) facilities. Overview talks were presented on each of these topics, followed by 1 1/2 days of intense parallel working group sessions. The final half day of the workshop was devoted to the presentation and discussion of the working group summary reports, closing remarks and a discussion of future plans for this effort.

Preface

This report contains the proceedings of a 2 1/2 day workshop on the Science of Intense Radioactive Ion Beams which was held at the Los Alamos National Laboratory on April 10-12, 1990. The workshop was attended by 105 people, representing 30 institutions from 10 countries. The thrust of the workshop was to develop the scientific opportunities which become possible with a new generation intense Radioactive Ion Beam (RIB) facility, currently being discussed within North America. The workshop was organized around five primary topics: (1) reaction physics; (2) nuclei far from stability/nuclear structure; (3) nuclear astrophysics; (4) atomic physics, material science, and applied research; and (5) facilities. Overview talks were presented on each of these topics, followed by 1 1/2 days of intense parallel working group sessions. The final half day of the workshop was devoted to the presentation and discussion of the working group summary reports, closing remarks and a discussion of future plans for this effort.

This workshop came about as a result of the recent Nuclear Science Advisory Committee (NSAC) Long Range Planning (LRP) activity during 1989. Town Meetings sponsored by the Division of Nuclear Physics of the American Physical Society were held in preparation for the LRP. The communities of nuclear scientists studying nuclei far from stability and those using low-energy beams as nuclear probes both strongly endorsed establishing a RIB facility within the next ten years. The case for such a facility was presented to the full NSAC Long Range Plan Working Group during its meeting in Boulder, Colorado on August 6-11, 1989, in which priorities for the field were discussed and recommendations formulated for the DOE and NSF. The scientific case for a RIB facility was well received by that group and several references to these scientific opportunities discussed can now be found in various sections of the Long Range Plan.

At this workshop we have concentrated our attention on outlining the scientific program that would be made possible by the development of such beams. We did not restrict our discussions to a particular production scheme or facility. As such, this workshop represents only our initial steps in preparing the case for such a facility -- further work will be needed to develop the scientific issues and to better define the type of radioactive beam facility which would best meet these new challenges.

The success of this workshop represents the hard work of many individuals. Of special note are the working group chairmen: Wolfgang Bauer, Rick Casten, John D'Auria, Jerry Garrett, Stan Hanna, Michael Howard, and Bob Stokstad, who took on the bulk of this undertaking by organizing the working groups and in preparing the summary reports; the invited overview speakers: Grant Mathews,

Mike Nitschke, Ingemar Ragnarsson, Jerzy Sawicki, and John Schiffer, who set the stage for our discussions and prepared manuscripts for these proceedings; the International Advisory Committee (listed below) for their help in preparing the workshop program and by encouraging more international participation at the workshop; and our fellow members of the Local Organizing Committee (also listed below) whose combined efforts were essential in the preparation and organization of the workshop. Moreover, we extend our thanks for a job well done to the conference secretary, Kathy Garduno; the LANL Protocol Office coordinators, Jan Hull and Mildred Saxman, for organizing the Study Center meetings; and Xiao-Lin Tu, Xiao-Gang Zhou, and Hardy Seifert for audio-visual and general assistance during the conference.

John B. McClelland

David J. Vieira

International Advisory Committee:

G. Bertsch (Michigan State)
R. F. Casten (Brookhaven)
J. M. D'Auria (Simon Fraser)
C. N. Davids (Argonne)
C. Detraz (GANIL)
W. Haxton (Washington)
W. Henning (GSI)
D. J. Horen (Oak Ridge)
S. E. Koonin (Caltech)
K.-L. Kratz (Mainz)
G. J. Mathews (Livermore)
J. M. Nitschke (Berkeley)
J. R. Nix (Los Alamos)
C. Rolfs (Munster)
B. M. Sherrill (Michigan State)
F. S. Stephens (Berkeley)
B. H. Wildenthal (New Mexico)
H. Wollnik (Giessen)
T. Yamazaki (INS)

Local Organizing Committee:

T. S. Bhatia
P. E. Koehler
C. J. Maggiore
J. B. McClelland, Co-Chairman
P. Möller
J. R. Nix
D. D. Strottman
W. L. Talbert
R. D. Taylor
D. J. Vieira, Co-Chairman

CONTENTS

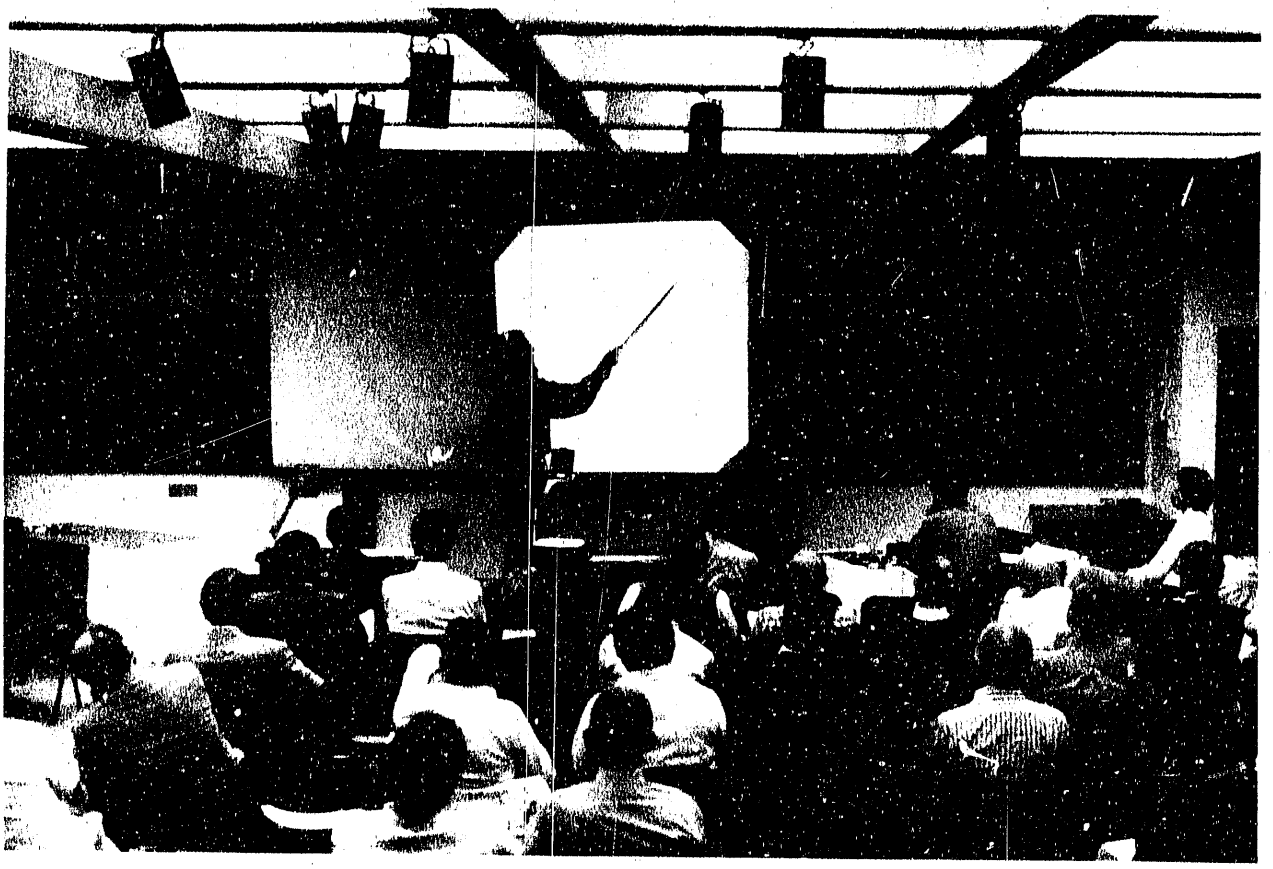

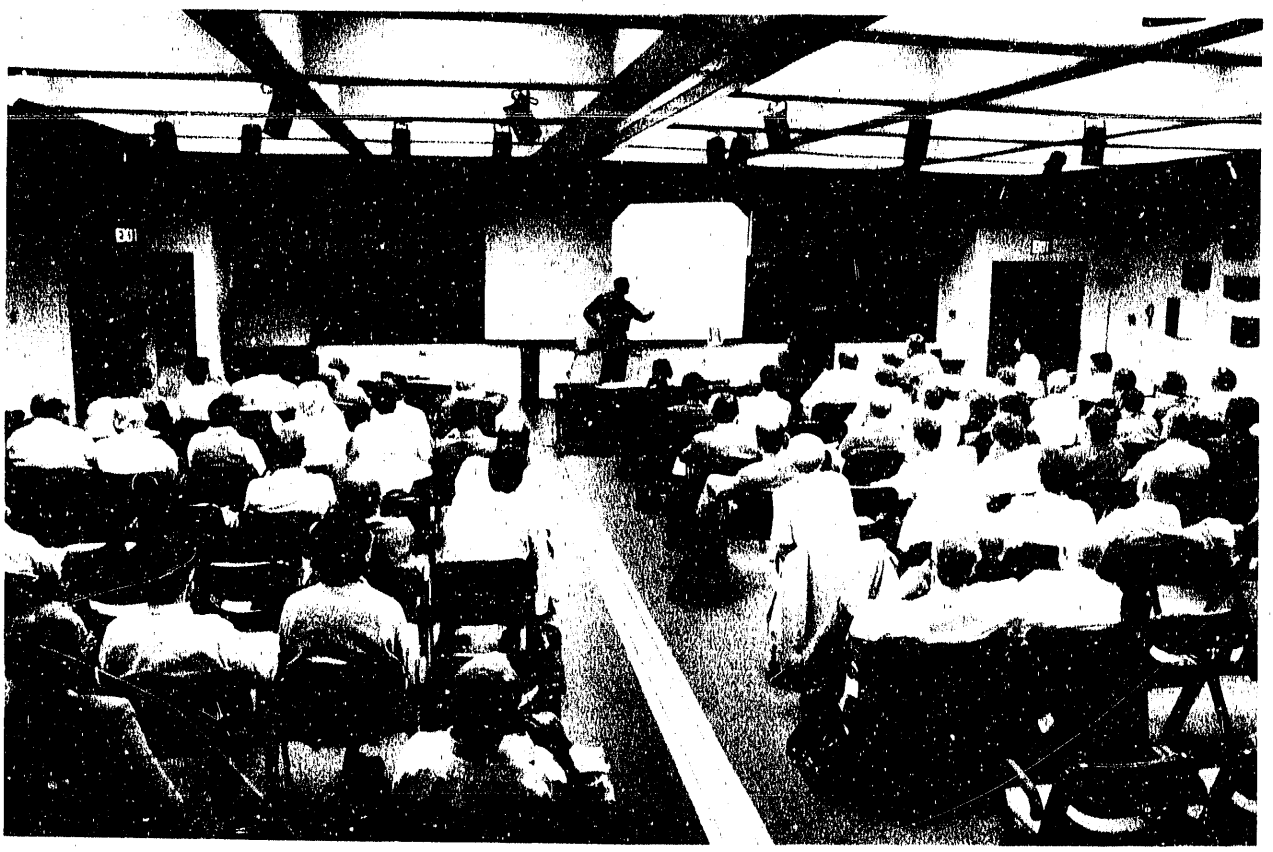
EXIT
EXIT


EXIT

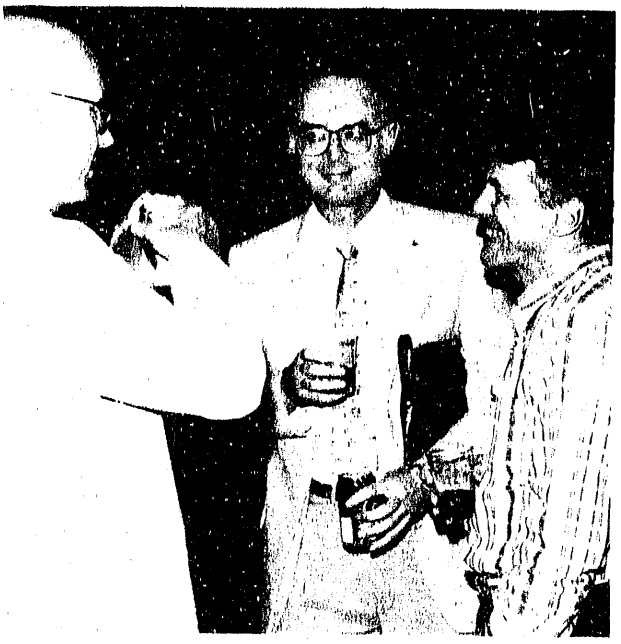


SMOKING
PROHIBITED

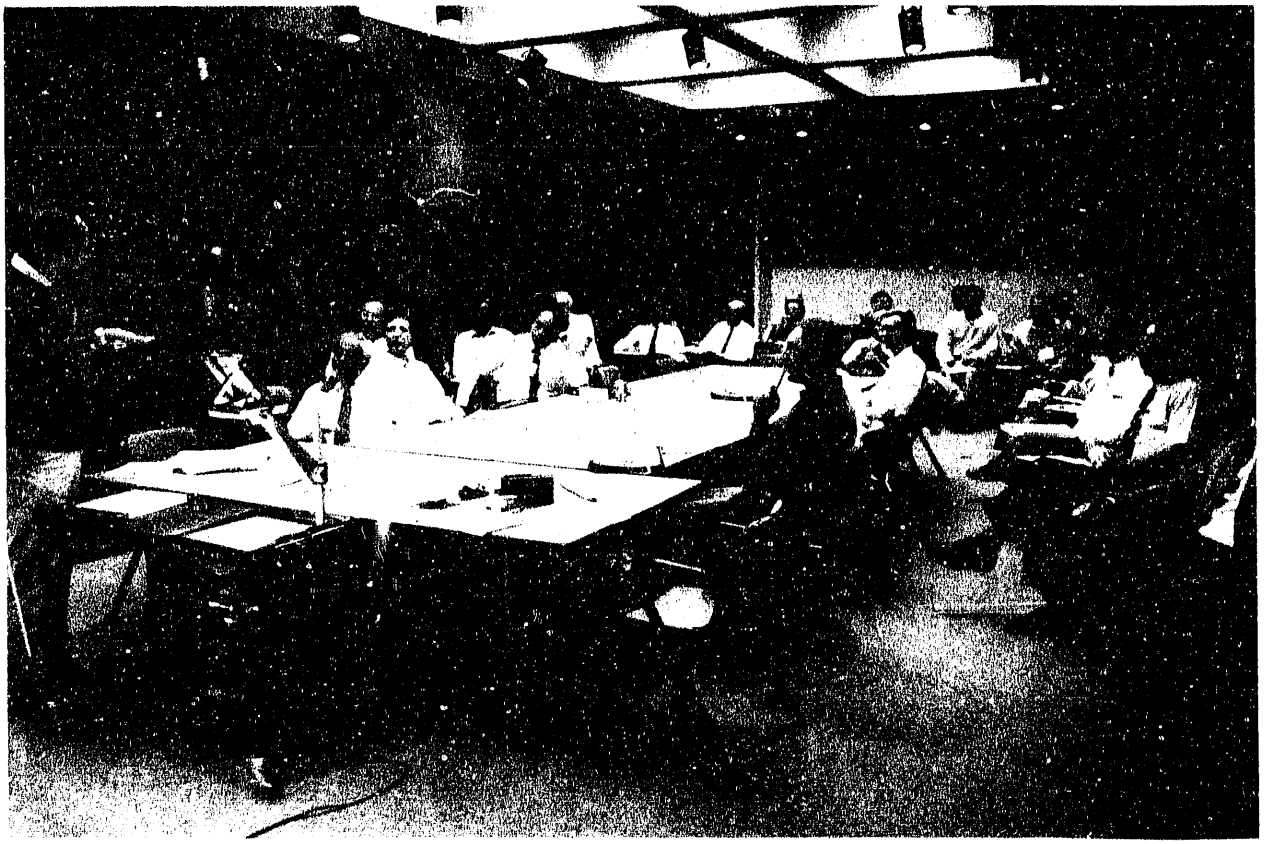

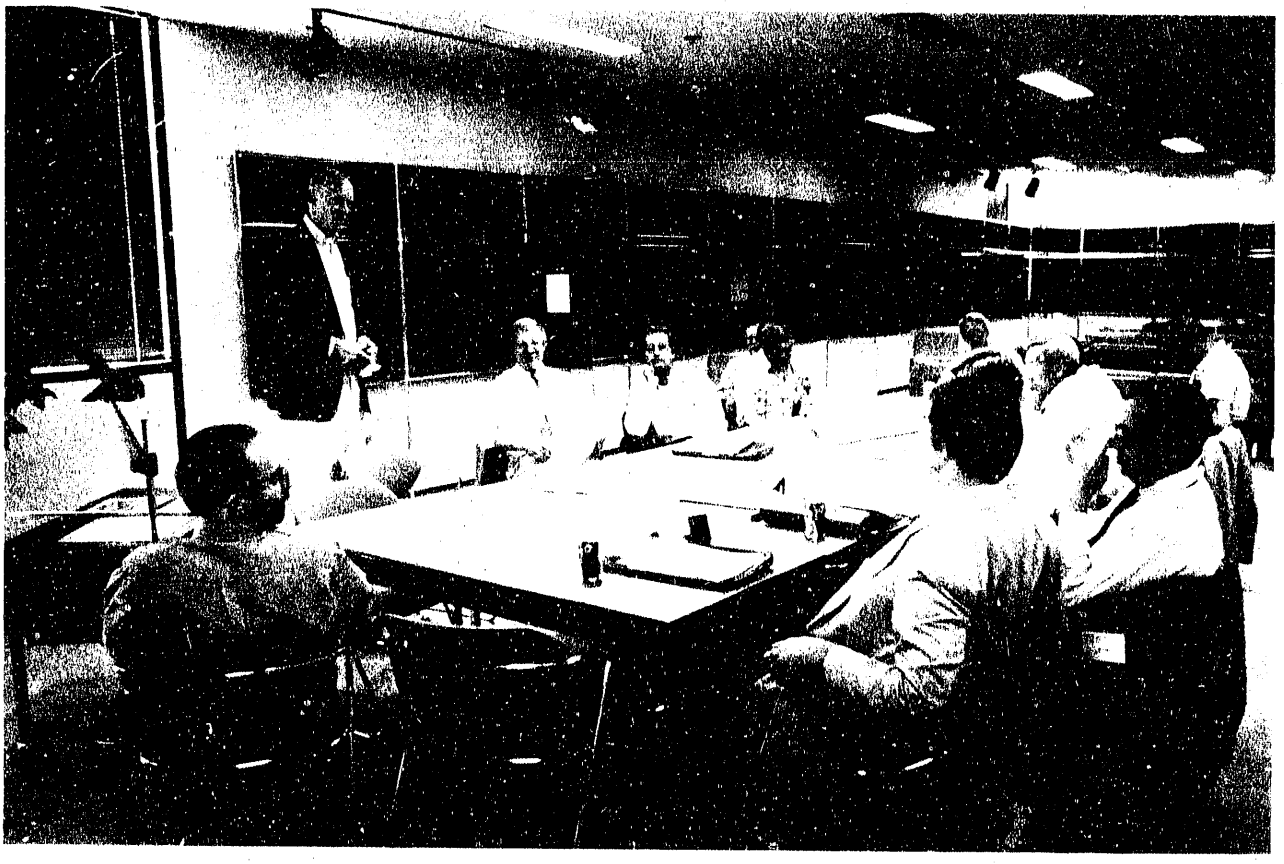

POSITION PAPER OF WORKING GROUP 1 ON REACTION PHYSICS

R. G. Stokstad, Chairman
D. D. Strottman and J. R. Nix, Coordinators

Contributions by F. Ajzenberg-Selove, W. W. Bauer, F. D. Becchetti, D. DiGregorio, C. D. Goodman, R. C. Haight, A. C. Hayes, D. J. Horen, H. J. Kim, S. Kubono, D. G. Madland, K. W. McVoy, P. Möller, D. M. Moltz, W. D. Myers, J. R. Nix, J. O. Rasmussen, J. P. Schiffer, B. M. Sherrill, E. R. Siciliano, K. P. Snover, R. G. Stokstad, D. D. Strottman, R. E. Tribble, D. J. Vieira, A. C. C. Villari, W. B. Walters, H. R. Weller, and J. B. Wilhelmy

1. Introduction

The limits of nuclear matter will be reached through nuclear reactions, just as much of what we know about nuclear structure has come from reaction studies. For studying the limits of nuclear matter, radioactive ion beams will both open up new vistas in several important dimensions and offer a fresh look at more familiar terrain. These will include extremes in the neutron-to-proton ratio (isospin), energy transfer, excitation energy, angular momentum, polarization, and nuclear shape.

We have divided the many reactions with radioactive ion beams that were suggested in our working group into four main categories. The first category involves nuclear matter in motion, or multidimensional reaction dynamics, and is discussed in sect. 2 of this position paper. The second category is concerned with the paths to neutron matter, which include neutron halos, or the physics of loosely bound nuclei, as well as the determination of the neutron drip line. Because of the intrinsic importance of this subject and its relation to both reaction physics and nuclear structure, it is included as a separate position paper. Section 3 continues with our third category, reactions that serve as probes of nuclear structure. Section 4 treats our fourth category, isomeric radioactive ion beams, where the projectile nuclei are in excited states.

It will be apparent in the following discussion that there is a wide range of difficulty in the suggested experiments. Some reactions will be extremely difficult, having small cross sections and even involving radioactive targets as well as radioactive beams, whereas others could be studied with existing instrumentation today, were the radioactive beams available. Furthermore, the experiments discussed below are only examples representing classes or categories of experiments. The requirements placed by the experiments on the radioactive beams—mass, energy, energy resolution, and other characteristics—are not dealt with systematically or in detail. But it will be

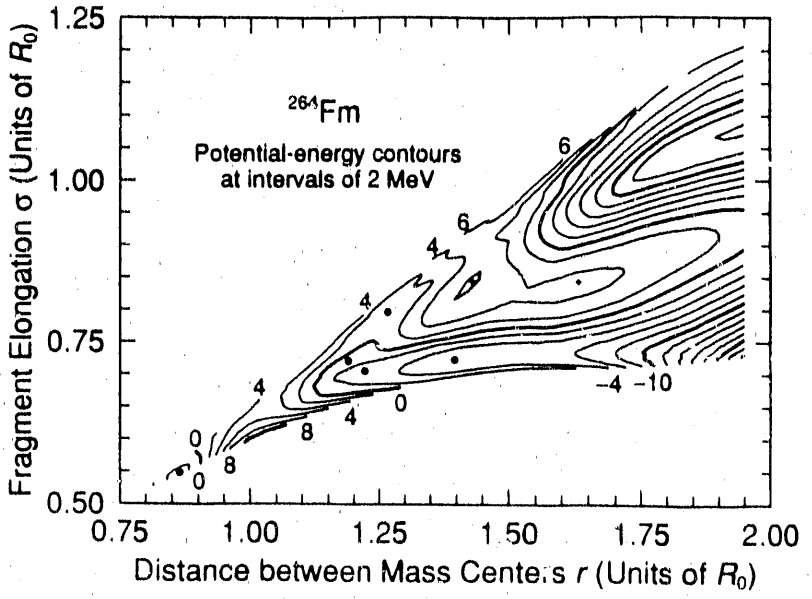

Figure 1: Calculated potential-energy surface for ^{264}Fm.

apparent that, just as with stable beams, more than one production method (e.g., ISOL or Fragmentation) is required if one is going to be able to perform the wide range of experiments illustrated below.

2. Nuclear matter in motion: multidimensional reaction dynamics

The opportunity afforded by radioactive ion beams to reach new regions of nuclei will help resolve many issues concerning collective nuclear motion. These include such diverse items as the effect of single-particle shell structure on the multidimensional nuclear potential energy of deformation, the flow and transfer of neutrons in subbarrier fusion, and isospin mixing at high excitation energies. New data provided by radioactive ion beams will assist in our quest for a fully microscopic understanding of nuclear collectivity.

2.1. PATHWAYS TO VERY HEAVY NUCLEI

Recent fission experiments [1,2]) have shown astonishingly abrupt transitions at ^{258}Fm in three separate properties: fission-fragment mass distributions, fission-fragment kinetic-energy distributions, and spontaneous-fission half-lives. All three of these phenomena are explained by the discovery of a new fission valley [3,4]) in ^{258}Fm and nuclei beyond. The calculated valley for ^{264}Fm is illustrated in fig. 1, which shows the potential energy as a function of the distance between mass centers r and fragment elongation σ of the two nascent fragments [3]). The lower left-hand corner of the diagram corresponds to the ground state of ^{264}Fm, and the lower right-hand corner corresponds to the configuration of two nearly spherical doubly magic

^{132}Sn nuclei. The long, narrow valley connecting these two configurations is separated from the traditional fission valley in the upper right-hand corner by a complicated topology involving saddle points, mountain tops (indicated by plus signs), and a high ridge. The solid circles in the diagram correspond to local minima.

Radioactive ion beams will provide important pathways to this region, through both very asymmetric transfer reactions and nearly symmetric fusion reactions. Examples of the former are ^{254}Es(^{11}Li,^{3}He)^{262}Fm and ^{254}Es(^{9}Li,^{3}He)^{260}Fm, involving ^{11}Li and ^{9}Li projectiles, with half-lives of 8.7 ms and 177 ms, respectively, incident on a ^{254}Es target, with half-life 276 d. An example of the latter is ^{132}Sn + ^{126}Sn $\rightarrow$ ^{258}Fm, involving a ^{132}Sn projectile, with half-life 40 s, incident on a ^{126}Sn target, with half-life 10^5 y. The reaction ^{132}Sn + ^{132}Sn $\rightarrow$ ^{264}Fm might ultimately be possible through the use of rapid-deposition target-production techniques.

These are only four examples of many reactions with radioactive ion beams that lead to especially large single-particle effects on the multidimensional nuclear potential energy of deformation. The resulting multiple minima and valleys separated by saddle points and ridges will significantly affect the reaction dynamics, especially at subbarrier energies. By increasing the bombarding energy, one will also be able to study the disappearance of single-particle effects with increasing excitation energy.

Just as the peculiar structure of ^{132}Sn is thought to influence the fission of the heaviest Fm isotopes, other aspects of nuclear structure may be at work in determining the mass distribution associated with fission. Robertson and Walters [5]) have suggested that a softness against octupole deformation for nuclei in the Cs-Ba mass-145 region might be responsible for the interesting phenomenon that the heavy partner in an asymmetric mass split is always a nucleus of about this mass, with the mass of the lighter fission fragment increasing or decreasing as the mass of the parent fissioning nuclide changes. Their argument is that an octupole deformation resembles the shapes fission fragments must acquire as they approach scission. Nuclei that can be easily deformed to an octupole shape will then be favored in fission. If this argument is correct, and if the Cs-Ba mass-145 nuclei have ground states that either have or are easily induced to acquire an octupole component, then the barrier for fusion might be lowered [6]) for heavy radioactive isotopes of Cs and Ba bombarding neutron-rich but stable targets around mass 100 to 120. Performing such a reaction would be similar to bombarding ^{126}Sn with ^{132}Sn—one would be working back up a fission valley in this multidemensional space toward a very heavy compound nucleus, taking advantage of the same nuclear-structure effects that cause the valley and the trajectory along it in the fission process.

2.2. FISSION IN THE PRE-ACTINIDE REGION

A real possibility exists to take advantage of reverse kinematics with radioactive beams in the Z = 84–94 region. There has been a lot of effort in the Fm region to exploit the rapid changes in fission properties. These changes are also present in the pre-actinide area as well. If we could have beams of neutron-deficient isotopes of these pre-actinides then we could do simple direct reactions with reverse kinematics

and measure the fission de-excitation channels. The reverse kinematics focuses the reaction products in the lab and therefore gives high geometric coverage and, since the decay products will have near beam velocities, they are much easier identified with counter techniques.

Another of these reverse reactions would be to study fission shape isomerism. In the light Th and Ra regions, the inner fission barrier should be around 3 MeV above the isomeric level, while the outer barrier is substantially above this value. This should be a condition which allows sufficient population of an isomeric state and also permits it to have a reasonable half-life (> ns). These isomers should decay by gamma branching back to the ground state. Cross sections will be small (on the order of microbarns) but one could take advantage of the reverse kinematics to move the products out of the reaction zone (i.e., recoil shadowing) and possibly see some of these decays.

2.3. NEUTRON TRANSFER IN SUBBARRIER FUSION

The transfer of nucleons among colliding nuclei on the path to fusion is one of several dimensions (deformation, vibration, and neck formation) that can influence the probability of fusion. At energies above the barrier a single dimension, the radial degree of freedom defining the separation of the two nuclei, is sufficient to describe the fusion of light to medium-mass nuclei. Particularly at subbarrier energies, though, the extra dimensions mentioned above can be very important in determining the cross section. Radioactive beams will give us a unique tool to study the importance of the ground-state Q-value for neutron transfer on the cross section for subbarrier fusion.

Just to give an example, systems like $^{15}O + ^{143}Nd$ and $^{14}O + ^{144}Nd$ possess very large ground-state Q-values (see table 1) for 1-neutron pickup (+9.5 MeV) and for 2-neutron pickup (+14.5 MeV), respectively. For comparison, the existing transfer data [7-10]) are for Q-values less than +2 MeV and +6.6 MeV for the 1n- and 2n-pickup reactions, respectively. The effect of the positive ground-state Q-value on the fusion at subbarrier energies can be illustrated by a simplified coupled-channel calculation [11]) for the fusion cross sections in the systems $^{15}O + ^{143}Nd$ and $^{14}O + ^{144}Nd$. These calculations, presented in fig. 2, show a large enhancement at low energies that has a different energy dependence than, for example, the coupling to a series of low-lying rotational states.

TABLE 1
Ground-state Q-values for one- and two-nucleon transfer reactions
(+ means pickup, − means stripping)

System	Neutrons				Protons			
	−1	−2	+1	+2	−1	−2	+1	+2
$^{15}O + ^{143}Nd$	−22.8	−5.4	+9.5	+3.9	−3.6	−2.6	−8.1	−12.2
$^{14}O + ^{144}Nd$	−26.9	−17.4	+5.4	+14.5	+5.3	+0.2	−10.3	−15.3

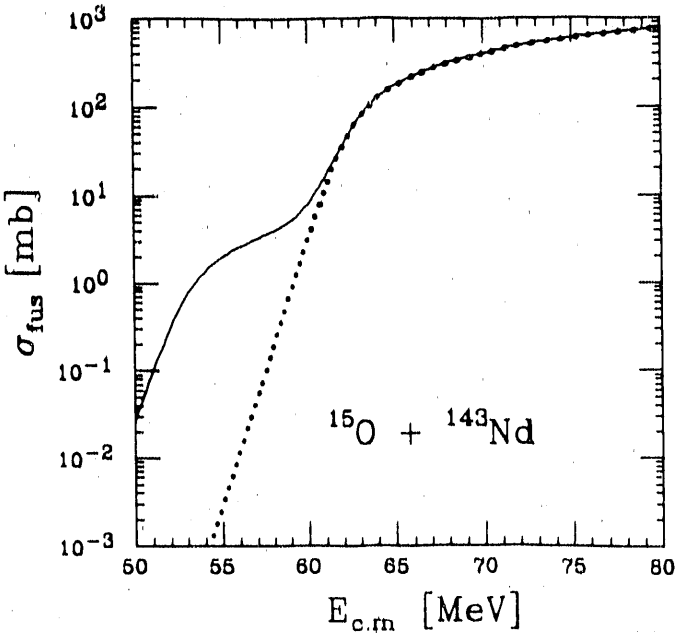

Figure 2: Cross sections for subbarrier fusion of ^{15}O + ^{143}Nd calculated with the coupled-channels code of Dasso and Landowne [11]). The dotted line is the result for no coupling in the entrance channel. The effect of the coupling of a neutron-transfer channel is shown by the full line. The large enhancement predicted below the barrier arises from the large positive Q-value for neutron transfer from ^{143}Nd to ^{15}O. While a useful guide for developing experiments, this estimate has been made with the simplified code CCFUS, which may overestimate the size of the effect compared to that predicted by a more refined calculation.

To study the correlation of positive Q-values with the enhancement of the subbarrier fusion as well as the relative effect of the different transfer channels, it would be interesting to make an experimental investigation of the fusion and transfer reactions in ^{15}O + ^{143}Nd and ^{14}O + ^{144}Nd. The measurements of the fusion cross sections as functions of bombarding energy can be achieved by detecting the evaporation residues with two low-pressure multiwire proportional counters. The identification of the evaporation residues will be made by their time of flight and the energy loss in any of the counters. This technique has already been used to measure the fusion cross sections for ^{12}C + ^{128}Te at different bombarding energies. It is worth noting [12]) that beam intensities required for these experiments are very modest (less than 10^7 particles/s). The transfer-reaction measurements can be made by detecting and identifying the reaction products at backward angles in a silicon surface-barrier ΔE-E telescope with a thin ΔE detector and good timing resolution, which provides mass resolution through time of flight and nuclear-charge resolution via energy losss. This technique has been succesfully used in $^{16,18}O$ + Sn transfer studies performed by Henning et al. [7]). Another technique will be to tag the various transfer channels through the observation of discrete-line gamma rays by an array of Compton-suppressed Ge detectors.

2.4. NEUTRON FLOW IN SUBBARRIER FUSION

A large body of data points to the beginning phase of heavy-ion fusion as proceeding through doorway processes such as those mentioned in the preceding section. The doorway provides extra degrees of freedom that enhance fusion cross sections at subbarrier energies. A process related to the effect of neutron transfer channels discussed above and that gives a good account of some of the observed fusion enhancements is the recently suggested free-flow of neutrons [13]). In this proposed process the transfer of a valence neutron, which proceeds via tunnelling at large internuclear separations, becomes a free-flow process once the colliding nuclei approach each other sufficiently close for the neutron barrier to disappear (due to overlapping tails of nuclear potentials). The internuclear distance where the neutron flow commences is intimately related to the binding energy of the least-bound neutron of the system and systematically lies outside (by about 2 fm for $40 < A < 100$) the corresponding distance where strong absorption occurs [13,14]). This neutron flow in turn precipitates the formation of a neck connecting the nuclei, e.g., via liquid-drop effects [15,16]). Coalescence of the neck leads to fusion, and re-separation leads to energy-damped multinucleon transfers. For the case of the ^{50}Ti + ^{93}Nb system [17]), the scission of the neck preferentially populates channels that involve transfers of up to four nucleons from the heavy to the light collision partner, i.e., the system tends toward symmetric partition, very reminiscent of familiar spontaneous fission.

Neutron flow is the key to this subbarrier process, and as the binding of the valence neutron weakens, the internuclear distance where the free flow commences becomes larger. Accordingly, radioactive beams of nuclides near the neutron drip line, where the neutron is weakly bound by less than about 1 MeV, would open an exciting new vista to explore this interesting subbarrier process.

2.5. ISOSPIN MIXING IN GIANT-DIPOLE DECAY OF COMPOUND NUCLEI

Compound nuclear isospin mixing at high excitation energies (50 MeV and higher) can be studied [18]) in light $N = Z$ nuclei by looking at GDR gamma-emission in heavy-ion fusion-evaporation in reactions with $T = 0$ entrance channels, e.g., ^{16}O + ^{12}C $\rightarrow$ ^{28}Si*. In such reactions, (isovector) GDR gamma-decay is strongly hindered for states of pure isospin, due to the low level density of $T = 1$ final states. There is a surprising result, viz., that very large mixing widths of 1 MeV or greater for the mixing of $T = 1$ states with $T = 0$ states are necessary to explain the data [18]). However, it is necessary to "calibrate" the statistical model by studying neighboring $N = Z$ compound nuclei. A much better calibration would be to look at the same $N = Z$ compound nuclei formed in a $T \neq 0$ entrance channel, for which GDR gamma-decay would not be hindered. This is not possible with stable heavy ions, for which one always has $N \geq Z$. With radioactive beams, proton-rich projectiles are possible that permit such reactions. For example, ^{28}Si* could be formed in the reactions ^{15}O + ^{13}C and ^{14}O + ^{14}C. Other $N = Z$ nuclei could be studied in a similar fashion.

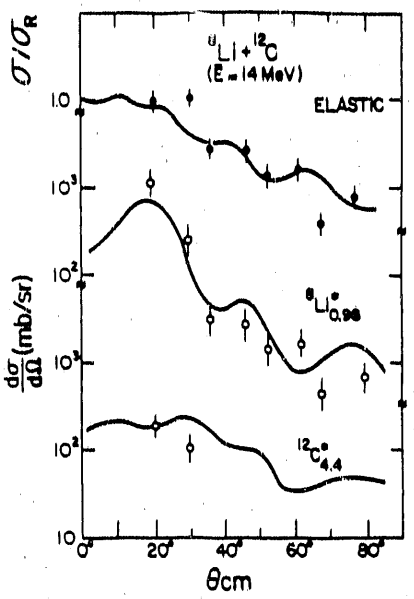

Figure 3: Differential cross sections measured for a beam of ^{8}Li scattered by a ^{12}C target [23]).

3. Reactions as probes of nuclear structure

3.1. TOTAL REACTION CROSS SECTION

The total reaction cross section or, closely related to it, the interaction cross section σ_I, is related to the most basic structural feature of the nucleus, its size. Some of the first measurements to be made with secondary beams of radioactive nuclei were the interaction cross sections [19]). These measurements at high energies (typically 800 MeV/A) revealed a remarkable change in interaction radius with changing isopspin. Measurements at lower energies and for a wide variety of radioactive nuclei also reveal interesting changes in the mean-square radius with isospin [20–22]). These results are considered in the section on neutron halos in a separate position paper.

3.2. ELASTIC SCATTERING

Like the total reaction cross section, the differential cross sections for elastic scattering are one of the most basic and important reaction quantities in nuclear physics. And because the cross sections can be large, they will also be among the first quantities to be measured when a new radioactive beam facility is developed. Figure 3 shows the cross sections [23]) for the elastic scattering of ^{8}Li by ^{12}C at an energy of 14 MeV. The full curves give the results of DWBA calculations using a deformed optical model form factor. The inelastic excitation for the projectile is significant and can be attributed to the peculiar properties of ^{8}Li (weakly bound, T, and J^{π}).

Another reason for the special role of elastic scattering is the degree to which this process is understood theoretically, particularly for elementary projectiles, where

extensive studies using optical-potential models have provided a data base from which microscopic information has been obtained.

Radioactive ion beams would allow us to test and extend the optical-potential models for elastic scattering into new extremes of spin and isospin. The types of projectiles that could be used for these new studies would include neutron-rich and proton-rich ground states, as well as excited (isomeric) states of these nuclei. Here we mention some of the new possibilities that would be provided by the elastic scattering of proton-rich ground states. The new opportunities that would be provided by the elastic scattering of neutron-rich ground states and of isomeric states are given in other sections.

With a RIB facility, one may have available light, $J^\pi = 0$ projectiles such as ^{10}C, ^{14}O, ^{18}Ne, and ^{22}Mg. Elastic-scattering experiments using these projectiles from a proton target would provide us with the opportunity to study the single-particle matter distributions for relatively simple cases where $N < Z$. In the case of ^{10}C and ^{14}O, the nuclei ^{11}N and ^{15}F that would be produced in compound-nucleus reactions lie beyond the proton drip line! We also may be able to test our understanding of the optical-potential models by comparing these results to the corresponding scattering from neutron-rich isotopes such as ^{14}C, ^{18}O, ^{20}Ne, and ^{26}Mg, in which case the Coulomb interaction would be fixed while the isospin part of the strong interaction would change from $T_z = -1$ to $T_z = 1$. Of course, the use of a polarized proton target would extend these studies to include the spin-isospin part of the interaction. Along the same lines as those mentioned above for *p*- and *sd*-shell nuclei, one may also consider the very interesting possibilities of studying the *d*-shell isotopes $^{36-39}$Ca.

3.3. INELASTIC SCATTERING

The inelastic scattering of radioactive beams affords the possibility of measuring transition matrix elements in nuclei that have heretofore been inaccessible. One example is shown in fig. 3 for the first excited state of ^{8}Li. Substituting a gold target for a carbon target should substitute electromagnetic excitation for nuclear excitation and determine the B(E2) value connecting the ground and first excited state [24]. Inelastic scattering of heavier beams from light targets, including hydrogen, could extend significantly our quantitative knowledge of collective transition strengths.

The assumption of time-reversal invariance imposes a reciprocity relationship for the unpolarized inverse reaction cross sections obtained at the same center-of-mass energy and scattering angle. Previously, this reciprocity relation has been studied by use of inverse transfer reactions such as ^{24}Mg(α,p)^{27}Al, and found to be accurate to within a fraction of a percent. The simultaneous availability of nuclear ground and excited states from a RIB facility would allow the reciprocity relation to be studied within the same nuclear environment, and possibly lead to a more stringent test. For example, inverse transitions such as ^{18}F(p,p$'$)^{18}F* could be used to study time-reversal invariance.

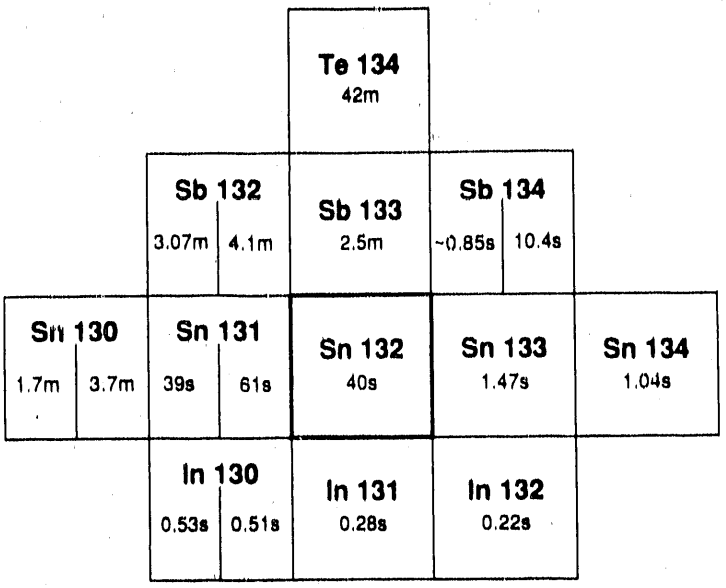

Figure 4: The doubly magic nucleus ^{132}Sn and its neighbors. The measurement of single- and few-nucleon transfer reactions in this region will map out the interaction energies among the single-particle orbitals [25]).

3.4. TRANSFER REACTIONS

The same measurements yielding elastic and inelastic scattering information from light targets (p, d, ^{3}He, and ^{4}He) would also provide a rich source of new information on single-particle motion. By observing the scattered target nucleus or target-like reaction product, the same kind of spectroscopic information can be obtained as has been gleaned from reactions such as (d,^{3}He), (d,t), (d,p), (p,d), and (^{3}He,d) using beams of hydrogen and helium isotopes. Indeed, measurements of this type are approved [25]) for the experimental storage ring, ESR, at GSI's new synchrotron, SIS-18. Here it will be of particular interest to map out the effective interaction among single-particle orbitals in the region of the double shell closure at ^{132}Sn. Figure 4 charts the region of the nuclides around ^{132}Sn. A beam of ^{132}Sn projectiles and targets of p, d, ^{3}He, and ^{4}He would enable the full arsenal of one- and two-nucleon transfer reactions to be applied to the mapping of particle and hole states in this region. This type of nuclear structure information in the vicinity of the doubly closed shell at ^{56}Ni shows a beautiful systematic behavior that is not well understood. Being able to obtain comparable information in the region of a different double shell closure may bring the clue for the solution of the problem in the Ni region, or it may raise new and unexpected questions.

The properties of single-particle orbitals in nuclei far from closed shells and in the regions of strong deformation are also of interest for study with radioactive beams in conjunction with multiple-high-resolution-gamma-detector arrays. Indeed, the latter have made possible a promising new class of nuclear reactions. Spherical actinide nuclei have produced neutron-transfer products at high spin. On the incoming path,

Coulomb excitation pumps the deformed partner to spins as high as 14, and one or more neutrons are transferred, giving rise to deformed transfer products, which are further excited to higher spins by Coulomb excitation on the outward path. These high-spin states reveal themselves through the de-exciting gamma-ray cascades. For example, the knowledge of the ground-state rotational bands in ^{160}Dy, ^{234}U, and ^{238}Pu has been extended to considerably higher spins.

At present a fundamental limitation on this powerful new spectroscopic tool in the actinides is that no stable, high-Z projectiles are available with neutron separation energies below those of the actinides, so that one can only extract neutrons but not add them to the actinides.

The addition of a neutron to a heavy target like ^{248}Cm at high spin could give unique information on Nilsson orbitals lying in the region of the possible superheavy island of stability. Learning the location of the $h_{11/2}$ or $k_{17/2}$ neutron levels would refine the half-life estimates of the superheavy elements. The experimental search would be similar to the experiments performed by Garrett and co-workers in locating the $i_{13/2}$ proton levels in the rare earths [26].

The best candidates seem to be ^{17}O and ^{210}Bi, although ^{137}Xe and ^{138}Cs may provide interesting possibilities. A beam of ^{17}O, because it does not excite ^{248}Cm to very high spins, would map the lower-spin orbitals while the heavier radioactive beams would reach the more interesting high-spin orbitals. And in addition to the spectroscopic goal of locating the nucleon orbitals, a study of the reaction mechanism—Coulomb excitation combined with neutron transfer—and further development of the calculational tools present important challenges.

3.5. CHARGE EXCHANGE

3.5.1. *General considerations.* Radioactive beams also provide unique opportunities for studing the charge-exchange reactions, again using reverse kinematics. Transitions induced by both the isospin and spin-isospin operators will yield information pertaining to $L = 0$ isospin transitions (Fermi) and spin-isospin transitions (GT) as well as higher-L transfer transitions. In a notation indicating reverse kinematics, the reaction on a hydrogen target is written p($_Z A_N$,$_{Z+1} A_{N-1}$)n, with the proton target being in the form of a plastic for a single pass beam or a gas if a circulation beam in a storage ring is used. A spectrometer (perhaps in conjunction with the magnetic elements of a storage ring) with particle identification will be required to measure the heavy-ion reaction product. In some cases, detection of the coincident neutron will be required.

Some advantages of using reverse kinematics for these particular experiments are: (1) The detector efficiency for the heavy fragment is close to unity. (2) The energy resolution of the heavy fragment could be much better than could be obtained from neutron time of flight. (3) One can measure the complete angular distribution with either one or a few angular settings of the spectrograph Crude calculations of counting rates indicate that such experiments will be feasible with particle fluxes expected from a RIB facility.

Measurements of isobaric transitions are expected to extend the data on Coulomb displacement energies and provide sensitive tests for isobaric mass formulas. Measurements of GT-strength distributions can be of value to both astrophysics and nuclear physics. Some other questions to be addressed are the distributions of $L = 1$, $S = 0$, and $S = 1$ strengths as functions of incident energy, as well as measurements of isospin splitting.

3.5.2. *Anomalies in Fermi and Gamow-Teller strengths.* It has been shown experimentally that cross sections for (p,n) reactions are proportional to beta-decay transition rates for initial and final states that are connected by allowed Fermi or Gamow-Teller transitions. In fact, when these transitions can be observed in (p,n) reactions at low momentum transfer, as, for example, at zero degrees and proton energy above 100 MeV, essentially the entire structure dependence of the cross section is contained in the beta-decay matrix element [27]). This fact is expected theoretically also. This simple structure dependence has been exploited not only in nuclear-structure studies, but also has been applied to determining neutrino detection cross sections for solar-neutrino detectors.

The (p,n) cross section also depends on kinematic factors that are easily calculated and on the nuclear mass A in a way that has so far defied calculation. Let us define the specific cross section as the (p,n) cross section per unit Fermi or Gamow-Teller transition probability, whichever is applicable to the transition in question. We also assume that correction has been made for kinematics and momentum transfer. Then we expect the specific cross section to have a smooth mass dependence. However, measured specific cross sections show large variations between adjacent A values. For example, the specific cross sections for $A = 13$ and $A = 15$ are nearly 1.5 times larger [28]) than those for $A = 12$ and $A = 14$. What is more puzzling is that the anomaly has not been observed in (n,p) reactions for the transition from ^{13}C to ^{13}B. The cross-section normalization for (p,n) reactions is done with isospin-related transitions but not exactly isospin-mirror transitions.

If one could bombard a proton target (it could be a plastic target) with a ^{13}N beam, for example, one could measure in reverse kinematics the (p,n) cross section for the transition between the ground state of ^{13}N and the ground state of ^{13}O, which is the isospin mirror of the measured beta-decay transition from ^{13}B to ^{13}C that was used to determine the GT matrix element to calibrate the specific cross section. This one measurement alone should be interesting because it addresses a case where a large anomaly is seen in the (p,n) cross section. Figure 5 illustrates the measurements needed for the $A = 13$ system.

In general, the availability of radioactive beams removes the severe restriction that GT and Fermi transitions can be studied with (p,n) reactions only for cases originating on nuclei that happen to be stable. The cross sections are typically large, a few millibarns per steradian. The energy should be about 100 MeV/A to get good selectability for F and GT transitions.

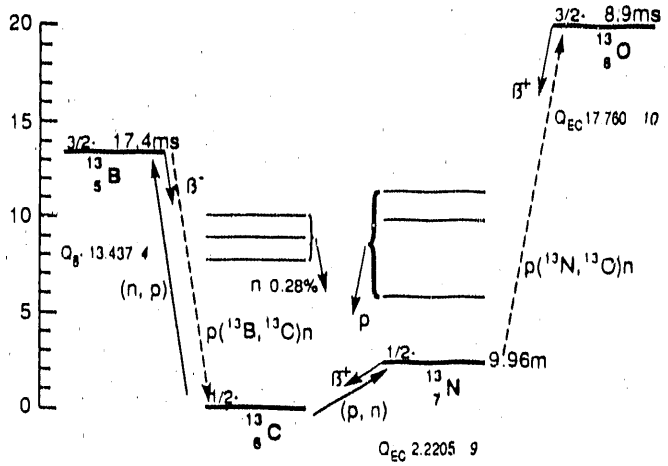

Figure 5: The mass-13 isobaric system. The ^{13}C(p,n)^{13}N reaction is anomalous with respect to the Gamow-Teller transitions in the $A = 12$ and $A = 14$ systems. The dashed arrows show the transitions that could be studied with radioactive beams.

3.5.3. *Double-beta decay.* Considerable theoretical and experimental effort has been invested in attempts to determine lifetimes of nuclei that double-beta decay. From this work one hopes to learn about extensions to the Standard Model. Thus far, there is only one laboratory measurement, that of ^{82}Se decaying to ^{82}Kr. For this case the theoretical predictions differ from the experimental data by factors of four to ten.

Double-beta decay can proceed with either zero or two neutrinos appearing in the final state; appearance of the former would signal lepton-number violation. The observed decay of ^{82}Se presumably is a two-neutrino decay. The dominant mechanism for the two-neutrino decay is the Gamow-Teller mechanism, with the transition proceeding through 1^+ states of the intermediate odd-odd nucleus. However, states of other spins may contribute, particularly in the case of zero-neutrino decay.

To understand the discrepancy between theory and experiment, and to provide additional tests of the nuclear wave functions, (p,n) and (n,p) reactions are being used to map out the Gamow-Teller strength. Additional constraints will result by using a radioactive beam composed of the intermediate nucleus. Such information is particularly important if one is able to measure double-beta decay to the 2^+ levels of the granddaughter nucleus. There are theoretical suggestions that such transitions are sensitive to extensions of the Standard Model such as right-handed currents.

Three of the most actively studied double-beta decaying nuclei are ^{76}Ge, ^{82}Se, and ^{100}Mo. The ground-state spins of the intermediate odd-odd nuclei are 2^- (^{76}As), 5^- (^{82}Br), and 1^+ (^{100}Tc), although there is a 6-minute isomer in ^{82}Br at 46 keV having angular momentum 2^-. Beams of either ^{76}As or ^{82m}Br would allow the measurements of transitions to states in neighboring nuclei, which would provide useful constraints

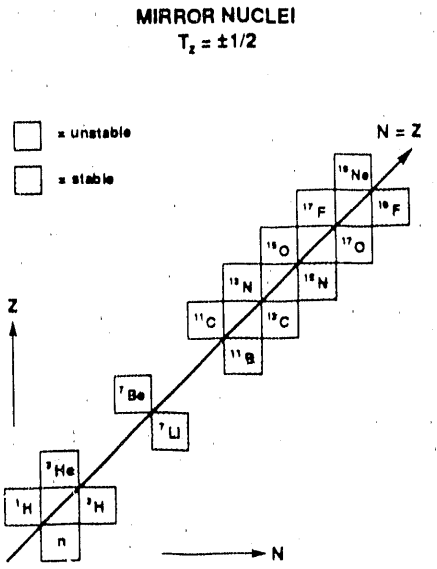

Figure 6: The $T_z = \pm 1/2$ mirror nuclei. Radioactive beams would enable the study of charge-exchange reactions among several mirror pairs and the contribution of this process to elastic scattering.

not otherwise attainable.

Particularly useful would be beams of ^{100}Tc since transitions induced by the (p,n) reaction from the ^{100}Tc 1^+ ground state to excited states of ^{100}Ru would provide information useful for calculating double-beta branching ratios that is not available from the beta decay of ^{100}Tc itself. This would in turn provide constraints on right-handed currents and massive neutrinos.

3.5.4. *Charge-exchange reactions between mirror nuclei.* Charge-exchange reactions between a stable projectile and a stable target are well established spectroscopic tools for studies of nuclear structure. If one could instead employ in a general way $T_z = \pm 1/2$ mirror nuclei for the projectile and target with the resulting interference between direct and exchange terms, a new type of charge-exchange reaction would become possible that could, in principle, probe unique parts of both ground-state and excited-state wave functions [29]). Utilizing mirror nuclei also has the property that the reaction Q-value ≈ 0, which enhances the possibility of observing non-perturbative effects (resonances). The basic idea behind such resonances is that two nucleon-equivalent cores elastically scatter off of each other and that the unpaired proton and neutron might resonantly interact via pion exchange terms between only these valence nucleons. The cross section for this process can be approximated by utilizing that for the elastic scattering of the two cores.

The only stable nucleus that has more protons than neutrons is ^{3}He. All other nuclei with $T_z = -1/2$ are unstable. Figure 6 illustrates this and points out the large number of such nuclei that become available with a radioactive beam facility. The only case of charge exchange among mirror nuclei studied to date is the ^{3}He–^{3}H(12 y) system [30,31]); an experiment to search for the effects predicted by

Vary and Nagarajan [29]) in the ^{7}Be(53 d)–^{7}Li system is underway [32]). The reactions ^{11}C(20 m) + ^{11}B and ^{13}N(10 m) + ^{13}C require radioactive beams because of the short half-lives of the $T_z = -1/2$ members.

In addition to the charge-exchange effects mentioned above, which are studied by the elastic scattering of a radioactive beam by its mirror nuclear target, there exists a specific comparison between mirror nuclear wave functions that could be uniquely investigated by utilizing an inelastic scattering process in reactions of mirror nuclei. Many years ago the Thomas-Ehrman effect was postulated [33,34]) to explain the energy difference between the $1/2^+$ first-excited states in ^{13}C and ^{13}N. The s-wave proton in the excited state of ^{13}N is unbound by about 0.4 MeV. The loosely bound proton experiences a lower Coulomb energy. This effect is most dramatic when an s-state is involved, and it has been invoked to explain the sudden extra stability of nuclei at the proton drip line [35]). By performing a mutual-excitation scattering measurement of ^{13}N on ^{13}C, it should be possible to identify changes in the mirror wave function. Furthermore, the technique can be calibrated by studying a case where the Thomas-Ehrman effect is not present, but which is otherwise similar. The ^{11}C–^{11}B system is such a case. Study of the elastic scattering of the $A = 11$ mirror nuclear system will also permit us to explore unresolved theoretical issues that are expected to arise from the presently incomplete theory [29]). The extension of these considerations to $T_z = -1$ nuclei, also available as radioactive beams, is clear.

The large cross sections expected for these reactions make this general type of experiment feasible with the beam intensities that would be initially available at a radioactive beam facility. The 590-keV energy difference between the $1/2^+$ and $3/2^-$ states in ^{13}C demands a beam with a well-defined energy.

4. Isomeric radioactive ion beams

4.1. PROJECTILES EXISTING IN HIGH-SPIN ISOMERIC STATES

Consider first a beam of ^{178}Hf ions existing in the $J^\pi, K, E^* = 16^+, 16$, 2.447-MeV state. Performing Coulomb-excitation experiments could lead to population of the excited members of a rotational band built upon this state. This would be the first observation of a rotational band built upon such a high-spin isomer. Questions of shape (moment of inertia), band termination, and influence of the large value of K would be addressed.

Consider next a beam of ^{18}F* existing in the 5^+, 1.119-MeV state. The production of this isomer in a primary nuclear reaction can lead directly to an aligned and even polarized 5^+ isomeric-state beam. Such a beam would allow exploration of polarization phenomena with very high projectile spin [36]).

Excited-state scattering studies lead to the possibility of energy-gaining transitions in competition with elastic scattering, implying changes in the reactive content of the optical-model potential [37]). Relatively simple total reaction cross-section measurements would shed light on this question. The high-spin isomeric state also leads to a re-examination of the question of the presence of a spin-spin term of the form

$\mathbf{J_t \cdot J_m}$ in the optical-model potential, where the subscripts t and m refer to target and isomeric state, respectively. A good example for studying changes in the reactive content of the optical-model potential may be the 16^+, 2.905-MeV state in ^{212}Po, which is a member of the ground-state rotational band that has a half-life of 45 s.

For the excitation of the giant-dipole resonance one may speculate on the exotic spectroscopy that becomes possible. Brink showed many years ago that a giant resonance can be built upon any state, not just the ground state. It would be extremely interesting to observe through, e.g., in-beam spectroscopy, the giant resonance built upon a high-spin isomeric state, and the splitting of the resonance for large values of K.

References

1. E. K. Hulet, J. F. Wild, R. J. Dougan, R. W. Lougheed, J. H. Landrum, A. D. Dougan, M. Schädel, R. L. Hahn, P. A. Baisden, C. M. Henderson, R. J. Dupzyk, K. Sümmerer, and G. R. Bethune, Phys. Rev. Lett. **56** (1986) 313

2. D. C. Hoffman and L. P. Somerville, Particle emission from nuclei, vol. **III** (CRC, Boca Raton, 1988) p. 1

3. P. Möller, J. R. Nix, and W. J. Swiatecki, Nucl. Phys. **A492** (1989) 349

4. J. R. Nix, Nucl. Phys. **A502** (1989) 609c

5. J. D. Robertson and W. B. Walters, Proc. Symp. on exotic nuclei, 198th American Chemical Society National Meeting, Miami Beach, Florida, 1989, to be published

6. F. Catara, C. H. Dasso, and A. Vitturi, J. Phys. G: Nucl. Phys. **15** (1989) L191

7. W. Henning, F. L. H. Wolfs, J. P. Schiffer, and K. E. Rehm, Phys. Rev. Lett. **58** (1987) 318

8. G. Montagnoli et al., Proc. Symp. on the many facets of heavy-ion fusion reactions, Argonne, Illinois, 1986, Argonne National Laboratory Report ANL-PHY-86-1 (1986) p. 555

9. K. E. Rehm, Proc. XII Workshop on nuclear physics, Iguazu Falls, Argentina, 1989 (World Scientific, Singapore) to be published.

10. Heavy ion interactions around the coulomb barrier, edited by C. Signorini et al., Lecture notes in physics, vol. **317** (Springer-Verlag, Berlin, 1988)

11. C. H. Dasso and S. Landowne, Phys. Lett. **183B** (1987) 141

12. D. DiGregorio and R.G. Stokstad, private comunication

13. P. H. Stelson, Phys. Lett. **205B** (1988) 190

14. P. H. Stelson, H. J. Kim, M. Beckerman, D. Shapira, and R. L. Robinson, Phys. Rev. **C41** (1990) 1584

15. C. E. Aguiar, V. C. Barbosa, L. F. Canto, and R. Donangelo, Nucl. Phys. **A472** (1987) 571

16. A. Iwamoto and K. Harada, Z. Phys. **A326** (1987) 201

17. H. J. Kim, private communication

18. M. N. Harakeh, D. H. Dowell, G. Feldman, E. F. Garman, R. Loveman, J. L. Osborne, and K. A. Snover, Phys. Lett. **176B** (1986) 297

19. I. Tanihata, T. Kobayashi, O. Yamakawa, S. Shimoura, K. Ekuni, K. Sugimoto, N. Takahashi, T. Shimoda, and H. Sato, Phys. Lett. **206B** (1988) 592

20. W. Mittig, J. M. Chouvel, W. L. Zhan, L. Bianchi, A. Cunsolo, B. Fernandez, A. Foti, J. Gastebois, A. Gillibert, C. Gregoire, Y. Schultz, and C. Stephan, Phys. Rev. Lett. **59** (1987) 1889

21. A. C. C. Villari et al., Proc. XXVII Int. Winter Meeting on Nuclear Physics, Bormio, Italy, 1989, University of Milan Report (1989) p. 74

22. M. G. Saint-Laurent, R. Anne, D. Bazin, D. Guillemaud-Mueller, U. Jahnke, J. G. Ming, A. C. Mueller, J. F. Braundet, F. Glasser, S. Kox, E. Liatard, T. U. Chan, G. J. Costa, C. Heitz, Y. El-Masri, F. Hanappe, R. Bimbot, E. Arnold, and R. Neugart, Z. Phys. **332A** (1989) 457

23. J. Brown, F. D. Becchetti, W. Z. Liu, J. W. Jänecke, D. A. Roberts, J. J. Kolata, A. Morsad, and R. E. Warner, Proc. First Int. Conf. on radioactive nuclear beams, Berkeley, California, 1989 (World Scientific, Singapore, 1990) p. 372

24. F. D. Becchetti, J. Brown, J. W. Jänecke, W. Z. Liu, D. A. Roberts, J. J. Kolata, R. Smith, K. Lamkin, A. Morsad, and R. E. Warner, Proc. First Int. Conf. on radioactive nuclear beams, Berkeley, California, 1989 (World Scientific, Singapore, 1990) p. 305

25. J. P. Schiffer, these Proceedings

26. C. X. Yang, J. Kownacki, J. D. Garrett, G. B. Hagemann, B. Herskind, J. C. Bacelar, J. R. Leslie, R. Chapman, J. C. Lisle, J. N. Mo, A. Simcock, J. C. Wilmott, W. Walus, L. Carlén, S. Jönsson, J. Lyttkens, H. Ryde, P. O. Tjøm, and P. M. Walker, Phys. Lett. **133B** (1983) 39

27. C. D. Goodman, C. A. Goulding, M. B. Greenfield, J. Rapaport, D. E. Bainum, C. C. Foster, W. G. Love, and F. Petrovich, Phys. Rev. Lett. **44** (1980) 1755

28. T. N. Taddeucci, C. A. Goulding, T. A. Carey, R. C. Byrd, C. D. Goodman, C. Gaarde, J. Larsen, D. Horen, J. Rapaport, and E. Sugarbaker, Nucl. Phys. **A469** (1987) 125

29. J. P. Vary and M. A. Nagarajan, Proc. Workshop on radioactive nuclear beams, Washington, D.C., 1984, Lawrence Berkeley Laboratory Report LBL-18187 (1984) p. 113

30. A. D. Bacher, R. J. Spiger, and T. A. Tombrello, Nucl. Phys. **A119** (1968) 481

31. R. F. Haglund, G. G. Ohlsen, R. A. Hardekopf, N. Jarmie, R. E. Brown, and P. A. Schmelzbach, Phys. Rev. **C15** (1977) 1613

32. R. N. Boyd, M. S. Islam, J. Kolnicki, M. Farrell, T. F. Wang, K. E. Sale, and G. J. Mathews, Proc. First Int. Conf. on radioactive nuclear beams, Berkeley, California, 1989 (World Scientific, Singapore, 1990) p. 311

33. R. G. Thomas, Phys. Rev. **80** (1950) 136; **88** (1952) 1109

34. J. B. Ehrman, Phys. Rev. **81** (1951) 412

35. E. Comay, I. Kelson, and A. Zidon, Phys. Lett. **210B** (1988) 31

36. F. D. Becchetti, private communication

37. D. G. Madland, private communication

NUCLEAR STRUCTURE/NUCLEI FAR FROM STABILITY

Report of Working Group II

Co-chairmen: R. F. Casten [1] and J. D. Garrett [2]

Local Coordinator: P. Moller

Members: W. W. Bauer, D. S. Brenner, G. W. Butler, J. E. Crawford, C. N. Davids, P. L. Dyer, K. Gregorich, E. G. Hagbert, W. D. Hamilton, S. Harar, P. E. Haustein, A. C. Hayes, D. C. Hoffman, H. H. Hsu, D. G. Madland, W. D. Myers, H. T. Penttila, I. Ragnarsson, P. L. Reeder, G. H. Robertson, N. Rowley, F. Schreiber, H. L. Seifert, B. M. Sherrill, E. R. Siciliano, G. D. Sprouse, F. S. Stephens, K. Subotic, W. Talbert, K. S. Toth, X. L. Tu, D. J. Vieira, A. C. C. Villari, W. B. Walters, B. H. Wildenthal, J. B. Wilhelmy, J. A. Winger, F. K. Wohn, J. M. Wouters, X. G. Zhou, and Z. Y. Zhou

1 Introduction

Our current knowledge of nuclear structure is confined to nuclei produced with projectiles and targets that have equilibrated for a significant fraction of the lifetime of the universe. Such a long equilibration (a few billion years) must evade many of the most exotic nuclear configurations, which due to their special properties, decrease the stability of the nucleus. The present basis of nuclear structure is phenomenlogical, that is, it is not derivable from a simple set of master equations. Not only is the structure of the nucleus sensitive to bulk properties, such as its mass and charge, but it also is strongly dependent on the details of the independent-particle quantal states that the protons and neutrons occupy and how these states interact with each other and modify the bulk nuclear properties. Far from stability the various possible combinations of exotic single-particle states make the problem

even more complicated. Therefore, it is not possible simply to extend the present knowledge theoretically to such exotic situations not accessible to experimental study. Thus the use of Radioactive Ion Beams (RIBs) should provide unique opportunities, not only to answer critical issues concerning some of the most fundamental current nuclear structure themes, but it also will allow the study of entirely new phenomena unavailable with current techniques and not derivable from our present knowledge of nuclear theory.

It is useful to highlight a few such possibilities in these introductory remarks in anticipation of the more detailed discussions given below: (i) The long-predicted island of superheavy stability may be established. Not only is this of interest as a long-standing, elusive, historic goal, but it also is perhaps the ultimate test of the predictive power of current nuclear models and, therefore, of our understanding of the interplay of independent-particle and macroscopic structure in nuclei. (ii) The nuclear equation of state will be refined and the enticing hints of the possible binding of pure neutron matter can be probed by mass measurements and the associated definition of the drip lines. (iii) New information in neutron-rich nuclei may finally provide sufficient detailed information to pin down the site, environment, and mechanism of r-process nucleosynthesis. (iv) Detailed measurements of the properties of predicted closed-shell nuclei, such as ^{78}Ni, ^{100}Sn, and ^{132}Sn, will offer a stringent test of the microscopic independent-particle quantum structure forming the foundation of the nuclear shell model itself. (v) New data and analyses of the spectrum of single-particle states will provide detailed new information on the fundamental single-particle structure of nuclei and on the residual interactions that modify that structure. (vi) New manifestations of collectivity, such as the long-sought stable triaxial nuclei, may be found and a better understanding of others (for example reflection asymmetric shapes, which only now are beginning to be probed) should be in the offing. (vii) The study of neutron halos, or skins, representing nearly-pure, low-density neutron matter is a most intriguing and exciting venture. (viii) Complete spectroscopy near stability will allow the first comprehensive connections between low- and high-spin physics to be forged making possible uniquely-sensitive tests of modern nuclear structure models. The exciting concept of quantal chaos in nuclei can be more readily studied in such nuclei and in others that can be formed with extremely-high beta-decay energies. (ix) In the realm of high spin, the increased fission barriers in newly accessible neutron-rich nuclei may allow the discovery of hyperdeformed nuclear shapes with a 3:1 ratio of major to minor nuclear axes. (x) Access to exotic hig-h-j, low-Ω configurations and the associated magnified Coriolis effects

should open unique new vistas in which the single-particle effects are dominated by rotation.

In the following pages we briefly outline some of these and other topics. It should be recognized that it is impossible to do justice to such a broad field in these few pages. Since this work represents the collective viewpoints of a diverse Working Group, and since it is not clear which of the topics discussed will in fact turn out to be the most interesting in an operating facility a number of years hence, we have resisted the temptation to discuss only a couple of topics in detail and rather try to present as broad a coverage as possible. At the other extreme we try to avoid making this report a mere listing of an even larger number of topics by attempting to present sufficient material to indicate an interest in each case. That is, in each subarea we try to identify the main themes, undercurrents, and motivations, and to identify a few experimentally-accesible examples. Finally, since this is the collective report of a Working Group discussing scientific applications, and is neither a complete nor a review paper, we have dispensed with a complete set of references. The field covered by this report is so vast and active that, to have done otherwise, would have highlighted a miniscule segment of the literature at the expense of numerous equally deserving accomplishments. A few "typical" references, however, are included to assist the nonexpert. For additional information the reader is referred to one of several recent reviews and/or conferences on this subject [3,4,5,6].

Although the scientific justification for further studies of nuclei far from stability with RIBs should be amply demonstrated below, and elsewhere in this report, it is interesting to reflect for a moment on the history of such studies. A few examples that come to mind include that of ^{146}Gd and the discovery that, for certain neutron numbers, Z = 64 acts as a closed shell [7]. This was one of the earliest additions to the traditional complement of magic numbers. Similarly, recent studies of deformation near ^{31}Na and ^{80}Zr show that N = 20 and Z = 40 does not ensure a spherical nuclear shape [8,9]. The discovery, in the early 1970's, of an abrupt spherical-deformed phase or shape transition region at N=60 near A=100 [10] and within a few mass units of a significant neutron subshell closure at N = 56,58 [11] hinted at the need for a more detailed understanding of the onset of collectivity in nuclei and led, several years later, to the Federman-Pittel mechanism [12] in which the valence p–n interaction modifies the underlying single-particle structure of one type of particle as a function of the number of nucleons of the other type. The discovery of beta-delayed nucleon, or few-nucleon, radioactivity (β–p,β–2p,β–n,β–2n,...), often near the drip lines [4], revealed

the spectroscopic richness of regions with high-decay energies and offered new insights into the structure and stability of nuclei at the extremes of isospin. Nearer stability, the discovery, in recent years, of examples of multiparticle radioactivity in which intact ^{14}C or even ^{24}Ne or ^{34}Si nuclei are emitted [13] pointed to the amazing complexities of the nuclear potential-energy surface and to the possibility of exotic-cluster formation near the nuclear surface. The discovery of symmetric fission in the heaviest known actinides [14] demonstrated the key role played by structure (extra binding) in the fission fragments. Finally, the discovery of superdeformation in rapidly-rotating neutron-deficient heavy nuclei [15] has opened up wholly new high-spin phenomena that continue to reveal remarkable discoveries, such as essentially identical rotational sequences in neighboring isotopes and isotones [16]. Together, these and other studies have led to new ideas on shell effects (e.g., Strutinsky shell corrections) and residual interactions, to the discovery of dynamical symmetries in nuclei, to the development of new generations of more sophisticated macroscopic-microscopic models, and to a more profound understanding of pairing and collectivity in nuclei.

2 Masses, Stability, Beta Decay, and the Heaviest Elements

Under this rubric gross nuclear properties are stressed. These properties reflect, in a sense, the most obvious and global characteristics of each nucleus and are, therefore, the net result of the single-particle motion, collective correlations, and interactions that are active. The motivation for studying such properties is, of course, to elucidate these facets but also, more specifically, to understand such important concepts as the nuclear equation of state, in particular its compressibility and charge distribution. Studies in this area are also of paramount importance to eradicating the nuclear uncertainties in the r-process of stellar nucleosynthesis. Finally, work here is also directed toward discovering and studying the heaviest elements and, possibly, a superheavy island of stability. Even work on nuclei far removed from this island is important, since it leads to improved modelling of nuclear masses and lifetimes and therefore to more sophisticated extrapolations to unknown nuclei.

2.1 Fission/Heaviest Elements

As noted, a prime interest is the creation and study of nuclei in the predicted superheavy island of stability [17]. This is a long sought goal of nuclear physics, which has often been thought to be unattainable. However, recent improvements in macroscopic-microscopic models offer greater confidence in predicting the existence and properties of superheavy nuclei [18] Such models are quite sophisticated and are capable of handling complex potential energy surfaces with multiple minima and saddle points. Moreover, they take into account the structure not only of the fissioning system, but also that of the daughter products, since this is the barrier to that fission which determines the stability of a given nuclear species. It is only with RIBs that any realistic chance exists to reach the superheavy island, thereby discovering the heaviest nuclei, and testing the ultimate single-particle bases for all nuclear structure. Aside from the general issue of producing superheavy nuclei there are other associated goals. The fission of excited nuclei in the lead region is symmetric, that is, the fission product masses are nearly equal. The spontaneous fission of most of the actinide nuclei, on the other hand, is highly asymmetric. Therefore, the identificaton of the onset of asymmetric fission near A = 220--230 is critical to the understanding of the fission process and an understanding of the competition among fission modes as a function of Z, N, excitation energy and angular momentum of the fissioning system in terms of both macroscopic, droplet behavior and modulations due to the underlying shell structure. Studies might center on the light Ra isotopes. A second area concerns heavy actinides with N > 160. Figure 1 shows a calculation of the fission barriers near A = 264 [19]. There is a fascinating competition between asymmetric and symmetric fission with very high kinetic energy associated with the fission of nuclei such as $^{264}No_{162}$, $^{264}Md_{163}$, and $^{264}Es_{165}$. In these nuclei the barrier to symmetric fission can be offset by the extra binding of the symmetric, doubly-magic, daughter nuclei $^{132}Sn_{82}$. (Incidentally, since fission probabilities depend not only on the structure of the parent but also on that of the daughter, this is yet another motivation for the study of nuclei in the vicinity of ^{132}Sn.) About 12 MeV of energy is gained for each Sn fragment, thereby opening a symmetric fission path characterized by an anomalously-high kinetic energy of the fission fragments. Conversely it is noted that the inverse process, the fusion of two nuclei in the vicinity of the ^{132}Sn closed shell, should have an enhanced cross section and might, indeed, be a method of synthesising some of the heaviest elements. Less complicated transfer reactions, using RIBs, to produce nuclei

with A $\approx$ 264 include $^{264}Es_{155} + {}^{96}Rb_{59} \rightarrow {}^{264}Fm_{164}$, $^{264}Md_{163}$, $^{264}No_{162}$, and $^{264}Lr_{161}$.

2.2 Drip Lines

The study of both proton and neutron drip lines is important in indicating the limits of particle stability of nuclei in general, in further testing of macroscopic-microscopic models and (see below) in gaining access to nuclei with extremely high decay energies which offer the possibility of exotic decay modes. The neutron drip line is a particularly-important regime which is of critical interest to the study of neutron halos and skins. The discovery of nuclei with halo properties such as ^{11}Li [20,21] hints that pure or nearly-pure neutron matter may even be bound under certain circumstances. Recent nuclear matter calculations directed toward this issue [22], therefore, take on renewed interest. They are parameterized in terms of a constant that can be fixed empirically by the precise location of the neutron drip line. (Additional information on neutron halos is contained in subsecton 3.2.1 and in a separate chapter in this report.) Finally, the locus of the proton and neutron drip lines is of interest in limiting possible nucleosynthesis scenarios.

2.3 Masses

The mass is a fundamental nuclear property. Since masses give binding energies and, therefore, neutron and proton separation energies, they are essential to the understanding and the modelling of the r-process for nucleosynthesis (discussed below). They also give indirect information on the nuclear equation of state, provide crucial tests of macroscopic-microscopic models, and yield information on the structure of the nuclear ground state.

Masses are particularly useful in delineating the nuclear equation of state. The concept of nuclear compressibility plays a key role here, determining, for example, the energy of giant monopole resonances and the "skin" properties of nuclei. Since the compressibility essentially reflects the restoring force against oscillations of the outermost nucleons, its determination relies on the empirical knowledge of nuclear masses. RIB studies will enable many new and critical mass determinations.

An interesting concept which has arisen in connection with nuclear halos as well as in other contexts is that of Coulomb redistribution, or the suppression of the proton density in the nuclear interior due to a combination of Coulomb repulsion and an associated in-filling of neutrons. This effect

has been empirically detected in electron-scattering experiments [24] and also appears in some Hartree-Fock calculations [25]. Liquid-drop models do not incorporate such proton-deficient cores, but droplet models, which agree better with the masses of the heaviest elements, do. Therefore, additional masses of heavy nuclei will aid the delineation of such models and refine the understanding of proton core suppression.

Certain double differences of nuclear masses can be used to extract empirical proton-neutron two-body residual matrix elements [26]. It has become increasingly evident recently that these matrix elements, representing a T=0 residual interaction, are of critical importance in understanding the evolution of nuclear shell structure as a function of particle number, isospin, and angular momentum and, therefore, of the onset and development of collectivity and phase transitions in nuclei. Such interactions will be considered in greater detail in the following section, but suffice it to say here that new mass determinations in certain critical regions would go far toward reducing the uncertainty in two-body residual interaction matrix elements.

Aside from specific theoretical reasons for measuring the masses of selected nuclei, there are several mass regions where no empirical data exists in which the various theories exhibit large deviations. Clearly, the measurement of even a few masses in these regions would help distinguish between the models and, inevitably, refine them. In particular, neutron rich nuclei with Z = 10–20, the Z = 28–36 nuclei with N > 50, and the Z = 44–50 nuclei with N $\approx$ Z are such examples.

A particularly enigmatic region occurs near ^{34}Na. Here, not only do significant deviations exist between theoretical and experimental masses, but the measured Na masses themselves have a different isotopic trend relative to the neighboring isotones. Some of these masses have sizable experimental uncertainties. Recently an "island of inversion" has been proposed for these nuclei [27] in which $0\hbar\omega$ and $2\hbar\omega$ excitations cross, leading to the sudden onset of deformation at N = 20, a neutron number previously considered as a classic magic number. Improved masses for the neutron-rich Na isotopes and new results for neighboring isotones would test these ideas and help to solidify our understanding of how and where nuclear deformation arises in terms of the detailed spectrum of single-particle states.

2.4 Beta Decay and Lifetimes

Beta decay is valuable for a variety of reasons: a measure of Gamov-Teller (G–T) matrix elements as a test of weak interaction theory, a source of

nuclear lifetimes, or as a means of access to interesting nuclear structure questions. In the present section we focus on the first two points leaving the discussion of the last topic with regard to the study of nuclei far from stability for the following section.

One of the interesting beta-decay puzzles is the apparent empirical quenching of G–T strength. G–T matrix elements are often substantially smaller than predicted, even in nuclei near closed shells where both parent and daughter configurations are simple and, presumably, well known [28]. Before the question can be fully addressed, though, it is necessary to determine that the full empirical strength has been found. Strength can be missed either if it is fragmented (by the mixing of states in the daughter nucleus) into too fine a structure to be observed or (again due to mixing) if some of it is pushed to excitation energies above the effective threshold for significant beta feeding. Both sources of error are minimized for nuclei with high beta-decay energies. More levels in the daughter nucleus are available for population; therefore, a more complete and reliable level scheme can be constructed and the range of excitation energies in which to search for the beta-decay strength is also increased. The use of RIBs to populate beta-decaying nuclei extremely far from stability with their associated higher beta-decay energies thus offers an opportunity to more thoroughly address the long-standing G–T quenching problem. Likewise access to neutron-rich nuclei just below the Pb closed shell using RIBs will allow the first measurement of beta-decay matrix elements connecting states differing by two major shells.

Beta decay far from stability with high Q_β values also can lead to particle-unstable daughter nuclei. A number of cases of such beta-delayed particle (β-p, β-2p, ...) emission have been discussed [4]. They are interesting because they provide structure information for the daughter nucleus, information on the position, strength, and distribution of the G–T giant resonance, and a study of super-allowed beta-decay matrix elements. Moreover, β^+ decay populates isobaric analogue states and, especially in light nuclei, or medium nuclei with N $\approx$ Z, allows a determination of the isotopic-spin purity. An example of the advantage of RIBs for populating exotic nuclei where such questions can be addressed is given by a comparison of fusion-evaporation calculations for various reactions leading to ^{51}Co. The ^{40}Ca(^{16}O,xp,yn) reaction at 170 MeV has a cross section of 0.004 mb. In contrast, the corresponding ^{14}O reaction, ^{40}Ca(^{14}O,xp,yn), at the more convenient lower energy of only 70 MeV has a cross section, 0.17 mb, over 40 times larger. The lower required beam energy helps to compensate for the

difficulty of providing ^{14}O beams.

The use of RIBs to make beta-unstable nuclei, either by reactions or as fission products of heavy actinides, allows the study of many new nuclei along the r-process path [29]. A critical issue in supernova r-process nucleosynthesis is the time scale ("cycle" time) needed for the production by neutron capture and beta decay, of the actinides from "seed region" nuclei near ^{56}Fe. This time scale is dominated by the half lives of the so-called waiting-point nuclei where the r-process abundance peaks cross a neutron magic number. At such points the r-process halts until these nuclei can beta decay. It is, therefore, crucial to determine the lifetimes and binding energies of nuclei in these waiting-point regions so as to determine, or set limits on, the required duration of the intense supernova explosion. Recently, some of these nuclei have been studied for the first time, but more information is needed on all three waiting point regions near ^{80}Zn, ^{130}Cd, and especially ^{195}Tm, where no experimental information exists. It may be possible to study such species either through reactions with RIBs or through the beta decay following the fission of heavy, very neutron rich actinides produced with RIBs.

In modern "network" r-process calculations [29], the waiting-point approximation (of ignoring all but the lifetimes of the waiting point nuclei) is bypassed by incorporating the properties ($T_{1/2}$, binding energies, etc.) of all nuclei along the r-process path into these complex calculations. Therefore, these data are needed so that a larger fraction of the information inserted into these calculations is empirical. This is especially important because, even though recent models are greatly improved over their predecessors, the discrepancies between measured and predicted lifetimes even near stability average at least a factor of 2–3 (in both directions) and can exceed an order of magnitude in selected cases. This constitutes a significant impediment to determining the site and environment (neutron flux, duration, and temperature) of the r-process.

2.5 Cluster Decay

A fascinating phenomenon, now known in several cases, is heavy-ion radioactivity, in which an unstable nucleus decays by emitting a massive chunk, such as ^{14}C, or even ^{25}Ne or ^{34}Si [13]. This process is clearly a major challenge to nuclear theory, since it requires an understanding of both the formation amplitudes of such fragments near the nuclear surface, as well as the probability of their emission through a complicated barrier. Though this decay

mode was actually predicted before its observation, it is still far from well understood and new empirical examples, and their systematics, would be valuable. There is the intriguing possibility that this decay mode may be even more prominent farther from stability in nuclei accessible with RIBs.

2.6 Laser Spectroscopy

The access to nuclei with extremes of isospin also introduces exciting possibilities for using laser-spectroscopic methods. Many of the most fundamental properties of a nuclear state, e.g. the mean-square radius $< r^2 >$, the magnetic moment μ, the magnitude and **sign** of the quadrupole moment Q, and in some cases the spin, can be measured using techniques based on lasers [30].

Laser techniques generally involve exciting ions resonantly and mapping out the isotope shifts and hyperfine structure by scanning the laser wavelengths. The use of radioactive beams circumvents the usual problem of producing and transporting short-lived nuclei to the laser beam. The exotic nuclei could be obtained either as a direct beam or as the residue of a reaction based on RIBs. Laser methods well matched to both production methods are available: e.g., the collinear method [31] for direct beams and recoil into gas [32] for less intense production by reactions.

Nuclear phenomena that can be studied include unusual distributions of nuclear matter, shape changes, and high-spin effects including superdeformation. Several of these possibilities are discussed in more detail in the following paragraphs:

Local deviations of the neutron to proton density ratio. Nuclei with a large deficit or excess of neutrons may minimize their energy by local variations in the properties of nuclear matter, e.g. the neutron "skins" or "halo" and Coulomb redistribution discussed elsewhere in this article. Indeed at the extremes of isospin, accessible with RIBs, even more extreme variations in the N/Z density ratio, e.g. a local "precipitation" may occur. Such effects could be studied by comparing results of laser spectroscopy, which measures properties of the proton distribution, and hadronic probes, that determine the matter distribution. Deviations of $< r^2 >$ from an $A^{1/3}$ dependence alone, can yield an indication of a separation of the neutrons from the protons.

Specific properties of exotic states. Measurements of $< r^2 >$, μ, and in some cases Q can be made using laser techniques for special nuclear states, such as the superdeformed and other exotically-deformed states described

elsewhere in this report.

Transitional nuclei. The most definitive signature of a nuclear shape transition is a sudden change in $< r^2 >$ and an associated change in the sign of Q. An example is that observed using laser techniques in the Pt, Au, Hg, and Tl isotopes [30,33]. The use of RIBs will allow an extension of measurements in this mass region to lighter nuclei and for similar measurement in the region of the more exotic shape transitions discussed elsewhere in this report.

Radii of closed-shell nuclei far from stability. Measurements of $< r^2 >$ would be a test of the proposed double-shell closure in, e.g. ^{100}Sn and ^{132}Sn. The charge radii for the tin chain studied thus far ^{108,125}Sn [34] show a smooth parabolic variation. Measurements and extrapolations indicate smaller values than calculated from microscopic theories for $^{118-132}$Sn.

3 Nuclear Shell Structure, Shapes, Collectivity, and Shape/Phase Transitions

Neglecting effects, such as quark degrees of freedom, coupling to baryon excitations (e.g., delta resonances), which appear to be superfluous for low-energy (say < 100 MeV/A) phenomena, the Fermion Shell Model is the most fundamental model of nuclear structure. This model is based on a mean field (mostly due to a central potential) leading to quantal single-particle states, and residual interactions that contribute in a many-body environment. Where calculations are practical, it is the paradigm. In general, it is the rationalization and microscopic justification for other models, models which are themselves generally simplifications or truncations of the Shell Model designed to avoid its calculational complexities and to focus on simple, often collective, excitation modes, symmetries and the like. In view of this theoretical hierarchy, tests of the fundamental properties of shell structure are vital to a profound understanding of nuclear physics and, ultimately, to providing the input for the development of a realistic nuclear theory which remains elusive. Nuclei in the new frontiers far from stability offer wholly new vistas leading toward this goal. In addition, access to new combinations of N and Z, the exploitation of high decay energies, and of opportunities for "complete spectroscopy" will reveal new manifestations of collective many-body behavior, symmetries, and afford a qualitative leap in our appreciation of the interplay of the single-particle and collective facets of nuclear structure.

3.1 Single-Particle Structure

The underlying microscopic basis for all nuclear structure is the Shell Model whose most important characteristic is a set of single-particle eigenstates and eigenvalues. This is fundamental to all other manifestations of single-particle and collective behavior. As alluded to earlier, however, the single-particle energies of nuclei do not constitute an immutable substructure. Rather, due to gross changes (e.g., radius) in the mean field and to the effects of residual interactions, the single-particle structure, and its attendant patterns of major and minor gaps, is an evolving, dynamic concept, which is dependent, separately and in concert, on the numbers of protons and neutrons and, in particular, on the numbers of valence particles of each type. Even the magic numbers are not sacrosanct in that some nuclei with N = 20 or Z = 40 (e.g., ^{31}Na and ^{80}Zr) are well deformed and nucleon numbers such as Z = 64 can provide strong inducements to spherical shapes. Thus one of the most important roles of RIBs in nuclear structure will be the study of such as yet unreachable doubly-magic nuclei as ^{78}Ni, ^{100}Sn, and ^{132}Sn and the mapping of single-particle structure in the neighboring odd-proton and odd-neutron nuclei. This can be done only by exploiting reverse kinematic stripping and pickup reactions using RIBs. Nickel-78, ^{100}Sn, and ^{132}Sn all are expected to be doubly closed-shell nuclei with properties similar to ^{208}Pb. If these expectations should turn out to be false, it would be a devastating assault on our most basic concepts of nuclear structure and, just as clearly, a challenge and mandate for a deeper understanding of the shell structure of nuclei, which results from the interplay of fundamental quantum degeneracies in central potentials and the critical residual interactions which modulate that shell structure.

The two most obvious and predominant components of these residual interactions are nucleon pairing and the valence p–n interaction. Though the former has been rather thoroughly studied, recent work suggests new features such as a possible dependence of pairing on neutron excess, (N–Z)/A. Whether such effects are due to a fundamental neutron-excess dependence of the pairing interaction or whether they arise from macroscopic effects or p–n interactions is an open, and basic, question. RIBs will make possible the production and study of new nuclei spanning extended isotopic or isotonic chains. One case where such chains have recently provided intriguing data is the set of neutron rich V–Fe isotopes where no isospin effects are observed [35].

The valence p–n interaction affects nuclear structure in several ways

[36]. It appears in two forms, as a T=1 interaction identical to the nuclear p–p and n–n forces, and, more importantly, as a T=0 force that leads to single-nucleon configuration mixing and hence, perforce, to collectivity and deformed nuclear shapes. The T=0 interaction appears, predominantly, in two guises, a monopole and a quadrupole component. The latter, which is dependent on the angular orientation of the respective proton and neutron orbits plays a key role in the evolution of collective behavior in deformed regions and contributes to the saturation of collectivity near midshell (where individual quadrupole p–n matrix elements vanish). The monopole component is, perhaps, even more crucial, and certainly less well known: depending on radial overlaps, it varies with the (nlj) single-particle quantum numbers of the interacting orbits and contributes effective shifts to their single-particle energies. These shifts can eradicate shell and subshell gaps, both for spherical and deformed shapes, and therefore, vitally affect the evolution of nuclear structure. An example is the A = 100 and 150 phase-transitional nuclei where the dynamics of the Z = 38 or 40 and Z = 64 gaps contributes to the sudden onset of deformation at N = 60 and to that at N = 90. This effect is particularly dramatic for the Sr isotopes where the onset of deformation is gradual below N = 50 but virtually instantaneous on the neutron-rich side at N = 60 [37]. Another example is the structure of the heavy N = Z nucleus ^{80}Zr which, despite having nucleon numbers of 40, is deformed rather than spherical in its ground state.

Unfortunately, the monopole p–n interaction matrix elements are not well known and it is not yet possible to account quantitatively for the known shifts of single-particle energies (e.g., the inversion of the neutron $2d_{5/2}$ and $1g_{7/2}$ orbits between Zr and Sn). Excellent empirical sets of two-body matrix elements are available for the 2s-1d shell in light nuclei but the reliability of such empirical sets falls off rapidly beyond the $1f_{7/2}$ shell. Partly, this is due to the lack of accessible nuclei where the appropriate combinations of proton and neutron single-particle states are available. As a specific example, the proton Z = 50–82 and neutron N = 82–126 shells have five and six orbits, respectively, and hence 30 two-body p–n T=0 matrix elements. However, since these shells tend to fill together near stability, empirical information is only available on the matrix elements between orbits occupying similar positions in each shell. Thus, for example, one can estimate the $\pi(2d_{5/2})$–$\nu(2f_{7/2})$ interaction, but not the $\pi(2d_{5/2})$–$\nu(3p_{1/2})$ or the $\pi(2d_{3/2})$–$\nu(2f_{7/2})$ interactions. Determination of the latter two interactions requires binding energies of the 0^+ ground states of even-even nuclei and single-particle energies in odd-mass nuclei that have, for example, two valence nucleons of one

type and many of the other (e.g., the neutron-rich Te, Z = 52, isotopes or the proton-rich N = 84 isotones). Such studies can revolutionize our knowledge of residual interactions. Combined with the capabilities of modern computers, this offers the hope that realistic *ab initio* microscopic nuclear-structure calculations in heavy nuclei may become possible for the first time.

Empirical p–n interactions of the last proton and last neutron may be estimated from double differences of binding energies of neighboring nuclei [26]. Figure 2 shows such empirical interactions for the ground states of even-even nuclei. The microstructure (see inset) reflects primarily the complementary contributions of the monopole and quadrupole components. In deformed nuclei, the behavior of the latter is usually understandable (at least qualitatively) in terms of the angular orientations of the respective Nilsson orbits. This gives the hope of another approach to extracting the monopole part. This is easiest in regions (near midshell) where the quadrupole component is small. However, to do this requires new data (binding energies) on such nuclei as ^{240}Cf, ^{244}Fm, ^{250}No, and ^{254}104, beyond point "A" in Fig. 2. A similar region may exist in the rare-earth region near N = 100, but it is less obvious empirically (region "B" in Fig. 2). Precise binding energies for such nuclei as ^{156,158}Er, $^{160-164}$Yb, ^{164,166}Hf, and ^{168}W, which should be accessible using RIBs, would be enormously useful. Indeed, measurement of these eight masses would immediately give p–n interactions in fourteen additional nuclei. Dysprosia–168,170 would fill in critical *lacunae* as well.

Lastly, it is known that T=0 p–n interactions in light N = Z nuclei are anomalously large (indeed, they appear as singularities in region "C" of Fig. 2), and also that they decrease in magnitude with increasing N or A. Shell-model calculations with realistic interactions reproduce this effect, as a consequence of the enhanced T = 0 matrix element in orbit combinations having high spatial symmetry that occur for N = Z. It will be especially interesting to extend such data (requiring sets of four adjacent masses) to still heavier N = Z regions where one might expect the spatial symmetry to be reduced due to the effects of the Coulomb force in altering the proton single-particle energies. Studies between Z = 40 and 50 would be particularly intriguing since ^{80}Zr has recently, and surprisingly (N,Z = 40 are often considered magic numbers), been discovered to be deformed [9] and ^{100}Sn is expected to be a good doubly-magic nucleus such as ^{208}Pb. With RIBs one can expect to form the entire N = Z sequence from ^{80}Zr to ^{100}Sn and perhaps beyond.

The overriding goal, which is now barely on the verge of achievement even in the phenomenological sense, is to achieve a truly unified macroscopic and

microscopic understanding of nuclear structure, collectivity, phase transitions, and deformation.

3.2 Access to New N,Z Combinations

Much of the discussion in the preceeding subsection, of course, relies on access to new regions of N and Z in the sense that the T = 1 and 0 residual interactions are dependent on the proton and neutron orbits; hence new effects and new information, often crucial not just incremental, can be obtained by extending the ranges of N and Z. Here we focus on different aspects of this, in particular on the interplay of single-particle and collective effects that may give rise, in uncharted nuclei, to new types of collective motion or shapes or to new examples of known types that will aid in an improved understanding of their structure and microscopic origins.

3.2.1 Neutron Halos and Skins

One of the most interesting and exotic new nuclear phenomena involves the concept of neutron skins or halos in extremely neutron-rich nuclei, such as ^{11}Li or ^{14}Be. Greatly-enhanced nuclear radii are observed for these cases [20,21] see Figure 3, where the last pair of neutrons is only barely bound. The opportunities for future studies here are many, ranging from the structure of the halos themselves to the exploitation of the loose binding and beta-decay lifetime of these nuclei in reactions, where such phenomena as neutron flow, large isospin transfer, and the like can be studied. The halo regions may be conceived of as an extremely low-density form of (neutron) nuclear matter. As such they are intermediate between free nucleons and normal-nuclear matter and one might think that they could provide a third regime in which to study nuclear interactions and medium modifications (e.g., EMC type effects). Clearly such experiments on halo nuclei will be extremely difficult at best, but measurements of, for example, the neutron magnetic moment in odd-neutron halo nuclei by laser spectroscopy, could be fascinating. The entire subject of neutron halos and skins is treated in greater detail in a separate chapter of this report [22].

3.2.2 New Collective Modes

Collective shapes are favored microscopically when single-particle orbits with that specific shape are occupied. Collective modes appear when orbits are occupied that have large matrix elements of the particular mode creation

operator with another nearby orbit. Therefore, access to new more exotic N,Z combinations affords the possibility to observe even more exotic shapes and collective excitations. Some of these, such as super and hyperdeformed shapes, which depend on large angular momentum for stability will be discussed in the next section.

Despite years of use of models of triaxial nuclei, there is essentially no firm evidence that nuclei exist with stable rigidly-asymmetric shapes [38]. Indeed, it is difficult to distinguish between stable triaxial shapes and fluctuations with respect to the triaxial (gamma) degree of freedom. Similarly, nuclei with oblate ground-state shapes are very few (e.g., some Pt and Au nuclei) and in those it also is likely that one is observing a gamma-soft configuration with a slightly oblate rms shape rather than a static oblate deformation.

Triaxial nuclei are likely to occur when the protons are filling prolate orbits and the neutrons oblate orbits or vice versa. In a Nilsson context these are, respectively, the downsloping and upsloping orbits that occur at the bottom or the top of a shell. In heavy nuclei examples of such "schizophrenic" nuclei are, therefore, to be sought in extremely neutron-poor or -rich species such as, isotopes of Hf – Pt nuclei with N $\approx$ 90 which could be produced with neutron deficient RIBs.

Oblate shapes occur when both protons and neutrons have nearly full shells. The Fermi surface then lies near highly oblate-driving orbits that cancel the normal prolate-driving preference that has been accumulated by the filled orbits. The oblate-prolate competition can often lead to two minima in the potential energy surface, one of each shape, and the nuclear ground state is then determined by rather subtle details. Coexistence is possible, as evidenced, for example, by nuclei with A $\approx$ 130 [39], as is gamma-softness (e.g., Pt, Au), if there is a path between the minima through the gamma plane. Interesting searches for oblate nuclei in the neutron deficient Se, Kr region, the light (N $<$ 82) Ba nuclei, and the light Au nuclei will again be facilitated by the use of fusion-evaporation reactions with neutron-deficient RIBs.

Of course, nuclear shape coexistence, just alluded to, is now known to be a widespread phenomena. Indeed the classic example is ^{152}Dy in which slightly-deformed oblate, "normally-deformed" prolate and superdeformed prolate states coexist at the same angular momentum [15,40]. Other beautiful examples of shape coexistence have been mapped out in the Pb, Tl, Hg region, down to neutron midshell (e.g., $^{182}Hg_{102}$ [41]) [see Figure 4]. The energy systematics of the intruding configuration shows a parabolic drop to-

wards midshell against N. This is consistent with the most popular interpretation of such states which predicts an energy minimum near midshell where the enhanced proton-neutron interaction in the intruder (particle-hole) excitation is a maximum. The Cd nuclei, known on both sides of neutron midshell, indeed suggest that the intruder energies rise roughly symmetrically about midshell. However, the absolute intruder excitation energies depend on the strength of the residual interaction relative to the energy gap that must be overcome and, in Cd, these energies happen to lie very close to the vibrational two-phonon states. While this gives a possibility to study the mixing of normal and intruder configurations, it also obscures the behavior of the latter. Therefore, a better testing ground would be even more neutron deficient-nuclei in the Hg region than can currently be populated. RIBs are crucial to further study of this issue. Another fascinating region centers on the N = 60 isotones near ^{100}Zr where the lowest known excited 0^+ states of any deformed nucleus have been discovered. The physics of intruder states is intimately linked with mechanisms for the onset of deformation and provides a unique view of those mechanisms.

In the last few years many examples of reflection-asymmetric nuclei [42] have been identified, usually by their signatures of parity-doublet rotational bands (0^+, 1^-, 2^+, 3^-, ... sequences, usually slightly displaced from each other), relatively enhanced E1 transitions and, in odd-mass nuclei, anomalous decoupling parameters. (An example [43] is shown in Figure 5.) Nevertheless, it remains an open question to what extent such fundamental shapes, which break an important spatial symmetry, are static or dynamic. Octupole shapes are expected in regions where both valence neutrons and protons filling the orbits of a "$\Delta l = 3$" pair (e.g., $\pi(2d_{5/2}$-$1h_{11/2})$ and $\nu(2f_{7/2}$-$1i_{13/2})$ in the rare earths). These orbits are strongly connected by the Y_3 operator. Octupole collective nuclei are known in the light Rn-Th region and in the rare earths near ^{146}Ba. With RIBs, other examples, in lighter nuclei, such as ^{90}Se and ^{94}Kr or their odd-mass neighbors, could be sought. Also, in many neutron-deficient nuclei formed in heavy-ion fusion-evaporation reactions, the low-j (especially the 3^-) states are not observed and therefore the octupole collectivity remains poorly established. Access to these nuclei by "softer" reactions using RIBs is an intriguing possibility. The light ($A \approx 120$) Xe, Te region would be especially interesting for such studies.

Higher moments in the nuclear shape, such as hexadecapole deformations, are also well established, especially in the stable W nuclei where diagonal Y_4 matrix elements among high-j, unique-parity, orbits are large. Hexadecapole vibrations are also a likely component of low-lying ($\approx$ 1 MeV)

K = 4 bands in Os. A positive ϵ_4 (barrel shape) is naturally expected when the configurations with the largest radii are filling mid-K Nilsson orbits. These orbits are oriented $\approx 45°$ relative to the nuclear equator and thus favor an infilling of nuclear matter in the "corners". Such shapes also should appear in lighter nuclei, for example, heavy Pd nuclei ($^{116-120}$Pd) which could be produced with very neutron rich RIBs or by fission of the heaviest actinides.

Finally, there are sporadic hints of even higher moments (e.g., β_5 and β_6 deformations [44]). Five-minus levels are often considered as rotational excitations built on lower-lying 3^- states. However, near the top of each shell in heavy nuclei, there is the possibility of a direct $\Delta l = 5$, two-quasiparticle, excitation, such as an $h_{11/2} \otimes s_{1/2}$, in the 50–82 shell. Indeed, the Te–Ba nuclei with N $\approx$ 70 have anomalously low 5^- states (relative to the 3^- states). In some cases even $E_x(5^-) < E_x(3^-)$. It is interesting to speculate whether the analogous $\Delta l = 5$ excitations in heavier nuclei, namely $i_{13/2} \otimes p_{3/2}$ and $j_{15/2} \otimes d_{5/2}$ in the 82–126 and 126–184 shells have sufficient degeneracy to allow the development of collective 5^- correlations. However, the present knowledge of 5^- states in the rare earth and actinide nuclei is limited, e.g. to Dy isotopes with A < 158, Ra with A $\leq$ 158, and Th with A $\leq$ 232, where the $i_{13/2}$ or $j_{15/2}$ are barely occupied. If substantially more neutron-rich Dy, Er, Ra, or Th nuclei could be studied using RIBs, this new collective mode might be disclosed.

The possibility of observing new collective modes or symmetries implies as well the likelihood of discovering new shape/phase transitional regions, or of extending existing ones. This is an attractive opportunity since, historically, more has probably been learned about (collective) nuclear structure, its manifestations and dynamics, from such regions than in any others. Recent work in the very neutron-deficient rare earth nuclei, especially the light Ce and Nd isotopes with A = 120–130, has provided evidence [45] for a new, gradual, spnerical to soft shape transition that has the earmarks of becoming stably-deformed for slightly-smaller neutron number. This region has only begun to be mapped out; the largest $E_x(4^+)/E_x(2^+)$ ratios in the region are still only $\approx$ 3.0, and the vibrational modes are as yet virtually unstudied). This region is interesting because its smooth evolution is in contrast with the sharp onset of deformation in the A = 100 and 150 mass regions. A thorough study, using proton-rich RIBs, will be helpful in understanding the mechanism for deformation and the interplay of the dynamics of the underlying single-particle structure and the collective correlations that develop.

Of course, one of the most exciting new regions centers on the heaviest known N = Z nuclei (discussed earlier in a different but related context). Zirconium-80 has recently been found [9] to be deformed despite having 40 protons and 40 neutrons (see Figure 6). Neighboring nuclei as well as the heavier N = Z species approaching ^{100}Sn will provide perhaps the most exciting opportunity yet to observe the evolution and coexistence of shapes and the persistence of magic numbers, since it is widely expected that the so far elusive ^{100}Sn will be doubly magic. Where, along the N = Z path, does the spherical configuration become the ground state? How stable are the 40 and 50 magic numbers? These are key questions at the heart of our understanding of shell and collective structure. Experimentally, these nuclei might be reachable with reactions on unstable, long-lived targets, such as ^{40}Ca + ^{56}Ni $\rightarrow$ ^{96}Cd* or ^{40}Ca + ^{44}Ti $\rightarrow$ ^{84}Mo*, or with neutron-deficient RIBs.

3.2.3 Other Issues

The Fermion Dynamical Symmetry Model [46] suggests sudden "breaks" in nuclear systematics (e.g., in the actinides when the normal-parity neutron shell is 1/3 filled) due to special Pauli effects. In simple terms, the filling of certain classes of states ultimately blocks some collective modes, causing others (in this scheme) to suddenly become the ground state. Concomitant effects in transition rates should accompany this phenomenon. The use of RIBs to establish either the existence, or the nonexistence, of such effects, for example in the neutron-rich actinides, could be a litmus test for these models.

Finally, other models, currently nearing the stage of practical calculations, attempt, for the first time, to encompass multi-$\hbar\omega$ spaces and to incorporate the collectivity of giant resonances and low-lying structures into a single unified framework, without effective charges [47]. The study of higher-spin states of stable nuclei (e.g., ^{168}Er), which is accessible with RIBs (see below), would provide the critical tests of these models.

3.3 Complete Spectroscopy and Chaos

The access to high decay energies far from stability allows numerous opportunities for extending spectroscopic studies as a function of N, Z, and E_x. Several of these possibilities have already been mentioned, e.g. the study of beta-delayed particle instability, cluster emission, and G-T quenching. How-

ever, one aspect of high decay energies remains to be considered: namely the possibility for "complete" spectroscopic studies [48]. This term refers to the experimental establishment of sets of levels, in certain ranges of excitation energy and spin, that are known to be essentially complete, and the further delineation of as many of their properties, e.g. decay routes, moments, lifetimes, etc., as possible. Such complete data not only provide the most strigent tests of nuclear models, they also provide a very detailed information base for a specific quantum system that can be utilized for understanding even more general physical ideas and for technical applications. A currently-fashionable example is analyses to determine whether nuclear levels are "ordered" or "chaotic."

3.3.1 Complete Spectroscopic Measurements

The classic tool for ensuring that the set of states populated is complete, only usable along the stability line, is the (n,γ) reaction, especially in the Average Resonance Capture (ARC) mode. However, other reactions, which feed the nucleus at suffiently-high excitations energies (temperatures) and which deexcitate statistically, also offer a virtual guarantee of completeness in the appropriate cases. One can cite, for example, the (n,n'γ) reaction for low-spin states, the ($\alpha, xn\gamma$) or (light heavy-ion,xnγ) reactions for intermediate spin states and (heavier heavy-ion,xnγ) reactions for still higher spins, as well as, to a lesser degree, beta-decay with extremely large Q_β values.

There are two conceptually-distinct areas of work here. One is the study of low-spin states very far from stability (primarily by beta decay), providing the first tests of nuclear models of, for example, collective modes, in such new N,Z regions. Perhaps even more intriguing is the opportunity to use neutron-rich RIBs to study high-spin states of stable or near-stable nuclei, in order to complement already existing, complete, low-spin data, and thereby, forging the first comprehensive links between high- and low-spin nuclear structure. Perhaps the best heavy case for this is ^{168}Er which is known, for I = 0–6, in an essentially complete form up to about 2 MeV. Here, the use of reactions, such as ^{130}Te(^{42}S,4n)^{168}Er, and/or ^{154}Sm(^{18}C,4n)^{168}Er, would provide a comparable completeness for high-spin levels and offer perhaps the only nucleus where the full panoply of nuclear structure models could be simultaneously tested. In general, low-spin data is abundant in rare earth nuclei near stability. Figure 7 shows the loci of nuclei that could be produced at high spin using RIBs with 6 neutrons beyond stability. Today's models aim at being more and more comprehensive but require correspondingly-

thorough data for their testing. This is not a program to be carried out on every possible nucleus, but as history has shown, such studies in isolated, well chosen, cases can be extremely valuable. Another example, this time an odd-mass nucleus, might be ^{109}Pd in which a nearly full set of unique-parity favored and unfavored anti-aligned states based on the $\nu(h_{11/2})$ orbit is known and where disclosure of the complementary aligned states would permit the best test to date of particle-rotor models.

3.3.2 Average Nuclear Properties

Complete spectroscopic data will provide a means of establishing average nuclear properties and thereby distinguishing these average properties from the "truely-novel" exceptions. For example, neither the low-lying collective states (the subject of much of the past two decades of low-spin experimental studies) nor the highly-aligned near-yrast high-spin states (likewise the main subject of the past two-decades of high-spin studies - see the following section) are representative of the average nuclear states. Both are strongly-populated in statistical reactions, hence available for study, because their special properties (correlations and the Coriolis force respectively) cause them to occur at low excitation energies. More complete data, however, will establish average quantities (e.g. level densities, transition rates, decay widths, ...) as a function of the experimentally accesible quantities N, Z, I, π, and E_x. Such information would be of considerable importance for a variety of applications.

3.3.3 Is the Nuclear Spectrum of States Ordered or Chaotic?

Finally, complete spectroscopy will provide a greatly-expanded opportunity to investigate seriously the issue of quantum chaos in nuclei [49]. Sufficient data exists to indicate that the spacing of nuclear states at the neutron and proton thresholds is describable by random-matrix theory [50], i.e. nuclei under these conditions are "chaotic." Yet special states (such as isobaric analogue states, molecular resonances, superdeformed states, very high-K states, ...) at the same excitation energy seem to remain "pure." They apparently do not mix with the background of strongly-mixed, "chaotic" states. Attempts at extending such analyses to lower excitation energies to study the temperature and angular-momentum dependence of the transition from ordered to chaotic systems have not been conclusive [51] because of the lack of complete nuclear data.

The description of the nuclear quantum system in terms of the currently-fashionable concept of "order" and/or "chaos" is by no means complete. Fundamental questions, such as: how the nuclear quantum system evolves from ordered to chaotic behavior, the coexistence of ordered and chaotic states, transition rates in chaotic systems, the role of symmetries in preserving order, more efficient (i.e. simpler) descriptions of chaotic quantal systems, and the relation between a chaotic nucleus and other chaotic quantal systems, remain to be answered. Detailed studies of nuclei like ^{26}Al [52] have already set the stage; however, complete data for selected nuclei sampling the variety of phenomena described in the previous sections are needed to answer the questions posed by this new approach to nuclear physics.

4 High-Spin Studies with Radioactive Ion Beams

The use of radioactive ion beams, not only will allow high-spin studies similar to those in vogue today (see e.g. [53,54]) to be extended to a wider range of nuclei testing our current understanding of rapidly-rotating nuclei, it also will allow new physical concepts to be studied. Some of these ideas are summarized in this section.

4.1 Exotic Nuclear Shapes at High Spin

The exotic equilibrium shapes, such as superdeformed (2:1 ratio of major to minor axis), octupole (pear-shaped), and triaxial that nuclei can assume in the extreme condition of rapid rotation are an excellent illustration of the intimate connection between independent-particle and collective degrees of freedom. Since these shapes depend on the details of the spectrum of single-particle quantum states, the greater variety of such states that nuclei at the limits of isospin will provide is desirable. The condition of minimum energy and the strong, attractive, short-ranged nuclear interactions tend to select "conventional" equilibrium shapes. By enlarging the variety of single-particle states by forming nuclei at the extremes of both isospin and angular momentum more exotic shapes become feasible. For example:

Superdeformed states occur [15] when large gaps (providing negative single-particle energy contributions) develop in the spectra of single-proton and single-neutron states for a 2:1 ratio of the major to minor axis. Calculations [55] indicate that such gaps occur in prolate nuclei for $Z \approx$14–17, 34, 39–42, 65–69, and 82–94 and $N \approx$ 30–47, 63–67, 78–92, 104–112, and 138–158. Superdeformed shapes already have been observed for (Z, N) =

(65–69,78–92), (82–94,104–112), and (82–94,138–158) corresponding to the ^{152}Dy region, the ^{192}Hg region, and the fission isomers, respectively [54]. The use of radioactive beams should provide other mass regions where both proton and neutron single-particle spectra favor superdeformed shapes, for example, (Z, N) = (65–69,63–67), (39–42,63–67), and (39–42,30–47), and extend the possible superdeformed studies in other regions only partly accessible to stable targets and beams.

Shell corrections also should occur for oblate superdeformed shapes (2:1 ratio of major to minor axis, but with two major axes *versus* one major axis for prolate superdeformed systems). As yet no oblate superdeformed nuclei have been identified. The nucleus ^{148}Sm, which is not accessible at high spin with (heavy-ion, xn) reactions using stable beams and targets, is predicted to be one of the most favorable cases for superdeformed oblate collective shapes.

Hyperdeformed equilibrium shapes (3:1 ratio of major to minor axes) also have been predicted, but not yet observed. The most favorable predicted [56] cases for experimental studies, rapidly-rotating nuclei near ^{166}Er, can only be populated at maximum angular momentum with radioactive ion beams. The increased neutron excess of this isotope relative to those accessible with the fusion-evaporation reaction using stable heavy-ion beams also increases the angular momentum that the compound system can accomodate and survive fission. Such an angular momentum increase is crucial for observing hyperdeformed states. The nucleus requires a great deal of angular momentum to stablize such enlongated nuclear shapes. Indeed the added angular momentum associated with the radioactive beams may be the difference between observing and not observing hyperdeformation.

4.2 Exotic Configurations Dominated by the Coriolis Force

Many of the current topics of high-spin physics (e.g. band crossings ("backbends"), loss of collectivity at high spin, and signature dependent energies and transition rates) are associated with high-j, low-Ω configurations that have a large projection of the intrinsic angular momentum, j_x, on the rotational axis. These phenomena are the result of modifications of the spectrum of single-particle states by the Coriolis plus centrifugal interaction leading to a term in the independent-particle hamiltonian equal to $-\omega j_x$. Configurations always exist in the next higher shell with even larger values of j_x. For prolate deformations these "exotic" configurations lie low in the higher shell. (For superdeformed and hyperdeformed systems they intrude into the

lower shell and are important components in producing the deformed shell gaps that lead to stability.) In a rapidly rotating system such orbits also can intrude into the lower shell for normal deformations. Anomalous moments of inertia [57] and band crossings [58] are associated with the few cases where such high-j_x intruders presently are observed in near transitional nuclei. Using neutron-rich radioactive beams, it should be possible to populate such configurations in stably-deformed nuclei testing whether the observed anomalies are associated with these orbits or the stability of the nuclear shape.

In the actinides such high-j_x intruders correspond to shell-model states from above the superheavy shell gaps, e.g. the $j_{15/2}$ proton state and the $k_{17/2}$ neutron state. The low-ω components of these configurations, which are predicted [59] to lie just above the Fermi level for the heaviest possible actinide targets (e.g. ^{248}Cm and ^{252}Cf), should become yrast at moderate spins, I =20–30. Because of Q-value considerations (see below) radioactive beams probably are necessary for the population of such states in Coulomb excitation plus transfer reactions.

4.3 Residual Proton–Neutron Interactions at High Spin

The major modifications of the single-particle quantal states at large angular momentum described in the preceeding paragraphs also will change the overlaps of the nucleonic orbitals thereby modifying the residual nucleon-nucleon interactions. Not only are the high–j, low–Ω orbitals most-strongly affected by the Coriolis and centrifugal forces, but they also are the most localized [60], and therefore, the most sensitive to residual interactions. Interesting attempts at extracting empirical estimates of such interactions are described in [60,61,62]. The possibility of studying even higher–j, low–Ω intruder orbitals using RIBs, as described in the preceeding subsection, should allow even more exotic nucleon-nucleon interactions to be studied as a function of rotation.

In the limit of very large angular momentum, where the single-particle structure of the nucleus is dominated by Coriolis and centrifugal forces, the occupation of configurations associated with nucleons moving in equatorial orbitals in the direction of the nuclear rotation is increased [60]. Such orbitals have large spatial overlap. This is a necessary, though not sufficient, condition for a new type of correlation that might be termed "Coriolis correlations." The increased localization associated with the various substates of the even higher-j "intruder" orbitals that should be available in selected

nuclei that can be populated with RIBs (see the preceeding paragraph) will enhance this possible new type of collectivity.

Residual p–n interactions also can affect the alignment of angular momenta with the rotational axis, and hence band crossings [63]. As with all residual p–n interactions such phenomena are largest where the protons and neutrons are filling, not only the same shell, but also similar orbits of the same shell. Therefore, these effects, which to date have been largely negelected will be largest in those neutron-defficient, deformed nuclei with $N \approx Z$ that can be studied using neutron-deficient RIBs.

4.4 Transfer Reactions

Many of the possibilities of using heavy-ion transfer reactions, for example, to populate neutron-rich nuclei or the high-spin states based on intruder orbits originating from above the superheavy shell, as described in the preceeding subsections, are limited by the reaction mechanism. Heavy-ion induced transfer reaction cross sections are strongly Q–value dependent. Positive Q values enhance such cross sections. This is especially true for proton transfer reactions. Unfortunately the decrease in the binding energy curve for $A > 56$ leads to negative relative binding in the target for stripping reactions and hence requires projectiles with very weakly-bound protons or neutrons to compensate. For example, heavy-ion beams with a single proton or neutron outside a doubly-closed shell are desirable for single-proton and single-neutron transfer reactions. However, except for light heavy ions, such as ^{17}O (and ^{209}Bi in which the proton remains quite strongly-bound) these nuclides are not stable. ^{37}S and ^{49}Ca seem ideal for single-neutron transfer, and ^{38}S and ^{50}Ca are interesting beams for two-neutron stripping. Likewise, ^{41}Sc and ^{57}Cu beams are optimal for single-proton stripping as is ^{42}Ti for two-proton stripping. It is emphasized that transfer reactions and Coulomb excitation are the most efficient methods of populating the actinides at high spin, since the dominant decay of the highly-excited actinide residues of the heavy-ion fusion reaction is fission.

4.5 Coulomb Excitation of Exotic Radioactive Beams

It would be possible to determine the magnitude of the quadrupole moment of any RIB nuclei by Coulomb exciting the beam nuclei using, for example, a ^{208}Pb target. This technique would be important in exploring the new shell closures, transitional nuclei, and regions of deformation described elsewhere

in this report. It also would allow the first comparison of transition rates obtained from Coulomb excitation and Doppler-shift lifetime measurement based on (heavy-ion,xn) reactions.

5 Summary

This report outlines some of the nuclear structure topics discussed at the Los Alamos Workshop on the Science of Intense Radioactive Ion Beams. In it we also have tried to convey some of the excitment of the participants for utilizing RIBs in their future research. The introduction of radioactive beams promises to be a major milestone for nuclear structure perhaps even more important than the last such advance in beams based on the advent of heavy-ion accelerators in the 1960's. RIBs not only will allow a vast number of new nuclei to be studied at the extremes of isospin, but the variety of combinations of exotic proton and neutron configurations should lead to entirely new phenomena. A number of these intriguing new studies and the profound consequences that they promise for understanding the structure of the atomic nucleus, nature's only many-body, strongly-inteacting quantum system, are discussed in the preceeding sections. However, as with any scientific frontier, the most interesting phenomena probably will be those that are not anticipated—they will be truly new.

References

[1] Brookhaven National Laboratory, Upton, N.Y. Brookhaven National Laboratory is operated by the Associated Universities for the U.S. Department of Energy. Work supported under Contract No. DE-AC02-76CH00016.

[2] Oak Ridge National Laboratory, Oak Ridge, TN. Oak Ridge National Laboratory is operated by Martin Marietta Energy Systems Inc. for the U.S. Department of Energy under Contract No. DE-AC05-850R21400.

[3] Treatise on Heavy-Ion Science, Volume VIII — Nuclei Far From Stability, ed. D.A. Bromley (Plenum, 1989, New York).

[4] C. Detraz and D. Vieria, Ann. Rev. Nucl. Sci. 39 (1989) 407.

[5] Proceedings of Fifth International Conference on Nuclei far From Stability, AIP Conf. Series Number 164, ed. I.S. Towner (AIP, 1988, New York).

[6] Proceeding of the First International Conference on Radioactive Nuclear Beams (World Scientific, 1990, Singapore).

[7] M. Ogawa, *et al.*, Phys. Rev. Lett. 41 (1978) 289.

[8] C. Thibault, *et al.*, Phys. Rev. C12 (1975) 644; X. Campi, et al., Nucl. Phys. A251 (1975) 193; and C. Detraz, in Proc. Fourth Int'l. Conf. on Nuclei Far from Stability, Helsingor, 1981, eds. P.G. Hansen and O.B. Nielsen,CERN Rep. 81-09 (CERN, 1981, Geneve) p.361.

[9] C.J. Lister, *et al.*, Phys. Rev. Lett. 59 (1987) 1270.

[10] E. Cheifetz, R.C. Jared, S.G. Thompson and J.B. Wilhelmy, Phys. Rev. Lett. 25 (1970) 38.

[11] S.W. Yates and R.A. Meyer, Phys. Rev. C33 (1986) 1843.

[12] P. Federman and S. Pittel, Phys. Lett. 69B (1977) 385; and 77B (1978) 29.

[13] H.J. Rose and G.A. Jones, Nature 307 (1984) 245; D.V. Alexandrov, *et al.*, Zh. Exp. Theo. Fiz. 40 (1984) 152, JETP Lett. 40 (1984) 909; S. Gales, *et al.*, Phys. Rev. Lett. 53 (1984) 759; P.B. Price, *et al.*, Phys. Rev. Lett. 54 (1985) 297; W. Kutschera, *et al.*, Phys. Rev. C32 (1985) 2036; Barwick, *et al.*, Phys. Rev. C31 (1985) 1984; and M. Paul, *et al.*, Phys. Rev. C34 (1986) 1980.

[14] J.P. Balagna, *et al.*, Phys. Rev. Lett. 26 (1971) 145; see also D.C. Hoffman, *et al.*, Phys. Rev. C 21 (1980) 972; and E.K. Hulet, *et al.*, Phys. Rev. Lett. 56 (1986) 313.

[15] P.J. Twin, *et al.*, Phys. Rev. Lett., 57 (1986) 811.

[16] T. Byrski, *et al.*, Phys. Rev. Lett., 64 (1990) 1650; and W. Nazarewicz, P.J. Twin, P. Fallon, and J.D. Garrett, *ibid.* pg. 1654.

[17] S.G. Nilsson, *et al.*, Nucl. Phys. A131 (1969) 1.

[18] P. Möller, G.A. Leander, and J.R. Nix, Z. Phys A323 (1986) 41; and K. Böning, Z. Patyk, A. Sobiczewski, and S. Cwiok, Z. Phys. A325 (1986) 479.

[19] P. Möller, J.R. Nix, and W.J. Swiatecki, Nucl. Phys. A492 (1989) 349.

[20] I. Tanihata, *et al.*, Phys. Letts, 160B (1985) 380; Phys. Rev. Lett. 55 (1985) 2676; and Phys. Lett. 206B (1988) 592.

[21] I. Tanihata, in Proc. of Conf. on Nuclear Structure in the Nineties, ed. N.R. Johnson, Nucl. Phys. A, in press.

[22] See W. Bauer, Cont. in these Proceedings; and refs. therein.

[23] W. Myers, in Proc. of First Int'l. Conf. on Radioactive Nuclear Beams (World Scientific, 1990, Singapore), in press.

[24] See, e.g., B. Frois, in Nuclear Structure 1985, ed., R. Broglia, G. Hagemann, B. Herskind (North Holland, 1985, Amsterdam) p.25.

[25] J. Decharge and D. Gogny, Phys. Rev. C21 (1980) 1568; and J.W. Negele, Rev. Mod. Phys. 54 (1982) 913.

[26] D.S. Brenner, C. Wesselborg, R.F. Casten, D.D. Warner, and J.-Y. Zhang, Phys. Lett. B, in press.

[27] E.K. Warburton, J.A. Becker, and B.A. Brown, Phys. Rev. C41 (1990) 1147; C. Thibault, *et al.*, Phys. Rev. C12 (1975) 644; and C. Detraz, *et al.*, Nucl. Phys. A394 (1983) 378.

[28] I.S. Towner, in Nuclei Far from Stability, ed. I.S. Towner, AIP Conf. Proc. 164 (AIP, 1988, New York) p. 593.

[29] V. Trimble, Rev. Mod. Phys. 47 (1975) 877; and G.J. Mathews and R.A. Ward, Rep. Prog. Phys. 48 (1985) 1371.

[30] E.W. Otten, in Treatise on Heavy-Ion Science, ed D.A. Bromley (Plenum, 1989, New York) vol VIII, p. 515.

[31] K.-R. Anton, *et al.*, Phys. Rev. Lett. 40 (1978) 642.

[32] G.D. Sprouse, *et al.*, Phys. Rev. Lett. 53 (1989) 1463.

[33] J.A. Bounds, *et al.*, Phys. Rev C36 (1987) 2560; G. Ulm, *et al.*, Z. Phys. A325 (1986) 247; U. Krönert, *et al.*, Z. Phys. A331 (1988) 521; J.K.P. Lee, *et al.*, Phys. Rev. C38 (1988) 2985; H.T. Duong, *et al.*, Phys. Lett. B217 (1989) 401; and Th. Hilberath, *et al.*, Z. Phys. A332 (1989) 107.

[34] G. Huber, in The Variety of Nuclear Shapes, ed. J.D. Garrett, *et al.*. (World Scientific, 1988, Singapore).

[35] X.L. Tu, X.G. Zhou, D.J. Vieira, J.M. Wouthers, Z.Y. Zhou, M.L. Seifert, and V.G. Lind, Z. Phys. A, in press.

[36] I. Talmi, Rev. Mod. Phys. 34 (1962) 704; and K. Heyde, Int. J. Mod. Phys. A4 (1989) 2063.

[37] F. Wohn, *et al.*, to be published.

[38] I. Hamamoto, in Microscopic Model in Nuclear Structure Physics, ed. M.W. Guidry, *et al.*(World Scientific, 1989, Singapore) p. 173.

[39] E.S. Paul, *et al.*, Phys. Rev. Lett 58 (1987) 984; and M.J. Godfrey, *et al.*, J. Phys. G 15 (1989) 671.

[40] B.M. Nyako, *et al.*, Phys. Rev. Lett. 56 (1986) 2680.

[41] P. Van Duppen, E. Coenen, K. Deneffe, M. Huyse, and J.L. Wood, Phys. Lett. 154B (1985) 354.

[42] G.A. Leander and Y.S. Chen, Phys. Rev. C37 (1988) 2744.

[43] M. Dahlinger, *et al.*, Nucl. Phys. A484 (1988) 337.

[44] P.D. Cottle, *et al.*, Phys. Rev. C, in press.

[45] B.J. Varley, *et al.*, in Capture Gamma-Ray Spectroscopy and Related Topics- 1989, ed. S. Raman, AIP Conf. Proc. 125 (AIP, 1984, New York) p. 709.

[46] C.L. Wu, *et al.*, Phys. Lett. 168B (1986) 213; and M. Guidry in Proc. of the Sym. on Exotic Spectroscopy, ed. W. McHarris (American Chemical Society, 1990), in press.

[47] O. Castanos and J.P. Draayer, Nucl. Phys. A491 (1989) 349.

[48] R.F. Casten, D.D. Warner, M.L. Stelts, and W.F. Davidson, Phys. Rev. Lett. 45 (1980) 1077; and J.D. Garrett, in Proc. Workshop on Nucl. Struct. in the Era of New Spectroscopy, Part B—The Nucleus at High Spin (Niels Bohr Inst., 1989, Copenhagen) pg. 159.

[49] O. Bohigas and H.A. Weidenmuller, Ann. Rev. Nucl. Part. Sci. 38 (1988) 421; and W.J. Swiatecki, Nucl. Phys. A488 (1988) 375c.

[50] R.V. Haq, A. Pandey, and O. Bohigas, Phys. Rev. Lett. 48 (1982) 1986.

[51] T. von Egidy, H.H. Schmidt, and A.N. Behkami, Nucl. Phys. A481 (1988) 189; and J.D. Garrett and J.M. Espino, in Nuclear Structure in the Nineties, ed. N.R. Johnson (ORNL, 1990, Oak Ridge) pg. 126.

[52] G.E. Mitchell, *et al.*, Phys. Rev. Lett. 61 (1988) 1473; and J.F. Shriner, Jr., *et al.*, Phys. Rev. C, in press.

[53] GAMMASPHERE Proposal, eds. M.A. Deleplanque and R.M. Diamond, (1988).

[54] Proceedings of the Conference on Nuclear Stucture in the Nineties, ed. N.R. Johnson, Nucl. Phys. A, in press.

[55] T. Bengtsson, M.E. Faber, G. Leander, P. Möller, M. Ploszajczak, I. Ragnarsson, and S. Åberg, Physica Scripta 24 (1981) 200.

[56] J. Dudek, T. Warner, and L.L. Riedinger, Phys. Lett. B211 (1988) 252.

[57] B. Cederwall, *et al.*, Phys. Lett. B, in press.

[58] See e.g., C.-H. Yu, *et al.*, Nucl. Phys. A511 (1990) 157.

[59] J.B. Wilhelmy, R.R. Chasman, A.M. Friedman, and I. Ahmad, in Opportunities

[60] J.D. Garrett, J. Nyberg, C.Y. Yu, J.M. Espino, and M.J. Godfrey, in Contemporary Topics in Nuclear Structure Physics, ed. R. Casten, *et al.*(World Scientific, 1988, Singapore) p. 699.

[61] S. Frauendorf, *et al.*, Nucl. Phys. A431 (1984) 511.

[62] J. Y. Zhang, *et al.*, in Proc. of the Conf. on Nuclear Structure in the Nineties, ed. N.R. Johnson, Nucl. Phys. A (1990), in press.

[63] J.A. Sheikh, N. Rowley, and M.A. Nagarajan, Phys. Lett. B240 (1990) 11; and Phys. Rev. Lett., in press.

Figure Captions:

Figure 1. Potential energy contours as a function of r, the distance between the mass centers, and σ, the fragment elongation, for $^{252}Cf_{154}$, middle portion, and $^{258}Fm_{158}$, lower portion. The family of shapes considered are shown as a function of r and σ in the upper portion of the figure. The two fission paths are illustrated by the arrows superimposed in the lower-portion of the figure. For further details see [19].

Figure 2. The empirical residual interactions, δV_{pn}, extracted from double differences of the ground-state binding energies in neighboring even-even isotopes and isotones, see [26], are shown as a function of the number of neutrons. The inset gives an expanded view for N = 40–160. The portions of the curve labelled "A", "B", and "C" are discussed explicitly in the text.

Figure 3. Measured interaction radii, R_I, of neutron-rich isotopes of He, Li, Be, B, and C as a function of A. Note the striking deviation of r_I from 1.18 $A^{1/3}$ for ^{11}Li, ^{11,12,14}Be, and perhaps ^{17}B. See ref. [21], the source of this figure, for reference to the original data.

Figure 4. Plot of the excitation energy of the intruding coexisting deformed states in the isotopes of Tl, Pb, and Bi. See ref. [41], the source of this figure, for reference to the original data.

Figure 5. Partial level scheme for the nucleus $^{223}Th_{133}$ [43] showing two "parity-doublet" rotational sequences, connected by enhanced E1 transitions, characteristic of stable octupole deformations.

Figure 6. Low-lying level schemes [9] of self-conjugate nuclei $^{76}Sr_{38}$ and $^{80}Zr_{40}$, indicating the rotational behavior of these nuclei, $E_x(4^+)/E_x(2^+) \approx 2.85$ for both nuclei.

Figure 7. Comparison of stable nuclei (circles) and all the nuclei (squares) that can be populated as compound nuclei using heavy-ion fusion reactions on stable targets and with beams of $Z \geq 13$ and six neutrons beyond the heaviest stable isotope. Note that even allowing for the emission of 4-5 neutrons in the (H.I., xn) reaction, it is possible to overlap low-spin studies near stabil ty and high-spin studies populated using (H.I.,xn) in the same nuclei.

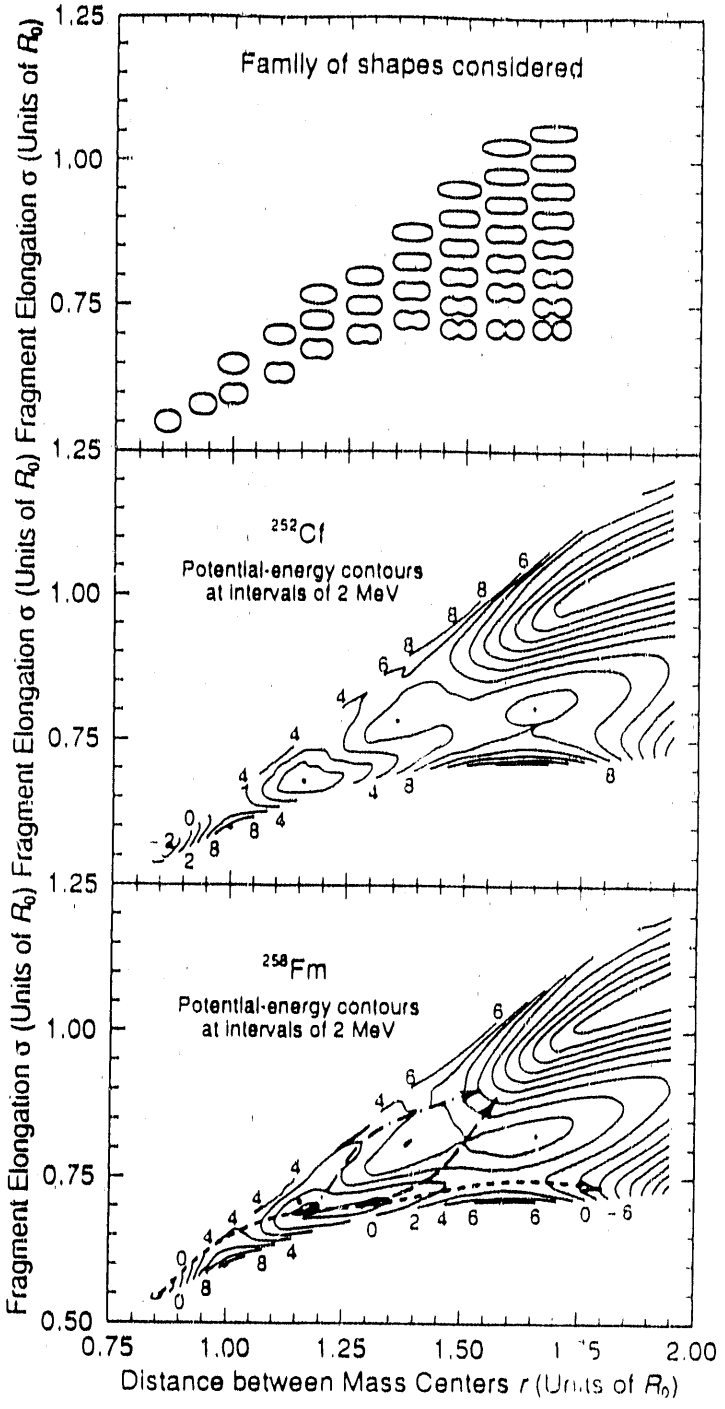
Family of shapes considered
^{252}Cf
Potential-energy contours
at intervals of 2 MeV
^{258}Fm
Potential-energy contours
at intervals of 2 MeV
Fragment Elongation σ (Units of R_0)
Distance between Mass Centers r (Units of R_0)
1.25
1.00
0.75
0.50
0.75
1.00
1.25
1.50
2.00

FIGURE 1

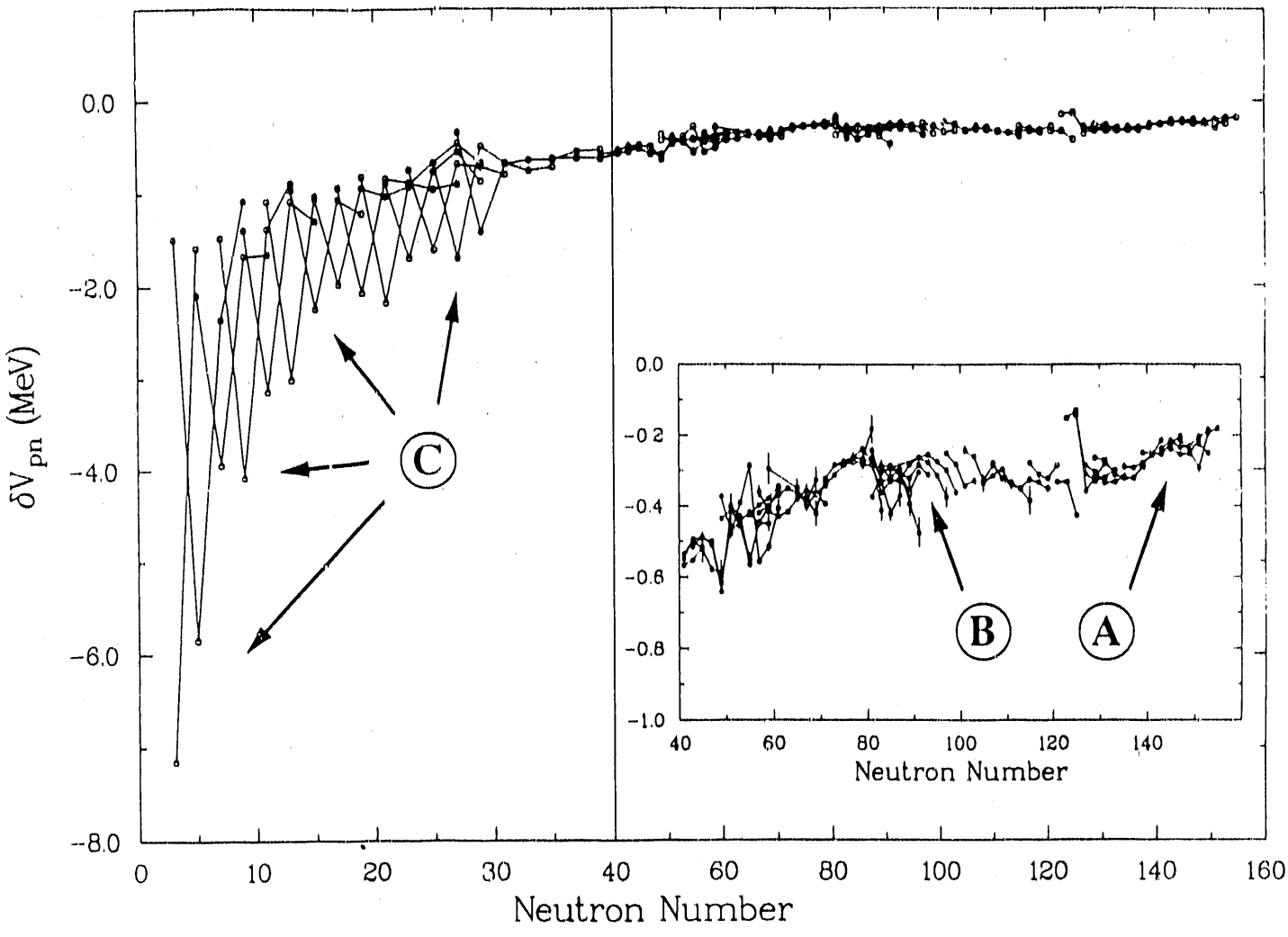
0.0
-2.0
-4.0
-6.0
-8.0
δV_{pn} (MeV)
0
10
20
30
40
60
80
100
120
140
160
Neutron Number
C
0.0
-0.2
-0.4
-0.6
-0.8
-1.0
40
60
80
100
120
140
Neutron Number
B
A

FIGURE 2

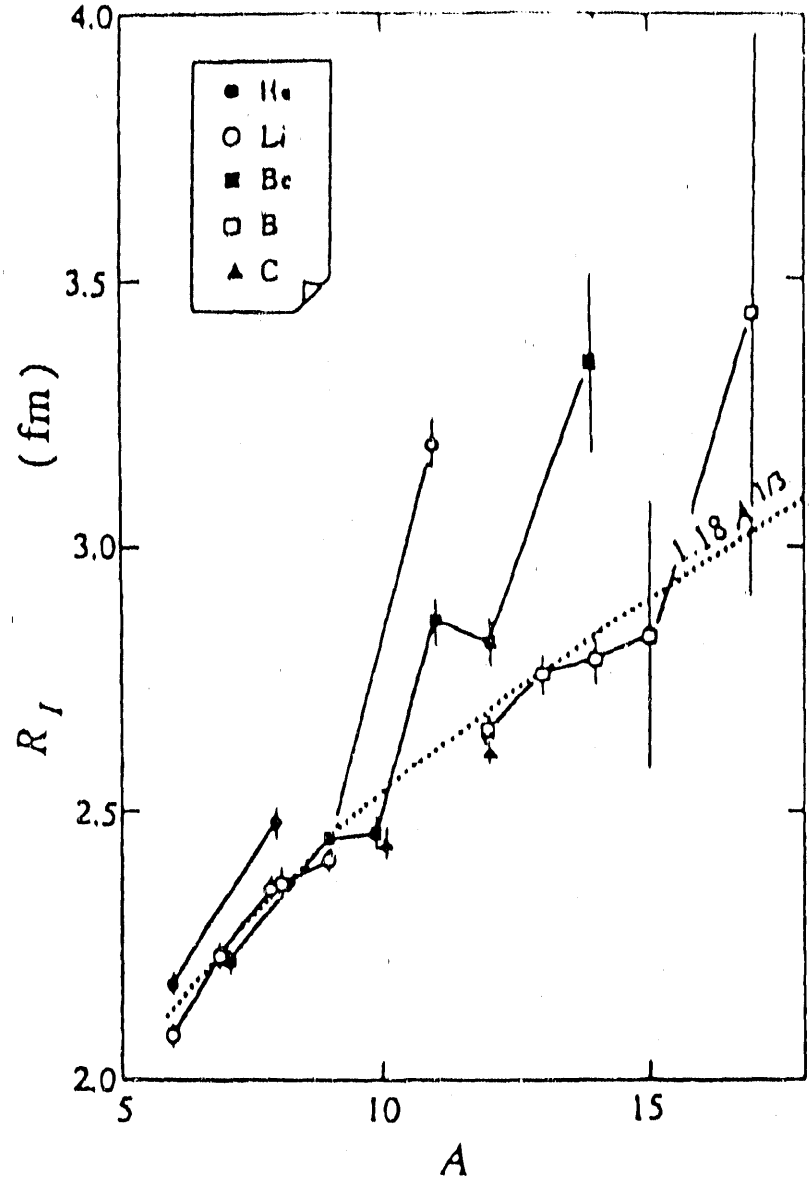

FIGURE 3

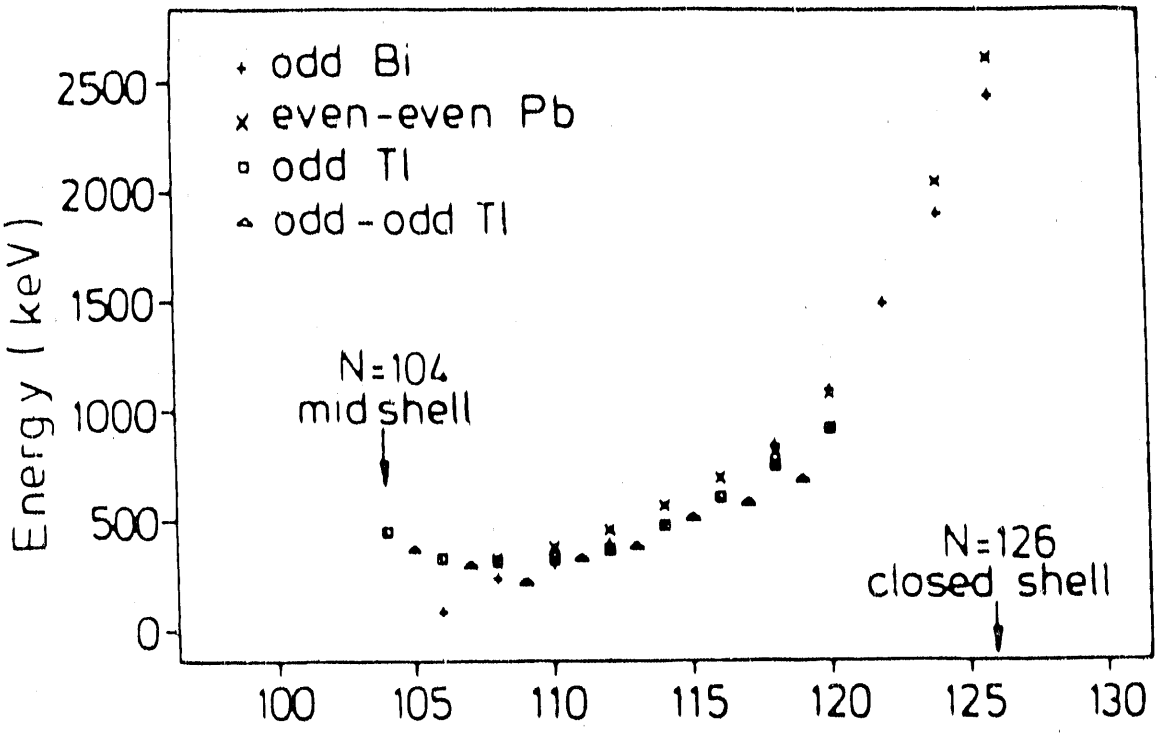
odd Bi
even-even Pb
odd Tl
odd-odd Tl
Energy (keV)
2500
2000
1500
1000
500
0
N=104
mid shell
N=126
closed shell
100
105
110
115
120
125
130

FIGURE 4

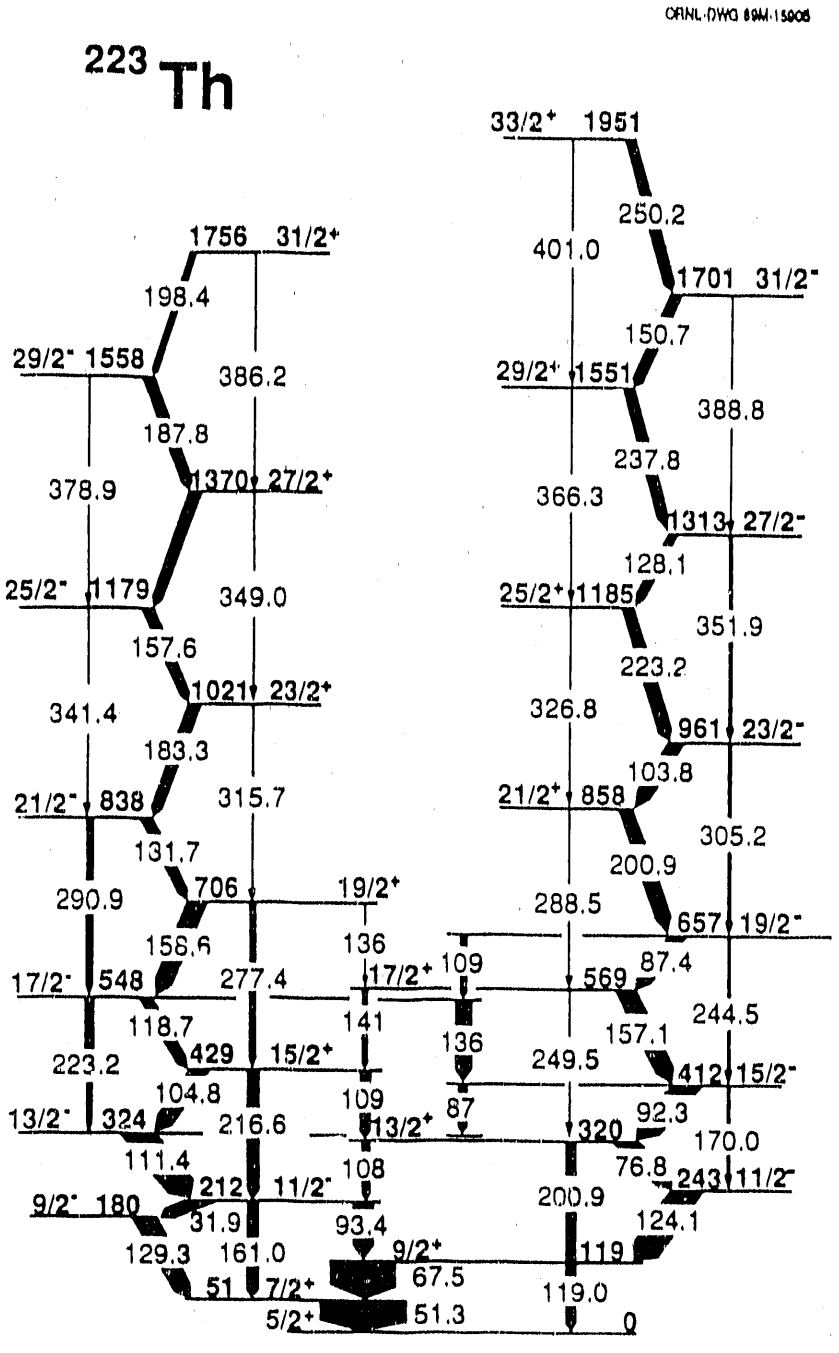
ORNL-DWG 89M-15905
223 Th
33/2+ 1951
250.2
401.0
1701 31/2-
150.7
29/2+ 1551
388.8
237.8
366.3
1313 27/2-
128.1
25/2+ 1185
351.9
223.2
326.8
961 23/2-
103.8
21/2+ 858
305.2
200.9
288.5
657 19/2-
87.4
569
244.5
157.1
249.5
412 15/2-
92.3
320
170.0
76.8
243 11/2-
200.9
124.1
119
119.0
0
1756 31/2+
198.4
29/2- 1558
386.2
187.8
378.9
1370 27/2+
349.0
25/2- 1179
157.6
341.4
1021 23/2+
183.3
21/2- 838
315.7
131.7
290.9
706 19/2+
158.6
136
17/2- 548
277.4
17/2+
109
118.7
141
136
223.2
429 15/2+
104.8
109
87
13/2- 324
216.6
13/2+
111.4
108
9/2- 180
212 11/2-
31.9
93.4
129.3
161.0
9/2+
67.5
51
7/2+
5/2+
51.3

FIGURE 5

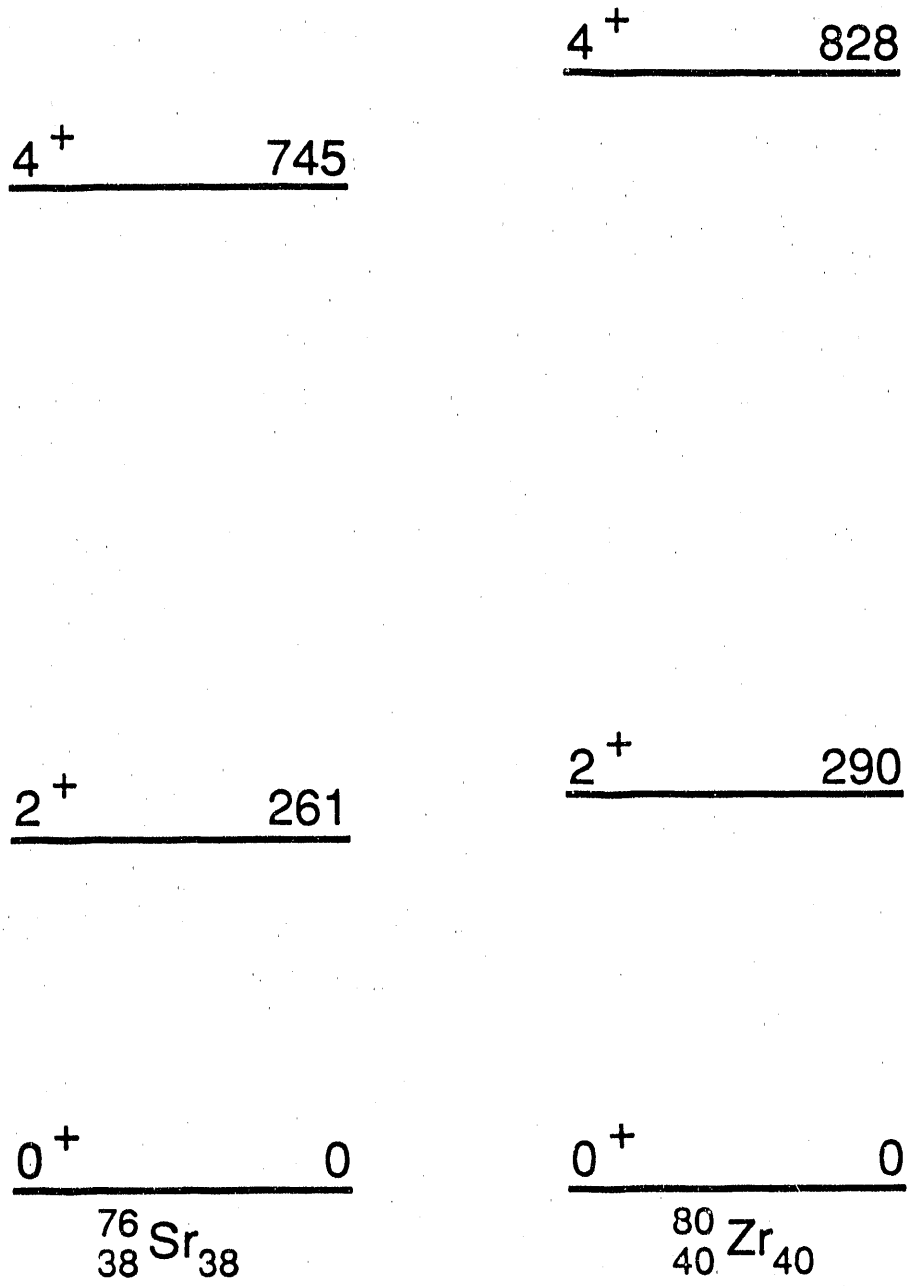

FIGURE 6

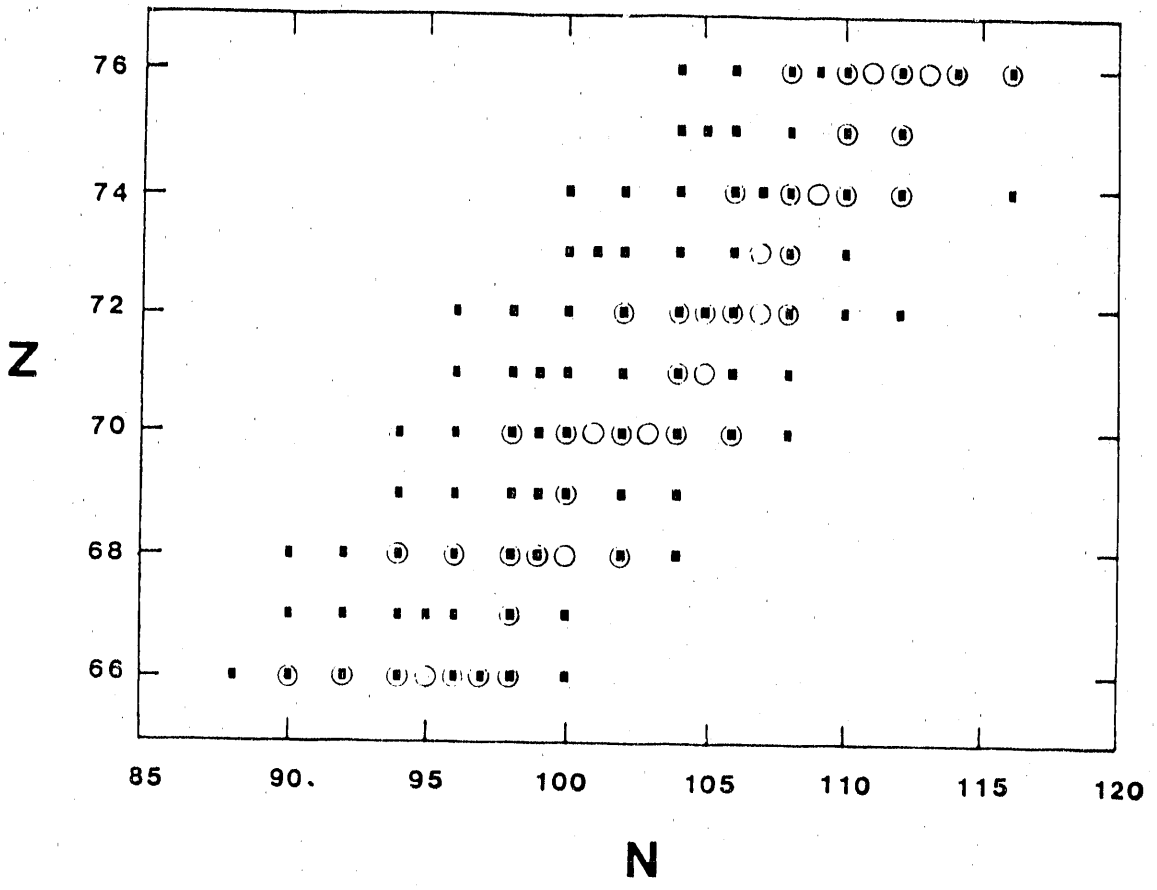

FIGURE 7

Position Paper on Neutron Halos and Drip Line Exotica

"At the Edge of Neutron Matter"

(Note: At the time of this workshop, it was felt that this paper should be written to combine material discussed in both Working Groups 1 and 2 to highlight this important aspect of a radioactive beam facility.)

W. Bauer[1], Chairman
D.J. Vieira[2], Coordinator

Contributions by: W. Bauer, G.F. Bertsch, F. Becchetti, B.A. Brown, A.C. Hayes, W.D. Myers, J.R. Nix, P.L. Reeder, D.D. Strottman, R.G. Stokstad, A. Sustich, D.J. Vieira, C.C. Villari

1. Introduction

Neutron matter exists in the cosmos in the form of neutron stars. It is kept stable by the interplay between the attractive gravitational interaction and the repulsive electromagnetic interaction which allows only very small proton admixtures. The minimum mass required for the gravitational interaction to become comparable to the nuclear interaction is approximately 1/10 of the mass of the sun. Therefore we cannot reproduce this state of matter in any laboratory on earth.

However, we can approach the edge of neutron matter by studying the properties of nuclear matter at the limits of neutron-stable nuclei. These nuclei are the last particle- stable nuclides and are located at the neutron "drip-line" - beyond which additional neutrons instantly break away. The large neutron excesses available in these nuclei will enable us to extrapolate to the neutron matter limit by studying their properties.

Radioactive ion beam facilities allow studies of these nuclei with the highest ratios of neutrons to protons achievable in the laboratory and thus

[1]NSCL, Michigan State University, East Lansing, MI 48824-1321
[2]LAMPF, Los Alamos National Laboratory, Los Alamos, NM 87545

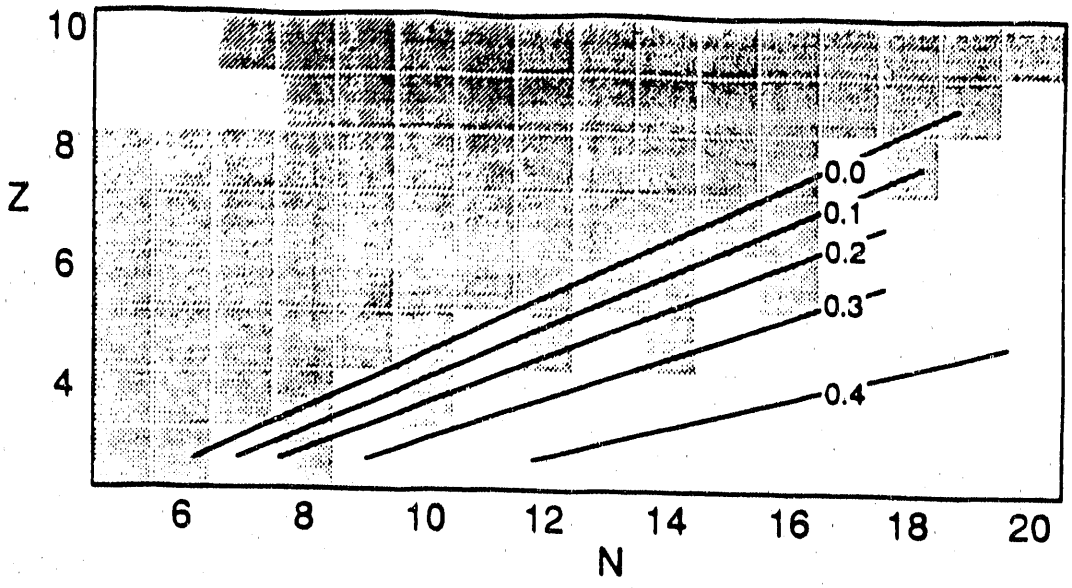

Figure 1: A portion of the nuclide chart showing as grey squares nuclei that are known to be stable against particle emission. The solid lines correspond to the predicted limits of stability for different values of a parameter r which determines by how much nuclear matter is unbound (taken from [1]).

provide the best data for extrapolations to the properties of neutron matter. In addition, neutron-rich nuclides near the drip line have unique structure and decay modes which extend our understanding of more normal nuclear matter.

2. Binding Energy of Neutron Matter

If neutron matter were bound, nuclear physics would be enriched by amazing structures. These structures, with life times limited only by beta decay, would include neutron balls of arbitrary size. Since the neutrons have no electrostatic repulsion from each other, the fission and alpha decay

channels would be closed to these neutron balls. Thus, their lifetime would not be limited by these strong processes, which proceed on a relatively fast time scale, and which constitute the main limitations on the life times of heavy chunks of normal nuclear matter.

These neutron balls might contain clusters of protons, with topologies not necessarily those of a single sphere, e.g. two or more fragments held apart by their Coulomb repulsion, or a hollow proton bubble filled with neutrons.

Since all searches for small bound clusters of neutrons have turned out negative thus far, we presently have to conclude that neutron matter is unbound in the absence of sizeable contributions of the gravitational interaction to the binding. However, it has to be stressed that we do not know exactly by how much neutron matter is unbound. This is, because we have no strict limits on the minimum size of neutron matter clusters from direct experimental observations. All of our knowledge is based on theoretical extrapolations from bound finite nuclei.

If neutron matter is only slightly unbound, we might expect to see precursors of such exotic neutron matter effects in phenomena that are observable at the neutron drip lines. The best way to proceed is to study nuclei with the largest possible neutron excess, both light and heavy nuclei, since even if bulk neutron matter were bound, small neutron balls would tend to be destabilized by their surface energy. Neutron matter is unbound and the maximum neutron excess for a given Z is limited by neutron drip. The actual location of the limit of stability is determined by the stiffness of the neutron matter equation of state [1] (compare Fig. 1).

One also expects the energy of the Giant Dipole Resonance to drop off at the limit of stability because the restoring force which comes mainly from the surface, will be affected by the neutron excess. It should also be mentioned that both the location of the limit of stability and the Giant Resonance energies are expected to depend on the overall excitation of the nucleus. Consequently, it may be possible to determine some of the temperature dependence of the nuclear equation of state.

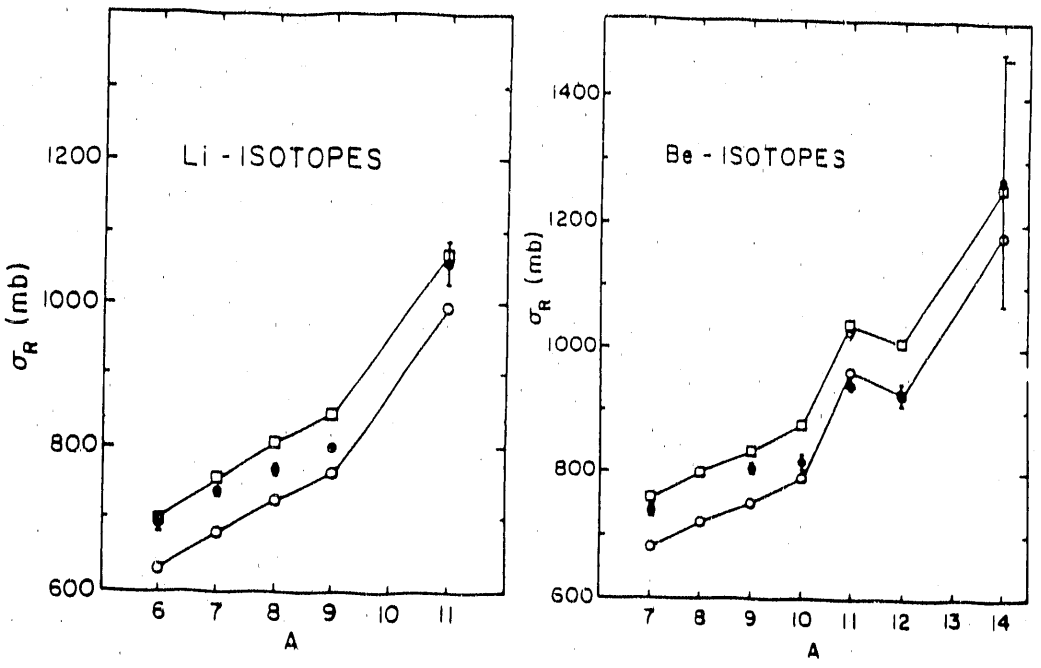

Figure 2: Reaction cross sections for Li and Be isotopes on a ^{12}C target. Filled symbols are the data (taken from [2]), and the solid lines and open squares (circles) are the results of calculations with finite (zero) range interactions (taken from [6]).

3. Microscopic Nuclear Properties: Neutron Halos

Beyond these macroscopic considerations there are significant opportunities for advancing our understanding of microscopic nuclear properties that also occur at the drip lines. The very last member of each isotopic sequence as we reach the limit of stability will be weakly bound. Due to this small binding energy and the Heisenberg uncertainty principle, the tail of the wave function is expected to extend far out beyond the normal nuclear matter radius obtained from an $A^{1/3}$ parametrization. This effect has already been seen in ^{11}Li and ^{14}Be [2,3,4] (see Fig. 2).

While there is nothing surprising in the increased reaction cross sections these nuclei have associated with their larger spatial extend, what is surprising is the fact that all Shell Model and Hartree-Fock calculations have

so far not quite succeeded to describe the properties of these nuclei. As a testing ground for established calculational approaches this has to be one of the best.

The effect of large neutron excess can most easily be seen among low Z elements. For example, modifications of the neutron density distributions can be observed by looking at elastic and inelastic scattering of all the Li isotopes from ^{8}Li to ^{11}Li. Our present understanding of ^{11}Li is that of a ^{9}Li core with 2 neutrons located predominantly in an extended surface region. These two neutrons are in essence responsible for the very large reaction cross section experimentally observed for ^{11}Li.

Similar neutron density trends can be studied by scattering experiments on boron isotopes from mass 8 to 19.

4. Nuclear Structure Physics with Neutron Halos

Because of this configuration of two neutrons interacting with each other and with the core, there exists the possibility of studying 3-body correlations in nuclear matter in an unusually clean manner.

Elastic and inelastic reactions at high beam energies can be used to establish the diffuseness of the neutron skin.

With radioactive ion beams, one can study neutron halos via sub-barrier transfer reactions such as (^{11}Li, ^{9}Li), (^{11}Li, ^{10}Li), etc. Important information will come from measurements of double differential cross sections as a function of beam energy and scattering angle. Such measurements also investigate the quantum mechanical nature of the neutrons in the halo, e.g. the important single particle configurations in the tail. One also can study a few excited states in these drip-line nuclides.

By using beams of these exotic nuclides, one can induce reactions to produce other unbound exotic nuclei such as (^{11}Li, ^{10}He), (^{11}Li, ^{10}Li), etc.

These exotic nuclides with neutron halos may lead to very cold fusion reactions via sub-barrier fusion. The neutron tails will give an assist to such reactions, because the neutrons in the halo are not subject to the

Coulomb interaction which is the major limiting factor in obtaining cold fusion reactions with normal nuclei.

The structure of ^{11}Li is of particular interest because of its unusually large ratio of neutrons to protons (8/3=2.67) and because of its unusually small binding energy. Existing measurements of the total reaction cross section for ^{11}Li and other neutron-rich light-mass nuclei have given the evidence for large matter radii [2]. No Hartree-Fock type calculation currently can explain the large radii [5]. One could expect Shell Model calculations to work better, but these calculations also fail. The only way in which theories are at present able to reproduce the reaction cross sections of light nuclei close to the drip line is by using densities which are artificially constrained to fit the empirical binding energies [6]. But it has to be stressed that self-consistent calculations have failed so far in this task. This may turn out to be not a failure in principle but only evidence for the finite accuracy of calculations for this type, because binding energies can rarely be predicted to an accuracy of less than one MeV. However, future studies from a theoretical as well as from an experimental standpoint are needed.

This raises a number of additional questions concerning the nature of such a halo.

1. Are nuclides such as ^{11}Li, ^{19}B, and/or other nuclei near mass 40 deformed or even superdeformed? It is possible that the huge neutron excess forces the neutrons to occupy high angular momentum states causing the nucleus to be deformed. This effect might be expected by examining the Nilsson model and observing the existence of intruder states from outer shells whose energy is lowered with increasing deformation. We estimate that a deformation of β=0.6 in ^{11}Li could have an effect of approximately 30% on the root mean square radius. A Shell Model calculation of the magnetic moment of ^{11}Li yields 2.997 μ_N for the superdeformed case and 3.793 μ_N for the closed neutron shell case [7]. From a comparison to the experimental data, which yield 3.6673(25) μ_N for the magnetic moment of ^{11}Li [8], a large deformation for this nucleus seems unlikely. However, a measurement of the quadrupole moment of this nucleus via in-beam laser spectroscopy should yield a more definitive answer.

2. Can beta decay life times be calculated from theory? In the case

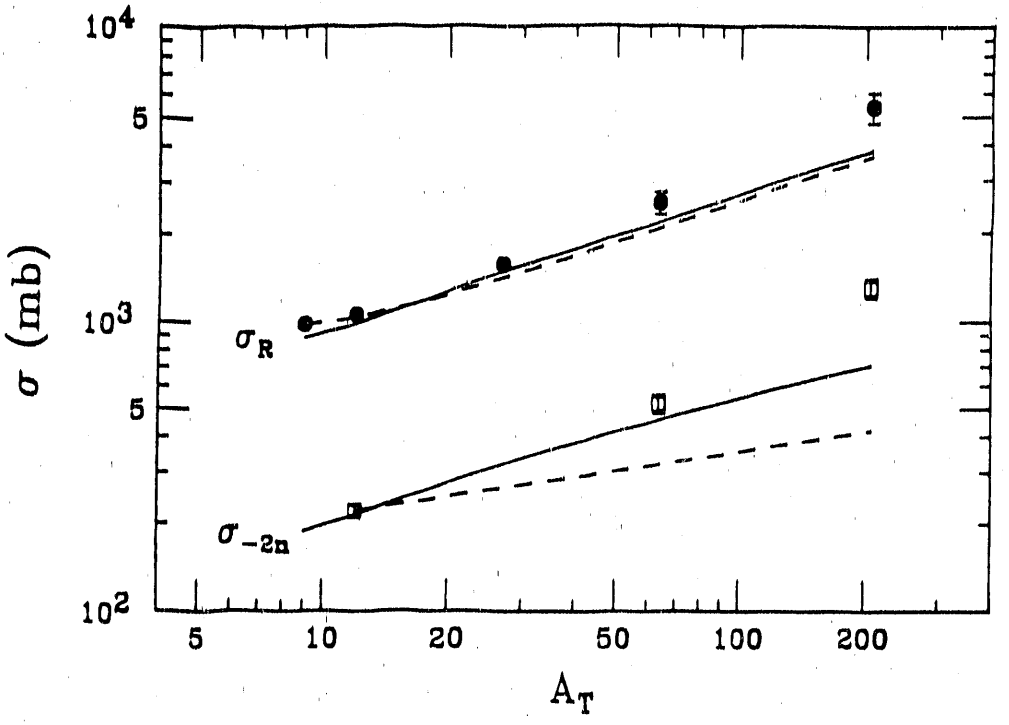

Figure 3: Reaction cross section for ^{11}Li as a function of target mass. Lines: Predicted nuclear contributions to the reaction cross section, using different models (taken from [10]).

of ^{11}Li, there is almost a factor of three discrepancy between the best Shell Model calculation and experiment [9]. It is important to perform measurements of decays to specific states with high Gamow-Teller transition probabilities, B(GT). This is because all low lying states in ^{11}Be with large branching ratios have only small B(GT) values for which small adjustments in the theory parameters have large consequences. By performing exclusive decay experiments to states with large B(GT) values, which cannot be freely adjusted by choice of the theoretical interaction parameters, a much more stringent test of existing theories can be performed. Because of the small branching ratios associated with these states, however, high radioactive beam currents are needed. Complementary information could be obtained by performing the ^{11}Li(p,n)^{11}Be reaction in reverse kinematics at sufficiently high beam energy ($\sim$ 100 MeV/nucleon). It seems also worthwhile to extend measurements and calculations to other exotic nuclides.

3. Can theory predict the electromagnetic dissociation cross sections?

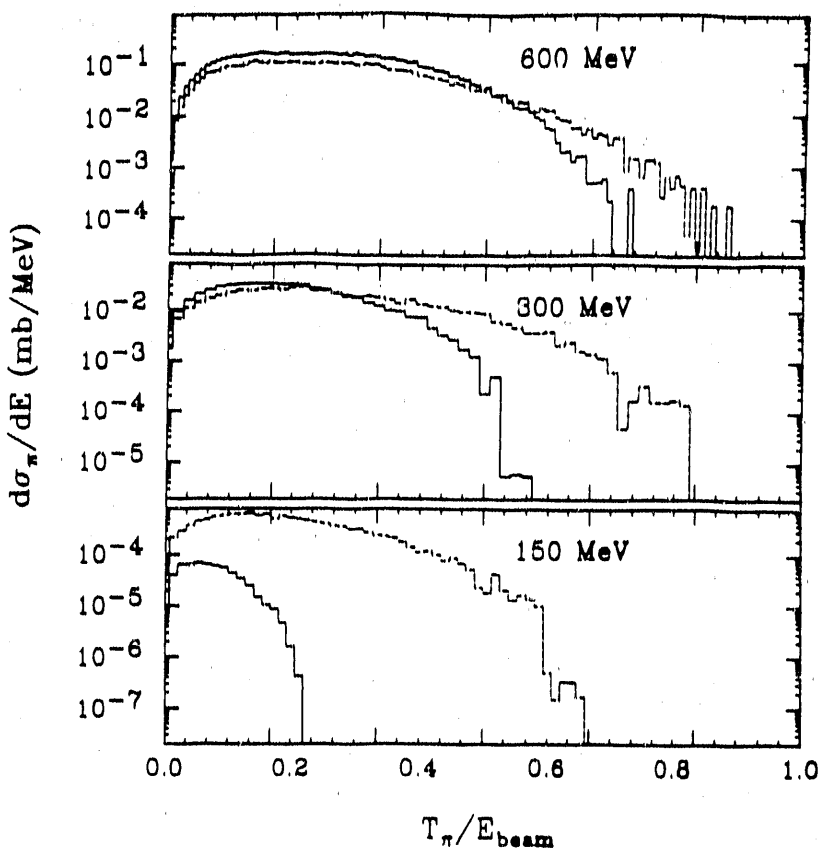

Figure 4: Predicted pion (π^+) energy distributions from one core (dashed histograms) and one halo neutron (solid histograms) of a ^{11}Li colliding with a proton from a ^{12}C target [13].

These can be measured by difference methods. However, these difference methods are model dependent, because one has to subtract the nuclear contribution from the total dissociation cross section in order to obtain the electromagnetic part. It turns out that a simple Glauber type approximation to the nuclear dissociation cross section is not sufficient. A better approach is the use of an eikonal approximation [10]. The inferred Coulomb cross section by using this method is **600** $\pm$ 100 mb for the reaction 790 MeV/nucleon ^{11}Li on ^{208}Pb (see **Fig. 3**).

This result has to be compared to a theoretical calculation using the Random Phase Approximation [11]. This theory predicts a softening of the dipole mode ("soft E1 resonances") as expected, and the response is sufficiently enhanced to explain the experimental data.

However, other theoretical investigations indicate a high sensitivity of the predicted E1 strength to the specific wave functions used [12]. Therefore the question if theory and experiment agree for the Coulomb dissociation cross section may still be open.

4. What is the momentum distribution of the halo neutrons? There are several methods which could be used to measure this distribution. One is to measure the ^{9}Li transverse momentum distribution from the reaction $^{11}\mathrm{Li} \rightarrow {}^{9}\mathrm{Li} + 2\mathrm{n}$. This yields two Gaussian components with different widths, 95 ± 12 and 23 ± 5 mb, respectively [4]. The smaller of the two is being attributed to the halo neutrons.

   Another way of obtaining similar information would be to measure pion momentum distributions from the reaction of a high energy beam of ^{11}Li on a ^{12}C target or on a ^{1}H target. The different neutron momentum distributions of core and halo neutrons in ^{11}Li would then show up as contributions to the pion energy distributions with different slopes (see Fig. 4). We estimate that a beam of 10^{5} ^{11}Li per second at a beam energy of 300 MeV/nucleon would produce about 10^{4} pions per second. With this production rate, a high quality experiment using a pion spectrometer could be performed. Alternatively, one can measure 2-neutron angular correlations at small angles by means of ^{11}Li stripping reactions.

Two other questions are related to the occurrence of soft E1 resonances for the neutron rich nuclei:

1. Are there soft E1 resonances for proton-rich nuclei? In proton-rich nuclei, there can be no proton "halo" due to the Coulomb barrier.

2. Is there a neutron halo in the presence of a low 1-neutron binding energy but a high 2-neutron binding energy? A first candidate for this effect appears to be the isotope ^{11}Be, but further studies are in order.

Both of these questions can be answered by studies near the particle drip-lines made accessible by radioactive ion beam facilities.

Another topic of great interest is how the nuclear surface (skin) changes as one approaches the drip-line either on the proton-rich or neutron-rich side of the valley of stability. This can be studied with the techniques of on-line laser spectroscopy discussed elsewhere in these proceedings.

As one approaches the neutron drip-line, the radioactive decay mode of beta-delayed two-neutron emission becomes more probable. The study of the two-neutron energy and angular correlation from such decays will provide information on the mechanism of two-neutron emission. The question is whether the neutrons come out sequentially or do they leave the nucleus as a di-neutron and break apart outside the nucleus?

Finally, studies at the neutron drip-line offer the possibility of discovering a postulated decay mode known as ground state two-neutron emission. This occurs when a given nuclide is stable with respect to one-neutron emission but is unstable with respect to two-neutron emission. This is analogous to the ground state two-proton emission being sought on the opposite side of the valley of stability. The protons feel a Coulomb barrier which retards the emission of the two protons and leads to predicted half-lives in the micro-second to milli-second range. However, neutrons do not have this barrier; so measurable life times will occur only if there is very low neutron energy available, there is an angular momentum barrier, and/or there are unfavorable transition matrix elements. By definition, ground state two neutron emission occurs only at the neutron drip line and thus requires the capabilities of a radioactive ion beam facility to produce such nuclides.

5. Conclusions

The topics listed above can only be viewed as a very preliminary glance at the amazing range of new possibilities for nuclear structure studies with radioactive beams. The phenomenon of the occurrence of neutron halos seems firmly established. Present and future suitable radioactive beam facilities will open new avenues for this kind of research and permit a detailed investigation of the edge of neutron matter.

References:

1. W. D. Myers, Proc. of the 1st Int. Conf. on Radioactive Nuclear Beams, 16-18 Oct. 1989, Berkeley, CA, World Scientific.
2. I. Tanihata et al., Phys. Lett. 160B, 380 (1985).
3. I. Tanihata et al., Phys. Rev. Lett. 55, 2676 (1985).
4. T. Kobayashi et al., Phys. Rev. Lett. 60, 2599 (1988).
5. H. Sato and Y. Okuhara, Phys. Lett. 162B, 217 (1987).
6. G.F. Bertsch et al., Phys. Rev. C 39, 1154 (1989).
7. B.A. Brown, unpublished.
8. E. Arnold et al., Phys. Lett. 197B, 311 (1987).
9. M.S. Curtin et al., Phys. Rev. Lett. 56, 34 (1986).
10. G.F. Bertsch et al., MSU preprint (1990).
11. G.F. Bertsch and J. Foxwell, Phys. Rev. C 41, 1300 (1990).
12. A.C. Hayes and D. Strottman, Los Alamos preprint (1990).
13. W. Bauer, work in preparation.

Report From Working Group 3: Nuclear Astrophysics

Chairman:
W. Michael Howard
Lawrence Livermore National Laboratory

Coordinator:
Paul Koehler
Los Alamos National Laboratory

Contributors:
M. Arnould, Institut d'Astronomie and d'Astrophysique
ULB, Bruxelles, Belgium
R. E. Azuma, CalTech, Pasadena
L. Buchmann, TRIUMF, Vancouver, B.C.
A. Champagne, Princeton University
G. M. Fuller, University of California, San Diego
S. Kubono, Institute for Nuclear Study, University of Tokyo
P. J. Leleux, University of Louvain, Belgium
M. Loiselet, Louvaine-La-Nueve, Belgium
G. J. Mathews, Lawrence Livermore National Laboratory
B. S. Meyer, Lawrence Livermore National Laboratory
P. Möller, Los Alamos National Laboratory
E. B. Norman, Lawrence Berkeley Laboratory
F.-K. Thielemann, Department of Astronomy, Harvard University
J. W. Truran, University of Illinois, Urbana
M. Wiescher, Department of Physics, University of Notre Dame
S. E. Woosley, University of California, Santa Cruz
J. M. Wouters, Los Alamos National Laboratory

The study of nuclear astrophysics involves the interaction of nuclei throughout the periodic table, both on the proton-rich and neutron-rich side of the valley of beta stability, over a range of energies from far below the Coulomb barrier to near the Coulomb barrier. In addition to nuclear reaction rates, nuclear astrophysicists need to know nuclear binding energies, fission properties and weak interactions rates of some very exotic nuclei. Calculation of these quantities imply detailed knowledge of nuclear levels and the nuclear level density, detailed nuclear structure information related to fission properties, and the statistical behavior of reaction rates for both neutron and charged-particle capture. To follow nature's evolution of the abundance of chemical elements requires knowledge of these nuclear properties for literally thousands of nuclei. Many important processes involve stable nuclei for which nuclear reaction rates can be measured. However, many more important processes involve radioactive nuclei which either are not easily produced in the laboratory, or up until now were impossible to produce. In this report we will make the case for a few selected examples for which an intense radioactive beam facility can be used to measure specific reactions and other nuclear properties of prime importance in astrophysics.

However, we will also make the case for the need to study the global properties of nuclei, both on the proton and neutron-rich sides of the valley of beta stability. Several processes in nuclear astrophysics, i.e. the p-process[1], the r-process[2] and the rp-process[3] depend on nuclear reaction rates, beta-decay rates, and nuclear masses for thousands of nuclei far from the valley of beta-stability. We need experiments to validate the statistical models of nuclear reactions and nuclear structure that are used for these calculations of nucleosynthesis. Of particular importance are Gamow-Teller strengths for neutron-rich isotopes in the mass range of A = 56 to 70[4] region and nuclear masses and beta decay rates for neutron-rich isotopes beyond the N = 50 neutron closed shell.[2]

This report draws contributions from various astrophysics groups. Included in the discussion are some of the nuclear physics needs for the astrophysical r-process, hydrogen burning[5] and the hot CNO cycle[3,6-8], the rp-process[3], and inhomogeneous big bang nucleosynthesis[9-15]. Also included is some discussion of intermediate mass nucleosynthesis, including the production of the radioactive nuclei ^{22}Na and ^{26}Al[7,16], as well as problems in supernovae calculations related to uncertainties in electron-capture rates[4]. The discussion is broad, but not comprehensive, and sometimes general rather than specific. The point of including the various discussions is to give a flavor for the wide range of problems that can be addressed for applications of radioactive ion beams to nuclear astrophysics. Although there are sometimes specific nuclear reactions that need to be measured, it would be a mistake to concentrate on a few light mass reactions, for example, when considering the design of a intense radioactive ion beam facility. Specifically, the rp-process and the r-process, as well as the p-process, are nucleosynthetic processes that require global nuclear structure and nuclear reaction rates for nuclei on both the proton and neutron-rich sides of the valley of beta stability. One break through with a radioactive ion beam facility for nuclear astrophysics would be the study of heavy neutron-rich nuclei that would be impossible to produce by other means. Although the study of individual nuclear reactions is always very important for nuclear astrophysics, we feel that more emphasis should be placed on the production of both proton-rich and neutron-rich heavy elements. This conclusion affirms the conclusion of Working Group 2 on Nuclei Far From Stability.

We will conclude the report with an analysis of the facilities required to meet the various experimental needs for nuclear astrophysics. This report also includes in an Appendix a description of radioactive ion beam experiments relevant for astrophysics presently underway in Japan and Belgium.

With the launch of the Hubble Space Telescope (HST), and the launch of the Gamma Ray Observatory (GRO) later this year, the science of nuclear astrophysics will become more exciting and more demanding in this decade. Nuclear physics learned from experiments with an intense radioactive ion beam facility could play an important part in pursuing our increased understanding of the nuclear reactions in the cosmos.

I. HYDROGEN BURNING AND THE HOT CNO CYCLE

An example of a particular reaction of importance involving a radioactive nucleus for the proton cycle in the Sun is $^{7}Be(p,\gamma)^{8}B$. This reaction governs the rate of ^{8}B neutrinos from the Sun, the ones measured by Dr. Ray Davis and his colleagues using a 100 000 gallon tank of C_2Cl_4 located at the bottom of the Homestake gold mine in South Dakota. The observed flux of neutrinos is about only one-third of the predicted flux. There appears to be a discrepancy outside the formal errors, with no agreed solution to the problem. Either the nuclear physics could be in error or the astrophysics associated with the determination of the physical conditions in the core of the Sun could be wrong. Although other neutrino experiments are planned that will detect neutrinos from the main p-p chain reactions, a new measurement of this reaction rate would be very important. Discordant measurements of this rate by different groups needs to be resolved.

As discussed in many places,[3,8] a major change in the classical CNO cycle occurs when the rate for $^{13}N(p,\gamma)^{14}O$ becomes more rapid than the ^{13}N beta-decay. Other proton capture rates on unstable species are involved in the hot CNO cycle are: $^{14}O(\alpha,p)^{17}F$, $^{17}F(p,\gamma)^{18}Ne$[17], $^{18}F(p,\gamma)^{19}Ne$, $^{18}F(p,\alpha)^{15}O$ and $^{19}Ne(p,\gamma)^{20}Na$.[18] The hot CNO cycle transforms into the rp-process when the rates for $^{15}O(\alpha,\gamma)^{19}Ne$ and $^{14}O(\alpha,p)^{17}F$ become more rapid than the corresponding beta-decays. In such a case the reaction $^{19}Ne(p,\gamma)^{20}Na$ may provide a breakout from the hot CNO cycle towards heavier elements. For the case of the study of hydrogen burning it is of prime importance to know detailed reaction rates for light-mass radioactive nuclei. These reaction rates are best studied in the energy range 0.2 to 1.0 Mev/nucleon. See the references for additional light reactions of importance. The reaction rates for many of these light reactions can also be determined by looking at inverse reactions, measuring spectroscopic factors or studying analog structures of mirror nuclei. However, these methods have various drawbacks, in determining the stellar rates, so that direct measurement with a radioactive ion beam may still be highly preferable.

II. INHOMOGENEOUS BIG BANG NUCLEOSYNTHESIS

Recently there has been considerable interest in baryon inhomogeneous cosmologies. Several processes such as a first order QCD phase transition, evaporating quark nuggets, or superconducting cosmic strings could have given rise to macroscopic baryon number fluctuations in the early universe. At later times, after weak decoupling, neutrons diffuse more readily out of high baryon density regions than do protons. In this way relatively neutron-rich and proton-rich regions could have formed prior to nucleosynthesis. The resulting light element yields from nucleosynthesis would then be different from those in a homogeneous universe.

One possible difference between homogeneous and inhomogeneous nucleosynthesis is that some elements with $A \geq 9$ could have been made in fairly substantial amounts in an inhomogeneous universe. This is to be contrasted with the homogeneous universe in which little production of elements with $A \geq 9$ occurs due to the lack of stable nuclei at mass five

and eight. Therefore, should relatively large quantities of A ≥ 9 nuclei be observed in extreme Population II stars, we would have good evidence for baryon inhomogeneity in the universe at the time of nucleosynthesis.

The formation of A ≥ 9 nuclei predominately occurs in neutron-rich regions in inhomogeneous universes. The important reaction sequence is $^{1}H(n,\gamma)\ ^{2}H(n,\gamma)\ ^{3}H(d,n)\ ^{4}He(t,\gamma)\ ^{7}Li(n,\gamma)\ ^{8}Li$. The nucleus ^{9}Be may be made by $^{8}Li\ (n,\gamma)\ ^{9}Li(\beta^{-})^{9}Be$ and $^{8}Li(d,n)^{9}Be$ (as well as by $^{7}Li\ (t,n)\ ^{9}Be$). Observations of the abundance of ^{9}Be in extreme Population II stars could provide constraints on inhomogeneous cosmologies. The chain leading to the intermediate mass elements is $^{8}Li\ (\alpha,n)\ ^{11}B(n,\gamma)\ ^{12}B(\beta-)\ ^{12}C(n,\gamma)\ ^{13}C$. Clearly, reactions on ^{8}Li are extremely important for formation of elements with A ≥ 9, and accurate ^{8}Li cross sections are necessary for reliable predictions of the nucleosynthesis of these nuclei. Subsequent evolution to higher mass is shown in Figure 1. As may be seen, one requires nuclear cross sections and nuclear masses for many neutron-rich light isotopes.

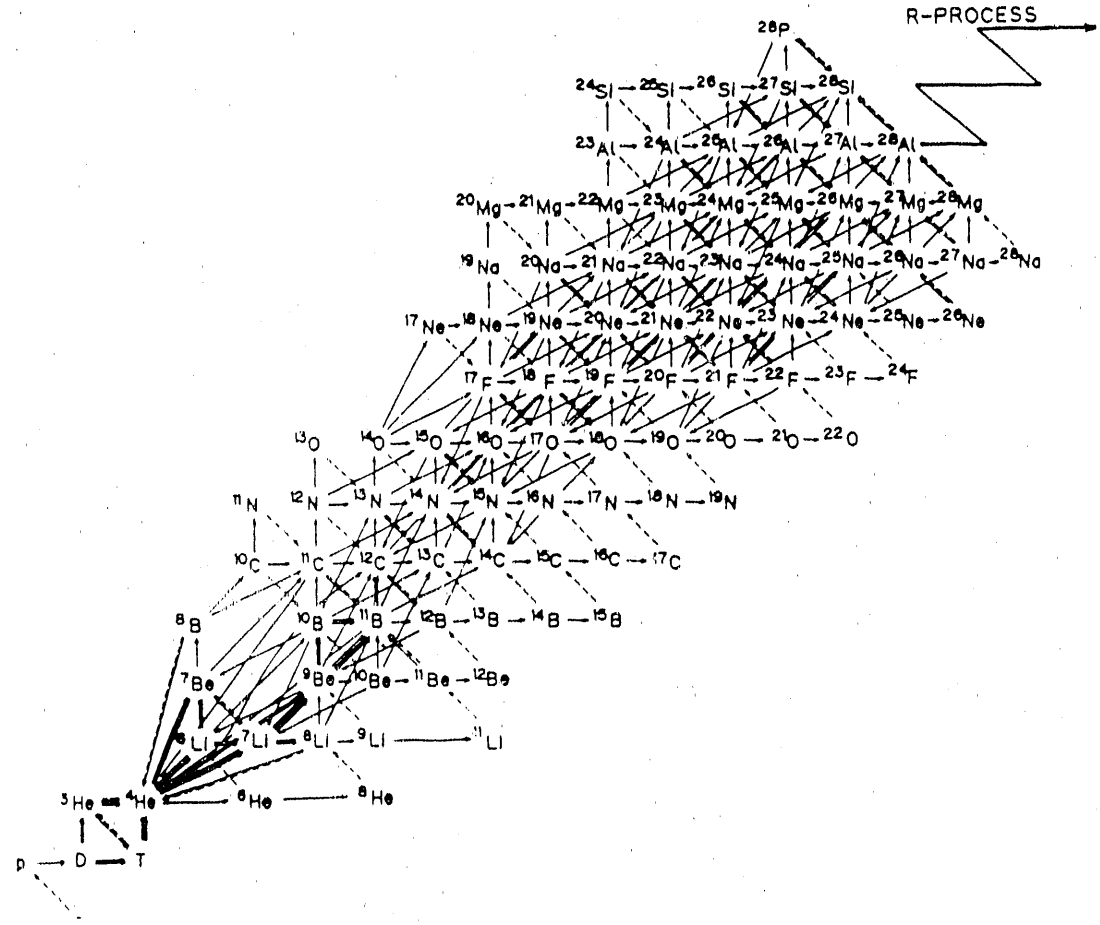

Fig. 1. A typical nuclear reaction network used in calculations of inhomogeneous big bang nucleosynthesis. From Ref. 15).

Aside from the possibility of formation of intermediate and heavy mass nuclei in the big bang, baryon inhomogeneous cosmologies may relax constraints on the present ratio of the baryon density to the closure density. Homogeneous nucleosynthesis provides the constraint $\Omega_b \lesssim 0.15$. Since inflation suggests $\Omega = 1$, the implication is that some 90% of the mass energy in the universe is in a form other than baryons (e.g. massive neutrinos, axions, etc.). In baryon inhomogeneous universes, Ω_b may be as large as 0.8, but only if the ^{7}Li constraint is relaxed. The nucleus ^{7}Li is overproduced in baryon inhomogeneous universes since it is made as ^{7}Li in the neutron-rich regions and as ^{7}Be in the proton-rich regions (^{1}H(n,γ)^{2}H(^{2}H,γ) ^{4}He(^{3}He, γ) ^{7}Be(β^+) ^{7}Li). It turns out, however, that late-time hydrodynamic dissipation of the density fluctuations during nucleosynthesis may have an important effect on ^{7}Li yields. In such a dissipation event, the high density, proton-rich region may be rapidly mixed with the lower-density, neutron-rich material. Destruction of ^{7}Be occurs via ^{7}Be (n,p) ^{7}Li (p, α) ^{4}He. When the mixing is instantaneous, the final ^{7}Li yield may be reduced by as much as two orders of magnitude. Also contributing to the destruction of ^{7}Li are the reactions ^{7}Li (t, α) ^{6}He and ^{7}Li(t,n) ^{9}Be$^* \rightarrow$ n + 2 ^{4}He. It would therefore be of great interest to have accurate cross sections for tritium capture reactions on ^{7}Li for energies in the range 10- 100 keV, as well as accurate reaction rates for the destruction of ^{8}Li.

III. GAMOW-TELLER STRENGTHS FOR INTERMEDIATE MASS NUCLEI

The extent of electron capture during the pre-supernova core collapse determines the resulting iron core and neutron star mass[19,20]. The more electron capture or neutronization, the smaller the value of Y_e, the number of electrons per nucleon, and the smaller the resulting core mass of the pre-supernova star. The dense core of the pre-supernova star tends to have a mass corresponding to a Chandrasakar mass. Most of the nuclei in the core are iron group nuclei in a range of mass $56 \lesssim A \lesssim 70$. High energy (n,p) reactions for neutron-rich nuclei in this mass region to deduce Gamow-Teller strength distributions would make a significant contribution towards understanding pre-supernova stellar evolution and also understanding the supernova explosion mechanism itself. A recent study[21] has determined that for pre-supernovae core evolution the most important electron captures are on ^{56}Ni,^{55,59,60}Co and ^{55}Fe, ^{52}V and ^{67,68}Cu, and the most important beta decays are for ^{56}Co, ^{55,57}Mn, ^{57,58}Cr and ^{67,69}Ni.

IV. ASTROPHYSICAL r-PROCESS

Although the mechanism of the astrophysical r-process has been studied for more than thirty years, we are still not sure of its site in nature.[1,22] Part of the reason for this is the complexity of the nuclear physics required to calculate the r-process, and the lack of experimental information. Recent years has seen great progress in the sophistication of the nuclear models used in the calculations. Except for a very few cases, we must rely on theoretical modelling for all of the necessary nuclear quantities that are used in the calculations. These quantities include, nuclear masses, nuclear partition functions, neutron

capture rates (including the effects of excited states), and beta decay rates (also including the effects of excited states). Of prime importance is the location of the neutron-drip line in the N-Z plane. Figure 2 shows a typical r-process path in the N-Z plane. Stable nuclei are included in black, while unstable nuclei which experimental mass determinations are shaded in grey. As one can observe from studying this figure, a radioactive ion beam facility that was capable of producing critical heavy neutron-rich nuclei could go a long way in providing information for the astrophysical r-process.

Current r-process calculations use macroscopic-microscopic models, such as the diffuse surface folded-Yukawa model of Möller and Nix[23,24] to consistently predict nuclear binding energies, fission and neutron emission probabilities,[25] and along with Gamow-Teller interactions,[26,27] and beta decay rates for neutron-rich heavy elements.[28] Experiments with radioactive ion beams to confirm or improve such models would be an important benefit to nuclear astrophysics.

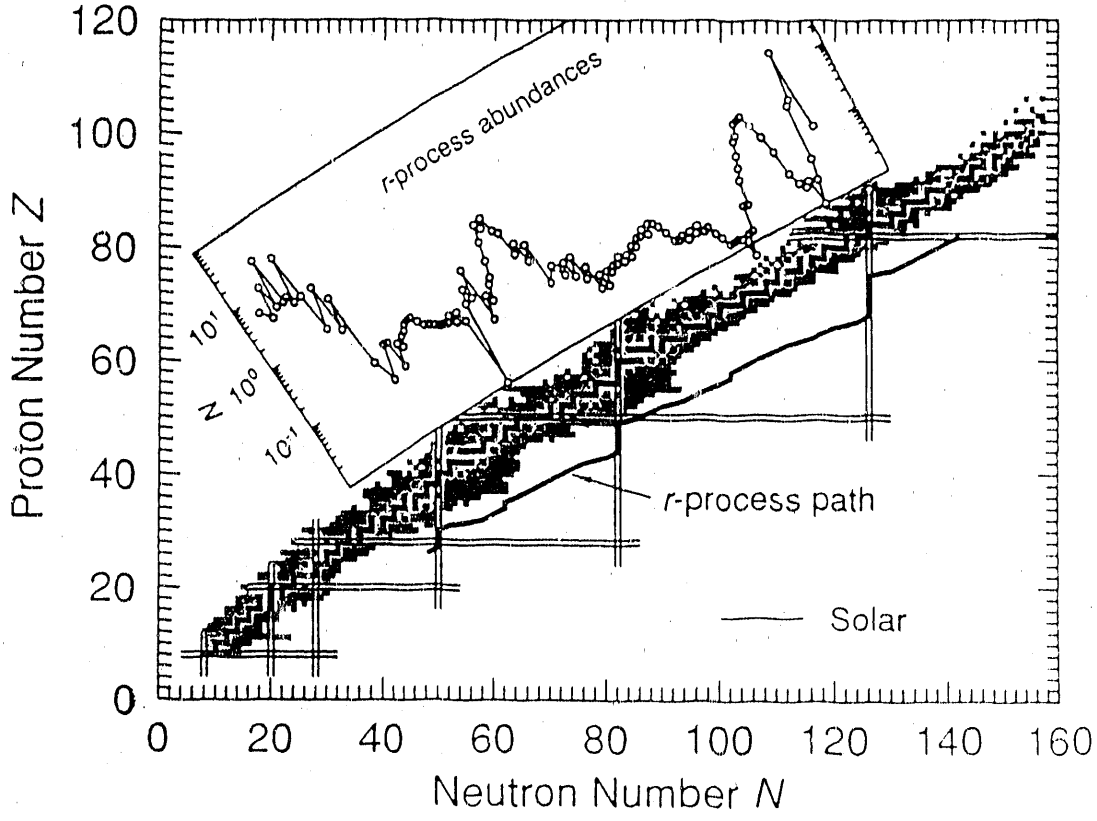

Fig. 2. Plot of the r-process path in the N-Z plane. Stable nuclei are shown in black, and unstable nuclei with experimental mass determinations are shown in grey. Also included is the abundance distribution of r-process nuclei as a function of A. (Figure due to P. Möller).

Of particular interest are the properties of nuclei near the r-process waiting points, or the neutron closed shells. Some r-process nuclei near the N = 82 closed shell are already studied. However, present heavy ion reactions are a long ways from producing r-process nuclei near the N = 126 closed shell. It is radioactive ion beams that could make an important impact in this region

The role of neutron-induced or beta-induced fission is important in terminating the r-process near the N = 184 closed neutron shell. The fragments from fission at the termination of the r-process may be responsible for the peak in the r-process distribution of isotopes in the rare-earth region. Beta-delayed fission and beta-delayed neutron emission rates for nuclei as they decay from the r-process path to the valley of beta stability in the mass region $232 \leq A \leq 260$ are important for studies of nuclear cosmochronolgy[25,29-31]. Such rates may influence the U/Th production ratios, which, in turn, coupled with models of Galactic evolution, help determine the age of the Galaxy.

It is not possible to measure neutron capture cross sections directly in radioactive ion beam facilities. Another method can, however, be applied which is presently widely used to predict proton capture reactions on unstable proton-rich nuclei. Reactions like (d,p) would produce the same compound nucleus as an (n,γ) reaction and allow one to investigate resonance energies and other properties (parity, partial widths) which then can be employed for an indirect calculation of the neutron capture cross sections. Independent of the individual cross section, such an investigation would also result in a systematic analysis of level densities in neutron-rich nuclei and their dependence on the distance from stability. A high nuclear level density is a prerequisite for the validity of statistical model calculations.[32,33] The (d,p) experiments should be performed at energies of about 20 MeV/nucleon.

V. INTERMEDIATE MASS NUCLEI -- AN EXAMPLE: ^{22}Na, ^{26}Al and ^{44}Ti

Classical novae explosions are known to provide an environment in which hydrogen-burning reactions proceed on carbon, nitrogen, and oxygen (CNO) nuclei, and heavier nuclei, at high temperatures and densities on a dynamical timescale. Weiss and Truran[16] recently suggested that for such conditions, the production of potentially interesting and detectable abundance levels of the radioactive isotopes ^{22}Na and ^{26}Al may occur. They conclude that novae may represent an important source of ^{26}Al in the Galaxy and that some nearby novae may be expected to produce detectable flux levels of ^{22}Na decay gamma rays. The detection of ^{22}Na in novae would provide critical constraints, both on their temperature and envelope convection histories and on their initial envelope composition. If one knows from early observations both that a nova is at a distance of less than one kiloparsec and that its envelope is significantly enriched in neon and magnesium, the Gamma Ray Observatory (GRO) to be launched late this year may have a chance to detect the gamma ray lines from the decay of ^{22}Na.[16]

The destruction rates of ^{22}Na and ^{26}Al, particularly the rate of the reactions $^{22}Na(p,\gamma)^{23}Mg$, $^{26}Al(p,\gamma)^{27}Si$ and $^{26m}Al(p,\gamma)^{27}Si$ are very important in determining how much ^{26}Al is produced in such novae explosions. Observations of ^{22}Na and ^{26}Al gamma ray lines from novae explosions could set constraints on the hydrodynamics, convection and initial compositions of such explosions. This is but one example, in light to intermediate mass nucleosynthesis, where the determination of a key reaction rates on radioactive nuclei can have important consequences. For nucleosynthesis of ^{44}Ca and γ-ray astronomy, the production and destruction rates for ^{44}Ti are important, as well as a measurement of its rather uncertain halflife.

VI. THE rp-PROCESS

The rp-process is the transmutation of CNO nuclei into iron group nuclei and beyond in hot ($0.3 < T_9 < 5.0$) proton-rich environments.[3] The reactions proceed through proton capture on light nuclei and alpha-particle capture on intermediate mass radioactive nuclei. At high temperature and density conditions, the reaction path will be close to the proton drip line. The result is that both nuclear binding energies and charged particle reaction rates on very proton-rich nuclei in the mass region $20 \leq A \leq 66$ will be necessary to accurately calculate this process. Such a process may have important consequences for nucleosynthesis, as well as being an important energy generation mechanism in novae explosions. As mentioned previously, the reaction $^{19}Ne(p,\gamma)^{20}Na$ is thought to govern the transition from CNO nuclei to intermediate nuclei.

Other important breakout reactions for the rp-process may include $^{27}Si(p,\gamma)^{28}P$, $^{31}Si(p,\gamma)^{32}Cl$, and $^{39}Ca(p,\gamma)^{40}Sc$.[34] These key reactions are mainly proton capture reactions on proton-rich radioactive nuclei with low Q values. In that case the cross sections and reaction rates are determined by single resonances and the direct capture process only and cannot be calculated by statistical methods (Hauser-Feshbach). The influence of the single resonances and the direct reaction contribution must be measured directly. In contrast, proton capture reactions on radioactive nuclei with $A > 26$ near the line of stability have typically rather high Q values and can therefore be estimated by Hauser Feshbach calculations.

The termination point of the rp-process depends crucially on whether the proton separation energy of ^{65}As is more than about 250 keV. If it is less than this value, the process halts at ^{64}Ge, if it is greater, the process continues up to approximately $A = 80$. The nucleus ^{65}As is so proton-rich that in order to produce it and have a charged-particle in the exit channel to detect, it is necessary to use a radioactive beam or target.

VII. REQUIRED FACILITIES

Experiments in nuclear astrophysics using radioactive ion beams will be among the most challenging in nuclear physics, because of the demand for either very proton-rich or

neutron-rich nuclei and the very small cross sections involved in the reactions. In the previous sections we have identified various astrophysical process and specific reactions of prime importance where the nuclear needs can be addressed with a radioactive ion beam facility. Regarding the required facility to meet these nuclear needs we define four major areas:

a) Nuclear capture reactions involving stellar processes.

b) Production of exotic nuclei for r-process or rp-process modelling.

c) Nuclear transfer reactions for simulating specific neutron, proton or alpha capture reactions.

d) Determination of Gamow-Teller strengths via (d,p) or (n,p) reactions on isotopes within the iron group.

The facility demands for these reactions are summarized in Table I. The processes a) and b) are quite distinct in intensity and energy from processes c) and d). The first two processes will require the highest intensities possible, as the cross sections involved are in general (for case a)) of order of microbarns. For target thicknesses of 10^{18} cm^{-2} and beams of order 10^{10} sec^{-1}, the resulting event rate for low-energy capture will be of order 10 hr^{-1}. Producing exotic nuclei will allow somewhat thicker targets, but the production cross section for the exotic nuclei will certainly be very small.

TABLE I. Facility Requirements

	a) Nucleon Capture	b)Exotic Nuclei	c) Nucleon Transfer	d) G. T.
Energy Range:	0.2-2 MeV/u	4-8 MeV/u	10-20 MeV/u	100-300 MeV/u
Intensity	$>10^9$ sec^{-1}	$>10^{10}$ sec^{-1}	$\geq 10^6$ sec^{-1}	$\geq 10^6$ sec^{-1}
Masses (Projectile):	7-200 (80)	40-100	7-200	40-70
Energy Spread:	< 1%	< 10%	< 10%	< 1%

The second class of experiments c) and d) will require more moderate beam intensities, but considerably high energies. Given the range and scope of proposed and existing

facilities, the first two reactions classes will require the highest intensities available at moderate energies, which requires an Isotope Separator On-Line (ISOL) facility. The second class of reactions seems to be well suited for heavy-ion fragmentation, especially when coupled to a storage ring. All experiments will require extensive detector development with high efficiency and high discriminatory capabilities. More attention should be given to the development of the required detectors for these proposed facilities.

VIII. CONCLUSIONS

We have outlined some of the needs of nuclear astrophysics that could be met with a radioactive ion beam facility. The nuclear needs cover the entire range of proposed facilities. We would like to emphasize the global natures of the nuclear needs for astrophysics. While individual reactions are always of prime importance in nuclear astrophysics, it is the reliability of the statistical and macroscopic-microscopic models that are used that provi understanding of the origin of the elements in nature. We would also like to point out t nuclear physics plays an important role not only in understanding the origin of the elements in nature, but also in processes like how supernovae or novae explode, or in putting constraints on cosmological models. With the launch of the Hubble Space Telescope (HST), and the launch of the Gamma Ray Observatory (GRO) late this year, many astronomical surprises await us in the next decade. Nuclear physics will undoubtly play an important role in understanding these phenomena. The understanding of the nuclear structure of a broad range of nuclei across the periodic table helps us understand the universe now and back to the big bang. A radioactive ion beam facility that will delineate this nuclear structure will play a key role in future astrophysical developments.

NUCLEAR ASTROPHYSICS EXPERIMENTS AT INS, TOKYO

S. Kubono
Institute For Nuclear Study, University of Tokyo

This is a brief description of the programs under way or in near future.

1. There are some experimental works under way at INS using two-body charged particle spectroscopy. These include the study of ^{21}Mg for the ^{20}Na(p,γ) ^{21}Mg stellar reaction rate.

2. There are three nuclear astrophysical experiments going on with using the projectile fragment separator RIPS at RIKEN.

   a. Measurement of the gamma width of the 2.637 MeV 1^+ state (the first excited state above the proton threshold in ^{20}Na), which is the critical physical parameter for the breakout problem from the hot-CNO cycle. So far, the ^{20}Mg yield was measured.

   b. Study of the reaction rate of ^{26m}Al(p,γ).

   c. Measurement of the gamma width of the 1^- state in ^{14}O is scheduled next month (May, 1990) by using Coulomb dissociation of ^{14}O which are collected by the RIPS.

STATUS REPORT ON THE RADIOACTIVE ION BEAM PROJECT AT LOUVAIN-LA-NEUVE

P. Leleux, M. Loiselet

Catholic University at Louvain
Chemin du Cyclotron, 2, B-1348 Louvain-la-Neuve, Belgium

The general layout of the Radioactive Ion Beam Project at Louvain-la-Neuve has been described elsewhere.[1,2] Recent advances have led to the acceleration of a $^{13}N^{1+}$ beam at 8 MeV with an intensity of 1.5×10^8 particles per second, i.e. 25 particles pA. This has been achieved through the following improvements: use of a ^{13}C target, bombarded with 100 μA, 30-MeV protons, with an efficiency for the release of the ^{13}N activity thereby produced of 10%; optimization of the efficiency of the ECR source for ionizing ^{13}N into the 1^+ Ionic state, raised to 5%; increase of the efficiency of the CYCLONE cyclotron for accelerating $^{13}N^{1+}$ ions, through an improvement of the vacuum and of other parameters, up to 4%. The next steps will be the lowering of the ^{13}C contamination in the ^{13}N beam, and a further increase of the accelerated intensity. The first reaction of astrophysical interest which will be studied is $^{13}N(p,\gamma)^{14}O$. The necessary apparatus has been built, and an overall test of its performances has been carried through a remeasurement of the cross section for the $^{13}C(p,\gamma)\ ^{14}N$ reaction at the 0.552-MeV resonance.

The coworkers are: Th. Delbar, W. Galster, I. Licot, E. Lienard, P. Lipnik, G. Ryckewaert, J. Vervier (University of Louvain-la-Neuve), P. Decrock, M. Huyse, P. Van Duppen (University of Leuven) J. Vanhorenbeeck (University of Brussels).

1. Th. Delbar, M. Huyse and J. Vanhorenbeeck, editors, The Radioactive Ion Beam Project at Louvain-la-Neuve, RIB-1988-01, Internal Report (1988).

2. Proc. First International Conference on Radioactive Nuclear Beams, Berkeley, USA, October 16-18,1989.

REFERENCES

1. S. E. Woosley and W. M. Howard, Astrophys. J. Suppl., 36, 285 (1978).

2. G. J. Mathews and R. A. Ward, Rep. Prog. Phys., 48, 1371 (1985).

3. R. K. Wallace and S. E. Woosley, Astrophys. J. Suppl. 45, 389 (1981).

4. M. B. Aufderheide, G. E. Brown, T. T. S. Kuo, D. B. Stout, and P. Vogel, Astrophys. J., in press (1990).

5. C. E. Rolfs and W. S. Rodney, Cauldrons in the Cosmos, (University of Chicago Press: Chicago, 1988).

6. W. A. Fowler, Rev. Mod. Phys., 56,149 (1984).

7. W. Hillebrandt and F.-K. Thielemann, Astrophys. J., 255, 617 (1982).

8. M. Arnould and W. Beelen, Astron. Astrophys. 33, 215 (1974).

9. R. A. Malaney, in Workshop on Primordial Nucleosynthesis, (ed. W. J. Thompson, B. W. Carney, H. J. K rwowski, World Scientific: Singapore, 1990).

10. R. A. Malaney and W. A. Fowler, in The Origin and Distributions of the Elements, (ed. G. J. Mathews, World Scientific: Singapore, 1987).

11. J. H. Applegate, C. J. Hogan, and R. J. Scherrer, Astrophys. J., 329, 572 (1988).

12. F.-K. Thielemann and M. Wiescher, in Workshop on Primordial Nucleosynthesis, (ed. W. J. Thompson, B. W. Carney, H. J. Karwowski, World Scientific: Singapore, 1990).

13. G. J. Mathews, B. S. Meyer, C. R. Alcock and G. M. Fuller, Astrophys. J., in press (1990).

14. H. Kuri-Suomio and R. Matzner, Phys. Rev. D, 39,1046 (1989).

15. T. Kajino, G. J. Mathews and G. M. Fuller, Astrophys. J., in press (1990).

16. A. Weiss and J. W. Truran, Astrophys. J., submitted, (1990).

17. M. Wiescher, J. Görres and F.-K. Thielemann, Astrophys. J., 326, 384 (1988).

18. S. Kubono, H. Orihara, S. Kato and T. Kajino, Astrophys. J., 344, 460 (1989).

19. G. E. Brown, ed.Theory of Supernovae, Phys. Rep. 163,1-203 (1988).

20. N. Strawmann, Particle Physics and Astrophysics, (Springer-Verlag: Berlin, 1988).

21. I. Fushiki, M. Aufderheide, S. E. Woosley and D. Hartmann, private communication, (1990).

22. G. J. Mathews and J. J. Cowan, Nature, submitted (1990).

23. P. Möller and J. R. Nix, At. Data Nucl. Data Tables 26, 165 (1981).

24. P. Möller and J. R. Nix, Nucl. Phys., A361, 117 (1981).

25. B. S. Meyer, W. M. Howard, G. J. Mathews, K. Takahashi, P. Moller, and G. A. Leander, Phys. Rev. C, 39,1876 (1989).

26. J. Krumlinde and P. Möller, Nucl. Phys., A417, 419 (1984).

27. K-I Kratz, J. Krumlinde, G. A. Leander, and P. Möller in Recent Advances in the Study of Nuclei Off the Line of Stability, (ed. R. Meyer and D. Brenner, American Chemical Society, Washington, 1985).

28. P. Möller and J. Randrup, Nucl. Phys., in press (1990).

29. F.-K. Thielemann, J. Metzinger, and H. V. Klapdor, Astron. Astrophys. 123, 162 (1983).

30. B. S. Meyer, P. Möller, W. M. Howard, and G. J. Mathews, in Proceedings of the 50 years with Nuclear Fission, (American Nuclear Society: Illinois, 1989).

31. F.-K. Thielemann, A. G. W. Cameron, and John J. Cowan in Proceedings of the 50 Years With Nuclear Fission (American Nuclear Society: Illinois, 1989).

32. F.-K. Thielemann, M. Arnould, and J. W. Truran, in Advances in Nuclear Astrophysics, (eds. E. Vangroni-Flam et al., editions frontures: Gifsur Yvette).

33. S. E. Woosley, W. A. Fowler, J. A. Holmes, B. A. Zimmerman, At. Data Nucl. Data Tables, 22, 371(1979).

34. M. Wiescher and J. Görres, Astrophys. J. 346, 1041 (1989).

THE BORDER REGIONS OF MEDICINE, CONDENSED MATTER, ATOMIC AND NUCLEAR PHYSICS

Report of Working Group IV

Chairman: S. S. Hanna

Local Coordinator: R. D. Taylor

Members: E. D. Arthur, J. E. Crawford, P. L. Dyer, W. D. Hamilton, S. S. Hanna, C. J. Maggiore, H. A. O'Brien, D. R. Phillips, J. Sample, J. A. Sawicki, G. D. Sprouse, R. D. Taylor, J. R. Tesmer, B. H. Wildenthal

1. Introduction

One of the great strengths of nuclear physics lies in the important contributions it has made to other fields such as medicine, biology, chemistry, atomic physics, and condensed matter physics. These contributions have come through (1) nuclear radiations and (2) interactions with the nuclear environment.

(1) Nuclear radiations such as the classical α, β, and γ radiations, fast and slow neutrons, and more recently the newer particles such as pions and muons have provided an incredibly rich and variable array of probes which have been adapted to diverse phenomena ranging from medical diagnosis and therapy to uncovering art forgeries. The richness of these probes has been due in large measure to the great number of available isotopes, each providing its own characteristic spectrum of particles and energies at isotopic lifetimes ranging between effectively zero and infinity. It is clear that the advent of a dedicated radioactive ion beam (RIB) facility would greatly enlarge the number of available isotopes and expand the richness and diversity of their isotopic properties.

(2) From a scientific standpoint the interaction of the nuclear moments with the electromagnetic fields of the nuclear environment - the hyperfine interaction - has provided a powerful tool, often inviting skill and ingenuity, for measuring these moments and fields. From a knowledge of the moments one can sometimes deduce the nuclear spins. The use of an RIB facility will greatly expand the scope of these measurements and could lead to

clever extensions or new techniques in these studies. In the following we examine some of the advantages that might accrue to isotope production and to the methods and techniques of studying hyperfine interactions with a dedicated RIB facility.

2. Laser spectroscopy

The most recent method to be applied to the measurement of nuclear moments through the hyperfine interaction is the technique of laser spectroscopy. At present the emphasis has been on measuring the E0 moments of nuclei which leads to a knowledge of the mean-square charge radii $\langle r^2 \rangle$. It is of particular interest to measure the radii of an isotopic sequence to observe the effect of adding neutrons on the charge (i.e., proton) distribution. Two distinct techniques have been employed in the experimental setup for obtaining the hyperfine spectra with laser excitation. In some cases the measurements also show the effect of an M1 moment which can lead to a measurement of the magnetic dipole moment μ of the nuclear state. The extension to the measurement of an E2 moment and thus the nuclear electric quadrupole moment is straightforward provided the electric field gradient of the hyperfine interaction is known. A more detailed account of studies of nuclear charge radii and the benefits to be derived from an RIB facility can be found in the report of Working Group III, paragraph 2.6, entitled Laser Spectroscopy.

3. Mössbauer spectroscopy

3.1. MÖSSBAUER EXPERIMENTS

The Mössbauer effect (ME), the recoil-free emission and resonant absorption of gamma-rays, is a well proven tool in many areas of condensed matter, atomic physics, and special aspects of nuclear physics. The Mössbauer spectrum often gives a rich picture of the Mössbauer nucleus in its host environment. Over 100 potential Mössbauer transitions exist involving isotopes of about half the elements[1]). The usual situation involves a long-lived parent (days to years) that populates some low-lying (< 150 keV) excited state that decays to the ground state. The lifetime of the excited state (typically 10^{-11} to 10^{-6}s) gives rise to an energy resolution $\Delta E/E = 10^{-11}$ to 10^{-16} for those events that are recoil free. That an ME exists is usually shown by observing the transmission of a resonant absorber as a function of Doppler velocity between source and absorber. The richness appears in the resolved hyperfine spectrum of the Mössbauer transition involving the magnetic moments, quadrupole moments and spins of both the excited and ground states. Thus, an energy analysis (Mössbauer spectrum) yields information about the isomer shift, and magnetic and

quadrupole hyperfine fields. The relative and absolute intensities of the Mössbauer lines are related to the polarization and lattice dynamics of the Mössbauer nucleus in its host environment. Effects of temperature, annealing, pressure, and applied magnetic field provide additional information about atomic structure, phase changes and transitions, chemical changes, impurities, radiation damage and multiple sites. In principle the ME study may be carried out as a source experiment or as an absorber experiment.

Radioactive ion beams (RIB) will broaden the scope of available Mössbauer sources by in-beam production of Mössbauer levels. In-beam implantation studies will provide new opportunities of controlling such phenomena as implantation depth, radiation damage and impurity levels. We present a few examples of cases in which an RIB will potentially enhance or enable the production of certain types of Mössbauer studies[2]). In general the advantages for producing ME sources by an RIB are those enjoyed by a conventional heavy ion beam, the RIB serving to enlarge the scope of ME source production.

3.1.1. Short lived parents

Most conventional ME experiments utilize a long-lived (weeks to years) parent to populate the Mössbauer level. Low specific activity (typical of reactor activations) and a long parent lifetime often result in rather weak sources. The source must also be thin to allow the soft ME gamma rays to emerge and be relatively free of the ground state ME isotope (to avoid resonant self-absorption). Enriched stable isotopes are often required for making either an ME source or absorber. Given these requirements, the RIB capability would broaden the possibility of obtaining short-lived ME parents (minutes to hours). Some short-lived parent isotopes feed the ME level more efficiently than their long-lived counterpart. Several ME isotopes are seldom used because there is no really convenient long-lived parent. The RIB facility has promise of contributing to the production of these and other new ME isotopes, e.g., ^{61}Ni, ^{73}Ge, ^{157}Gd, ^{161}Dy, ^{189}Os, ^{191}Ir, and ^{197}Au. For these examples, the conventional parent lifetimes are longer than an hour but on-line production at the RIB facility should allow shorter parent lifetimes to be considered, such as the 1.7-m lifetime of ^{57}Mn parent of ^{57}Fe.

3.1.2. Low concentrations

Often the ME is used as an impurity probe of its host to study phase changes, magnetism, inequivalent sites, and lattice dynamics of the host. Source (parent) concentrations of a few ppm are usually sufficient; nevertheless, suitable ME sources in many host

materials cannot be readily prepared because of lack of available parent material of sufficient specific activity, chemical incompatibility, volatility, and/or lack of facilities for radioactive doping. Isotope separators have been used to implant radioactive parents, but the process is very inefficient, and the present acceleration potentials are rather low so their use has been mostly confined to surface studies[3]).

Source implantation via the RIB (or other heavy ion beam) circumvents many of the problems encountered in preparing conventional ME sources. One can expect a rather homogeneous target area with a well defined depth profile for a given host. Low-temperature targets are often used. Required post heat-treatment of most sources will be minimal. This situation can be contrasted to the conventional (non-uniform) emplacement of the activity on the surface of a host followed by various chemical/thermal/diffusion treatments. The expected high purity of the RIB implies a higher specific activity of the dopant and relatively lower noxious impurity concentrations. Of course, the intensity of the RIB is a prime consideration.

3.1.3. High specific activity sources

Whenever appropriate stable isotopes exist, the most effective way to produce ME source activity is in a reactor. Characteristically this activity has rather low specific activity, and there is no ready means to separate the desired product. Accelerator-produced activity usually requires rather complex chemical purification or separation. Sources made with low specific activity tend to be rather large in diameter in order to meet the thinness requirement. Intense "point sources" are an identified need in many ME experiments such as source or absorber experiments in high pressure diamond anvil cells[4]), where the samples are only 50-400 microns in diameter. The promise of the RIB to introduce activity into a small volume would greatly expand the scope of high pressure ME physics.

3.1.4. Exotic chemistry

The study of rare gases and their binding in solids has been an ME specialty. Two isotopes are excellent candidates for ME studies: ^{83}Kr has a 9.4-keV, 150-ns first excited state and ^{129}Xe a 39.6-keV, 1.0-ns level. Neither have convenient parents for conventional ME spectroscopy. However, 1.9-h ^{83m}Kr and 8.0-d ^{129m}Xe feed the ME levels. The RIB implantations of these rare gas atoms and the subsequent ME experiments should provide unique microscopic information on the binding, valence, lattice dynamics and hyperfine interactions of rare gases in selected hosts. The ME levels are also fed by 2.4-h ^{83}Br

and by 2.2-h ^{129}Cs. With these sources the dynamics of the implantation and annealing may well be different and the ME measurements might well distinguish the various sites and processes.

3.2. ON-LINE MÖSSBAUER SOURCES

Most of the ME cases considered so far have involved producing sources at the RIB facility with lifetime in the minutes to days range. With such sources there would be time for processing the source with or without removal. Beam chopping would facilitate such procedures. A truly on-line implantation ME facility also has much appeal. In addition to allowing use of shorter lifetime parents (ns - ms), one could study the immediate effects of radiation damage and self annealing and other solid state phenomena such as implantation site location of the ME atom. On the other hand, for ME sources the recoil-free fraction is enhanced by lowering the temperature and annealing may be necessary to reduce source broadening due to multiple sites. The ability to control the target temperature during the implantation is important for source preparation as well as solid state studies.

In the following the in-beam implantation Mössbauer experiment (INBIME) is illustrated by the implantation of excited ^{57}Fe nuclei into single crystals of semiconductors[5]). The application to ME nuclei which cannot be produced by radioactive sources is illustrated by a study of the isomer shifts in isotopic series of rotational nuclei[6,7]). The microscopic theory of Meyer and Speth[8]) gives dramatic agreement with the isomer shift experiments, especially in giving the shrinking observed for some of these rotational levels.

A simple arrangement for INBIME in which the temperature can be varied is shown in fig. 1 (low temperatures can be obtained by replacing the heating element by a liquid nitrogen or helium reservoir). Figure 2 shows spectra obtained for implantation of ^{57}Fe into single crystals of germanium as a function of temperature. Two well-defined sites are observed. The right hand resonance can be identified with a substitutional site, while the left hand resonance is produced by either an interstitial or a "damage" site.

The use of INBIME to produce high-quality, single-line, short-lived sources which cannot be produced by radioactive parents is illustrated by an experiment which measures the isomer shifts in a series of isotopes. Usually only the proton-rich isotopes can be measured with radioactive sources; in-beam implantation can then be used to complete the series. Both the Gd and Yb series of isotopes have been completed in this way[6,7]).

Following are the important features of the Yb experiments:

(1) Only single-line sources and absorbers were used.

(2) Enriched targets and absorbers, while not essential, were used for the rarer isotopes in order to conserve accelerator time.

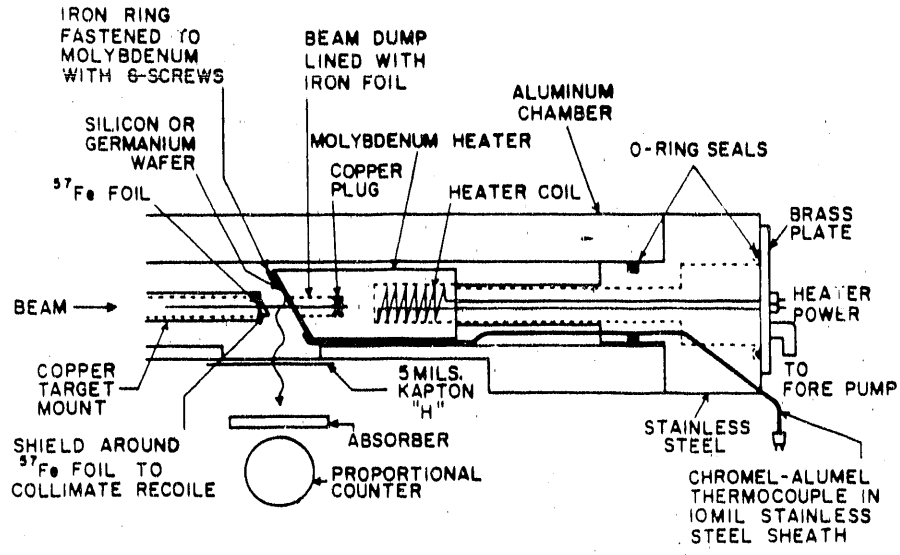

Fig. 1. Apparatus used for varying the temperature in in-beam implantation Mössbauer experiments (INBIME).

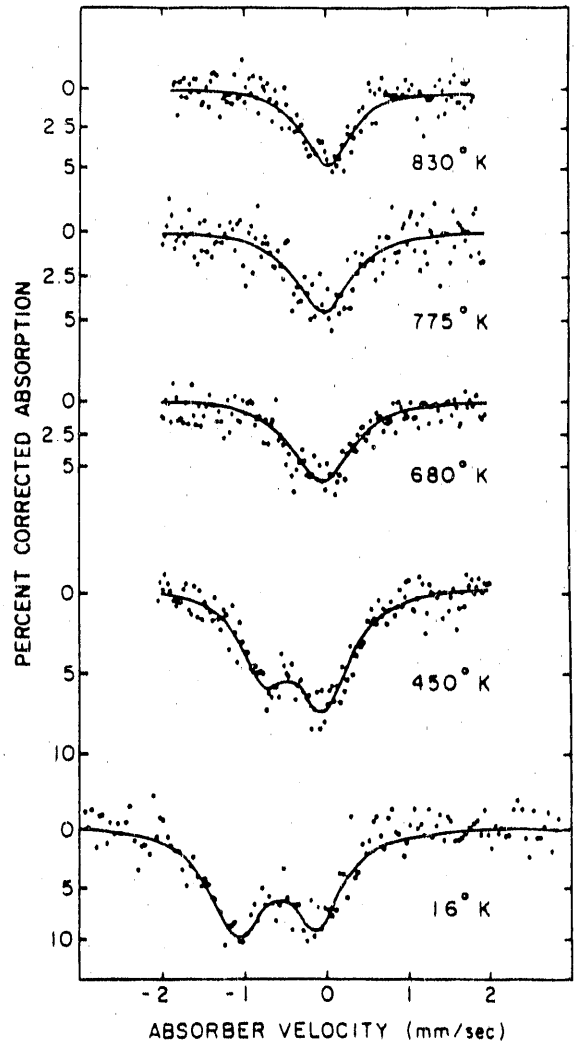

Fig. 2. Mössbauer spectra of ^{57}Fe implanted into germanium by means of a 64-MeV ^{35}Cl beam, at various temperatures.

(3) High purity (99.999%) Al was used as the implantation medium for the source.

(4) To tie the implantation measurements on $^{172,174,176}Yb$ to previous source experiments, ^{170}Yb was included in the ..ies as a source experiment, using neutron-irradiated $TmAl_2$ as the source. These latter runs were carried out in a "conventional" Mössbauer cryostat.

(5) The implantation runs were made in an in-beam, nitrogenless, helium cryostat to expedite changing absorbers. Two target-catcher assemblies were used in series, as shown in fig. 3, to increase the source strength.

(6) The basic feature of the method was to compare absorbers A and B (see fig. 3) simultaneously. After a run in the configuration AB the absorbers were interchanged and a run of equal duration was made in the configuration BA. In this way each absorber was exposed symmetrically to any possible imperfections in the Mössbauer drive.

(7) A large number of absorbers were measured so as to be able to select a suitable pair producing the maximum isomer shift. The results indicated that Yb_2S_3 and YbF_2 produced the maximum shift and they also gave good symmetric single-line spectra.

(8) The absorbers used in the implantation runs were "calibrated" with the ^{170}Yb radioactive source.

A typical result is shown in fig. 4. The most interesting feature of this experiment can be seen in this figure. Whereas the isotope ^{170}Yb shows a large shift between YbF_2 and Yb_2S_3, in ^{176}Yb the shift is essentially zero. Thus, the addition of a few neutrons produces a profound effect on the nuclear size of the rotating 2^+ level relative to that of the ground state. The final results are shown in fig. 5 and compared with other experiments

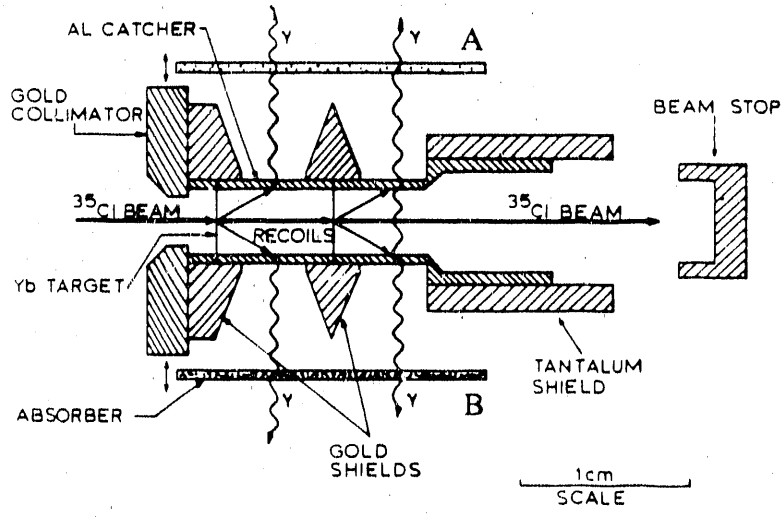

Fig. 3. Principal features of the apparatus used for nuclear excitation and recoil implantation through vacuum in a Mössbauer isomer-shift experiment. Note the series arrangement of two targets and two catchers used to increase the effective source strength.

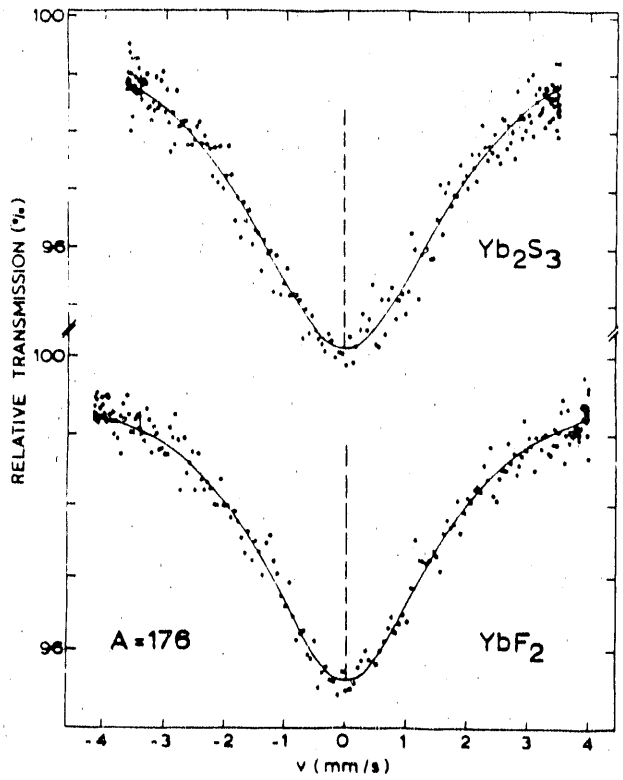

Fig. 4. Mössbauer absorption spectra of the 84 keV γ-rays of ^{170}Yb for the indicated ytterbium absorbers. The solid lines are least-squares fits of symmetrical Lorentzian lines to the data. The dashed lines indicate the centroids of the resonance dips.

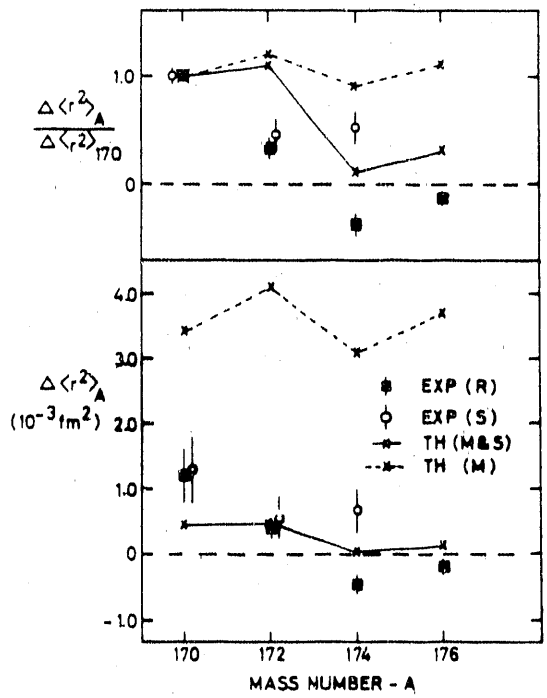

Fig. 5. Comparison of experimental and theoretical values of $\Delta\langle r^2\rangle_A$ and of the ratios to $\Delta\langle r^2\rangle_{170}$ for the $2^+ \rightarrow 0^+$ transitions in the even-even ytterbium isotopes. The letters (R) and (M&S) signify the present results and those of ref. 8), respectively. Other symbols refer to earlier work.

and with theory. At the top are plotted the ratios $\Delta\langle r^2\rangle_A/\Delta\langle r^2\rangle_{170}$ which need no calibration. At the bottom the values of $\Delta\langle r\rangle_A$ are given which require knowing the value of $|\psi(YbF_2)^2 - |\psi(Yb_2S_3)|^2$ at the nucleus.

In some cases an RIB facility would allow these isotopic series to be extended. Other dramatic changes in isomer shifts have been predicted[8]).

4. NMR spectroscopy

4.1. GENERAL

A radioactive ion beam would be very useful in nuclear magnetic resonance (NMR) spectroscopy in two respects. First, it would extend the very precise and relatively simple NMR method to the large number of new nuclides that would become available by the use of an array of new beams of nuclei. All the established techniques of the accelerated beam-NMR method[9,10]) would still be available. Moments of nuclei further from the valley of stability than heretofore measured would become accessible. Second, if polarized RIB's were available (see Section 8 below) the polarized beam-NMR method would become directly applicable to the beam nuclei and, by polarization transfer, to the products of reactions initiated by the polarized beam nuclei. In the following we discuss briefly some results of the polarized beam-NMR method in which polarized protons and radioactive tritons were used.

4.2. THE POLARIZED BEAM - NMR METHOD

Work has been carried out at the Ion Beam Facility of the Los Alamos National Laboratory to continue the measurement of magnetic moments of beta unstable nuclei using the polarized beam-NMR method. The polarized triton beam which is available at Los Alamos makes it possible to produce several nuclei whose magnetic moments are unknown. Using the polarized triton beam to initiate a nuclear reaction, the following nuclei have been produced: ^{8}Li, ^{11}Be, ^{12}B, ^{15}C, ^{16}N, and ^{20}F. Also, a polarized proton beam has been used to produce ^{23}Mg and ^{27}Si. Moments of the underlined nuclei have not been measured.

In the polarized beam-NMR method, the nuclei of interest are produced from the interaction of the polarized triton beam with a thick target, via (t,p) and (t,α) reactions. Polarization transfer in the reaction leaves the resulting beta-unstable nucleus polarized. The beta-decay asymmetry due to parity violation is used to detect this polarization. The target is maintained in a large homogeneous magnetic field to separate the Zeeman levels for the NMR measurement. The field also serves to decouple the polarization from depolarizing

mechanisms in the solid state environment. An RF field applied at the Larmor precession frequency induces transitions between the Zeeman levels and eliminates the beta-decay asymmetry. By simultaneous comparison of this frequency with the proton Larmor frequency in the same field, the unknown moment can be determined.

The experimental setup is similar to that used at Stanford in previous work with this technique[10]). Figure 6 shows the arrangement of the target chamber. The tandem source is a Lamb shift type polarized source which typically produces 100 nA of current, with a polarization of 75-85%. The source can be used to produce either polarized tritons or protons.

In searching for the NM resonance the data acquisition is completely automated allowing long frequency scans to be taken without any intervention from the experimenter. The Los Alamos polarized ion source is interfaced to the data acquisition computer so the spin of the polarized beam can be flipped as desired to offset instrumental effects. In addition, the value of the magnetic field is periodically measured by the data acquisition computer to monitor the stability of the field.

Many different targets have been examined to look for beta decay asymmetries. The measured experimental beta decay asymmetry is a function of the polarization transfer in the nuclear reaction, the beta decay asymmetry coefficient, and the relaxation time of the polarization in the solid state environment. This means that often a large number of combinations of target material, temperature, and beam energy must be tried to find a measurable beta decay asymmetry for a particular nucleus.

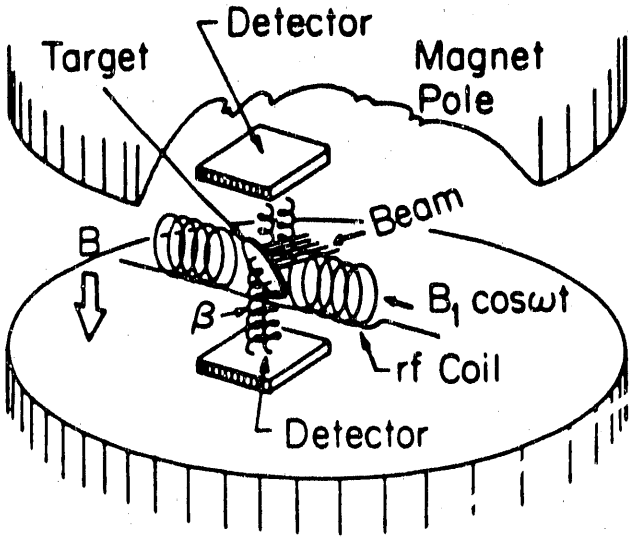

Fig. 6. Target chamber for beta-decay asymmetry measurements and NMR determination of nuclear moments.

As an example of the method fig. 7 shows the resonance curve for ^{8}Li implanted in ^{9}Be. The value obtained for the moment of ^{8}Li is in agreement with previously reported values[11]).

An NMR response was found at twice the normal Zeeman frequency for ^{12}B in an amorphous ^{13}C target. See fig. 8. This resonance is attributed to the cross-over transition between the +1 and -1 substates of the 1^{+} ground state of ^{12}B induced by the mixing of the ±1 and 0 substates in the large electric quadrupole field in the amorphous ^{13}C sample.

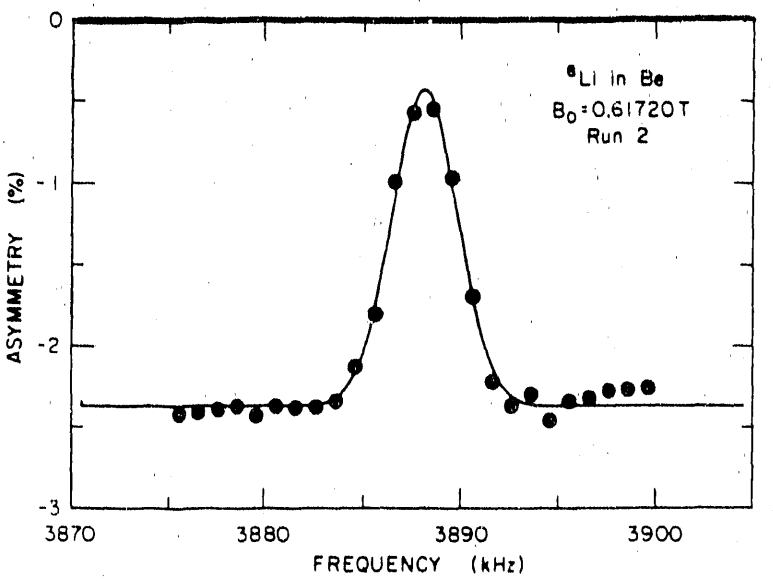

Fig. 7. Beta-decay-asymmetry/NMR curve for ^{8}Li implanted in polycrystalline Be metal. The frequency modulation is ± 5 kHz.

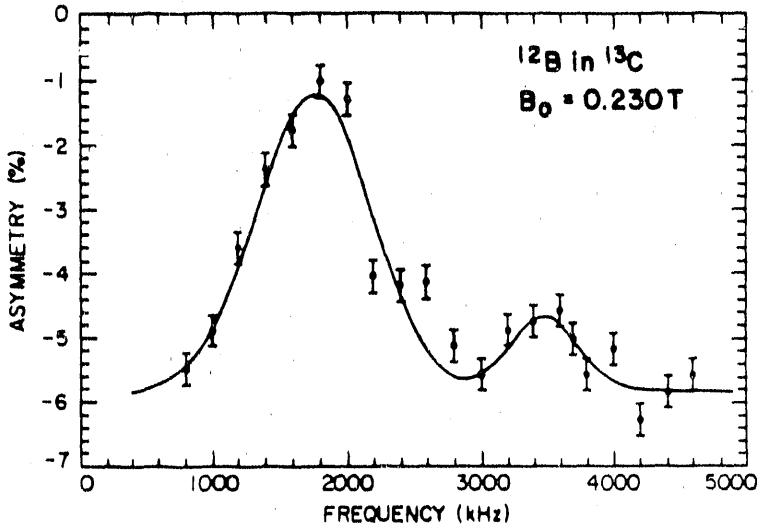

Fig. 8. The $\Delta m = \pm 1$ and $\Delta m = \pm 2$ NMR's of ^{12}B in amorphous ^{13}C at B_0 = 0.23T.

5. Low temperature nuclear orientation

The operation of a ^{3}He:^{4}He refrigerator coupled on-line to a mass separator is now an established means for orienting short-lived isotopes. The usual method of orientation is by the interaction of the nuclear magnetic moment with a magnetic field and the necessary condition is that the interaction strength μB is comparable to the Boltzman energy kT. The degree of orientation is proportional to $\exp(-\mu B/IkT)$. The low temperature is provided by the refrigerator while large magnetic fields may be obtained for most elements by including them in a suitable ferromagnetic host, such as iron or gadolinium, in which they experience the nuclear hyperfine field. An advantage of the method is that a relatively small external field is adequate to align the hyperfine field and specify its direction. Except for a few elements, e.g. those occurring in group II or those with $A < 20$, adequate fields can be achieved, and in general these far exceed a field that may be directly obtained from a superconducting magnet.

An extensive range of nuclear spectroscopy measurements may be carried out; α, β and γ-ray distributions may be measured and also static moments determined. Nuclear orientation (NO) experiments have an advantage over other equivalent methods. This is best illustrated by comparing γ-ray directional distributions from oriented nuclei to γ-γ directional correlations from a random nuclear ensemble. Both methods give information about the spin of nuclear states and the multipolarities of linking transitions. In the NO experiment the quantization axis is specified by the magnetic field direction rather than the emission direction of the first γ-ray in the cascade. Then the NO measurement has the considerable advantage that all γ-ray singles are counted, rather than selected coincidence cascades. This high counting rate is an important advantage since high precision data may be obtained in a comparatively short time which is very useful for accelerator based experiments. The same point can be made for distributions and correlations involving α and β particles.

Base temperatures as low as 5 mK are typical when a refrigerator is closed to all external heat sources. However, when implanting activity into the cold collecting foil, this foil is exposed to thermal radiation which enters along the path of the ion beam. It is this radiation, rather than the kinetic energy of the low intensity implanted ions, which limits the base temperature. In the on-line mode the temperature is limited by the cooling power to about 10 mK. This favorable operating condition is achieved by admitting the beam through a small aperture, a few mm in diameter, which is kept cold and which is about 1 m from the cold host foil. The beam is transported over this final section through a cold (4K), blackened tube containing several diaphragms. In this way radiation scattering is reduced and exposure of the host foil to thermal radiation is minimal.

The degree of orientation of the implanted nuclei depends on the nuclear spin-lattice relaxation time. If the half-life of the implanted nuclei is less or comparable to the relaxation time, the degree of orientation will be small. The orientation depends on both the strength of the hyperfine interaction and the temperature. For typical operating conditions most nuclei with $T_{1/2} > 1$ min will have a substantial orientation which often is unknown; however, this will not prevent useful nuclear spectroscopy information being obtained. For much shorter lived activities it may become necessary to orient the nuclei before implantation.

Radioactive beams, because of their anticipated low intensity, will pose further restrictions on the method and, in order to obtain a sufficient activity, it may be necessary to eliminate the mass-separation component from the system. In principle it should be possible to place a target foil in front of the cold ferromagnetic host. This target foil would be held at as low a temperature as possible and effectively close the system to thermal radiation. Recoils from the target could now enter the host foil and although these would be energetic their probable small intensity should not lead to a serious heating problem. However, the fraction of the beam that did not stop in the target foil could be a serious problem, and some simple selection of the ion species emerging from the target may be necessary.

The spectroscopy of short lived activities will undoubtedly depend on nuclear orientation techniques and, though often complex, these may offer many advantages which far outweigh their difficulties.

6. Few electron ions

6.1. ONE ELECTRON IONS

In the Recoil-Into-Plunger (RIP) method the nuclear state under study is produced by a nuclear reaction, which causes the excited nucleus to recoil forward out of a thin target at velocities that are several percent of the speed of light. The nucleus is stopped by a plunger (stopper), which can be set at a variable distance from the target. The γ-rays from a nucleus that decays in flight will be Doppler shifted, while those that come from a nucleus that has stopped in the plunger will be unshifted. This allows the stopped nuclei to be distinguished from the ones in motion.

When the nucleus is recoiling in vacuum, its spin also experiences a Larmor precession induced by the hyperfine field of the atomic electrons. For one electron ions the hyperfine field can be calculated exactly, since it is due to a single 1s electron. The Larmor precession can be measured by observing the destruction and restoration of the γ-ray angular distribution as the plunger is moved. The angular distribution is attenuated as the spins

precess but is restored at plunger settings that allow all the spins to precess through 180°, thus reproducing the original spin alignment. From the precession curve thus obtained the g-factor of the state can be extracted[12]).

A moment measurement was recently made[13]) on the 297 keV, 3⁻ state in ^{16}N. The state was populated with the reaction d(^{15}N,p)^{16}N. By inverting the reaction with a ^{15}N beam large recoil velocities were obtained. Measurements were made in coincidence with the outgoing protons at a beam energy of 34 MeV. A precession curve for the 3⁻ level, which shows the change in angular distribution as a function of plunger distance, is reproduced in fig. 9. Analysis of this curve gives: $g(^{16}N; 297, 3^-) = 0.409 \pm 0.025$.

6.2. FEW ELECTRON IONS

Previous experiments[14,15]) have demonstrated the feasibility of using external magnetic fields to decouple the magnetic hyperfine interaction in free ions as a means of measuring nuclear g factors. Here we report the use of this method on hyperfine interactions involving mainly the atomic M shell to measure the g factor of the second excited state of ^{40}Ca($I^\pi = 3^-$, $E_x = 3.737$ MeV, $\tau = 61$ psec)[16]). We believe this method could become very useful for radioactive ions with Z values so large that single electron ion production would be difficult.

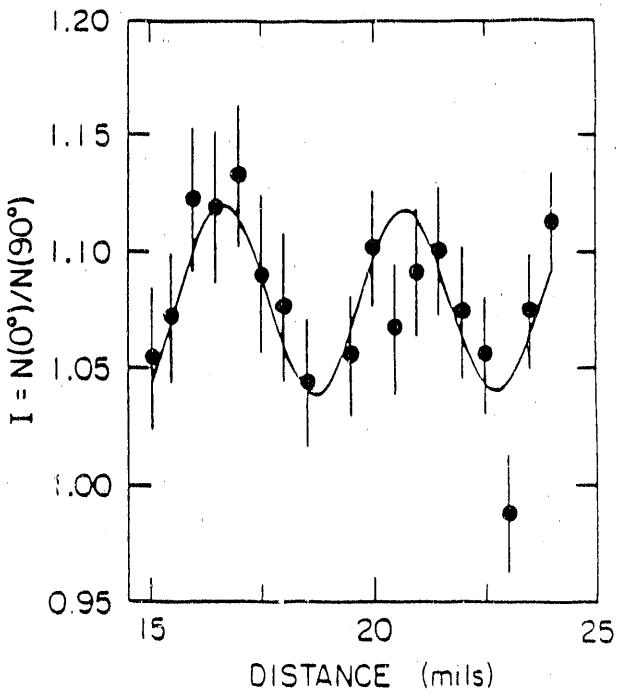

Fig. 9. Oscillation curve of the 297 keV, 3⁻ state of ^{16}N, showing the ratio of counts at 0° to those at 90° as a function of stopper distance. The solid curve is a least squares fit to the data giving $|g| = 0.50 \pm 0.03$.

As for one electron ions the method consists of exciting and orienting the nuclear state of interest by means of a nuclear reaction which also ejects the ions into vacuum from a thin target. The velocities imparted to the atoms are selected so that when they emerge from the target they are sufficiently ionized to produce hyperfine fields large enough to cause observable rotations of the nuclear spin and corresponding perturbations of the γ-ray angular distribution of the excited state. An external magnetic field is applied along the orientation axis (i.e., the beam direction) and increased until the nuclear moments are decoupled from the hyperfine fields (i.e., the Larmor precession of each atomic moment becomes so rapid that the nuclear moment can no longer follow it). The decoupling process can be observed through the perturbation of the angular distribution, and its dependence on the external field (the "decoupling curve") is a sensitive measure of the product of the nuclear moment and the atomic hyperfine fields.

The decoupling curve for the 3^- state of ^{16}O is shown in fig. 10. At the present time, the precision of the method for measuring moments rests primarily on the accuracy with which the atomic fields can be determined. Fortunately, it is usually possible to produce ionization states by appropriate velocity selection in which a single atomic configuration dominates the hyperfine interaction. These configurations are usually unpaired s states

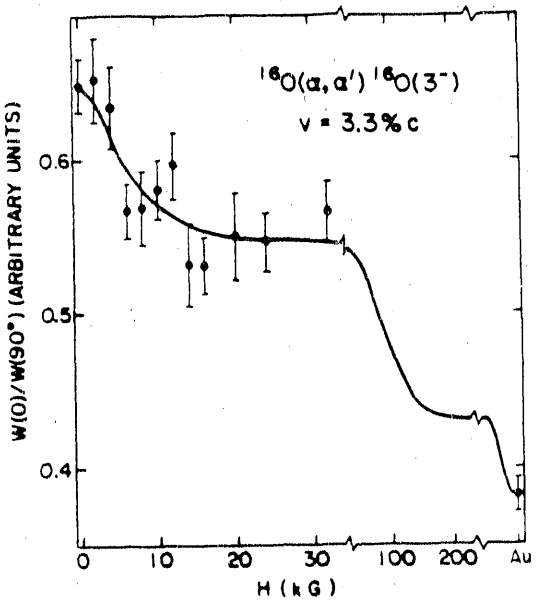

Fig. 10. Decoupling data for the 3^- state of ^{16}O. The drop above H = 30 kG is due to the 1s field.

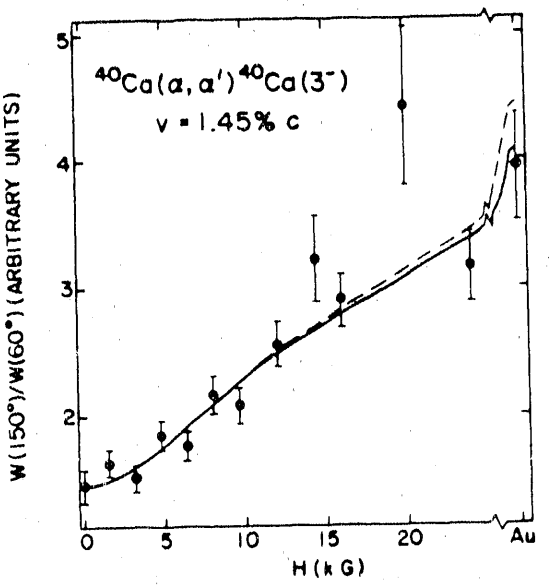

Fig. 11. Decoupling data for the 3^- state of ^{40}Ca. The curve is drawn for g = 0.56.

for which fairly reliable calculations can be made. Moreover, as the decoupling field is increased, the weak fields decouple first and the strong fields later on so that, to some extent, the various hyperfine fields are treated separately. This partial separation of the decoupling fields improves the accuracy of the analysis. In fig. 11 a decoupling curve is shown for the 3^- level of ^{40}Ca. Analysis of this curve gave a g-factor of 0.56 ± 0.13.

7. Transient fields

The large transient magnetic field that acts on fast ions passing through ferromagnetic media may be used to measure the magnetic moments of nuclear excited states with picosecond lifetimes. The magnetic precession of a gamma-decay angular correlation is a direct measure of the excited state g-factor if the transient field is known from empirical determinations or by calibration with a magnetic moment as measured by an independent technique. The large transient fields observed could most easily be explained by the capture of polarized electrons into s states of the fast ion; however, a detailed calculation of this process has not yet been given.

The transient field technique has recently been used to measure[17,18]) the g-factors of the 2^+ excited states in the isotopic sequence $^{122,124,126,128,130}Te$. The magnetic moments of the 2^+ states of ^{122}Te and ^{124}Te are known from independent experiments and these values were used to calibrate the transient field acting on fast Te ions in iron. With this calibration the g-factors of the other Te isotopes were obtained.

The results are compared with other measurements[19]) and with theory in fig. 12. The Te g-factors lie below the hydrodynamical values of $g = Z/A$, but are in better agree-

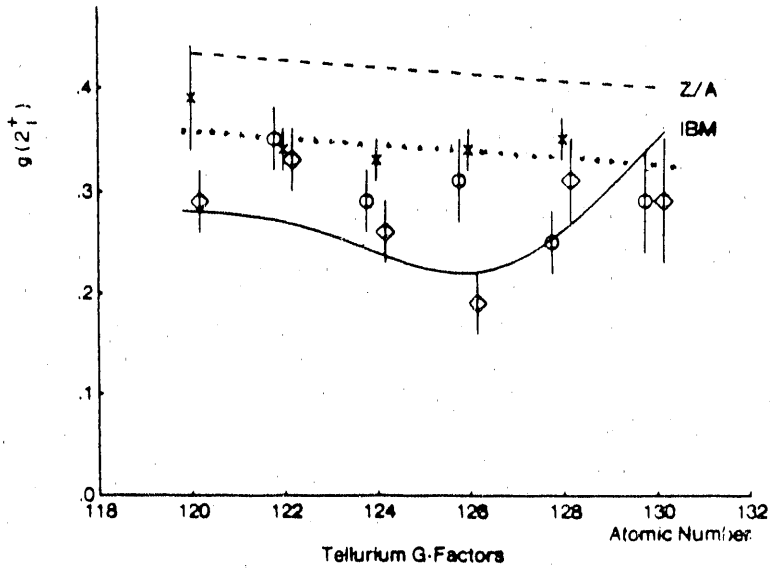

Fig. 12. The g-factors for the Te isotopes. The crosses, circles, and diamonds represent the data of ref. [18]), [17]), and [19]), respectively. The dotted and solid lines are from refs. [20]) and [21]), respectively.

ment with a calculation by Greiner[20]) that includes the effect of different pairing strengths for protons and neutrons. However, the agreement with the results of ref. [19]) is not good and leaves open whether there is a minimum in the trend as predicted by the IBM[21]).

It was this question that led to the modification of the standard transient field method[18]) in an attempt to reduce greatly systematic and in particular target related errors. In the new method magnetic moments for several isotopes are measured simultaneously by combining the isotopes in one target and then using Ge(li) detectors to separate the resulting γ-ray lines. In contrast to the standard method which measures the isotopes one at a time, errors arising from beam damage or target fabrication uncertainties are virtually eliminated since these now affect the isotopes uniformly. In addition the greatly increased resolution of the Ge(Li) detectors over the NaI detectors used previously eliminates many possible contaminants and uncertainties due to lineshape in the γ-ray spectra.

The advantages of the method are illustrated in fig. 13. The high resolution, the cleanliness of the spectrum, the insignificant background, and the almost complete lack of contaminant lines are clearly apparent. Also, the relative intensities of the lines can be pre-selected by mixing the isotopes in the target in the desired proportion.

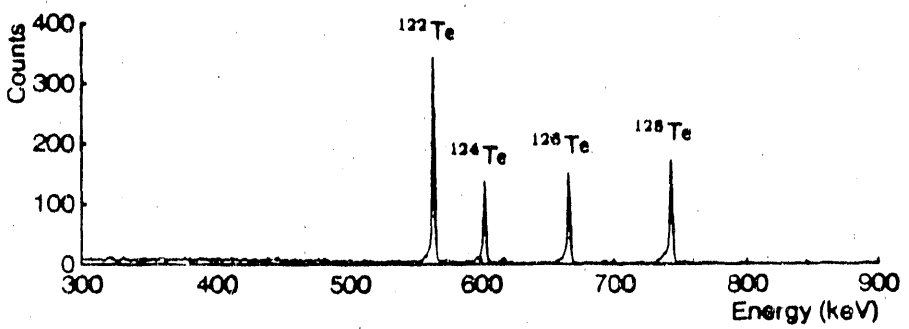

Fig. 13. Gamma rays from four Te isotopes observed in the method of ref. [18]).

8. Polarized beams

In planning any new accelerator facility for nuclear physics, the desirability of producing polarized beams arises because of the many important phenomena that polarization produces or elucidates. The only significant requirement that polarization introduces into the technology of producing polarized short-lived radioactive beams is the obvious one that the polarization process must be essentially on-line with the production of the beam. Since

the possibility exists of making all polarization processes used so far on-line we shall discuss the general question of producing polarized beams while pointing out, when necessary, the modifications required by the radioactivity.

Two successful approaches have been made to the production of polarized beams of nuclei. In the first, the nuclei are polarized before being accelerated to form polarized beams; in the second, the polarized beams are produced from nuclei that have already been accelerated. We start with the first approach.

8.1. POLARIZATION BEFORE ACCELERATION

There have been two successful types of polarized ion sources developed over the past 25 years: the atomic beam source[22]) and the Lamb-shift source[23]). The basic source in either case is the hydrogen source which has been extensively developed and widely used[22,24]). In fact, the production of polarized radioactive tritium beams has been achieved with the Lamb-shift source[25]) but could just as well be produced by atomic-beam sources. In recent years progress has been made in developing laser driven or laser assisted ion sources[26,27]). Since atomic beam sources can be used for a large variety of nuclear species and are amenable to the use of lasers we shall restrict the discussion to atomic beam sources.

In a typical gaseous atomic beam source neutral atoms are produced by dissociating molecular gas in a discharge excited by a radiofrequency oscillator. A supersonic flow of atoms emerges from the dissociator nozzle and is collimated by an aperture. Atoms not passing through the aperture are removed from the system by large capacity diffusion pumps.

The collimated atomic beam is then passed through the strong, inhomogeneous magnetic fields of two sextupole magnets. In the large field gradients of the sextupole magnets atoms with spin projections along the field $M_J > 0$ are deflected towards regions of weaker fields and are thereby focused onto the sextupole axis. Atoms with $M_J < 0$ are deflected away from the sextupole axis and hence out of the beam. In the region of this defocused beam, non-focused contaminants and surplus gas are removed by large capacity diffusion pumps in the sextupole region. The result is a beam of polarized neutral atoms.

the possibility exists of making all polarization processes used so far on-line we shall discuss the general question of producing polarized beams while pointing out, when necessary, the modifications required by the radioactivity.

Two successful approaches have been made to the production of polarized beams of nuclei. In the first, the nuclei are polarized before being accelerated to form polarized beams; in the second, the polarized beams are produced from nuclei that have already been accelerated. We start with the first approach.

8.1. POLARIZATION BEFORE ACCELERATION

There have been two successful types of polarized ion sources developed over the past 25 years: the atomic beam source[22]) and the Lamb-shift source[23]). The basic source in either case is the hydrogen source which has been extensively developed and widely used[22,24]). In fact, the production of polarized radioactive tritium beams has been achieved with the Lamb-shift source[25]) but could just as well be produced by atomic-beam sources. In recent years progress has been made in developing laser driven or laser assisted ion sources[26,27]). Since atomic beam sources can be used for a large variety of nuclear species and are amenable to the use of lasers we shall restrict the discussion to atomic beam sources.

In a typical gaseous atomic beam source neutral atoms are produced by dissociating molecular gas in a discharge excited by a radiofrequency oscillator. A supersonic flow of atoms emerges from the dissociator nozzle and is collimated by an aperture. Atoms not passing through the aperture are removed from the system by large capacity diffusion pumps.

The collimated atomic beam is then passed through the strong, inhomogeneous magnetic fields of two sextupole magnets. In the large field gradients of the sextupole magnets atoms with spin projections along the field $M_J > 0$ are deflected towards regions of weaker fields and are thereby focused onto the sextupole axis. Atoms with $M_J < 0$ are deflected away from the sextupole axis and hence out of the beam. This defocused beam, non-focused contaminants and surplus gas are removed by large capacity diffusion pumps in the sextupole region. The result is a beam of polarized neutral atoms.

8.1.1. Polarized hydrogen beams

For ^1H the splittings of the atomic hyperfine states as a function of the applied magnetic field are shown in fig. 14. In the strong inhomogeneous fields of the sextupole magnets only states 1 and 2, with $M_J = 1/2$, have a high probability of transport through the sextupole region. Two methods exist for converting the atomic polarization to nuclear polarization: the weak field and the strong field (or adiabatic passage) techniques. In the former method the polarized atoms pass from the region of strong field in the sextupoles ($B > B_c$) to an applied weak field ($B \lesssim B_c$) where the states with rearranged spins are designated by $M_F = +1,0$ to produce a net nuclear polarization of 50% (see fig. 14).

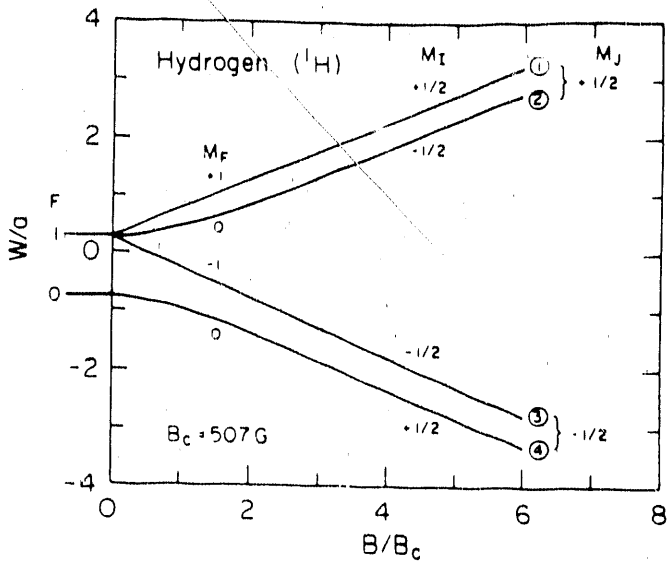

Fig. 14. The hyperfine levels of ^1H ($I = 1/2$, $J = 1/2$) as a function of applied magnetic field B. Energies are in units of $a = \Delta\upsilon[F = 1 \rightarrow F = 0] = 1420.4$ Mhz.

For ^1H a theoretical nuclear polarization of 100% can be attained by the use of the adiabatic passage technique. In this method a single rf transition unit is tuned to induce transitions in a strong field from state 1 to state 3. State 3 with $M_J < 0$ produces the same 100% nuclear polarization as state 2 in a strong magnetic field (see fig. 14). This technique is now widely used.

Following the creation of the nuclear polarization the neutral beam is then appropriately ionized and accelerated for injection into an accelerator. The properties of the beam should be carefully matched to the type and input parameters of the accelerator: tandem, cyclotron, linac, etc. This type of ion source is also routinely used for polarized ^2H with adjustments made for the change in the hyperfine diagram resulting from the change in the nuclear spin ($1/2 \rightarrow 1$). With ^2H tensor polarization is possible and readily achieved.

8.1.2. Other polarized beams

Polarized beams of other nuclear species have now been produced[27,28]). In the following we discuss briefly the ^{19}F, ^{14}N, $^{6,7}Li$, and ^{23}Na cases, all of which, with appropriate modifications, could be applied to radioactive species, e.g., ^{20}F, ^{13}N, ^{8}Li and ^{24}Na. An obvious but significant modification in each case arises from the change in the hyperfine diagram caused by the different spin of the radioactive isotope.

Atomic fluorine has the electronic ground-state configuration $^2P_{3/2}$ and a nuclear spin + 1/2 leading to the hyperfine levels shown in fig. 15. Passage of atomic ^{19}F through the sextupole magnet system separates the states with electron spin projection numbers M_J = 1/2, 3/2 from those with M_J = -1/2, -3/2.

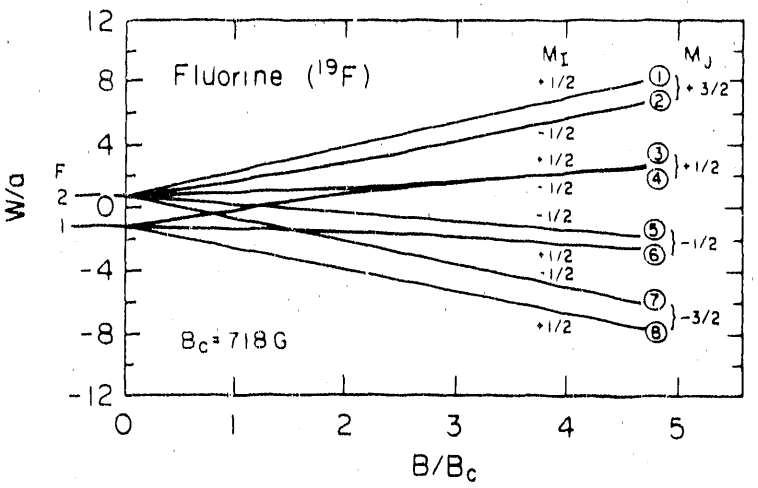

Fig. 15. The hyperfine levels of $^{19}F(I = 1/2, J = 3/2)$ as a function of applied magnetic field. Energies are in units of $a = 0.5\ h\Delta\upsilon(F = 2 \rightarrow F = 1) = 8.31 \times 10^{-6}$ eV.

Molecular fluorine possesses a low dissociation energy, making it attractive for dissociation in an rf discharge. Preliminary tests and calculations showed that polarized atomic fluorine could be produced and if suitable rf transitions (two, in this case) were applied in a strong field a sizable nuclear polarization would be obtained[28]). The chemical reactivity of atomic and molecular fluorine does necessitate some modifications in the atomic beam apparatus[28]).

Having an electronic configuration $^4S_{3/2}$ and nuclear spin I = 1, ^{14}N presents a more complex level diagram in an applied magnetic field (fig. 16). Still, in passing through a sextupole magnet, nitrogen atoms in states of M_J = + 3/2, + 1/2 (states 1 through 6 in fig. 16) will be focused along the beam axis whereas those with M_J = -1/2, -3/2 (states 7 through 12) will be defocused. The possibility of inducing rf transitions (four in number) between appropriate states to produce nuclear polarization, has been investigated theoretically in some detail[28]).

The obvious choice for producing atomic ^{14}N, nitrogen gas, is not useful because of the relatively high molecular dissociation energy of 9.76 eV, which is considerably larger than plasma electron energies in a typical rf discharge. After considering several other gases containing nitrogen, ammonia (NH_3) was singled out as the most likely candidate for efficient dissociation[28]). It seemed plausible that ammonia molecules could be dissociated by electron impact in three steps: $NH_3 \rightarrow NH_2 + H$, $NH_2 \rightarrow NH + H$, $NH \rightarrow N + H$, each step requiring only about 3 eV. Tests showed that a good beam of atomic N was produced with NH_3 in the dissociator.

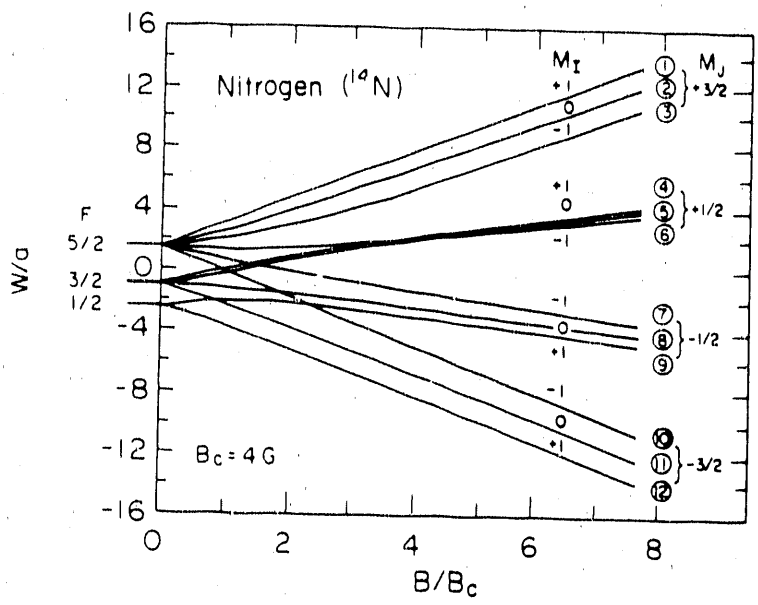

Fig. 16. The hyperfine levels for ^{14}N(I = 1, J = 3/2) as a function of applied magnetic field B; a = 10.45 MHz.

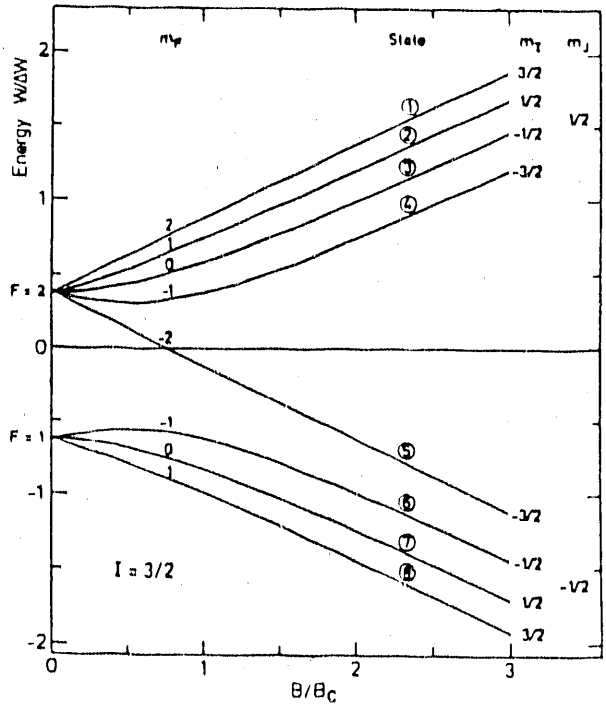

Fig. 17. The hyperfine levels of alkali atoms, ^{7}Li, ^{23}Na, ^{39}K, ...(I = 3/2, J = 1/2) as a function of applied magnetic field; a = $\Delta\upsilon$ [F = 2 $\rightarrow$ F = 1].

A partial list of other nuclei that can be polarized by the atomic beam method is given in table I, together with some of their important hyperfine and nuclear properties. The Heidelberg-Marburg group[29]) has produced beams of polarized ^{6} Li and ^{23}Na for injection into a tandem accelerator[27,29]). The hyperfine level diagram appropriate for the alkali atoms with I = 3/2 (^{7}Li, ^{23}Na, ^{39}K ...) is shown in fig. 17.

The Heidelberg-Marburg ^{23}Na source is also optically pumped in order to enhance the polarization. The principle[26,27]) is shown in fig. 18. Optical pumping with circularly polarized light induces transitions with $\Delta M_F = +1$ for right-handed polarization and vice versa for opposite polarization. In the ideal case this results in pumping all the levels into one hyperfine state with the maximum value of $|M_I|$ (see fig. 18).

8.1.3. Interface to source of radioactive species

In order to use the atomic beam method in conjunction with radioactive species produced by an accelerator three problems will need to be addressed:

(1) The atomic beam (or other type of) source will need to be made just as efficient as possible to balance the inherent low intensities of the radioactive isotope production. This will mean maximizing both the intensity and polarization of the source. Ideas for achieving the former are discussed elsewhere[28]); the latter will almost certainly require the use of laser techniques, including the possibility of a completely laser driven procedure[30]). An attempt to achieve these goals is being made at Heidelberg where a super high intensity, large polarization source is being developed for use in producing a polarized hydrogen je target for a $\bar{p} + \vec{p}$ experiment[31]).

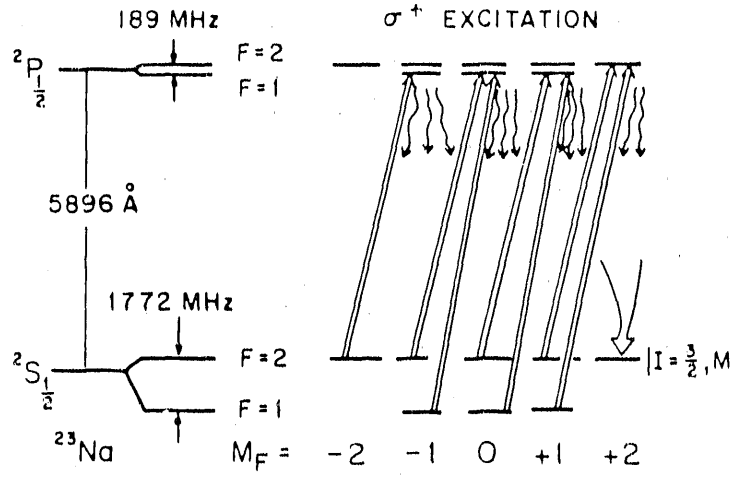

Fig. 18. Principle of laser driven polarization of ^{23}Na. The optical pumping diagram for ^{23}Na is shown. The atoms are pumped to the M_F = 2 (M_I = 3/2) Zeeman substate. Ref. [26]).

TABLE I.

List of possible polarized heavy ion beams. Q/ZeR^2 gives the deformation of the nucleus. f is the ratio of spin precession angle and deflection angle in a magnetic field for singly charged ions. Ref. [29].

Nucleus	I^π	$B_{crit.}$ (mT)	$f = gA/2$	Q/ZeR^2
^{6}Li	1^+	8.2	2.5	0.00
^{7}Li	$3/2^-$	28.8	7.6	-0.23
^{23}Na	$3/2^+$	63.3	17.0	0.15
^{39}K	$3/2^+$	16.5	5.1	0.03
^{133}Cs	$7/2^+$	328	49.0	0.00
^{19}F	$1/2^+$	71.7	50.0	-
^{35}Cl	$3/2^+$	21.0	9.6	-0.04
$^{79(81)}$Br	$3/2^-$	102 (108)	55.5(61.3)	0.05(0.04)
^{127}I	$5/2^+$	124	71.3	-0.06
^{115}I	$9/2^+$	12021	70.7	0.08

(2) Proper hyperfine techniques and parameters for each desired radioactive isotope and appropriate rf and laser transitions will need to be worked out and implemented.

(3) A suitable interface between the production of the radioactive isotope and the polarized ion source must be developed. Preliminary thought has been given to this problem[32]. However, techniques for collecting, thermalizing and transporting desired isotopes from high energy production facilities, such as GSI, ISOL, and the input to the proposed RIB, have yet to be worked out.

8.2. POLARIZATION AFTER ACCELERATION

We now turn to the problem of producing polarized radioactive nuclei and beams from accelerated beams of polarized or unpolarized particles. Since the available processes are inherently on-line they are generally quite suitable for radioactive isotopes.

There have been three methods developed to produce polarized nuclei from accelerated beams.

(1) Very early the so-called double scattering experiments were carried out, in which polarized nuclei were produced in a nuclear reaction and then analyzed in a second reaction. The Osaka school has developed this concept to produce polarized radioactive beams from nuclear reactions[9]) (see fig. 19) that have been used in a variety of applications. In this technique the intensity of the beam is limited by the necessity to restrict the angular spread of the polarized recoil beam because it is a secondary beam. On the other hand, very intense unpolarized primary beams are now available and suitable lenses can be used to concentrate the recoil beam.

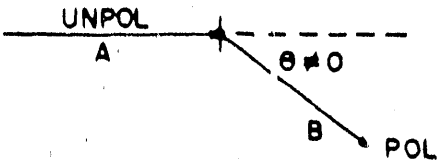

Fig. 19. Production of polarized nuclei from nuclear reactions.

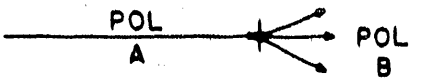

Fig. 20. Production of polarized nuclei from polarized beams.

(2) At Stanford the approach has been to collect all the polarized reaction products that are produced by polarization transfer in a nuclear reaction induced by a polarized beam[33]) (see fig. 20). The polarized recoils can be collected in the target itself or in a separate implantation medium; or they can be formed into a beam by selecting appropriate (endothermic or inverse) reactions that produce restricted kinematic cones in the forward direction and then further concentrated by suitable lenses if desired. Polarized beams of relatively high intensity can be produced in this way.

(3) A very promising development is the use of tilted surfaces to polarize ion beams. Two manifestations of this phenomenon have been utilized. In one, the ion beam passes through a tilted foil[34]) (see fig. 21). Upon emergence from the second surface the unequal drag produced by the tilt of the surface on the electrons of the ion produces a col-

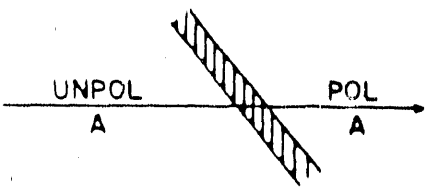

Fig. 21. Production of polarized nuclei from a tilted foil.

Fig. 22. Production of polarized nuclei from grazing reflection.

lective electronic polarization that is subsequently converted to nuclear polarization by the hyperfine interaction. An important feature is that the atomic polarization (of opposite sign) produced in the first surface is destroyed by the multiple collisions inside the foil.

In the second type of surface interaction the ion beam is reflected at grazing incidence from a surface[35]) (see fig. 22); again the drag produced by the interaction of the ionic electrons with the surface induces a polarization that is then transferred to the nucleus. Both these techniques can be used at low or high velocity, i.e., before or after acceleration. In practice, it is found necessary to use many successive surface interactions in order to build up usable polarizations.

In the following we shall discuss examples of these methods of producing polarized nuclei.

8.2.1. Polarization by nuclear reaction

An Osaka group[36]) has produced a polarized beam of radioactive ^{15}C ions from the reaction $^{232}Th(^{15}N, ^{15}C)$. The reaction products including ^{15}C, ^{16}N, and ^{17}N ions are selected at $\theta = 25°$ and passed through a large spectrometer which separates ^{15}C from the other products (see fig. 23). The polarization produced at the chosen angle and retained after passage through the spectrometer is sufficient (~4%) to produce a measurable β-decay asymmetry from ^{15}C after it is implanted into high-purity graphite.

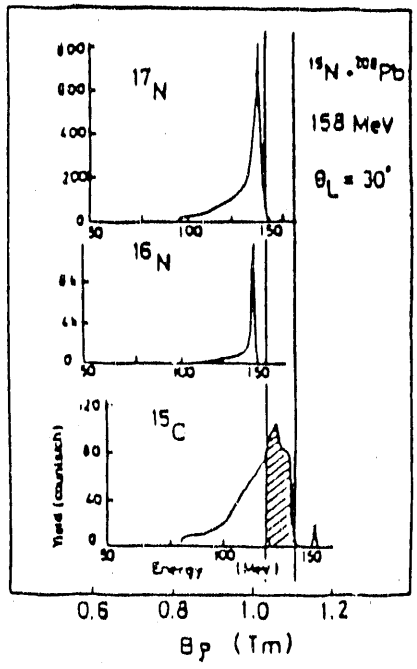

Fig. 23. Separation in a spectrometer of nuclei polarized in a nuclear reaction.

8.2.2. Polarization by polarization transfer

An example of the use of a polarized beam to produce polarized nuclei by polarization transfer can be found in the experiment that measures the β-decay asymmetry of ^{8}Li as a function of the β energy. Polarized ^{8}Li nuclei are produced by means of the $^{7}Li(\vec{d},p)^{\overrightarrow{8}}Li$ reaction. This experiment was first carried out at Stanford[37]) and has since been continued at Wisconsin[38]). The method of

producing the polarized nuclei provides a significant improvement over previous measurements of this kind since it provides significantly larger counting rates which allow much better statistics to be obtained. The greater precision not only makes it possible to decrease systematic errors (by facilitating tests) but also makes the result sensitive to details of the β-decay interaction that were not accessible before. The result of these experiments can be fitted with "good" shell-model wave functions for the pertinent states and is based on CVC but no second class currents in the beta decay. However, the test for second class currents is not very stringent as the result is not very sensitive to them in this case.

A further example of the use of a polarized beam to produce polarized nuclei whose moments were then measured by NMR[33]) is shown in fig. 24. Polarized ^{8}Li nuclei were produced from ^{7}Li($\vec{d}$,p)$\vec{^{8}\text{Li}}$ and allowed to implant in a target of $LiIO_3$. In this solid state medium the ^{8}Li nuclei are subject to an electric field gradient which perturbs the Zeeman splitting in the field B_0, as shown in the insert in fig. 24. The polarization is observed by measuring the β-decay asymmetry of $^{8}\vec{\text{Li}}(\beta)^{8}$Be. The rf field applied to the sample partially destroys the asymmetry when its frequency comes into resonance with one of the transitions in the Zeeman diagram. The technique is enhanced when three of the transitions are already saturated while the fourth is probed by the rf field. The resulting four resonances are shown in fig. 24. A knowledge of the electron field gradient allows the quadrupole moment of ^{8}Li to be extracted, $|\,Q(^{8}\text{Li})/Q(^{7}\text{Li})\,| = 0.77(6)$, where $Q(^{7}\text{Li})$ is known.

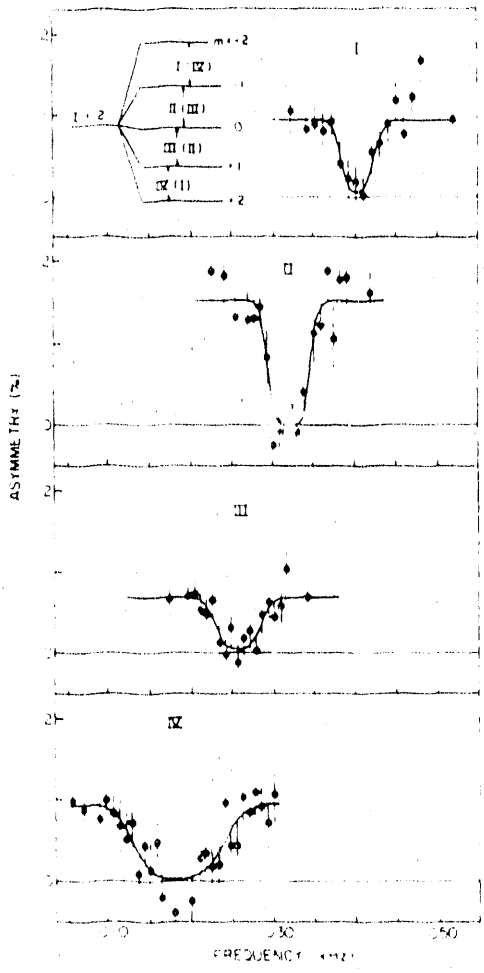

Fig. 24. The four resonances of the quadrupole perturbed NMR spectrum of polarized ^{8}Li implanted in $LiIO_3$. The level splittings corresponding to the resonances are shown in the insert.

8.2.3. Polarization by tilted surfaces

We begin with an experiment[39]) in which a heavy ion beam is polarized by a tilted foil polarizer and the polarized beam is then used in a subsequent reaction. A beam of ^{27}Al ions from an accelerator is passed through a multifoil assembly tilted at +60°. The direction of the polarizer can be easily reversed by rotating it through 180° to make the tilt angle -60°. The polarized beam interacts with a thin C target and ^{27}Al projectiles are Coulomb excited. The polarization sensitivity of this interaction is observed by detecting the left-right asymmetry of the C recoils responsible for the interaction. This is accomplished by tagging the recoils with de-excitation γ rays from the Coulomb excited ^{27}Al states. This successful experiment not only demonstrates the feasibility of making heavy-ion polarimeters in this way, but also points the way for the routine use of tilted foils in the production of polarized heavy-ion beams.

Another example of separating and forming a beam of heavy ions from a nuclear reaction by means of a spectrometer is afforded by work at Rochester[40]). In this experiment ^{33}Cl nuclei were produced in the reaction ^{2}H(^{32}S,^{33}Cl)n and separated in a recoil mass spectrometer (RMS). They then were polarized by passage through an assembly of 10 tilted foils (see fig. 25). The ^{33}Cl polarization was determined by observing the asymmetry in the β decay from the ^{33}Cl ions implanted in a NaCl single crystal. The magnetic moment of ^{33}Cl was then measured by the method discussed in Section 4 above. This was the first use of tilted foils in this type of experiment.

The possibility of using tilted foils (or grazing surface reflections) in a dedicated manner to polarize heavy-ion beams that have already been accelerated is strengthened by

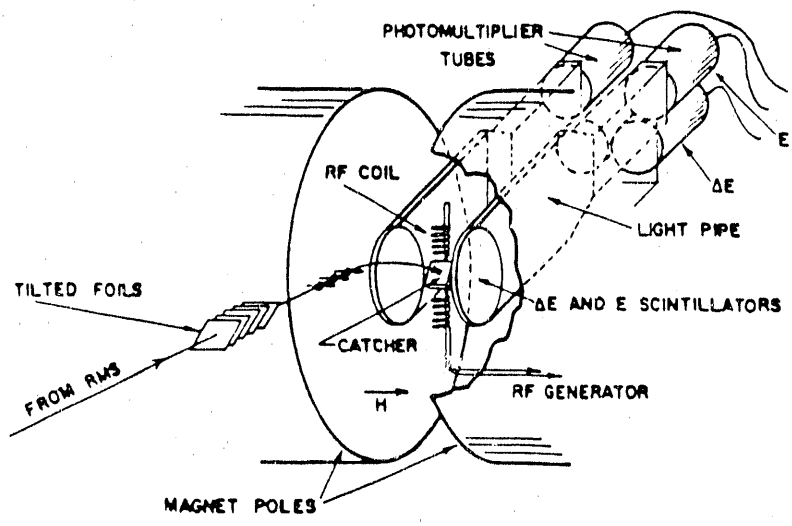

Fig. 25. Polarization by tilted foils of nuclei separated by a recoil-mass-spectrometer.

the successful use of large numbers of tilted foils[41]). In arrangements such as shown in fig. 26 up to 40 tilted foils have been used and nuclear polarizations up to 20% have been attained. In these applications the basic foil has been made of carbon with thicknesses in the few $\mu g/cm^2$ range. Clearly, in a dedicated use of tilted foils to produce polarized beams in a routine manner, the foils will need to be reliable and to withstand prolonged bombardment by heavy ions. It will therefore be necessary to carry out R and D to find the strongest a... most resilient foils and to develop the technique of rotating or oscillating the foils to prolong their life. The use of grazing reflection from a surface would clearly be much less subject to breakage and damage and multiple reflections might be achieved by use of a suitably curved surface (see fig. 27).

In summary we believe that, if the production and acceleration of radioactive nuclei becomes a reality, it will be possible to polarize these beams either by pre- or post-acceleration processes. We would predict that in the case of vector polarization the standard

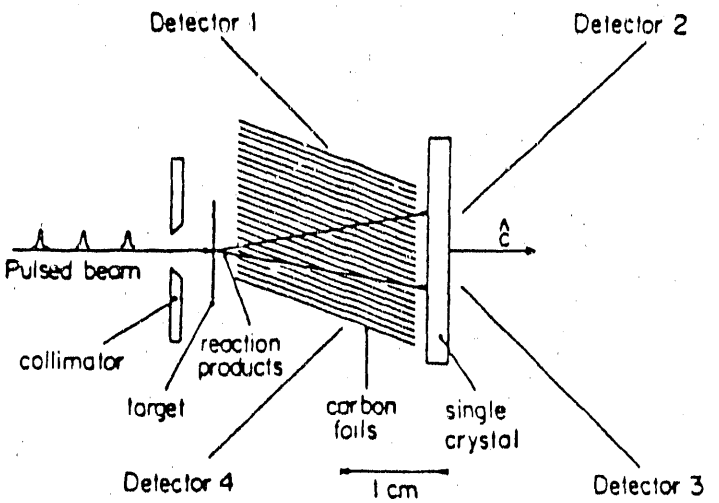

Fig. 26. Use of many tilted foils to polarize recoil ions.

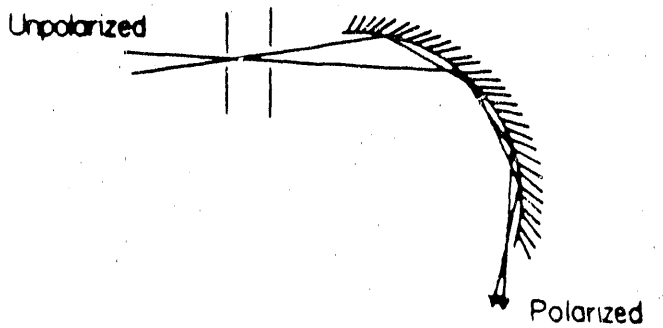

Fig. 27. Schematic representation of a possible scheme for producing polarization by multiple grazing reflections from surfaces.

method might well become the dedicated use of multiple interactions with tilted surfaces, either by transmission or reflection. This technique is both relatively simple and inexpensive. For larger polarizations and production of tensor polarization, a laser assisted atomic beam source might prove to be the best choice. Finally, it might well be desirable to combine both pre- and post-acceleration polarizers in order to produce the maximum polarization, which is of crucial importance in the use of low intensity beams, since the appropriate figure of merit is P^2I.

9. Radioisotopes

The discipline of nuclear medicine is comprised of that segment of the health sciences devoted to the development of radioactive tracer methods for the study of diseases, and the development of diagnostic and therapeutic procedures which influence the care of patients afflicted with various diseases. The field of nuclear medicine had its genesis in the 1930's when radioactive isotopes became available from early models of the cyclotron in Berkeley. Following the second world war, reactor produced radioisotopes were distributed from Oak Ridge for research in the physical sciences and medicine. Since then nuclear medicine has grown at a rapid pace, spurred by the development of the rectilinear scanner, the gamma camera, the Mo/Tc radioisotope generator, commercial cyclotrons, and positron emission tomography.

Federal support and leadership, under the auspices of the AEC and its successors, have been responsible for the development of the field. The DOE nuclear medicine program overlaps significantly other federal basic and applied chemistry, engineering and physics programs, and NIH programs which emphasize the study of disease processes. The major advantage derived from conduct of nuclear medicine programs under DOE auspices is the opportunity for utilization of major investments by DOE in facilities and personnel in the fields of basic physical research and engineering. This has allowed the conduct of productive nuclear medicine research and efficient technology transfer at a cost that is small relative to the investments and to costs that would be required in the absence of close programmatic relationships. The essential multidisciplinary character of nuclear medicine research has benefited greatly from the close interaction of many technical and clinical disciplines.

Most radionuclides used in clinical medicine are now produced by industry. A recent marketing and forecast report by the Market Intelligence Research Corporation suggests that the radiopharmaceutical market will experience exponential growth during the next five years, approaching $3 billion in 1995 as compared to $200 million in 1990.

Meanwhile, research on new radionuclide production technology is being conducted at advanced accelerator facilities at Los Alamos and Brookhaven. The Society of Nuclear Medicine and The American College of Nuclear Physicians have expressed concern that DOE support for isotope production is decreasing and that this could have a serious negative impact on field of nuclear medicine[42-44]).

In addition to nuclear medicine, radionuclides are also applied in numerous other ways to facilitate scientific investigations. They are used by biologists, nutritionists, and biochemists to study biochemical processes in healthy and diseased physiological systems. They can be used to trace geochemical pathways and to assess models of elemental economies within the earth's ecosystem. Radionuclides have been used to investigate the mode of action and environmental fate of pesticides. They are being used to evaluate and monitor environmental protection and clean-up systems. Several nuclides are used as x-ray sources for analytical and medical applications. The nuclear power industry depends upon specific radioisotopes for the calibration and quality assurance of their radioassay instruments and procedures. Other industries use them to develop and evaluate chemical processes. Physicists have used them to experimentally assess nuclear and astrophysical models, measuring reaction cross-sections, studying hyperfine interactions, and performing other basic studies.

It is apparent that radionuclides serve a major function in advancing all areas of science. It is therefore quite appropriate to evaluate how any new beam facility could incorporate radioisotope production for these applications. For the nuclear medicine applications isotopic half-lives range from a few seconds (usually obtained from radioisotope generator systems) to years. However, the most commonly used nuclides have half-lives in the range of hours to a few days. Monthly demand is generally in the millicurie to kilocurie range. It is often important that the isotopes be produced in very high specific activity. Perhaps the most important criteria to be met is that medical radioisotopes must be available throughout the entire year. Thus for medical applications the most important considerations are the radioisotope yield and regular availability. Post separator acceleration does not appear to be an important factor.

An RIB facility designed to incorporate on-line mass separation of nuclides could be used very effectively to measure spallation production "cross-sections" of radioisotopes identified as valuable or potentially valuable. Thick-target yields for a variety of isotopes have been measured, with the ISOLDE facility. These data indicate that some nuclides can be collected in significant quantities. For example, ^{153}Sm is a beta emitting isotope with significant potential as an in-vivo therapeutic agent. The quoted ISOLDE yield for this isotope is 8.70×10^7 ions per second per microampere of proton current on a Gd/La alloy

target. At this rate, it would be possible to produce about 0.5 Ci of ^{153}SM per day, with high specific activity, on a high current proton accelerator. This could be collected prior to post acceleration in an RIB facility, while passing some other isotope into the ion accelerator. The isotopes ^{127}Xe (0.2 Ci/day) and ^{68}Ga (1 Ci/day) are two other examples of medically important isotopes that could likely be recovered in significant quantities after on-line separation as part of an ion-beam facility. The collection of separated ^{123}X and subsequent recovery of ^{123}I is another example that was discussed.

In the event the RIB facility were to employ a thin production target as the source of materials for the separator and post accelerator, it would be possible to incorporate a radioisotope production targeting system immediately downstream that would utilize the excess primary beam. Very high specific activity radioactive targets and/or sources could be prepared by post-separator deceleration and collection on a suitable backing material. These targets and sources, which are difficult to prepare using currently existing techniques, would be extremely useful for important on-line nuclear reaction cross-section measurements or as x-ray sources for analytical and medical applications.

It was apparent from the discussions held during the RIB Workshop that the design of the future facility should incorporate capabilities to accommodate the separation and recovery of separated isotopes for subsequent applications in medicine and physical research. It is believed that including "practical" applications in the proposal would strengthen the justification for building the facility.

References

1) J.G. Stevens and V.E. Stevens, Mössbauer Effect Data Index, vol. 1975 (Plenum, New York, 1976)
2) J.A. Sawicki, Proc. Accelerated Radioactive Beams Workshop, Parksville, Canada, 1985, ed. L. Buchmann and J.M. D'Auria, TRI-85-1 (TRIUMF, Vancouver, 1985) p. 307
3) H. de Waard and L. Niesen, Mössbauer Spectroscopy Applied to Inorganic Chemistry, vol. 2, ed. G.J. Long (Plenum, New York, 1987) p. 1
4) R.D. Taylor and M.P. Pasternak, Hyperfine Interactions (1990), to be published.
5) G.L. Latshaw, P.B. Russell and S.S. Hanna, Hyperfine Interactions **8** (1980) 105
6) P.B. Russell, G.D. Sprouse, G.L. Latshaw, S.S. Hanna and G.M. Kalvius, Phys. Lett. **32B** (1970) 35
7) P.B. Russell, G.L. Latshaw, S.S. Hanna and G. Kaindl, Nucl. Phys. **A210** (1973) 133
8) J. Meyer and J. Speth, Nucl. Phys. **A203** (1973) 17
9) K. Sugimoto, A. Mizobuchi, K. Nakai, and K. Matuda, Phys. Lett. **18** (1965) 38.
10) T. Minamisono, J.W. Hugg, D.G. Mavis, T.K. Saylor, H.F. Glavish and S.S. Hanna, Phys. Lett. **61B** (1976) 155
11) D. Connor, Phys Rev. Lett. **3** (1959) 429
R.C. Haskell and L. Mandansky, Phys. Rev. C **7** (1973) 1277
12) W.L. Randolph, N Ayres de Campos, J.R. Beene, J. Burde, M.A. Grace, D.F.W. Start and R.E. Warner, Phys. Lett. **44B**, 36 (1973)
13) B.T. Neyer, Ph.D. thesis, Stanford University, 1984
14) G.D. Sprouse, S.S. Hanna and G.M. Kalvius, Phys. Rev. Lett. **23** (1969) 1014
15) W.A. Little, H.C. Jain, B.B. Triplett, S.M. Lazarus, T.K. Saylor, P.D. Bond and S.S. Hanna, Bull. Am. Phys. Soc. **18** (1973) 1602
16) H.C. Jain, A. Little, S.M. Lazarus, T.K. Saylor, B.B. Triplett and S.S. Hanna, Phys. Rev. C **14** (1986) 2013
17) J.S. Dunham, R.T. Westervelt, R. Avida and S.S. Hanna, Phys. Rev. C **37** (1988) 2881
18) J.L. Thornton, Ph.D. thesis, Stanford University, 1985
19) N.K.B. Shu, R. Levy, N. Tsoupas, A. Lopez-Garcia, W. Andrejtscheff, and N. Benczer-Koller, Phys. Rev. C **24** (1981) 954
J.M. Brennan, M. Hass, N.K.B. Shu, and N. Benczer-Koller, Phys. Rev. C **21** (1980) 574

20) W. Greiner, Nucl. Phys. **80** (1966) 417
21) M. Sambataro and A.E.L. Dieperink, Phys. Lett. **107B** (1981) 249
22) H.F. Glavish, Proc. Third International Symposium on Polarization Phenomena in Nuclear Reactions, Madison, Wisconsin, 1970, ed. H.H. Barschall and W. Haeberli, (University of Wisconsin Press, Madison, 1971) p. 267
23) B.L. Donnally, Proc. Third International Symposium on Polarization Phenomena in Nuclear Reactions, Madison, Wisconsin, 1970, ed. H.H. Barschall and W. Haeberli, (University of Wisconsin Press, Madison, 1971) p. 295
24) W. Haeberli, Ann. Rev. Nucl. Sci. **17** (1967) 373
25) R.A. Hardekopf, Proc. Fourth International Symposium on Polarization Phenomena in Nuclear Reactions, Zürich, 1975, ed. W. Grüebler and V. König (Birkhäuser, Basel, 1976) p. 865
26) D.E. Murnick and M.S. Feld, Proc. Fifth International Symposium on Polarization Phenomena in Nuclear Reactions, Santa Fe, 1980,ed. G.G. Ohlsen, R.E. Brown, N. Jarmie, W.W. McNaughton and G.M. Hale (American Institute of Physics, New York, 1981) p. 804
27) D. Krämer et al., Nucl. Instr. and Meth. **220** (1984) 123; Proc. Sixth International Symposium on Polarization Phenomena in Nuclear Reactions, Osaka, 1985, ed. M. Kondo, S. Kobayashi, M. Tanifuji, T. Yamazuki, K.-I. Kubo and N. Onishi, Supplement Jour. Phys. Soc. Japan **55** (1986) p. 1080
28) J.S. Dunham, C.S. Galovich, H.F. Glavish, S.S. Hanna, D.G. Mavis, and S.W. Wissink, Nucl. Instr. and Meth. **219** (1984) 46
29) E. Steffens, Nucl. Instr. and Meth. **184** (1981) 173
30) H.-J. Kluge, F. Ames, W. Ruster and K. Wallmeroth, Proc. Accelerated Radioactive Beams Workshop, Parksville, Canada 1985, ed. L. Buchman and J.M. D'Auria, TRI-85-1 (TRIUMF, Vancouver, 1985) p. 119
31) D. Fick, private communication
32) J.S. Dunham, private communication
33) T. Minamisono, J.W. Hugg, D.G. Mavis, T.K. Saylor, S.M. Lazarus, H.F. Glavish, and S.S. Hanna, Phys. Rev. Lett. **34** (1975) 1465
34) H.G. Berry, L.J. Curtis, D.G. Ellis, and R.M. Schectman, Phys. Rev. Lett. **32** (1974) 751
35) H.J. Andrä, R. Frohling, H.J. Plohn, and J.D. Silver, Phys. Rev. Lett. **37** (1976) 1212

36) K. Asahi et al., Proc. Sixth International Symposium on Polarization Phenomena in Nuclear Reactions, Osaka, 1985, ed. M. Kondo, S. Kobayashi, M. Tanifuji, T. Yamazuki, K.-I. Kubo and N. Onishi, Supplement Jour. Phys. Soc. Japan **55** (1986) p. 1032

37) J.R. Hall, D.L. Clark, S.J. Freedman, and S.S. Hanna, Nucl. Phys. **A483** (1988) 1

38) R.A. Bigelow et al., Proc. Sixth International Symposium on Polarization Phenomena in Nuclear Reactions, Osaka, 1985, ed. M. Kondo, S. Kobayashi, M. Tanifuji, T. Yamazuki, K.-I. Kubo and N. Onishi, Supplement Jour. Phys. Soc. Japan **55** (1986) p. 1030

39) H. Ohsumi et al., Proc. Sixth International Symposium on Polarization Phenomena in Nuclear Reactions, Osaka, 1985, ed. M. Kondo, S. Kobayashi, M. Tanifuji, T. Yamazuki, K.-I. Kubo and N. Onishi, Supplement Jour. Phys. Soc. Japan **55** (1986) p. 278

40) W.F. Rogers, D.L. Clark, S.B. Dutta, and A.G. Martin, Phys. Lett. **177** (1986) 293

41) G. Goldring et al., Proc. Sixth International Symposium on Polarization Phenomena in Nuclear Reactions, Osaka, 1985, ed. M. Kondo, S. Kobayashi, M. Tanifuji, T. Yamazuki, K.-I. Kubo and N. Onishi, Supplement Jour. Phys. Soc. Japan **55** (1986) p. 1146

42) Proceedings DOE Workshop on The Role of a High-Current Accelerator in the Future of Nuclear Medicine, compiled D.C. Moody and E.J. Peterson, ed. J.H. Heiken, LA-11579, UC-408 and UC-414, May, 1989

43) Review of Office of Health and Environmental Research Program, Nuclear Medicine, prepared by Subcommittee of Health and Environmental Research Advisory Committee, Office of Energy Research, DOE, August, 1989

44) W.H. Briner and R.P. Spencer, Statement on behalf of the The Society of Nuclear Medicine and The American College of Nuclear Physicians Concerning the Fast Flux Test Facility, Before the Subcommittee on Energy Research and Development of the House Committee on Science, Space, and Technology, March, 1989

Mossbauer Effect -- R. D. Taylor, Los Alamos National Laboratory

The Mössbauer effect (ME), the recoil-free emission and resonant absorption of gamma-rays, is a well proven tool in many areas of condensed matter and special aspects of nuclear physics. The Mössbauer spectra often give a rich picture of the Mössbauer nucleus in its host environment. Over 100 potential Mössbauer transitions exist involving isotopes of about half the elements[1]). The usual situation involves a long-lived parent (days to years) that populates some low-lying (<150 keV) excited state that decays to the ground state. The lifetime of the excited state (typically 10^{-11} to 10^{-6}s) gives rise to an energy resolution $\Delta E/E = 10^{-11}$ to 10^{-16} for those events that are recoil free. That a Mössbauer Effect exists is usually shown by observing the transmission of a resonant absorber as a function of Doppler velocity between source and absorber. The richness comes about from the resolved hyperfine spectra arising from allowed transitions involving the magnetic moments, quadrupole moment and spin of both the excited and ground states. Thus, an energy analysis (Mössbauer spectrum) yields information about the isomer shift, valence, magnetic and quadrupole hyperfine fields, polarization, and lattice dynamics of the Mössbauer nucleus in its host environment. Effects of temperature, pressure, and applied magnetic field provide additional information about the phase changes and transitions, chemical changes, texturing and multiple sites. In principle the ME study may be carried out as a source experiment or as an absorber experiment. Nuclear moments, nuclear radius change, and spin of the excited state are derivable from the Mössbauer spectra.

Radioactive ion beams (RIB) broaden the scope of available Mössbauer isotopes and provide new opportunities through the capability of controlling the implantation depth and the impurity levels. We present a few examples of cases in which RIB potentially enhance or enable certain types of Mössbauer studies[2]).

1.1 SHORT LIVED PARENTS

Most conventional ME experiments utilize a long-lived (weeks to years) parent(s) to populate the Mössbauer level. Low specific activity (typical of reactor activations) and a long parent lifetime often result in rather inefficient sources. The source must be thin to allow the soft ME gamma rays out and be relatively free of the ground state ME isotope (resonant self absorption). Enriched stable isotopes are often necessary for making either sources or absorbers. The RIB capability would allow "conventional" ME for (alternate) short-lived parents (minutes to hours) where the lower concentration required to obtain a given count rate may be important. Some short-lived parent isotopes feed the ME level more efficiently than their long-lived counterpart. Several ME isotopes

are seldom used because there is no really convenient long-lived parent. The RIB has promise in this and in new areas e.g. ^{61}Ni, ^{73}Ge, ^{157}Gd, ^{161}Dy, ^{189}Os, ^{191}Ir, ^{197}Au. For these examples parent lifetimes are longer than an hour but "on Line" ME spectrometers at the RIB facility should allow shorter parent lifetimes to be considered, such as the 1.7-m ^{57}Mn parent of ^{57}Fe[2]).

1.2 LOW CONCENTRATIONS

Often the ME is used as an impurity probe of its host to study phase changes, magnetism, inequivalent sites, and lattice dynamics of the host. Source (parent) concentrations of a few ppm are usually sufficient; nevertheless, conventional ME sources in many host materials cannot be readily prepared because of lack of available parent material of sufficient specific activity, chemical incompatibility, volatility, and/or facilities for radio- active doping. Isotope separators have been used to implant radioactive parents, but the process is very inefficient, and the present acceleration potentials are rather low so their use has been mostly confined to surface studies[3]).

Implantation via the RIB circumvents many of the problems encountered in preparing conventional ME sources. One can expect a rather homogeneous target area with a well defined depth profile for a given host. Low-temperature targets are often used. Post heat-treatment of most sources will be minimal. This procedure can be contrasted to the (non-uniform) emplacement of the activity on surface of the host followed by various chemical/thermal/diffusion treatments. The expected high purity of the RIB implies a higher specific activity of the dopant and relatively lower noxious impurity concentrations.

1.3 HIGH SPECIFIC ACTIVITY SOURCES

Wherever appropriate stable isotopes exist, the most effective way to produce ME source activity is in a reactor. Characteristically this activity has rather low specific activity, and there is no ready means to separate the desired product. Accelerator-produced activity usually requires rather complex chemical purification/separation. Sources made with low specific activity tend to be rather large in diameter in order to meet the thinness requirement. Intense "point sources" are an identified need in many ME experiments such as source or absorber experiments in high pressure diamond anvil cells[4]), where the samples are only 50-400 microns in diameter. The promise of the RIB to introduce activity separated in both M and Z onto a variety of small targets would greatly expand the scope of high pressure ME physics.

1.4 EXOTIC CHEMISTRY

The study of rare gases and their binding in solids is rather new. Two isotopes

are excellent candidates for ME studies. ^{83}Kr has a 9.4-keV, 150-ns first excited state and ^{129}Xe a 39.6-keV, 1.0-ns level. Neither have convenient parents for conventional ME. 1.9-h ^{83m}Kr and 8.0-d ^{129m}Xe feed the ME levels. The RIB implantations of these rare gas atoms and the subseequent ME experiments should provide unique microscopic information on the binding, valence, lattice dynamics and hyperfine interactions of rare gases in selected hosts. The ME levels are also fed by 2.4-h ^{83}Br and by 2.2-h ^{129}Cs; the dynamics of the implantation/anneal process may well be different and the ME measurements likely will distinguish various sites and processes.

1.5 ON-LINE ME FACILITIES

Most of the ME cases considered so far have involved producing a source at the RIB facility that would then be removed for further processing and use. An on-line ME facility has much appeal. In addition to allowing use of shorter lifetime parents, one could study the effects of radiation damage and self annealing on the spectra. The recoil-free fraction of the ME is enhanced by lowering the temperature. Annealing may be necessary to reduce source broadening due to multiple sites. A suitable furnace/cryostat with the necessary ME absorber, Doppler velocity drive, windows, detectors, and data acquisition system could be located on-line[5]). The ability to control the target temperature during the implantation has important applications.

References

1. J. G. Stevens and V. E. Stevens, Mössbauer Effect Data Index, Vol. 1975 (Plenum Publishing Corp, New York, 1976).
2. J. A. Sawicki, Proc. Accel. Radioactive Beams Workshop, L. Buchmann and J. M. D'Auria, Editors, Parksville, Canada, 1985 (TRIUMF, Vancouver, TRI-85-1, 1985) p 309.
3. H. de Waard and L. Niesen, Mössbauer Spectroscopy Applied to Inorganic Chemistry, Vol. 2, G. J. Long, Editor (Plenum Press, New York, 1987) p. 1.
4. R. D. Taylor and M. P. Pasternak, Hyperfine Int. (1990) to be published.
5. G. Weyer, Nucl. Instr. Meth. 186 (1981) 201; Hyperfine Int. 29 (1986) 249.

A Radioactive Ion Beam and Isotope Production

Dennis R. Phillips and Harold A. O'Brien
Los Alamos National Laboratory

The discipline of nuclear medicine is comprised of that segment of the health sciences devoted to the development of radioactive tracer methods for the study of diseases, and the development of diagnostic and therapeutic procedures which influence the care of patients afflicted with various diseases. The field of nuclear medicine had its genesis in the 1930's when radioactive isotopes became available from early models of the cyclotron in Berkeley. Following the second world war, reactor produced radioisotopes were distributed from Oak Ridge for research in the physical sciences and medicine. Since then nuclear medicine has grown at a rapid pace, spurred by the development of the rectilinear scanner, the gamma camera, the Mo/Tc radioisotope generator, commercial cyclotrons, and positron emission tomography. Federal support and leadership, under the auspices of the AEC and its successors, have been responsible for the development of the field. The DOE nuclear medicine program overlaps significantly other federal basic and applied chemistry, engineering, and physics programs, and with the NIH programs which emphasize the study of disease processes. The major advantage derived from conduct of nuclear medicine programs under DOE auspices is the opportunity for utilization of major investments by DOE in facilities and personnel in the fields of basic physical research and engineering. This has allowed the conduct of productive nuclear medicine research and efficient technology transfer at a cost that is small relative to the investments and to costs that would be required in the absence of close programmatic relationships. The essential multidisciplinary character of nuclear medicine research has benefited greatly from the close interaction of many technical and clinical disciplines.

Most radionuclides used in clinical medicine are now produced by industry. A recent marketing and forecast report by the Market Intelligence Research Corporation suggests that the radiopharmaceutical market will experience exponential growth during the next five years, approaching $3 billion in 1995 as compared to $200 million in 1990. Meanwhile, research on new radionuclide production technology is being conducted at advanced accelerator facilities at Los Alamos and Brookhaven. The Society of Nuclear Medicine and The American College of Nuclear Physicians have expressed concern that DOE support for isotope production is decreasing and that this could have a serious negative impact on field of nuclear medicine.[1,2,3]

In addition to nuclear medicine, radionuclides are also applied in numerous other ways to facilitate scientific investigations. They are used by biologists, nutritionists, and biochemists to study biochemical processes in healthy and diseased physiological systems. They can be used to trace geochemical pathways and to assess models of elemental economies within the earth's ecosystem. Radionuclides have been used to investigate the mode of action and environmental fate of pesticides. They are being used to evaluate and monitor environmental protection and clean-up systems. Several nuclides are used as x-ray sources for analytical and medical applications. The nuclear power industry depends upon specific radioisotopes for the calibration and quality assurance of their radioassay instruments and procedures. Other industries use them to develop and evaluate chemical processes. Physicists have used them to experimentally assess nuclear and astrophysical models, measuring reaction cross-sections, studying hyperfine interactions, and performing other basic studies.

It is apparent that radionuclides serve a major function in advancing all areas of science. It is therefore

quite appropriate to evaluate how any new beam facility could incorporate radioisotope production for these applications. For the nuclear medicine applications isotopic half-lives range from a few seconds (usually obtained from radioisotope generator systems) to years. However, the most commonly used nuclides have half-lives in the range of hours to a few days. Monthly demand is generally in the millicurie to kilocurie range. It is often important that the isotopes be produced in very high specific activity. Perhaps the most important criteria to be met is that medical radioisotopes must be available throughout the entire year. Thus for medical applications the most important considerations are the radioisotope yield and regular availability. Post separator acceleration does not appear to be an important factor.

A RIB facility designed to incorporate on-line mass separation of nuclides could be used very effectively to measure spallation production "cross-sections" of radioisotopes identified as valuable or potentially valuable. Thick-target yields for a variety of isotopes have been measured, using the ISOLDE facility. These data indicate that some nuclides can be collected in significant quantities. For example, Sm-153 is a beta emitting isotope with significant potential as an in-vivo therapeutic agent. The quoted ISOLDE yield for this isotope is 8.70×10^7 ions per second per microampere of proton current on a Gd/La alloy target. At this rate, it would be possible to produce about 0.5 Ci of Sm-153 per day, with high specific activity, on a high current proton accelerator. This could be collected prior to post acceleration in an RIB facility, while passing some other isotope into the ion accelerator. Xenon-127 (0.2 Ci/day) and Ga-68 (1 Ci/day) are two other examples of medically important isotopes that could likely be recovered in significant quantities after on-line separation as part of an ion-beam facility. The collection

of separated Xe-123 and subsequent recovery of I-123 is another example that was discussed.

In the event the RIB facility were to employ a thin production target as the source of materials for the separator and post accelerator, it would be possible to incorporate a radioisotope production targeting system immediately downstream that would utilize the excess primary beam.

Very high specific activity radioactive targets and/or sources could be prepared by post-separator deceleration and collection on a suitable backing material. These targets and sources, which are difficult to prepare using currently existing techniques, would be extremely useful for important on-line nuclear reaction cross-section measurements or as x-ray sources for analytical and medical applications.

It was apparent from the discussions held during the RIB Workshop that the design of the future facility should incorporate capabilities to accommodate the separation and recovery of separated isotopes for subsequent applications in medicine and physical research. It is believed that including "practical" applications in the proposal would strengthen the justification for building the facility.

References

1. Proceedings of the DOE workshop on The Role of a High-Current Accelerator in the Future of Nuclear Medicine, Compiled by David C. Moody and Eugene J. Peterson, Edited by Jody H. Heiken, LA-11579, UC-408 and UC-414, May, 1989.

2. Review of the Office of Health and Environmental Research Program, Nuclear Medicine, Prepared by a Subcommittee of the Health and Environmental Research Advisory Committee, Office of Energy Research, U. S. Department of Energy, August, 1989.

3. Statement of Capt. William H. Briner, (Ret.) and Richard P. Spencer, On behalf of the The Society of Nuclear Medicine and The American College of Nuclear Physicians Concerning the Fast Flux Test Facility Before the Subcommittee on Energy Research and Development of the House Committee on Science, Space, and Technology, March, 1990.

Condensed Matter -- C. Maggiore, Los Alamos National Laboratory

The overview paper "Applications of Radioactive Ion Beams in Materials Science" by Jerzy A. Sawicki in these proceedings discusses the majority of possible applications in the field of condensed matter. In general, the practical use of these beams can be thought of as the inverse of nuclear physics experiments. The techniques of surface layer activation, nuclear reaction analysis, channeling, conversion electron spectroscopy, Mossbauer spectroscopy, on line nuclear orientation, perturbed angular correlation, nuclear magnetic resonance, and positron emission and annihilation are able to give information about the targets in those cases where the nuclear physics is completely understood. The deviations from an ideal response are related to the local environment in the sample which you are trying to measure. An intense radioactive ion beam facility will vastly increase the number of probe nucleii and therefore the materials systems available for study.

In addition to the applications listed above, an RIB facility would enable transmutation doping experiments to be performed. An example of such an experiment is the study of Ga diffusion in Si. Ga is not stable in Si and it is not possible to study its behavior over a wide range of concentrations. However by implanting 71As into Si at high concentrations and watching its decay through 71Ge into 71Ga, the precipitation of Ga from a supersaturated solution could be observed over a wide concentration range. The Ge is infinitely soluble in the Si lattice and its 11.2 day half life allows ample time for annealing and sample prepararion.

Another example of the need for an RIB facility is the preparation of ultra clean alpha particle standards for the semiconductor industry. Almost all semiconductor factories screen for radioactive contamination of VLSI circuits for alpha emitters. The wafers are scanned in process, but no one will allow normal alpha particle standards into the clean room environment. Implantation of radioactive ion beams below the surface of a silicon wafer would allow the needed clean standards to be prepared. A related application is the testing of VLSI circuits for Single Event Upset. Modern chips are mounted and packaged in such a way that it is not possible to test their sensitivity to alpha particles with an external source. Direct implantation of the alpha emitter into the chip at the appropriate depth would make it possible to test these circuits for radiation sensitivity.

The routine use of radioactive ion beams in the field of condensed matter will ultimately depend on the routine, reliable, and inexpensive availability of such beams. These requirements are often at odds with a normal nuclear physics research environment, but they should be kept in mind as much as possible during the planning stages of such a facility.

POSITION PAPER OF WORKING GROUP 5 ON FACILITIES

J.M. D'Auria, Chairman
T.S. Bhattia, Coordinator

Contributions by F. Becchetti, U. of Michigan, D.J. Clark, LBL, M. Fujioka, Tohohu U., W.D. Hamilton, Oak Ridge, M. Loiselet, Louvain-La-Neuve, G.E. McMichael, CRNL, D.J. Morrissey, NSCL, J.M. Nitschke, LBL, H.T. Pentilla, U. of Jyväskylä, B.M. Sherrill, MSU, T. Shinozuka, Tohohu U., R.G. Stokstad, LBL, K.M. Subotic, Boris Kidrich Inst., W.L. Talbert, Jr., LANL, D. Vieira, LANL, T.G. Walker, RAL, T.E. Ward, BNL, J.A. Winger, NSCL, H. Wollnik, U. Giessen

Abstract

As indicated by the response at this workshop, there is a great deal of of interest in the world and in North America in the possibility of building and using an accelerated radioactive beams facility to explore new regions of sub-atomic physics (basic and applied). At this workshop it was agreed that the optimal method of producing such beams in the energy region from 0 to about 10 MeV/u is the ISOL/Post-Accelerator approach while the optimal method above 10 MeV/u is the Projectile Fragmentation Recoil Method (PFRM). The choice of the appropriate approach for a facility based in North America should be primarily dictated by the priorities of the scientific program, but a set of criteria upon which these two approaches could be compared has been developed. There is clearly room for more than one such major facility in the world. Areas requiring additional research and development particularly for the ISOL/Acc program have been identified and pilot studies for a number of these, which are in progress or proposed, are discussed.

1. Introduction

Prior to the start of the workshop, a set of goals were developed to attempt to focus the discussion of the working sessions. These were

* status of the ISOL/Accelerator approach
* status of the PFRM approach
* comparison of these two approaches
* identification of key areas requiring study
* pilot development studies (planned or in progress)

While in retrospect there was insufficient time to cover properly all of these, nevertheless a great deal was achieved and in turn these formed the basis for this report of the achievements of the working group for facilities.

The working sessions in general were well attended (approx. 20 per session) and a good mix of experimental nuclear scientists and accelerator physicists were in attendance to deal with most types of questions raised. Twenty one oral presentation were given (approx. 15

min per presentation) covering many of the facilities in the world today in the field of accelerated radioactive beams. A series of written reports were also prepared, which are attached in the Appendix of this report.

Two events or non-events significantly affected the deliberations of the working group on facilities. The first was the very thorough and complete overview talk on the present status of producing radioactive beams in the world today, given by M. Nitschke. This minimized the need to repeat such material in the sessions themselves and was used as a base upon which the discussions could build. Since this talk will be presented as part of the written proceedings, this facilities report will attempt not to duplicate this material herein. The second event was the lack of communication from the sessions on the scientific program and related experimental requirements. While this non-communication was not unexpected nevertheless it did not allow the group to focus on the particular needs of the experiments considered of highest priority. Future meetings should avoid this if possible.

2. Different Methods of Producing Radioactive Beams

2.1. The ISOL/Accelerator Method

In this approach the desired radioactive species is produced using intermediate energy protons (or other energetic light ions) (> 500 MeV) in thin or thick targets. The species leaves the target, is ionized, extracted as an ion at about 60 keV and the subsequent ion beam mass analysed. It is then further accelerated to some desired higher energy. Details of this method can be found later in this report, in the overview report of M. Nitschke, or in refs. 1 and 2.

Prof. Shinozuka of Tohoku University presented a status report of the proposed accelerated radioactive beams facility at the JHP (3). This facility based on using the 1 GeV proton beam at the KEK LINAC will produce beams up to 6.5 MeV/u for masses up to 120. Various pilot projects are either in progress or are pending depending upon funding. These include studies of the RFQ split vane system, a small separator system using high resolution isobaric separation, and coupling of the ISOL system with the RFQ system. These will be tested at the INS laboratory.

Dr. T. Gordon Walker of the Rutherford Appleton Laboratory indicated that a conceptual design was completed for a proposed Accelerated Beams facility based upon using the high intensity (up to 100 μA, 800 MeV) proton beam at the synchrotron, ISIS. A thick target, vertical ISOL system based upon the ISOLDE design will be used to extract the radioisotopic ion beam of interest. The scientific program is in place and they will seek funding to perform a detailed design study and proper proposal preparation this year. A summary copy of their report is attached in the Appendix.

Dr. M. Loiselet of Louvain la Neuve indicated that improvements in the observed beam of ^{13}N had been observed at the RIB facility based on two cyclotron system (30 MeV production cyclotron) at Louvain (4). A

beam of 25 pA had been observed and this is expected to be increased to 100 pA by the summer. The large (1000:1) contamination of ^{13}C is expected to be reduced significantly by the use of chemical traps to remove CO and CO_2 before injection into the ECR ion source. There are plans to revise this system to use the larger K=120 Cyclone cyclotron as a production source and a new post-accelerator system to provide a greater variety of radioactive beams.

J. D'Auria indicated that the proposed ISAC radioactive nuclear beams facility (1) at the TRIUMF 500 MeV proton cyclotron laboratory is awaiting a decision on the much larger, more encompassing KAON proposal.

Dr. D. Clark from LBL discussed the energy ranges for producing the radioactive isotopes of interest using protons. The optimal energy for most species especially far from stability is of the order of 1-2 GeV although there are instances when lower energies can be an advantage. Dr. W. D. Hamilton (Oak Ridge)presented the option that an intense neutron source (10^{16}n/s/cm^2) will be available soon at Oak Ridge and should also be considered for producing radioactive beams of very neutron rich, medium mass fission products.

Dr. W. Talbert (LANL) discussed expected production yields from a thin target system in a high intensity beam (1 mA) using a gas jet system to transport the species recoiling out of the target. Given an assumed average ionization efficiency of 10 % using a mono cusp source, calculated yields especially for fission products seemed quite competitive with observed thick target yields at ISOLDE. A written report is attached in the Appendix. Dr. J. D'Auria (SFU) prepared a written report on observed production yields of a variety of radioactive ion beams from thick target facilities at ISOLDE at CERN and TISOL at TRIUMF (see Appendix).

2.2. The Projectile Fragmentation Recoil Method

In this approach a very energetic (> 50 MeV/u) heavy ion projectile with (A,Z) composition as close as possible to the desired radioactive beam is directed to a thin low-Z target. The desired recoiling fragment is captured, and mass/charge analysed with appropriate electromagnetic devices, resulting in an energetic radioactive nuclear beam. Additional details of this method can be found in the overview report of M. Nitschke, and in an attached report from B. Sherrill et al., and in reference 5.

Dr. B. Sherrill (MSU)gave a review of this method along with status and plans at the MSU NSCL Lab, at RIKEN and at the FRS system at GSI/SIS (6). In a related presentation Dr. J. Winger discussed a set of calculations for estimating expected production yields for this method. Additional details for both are given in a report in the Appendix. It is apparent that the expected production yields for the PFRM are almost competitive with the thick target ISOL method although they are in a very different energy regime. Also the facility at GSI will be operational this summer producing such energetic radioactive beams.

Dr. S. Harar of GANIL presented a status report of this facility in France with particular emphasis on the LISE spectrometer system (7). A number of upgrades are in progress on the system which will lead to even higher radioactive beam intensities in the near future.

Prof. F. Becchetti of MSU discussed the radioactive beams facility at Notre Dame University (8). This simple, relatively inexpensive system is based upon single nucleon transfer reactions at low energies, resulting in certain beams such as ^{8}Li with energies as low as 1 MeV/u. Simple nuclear reaction studies have been performed with this exotic beam and further, the first isomeric beam, ^{19m}F, is now available for use in limited studies.

3. Comparison of the Two Main Methods

When considering the type of major facility that could prove of value to the scientific community in North America over the next 10 years, it could be useful to attempt to compare these two quite different methods of producing radioactive beams. In his overview talk M. Nietschke does make such an reasonable attempt to compare what are presently considered the operating parameters of both approaches. Unfortunately a direct comparison to decide upon what would make the "best" facility is not an easy task to achieve and to a great extent depends upon the needs and priorities of the scientific program. During the working sessions of the Facilities group this topic was discussed and essentially two points were agreed upon

a. The optimal method to produce RB in the energy range below 10 MeV/u is the ISOL/Acc approach and the best method to produce RB with energies higher than 10 MeV/u is PFRM.

b. A set of criteria upon which the needs of the experimental program can be compared against the projected specifications of the different types of facilities should include beam energy and resolution, beam intensity, time structure, purity, (A,Z) of the required beam, and transverse emittance.

In addition it is clear that in the very near future there will be a number of good radioactive beams facilities of both types able to undertake good physics and science programs. There is not necessarily only one "best" approach, but it is possible at this time to indicate the limits on the operational parameters of the different types of facilities as dictated by technology today.

4. Identification of Areas Requiring Study

While it is clear that radioactive beams facilities can be built today and indeed a number of them are in operation, there are particular areas that do require additional developmental study especially for the ISOL/Acc approach. The PRFM approach will be studied at existing facilities over the next few years and future needs will be clarified. During the following working sessions, relevant presentations were given by Dr. D. Clark (LBL), Dr. G. McMichael (CRNL), Prof. Shinozuka (Tohoku Univ.), Prof. Wollnik (Giessen Univ.),

W. Talbert (LANL), D. Vieira (LANL), J. D'Auria (TRIUMF) and Dr. H. Penttila (Jyväskylä Univ.).

4.1. Suggested areas of study for the ISOL/Accelerator approach.

a. As indicated earlier the projected yields from a thin target gas jet ISOL system operating in a very intense (1 mA), intermediate energy proton beam are competitive with the thick target approach. Given the relatively simpler in-beam configuration, reducing the need for cumbersome remote handling apparatus, it is clear that actual production yields of both fission products and spallation products from such a system which includes the appropriate ion source should be measured. Included in the area studied should be the long term operational stability of such a system in the intense proton beam. Special material may be needed. Since the useful chemistry step (Z separation) provided by a thick target is missing, the usefulness of this approach is critically dependent on a working, user friendly high resolution isobaric mass separation system and developments in this area should be followed.

b. It is clear that a crucial element in this method is the availability of high efficiency ion sources which display long term stability in the intense radiation fields of the thick targets. Of particular interest are new developments in the area of ECR (Electron Cyclotron Resonance) sources and laser ion sources. In the former case these have demonstrated that they are capable of high efficiencies of a variety of elements and in particular can lead to high charge states efficiently. Given that the cost of the subsequent post-accelerator can be reduced significantly if multiple charged ions are injected, it is clear that such ECR systems used on-line needed to be thoroughly studied in various configurations. Recent developments of laser ion sources indicate that they can be quite efficient and of course isotope specific. Given that they could be operated in areas removed from the intense radiation field, the development and use of laser sources on-line should be pursued vigorously.

c. A key element in this method is the use of appropriate remote handling apparatus to both remove and service the sensitive front end (target and ion source systems) of the ISOL. While some laboratories do have such experience handling objects removed from intense radiation fields, nevertheless it should be remembered that an ISOL device has never been used in beams of intensity higher than about 2-3 μA. Given that beams as high as 1 mA are being proposed to be used, and given the rather fragile nature of the front end of an ISOL, development and experience is clearly needed to properly design an truly operational production system.

d. In order to provide the desired radioactive beam in this approach using thick targets, the proper target and target matrix must be used. Since the product does not recoil out of the target but rather it diffuses or desorbs from the surface, selection of the appropriate target is not always obvious. While considerable knowledge is available from the ISOLDE (CERN) laboratory, nevertheless development efforts in this area are always needed. Further, this type of knowledge is gained more from "hands-on" experience rather than from publications. Thus it is important that thick target research and development studies be pursued, ideally in collaborative efforts between the various laboratories around the world. This minimizes "reinventing the wheel".

e. While it is generally agreed that the only types of accelerators that are optimal for a post-accelerator (at least first stage) are the LINAC and the cyclotron, and while the LINAC does have a number of advantages over the cyclotron, nevertheless both types should be studied prior to actual funding to insure that an optimal final choice. In a situation of high yields of high charged states, cyclotrons indeed may have the advantage as discussed in an attached report by D. Clark (Appendix). Regardless, both require a low beta RFQ LINAC to efficiently capture and accelerate the 1 keV/u ion to about 60 keV/u. The actual selection of appropriate RFQ between 4-rod, 4-vane, and split vane is still not clear and requires additional modeling studies. Single stages of different types should be constructed and studied. In addition there is some question about the appropriate duty factor at which such RFQ systems should and could be operated at. This also requires modeling.

f. Additional questions requiring some attention include
-what is the highest voltage at which an ISOL can operate with minimal discharging? ISOLDE operates at 60 kV but higher acceleration voltages may be feasible?
-can an IGISOL (9) system operated properly in the high intensity production beams needed to produce high intensities for the radioactive beams?
-can an high intensity reactor with an ISOL system similar to TRISTAN (at BNL), coupled to an appropriate high resolution mass separator lead to the production of useable intensities of selected neutron rich, medium mass radioactive projectiles for subsequent acceleration ?
-will target materials composed of enriched stable isotopes as are presently available from Oak Ridge be needed to enhance the production of very exotic radioactive beams far from stability ?

4.2. The PFRM approach

a. Efficient cost effective cooling or decelerating techniques should be studied to reduce the radioactive beam

energies from the tens to hundreds of MeV/u at which they are produced. Dr. K. Subotic (Yugoslavia) gave an interesting presentation on the use of a cyclotron in reverse for such a purpose (see Appendix).

b. Methods of reducing the impurity component of such beams and minimizing the momentum resolution of the beam should continue to be studied.

c. Measurements of fragmentation yields and fragment distributions should be studied to determine how useful the PFRM approach will be for producing heavy nuclei and nuclei near driplines.

d. Studies on increasing the intensity of the MSCL primary beam should be encouraged.

5. Pilot Studies (Planned or in Progress)

A number of pilot studies are planned or are in progress in North America to study some of these areas. Below are those which were presented at this workshop.

a. A proposal has been prepared at LBL to couple two cyclotrons to produce a number of radioactive beams. This system would use a high current 30 MeV p production beam as at the facility at Louvain la Neuve and then post-accelerate using the 88" cyclotron. Additional details are in the attached report. This proposal would develop and use an ECR source as suggested above and would also develop new remote target and ion source handling apparatus. In addition it could also do unique physics studies and lead to the development of a strong community of radioactive beam users.

b. A proposal (attached) had been made to perform thin target production yield studies at LAMPF. As indicated above such results seem needed at this time to assess as soon as possible the validity of this approach given some of the attractive features mentioned above. Given a working system it is not inconceivable that this system could produce some interesting new physics as well as lead to the increased development of a radioactive beams user group at this high intensity proton intensity proton facility. A pilot thick target system had been initially considered for development and installation at the intense p beam at LAMPF. While such studies should be encouraged simply for the needed experience they provide, this study seemed particularly difficult given the intensity of the beam, the lack of prime user control of the beam, and the expensive apparatus needed for just a test system. One aspect of this study does involve development and use of a laser ion source. This would involve a very new and unique system requiring considerable development effort at this time. This study could proceed using off-line non-

radioactive materials and lead to quite useful and exciting results.

c. A thick target ISOL system has been installed at the high intensity, intermediate energy proton facility, TRIUMF. This facility called TISOL (10) is being used to indeed test new target materials, and new ion sources including the first on-line (to an ISOL device) ECR ion source for the production of radioactive species important for any future beams facility. In addition an active physics program has been started which will necessitate the development of appropriate remote handling apparatus of the sensitive front end systems.

d. The booster at BNL could be used as a production source given the near future availability of a 4 μA, 1.5 GeV proton beam. These parameters are ideal for a production source for a wide range of radioisotopes. At present a pilot study is in progress developing and using new remote handling apparatus in high radiation fields. Development of such technology is important for any future ISOL/Acc type facility.

e. The National Superconducting Cyclotron Lab (NSCL) at Michigan State University is constructing an analysis beamline called the A1200 which will be able to produce radioactive beams from the PFRM method (11). The beam energies will be in the range of 30 to 150 MeV/nucleon with intensities ranging from 10^3 to 10^7 pps. Generally these beams will be limited to light masses, A<100, but heavier masses could be possible with reduced intensity and purity. The device should begin operation in the fall of 1990. Some of the priorites for operation will be to study yields of the PFRM approach as well as techniques for radioactive beam experiments with large energy spreads and emittances.

There are a number of exciting pilot development studies in progress or planned outside of North America some of which were discussed at this workshop. These are not presented in this reportsince not all were available but the information transfer between members of the international community of radioactive beam users should be continued as it has traditional been encouraged, especially by the group at the ISOLDE facility (CERN). It is also useful to remember that the operating high energy heavy ion facilities including GSI/SIS, GANIL, and RIKEN are constantly performing pilot studies to improve the PRFM approach.

6. Conclusions

It is clear that there is now a great interest around the world in producing accelerated beams of radioactive species to perform a wide variety of basic and applied scientific studies. The technology is generally in place to build appropriate facilities to meet the needs of the experimental programs although a number of areas do need some

research and development studies. For a major facility there are two main methods of producing such radioactive beams, namely the ISOL/Accelerator approach and the Projectile Fragmentation Recoil Method. These approaches are complementary with the former optimal for producing projectile below approximately 10 MeV/u and the latter optimal for higher energies. A direct comparison of the two approaches can be made given a set of criteria but is only useful within the context of the requirements of the desired experimental program. There are a number of major PFRM type facilities in operation or about to start operation in the world at which high priority experiments will be performed within the next 5 to 10 years. There are several proposals to build major ISOL/Accelerator type facilities in the world although none yet have received full funding. The best facility for North America depends primarily upon the specified needs of the scientific program, but at this time an edge is given to an ISOL type facility as important experiments requiring this approach cannot be completed within the next 5 years. A number of excellent pilot studies have been proposed or are in progress to address some of the areas identified as requiring attention especially with the ISOL/Accelerator method.

References

1. L. Buchmann, et al., Nucl. Instru. and Meth., B26 (1987) 151.
2. H.L. Ravn and B.W. Allardyce, in Treatise on Heavy Ion Science, Volume 8, Nuclei Far From Stability, ed. by D.A. Bromley,(Plenum Press, New York, 1989), p. 363.
3. T. Nomura, Proc. of Int. Sym. on Heavy Ion Physics and Nuclear Astrophysical Problems, ed. by S.Kubono, M. Ishira, T.Nomura, Tokyo, July, 1988 (World Scientific Pub. Co., New Jersey, 1989), p. 295.
4. M. Arnould, et al., ibid., p. 287
5. I. Tanihata, in Treatise on Heavy Ion Science, Volume 8, Nuclei Far From Stability, ed. by D.A. Bromley, (Plenum Press, New York, 1989), p. 443.
6. P. Armbruster, H. Geissel and P. Kienle, Proc. of Int. Sym. on Heavy Ion Physics and Nuclear Astrophysical Problems, ed. by S.Kubono, M. Ishira, T.Nomura, Tokyo, July, 1988 (World Scientific Pub. Co., New Jersey, 1989), p. 247.
7. C. Detraz, ibid, p. 151.
8. F. Becchetti, et al., ibid, p. 277.
9. J. Arje, et al., Nucl. Instrum. Methods, A247 (1986) 431.
10. J. D'Auria, et al., Nucl. Instrum. Methods, B40/41 (1989) 418.
11. B.M. Sherrill, et al., 1st Int. Conf. on Radioactive Nuclear Beams, ed. by Myers, Nitschke, Norman, (World Scientific, Singapore, 1990), p. 72.

Working Group 5 -- Appendices

A. David J. Clark, ECR Ion Sources for ISOL Radioactive Beams Systems.

B. David J. Clark, The Cyclotron as a Secondary Accelerator in an ISOL System.

C. John M. D'Auria, Expected Intensities from a (Thick Target) ISOL/ Accelerator Radioactive Beams Facility.

D. W.D. Hamilton, A Reactor Based Source of Neutron Rich Radioactive Ions.

E. B.M. Sherrill, D.J. Morrissey and J.A. Winger, Radioactive Beams by Projectile Fragment Separation.

F. R.G. Stokstad, Production of Exotic Beams at the LBL 88-Inch Cyclotron by the ISOL Method.

G. K.M. Subotic, Fragment Deceleration in Cyclotron.

H. W.L. Talbert, Jr., Activity Expectations from a Thin-Target Ion Beams Facility for Short-Lived Nuclei.

I. W.L. Talbert, Jr., A Research and Development Program at Los Alamos for Production of Ion Beams of Short-Lived Nuclei.

J. Gordon Walker, The Proposed Radioactive Nuclear Beam Facility at RAL.

K. H. Wollnik, Separation of Short Lived Nuclei Within One Isobaric Chain.

ECR ION SOURCES FOR ISOL RADIOACTIVE BEAM SYSTEMS*

David J. Clark
Nuclear Science Division, Lawrence Berkeley Laboratory
1 Cyclotron Road, Berkeley, CA 94720, USA

Wide Range of Species. The ECR ion source (1) can produce many of the radioactive species of interest for experiments. This plasma source works well with most gases. Solid feed systems produce ions of elements throughout the periodic table, using ovens heated either by the plasma or by an external current through a resistive heater; sputtering of rods or foils inserted into the plasma is also used. Tantalum ovens have been used to produce ions of Be, Fe, Cu, Sc, U, etc. For radioactive beams of solid materials, the source walls will have to be made of a material like tantalum, and kept at temperatures high enough to vaporize the materials.

High Charge States. One of the important advantages of the ECR source for radioactive beams, as well as for stable beams, is the high charge states produced. This is a great advantage if one is injecting into an existing accelerator, such as a cyclotron or linear accelerator, which requires a charge state greater than one for acceleration to the desired energy. In a new accelerator system, the size of the accelerator can be reduced if the initial ion charge state is greater than one. This normally results in a lower intensity. But if the ions are stripped to a higher charge state between accelerating sections the loss can be a factor of 5 for masses of 100-200, or a factor of 25 for 2 strippings. It is thus possible that the ECR source using charge 20-25 for mass 100-200, and no stripping, could produce a system efficiency comparable to that of a system starting with charge 1 and using 2 strippings. This will depend upon keeping the gas flow low and the efficiency high, as described below.

Long Lifetime. The ECR source is a long-lived source, operating many weeks without maintenance, since there are no filaments or cathodes to replace. This is important in a high radiation environment near the target, where we are required to use very short personnel access times or remote handling. The source operates either continuously or pulsed, matching either cyclotrons and CW linacs, or pulsed linacs.

Efficiency and Delay Time. One of the crucial requirements for radioactive beam production is high efficiency for the conversion of feed material to ions of the desired charge state. Development thus far has been concentrated on charge state 1, and the results have been encouraging: efficiencies have been in the 30-60% range for ions of N, O, Ne and Xe. More R&D is necessary to fully optimize the temperature of the liner around the

plasma. For charge states greater than 1 very little work has been done. Eventually, after more R&D, one might hope to approach an efficiency of 50% conversion of feed material to total ion output, giving a gas conversion efficiency of about 3% for Xe^{20+}, for example.

The delay time through the source is also important. This time needs to be kept short for production of radioactive species with short half lives. The times observed thus far in ECR sources are in the few second range for neon and argon, and several minutes for nitrogen. R&D is needed here also.

Gas Flow. A limitation of the ECR source is that the gas flow must be limited to about 1 std. cc/hr, or 1 mg/hr of solid material for high charge state operation. This means that the amount of carrier gas at the target must be limited, or the excess trapped out before reaching the source. A helium jet system has a high flow rate, most of which can be skimmed away with differential pumping, but the aerosol remains and may give too high a gas load for the source. The gas flow matching must be studied in an R&D program.

Beam Optics. The exit aperture of the typical high charge state ECR source is 8 mm diameter. This serves as an object for the following isotope separation stage. The emittance is typically 200π mm mrad at 10 kV, un-normalized.

Reference:

1. C. M. Lyneis and T. A. Antaya, Rev. Sci. Instr. 61, 1, Part II, p. 221 (1990)

*This work was supported by the Director, Office of Energy Research, Division of Nuclear Physics of the Office of High Energy and Nuclear Physics of the U.S. Department of Energy under Contract DE- ACO3-76SF00098.

THE CYCLOTRON AS A SECONDARY ACCELERATOR IN AN ISOL SYSTEM*

David J. Clark
Nuclear Science Division, Lawrence Berkeley Laboratory
1 Cyclotron Road, Berkeley, CA 94720, USA

The Secondary Accelerator. The secondary accelerator in an ISOL system is injected with beam from the isotope separation stage which follows the ion source. This accelerator then accelerates the beam to the energy required for experiments. This energy can be around 1 MeV/u for some astrophysics experiments, or up to 5-10 MeV/u or more for nuclear physics experiments. The main candidates for this accelerator are a linear accelerator and a cyclotron.

The Modern Cyclotron. The cyclotron best suited to this purpose is the modern sector-focused cyclotron, which can accelerate light and heavy ions to any selected energy up to its magnet, rf or focusing limit. It has 100% macroscopic duty factor because of the CW rf system. These cyclotrons can use either the single pole or the separate sector design. Examples of single pole designs in the USA are those at Oak Ridge (ORIC), LBL (88-Inch) and the superconducting cyclotrons at Michigan State Univ. (NSCL). Indiana Univ. has a separated sector design. The single pole cyclotrons can be injected axially at an energy as low as a few kV, and so can be fed directly from the isotope separator stage of the radioactive beam system. So the single pole cyclotron appears to be the best choice of cyclotron for the radioactive beam secondary accelerator, with an injection energy of 5-20 kV.

The external beam emittance of the typical single pole cyclotron is 10-20 π mm mrad, un-normalized, for the K=100-150 size. It is about 3 π mm mrad for a K=500-1200 superconducting cyclotron. These emittances are determined by the ion source emittance and by the multiturn extraction mode used in these compact designs. The energy spread is typically .3% for the K=100-150 size.

Cyclotron Energy. The size of a cyclotron is described by its energy constant K, defined by $E/A = K\,Q^2/A^2$, where E is energy (MeV), A is mass (AMU) and Q is charge state (electron charges). K values are 140 for the LBL 88-Inch Cyclotron and 500 or 1200 for NSCL for example. The magnet axial focusing usually limits the energy of the lighter ions to less than that given by the K value. With a K=130 cyclotron we can accelerate $^{13}N^{1+}$ to .8 MeV/u for astrophysics experiments, as at Louvain-la-Neuve. This low energy uses the feature of harmonic acceleration, in which the rf frequency runs at H times the particle revolution frequency, where H is the harmonic number. With its wide frequency range rf system the LBL 88-Inch Cyclotron can accelerate ions from a fraction of an MeV/u up to 32 MeV/u for alpha particles, deuterons and fully stripped carbon, nitrogen and oxygen ions.

Initial Charge State. To accelerate radioactive beams to an energy of 5-10 MeV/u we may need to start with a charge state of more than one. For example, if we want A=20 ions at 5 MeV/u, we need charge state 4 (actually 3.8) for K=140, and charge 2 (1.3) at K=1200. So the efficiency of the system is critically dependent on the efficiency of the ion source for producing charge states 2,3 4, ... R&D on improving efficiency for all charge states is very important. The ECR ion source is described in a separate contribution to this workshop.

Transmission with Axial Injection. The cyclotrons at LBL and NSCL operate with axial injection systems giving 10% typical transmission of the selected charge state to external cyclotron beam. The transmission ranges from 5-20% for various beams in systems like this. The losses include the rf bunching characteristic of a sine-wave, the matching into the cyclotron center region, the charge exchange losses during acceleration and the extraction through an electrostatic channel.

Comparison with a Linac. The comparison with a linear accelerator shows that the linac can have a high acceptance of 80-90% if the first section is an RFQ. This gives the linac an advantage over the cyclotron with its 10% transmission, assuming that the linac has no other losses such as charge exchange or emittance matching. The advantage of the cyclotron is that it may accelerate the lighter ions to higher energies, as given by its K and the Q available from the ion source. For example an $^{16}O^{6+}$ ion can be accelerated to 20 MeV/u at K=140. With radioactive beams, efficient ion source production for the higher charge states is extremely important, as mentioned above.

Two Stage Cyclotron Systems. A two-stage cyclotron system can be used, with stripping between stages, to reduce the size of the accelerator needed to reach a given energy. This principle is used with heavy ion linacs and with the GANIL cyclotrons. With cyclotrons the second cyclotron would be injected radially rather than axially. It could be either a separate sector cyclotron like GANIL, or a single pole design like the 88-Inch or the NSCL superconducting cyclotrons. The simplest design would be a single pole type, injected with a low charge state, stripping at a foil near the center to place the stripped ion with a higher charge state on a centered orbit. The result would be a system like the proposed NSCL coupled cyclotrons. The transmission loss through the second cyclotron would be the stripping factor (5 for A=100-200), the charge exchange loss during acceleration, and the extraction loss, a total factor of about 10. But a 1 cyclotron system with higher charge states from the ion source can approach this performance, as was concluded at NSCL. The same will be true for a radioactive beam system, if the source efficiency can be optimized for high charge states. The ion source must be developed to its full potential for high efficiency at high charge states to make a decision on the optimum type of system.

*This work was supported by the Director, Office of Energy Research, Division of Nuclear Physics of the Office of High Energy and Nuclear Physics of the U.S. Department of Energy under Contract DE- AC03-76SF00098.

EXPECTED INTENSITIES FROM A (THICK TARGET) ISOL/ACCELERATOR RADIOACTIVE BEAMS FACILITY

John M. D'Auria
Simon Fraser University
Burnaby, B.C., Canada

1. FACTORS AFFECTING RADIOACTIVE BEAM INTENSITIES

The radioactive beam intensities expected from a thick target ISOL device coupled to a linear accelerator to form an ISAC device as has been proposed at TRIUMF (Canada), at the JHP (KEK, Japan) and at ISOLDE (CERN, Switzerland) is dependent on a number of factors including:

a) energy and intensity of the primary production beam;
b) target factors (thickness, operating temperature, release efficiency);
c) ion source factors (type, ionization efficiency);
d) ion beam transmission through system including post accelerator;
e) stripping losses if higher charge state needed.

1.A Role of Primary Proton Production Beam

In general it is acknowledged that the optimal projectile to produce the highest quantities of the widest variety of radioisotopes are intermediate energy protons, although there have been some advantages demonstrated at ISOLDE for the use of intermediate energy ^{3}He beams for particular products. Nevertheless, the remaining discussion will assume only incident proton beams with energies greater than 500 MeV. The three types of nuclear processes by which intermediate energy protons are used to make radioisotopes are spallation, fragmentation and fission.

The first reaction mechanism of interest are spallation reactions which result in highest yields for products close to the target and decrease with increasing separation from the target. These reactions are dominant at energies greater than 100 MeV/u. The recoil energies of such species is generally rather low. In general neutron deficient products are preferred and the isotopic yield as a function of mass can be approximated by a gaussian distribution with the some nucleons removed from the target. Semi-empirical formulas exist to allow predictions of such cross sections with some success. The dependence of spallation cross sections with increasing energy is not always predictable but can indeed increase, decrease, or remain constant. The further the desired isotope is from stability, the higher the incident proton energy needed to optimize the observed yield. Typically the maximum spallation cross sections are of the order of tens of millibarns.

The second reaction mechanism of interest is referred to as fragmentation and leads to the production of very light products with reasonably energetic recoil energies from very heavy targets. The isotopic mass distribution of the products is generally similar to those of spallation processes but the maximum occurs for heavy or neutron rich products. Fragmentation cross section increases strongly with energy up to about 2 GeV and then becomes approximately constant. Typically, cross sections for fragmentation processes is at most of the order of millbarns.

Fission is used to produce neutron rich isotopes in the middle Z region with again a gaussian mass distribution. The width of the distribution increases with incident proton energy, with the maximum moving slightly closer to stability with increasing proton energy. In general fission cross sections increase with increasing energy but not significantly. Recoil energies of fission products are quite high as compared to the processes above.

At present the intensities available at the meson facilities vary from about 200 μA (at 500 MeV) at TRIUMF to about 2 μA (800 MeV) at LAMPF and PSI. At the SC at CERN, ISOLDE has had access to a 600 MeV beam with intensities approaching 2-3 μA, but with their move to the PS Booster they will have access to a proton beam of similar intensities but higher energies (1 GeV). At the proposed radioactive beams facility at the JHP (KEK, Japan) a 1 GeV proton beam with intensities of the order of 10 μA are planned which is similar to that planned at the booster at BNL.

1.B. Target Factors

The main advantage of using intermediate energy protons with relatively long interaction depths is that reasonably thick targets can be used and in turn can lead to the production of high quantities of radioisotopes. At ISOLDE targets wtih thicknesses up to about 200 g/cm^2 have been used. Given a cross section of 10 mb for the production of a desired radioisotope from such a target (A=100) with a beam of 10 μA can lead to a saturation activity of the order of 8 x 10^{11} nuclei per sec.

Optimally the target thickness can be approximately one interaction length for the incident proton and thus dependent to some extent on the incident energy. The thicker the target the higher the yields, but also the higher the radiation levels produced in the target. Based upon the ISOLDE experience these targets can be essentially any form, e.g. molten metals, powder, alloys, and metallic foils. Also of importance is the amount of energy deposited into the target from the beam and how this relates to the temperature at which the target should be run to optimize the efficient release of the species of interest. For example, calculations by Eaton and Ravn (ISOLDE) indicate that a proton beam (~600 MeV) of 100 μA will deposit a power of about 8 kW on a target of Ti foils (20 cm in length) and raise the target to a temperature of about 1900°C (assuming only radiation cooling). Some materials such as magnesium oxide powder are predicted to accommodate such conditions, while special cooling may be needed for others (e.g., m.p. of titanium is 1600°C). The power deposited in the different materials does vary.

An important factor in the choice of an appropriate target is not only the production of the species of interest but its efficient release in a timely fashion so as not to lose any of the produced species. Different target materials release different elements with different efficiency and release times, and this is not necessarily predictable. There is considerable practical experience based upon what has been learned primarily at the ISOLDE and ISOCELE laboratories. Species with half lives in the millisecond region and even shorter have indeed been observed at these labs although there is some loss due to delay in the target. In general foils appear to release many elements when the foils are operated at a temperature close to their melting points. In some cases, however, molten metals only release specific elements, for example, molten lanthanium releases only cesium and to some extent barium efficiently. Powders are more specific although in general graphite powders

do appear to release a wide spectrum of elements. In the production yields given at the end of this report some of the elements released by certain target materials are indicated.

1.C Role of the Ion Source

Clearly an essential part of the generation of radioactive ion beams is the type of ion source. There are several different types that have been used in on-line isotope separators. These include the well studied heated surface/thermal ion source in which a hot surface of a material with a high work function is used to ionize elements of low ionization potential. This source is quite efficient for such elements as alkali elements with efficiencies approaching 60%. A second major type of ion source is the so-called plasma source and there are several different variations, referred to as the Bernas-Nier source, the FEBIAD source and others. Almost any element can be ionized in such sources with a wide range of observed efficiencies. A third type of source is the newly developed ECR (electron cyclotron resonance) source. While this source is only now receiving attention on ISOL devices, it appears that it can be quite efficient for elements reaching it. At present only gaseous species can be transported from the target to the plasma region of this source efficiently. A new type of source being developed is a laser ion source which can be quite specific for particular isotopes. While only a few studies have been performed, it appears that it can be reasonably efficient. In general these sources produce primarily singly charged ions but multiple charged ions could be of advantage to minimize the cost of the secondary accelerator system.

In all of these sources some relevant questions are stability, especially over a reasonably long time and in the presence of the very hot thermal and radioactive conditions present in the front end of the ISOL device. Depending upon the materials used in the ion source the longevity of the source can be a significant problem.

1.D Transmission Factors in the System

In general transmission in an ISOL/Accelerator system should be quite high approaching 80-90% especially if a LINAC system is used and no stripping is needed. The production of multiply charged ions and the use of a cyclotron as the secondary accelerator could increase transmission losses significantly.

2. OBSERVED RADIOACTIVE BEAM INTENSITIES

A wide range of radioactive beams have been generated at the various thick target ISOL devices in the world (ISOLDE, ISOCELE, TISOL). In summary, technology exists for producing beams from about 75 elements. Figure 1 displays the standard periodic table on which these elements are shown. Actual production yields have been measured from over 2000 isotopes and these cannot all be reproduced here. The best reference for most of these is ISOLDE USER'S GUIDE available from CERN, (CERN Report 86-05 along with updates). Composite figures for elements Li, Na, F, K, Rb, Cs, Yb, Hg, and Ra are included here to display what some of the production yields are. The units for all of these are particles per sec per microamp of proton in the incident production beam.

3. FUTURE DEVELOPMENTS AND PROBLEM AREAS

Clearly if incident photon beams with higher intensities can be accommodated, then higher final beam intensities can be achieved directly. It is believed that present technology can handle beams at least up to 10 μA, if not up to 50 μA. The targets at ISOLDE are of the order of 50 g/cm^2 and are handled by a robotic system after a run, although in the early days of ISOLDE they were handled by personnel for short periods of time. At the TISOL facility (TRIUMF) a medium Z target of the order of a 10 g/cm^2 exhibits fields of about 100 R/h on contact (or about 40 mR/h at 0.5 m) after a run of about 0.5 μA for a period of 8 h. A person can only work with such a source for a few minutes safely. Clearly, sophisticated target handling apparatus, remotely operational will be required to handle the proposed very thick targets after a run of 200 h with a beam of up to 50 μA. While such developments can follow closely present technology, nevertheless time and effort will be needed to properly develop and test such systems.

Higher ion source efficiences for some of the elements of interest will also lead to higher yields. Again, developmental studies are needed. Such sources will also be demanded to run stably for relatively long periods of time so that some of the studies involving small cross sections can be performed.

4. BIBLIOGRAPHY

There is a great deal of material that has been published on the operation and performance of thick target ISOL devices in operation at intermediate energy proton accelerators. Below is given only some of those which could be of value to prospective experimenters in this field.

A. For a comprehensive, thorough, and recent review of this entire area, consult "On-Line Mass Separators", Helge L. Ravn and Brian W. Allardyce in Treatise on Heavy Ion Science, ed. by D. Allan Bromley, Vol. 8, Nuclei Far From Stability (Plenum Press, New York, 1989) pp. 363-431.

B. A complete summary of productive yields observed at the ISOLDE facility can be found in, "ISOLDE USER'S GUIDE", ed. by H.-J. Kluge, CERN 86-05, 1986; and updates.

C. Comprehensive description of most ion sources useful for on-line mass separators can be found in,
   1. R. Kirchner, Nucl. Instr. Meth. 186:275 (1981).
   2. H.L. Ravn, Nucl. Instr. Meth. 139:281 (1976).

D. Estimates of cross-section using semi-empirical approach useful for intermediate energy proton can be found in,
   1. G. Rudstam, Z. Naturforsch. 21A:1027 (1966).
   2. R. Silberberg and C.H. Tsao, Naval Research Lab., Washington, D.C. NRL Report 7593 (1973); Astrophys. J. 25:315 (1973).

E. Most, if not all, of the recent work achieved with such thick target ISOL devices has been published at one of the EMIS (Electromagnetic Isotope Separators and Techniques Related to their Application) conferences. The Proceedings are published as NIM reports and the last one was held in 1987; Proceedings published in Vol. B26.

FIGURES

Periodic table of elements

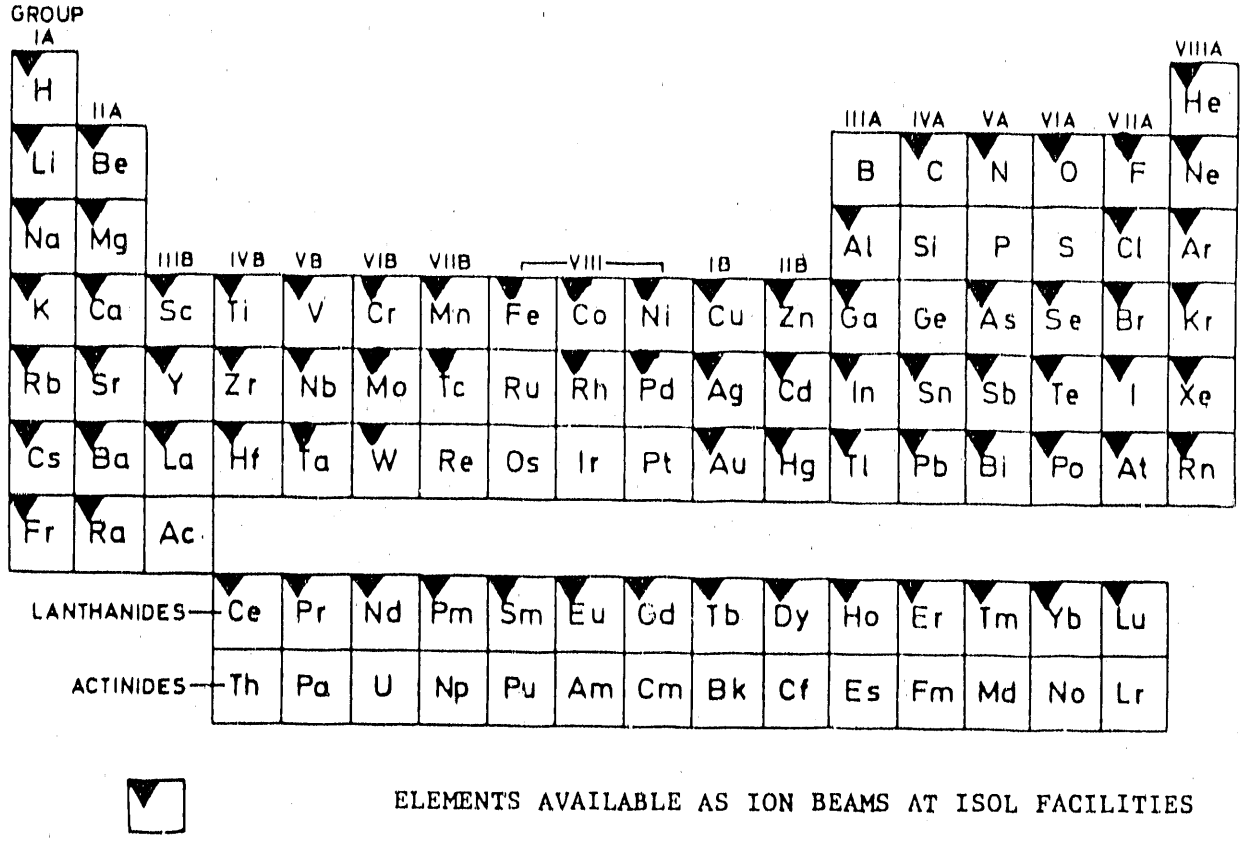

ELEMENTS AVAILABLE AS ION BEAMS AT ISOL FACILITIES

In the above standard periodic table of the elements, those for which ion beams have been generated at on-line mass separators are indicated by inverted triangles.

The figures on the following pages display typical production yields as measured at ISOLDE and TISOL for several different elements and different targets.

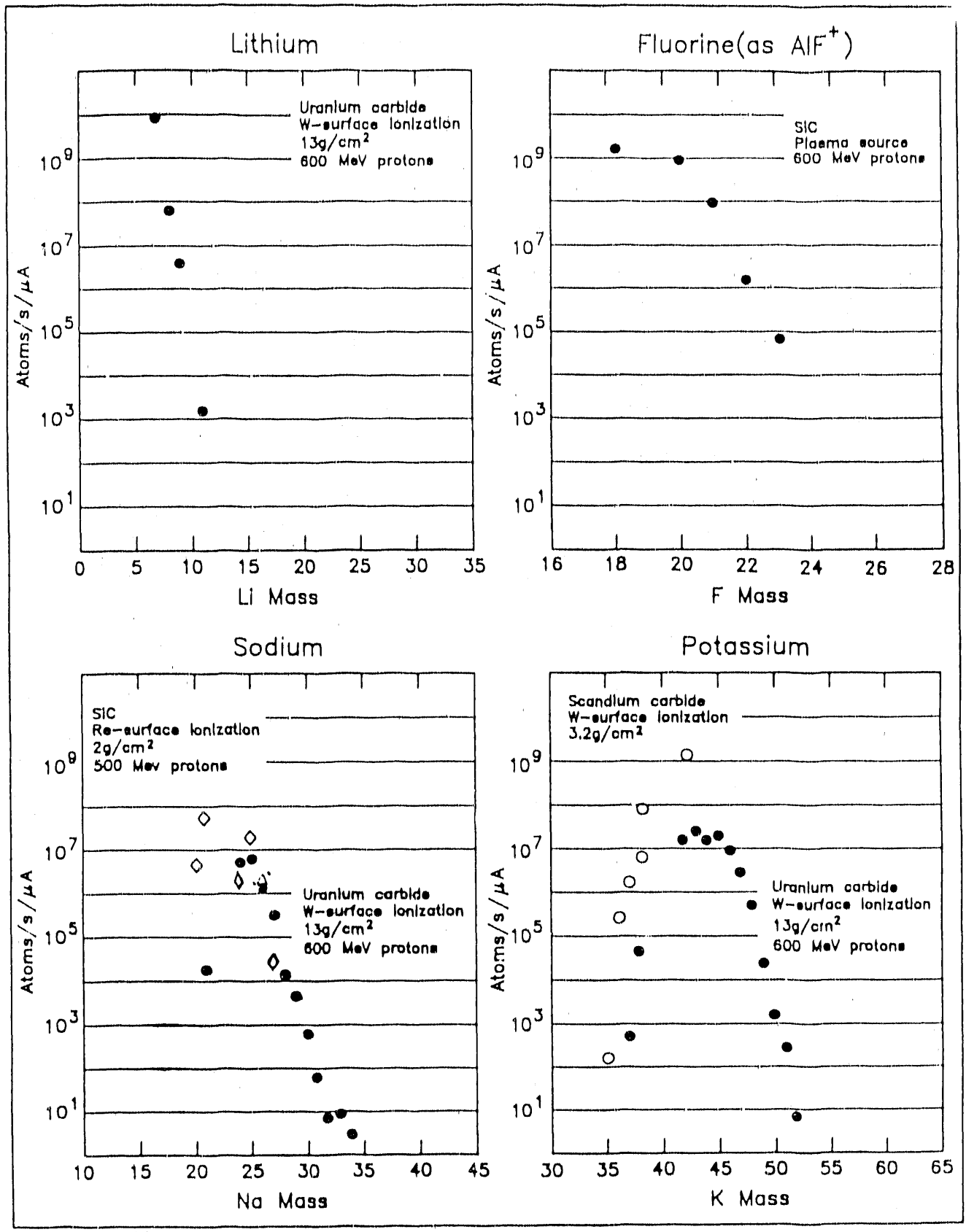
Lithium
Uranium carbide
W-surface ionization
13g/cm²
600 MeV protons
Atoms/s/μA
Li Mass
Fluorine(as AlF⁺)
SIC
Plasma source
600 MeV protons
F Mass
Sodium
SIC
Re-surface ionization
2g/cm²
500 Mev protons
Uranium carbide
W-surface ionization
13g/cm²
600 MeV protons
Na Mass
Potassium
Scandium carbide
W-surface ionization
3.2g/cm²
Uranium carbide
W-surface ionization
13g/cm²
600 MeV protons
K Mass

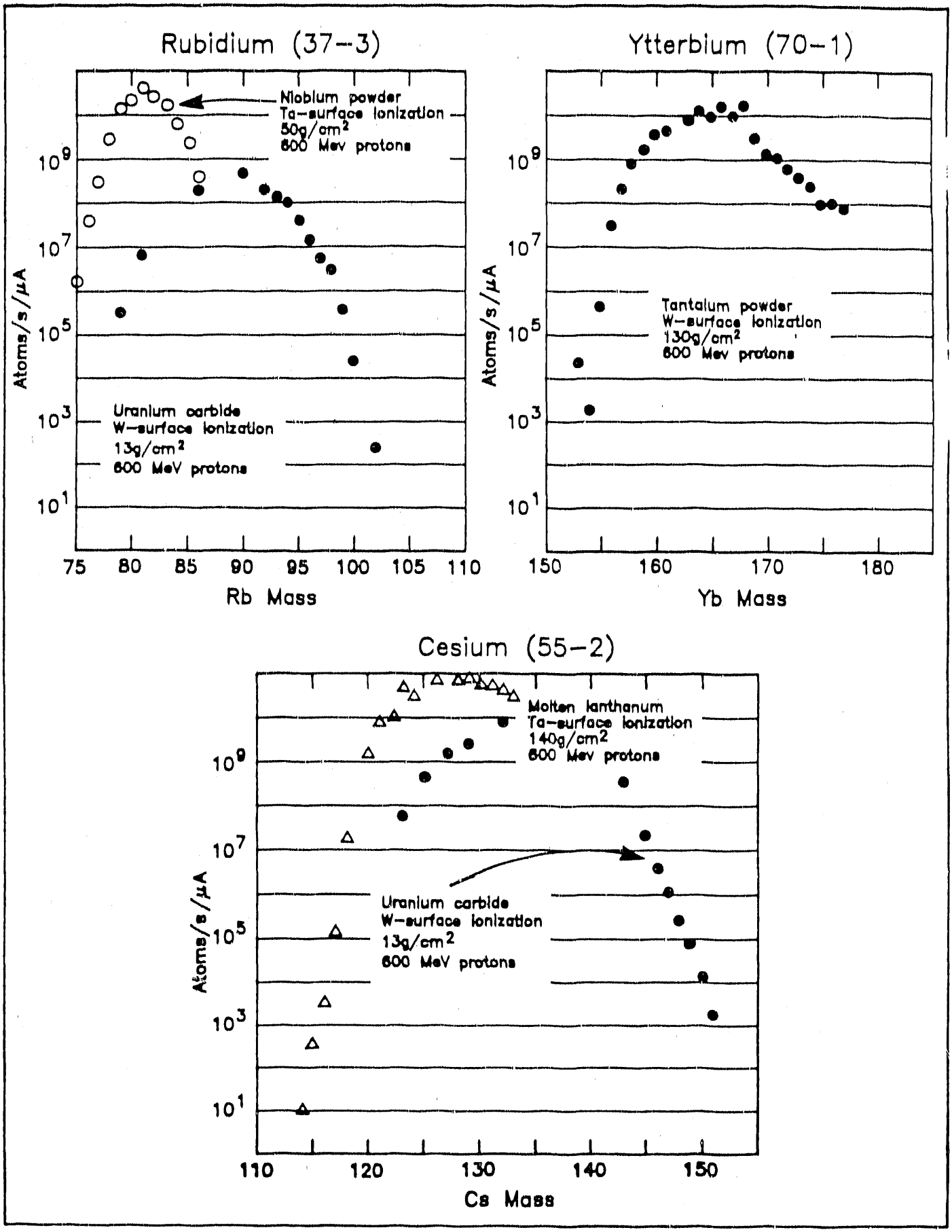
Rubidium (37–3)
Niobium powder
Ta–surface ionization
50g/cm²
600 Mev protons
Uranium carbide
W–surface ionization
13g/cm²
600 MeV protons
Atoms/s/μA
Rb Mass
Ytterbium (70–1)
Tantalum powder
W–surface ionization
130g/cm²
600 Mev protons
Yb Mass
Cesium (55–2)
Molten lanthanum
Ta–surface ionization
140g/cm²
600 Mev protons
Uranium carbide
W–surface ionization
13g/cm²
600 MeV protons
Cs Mass

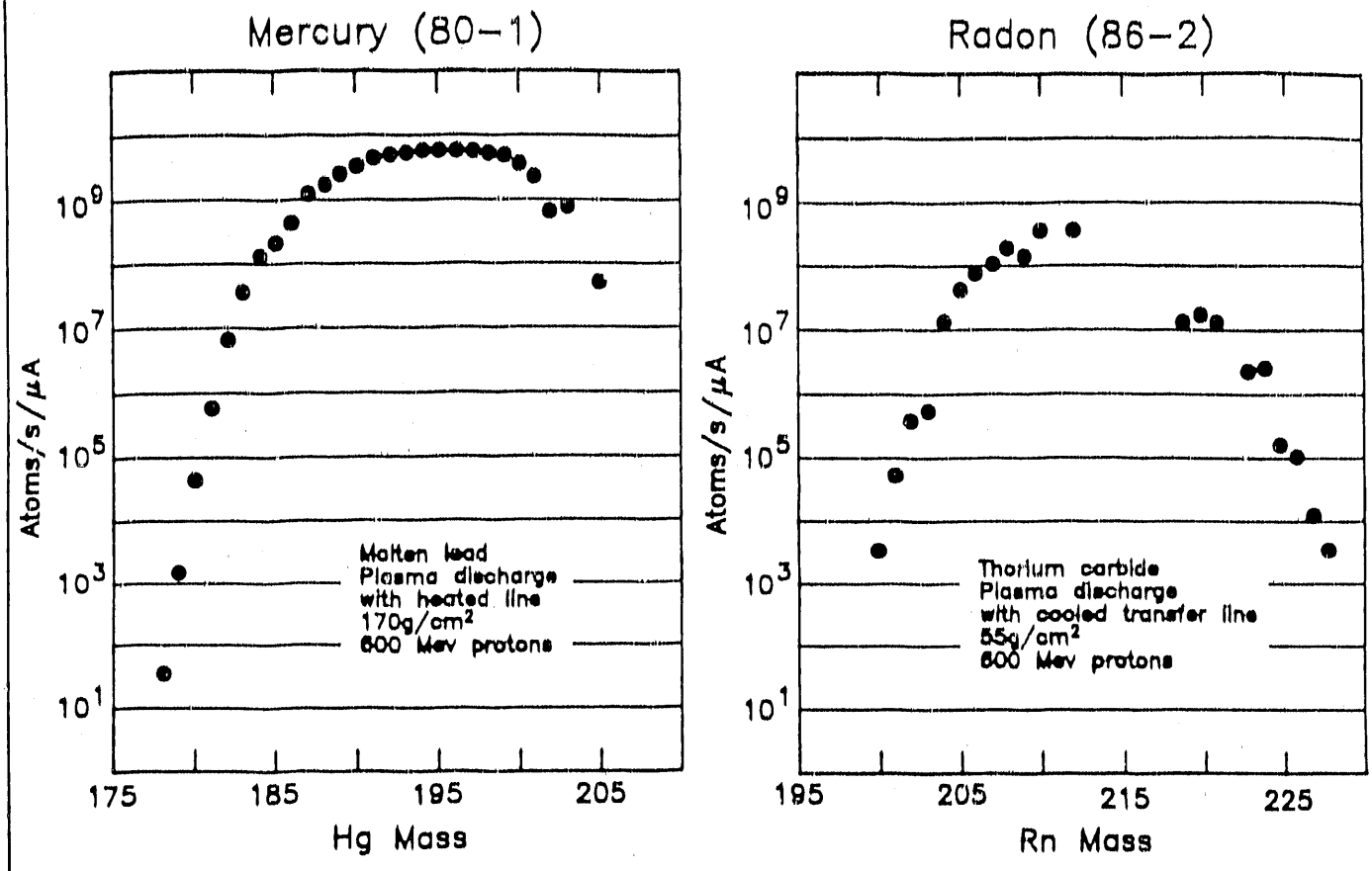
Mercury (80–1)
Atoms/s/μA
10^9
10^7
10^5
10^3
10^1
Molten lead
Plasma discharge
with heated line
170g/cm²
600 Mev protons
175
185
195
205
Hg Mass
Radon (86–2)
Atoms/s/μA
10^9
10^7
10^5
10^3
10^1
Thorium carbide
Plasma discharge
with cooled transfer line
55g/cm²
600 Mev protons
195
205
215
225
Rn Mass

A Reactor Based Source of Neutron Rich Radioactive Ions

W. D. Hamilton

Joint Institute for Heavy Ion Research
Oak Ridge National Laboratory
and
Vanderbilt University

The proposed provision of an Advanced Neutron Source, ANS, at Oak Ridge offers an excellent opportunity to develop an intense source of radioactive fission products.

This high flux reactor is planned to operate at a power of 350 MW and will have a peak unpreturbed flux of 8.5×10^{15} n cm^{-2} s^{-1}. Thus an ISOL source, located within the moderator, will provide a copious supply of fission products.

A reactor based source of radioactive ions offers several significant advantages:

- The reactor shielding also shields the source.
- The stable long-term operating conditions of a reactor in turn leads to a stable source production rate.
- Remote handling techniques for target servicing and changing are well developed at a reactor, as is the experience for dealing with high specific activities.
- The life-time of a source should be long and comparable to the reactor operating cycle.
- The mass distribution of fission products will be influenced by the neutron spectrum and the target. Epithermal neutrons will increase the yield in the valley that is typical of a ^{235}U target, while a ^{249}Cf or ^{251}Cf target will effectively eliminate the valley. A higher mass target will also increase the yield on the high mass side and extend the useful mass range by as much as ten units.

- The large capture cross-section means that a comparatively thin target, perhaps with a multi-foil structure, will appear black to neutrons and yet have the physical characteristics that will allow a helium jet to extract efficiently the fission products.
- Target heating may be sufficiently great from fission that little additional power will be required. Indeed, source heating in a high flux environment may limit the quantity of target and its structure.
- The range of fission products with a yield exceeding 0.01%, with is the useful limit, can extend from A=75 to A=167. The Yield contour on the neutron rich side corresponds roughly to the $T_{1/2}$=1s isochron.
- Such a source would be only a small part of the total research effort about a research reactor and would appear to be very cost effective.

Some of these features might also be considered to be disadvantages e.g. only neutron rich nuclei over a limited mass range of 92 units are available.

A further, and not insignificant, aspect of a fission source is that the two regions of maximum yield are several neutrons beyond the heaviest stable isotopes. Many of these fission products have $T_{1/2}$ ≈ 1d and it is thus feasible to collect them for subsequent used as neutron rich targets.

Radioactive Beams by Projectile Fragment Separation

B. M. Sherrill, D. J. Morrissey, and J. A. Winger
National Superconducting Cyclotron Lab, East Lansing, MI 48824

Contribution to the Workshop on the Science of Intense Radioactive Ion Beams, Los Alamos April 10-12, 1990.

Abstract

The production and separation of radioactive beams using direct separation techniques is discussed. Radioactive nuclei produced by projectile fragmentation, nucleon transfer, or Coulomb excitation and breakup can be collected and separated using magnetic fields. Secondary beam intensities of up to a few percent of the primary beam intensity are possible, although, depending on the production mechanism the beam emittance may be poor. The advantages of this method are that very short lived isotopes can be separated, there is no chemical sensitivity, the production target is relatively simple to operate, and the secondary products are produced at high energy and thus do not need to be reaccelerated. The disadvantages are poor beam emittance and the difficulties in slowing the ions for experiments which require energies much lower than the optimal production energy.

1. INTRODUCTION

A technique for producing radioactive beams is to take advantage of the forward focussing present in certain types of peripheral nuclear reactions. For example, at LBL as much as 1.0 % of the primary ^{12}C beam was converted to ^{11}C and separated[1,2] for biomedical applications. Such techniques have been pioneered using beamline elements at LBL[3] , and with the LISE spectrometer at GANIL.[4,5] Studies on radioactive beam production have been carried out at GANIL by Bimbot.[6] Several new devices have now or will shortly begin operation, including the FRS separator at GSI,[7] the RIPS separator at RIKEN,[8] and the A1200 at Michigan State University.[9] A general feature of fast recoil devices is the use of heavy ion beams with energies more that 50 MeV/nucleon. Most of the information in this paper is taken from the above references.[4,5,10] The prototype for future generations of fragment separators and radioactive beam facilities at high energy is the GSI-FRS-ESR system.[7] A useful and complete discussion of radioactive beams has been given by Tanihata.[11]

The important considerations that determine the usefulness of secondary beams are:

1. Secondary beam rate

2. Purity

3. Emittance and energy spread

4. Total energy, and

5. Limits on beam type from halflife or chemical selectivity.

These considerations will be discussed in this paper in connection with a comparison to beams produced by ISOL techniques in section 5.

Achromatic devices such as mentioned in the first paragraph are generally most useful for efficient separation at fragmentation energies, since they can collect a large fraction of all the produced fragments due to the forward kinematic focussing of the fragmentation reaction mechanism. Electric fields, although desirable, are generally not useful at fragmentation energies because the attainable fields can not sufficiently bend high rigidity fragments. Many lower energy devices use electric fields to cancel the velocity dispersion of magnetic dipoles leaving only mass dispersion.[12-15] A discussion of this has been given by Wollnik.[16] These devices still suffer from some contamination since the separation is only sensitive to the mass-to-charge ratio of the ion and not strictly the mass and proton number of the ions. An advantage of the fast-ion magnetic achromatic devices is that the purity of the secondary beams can be improved by the use of profiled energy degraders at an intermediate dispersive point.[4,5,10] This can, in most cases, eliminate mass-to-charge ambiguities, and provide pure secondary beams for even the heaviest isotopes. A recent upgrade of the LISE separator will take advange of a high electric field Wien filter and combine techniques.[17] It is also possible to use solenoid lenses for very high solid angle collection, but the field strength of current superconducting solenoids probably limits these to fragment energies below 100 MeV/nucleon. Such devices are being considered by Becchetti at the NSCL[18] and by Mittig at GANIL.[19]

One of the biggest problems with beams produced by projectile fragmentation is that the energy and angular spread of the beam is much larger than that of a standard beam from an accelerator (by a factor of 10 or more). The emittance of secondary beams is determined by a combination of nuclear reaction kinematics and atomic processes such as multiple angular scattering and energy loss straggling in the target and degrader. Secondary beam emittance is unavoidably large, except at very high beam energies. The use of profiled degraders also increases the emittance by a factor of 4 or so for a standard degrader.[10] The beam energy spread is also relatively large, on the order of several percent, but can be compensated for by a flight time measurement of the ions, or by the use of a monokinetic degrader which leaves all ions with the same energy. A review of degrader shapes, uses and effects has been published.[20]

The production target for fast recoil techniques need only be able to dissipate some fraction of the beam power. Radiation shielding is relatively simple since the enclosed volume can be kept small. The particle identification of fast ions is relatively simple, and the contaminant level can be easily checked. One final significant feature of direct separation is that it is not sensitive to chemical properties or halflife of the ion of interest.

The halflife limitation is only given by the flight time of the ions in the device (on the order of microseconds).

2. PRODUCTION METHODS

2.1 Projectile Fragmentation

In the energy range of 100 MeV/nucleon to a few GeV/nucleon the primary reaction mechanism for peripheral reactions is projectile fragmentation. A simple picture of this reaction is the participant spectator model where the target nucleus is imagined to shear off part of the projectile, leaving the rest of the projectile traveling forward at the initial beam velocity, with little angular divergence. The remaining projectile fragment then deexcites. Goldhaber[21] has shown that the momentum width of the fragments is given by the Fermi momentum of the removed nucleons, and can be written as:

$$\Delta P_{\|}[MeV/c] = 90 * \sqrt{\frac{A_f(A_b - A_f)}{A_b - 1.0}} \quad (1)$$

and

$$\Delta P_{\perp}[MeV/c] = \sqrt{\Delta P_{\|}^2 + \sigma_N^2} \quad (2)$$

where σ_N is approximately 200 MeV/c and is added to account for nuclear reactions which spread the fragments in angle; A_f and A_b are the fragment and beam masses, respectively. For example, at 500 MeV/nucleon ^{11}Li produced from ^{15}N is expected to have a Gaussian momentum distribution with a sigma of 1.3 percent, and a Gaussian angular cone with a sigma of 21 mr. The distributions are even narrower for heavier nuclei. For example from a ^{112}Sn beam of 500 MeV/nucleon ^{106}Sn fragments have an expected momentum spread of 0.18 percent with an angular cone of 2.4 mr. The variation of the widths of these distributions is a straight forward consequence of momentum conservation in the projectile rest frame.[22]

Projectile fragmentation is a generally more viable mechanism for producing a wide variety of beams, so the rates possible will be discussed in more detail below. The rates from transfer and Coulomb disossociation reactons will be discussed briefly in the following sections.

2.2 Transfer Reactions

Transfer reactions have been used at low energies to produce radioactive beams, for example at Osaka,[23] LLNL,[24] and Notre Dame University.[25] The idea is to use a very specific, high cross section reaction to convert a significant fraction of the beam into a single product in a specific nuclear state. Even at several hundred MeV/nucleon the transfer cross sections for one nucleon transfer can be tens of millibarns per steradian. One advantage of this technique is that in the case where only one final state is populated the energy spreads can be kept very low and are then determined mainly by the thickness of the production target. If a low mass target is used, such as LH_2, in a single nucleon transfer reaction, e.g. (p,d), the forward kinematic focussing yields a factor of 10 or more compression in the CM angle when transformed into the laboratory. It may be possible to produce beam intensities of up to 10^9 radioactive ions per second with this technique, although it will be limited to specific nuclei near stability.

2.3 Coulomb Dissociation

At energies above 500 MeV/nucleon, the equivalent photon flux present as a ion moves past a heavy target is so large that the cross section for excitation of the giant dipole resonance becomes very large.[20] The excited nuclei decay primarily by neutron emission from the Giant Dipole Resonance (GDR), producing nuclei one neutron less than the stable beam. For example, the electromagnetic disossociation cross sections are several barns for heavy nuclei on heavy targets at energies in the range of a GeV/nucleon.[27,28] The beams formed in this way have energy and angular widths determined only by the decay energy of the neutron from the GDR. For GeV/nucleon very-heavy ions this is a small effect. Thus beams of heavy nuclei with good emittances could be produced. An interesting related speculation is that multiple GDR excitations may occur leading to a polarized nucleus with the protons separated from the neutrons. If this excitation happens before fragmentation, then very neutron or proton rich nuclei may be produced. It should be noted that this production mechanism has not been studied.

3. SEPARATION TECHNIQUES

3.1 Fragment Separation with Profiled Degraders

As mentioned in the introduction, it appears the optimum separation technique for fast projectile residue ions is with magnetic "momentum loss achromats".[10] At energies below 100 MeV/nucleon or so electric fields and solenoids are also useful. The present discussion will concentrate on describing the momentum loss achromat technique.[4,5,10]

The term achromatic means, in practice, that at the end of the separator the horizontal position does not depend on momentum. Achromatic systems have the advantage of keeping the final spot sizes small for even large momentum acceptances. Figure 1, taken from Schmidt et al.,[10] shows the basic ideas of the method. Since the fragmentation mechanism produces nuclei at nearly the same velocity, the first dipole will separate the products according to their mass-to-charge ratio. In order to eliminate ions which have the same mass-to-charge ratio as the fragment of interest but different nuclear charges, an energy degrader is inserted into the beam after the first selection. Ions with different Z lose different amounts of energy and no longer have the same $B\rho$ as the ions of interest. These contaminents can then be separated with an additional set of dipoles.

Figure 2, also taken from Schmidt et al., shows schematically the two parts of the selection. The first selection is made by A/Z, and the second selection is made by a combination of energy loss (which depends on the ion velocity, as shown in the figure) and a second $B\rho$ selection. An example of how well the technique might work is shown in Figure 3. The figure is taken from a paper by Geissel[29] where they calcuated the separation of ^{205}Au from fragmentation of ^{208}Pb at 1 GeV/nucleon, using the program MOCADI.[30] The position is at the end of the GSI FRS. The various parts of the figure are labeled by the shape of the degrading material. The homogeneous degrader has a flat shape and is the easiest to construct, the achromatic degrader has a shape which maintains the achromaticity of the device after its insertion, and the monoenergetic degrader shape is such that all ions have the same kinetic energy after leaving the wedge.[20] The figure also illustrates the effects of range straggling for ions using the various degrader shapes.

The mass and charge resolving power of a fragment separator can be expressed in

Figure 1: Schematic illustration of the momentum loss achromatic technique taken from the paper by Schmidt et al.[10]

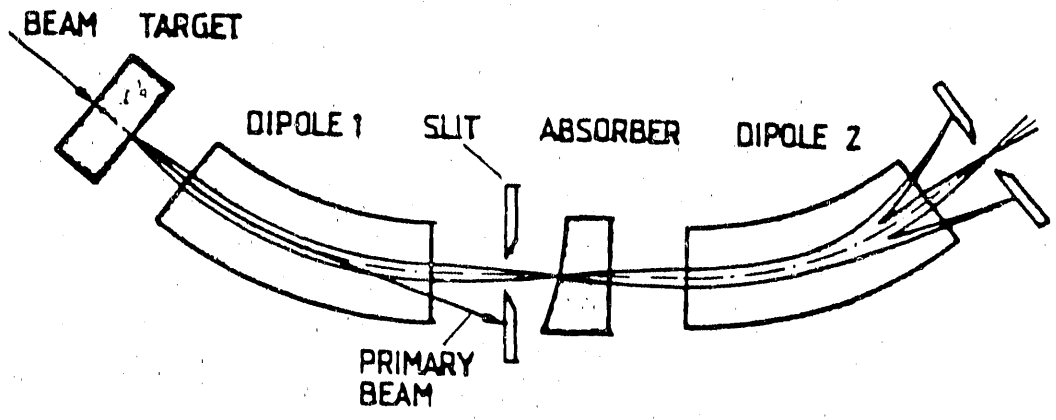

first order as:

$$R_{mass} = \frac{(x/\delta)_1}{(x/x)_1 \cdot x_0} \cdot \frac{(\delta/\delta_m)}{(\delta/\delta_0)} \; and \; R_{charge} = \frac{(x/\delta)_1}{(x/x)_1 \cdot x_0} \cdot \frac{(\delta/\delta_z)}{(\delta/\delta_0)} \tag{3}$$

where $(x/\delta)_1$ is the dispersion of the first set of dipoles; $\delta_m = \frac{(m-m_0)}{m_0}$, and $\delta_z = \frac{(Z-Z_0)}{Z_0}$; $(\delta/\delta_{z(m)})$ is the percent change in the momentum caused by a percent change in Z(m) at the degrader, with the mass(charge) and momentum held constant; x_0 is the initial spot size, and $(x/x)_1$ is the magnification at image 1. The above expressions are valid when using an achromatic system with

$$(x/\delta)_2 = -(x/x)_2 \cdot (x/\delta)_1 \tag{4}$$

and a degrader with a profile to preserve the achromatism.[10] The important point to notice is that the first term in both of these equations is just the momentum resolving power of the first half of the system. Hence, lower momentum resolving power implies a less pure secondary beam. For mass resolving power on the order of 200, the intrinsic momentum resolving power of the device should be 1000 or greater. This has important consequences for the design of the separator. It also indicates that the emittance of the primary beam should be as small as possible in order to reduce x_0 and thus increase the resolving power.

For illustration of typical parameters, a comparison of the various fragment separators is listed in Table 1. The LISE separator has been used over the past 5 years for a variety of experiments. The other devices are second generation systems in which some improvement has been made. The RIPS device has the largest solid angle and momentum acceptance. The A1200 is positioned at the beginning of the beam distribution lines for the NSCL K1200 cyclotron. The GSI device has been designed for much higher kinetic energies, where the fragmentation cone and energy spread are smaller and therefore allow smaller acceptances for the device. If one wished to optimze secondary rates it should be

Figure 2: Illustration of the two selections of a momentum loss achromat taken from the paper by Schmidt[10]. The solid line is the effect of the first dipole which selects according to A/Z. The second selection, represented by the dashed line is determined by the $B\rho$ change of an ion after passing though an absorber.

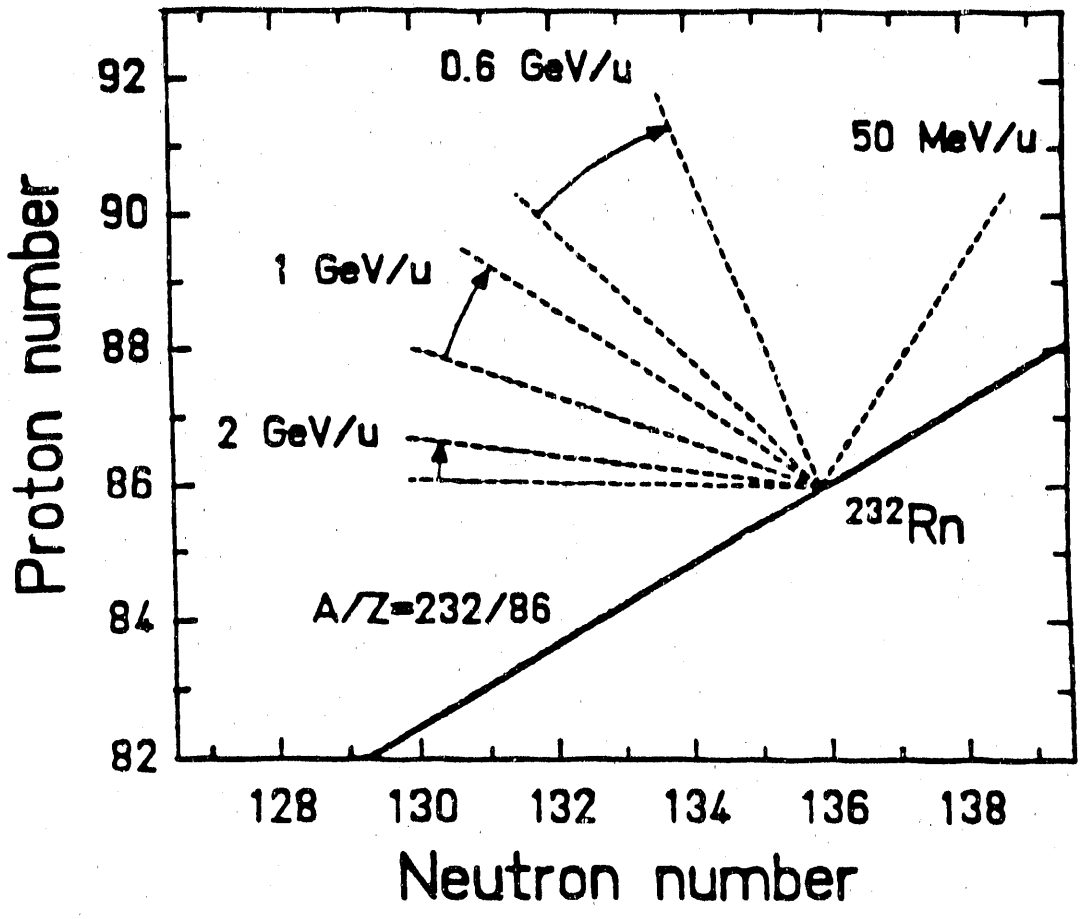

possible to construct a device for 18 Tm ions with a solid angle of 5 msr, a momentum acceptance of 6 percent, and the desired momentum resolving power. The larger solid angle and momentum acceptance are important if the device would also be used to separate light ions produced at 100 to 200 MeV/nucleon. At energies of 500 MeV/nucleon or higher the GSI FRS parameters are sufficient. An important consideration is: the larger the acceptance of the separator the lower the primary beam intensity must be to achieve 100 percent collection efficiency. It should be possible to construct separators which limit the optimum production energy to between 300 and 500 MeV/nucleon (neglecting charge state problems for the heaviest beams).

3.2 Cooling and Stopping Techniques

Experiments which require good secondary beam emittance, or energies well below the production energy will require that the secondary beam to be cooled and or deaccelerated. GSI is building such a system.[7] A problem with cooling is that the time scale for the process is on the order of seconds and hence short halflife ions will be lost. The inten-

Table 1: Comparison of Fragment Separators.

Parameter	LISE	A1200		GSI FRS		RIPS
		medium	large	medium	large	
Ω[msr]	1.0	0.8	4.3	0.71	2.5	5.0
$\Delta\theta$[mr]	30	20	54	30	160	80
$\Delta\phi$[mr]	30	40	80	30	20	80
$\Delta P/P$[%]	5.0	3.0	3.0	2.0	2.0	6.0
K-value	700	1600‡	1200	4000	2100	1300
Resolution	800†	3400	1300	8000	1300	1500
Length [m]	18	22	19	74	73	21

†monochromatic resolution.
‡($E/A = 100 MeV/nucleon\ ^8He$)

sities will also be reduced by at least an order (and typically two orders) of magnitude for deceleration due mainly to limitations in the number of nuclei which can be cooled, space charge limits, matching pulse structures, and the time associated with deceleration. Such techniques however, appear feasible and will be explored at GSI. The typical intensities of ions decelerated to the Coulomb barrier would probably be in the range of 10^5 to 10^6 ions per second.

Decay spectroscopy experiments generally require stopped ions. Stopping GeV/nucleon ions is not easy since the ranges are very long. If electromagnetic disossociation can be neglected then a heavy stopping material is desirable so the number of secondary interactions can be keep low. The range straggling of secondary ions can be keep low by the use of a monokinetic wedge rather than the standard achromatic wedge.[20] In this case after the degrader all ions have the same energy (the limit is set by the momentum resolution of the device and energy loss straggling). Figure 4 shows the effectiveness of this technique for a sample system stopping ^{20}Ne ions. The range straggling limit is only 10% above that for a monoenergetic ^{20}Ne beam with the same central energy as that of the degraded beam energy. It is also helpful to produce the nuclei of interest at as low an energy as possible. Hence it is desirable to have a large acceptance mode of the spectrometer available.

4. RADIOACTIVE BEAM RATES

In order to estimate the expected secondary beam rates, and evaluate the usefulness of the profiled degraders, we have written a simulation program called INTENSITY. The program calculates the angular and momentum acceptance of a fragment separator for a given ion assuming momentum and angular spreads of the fragments from the Goldhaber model[21] described above. The program uses production cross sections from the parameterization of Suemmerer,[31] and includes multiple scattering and energy loss in the target and degrader. The energy loss is calculated with the relativistic Bethe-Block formula, and the energy loss straggling from the Bohr formula[32] The program also includes a calculation of the charge state distribution for ions which are not fully stripped,[33] and the nuclear reaction losses of the beam and secondary fragments.[10] The

Figure 3: Calculated separation for ^{205}Au produced by fragmentation of 1 GeV/ nucleon ^{208}Pb. The nuclear cross sections are convoluted in the distributions[31]. Shown are the horizontal distributions at the end of the GSI FRS.

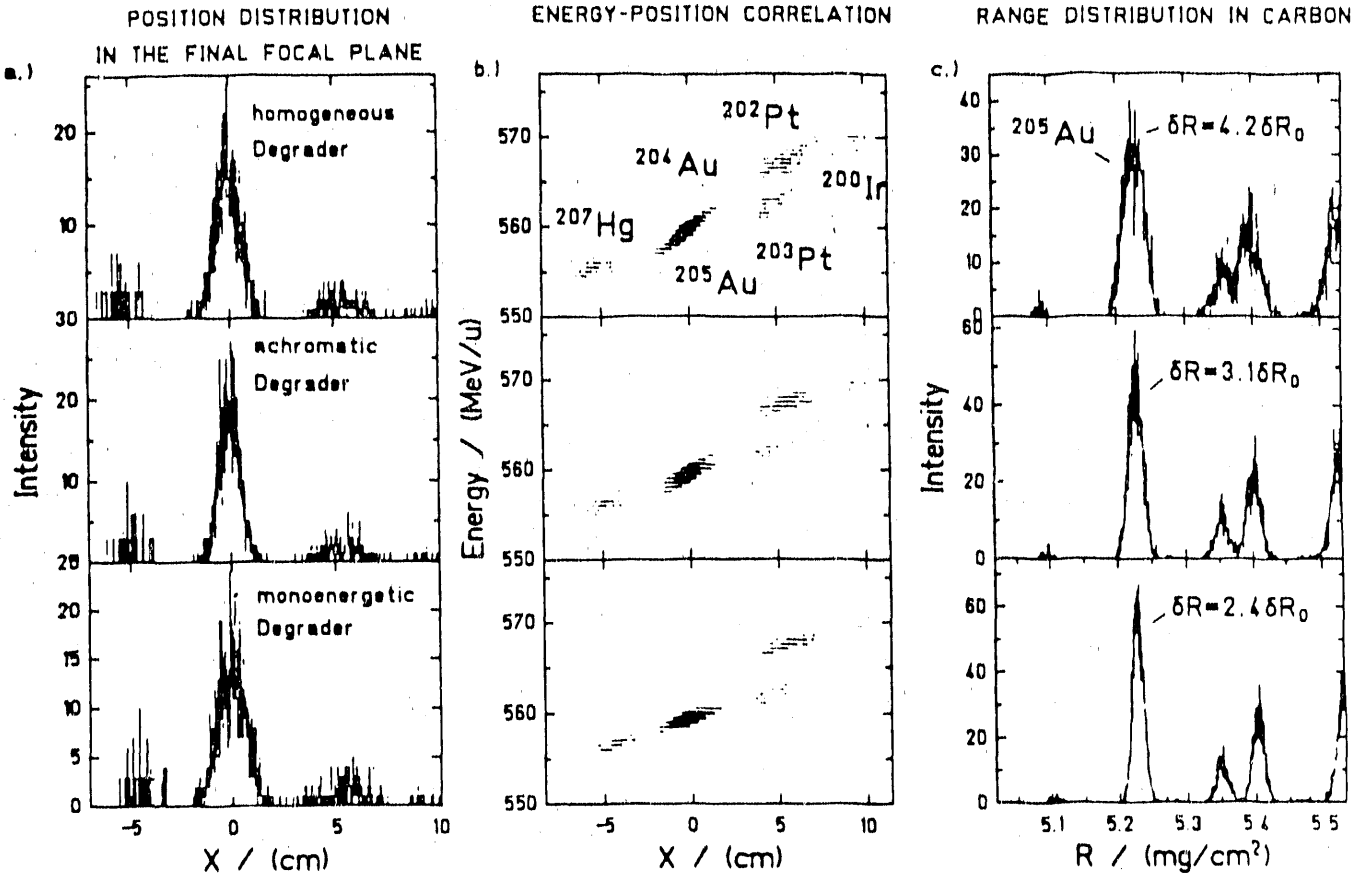

simulation assumes that ion-optical abberations and the initial beam spot are small.

Table 2 gives the expected secondary beam intensities for a sample fragment separator with a solid angle of 5 msr and a momentum acceptance of 6 percent, typical of what should be possible. An initial beam intensity of 1 pμA was assumed unless noted, and the target thickness was chosen to maximize the radioactive beam rate. In all cases calculated in the table, no significant increase in intensity was found in increasing the production energy to 800 MeV/nucleon. This is a consequence of the large acceptance assumed for the separator.

5. COMPARISON WITH OTHER TECHNIQUES

The two primary production schemes which can be compared are fast separation, and production schemes from high intensity proton bombardment of thick targets, such as is used at ISOLDE. These process are, in fact, complimentary since they use the same nuclear reaction mechanism, but one observes the residues of the projectile (rapidly moving in the laboratory frame) or the residues of the target (nearly at rest in the laboratory frame).

For ISOLDE type production the rate of secondary ions out of an ion source can be

Table 2: Estimates of the secondary beam intensities from the program INTENSITY described in the text. The production target is ^{9}Be, of thickness t in g/cm^2. The beam intensity was 1 pμA for all beams except Cd and Sn which were assumed to be 100 pnA, the production energy is 400 MeV/nucleon.

B	F	t(g/cm^2)	σ_S(mb)†	Rate(pps)	σ_G(mb)‡	Rate(pps)
^{7}Li	^{8}He	18.2	13.4	1.9×10^{10}	20.0	2.8×10^{10}
^{11}B	^{8}He	10.5	.05	5.2×10^{7}	0.5	5.3×10^{8}
^{14}C	^{11}Li	9.5	.01	1.5×10^{7}	0.1	1.4×10^{8}
^{20}Ne	^{19}Ne	13.8	20.3	4.6×10^{10}	65.6	1.5×10^{11}
^{106}Cd	^{104}Cd	5.0	2.7	2.3×10^{8}	28.0	2.4×10^{9}
^{112}Sn	^{100}Cd	4.4	.05	4.1×10^{6}	.05	4.0×10^{6}

†Based on cross sections calculated with the parameterization of Suemmerer.[31]
‡Based on measured cross sections or trends from the same number of removed nucleons from the data of Webber et al..[34]

written

$$R_{isol} = \frac{I_{beam}\sigma_f t N_A}{A_t}\epsilon \tag{5}$$

where I_{beam} is the proton beam intensity in particles per second, σ_f is the fragment production cross section in cm^2, t is the target thickness in g/cm^2, N_A is Avagodro's number, and A_t is the production target atomic mass in g/ mole. The ion source efficiency is ϵ. For heavy ion fragmentation this equation is

$$R_{FRS} = \frac{N_A\sigma_f}{A_t(\mu_b - \mu_f)}(e^{-\mu_b t} - e^{-\mu_f t}) \tag{6}$$

where $\mu_{f(b)}$ is the fragment(beam) attenuation length in the production target. The collection efficiency can be assumed to be close to one. If the beam and fragment have the same attenuation length (as is approximately the case for ^{11}C and ^{12}C), then the above equation simplifies to

$$R_{FRS} = \frac{N_A\sigma_f}{A_t} t e^{-\mu_f t} \tag{7}$$

where now the target thickness will be limited to the order of the interaction length of the ions. This equation is actually an underestimate of the rate since, in fact, other secondary ions will interact and may produce the fragment of interest. For fragments far from stability there is certainly an enhancement in the rate for thicker targets, whereas the above equation is probably more valid for fragments close to the beam.

If we assume that the product of the production cross section and target thickness (in atoms/cm^2) are the same for both methods then the ratio of rates is

$$\frac{R_{FRS}}{R_{ISOL}} = \frac{I_{HI}}{I_{pbeam}}\frac{e^{-\mu_f t}}{\epsilon} \tag{8}$$

The above assumption is justified if a hydrogen target is used for the III fragmentation production; then the nuclear reactions are identical in the rest frame of the heavy nucleus.

For heavy-ions in light targets the nuclear interaction length is shorter than the eletronic stopping length. The assumption is also approximately true for Be or C targets since the fragmentation cross section would be larger than the spallation cross section because a beam can be used which is selected for producing the fragment of interest and the ISOL facility is limited to certain target materials. ISOL facilities have the big advantage of high proton fluxes. The proton beam intensities are in the range of 10^{14} while HI intensities are in the range of 10^{13} for light ions and up to two orders of magnitude lower for the heaviest ions. The last factor, which is a ratio of efficiencies, can favor HI production by a factor of 1.5 or so for alkali ions, and a factor of 1000 or more where ISOL facilities have halflife or chemical problems with separation efficiency. Hence in the case of short halflives or chemically stubborn elements, HI separation can give higher rates despite the large difference in primary beam intensities.

ISOL beams must also be reaccelerated and HI beams must be slowed, depending on the experiment. The losses may be similar in both cases, but clearly if the fast HI beams can be used or are desired then they present an advantage over ISOL beams which must be accelerated to above 10 MeV/ nucleon, in which case an additional acceleration efficiency and the accelerator cost must be taken into account.

Fast HI fragment beams have the serious disadvantage of poor emittance and large energy spreads in most cases. Some experiments can compensate for these effects, but may become more complicated. In addition, if the HI fragments are to be stopped, depending of the fragment energy, the range can be very large and the possibility of the once pure fragments interacting in the stopper adding background. The poor emittance also makes the produced source sizes large and might complicate decay measurements. Such problems are not present for ISOL beams which have been used to make sources at low energy and with acceptable source sizes. The accelerated beams will have energy spreads and emittances which are a factor of 10 or more better than the fast HI fragment beams.

Finally, the purity of the beams can be expected to be equivalent. The requirement to achieve this level of separation is a fragment separator with sufficient momentum resolving power. For ISOL beams a high resolving power mass separator is also required.

6. CONCLUSION

Fast projectile fragment recoil separation is a very useful technique for producing high intensity radioactive beams. Given the number of facilities which are operating and are under construction, this technique will make a significant impact on radioactive beam physics. A high intensity radioactive beam facility would require primary beams of at least 1 pμA and energies in the range of 300 to 1000 MeV/ nucleon. The highest energies are needed due to charge state problems with the highest Z ions. The energy of the primary beam would be determined by the physics goals, and most likely will vary depending on the need. For spectroscopy studies, lower production energies are desirable, but for more efficient collection and separation, higher energies are desirable. Cooling and deceleration of fast radioactive beams may be necessary for some experiments, but is difficult, slow, and would limit beam intensity. However, for experiments which require certain elements or ions with short halflives, fast recoil separation is in any case the optimal technique.

REFERENCES

1) J. Alonso, A. Chatterjee and C.A. Tobias, IEEE Trans. on Nucl. Sci. **NS-26**,3003 (1978).

2) J. Alonso, Proc. of the Workshop on Research with Radioactive Beams, Washington DC (1984), LBL Report 18187.

3) I. Tanihata, et al., Phys. Rev. Lett. **55**, 2676 (1985).

4) J.P. Dufour, et al., Nucl. Instr. and Meth. **A248**, 267 (1986).

5) R. Anne, et al., Nucl. Instr. and Meth. **A257**, 215 (1987).

6) R. Bimbot, IPN Orsay Report, IPNO-DRE-87-35 (1987).

7) H. Geissel, et al., Projectile-Fragment Separator, a proposal for the GSI SIS-ESR Experimental Program.

8) T. Kubo, M. Ishihara, N. Inabe, T. Nakamura, H. Okuno, S. Shimoura, K. Yoshida, K. Asahi, H. Kumagai, and I. Tanihata, RIKEN Priprint, RIKEN-AF-NP-83, Dec. 1989.

9) B.M. Sherrill, et al., Proc. Int. Conf. on Radioactive Nuclear Beams, World Scientific Publ., in press, ed. J.M. Nitschke, Berkeley CA, 1989.

10) K.H. Schmidt, E. Hanelt, H. Geissel, G. Muenzenberg, J.P. Dufour, Nucl. Instr. and Meth. **A260**, 287 (1987).

11) I. Tanihata, Treatise on Heavy-Ion Science, Vol. 8 New York:Plenum (1989), p. 443.

12) J.A. Nolen, et al., in Instrumentation for Heavy Ion Nuclear Research, ed. D. Shapiro (Harwood, New York, 1985) p. 171.

13) C.N. Davids and J.D. Larson, Nucl. Instr. and Meth. **B40/B41**, 1224 (1989).

14) T.M. Cormier and P.M. Swertka, Nucl. Instr. and Meth. **184** 423 (1981).

15) R.E. Tribble, R.H. Burch and C.A. Gagliardi, Nucl. Instr. and Meth. **A285** 441 (1989).

16) H. Wollnik, Optics of Charged Particles, Achademic Press: Boston (1987).

17) A. Mueller private communication.

18) F. Becchetti, et al., A Proposal to the DOE for a Large Superconducting Solenoid, Univ. of Michigan, and private communication.

19) W. Mittig, GANIL, private communication.

20) H. Geissel, et al., Nucl. Instr. and Meth. **A282** 247 (1989).

21) A.S. Goldhaber and H.H. Heckmann, Ann. Rev. Nucl. Part. Sci. **28**, 161 (1978).

22) D.J. Morrissey, Phys. Rev. **C39** 460 (1989).

23) T. Yamagata, et al., Phys. Rev. **C39**, 873 (1989).

24) G.J. Mathews, R.C. Haight, R.W. Bauer, Proc. of the Workshop on Prospects for Research with Radioactive Beams from Heavy Ion Accelerators, Washington DC, April 1984, LBL Report LBL-18187, 21 (1984).

25) F.D. Becchetti, W.Z. Liu, D.A. Roberts, J.W. Jaenecke, J.J. Kolata, A. Morsad, X.J. Kong, and R.E. Warner, Proc. Int. Symp. on Heavy Ion Physics and Nucl. Astr. Problems (Tokyo, July 1988); and the contributions to the Proc. Int. Conf. on Radioactive Nuclear Beams, Berkeley (1989).

26) C.A. Bertulani and G. Baur, Phys Rep. **163**, 299 (1988).

27) M.T. Mercer, et al., Phys. Rev. **C33** 1655 (1986).

28) J.C. Hill, et al., Phys. Rev. **C38** 1722 (1988).

29) H. Geissel, et al., Proc. Int. School Seminar on Heavy Ion Physics, Dubna USSR, Oct. 1989, and GSI report GSI-89-30.

30) Th. Schwab, Ph.D. Thesis, Univ. of Giessen, FRG, in preparation; and Th. Schwab et al., GSI Scientific Report 88-1 (1988), p. 284.

31) K.Suemmerer and D.J. Morrissey, Proc. Int. Conf. on Radioactive Nuclear Beams, World Scientific Publ., in press, ed. J.M. Nitschke, Berkeley CA, 1989.

32) H. Geissel, Proc. of Semiclassical Description of Atomic and Nuclear collisions, ed. J. Bang and J. DeBoer (North Holland, 1986).

33) J.A. Winger, Michigan State Univ., private communication.

34) W.R. Webber, J.C. Kish, and D.A. Schrier, Phys. Rev. **C41**, 547 (1990).

Figure 4: Energy bunching of an energy degraded ^{20}Ne beam using a dispersive ion- optical system in combination with a monoenergetic degrader at the dispersive image position. The results are given in terms of the range straggling δR_0 of a monoenergetic ^{20}Ne beam with the same energy as the degraded fragments.

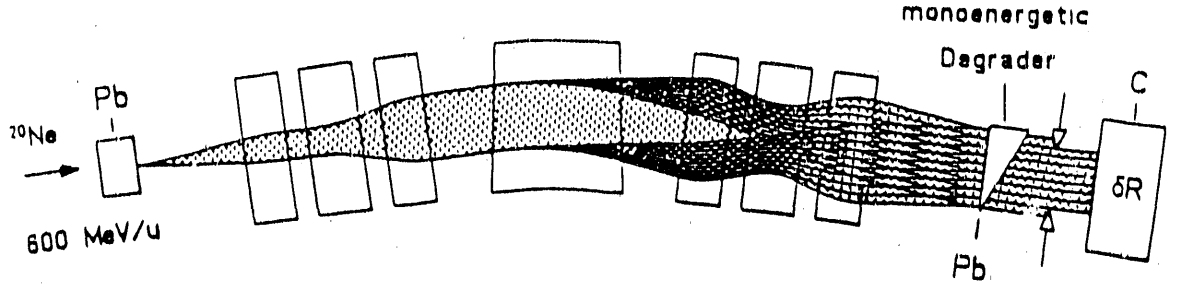

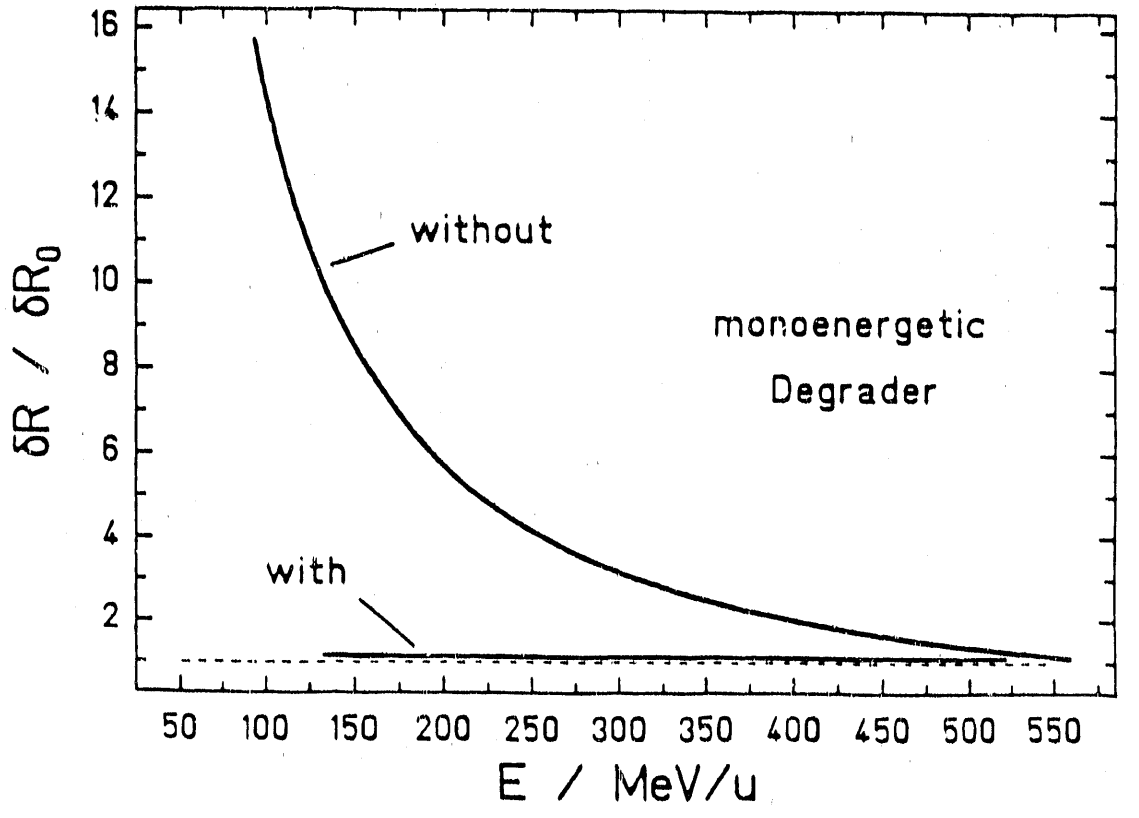

Production of Exotic Beams at the LBL 88-Inch Cyclotron by the ISOL Method†

The EB-88 Collaboration*

Abstract

The Users of the LBL 88-Inch Cyclotron are preparing a proposal to produce exotic, i.e., radioactive beams. The facility will consist of a high-current 30 MeV cyclotron to generate the radioactive nuclei, an ECR source that can be coupled to different production targets, and the 88-Inch Cyclotron to accelerate the radioactive ions. Thus, the basic concept is that of the double cyclotron system pioneered at Louvain-la-Neuve, although the initial emphasis will be on producing a variety of light proton-rich beams at energies up to 10 MeV/A. At this workshop we wish to outline what is being planned, to invite comments and suggestions, and, especially, to encourage participation. We believe that this facility will be an important step toward establishing the scientific and technical basis for a National High Intensity Facility. This can be achieved through active participation by members of the radioactive beam (RB) community in (i) experiments with high quality radioactive beams of moderate intensity and, (ii) R&D on high beam-power targets and highly efficient ion sources.

1. Introduction

There are several ways to make radioactive beams and, as is the case with stable beams, no single method satisfies all needs. The ISOL approach is capable of producing beams of nuclei with half-lives longer that about 0.1 sec, with moderate to high intensity (10^6-10^{11}/sec), high energy resolution, and low emittance. The energy depends on the second accelerating system but is typically ≤10 MeV/A. Thus, this approach makes possible a wide range of experiments in nuclear structure, nuclear reactions, and nuclear astrophysics. A high intensity ISOL facility in the United States, while receiving very favorable mention in the NSAC Long Range Plan, still lies well in the future because of its cost and the financial commitments already made to CEBAF and RHIC. Along with developing the scientific case for a major future facility (whether ISOL or something else) at this workshop, it is essential to begin a stepwise approach that includes both experimental nuclear physics and R&D on the critical components of RB production. This will help develop and strengthen the community of scientists that must exist in order to justify a major RB facility. For these reasons we believe that a smaller scale and shorter term ISOL project should go forward in the U.S. The recent progress at Louvain-la-Neuve [1] demonstrates that the double cyclotron concept works and has excellent potential for further development. In the following we show how this could be accomplished at the 88-Inch Cyclotron.

2. Concept

A schematic reminder of the main components in the system and the order-of-magnitude intensities in the different stages is shown in Fig. 1. There are at least two providers[2,3] of compact 30 MeV H^- and 15 MeV D^- cyclotrons, with prices starting at \$3M. The typical thick-target yields for (p,n) reactions leading to the lighter isotopes of carbon, nitrogen and oxygen vary from 10^{-4} to 10^{-3} per proton. Depending on the fraction of these atoms that can be extracted from the target and ionized in the ECR source to the desired charge state (2^+ - 4^+), the intensities of ions injected into the 88-Inch Cyclotron should vary from 10^7 to 10^{10}/sec. The cyclotron has an acceleration efficiency of typically 10%, which leaves 10^6 to 10^9 ions/sec for experiments.

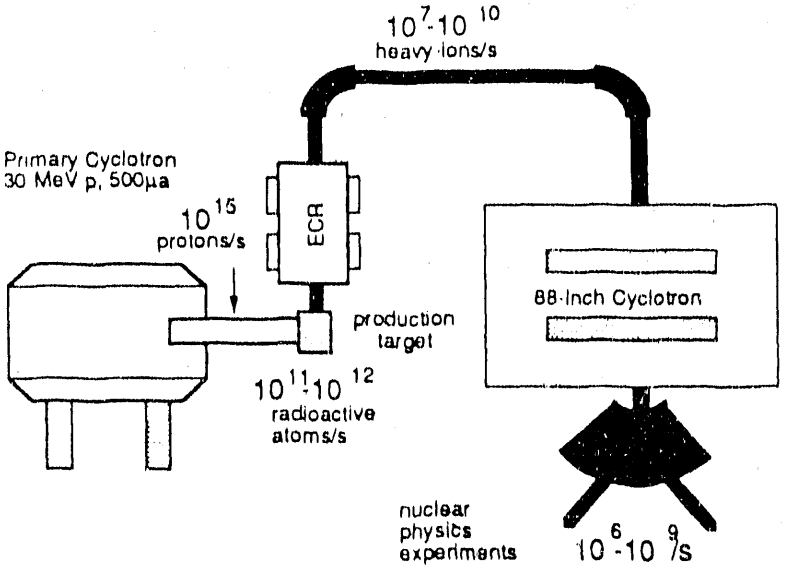

Figure 1.

3. Beams

There are about twenty proton rich isotopes from ^{7}Be through ^{30}P having half-lives of a second or longer that might eventually be obtainable as beams. But the approximately ten species with $Z \leq 11$ seem to be the ones to develop first, and of these, experimenters have so far expressed the most interest in ^{10}C(19s), ^{11}C(20m), ^{13}N(10m), ^{14}O(1.2m), and ^{15}O(2m). Neutron-rich beams could be developed in time as manpower and interest permit, and could be obtained in two ways: via the (n,p) reaction using neutrons produced by deuterium bombardment of ^{9}Be, or via the (p,3He) and (d,3He) reactions. These beams are expected to have intensities lower by one or perhaps two orders of magnitude.

The maximum beam energy of the 88-Inch Cyclotron (in MeV/A) is 140 $(q/A)^2$, the energy resolution is 0.3%, and the emittance is 20 π mm mrad.

4. Science

There is a wide range of possible experiments, even when considering only the proton-rich species. A number of scientists interested in EB-88 have suggested specific experiments in:

•Nuclear Astrophysics ($^{14}O+\alpha->^{17}F+p$)	(E. Norman)
•Reactions and Structure of Mirror Nuclei ($^{11}C + ^{11}B$ and $^{13}N + ^{13}C$)	(J. Cerny)
•Nuclear Physics at the Proton Drip Line (e.g., studies of $^{11,12}N$, $^{15,16}F$, etc.)	(H. Weller; F. Ajzenberg-Selove))
•Isospin Mixing in the GDR ($^{13}N + ^{13}C$, $^{4}N + ^{12}C$)	(K. Snover)
•Spectroscopy of Proton-Rich 1f-2p Nuclei (e.g., $^{14}O + ^{40}Ca$ ->)	(P. Haustein; F. Stephens; J. Becker)
•Subbarrier Fusion and Transfer ($^{15,16}O + ^{143,142}Nd$)	(R. Stokstad)

Some of these experiments are quite new, others are not, and collectively they represent only a beginning. We hope that through this workshop more people will become involved in the generation of ideas for experiments with EB-88.

With its present high efficiency ECR sources the 88-Inch Cyclotron has accelerated stable beams that, because of their isotopic rarity, can also be considered "exotic". Examples are $^{29,30}Si$, ^{34}S, ^{36}Ar, ^{48}Ca, and ^{136}Xe. The combination of radioactive and exotic stable beams made possible by EB-88 would provide unique opportunities for experiments with existing instrumentation (the Ge-detector array HERA, the large NaI spectrometer, particle detector arrays, etc.).

5. Physical Layout

A primary consideration in the design has been flexible operation for both experiments and R&D, and the ability to handle highly activated targets. This necessitates having several high-level caves instead of just one, and adequate shielding to prevent activation of adjacent caves during a production run. Fig. 2 shows the primary cyclotron enclosed in a vault having walls of boron-doped concrete, about four feet thick [4]. There are three beam lines, each equipped with a quadrupole triplet and ending in one of three caves. The cave doors move vertically on hydraulic lifts. The experimental area adjacent to the caves has controlled access through double doors. Provision for storage and remote handling of targets is included, although the details of this have yet to be designed. Since negative ion cyclotrons offer the possibility of extraction on either side of the

cyclotron, ports for testing of targets or production of isotopes at lower intensities are indicated, and could be developed as needed.

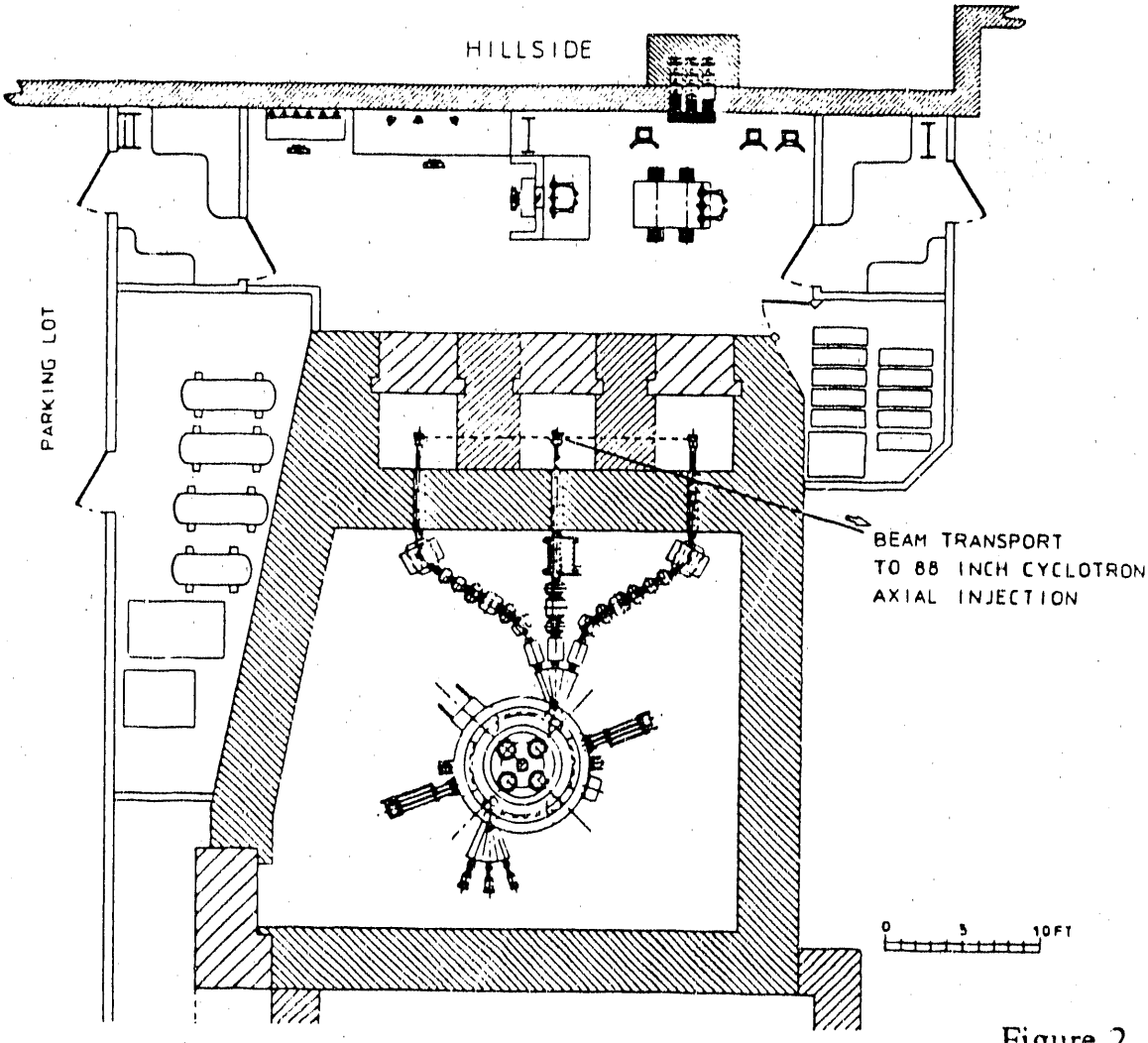

Figure 2.

6. Targets and Ion Source

The ECR ion source is mounted vertically and located in the middle cave, as shown in the elevation drawing of Fig. 3. Thus, the ECR source can be fed by a gas transport system from a target in the adjacent cave on either side, or can be operated in an integral mode with the target in the center cave. Some shielding between this target and the ECR source would be possible at the expense of a slightly longer distance between target and source. Provision has been made for local servicing or removal of the ECR source through movable roof blocks. Fir ally, Fig. 4 shows a schematic design of a target that is essentially integral with the ECR source, the connection being made by a heated transfer tube. The ECR source has a heated liner for high efficiency and short hold-up times.

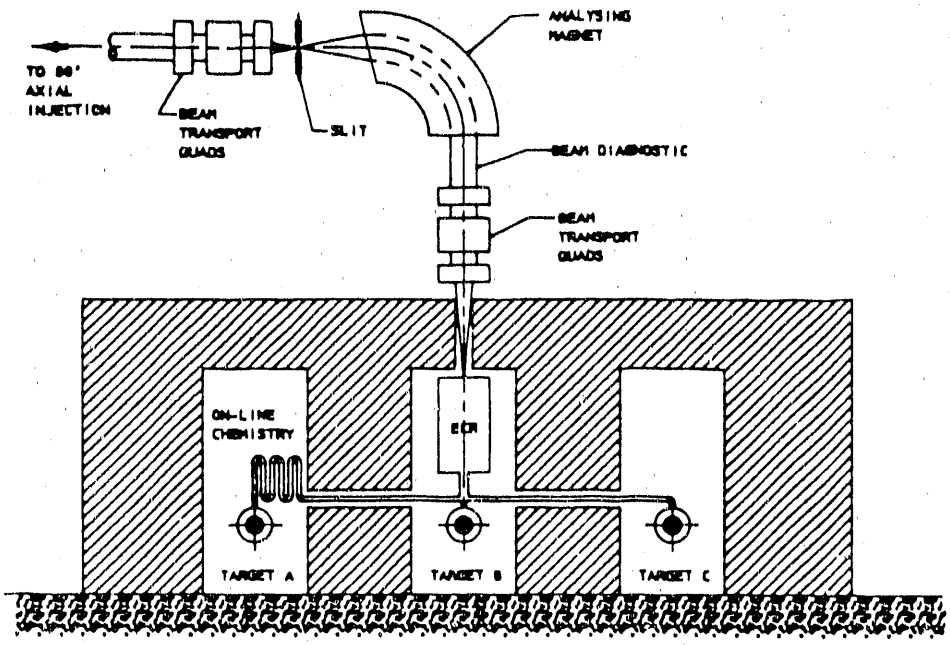

EB-88 TARGET CAVES
ELEVATION VIEW

Figure 3.

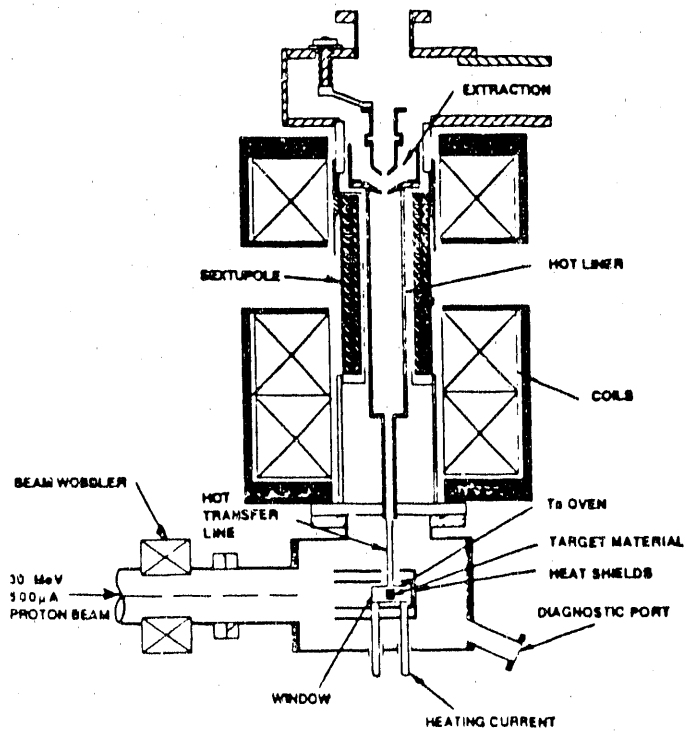

Figure 4.

7. Research and Development

There are three levels of R&D in this project. The first level uses existing equipment and is therefore near-term, while the second and third require EB-88.

1.(a) *Studies of target characteristics at moderate beam-power levels, up to 1.5 kW, using the proton beams from the 88-Inch Cyclotron.* (Initial investigations of a boron nitride target have been made with beams of a few microamperes [5]). This R&D can begin in earnest in the very near future with the design of a prototype target for studying different materials, temperatures, production reactions, etc. Presently, this activity is manpower limited: wider participation is most welcome.

(b) *Investigations of ECR source efficiency and hold-up times using the existing LBL-ECR source.* The Advanced ECR source will be connected to the 88-Inch Cyclotron this summer, freeing the present source for this work. Manpower here is also in short supply.

2. *R&D at higher power levels and with the dedicated ECR source once the facility is constructed.* This would support mainly the development of different beams and higher intensities at this facility, though it would obviously have wider relevance. This type of R&D would go on continuously.

3. *R&D directed specifically toward the problems of a future high intensity facility.*

There are many ways in which the use of this facility for experiments and for R&D is relevant for a future high-intensity facility, especially of the ISOL type. For brevity these are summarized as follows:

Relevance of EB-88 to a future high intensity RB facility

- Primary Beam:
  handling, diagnostics, safety, total power = 15(50)kW,
  longitudinal power density = 20(1) kW/cm. (The values in parenthesis are for a high intensity facility.)
- Targets:
  element-specific target matrices,
  fast diffusion and surface desorption,
  high yield, low vapor pressure, temperature control,
  beam power distribution.
- Beam Purity:
  element selective transport from target to ion source,
  fast on-line chem./phys. separation techniques.

- Ion Sources:

  high efficiency ECR for intermediate 2^+ - 4^+ charge states (charge state influences design and cost of second accelerator!), radiation hardened materials/components.
- Experiments:

  working with low RB intensities, beam impurities, background from RB itself, detector efficiencies.
- Safety Issues:

  primary beam, target/ion-source handling, robotics, post-accelerator contamination, shielding, containment.
- Education:

  training of the next generation of students and postdocs in the science and technology of radioactive beams.

In brief, R&D questions can be addressed today, and R&D flourishes when science can be done simultaneously.

8. Cost and Schedule

The cost is estimated at $7.5 M (FY90), which includes about $3.2 M for the high current cyclotron. With FY93 capital funding, operation for research would begin in FY '95.

Questions, comments, and inquiries about participation are most welcome, and can be addressed to any of the following people at the Workshop: D. Clark, K. Gregorich, P. Haustein, D. Hoffman, D. Moltz, M. Nitschke, F. Stephens, and R. Stokstad

References

1. Marc Loiselet, contribution to this workshop. J. Vervier, et.al., Proc. First Int. Conf. on Radioactive Beams, Berkeley, 1989
2. Ion Beam Applications, Louvain-la-Neuve, Belgium
3. Ebco Technologies, Richmond B.C., Canada
4. K. Erdman, private communication
5. P. Haustein, private communication.

† Nuclear Science Division, Lawrence Berkeley Laboratory, Berkeley, CA 94720

Work supported under contracts DE-AC03-76SF00098 and DE-AM03-76SF000326 with the U.S. Department of Energy

* EB-88 stands for "Exotic Beams at the 88-Inch Cyclotron", and the Collaboration, not a formal organization, consists of people from several institutions who devote, or would like to devote, time to this collective effort.

R. G. Stokstad,
for the EB-88 Collaboration

Fragment Deceleration in Cyclotron

K.M. Subotic
Boris Kidrich Institute

Nuclear structure and astrophysics experiments with radioactive ion beams (RIB) imply the RIB projectile energy range between 5-10 MeV/amu. RIBs may be produced using ISOL (isotope separator on-line) or PF (projectile fragmentation) method. In both cases RIBs are produced in nuclear reactions induced by fast projectiles (500-1000 MeV protons in ISOL or 100-400 MeV/amu in PF method). Cyclotrons may be efficiently used for primary beam production as well as a second stage machine for RIB selection, acceleration and/or deceleration of the in-phase RIB component[1] in both methods. In the first method zero-energy RIB, after selection, should be reaccelerated in post accelerator along the low energy (0-5 MeV/amu) trajectory characterized by extremely low pressure transparency.

At projectile fragmentation (PF) method RIBs are produced at high energies (50-400 MeV/amu). The RIB constituents are fully stripped interacting efficiently with cyclotron magnetic and accelerating guiding fields. The PF RIBs may be used directly at isotope identification and decay measurements or they should be decelerated to low energies for the purpose of nuclear structure and astrophysics experiments. At cyclotron based deceleration methods RIB should be injected at what is usually called cyclotron extraction radius. If injected at Accelerated Equilibrium Orbit at negative RF phase RIB will be decelerated along the inverse (high energy - high pressure transparency part of AEO trajectory). The RIB stability requirements could be derived from the analysis of the RIB radial phase space behaviour[2].

The RIB deceleration spoils its emittance proportionally to the square root of the ratio of the initial to the final RIB energies. The RIB intensity losses at deceleration may be estimated after determining the acceptance/emittance ratio at final beam energy. The RIB deceleration concerns only the high energy part of the cyclotron trajectory, at which the average value of charge-exchange cross-section could be up to 10^3 times lower [3] than that corresponding to the relevant low-energy trajectory at ISOL RIB acceleration. Thus the unavoidable RIB intensity losses caused by the emittance spoiling at RIB deceleration in PF method are expected to be compensated by improved pressure transparency along high energy trajectory.

For the typical ^{15}O RIB having energy 388 MeV/amu at angular divergency characterized by standard deviation of 4.25 mrad [4] the RIB oscillation amplitude is of the order of 10 mm [5] at cyclotron with extraction radius of 100", (being able to accelerate Z/A=.5 heavy ion species up to energies of 450 MeV/amu). The resulting RIB emittance is of the order of 40 π mm mrad. Acceptance of the typical iron cored superconducting cyclotron at 5 MeV/amu is of the order of 100 π mm mrad [6]. At this energy the ^{15}O RIB emittance will be of the order of

352 π mm mrad suggesting the reduction of beam intensity for a factor of 3.5. The pressure transparency of the machine is determined by $T_p = \exp-(C\Sigma\sigma_i L_i) = \Pi T_{pi}$ where $\sigma_i L_i$ are the products of charge-exchange cross-sections and respective trajectory segments, while C represents the respective dimension conversion factor. In 100" cyclotron the ratio of the pressure transparencies for low-energy (0-5 MeV/amu) and high-energy (388-5 MeV/amu) RIB path indicates 8 times better pressure transparency for RIB high energy deceleration path at PF approach than at the RIB low energy acceleration at the ISOL approach method for obtaining of low energy 5 MeV/amu RIB projectiles. Such an improvement of pressure transparency along the RIB deceleration path opens the possibility for compensation of the beam intensity losses caused by RIB emittance spoiling.

Finally it is relevant to note that aforegiven considerations are not based on the performances of the cyclotrons dedicated to the RIB deceleration, requiring the high-acceptance, high energy gain/turn and the sophisticated RIB extraction machine capabilities. The air-core superconducting cyclotrons[7] in the class of the machines with extraction radius of 100", being able to guide and accelerate the proton beams up to 1000 MeV and Z/A=.5 heavy ion species up to energies of 450 MeV/amu could be excellent candidates to meet these design criteria.

References:

1. K.M. Subotic et al: Superconducting mini cyclotrons in AMS; Nucl. Instr. and Meth., (1990).

2. Lj. Milinkovic, K. Subotic and E. Fabrici: Properties of centered accelerated equilibrium orbits, Nucl. Instr. and Meth. A273 (1988) 87-96.

3. R. Janev, L. Presnikov, V. Shevelko: Physics of highly charged ions, Springer-Verlag 1985.

4. R. Bimbot: Production of 400/n radioactive ion beams, IPN Orsay Report 1988.

5. M. Gordon (private communication).

6. Lj. Milinkovic, E. Fabrici and K. Subotic: The effects of the beam centering using first harmonic magnetic field component, Nucl. Instr. and Meth. A276 (1989) 418-426.

7. K. Subotic: Multipurpose air core cyclotron, Proceedings of EPAC, Rome 1989, 484-486.

Activity Expectations from a Thin-Target Ion Beams Facility for Short-Lived Nuclei

W. L. Talbert, Jr.
Los Alamos National Laboratory

I. INTRODUCTION

The existence of on-line mass separators at major accelerators or reactors for more than 2 decades has had a major impact on nuclear structure research. It has recently been suggested that an exciting new thrust in nuclear physics research would result from the availability of intense ion beams of short-lived nuclei. These beams could either be accelerated for use in nuclear reaction studies and materials science, or be used directly as in the past for nuclear structure studies. This new thrust has the requirement, however, that the short-lived species be available with the highest possible intensities, in order that reaction studies be realistically conducted, and so that exotic decay properties can be studied.

Short-lived nuclei can be produced by deep inelastic reactions with heavy-ion projectiles; however, much higher intensities of such nuclei are typically realized from the use of a high-energy proton beam through the processes of spallation, fission, and fragmentation. There are two basic approaches with high-energy proton beams to provide intense beams of short-lived nuclei:

1) Interaction of the proton beam with a thick target, for which the recoiling reaction products thermalize and diffuse to the surface of the target and then are released by desorption for subsequent transport and ionization in a co-located ion source. This approach is attractive for species that diffuse quickly in hot solid or liquid target material. However, this approach is element-specific and seriously constrains the study of reaction products with half-lives shorter than the diffusion/desorption times.

2) the second basic approach uses high-energy proton beams interacting with a thin target, from which the reaction products freely recoil, thermalize in a high-pressure gas and are then transported to a remotely located ion source. This transport can be achieved with thermalized, charge-stabilized recoil atoms directly (the ion guide concept[1]) or by attaching the thermalized recoils to the surfaces of aerosols which are transported by the gas stream (the He-jet concept[2]).

The thick-target approach is discussed in another contribution to this Workshop, along with a description of the production reaction processes available.[3] We concentrate here only on the thin-target approach. Because, in this approach, the intensities of ion beams of short-lived nuclei depend directly upon the production rates in the thin targets, the limits in production and the efficiencies for transporting the activities provide some interesting comparisons to the intensities possible for the thick-target approach. In comparing the end-of-system availability of the two approaches, the reader should keep in mind that the they are basically complementary and each has its place in providing ion beams of short-lived nuclei.

II. He-JET APPROACH *vs.* ION GUIDE APPROACH

The He-jet activity transport approach is schematically depicted in Fig. 1, in which the steps of the technique start from a helium supply, through an aerosol generator, a target chamber, a transport line (in practice a capillary), and into an ion source. In this approach, a stream of helium is "loaded" with aerosols and introduced into a target chamber (here shown as a chamber containing multiple targets). The recoiling activities

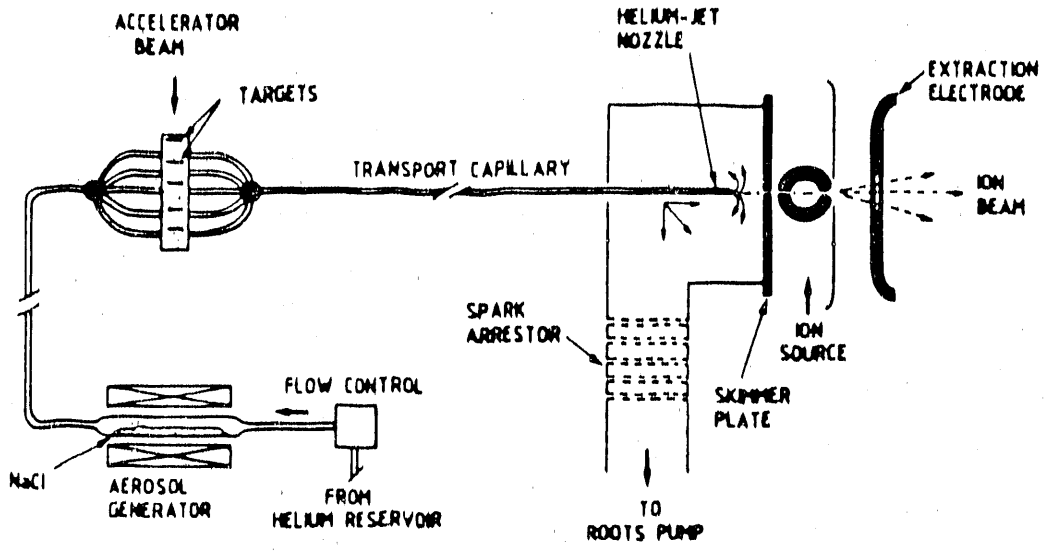

Fig. 1. Schematic of a He-jet activity transport system

produced by the beam interactions in the target foils are stopped in the helium and, once thermalized, become attached to the aerosols by surface forces. The activity-loaded aerosols are then directed, along with the helium, through the transport capillary to a skimmer chamber, where the helium is pumped away and the heavy aerosols, along with a small amount of helium, penetrate into an ion source. The skimming function is made possible by emergence of the helium gas from the end of the capillary in a Mach cone that has a much larger angle than the one for the heavy aerosols. The ion source serves the double function to volatilize the activities from the aerosols and ionize them for extraction into an ion optical system for mass analysis of the resulting ions.

The ion-guide approach parallels the He-jet approach, but employs the charge-stabilization properties of the helium for thermalized recoils, and uses an electric field to guide the ions into an ion optical system.

We favor the He-jet approach over the ion guide for thin-target production because of the following arguments:

1) The ion-guide approach has not been used in high-intensity beams;

2) The transport length for the ion guide is too short to be effective in transporting the stopped recoils through the beam-line shielding;

3) There is a relatively large body of experience for the He-jet; and

4) The efficiency of the ion guide is highly dependent upon the relative ionization properties of the working gas and recoiling products, whereas the He-jet has virtually the same efficiency for all non-volatile recoil products.

Comparison of the thin-target and thick-target approaches include:

1) The He-jet approach has prompt activity release, the transport to the ion source is rapid (of the order of 10's of msec for a 4-m long capillary), and the efficiencies are virtually independent of the nature of the produced species. The thick-target activity release, in contrast, is susceptible to delay by diffusion/desorption processes and exhibits strong dependence on the chemical and physical properties of the activity of interest.

2) The production rate of exotic nuclei can be large in the thick-target approach, but the deposit of significant beam energy in the target constrains the size and form of the target usefully employed. The thin-target approach, by contrast, requires as much production beam intensity as possible in order to make up for the target thinness. Both approaches, therefore, impose practical limits on the production rate.

3) The He-jet technique separates the highly-activated target chamber from the rest of the system, enabling ion source changes/maintenance to be accomplished with relative ease. The thick-target experience requires robotic handling for the integrated target/ion source, even at the few uA level, which poses a real challenge in planning for a significantly increased production beam intensity.

4) The thin-target approach allows the use of rare target materials, such as separated isotopes or transuranic elements, to enhance production rates in selected mass regions.

The thin-target approach is not intended to compete with the thick-target approach for those activities but are easily released from a thick target. In assessing the activities potentially available at a facility for intense beams of short-lived nuclei, however, the thin-target approach offers an attractive complementary capability to that using a thick target, and it is for this reason that the thin-target approach deserves to be pursued — after all, not all interesting nuclear physics is confined to those species that are easily released from a thick target.

III. ION BEAM INTENSITY FACTORS

A. Cross Section Estimates

The most important factor in estimating yields of ion beams of short-lived nuclei using the thin-target approach is the production rate, related to the reaction cross sections. Estimation of the thin-target production rates requires cross section models that are largely unvalidated by direct measurements. Thick-target activity availabilities have been determined for a large number of elements at the ISOLDE facility (see Ref. 3), but these available intensities cannot be related to the production cross sections except by a complex deconvolution of diffusion/desorption effects that are only primitively understood.

For spallation reactions, a set of semi-empirical relations exists to predict spallation product yields.[4] For the purpose of estimating thin-target yields, we have chosen the IDED and IDED-G models of Ref. 4, which result in reasonably accurate cross-section estimates for proton-induced spallation in the energy range of 600 MeV to 1 GeV.

For high-energy proton-induced fission reactions, we developed an empirical approach,[5] fitting two gaussian mass distributions to existing data for Rb and Cs, one for the neutron-rich portion of the data, and one for the neutron-deficient portion of the data. The gaussian parameters were adjusted for the mass yield variations and differences between the Rb and Cs data, and the parameters were interpolated for 800-MeV protons from the existing data for protons at 156 MeV, 170 MeV, and 1 GeV.[6,7] We expect these cross-section predictions to be reasonably accurate for the mid-mass range of fission products, but do not expect them to accurately predict cross sections resulting in the highly asymmetric fission distributions that yield low-mass and high-mass fragments.

B. He-Jet Transport Efficiency

An important element of the efficiency for the He-jet technique is the overall transport efficiency, which combines the efficiency of attachment of the produced activities and that of the transport down the length of the capillary. This efficiency was measured for conditions at LAMPF by comparing the activity collected at the end of the capillary to that generated in the target foil.[8] This measurement gave a combined efficiency for the target assembly and He-jet (45-m long capillary) of about 60% for all non-volatile elements.

C. Transport Time, Target Chamber Sweep Time

It is possible to calculate the activity transport time through the capillary, using an adiabatic flow theory.[9] Experiments have shown that the predicted transit times are realistic[8] and have a strong dependency on the flow conditions. For a 4-m long capillary required to penetrate the LAMPF beam-line shielding, a transit time as short as about 20 msec is predicted for strong flow.

Under the flow conditions for the capillary above, the sweep time (for a 10-cm long target chamber) calculates to be about 30 msec, yielding a total transport and sweep time of about 50 msec. This short delay is very attractive, and most short-lived neutron-rich nuclei will survive nicely under these conditions.

D. Ion Source Coupling and Efficiency

The least experience in He-jet technology is in coupling a He-jet activity transport system to a mass separator ion source with acceptable efficiency. Nevertheless, several laboratories have succeeded in obtaining useful coupling and ionization efficiencies.[10-13] The success of these efforts is illustrated nicely in Fig. 2, which shows that efficiencies of a few percent have been achieved, and it is reasonable to expect efficiencies of 10%, despite the common impression that the He-jet technique does not allow for moderately-high ion source efficiencies. This form of plot is suggested by the discussion in Ref. 14.

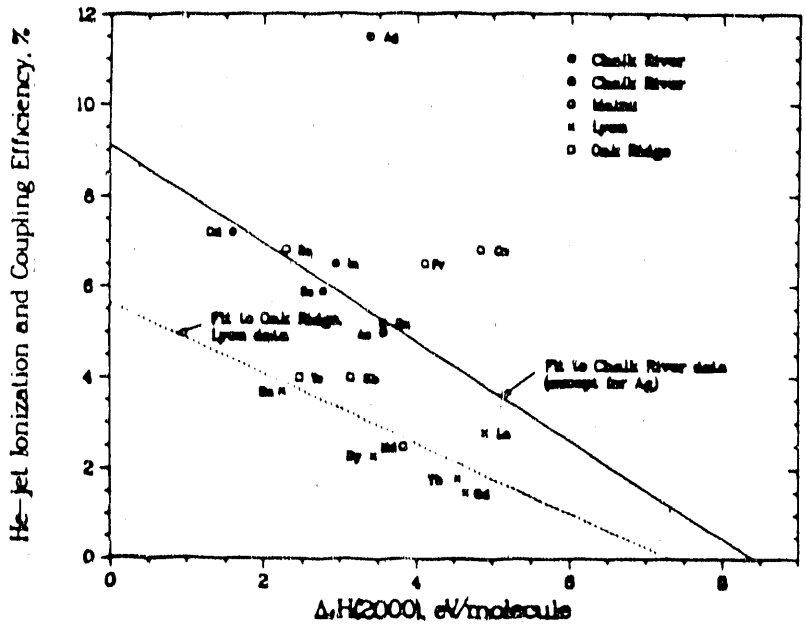

Figure 2. Ion source efficiencies reported for the He-jet technique

In Fig. 2, the abscissa is the free enthalpy of the chemical species at 2000° C, and the fits to the data indicate that, for the ion sources employed, the ionization was a two-step process with the first step being desorption from the hot surfaces of the ion source. An alternative approach may be to use a "once-through" ion source with the aerosols entering the plasma directly and not impinging first on a hot surface — this approach may be possible using a cusp-type ion source, such as the mono-cusp source.[15]

IV. EXPECTED ACTIVITY INTENSITIES FOR A HIGH-INTENSITY PROTON BEAM (LAMPF PARAMETERS)

Estimates of expected ion beam intensities for short-lived nuclei have been made for a number of nuclei that have interesting N/Z ratios or contain nucleon numbers of possible interest for reaction or nuclear structure studies. In deriving these estimates, the cross sections are estimated as indicated in Sec. III.A. The He-jet transport efficiency is given a conservative value of 60%; it is, however, reasonable to expect a somewhat higher value for shorter capillaries. The He-jet transport time is ignored for activities with half-lives larger than a few tenths of a second. Finally, the ion source coupling and ionization efficiency are considered to be of the order of 10%.

In addition, the possibility of multiple target chambers in the LAMPF beam allows the effective target thickness to be increased from the nominal 20 mg/cm^2 for fission products by a factor of five or more — for spallation products, it is presumed that an equivalent target thickness is possible by using multiple target foils or, possibly, wrapping one thin target foil in a spiral. Under the above conditions, a 1-mA beam intensity from LAMPF would yield an ion beam intensity of 1 x 10^8 ions/sec per mb of production cross section.

Some fission-product intensity expectations are shown in Fig. 3 for the "valley" elements and the heavier rare-earth elements with half-lives <100 sec. These activities are also not generally available using thick targets. The use of these ion beams, which are expected to be deformed, offers interesting new capabilities.

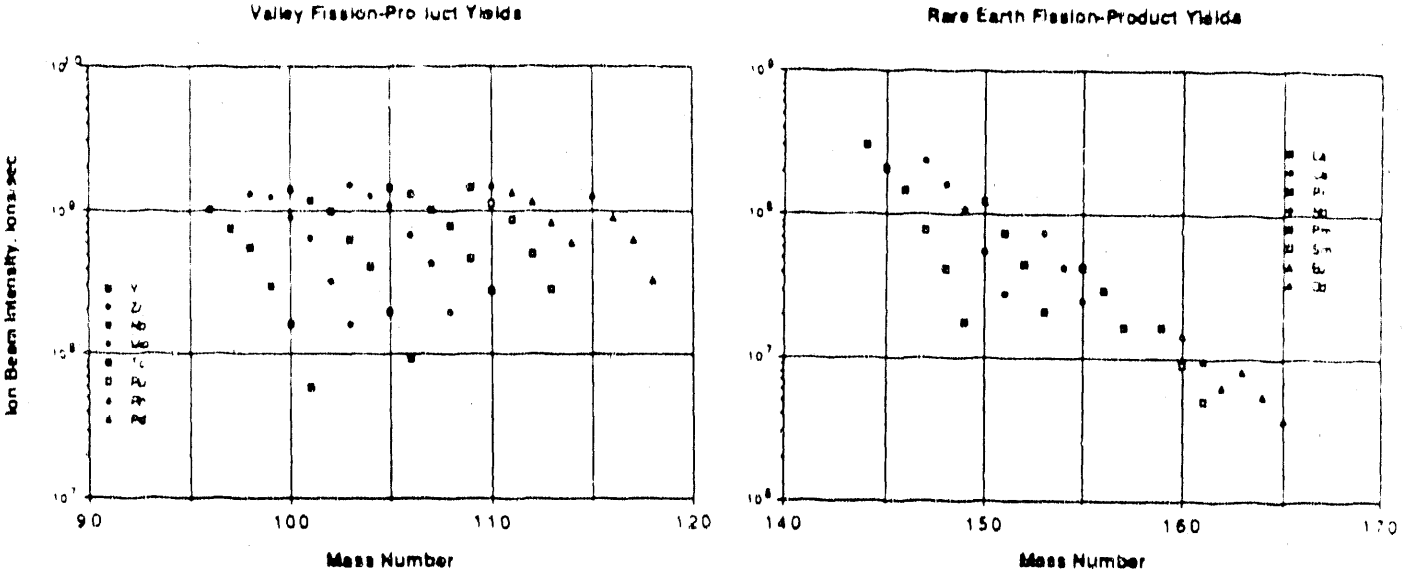

Figure 3. Expected ion beam intensities for selected fission products

Examples of expected spallation-product intensities are provided in Fig. 4, for which yields from several targets were estimated. These activities were selected to illustrate possibilities for ion beams in the general vicinity of N=Z, with half-lives >100 msec, for a number of elements not generally available using thick targets. It is worth noting that these species are many units away from stability and offer special capabilities in nuclear reaction studies requiring beam intensities of pA or higher.

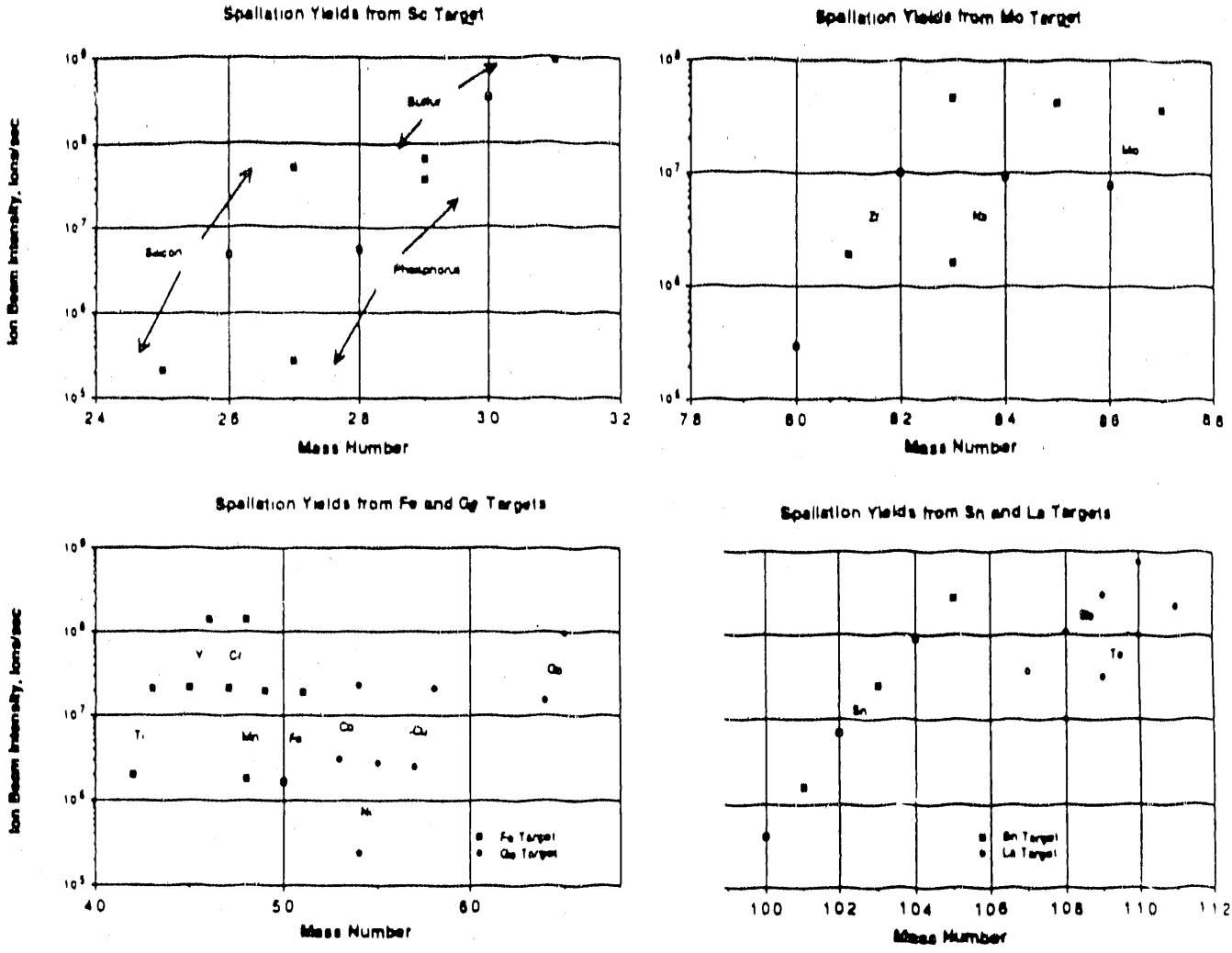

Figure 4. Expected ion beam intensities for selected spallation products

REFERENCES

1. J. Arje *et al.*, Nucl. Instr. and Meth. **B26**, 384 (1987).
2. H. Wollnik, Nucl. Inst. and Meth. **139**, 311 (1976).
3. J. M. D'Auria, "Expected Intensities from an ISOL/Accelerator Radioactive Beams Facility," these proceedings.
4. G. Rudstam, Z. Naturforsch. **21a**, 1027 (1966).
5. W. L. Talbert, Jr., M. E. Bunker and J. W. Starner, "Feasibility Studies of a Helium-Jet-Coupled Isotope Separator at LAMPF," in Proceedings of the TRIUMF-ISOL Workshop, Mr. Gabriel, Canada, eds. J. Crawford and J. M. D'Auria, TRIUMF Report TRI-84-1 (November, 1984), p. 179.
6. B. L. Tracy *et al.*, Phys. Rev. C5, 222 (1972).
7. B. N. Belyaev *et al.*, Nucl. Phys. **A348**, 479 (1980).
8. W. L. Talbert, Jr., M. E. Bunker and J. W. Starner, Nucl. Instr. and Meth. **B26**, 345 (1987).
9. H. Dautet *et al.*, Nucl. Instr. and Meth. **107**, 49 (1973).
10. H. Schmeing *et al.*, Nucl. Instr. and Meth. **B26**, 321 (1987).
11. A. Plantier *et al.*, Nucl. Instr. and Meth. **B26**, 314 (1987).
12. R. A. Anderl, J. D. Cole and R. C. Greenwood, Nucl. Instr. and Meth. **B26**, 333 (1987).
13. Y. Kawase, K. Okano and K. Aoki, Nucl. Instr. and Meth. **B26**, 341 (1987).
14. R. Kirchner, Nucl. Instr. and Meth. **B26**, 204 (1987).
15. J. P. Brainard and J. B. O'Hagen, Rev. Sci. Instr. **54**, 1497 (1983).

A Research and Development Program at Los Alamos for Production of Ion beams of Short-Lived Nuclei

W. L. Talbert, Jr., J. M. Wouters, D. J. Vieira,
E. L. Fearey, and J. B. McClelland

Los Alamos National Laboratory

I. INTRODUCTION

In the past few years, we have examined the feasibility of using a He-jet activity transport system[1] at LAMPF to provide intense sources of nuclei far from stability. These feasibility studies were carried out to assess potential capabilities for studying exotic properties of nuclei far from stability, as a complementary approach to more traditional thick-target techniques used at, for example, the ISOLDE facility at CERN.

We have reported[2] on the results of He-jet studies with attention to aerosol type and production conditions, target chamber flow conditions, and efficiencies for activity transport through a long (up to 45 m in length) capillary. Many of these studies were conducted using a neutron beam from the Omega West Reactor (OWR) to produce fission-product activities, but additional studies at LAMPF reinforced the conclusions of the OWR experiments. However, we have not completed a series of experiments using the main 1-mA beam at LAMPF to illustrate that the He-jet approach is a viable and predictable means to provide intense sources of exotic nuclei.

There exist many reports[3-7] on the use of a He-jet activity transport system to study nuclei far from stability and, based on these reports, we can be assured of modest, yet attractive, performance characteristics for a thin-target, He-jet activity transport system, coupled to a mass separator ion source[3-6] to provide ion beams as well as use in fast radiochemical studies.[7]

The thin-target approach is especially attractive for study at Los Alamos because of the unique availability of the high-intensity proton beam at LAMPF. The use of a high-intensity beam for production of short-lived activities allows the target thickness to be reduced to achieve the prompt activity release of reaction products that recoil from the target, thus avoiding one of the major limitations of thick targets, the time delay from desorption of products that diffuse to the target surface. In addition, the use of a thin target in the proton beam reduces significantly the radiative handling requirements in target replacement and maintenance. The He-jet transport system separates the target from the separator ion source so that the ion source is not subjected to the intense radiation fields present in production beam environments.

The thin-target approach is not intended to compete with the thick-target approach for those activities easily desorbed from a thick target. However, the use of thin targets offers an attractive, complementary capability for many species of desired short-lived nuclei that could subsequently be studied or accelerated, and are unavailable using thick targets because of desorption delays.

II. FUTURE STUDIES OF A He-JET SYSTEM

The use of the OWR to produce short-lived fission-product activities is attractive in He-jet feasibility studies because the experiments are absolutely parasitic to the normal operation of the reactor, and can be conducted without constraints from the complex schedules at LAMPF. Studies carried out at the OWR have resulted in evaluating the effects of changes in aerosol type and aerosol production (e.g., furnace temperature), and in helium flow conditions. Before using the He-jet approach on the main beam line at LAMPF to provide ion beams of short-lived nuclei, additional studies are necessary using the existing OWR arrangement.

A. Helium Flow and Activity Studies

In the He-jet approach, the major delay for produced activities is the combined result of (1) the time required for the helium flow to sweep out the gas volume of the target chamber and (2) the transit time through the capillary. In the previously-reported experiments,[2] the transit time through a 22-m long capillary was observed for a variety of flow conditions, and it was determined (see Fig. 1) that the predictions of the laminar flow calculations[9] were essentially verified to a Reynolds Number of about 6000 (occurring at the flow for which the chamber pressure is 370 kPa — at 225 kPa pressure, the flow is at the traditional laminar limit, R_E= 2200). Such high Reynolds Numbers are acceptable because the onset of turbulence in the laminar flow starts at the walls of the capillary, while the aerosols proceed mainly in the center of the gas flow. In Fig. 1, a slight deviation of observed transit times from the predicted values is noted at the higher flow rates, as expected if the flow were disturbed by turbulence.

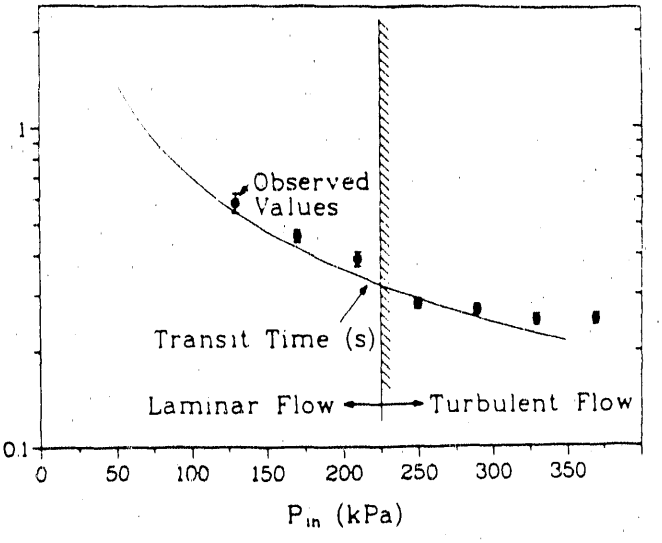

Figure 1. Transit time for a 22-m, 2.4-mm diameter capillary

For a system optimally located at LAMPF, the capillary length could be decreased to about 4 m. An idealized chamber for a fissioning target would be in the form of a cylinder with its axis oriented perpendicular to the proton beam and with a diameter equal to the range of fission fragments in helium at the working pressure. The fissioning target is deposited on the inner surface of the cylinder. It is a straightforward calculation to obtain the sweep time of the chamber (for a chamber of given active length — in this case, 10 cm), as well as the transit time through the capillary (see the approach in Ref. 9). The combined sweep and transit time is a strong function of the flow parameters, conveniently indexed by the Reynolds Number of the flow. As an example, for a capillary of 4-m length and idealized cylindrical target chamber, the traditional laminar-flow limit of R_E=2200 results in a time for sweep plus transit (for a 0.8-mm diameter capillary) of 315 msec, whereas

for R_E=7000, the combined time is 50 msec. Intermediate times would be expected for intermediate Reynolds Numbers.

An experiment conducted at the OWR can confirm this prediction without requiring the large efforts of a test at LAMPF. Using a series of target chambers with dimensions matching a range of flow rates (and helium pressures), the observation of short-lived activities collected on a moving tape collector would give direct confirmation of the flow predictions. In addition, the neutron beam can be shuttered in a few milliseconds, and the transit and sweep times can be measured directly by observing the time dependence of the pulse-produced activities as collected on the moving tape.

The experiments at the OWR have provided valuable experience and target chamber design information for studies based at LAMPF. Three experiments have been conducted at LAMPF, the first two at a low-intensity side beam ($\leq 6\ \mu A$) with the objective of measuring the transport efficiency of the He-jet activity transport system, and the third to evaluate the transported activity levels and survivability of the target chamber in the main LAMPF beam. The transport efficiency was measured for a number of product activities to be about 60% through a 22-m long capillary, and the transport was demonstrated to be unaffected by large beam-current densities (the low-intensity beam was focused to have a higher areal current density than is expected for the main beam).

The third experiment illustrated a difficulty in maintaining adequate target chamber cooling (the target chamber walls/windows reached temperatures exceeding 500° C), and the transported activity lost linearity with incident current at about 300 μA for the main beam current, presumably due to thermal-induced turbulence in the target chamber.

B. Target Chamber Studies

Based on the experience of the previous experiments, the LAMPF target chamber has been redesigned (see Fig. 2) with coaxial walls with annular cooling

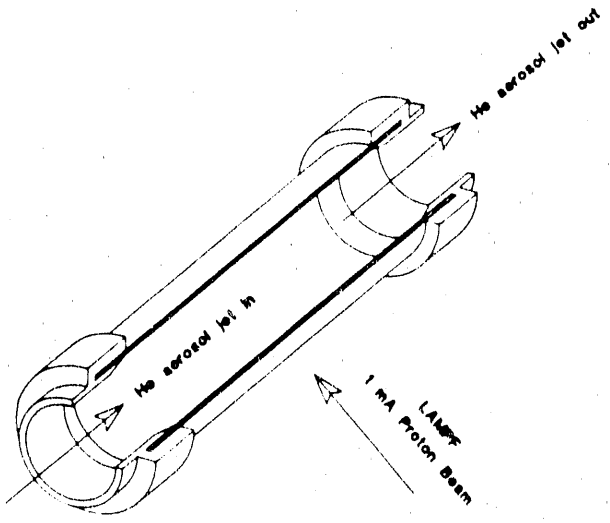

Figure 2. Target chamber design for use at LAMPF

to avoid the thermal effects observed earlier. This design features a minimum of mass in the region of the highest proton flux, and places the helium inlet and outlet in reduced radiation fields. The inner wall is expected to rise to a maximum temperature of about 150° C, a considerable improvement over the previous design. With this new chamber design, we expect to demonstrate survivability from the effects of the full beam intensity and maintain the activity transport efficiency observed previously. The eventual goal of this work is to determine the yields of exotic nuclei after transport and skimming for operation in the full LAMPF beam (>700 μA).

C. Ion Source and Ion Optical Development

1. Ion source development

An ion source test stand coupled to a He-jet skimmer chamber exists at the OWR for the purpose of examining ion source designs and optimizing ion-source parameters for efficient coupling to a He-jet. It is important that the ion source operate reliably under conditions of helium flow rates dictated by the previous studies, and provide ions of the activities transported by the He-jet with good efficiency (it has been shown that coupling and ionization efficiencies of a few percent are attainable,[4-7] and we believe that efficiencies approaching 10 percent are possible).

An ion source will be constructed from existing, well-documented concepts for sources in operation at other He-jet facilities. Coupled performance will be evaluated for subsequent staging at LAMPF to demonstrate operational parameters of the conceptual thin-target system to provide ion beams of exotic nuclei. In addition, we have been impressed with the results of preliminary studies with a mono-cusp source[10] and intend to continue these studies for a redesigned source.

2. Laser resonance ionization

Because of the inherent chemical non-selectivity of the He-jet activity transport system, a promising method for selective ionization of an activity of interest is the application of laser resonance ionization.[11,12] This approach potentially offers additional advantages, such as high ionization efficiency, pulsed operation (perhaps for better matching to the accelerator), and production of polarized ions. In this approach, a high-power laser would be used to desorb the activities from the aerosols and then a two- or three-color laser system would resonantly ionize selected species. This system could be pulsed or CW, and with circularly polarized light. We plan to investigate the suitability of this proven technique applied to the specific case of the He-jet activity transport system.

3. Prototype mass separator

A prototype mass separator will be designed for the purpose of providing diagnostic capabilities of the performance of He-jet coupled ion sources, This separator is envisioned to have two stages, the first a low-resolution stage primarily intended to separate out the expected intense He^+ ion beam, and the second stage to study the ion source performance characteristics. This separator will be used in experiments both at the OWR and at LAMPF.

III. CONCLUSIONS

Our intention with this R&D program is to address aggressively the question of a thin-target, high-intensity option for the production of exotic beams. It is envisioned that the essential elements of this program could be carried out in a time frame of about three years, given adequate resources. The compelling case for such efforts is presented in another paper in this Workshop addressing expected yields of activities and the advantages of a thin-target approach at a high-current proton accelerator such as LAMPF.

REFERENCES:

1. H. Wollnik, Nucl. Instr. and Meth. **139**, 311 (1976).
2. W. L. Talbert, Jr., M. E. Bunker and J. W. Starner, Nucl. Instr. and Meth. **B26**, 345 (1987).
3. A. Plantier *et al.*, Nucl. Instr. and Meth. **B26**, 314 (1987).
4. H. Schmeing *et al.*, Nucl. Instr. and Meth. **B26**, 321 (1987).
5. R. A. Anderl, J. D. Cole and R. C. Greenwood, Nucl. Instr. and Meth. **B26**, 333 (1987).
6. Y. Kawase, K. Okano and K. Aoki, Nucl. Instr. and Meth. **B26**, 341 (1987).
7. E. Stender, N. Trautmann and G. Herrmann, Radiochem. Radioanal. Lett. **42**, 291 (1980).
8. J. Ärje *et al.*, Nucl Instr. and Meth. **B26**, 384 (1987).
9. H. Dautet *et al.*, Nucl. Instr. and Meth. **107**, 49 (1973).
10. J. P. Brainard and J. B. O'Hagen, Rev. Sci. Instr. **54**, 1497 (1983).
11. G. S. Hurst *et al.*, Rev. Mod. Phys. **51**, 767 (1979); also G. D. Alkhazov *et al.*, Nucl. Instr. and Meth. **A280**, 141 (1989).
12. C. M. Miller and N. S. Nogar, Anal. Chem. **55**, 1606 (1983); also B. L. Fearey *et al.*, J. Opt. Soc. Am. B, **7**, 3 (1990).

The Proposed Radioactive Nuclear Beam Facility at RAL

Gordon Walker
Rutherford Appleton Laboratory

1. In the United Kingdom we are studying a Radioactive Nuclear Beams Facility which will have as its major experimental goal the extension of the study of the nucleus through spectroscopic studies at and near the neutron and proton drip lines and in the region of superheavy nuclei. This facility will separate and accelerate radioactive fragments with half-lives down to tens of milliseconds produced in spallation, fission and fragmentation processes using a primary beam of high intensity protons from the ISIS proton synchrotron at Rutherford Appleton Laboratory. The range of science that can be studied by such a facility includes nuclear physics, nuclear astrophysics, atomic physics, solid state physics and nuclear medicine.

2. The physics case for an RNB facility has been prepared by the UK nuclear structure community. The report of the year long study by the Working Group led by Bob Chapman of Manchester University is at this moment being considered by the National Nuclear Structure Committee. With the availability of beams of radioactive nuclei, access will be opened up for the first time to the study of a wide range of nuclei near the proton and neutron drip lines and to the region of the highest-Z nuclei.

3. The conceptual design of the RNB facility is based on present technology and comprises the following major components:

800 MeV proton beam of up to 100 μA current
target/ion source station
on-line isotope separator
post acceleration complex

The 800 MeV proton facility ISIS already exists at the Rutherford Appleton Laboratory for the production of neutrons for condensed matter research. The on-line isotope separation will follow the principles of the ISOLDE facility at CERN. Provision is provided for further acceleration up to energies of several MeV per nucleon using either a linear accelerator system or a linac plus race-track synchrotron.

4. A staged development is being considered. The first stage includes the target, ion sources, separator and experimental area, as at ISOLDE, but at incident proton current of say 10 μA. It is technically feasible to take up to 100 μA of ISIS protons for radioactive beams and the facility will be designed for this. The second stage includes the construction of the post accelerator and further experimental areas. An RFQ would be used to take the ions to 50 keV/nucleon to be followed either by a synchrotron-storage ring or a high energy linac system. A third stage may be considered for the former, to extend the energy range for heavy ions. In this stage, transfer lines are built between

the synchrotron and the ISIS ring. Heavy ions may then be injected and accelerated in the first ring, transferred to and accelerated in the ISIS ring before being stripped and returned to be re-accelerated in the first ring. In this way energies up to 40.6 MeV per nucleon may be obtained for the heavy ions and over 120 MeV per nucleon for the light ions.

5. It is proposed that the primary proton beam, target/ion sources (two) and beam dumps should be below ground for reasons of economy. Sufficient shielding between the two target stations would be provided to enable access to one station while the other is in use. The beam dumps would be of water to minimise activation problems. This not only simplifies the dump cooling but also results in a very inexpensive device. The straight-through primary proton line would also be placed underground. The ion beams from the source would be directed up to ground level where the separator and accelerator complex would be sited in the experimental hall.

6. Removal of the active target/ion source assembly would be carried out below ground by remote operation. The active components would be stored in flasks, which when full, would be transported to the disposal agency. It is expected that the same flask design that is currently used for the neutron facilities targets could be used for the radioactive beam target assemblies. Most of the water cooling facilities for the target would also be housed below ground. Thus all the main activity would be confined to below ground. The production and disposal of targets will be a significant running cost of the facility. RAL has already considerable experience in the handling and disposal of targets from the pulsed neutron source.

7. Mass separators and beam lines similar to the CERN ISOLDE 3 arrangement are considered for the low energy radioactive beams and provision is made to take the beams on to an accelerator system (linac or synchrotron) to produce energies of several MeV per nucleon for all ion species. No detailed design work has been carried out in the target/ion source area. It is hoped to learn the necessary skills involved by collaboration with CERN.

8. For elements up to mass number A=80 it is assumed that conventional ion sources, surface ionisation or plasma discharge types, with the ion charge state q=1 will be used. Charge state 2 is required for elements in the mass range 81 to 160 and charge state 3 for the mass range 161 to 240. This allows the use of a single RFQ for the first stage of post acceleration. The development of high charge state ion sources has been identified as a topic requiring study.

9. In the synchrotron option for post-acceleration, the RFQ linac will feed directly into a synchrotron. Major requirements for the ring are a very efficient multi-turn injection system and obtaining an adequate beam lifetime for the various radioactive ion species. A design has evolved for a fast-cycling synchrotron with a racetrack magnet lattice that encloses most of the available area of the hall. The design meets the required specification for light ions of an energy range of 0.2 to 6.0 MeV per nucleon, with the possibility of reaching 20.0 MeV. It

does not meet the specification, however, for very heavy ions where the energy range in MeV per nucleon is restricted between 0.2 and 2.6 until the third stage of the proposed development.

The synchrotron-storage ring has a 12.5 Hz magnet power supply with the 80.0 ms cycle divided equally for injection, field rise, extraction and field fall. Modified waveforms are required for the higher energy third stage which involves transferring ions to and from the ISIS ring for further acceleration up to 40 MeV/nucleon for mass number 238.

10. In the linac option, the facility would comprise an on-line isotope separator followed by a heavy ion linear accelerator system consisting of three main sections. Nuclear reaction products produced by the energetic protons via mainly target spallation are ionized in the ion source of the separator. The nuclide of interest is separated by momentum analysis and injected into the linac at an energy of 1 keV/u. Acceleration is carried out in three stages using an RFQ accelerator based on the TRIUMF design, an Interdigital H linac and either an Alvarez drift tube linac or independently phased resonators (warm or superconducting) as the third stage. By using stripping between these three stages for heavier ions the machine can cover the mass range M=10-80 assuming singly charged ions from the ion source, producing an output energy 6.5 MeV/u. By using doubly and triply charged ions from the sour and increasing the IH linac and final stage acceleration by approximately 25% over that required for the M=80 case it is possible to cover the mass range up to approximately 150.

11. In the course of producing this conceptual design for a radioactive nuclear beam facility we have recognised in addition to a detailed design study the need for further developments on the following topics:

1. High charge state ion sources
2. Low beta superconductivity cavities
3. Targets and ion sources
4. Synchrotron magnet, gas stripper and vacuum vessel design

Acknowledgement

The joint Daresbury Laboratory and Rutherford Appleton Laboratory team who carried out the conceptual design study are:

T.W. Aitken, J.R.J. Bennett, R.J. Elsey, I.S.K. Gardner, M.R. Harold, C.W. Planner, H.G. Price, G.H. Rees and N.D. West.

Separation of Short Lived Nuclei within one Isobaric Chain

H. Wollnik

II. Physikalisches Institut der Justus-Liebig-Universität
6300 Giessen, W-Germany

ABSTRACT

Principles and limits of mass separators are discussed that should achieve an element separation within an isobaric chain simply by using the small mass differences between those ions.

1 Introduction

To separate short lived nuclei commonly on-line mass separators are employed that consist of a not too small magnetic sector field and an ion source to which the short lived nuclei are rapidly transported from the production target [1]. Typically mass separators are fed with ions of one element and require mass resolving powers of $m/\Delta m > 250...500$ to separate the different isotopes of this element. However, if - as is always the case in on-line mass separators - several elements are present in the feed material to the ion source, each mass peak consists of ions of several neighbouring elements. Thus any element-specific chemical separation effect is welcome as there would be for instance chemical reactions in the ion source or the use of positive or negative surface ionization which favours alkali elements or halogens over all others.

In principle one can also use the small mass differences between ions of Z protons and N neutrons and ions of $Z \pm 1$ protons and $N \mp 1$ neutrons to distinguish between the ions of the isobaric chain $A = N + Z$. For stable

nuclei these mass differences are considerably below 1 MeV, while for short lived nuclei these mass differences increase to 5, 10 and more MeV. To separate ions of 100 amu, i.e. of $\approx$ 100 000MeV thus mass resolving powers $m/\Delta m \approx$ 10 000 or $m/\Delta m \approx$ 20 000 are required [2,3]. Unfortunately such mass resolving powers commonly can not be achieved by existing on-line mass separators.

2 Postulates to on-line Mass Separators of high Mass Resolving Powers

Though existing on-line mass separators can not achieve mass resolving powers of $m/\Delta m \approx$ 20 000, such mass resolving powers are commonly achieved by double-focusing mass spectrometers designed for the mass analysis of large molecular ions. In principle thus mass separators should be capable of achieving similar performances. Here two aspects are of importance

1. The final image of the x-extension of the area from which ions seems to originate, must be at least 20000 times smaller than the mass dispersion of the mass separator. Usually one even should ask this ratio to be 40000 or at least 30000 times smaller in order to allow for some misalignments and some residual image aberrations.

2. The aberrations of the system must be reduced so as to become insignificant as compared to the first-order size of the image of the entrance slit. Usually an active correction is necessary by using electrostatic or magnetic multipole elements [4] and/or by using surface coils in the sector magnets [5].

3. The different sources of mass cross contamination [3,6] must be counterbalanced sufficiently as to allow the investigation of a low yield isotope in the presence of intense beams of neighbouring masses.

2.1 Matching of the ion source to the mass separator

If one wants to achieve a high mass-separation power it is advisable not to image the ion-source orifice directly by the mass-separator optics to the

corres, onding image plane, - though this is done in most existing on-line mass separators -, but rather have another optical transfer system inserted in between. This transfer system should image the ion source orifice to an intermediate image at which a variable entrance slit of width $2s_1$ can be placed. The advantage here is that the system performance becomes considerably less dependent on the ion source performance which especially in on-line systems is not fully controllable.

Since the dispersion of a mass separator in most cases is $\approx \rho_0$, the radius of deflection of the separator sector magnet, and since the separator magnification mostly is about unity, the ratio of $2s_1/\rho_0$ should be $\approx 1/40000$ or at least $\approx 1/30000$. For an entrance slit of width $2s_1 \approx 100...200$ *microns* thus the radius of the sector magnet needs to be quite large. Thus a mass separator of high mass-resolving power is always a relatively large precision instrument which inevitably is a technically difficult device[7].

In case the requirements for the experimental system are not fixed over time, as is the case for most on-line mass separator, it is desirable that the transfer system between the ion source and the entrance slit be as flexible as possible. Thus at least the x-magnification should be variable within limits in order to adjust the beam width to the width of the entrance slit which on the other hand needs to be varied in order to achieve different mass-resolving powers for a fixed dispersion of the mass separator.

Since because of Liouville's Theorem the product of the beam width and the angle of divergence is constant for a given system, the beam divergence will decrease with a wider beam at the position of the entrance slit. This in turn will reduce the width of the ion beam in the separator magnet and thus reduce the mass resolving power [7] but also the demands on the mechanical alignment precision of all parts involved. Thus in all cases in which the mass resolving power can be decreased it is worthwhile to widen the entrance slit appropriately and adjust the optical transfer system such that the full slit width is used by the beam.

For an optimal design this transfer system should contain at least five quadrupoles [8,9] so that

1. the x- and y-focusing conditions can be met,

2. the x- and y-magnifications can be adjusted and

3. still one adjustable variable is free to help the beam stay within limits within the transfer system.

Furthermore this transfer system should form [8,9] an astigmatic image with the x-image coinciding with the entrance slit. This is rather important in order that the ion beam density stays within limits everywhere and thus are the difficult to control space-charge forces.

2.2 Mass Separators with low mass cross contamination

Assume that there are desired ions of mass to charge ratios m_0/q_0 as well as abundantly available ions of mass to charge ratio $m_1/q_1 = (m_0/q_0)(1+\delta_m)$. Then both types of ions will be focused to their appropriate positions on the image plane but both will have long tails which fall off exponentially but nonetheless extent to infinity.

These long tails come from two effects [6]:

1. angle scattering of m_1/q_1 ions on residual gas atoms and on surfaces. All ions which are scattered under such angles that they can pass through the exit slit positioned properly for the m_0/q_0 ions cause the undesired contamination.

2. charge exchange processes in the acceleration region in which an m_1 ion -after being accelerated to an energy $K_0\delta_K$- exchanges its charge with an m_1 atom that was at rest at this position thus allowing this now ionized atom to be accelerated to an energy $K_0(1-\delta_K)$. Ions for which $K_1 m_1/q_1 = K_0 m_0/q_0$, i.e. for which $(1+\delta_m)/(1-\delta_K) = 1$, so that a magnetic field can not distinguish them.

In the first case the contaminating ions have the wrong momentum, so that a second magnetic separator stage can eliminate them [10]. In the second case the contaminating ions have the correct momentum but a too low energy. Thus they can be eliminated only by some electrostatic field arrangement. Assuming singly charged ions of masses $m_0 = 200amu$ and $m_1 = 201amu$ one finds that $K_1 = 200/201 K_0$, i.e. K_0 is 0.5% larger than K_1. Such ions of too low energy can be removed

1. by an electrostatic sector field [10]

2. by placing the two magnetic sectors, i.e. in practice only [8] their vacuum chambers, at different electrostatic potentials or

3. by passing the ions through an Einzellens with its center electrode being at a retarding potential where the lens must be designed such that the ions on axis must move at least for a very small distance at less than 0.5% of their initial energy.

Note here also that the number of ions which can undergo charge exchange effects reduces with a r duced gas pressure in the acceleration region. Such a reduction can be considerably assisted by a properly designed transfer system [11].

3 Conclusion

An on-line mass separator that is capable of separating neighbouring elements within one isobaric chain from each other simply by their mass differences is possible. As outlined above, such a mass separator should consist of at least two large magnetic sector fields, a versatile transfer system between the ion source and the first sector magnet (see Fig.1) and some type of an energy analyzing system. The whole system must be build rigidly and with high precision. A correction of aberrations is necessary in most cases.

In case ion sources must be used that have a large energy spread, one should consider to build the separator as an angle- and energy- focusing system. In this case additionally relatively large quite precise electrostatic sector fields must be included in the design [7].

4 Captions

Fig.1 A layout of ISOLDE-3 the on-line mass separator described in refs. [8,9] is shown in a projection on the horizontal plane of deflection and on a surface that includes the beam axis and that is perpendicular to this plane. Note the position of the ion source at the upper right corner from where

a transfer system transports the ion beam to the entrance slit (first intermediate image) where an x-image exists but where the beam is wide in the perpendicular direction. Note also that because of building constraints the two magnetic sectors had to bend the ion beam in the same direction which required an intermediate lens system was required so that the dispersions of the two magnetic sectors would add.

5 references

1. H.L.Ravn et al.; Nucl. Instr. and Methods **A139**(1976)267
2. H.Wollnik; "Applied Charged Particle Optics, Part B", ed. A. Septier, Acad. Press (1980)
3. H.Wollnik; Nucl. Instr. and Methods **A258**(1987)289
4. M.Antl and H.Wollnik; Nucl. Instr. and Methods **A274**(1989)45
5. H.Wollnik; Nucl. Instr. and Methods **A103**(1972)479
6. H.Wollnik; Int. J. Mass Spectr. and Ion Proc. **30**(1979)137
7. H.Wollnik; Nucl. Instr. and Methods **95**(1971)453
8. H.Wollnik and K.Becker; Nucl. Instr. and Methods **238**(1985)206
9. C.Geisse, H.Wollnik, B.Allardyce, E.Kugler and K.Schlösser; Nucl. Instr. and Methods **B26**(1987)120
10. L.Cassignol, Proc. Isot. Sep. Conf. (19570137
    R.Bernas, S.C.Sarrouy and J.Camplan; Rev. Sci. Instr. **3291961)96**
11. E.P.Chamberlin and H.Wollnik; Los Alamos internal report, in preparation
12. H.Wollnik, S.Meuser, M.Fujioka, T.Nomura nd H.Kawakami; Nucl. Instr. and Methods in print

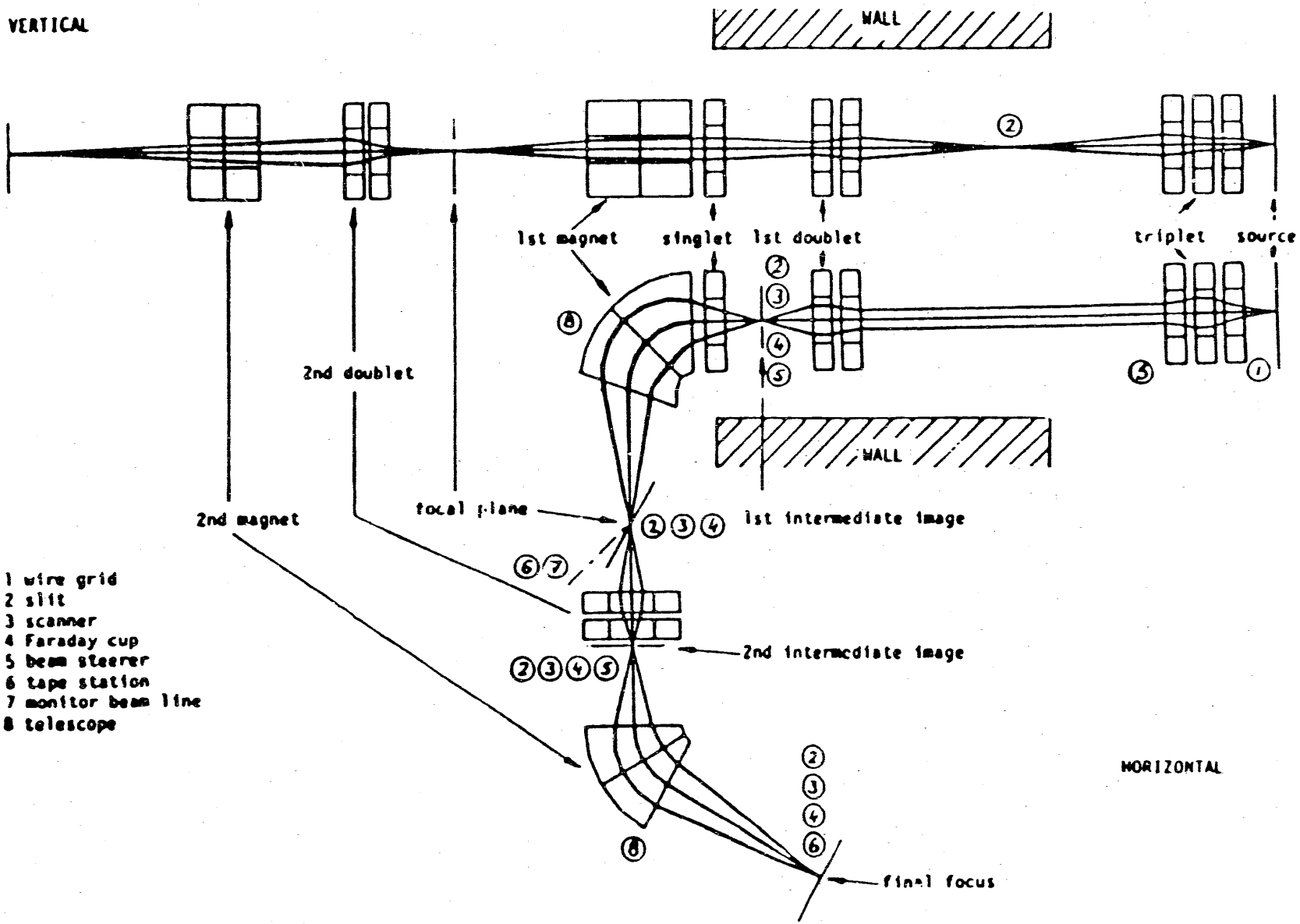
VERTICAL
WALL
1st magnet
singlet
1st doublet
triplet
source
2nd doublet
WALL
2nd magnet
focal plane
1st intermediate image
2nd intermediate image
final focus
HORIZONTAL
1 wire grid
2 slit
3 scanner
4 Faraday cup
5 beam steerer
6 tape station
7 monitor beam line
8 telescope

SOME THOUGHTS ON OPPORTUNITIES WITH REACTIONS USING RADIOACTIVE BEAMS

JOHN P. SCHIFFER
Argonne National Laboratory, Argonne, Illinois 60439-4843
and
The University of Chicago, Chicago, Illinois 60637

1. Introduction

I was asked to talk about the use of radioactive beams for nuclear reactions. My overall perspective is that the scientific justification for such studies must be done carefully. To go to the added complexity of radioactive beams one must clearly demonstrate the need for obtaining new information about nuclear structure or processes, information that is not otherwise available.

On the other hand, much of what we know about nuclear structure comes from nuclear reactions with stable nuclear beams and targets. While a certain amount of information about nuclei far from stability may be obtained from the study of their radioactive decays, this is limited. Our knowledge and understanding of nuclear structure comes from stable nuclei: energy levels, their spins and parities, and very importantly the matrix elements characterizing them (e.g. the single-particle strength, various kinds of collectivity, pairing, etc.). These are largely determined by reaction studies with normal stable nuclei. The extension of such studies to unstable nuclei, far from stability, may well hold qualitative surprises, or at the very least give a firmer basis to our understanding of nuclear structure.

Perhaps it is a matter of taste, but if one wishes to start on this endeavor then it is best to begin with simple, easily accessible features. The simplest nuclei are the ones that form doubly-closed shells and the easiest features to explore initially are the single-particle states and the collective excitations that one can build on these.

I would like to emphasize that a unique facility for this type of study is about to come into operation in Darmstadt where the ESR storage ring will capture radioactive beams from fragmentation products and cool them to useful energies for reaction studies. Circulating beams of many unstable nuclei are expected in the 10^{10} to 10^{16}/sec regime.[1] With an internal gas target, integrated luminosities should be achievable that are within a few orders of magnitude of those used in typical stable-beam experiments. With detectors of large solid angle very useful rates are likely to be within reach in the near future.

2. Nuclear Structure Studies Near Closed-Shell Nuclei

A specific case of such studies is represented by an experiment we hope to do at the ESR: A proposal for studying simple collective modes and single-particle states based on magic nuclei such as ^{56}Ni and ^{132}Sn.[2] With beams of such nuclei, one can pass them through a thin gas deuterium target in which reactions may take place -- for the ^{132}Sn(d,p) reaction for instance, one would be able to detect protons in an array of solid state detectors and establish the single-neutron states based on a doubly magic core. Data on (d,t)and (d,^{3}He) reactions may be accumulated simultaneously, yielding data on hole states. Proton states may require a He target but otherwise the technique is the same. The ideal energy for such reactions is around 10 MeV/u, where these transfer reactions are well calibrated and where momentum matching is relatively good. Prototype measurements on such inverse reactions with stable Xe beams shown in Figure 1 have been carried out at GSI during the past year in order to demonstrate their feasibility.[3]

Inelastic scattering may also be carried out, and here substantially higher energies may be used (e.g. several 100 MeV/u on a ^{4}He or ^{1}H target) since small momentum transfer is achievable even at high energies.[4]

Once the single-particle states are observed, the next step is to study the adjacent nuclei for particle-particle and particle-hole energies. The data base on such states is very limited, since there are precious few stable doubly-closed-shell nuclei, but the data indicate that the similarity in such states between different parts of the periodic table is very striking.[5] A subset of these data are shown in Figure 2. It would be very interesting to add data from the vicinity of the hitherto inaccessible closed shells. Such studies should also become feasible in time, though they would have to follow the observation of single-particle states, and be somewhat more difficult.

3. Reactions with Exotic Beams

There are some exotic phenomena, such as those associated with very loosely bound nuclei such as ^{11}Li where the loose binding results in the tail of the neutron wave function extending out to exceptionally large radii. It is likely that there are other nuclei, near the neutron drip line, that show such a wispy neutron halo. The ones where a neutron pair's separation energy is small are particularly interesting as has been emphasized by Bertsch for instance. But the pairing correlation with the other tightly bound pairs is not likely to be a significant feature.

As shown by the work of Tanihata and collaborators,[6] ^{11}Li and ^{14}Be are somewhat unique in their anomalously large interaction radii. They also may have the feature of a split giant dipole resonance, that would

contribute to the large interaction cross section. However, here it is likely to be important that in ^{11}Li two of the 8 neutrons are loosely bound -- while in heavier nuclei the fraction of loosely bound neutrons will inevitably be less, and such phenomena as the splitting of the giant resonance will be less pronounced. I also want to point out that similar effects are NOT to be anticipated for protons -- since even very loosely bound protons have a huge Coulomb barrier to penetrate, and therefore are not likely to show a comparable "proton halo". After all, we have nuclei unstable against alpha emission with no perceptible modification in their density distribution.

If one does a simple statistical estimate it seems likely that near the neutron drip line there will be some nuclei where the last neutron or neutron pair is bound by even less (perhaps 10 keV) than in ^{11}Li. It would be fascinating to try for sub-sub-Coulomb transfer reactions at energies even as low as half the Coulomb barrier, with nuclei that have such a wispy halo, and even to look for fusion enhancement. But we should remember that only the loosely bound neutron or neutron pair will have a special role.

4. Some Studies of Reactions with Astrophysical Interest

A number of reaction cross sections for proton or alpha-particle capture are of interest for stellar processes with nuclides that are unstable. Some such studies have been proposed recently to be carried out with radioactive beams at existing facilities without major investment of resources. An example is the study of the $^{14}O(\alpha,p)^{17}F$ reaction, which has an important role in the initiation of the rapid proton capture process. Since both ^{14}O and ^{17}F are unstable, the reaction may only be studied if one can prepare one or the other species in sufficient numbers. A recent proposal is to produce a beam of ^{17}F, using ^{17}O as the primary beam on a hydrogen target slightly above the $^{17}O(p,n)^{17}F$ threshold, where the ^{17}F particles would be emitted in a narrow forward cone. Since the energy of the ^{17}F is above the energy regime of interest for the astrophysical measurements, the particles have to be decelerated. With the independent resonators of a superconducting linac (ATLAS) this is readily achievable, and sufficient intensities of ^{17}F may be obtained to allow the experiment to proceed.[7] Some test measurements of deceleration have been carried out, and the experiment awaits the construction of a suitable hydrogen target that could be bombarded with several micro-amperes of oxygen beam.

5. Conclusions

There are interesting new aspects of nuclear properties that may become available through the use of radioactive beams. But these experiments are likely to be very expensive -- not only in terms of money

but in terms of effort. Radioactive beams are not an end to themselves. The scientific justification is probably there, but it has to be thought through carefully and preliminary experiments should be done whenever possible.

At present there is a major facility at which radioactive beams will be available: the ESR at Darmstadt, which is undergoing its initial tests now. It behooves those of us who profess to be interested in the use of radioactive beams for nuclear reaction or nuclear structure studies to go beyond attending workshops and start to become involved in real measurements in order to better appreciate the dimensions of opportunities, technical problems and of the scientific payoff. Surely, if a major new facility whose capabilities are to supplement those of the ESR is to be justified, it will have to build on what will be learned in Darmstadt in the near term future.

This research was supported by the U. S. Department of Energy, Nuclear Physics Division, under Contract W-31-109-Eng-38.

References

1) See for instance Proceedings of the Workshop on Experiments at SIS/ESR GSI-87-7 (1987)

2) SIS/ESR proposal no. 56, GSI (1987)

3) G. Kraus et al., GSI Scientific Report 1989, GSI 90-1 (1990)

4) P. Egelhof et al., SIS proposal (1990)

5) J. P. Schiffer and W. W. True, Revs. Mod. Phys. 48, 191 (1975)

6) T. Kobayashi et al., Phys. Rev. Lett. 60, 2599 (1988)

7) T.-F. Wang, ATLAS proposal (1990); W. Kutschera, private communication

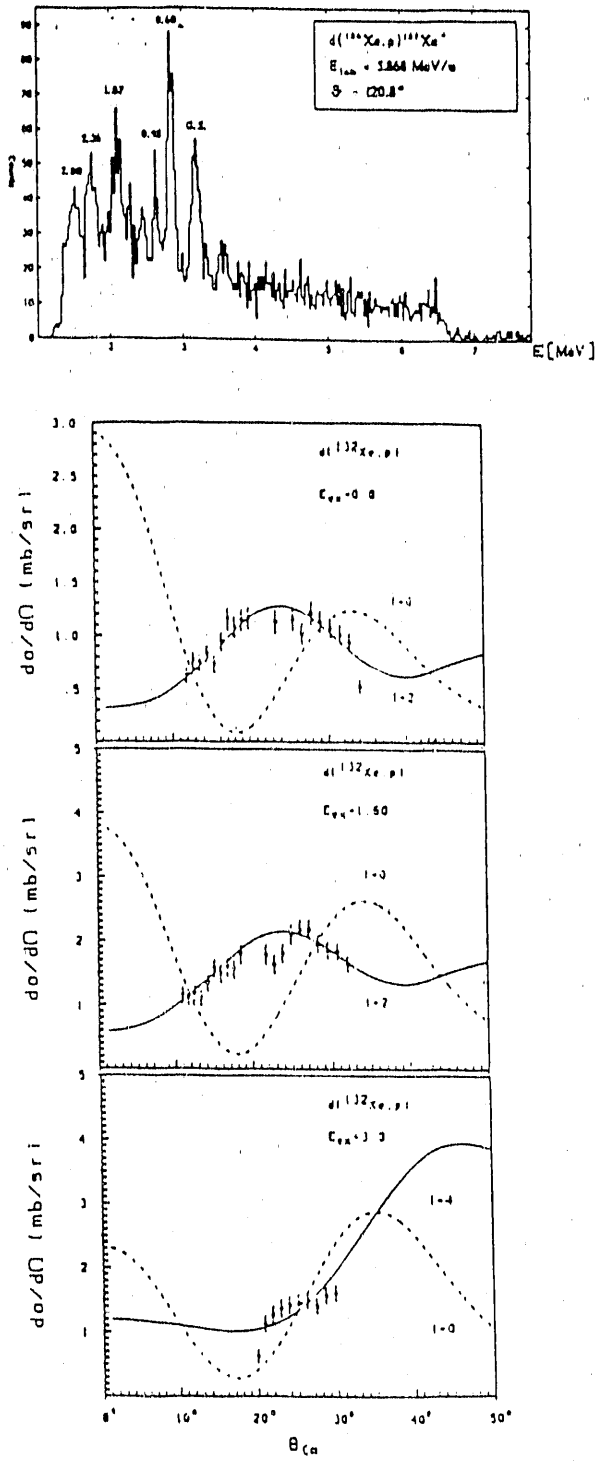

Figure 1: Study of the feasibility of measuring a (d,p) reaction with a heavy ion beam incident on a gas target from Kraus et al. ref. 3. This measurement was carried out as a prototype for experiments with radioactive nuclei in a storage ring. The upper figure shows a spectrum and the lower ones angular distributions for various peaks together with calculated shapes.

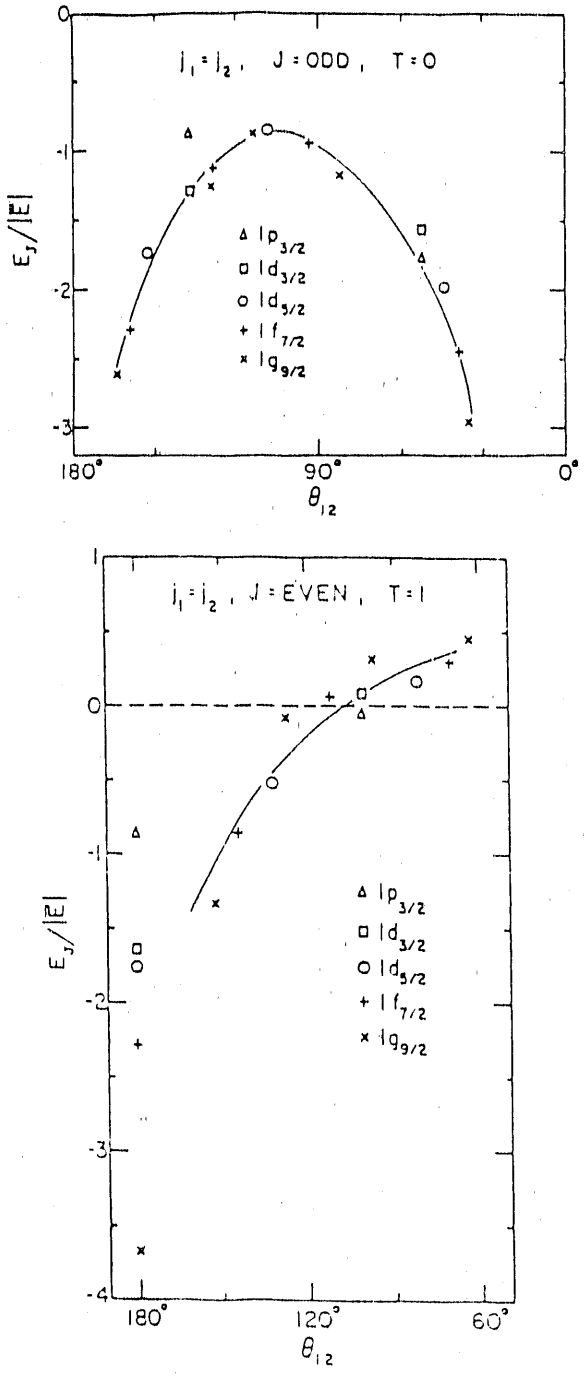

Figure 2: Matrix elements of the NN effective interactions, representing the energies of states in the immediate vicinity of closed-shell nuclei from throughout the periodic table from ref. 5. The angle θ_{12} represents the total angular momentum to which two nucleons are coupled. It would be of considerable interest to extend this data base with information from reactions with unstable nuclei in the vicinity of hitherto inaccessible closed shells, such as ^{132}Sn or ^{56}Ni.

EXOTIC NUCLEAR DEFORMATION AWAY FROM STABILITY

INGEMAR RAGNARSSON
Lund Institute of Technology
Department of Mathematical Physics
P.O.Box 118, S-221 00 Lund, Sweden

Abstract

We discuss the fact that to find shell effects which are in phase for protons and neutrons, nuclei far from stability must often be considered. Especially, with $Z = N$, the two systems will strive in the same directions. For heavier nuclei, it is necessary to consider systems with neutrons one shell higher than the protons where this condition will be different at superdeformation and at normal deformation. We exemplify with superdeformation in $^{60}_{30}Zn_{30}$ and $^{98}_{44}Ru_{44}$, $^{74}_{30}Zn_{44}$ and $^{110}_{44}Ru_{66}$ in addition to the regions already established around $^{152}_{66}Dy_{86}$ and $^{194}_{80}Hg_{104}$. In light nuclei, the shell effects are very strong compared with macroscopic energies. We argue that the nucleus ^{11}Be and some neighbouring nuclei have large triaxial deformation in contrast to the neutronhalo in some other neighbour nuclei.

For a general understanding of the nuclear properties in different regions, the shell energy landscape drawn as function of deformation and particle number is very illustrative. As seen in fig. 1, the variation is very regular with intersecting valleys and ridges. Therefore, in the same way as one may combine the spherical magic numbers to get doubly-closed nuclei, one may combine favoured proton and neutron shell effects for deformed shape to find other favoured (or unfavoured) configurations. This has recently been illustrated in a very convincing way by the observed superdeformed high-spin states around ^{152}Dy and ^{194}Hg. These findings complement previous observations of fission isomers for neutron numbers $N = 140$–150.

1. Superdeformation at an approximate 2:1 axis ratio

1.1. THE REGION AROUND THE DOUBLY-CLOSED ^{152}Dy NUCLEUS

The shape at superdeformation with an axis ratio of 2:1 constitutes a second symmetry in addition to the 1:1 shape for spherical nuclei and it seems that ^{152}Dy can be considered as doubly closed in a similar way as e.g. ^{208}Pb. The recent findings [1]) of almost identical transition energies (within 1-2 keV) when one particle is added or removed from ^{152}Dy might be taken as a support for such an assumption. The very interesting experimental fact is that one excited band has been observed in ^{151}Tb with essentially identical transition energies as in the superdeformed (SD) ground band of ^{152}Dy. In a similar way, one excited band has been observed in ^{150}Gd with essentially the same transition energies as in the SD ground band of ^{151}Tb. As noted by several participants at the recent Copenhagen workshop [3,4]), this can be understood if the orbital which is emptied has a decoupling factor a close to one while the core remains

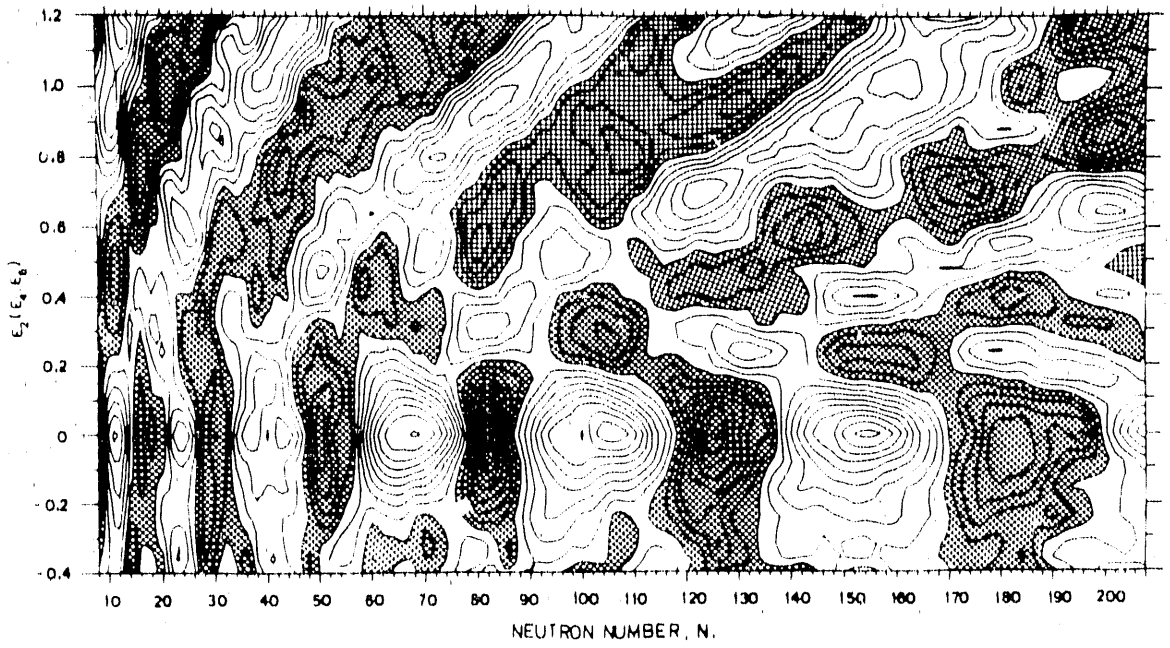

Figure 1: Neutron shell energy calculated in the modified oscillator drawn as function of quadrupole deformation and particle number[2]). The contour line separation is 1 MeV and regions of negative shell energy are shaded. Note especially the pronounced ridges which can be traced back to the $n_z = 0$ orbitals indicated in fig. 3. The ridges are separated by valleys which become especially pronounced at spherical shape ($\varepsilon = 0$) and 2:1 deformation ($\varepsilon \simeq 0.6$). We thus note approximate 2:1 magic numbers as indicated also in fig. 6, but also low shell energy and thus prediction of stable configurations for a variety of other combinations of particle number and deformation. The diagram is drawn for no rotation but, at large deformation, the general features of the shell energy turn out to be insensitive to collective rotation and also to be about the same for protons as for neutrons.

unchanged. Thus, the band can be parametrized as

$$E = (\hbar^2/2\mathcal{J}) \cdot R(R+1) = (\hbar^2/2\mathcal{J}) \cdot (I-i)(I-i+1) \qquad (1)$$

where thus $i = 0$ in the core and $i \approx 1/2$ (corresponding to $a \approx 1$) in the excited band while $\mathcal{J}$ (which is slightly R-dependent) is essentially identical. The decoupling factor of $a \approx 1$ shows almost unambiguously that it is the [301 1/2] Nilsson orbital which is being emptied which is certainly a very important observation. The calculated decoupling factor comes out somewhat too small and for example pseudo-oscillator symmetry has been invoked[3]) to understand this discrepancy.

What we will discuss here is rather the problem how the inert core could be understood. In fact, a similar observation[5]) has been made for the nucleus ^{153}Dy with one signature degenerate band, which has essentially the same moment of inertia as the core, i.e. if one corrects for the fact that the spins are integer and half-integer, respectively, the transition energies are identical to within 1-3 keV. In general one would expect different kinds of residual interactions (e.g. pairing) to disturb the bands much more.

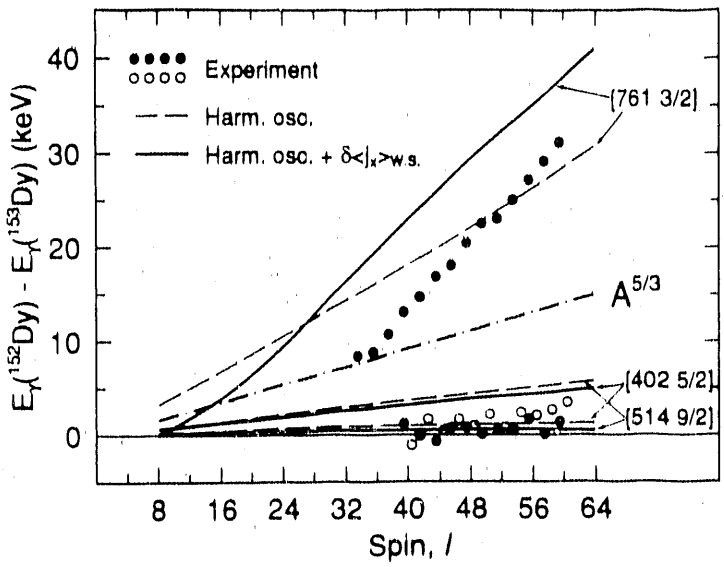

Figure 2: Observed differences in transition energies (filled and open circles) between ^{153}Dy [5]) and ^{152}Dy [7]) compared with calculations. With the highest spin in ^{152}Dy set to 60, the highest spins in the three bands of ^{153}Dy are assumed 119/2, 117/2 and 115/2, respectively. When the differences are taken, the transition energies in ^{152}Dy are interpolated to half-integer spins. The dot-dashed line shows a pure $A^{5/3}$ dependence, the dashed lines show the result from the pure oscillator and the full lines if the alignment is corrected to that obtained in Woods-Saxon calculations (e.g. [8])). The signature degenerate band in ^{153}Dy is well described by either [514 9/2] or [402 5/2] and the other band by [761 3/2]. The similar features obtained in experiment suggest that essentially pure single-particle effects are involved and that no "local crossings" caused by pairing are of importance.

Leaving the difficult question of residual interaction aside, it turns out that one possible explanation [9]) of these identical moments of inertia can be found in the pure single-particle model. In such a model, an added particle will disturb the core in essentially two ways, namely it will polarize the deformation and it will bring in an alignment. An additional small effect is the increase of mass which will lead to a scaling of entering quantities so that the size of the nucleus on the average will increase as observed experimentally. The mechanism is most easily understood in the pure oscillator model as illustrated for addition of a neutron in fig. 2. What one notes here is that for an upsloping equatorial orbital, having a negative alignment, the different effects will essentially compensate each other leading to almost identical transition energies. Indeed, the proton [301 1/2] orbital discussed above is of this upsloping character as are also the neutron orbitals [402 5/2] and [514 9/2].

Fig. 2 shows also the changes in transition energies with $< j_x >$ taken from the Woods-Saxon potential [8]). With this correction, we obtain a qualitative agreement not only for the upsloping orbitals but also for the high-j (high-N) [761 3/2] orbital. Once we know the changes in transition energies, we can also calculate for example

the second moment of inertia $\mathcal{J}^{(2)}$. This means that our calculations give an expression of how the addition (or removal) of a particle will influence the $\mathcal{J}^{(2)}$ moment of inertia where not only the alignment of the particle is considered (as was done in ref.[9])) but also the shape polarization is taken into account.

1.2. GENERAL FEATURE OF THE SHELL STRUCTURE

Before we continue to discuss other regions of approximate 2:1 deformation it is instructive to consider large deformations somewhat more generally. Thus, in fig. 3 we show a single-particle diagram for neutrons where stripes of equatorial orbitals (especially $n_z = 0$ and $n_z = 1$) have been marked out (fig. 3 is drawn for the W.S. potential but a M.O. diagram would have the same general features as noted long ago[11])). The stripes give rise to a high level density and the 2:1 magic numbers are then seen in between these stripes. In a similar way as for spherical shape, however, the magic numbers are shifted to somewhat larger particle numbers than in the pure oscillator where the 2:1 gaps are $N = \ldots, 16, 28, 40, 60, 80, 110, 140, \ldots$. Furthermore, some down-sloping high-j (or high-N) orbits tend to intersect the 2:1 shell gaps. Due to the low density of such states, they are not very important for the overall level density. However, instead of well localized 2:1 shell gaps, we will observe regions around $\beta = 0.6$ with no orbitals except the strongly down-sloping ones[11]). This means that the smaller is the particle number, the smaller is the favoured β-deformation. This is due to the β-dependence of the orbitals involved. For example, in fig. 3, there is a shell gap at $N = 64$ and $\beta = 0.6$ but then, if we take away the two particles in the lowest $N = 6$ orbital, we get another gap at $\beta = 0.50 - 0.55$ while if two particles are added to the second $N = 6$ orbital, a gap is created for $\beta \approx 0.65$. Furthermore, around $N = 86$, $N = 44$, $\ldots (\beta \simeq 0.6)$ the same general structure as around $N = 64$ is observed. The features are clearly born out in explicit calculations as illustrated for the M.O. in fig. 4. There, we plot the calculated equilibrium deformations for some yrast superdeformed configurations in the $A = 150$ region. The configurations are specified by the number of $N = 6$ protons and $N = 7$ neutrons. It is evident that the ε-value is correlated with the number of particles in these orbitals just in the way as expected from the single-particle diagram. Note also that these trends appear consistent with experiment[7]).

The high-j particles contribute strongly to the angular momentum not only at small deformation but also at superdeformation. Furthermore, they get aligned as a function of rotational frequency in a typical way leading to special features in the observed spectra. This can be seen in the $\mathcal{J}^{(2)}$ moment of inertia[8,9]) or the differences in transitional energies discussed above.

1.3. OTHER REGIONS OF APPROXIMATE 2:1 DEFORMATIONS

One could note that if one wants a deformed shell gap to survive with increasing

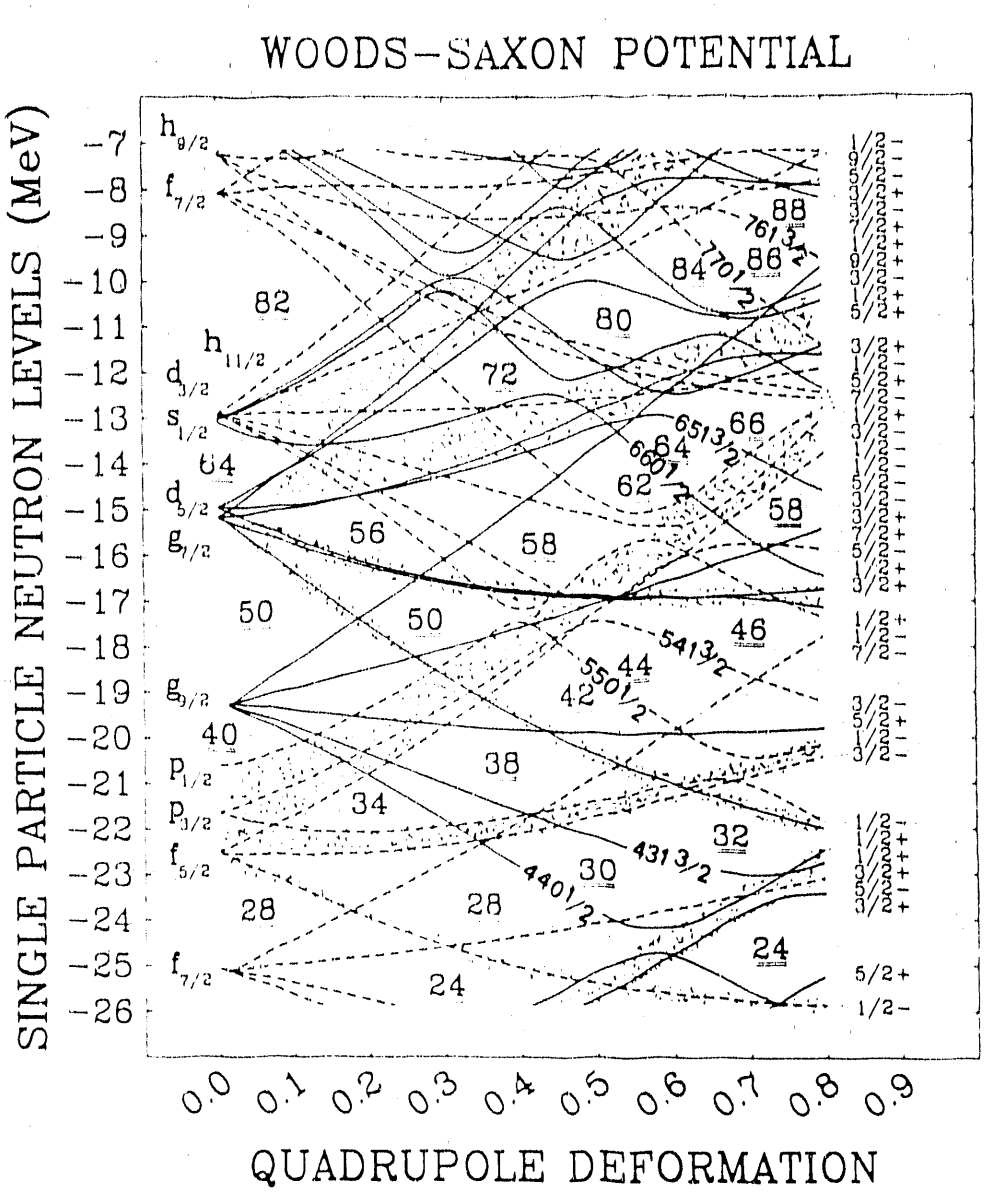

Figure 3: Single-neutron orbitals calculated in the Woods-Saxon potential drawn as functions of quadrupole deformation. Regions of equatorial orbitals with small values of n_z are indicated. Especially the $n_z = 0$ orbitals are important for the formation of the ridges seen in fig. 1. Note the regions of low s.p. density for $\beta = 0.5 - 0.6$ intersected by some down-sloping easily alignable orbitals whose asymptotic quantum numbers, $[Nn_z\Lambda\Omega]$, are given, cf. fig. 5. The figure is a slightly updated version of a figure originally published in ref. [10]).

frequency, it is favourable to be just above the first orbital of some N-shell. This is illustrated for the $N = 30$ and $N = 44$ shell gaps in fig. 5 where we see how these gaps rather become more pronounced at high spin because the orbitals just below are the first $N = 4$ [440 1/2] and $N = 5$ [550 1/2] orbitals, respectively. These orbitals get aligned and thus bend downwards with increasing ω. Consequently, as

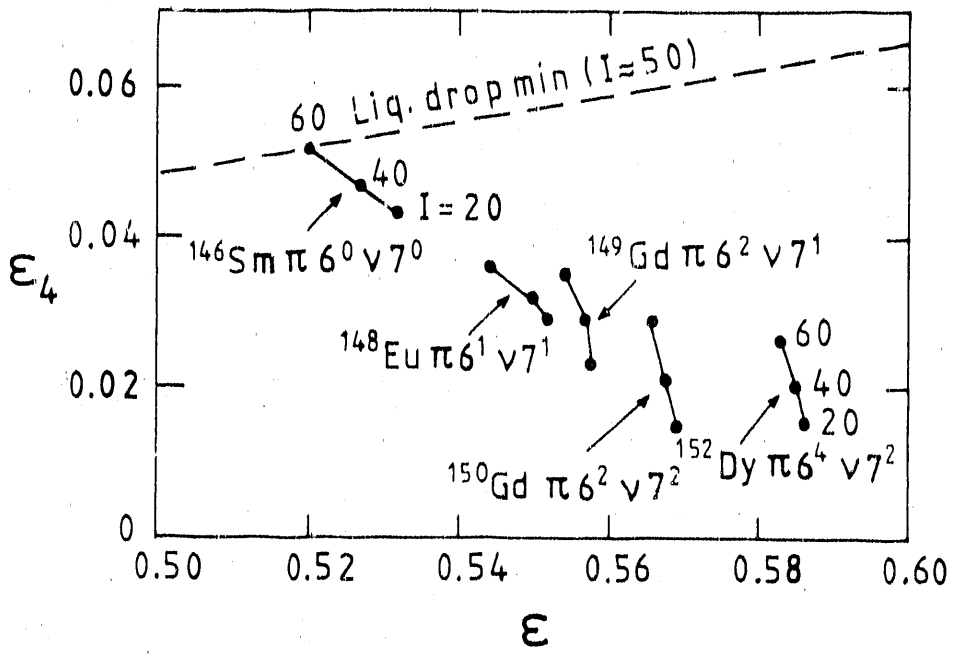

Figure 4: Calculated equilibrium deformations [9]) for superdeformed configurations of ^{146}Sm ($\pi 6^0 \nu 7^0$), ^{148}Eu ($\pi 6^1 \nu 7^1$), ^{149}Gd ($\pi 6^2 \nu 7^1$), ^{150}Gd ($\pi 6^2 \nu 7^2$) and ^{152}Dy ($\pi 6^4 \nu 7^2$) where ($6^n 7^m$) indicates that n protons occupy $N = 6$ orbitals and m neutrons occupy $N = 7$ orbitals. The dashed line shows for different ε-deformations the ε_4-deformation favoured by the rotating liquid drop at $I \approx 50$. Note the decreasing deformation when fewer high-N orbitals become occupied.

favourable SD cases below the Gd/Dy region, we would suggest ^{88}Ru, ^{108,110}Ru, ^{60}Zn and ^{74}Zn. As illustrated in fig. 6 these are all rather far from stability where, with present techniques, the neutrondeficient ones should be more easy to populate at high spins. Thus, we give in fig. 7 one calculated energy surface for the two $N = Z$ nuclei, ^{60}Zn and ^{88}Ru, in the spin region where the superdeformed minimum becomes yrast. We see that this happens for comparatively low spins for both of these nuclei and also that the SD minimum is separated from states at smaller deformation by a substantial barrier. A study of the ^{60}Zn nucleus is presently underway at Nordball [12]).

It is interesting to note that there is a supershell structure connected with 2:1 shell gaps [11]) so that each second gap can be put into one group and those in between into another group. It is associated e.g. with the fact that for the H.O. gaps, $N = 4$, 16, 40, 80, 140, ... the $n_z = 0$ orbitals are just above and the $n_z = 1$ orbitals just below while for the other gaps, $N = 2$, 10, 28, 60, 110, ... the situation is reversed. As one can see from fig. 3, the $n_z = 0, 1$ orbitals will then tend to push the former gaps towards larger ε-values and the latter towards smaller ε-values. Furthermore, ε_4 deformations will tend to make the former gaps more pronounced [11]). Thus, it seems that in the Dy/Gd region, it is the $N = 86$ neutrongap which is more pronounced than the $Z = 66$ gap while the fission isomers are formed mainly because of the $N = 140$–150 shell structure. Furthermore, the calculated super-deformation in ^{88}Ru is substantially larger than in ^{60}Zn where the minimum in the latter nucleus has some

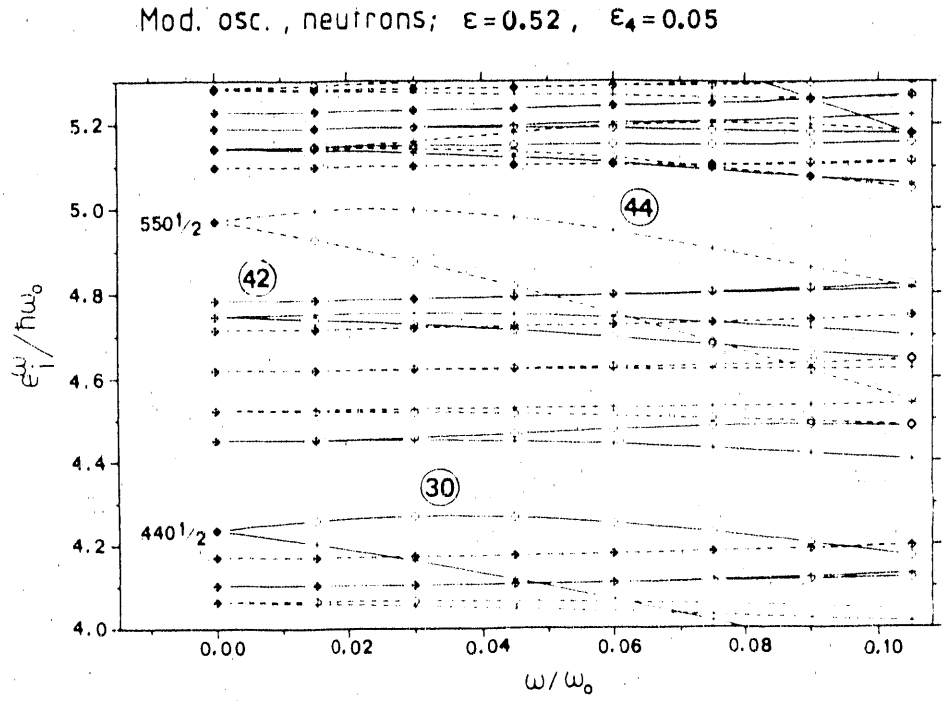

Figure 5: Single-neutron orbitals close to prolate 2:1 deformation drawn as functions of rotational frequency, ω. Note the shell gaps, $N = 30$ and 44, just above the first $N = 4$ [440 1/2] and $N = 5$ [550 1/2] orbitals, and how these gaps survive and even become more pronounced at large ω.

resemblance of the ^{20}Ne ground state which is formed because of the $Z = N = 10$ gap at 2:1 shape but leading to $\varepsilon \lesssim 0.40$ in ^{20}Ne. Similarly, the minimum we calculate in ^{88}Ru can be compared with the secondary minimum calculated (e.g. [11])) in ^{32}S at $\varepsilon \gtrsim 0.6$.

The next heavier region beyond ^{152}Dy should correspond to $Z \approx 86$ and $N \approx 116$. The general systematics then suggest a lower end of this region with deformations substantially smaller than $\varepsilon = 0.6$ corresponding to $Z \approx 80$ and $N \approx 110$. This is roughly consistent with the fact that a strongly deformed band [13]) with $\varepsilon = 0.45-0.50$ was recently discovered in ^{191}Hg. There is now a very large activity in the search for other similar bands in the Hg/Pb region and several cases have been identified in experiments carried out in Argonne, Berkeley and Liverpool, see e.g. [14]).

Fig. 1 suggests that for neutron numbers $N = 110$–130 we will stay away from deformations larger than $\varepsilon = 0.5$ but that there exists a shell energy minimum for $\varepsilon = 0.4-0.5$ for all these neutron numbers. Similarly, the proton shell energy appears to survive in the whole region $Z = 80$–90. Indeed, early calculations [15]) did predict a lot of nuclei with secondary minima for $Z = 80$–90 and $N = 110$–130, see fig. 8. Important for this is not only the shell energy but also the soft liquid drop energy. Many other calculations have followed with, to our knowledge, the first detailed high-spin study (carried out for ^{187}Au) in ref. [16]), while more general overview calculations at high spin can be found in e.g. [17,18]). As we expect a large region of secondary minima around and beyond $^{190-194}$Hg, it seems that it would be of great value to try

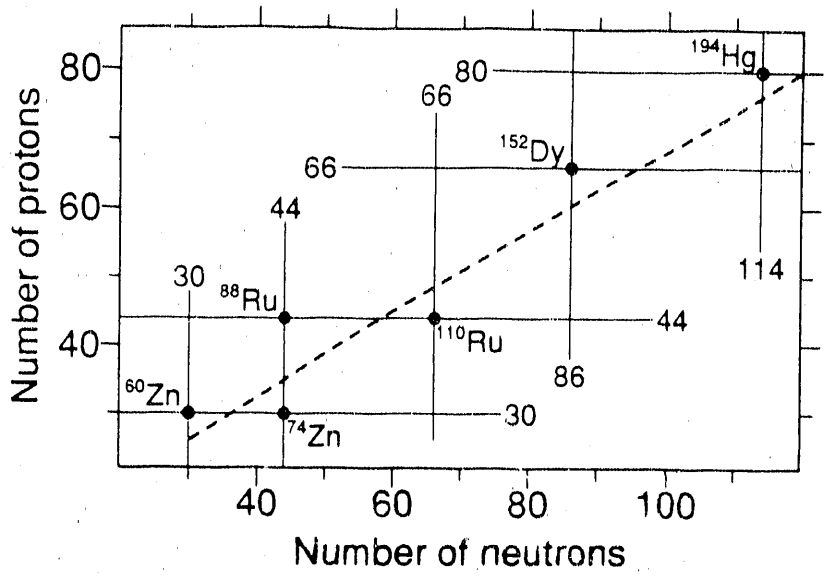

Figure 6: Part of the (N,Z) chart with the line of β-stability and suggested or observed magic 2:1 numbers indicated. Some doubly closed nuclei are then suggested where $(Z, N) = (80, 114)$ is of a somewhat different character with a favoured deformation $\varepsilon \leq 0.5$ as discussed in the text.

to estimate fissionbarriers, the height of the secondary minima,etc. with the most reliable models available today.

Important experimental facts in the Hg-region are that the rotational bands tend to stay populated down to spin 10 or even below but not to higher spins than around 40. These values are substantially lower than in the Gd/Dy region and appears correlated with the softer liquid drop energy in the heavier region. Secondly, while a single particle model without pairing always gives an $\mathcal{J}^{(2)}$ moment of inertia which decreases slightly with spin (increasing differences in transition energies), the opposite

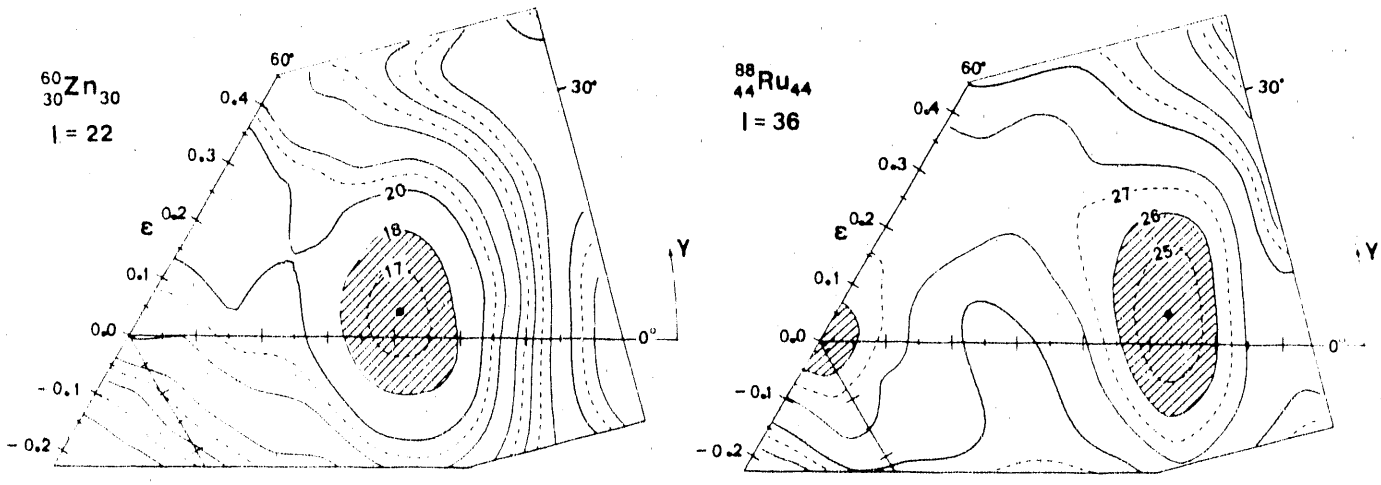

Figure 7: Calculated potential energy surfaces of ^{60}Zn at $I^{\pi} = 22^{+}$ and ^{88}Ru at $I^{\pi} = 36^{+}$. The minima at large deformation correspond to the gaps seen in fig. 5.

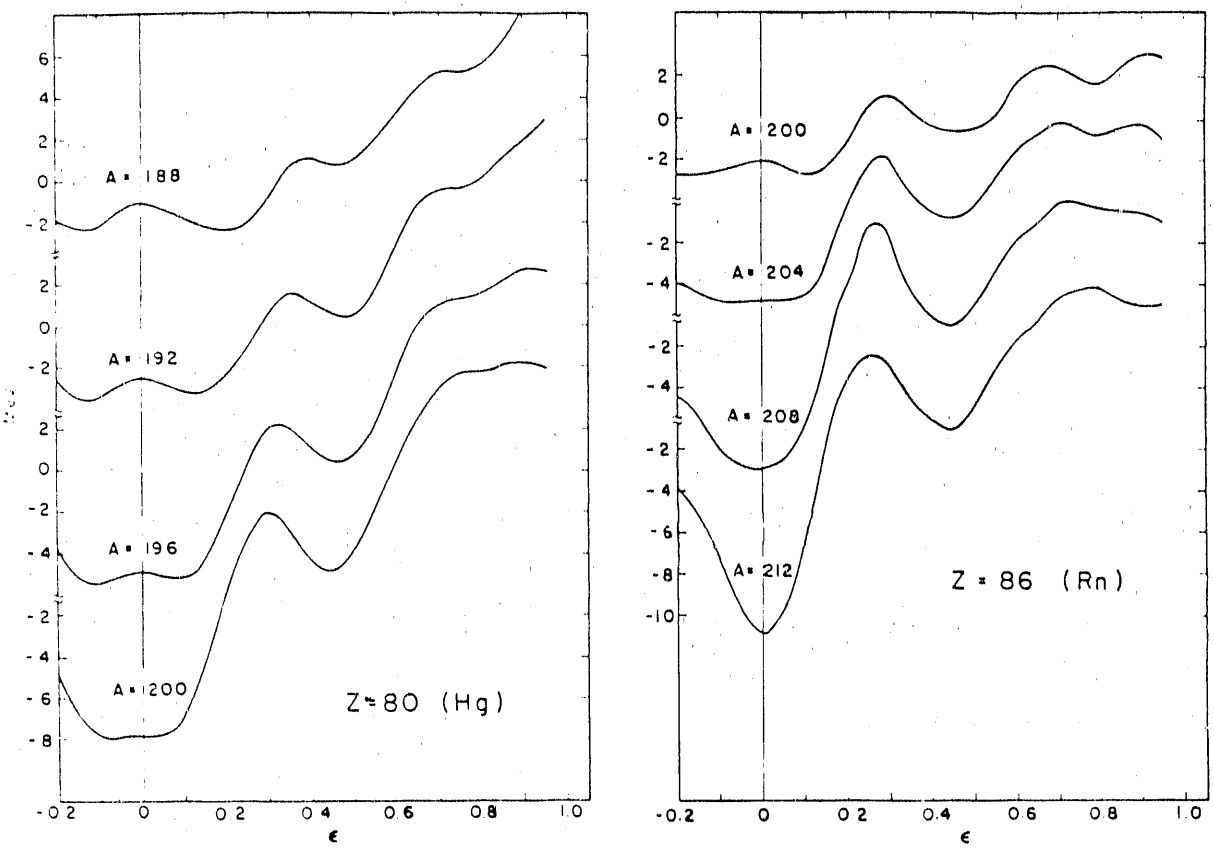

Figure 8: Potential energy calculated as a function of ε, with minimization in ε_4, for a number of Hg and Rn isotopes. The figure is taken from ref.[15]) but similar results with a secondary minimum at $\varepsilon \simeq 0.45$ has been obtained in several subsequent calculations.

effect is found experimentally with increases of typically 30% in the $I = 10$–40 range. It seems as if a weak band-crossing caused by pairing is involved[19]) even though it is difficult to understand why the experimental increase is so smooth up to the highest spins. A third very interesting observation is the very similar transition energies in different bands in an analogous way as discussed above around ^{152}Dy. Due to the expected importance of pairing in Hg nuclei, it is questionable if the ideas presented above can be applied here.

3. Deformations other than 2:1 in heavy nuclei

From fig. 1 one may also conclude that other large deformations than those close to 2:1 might give favoured configurations becoming yrast at high spins. Indeed, we get rather precise predictions of favoured combinations of proton number, neutron number and deformation. For example, it seems very probable that several large deformation states will be observed for $N = 130$–150 nuclei forming a bridge between the Ce/Nd region (e.g.[7])) and the Gd/Dy region. Let us also mention the so called hyperdeformed states predicted in ref.[20]) around ^{168}Yb noting that this is only one of many possibilities which would come out from more detailed calculations. With

the new experimental equipment being built or planned, we would thus expect that it will become possible to explore large regions of the space covered in figs. 1 and 3. Note that in many cases it will be necessary to go to nuclei far off stability to find (Z,N) combinations where the shell effects add coherently.

In fig. 1 we only consider axial shape leaving out the possibility of triaxiality. Indeed, because of the higher symmetry for axial shape, we expect more pronounced shell effects there but even so, one would expect that high-spin configurations at large deformation and with a well-defined triaxiality will be identified in the near future. One possible region is the Hf-isotopes with $N = 88$–100 where calculations [21,22]) give a minimum at $\varepsilon = 0.45$ and $\gamma = 20$ which becomes yrast for spins $I = 40$–50.

3. Large deformations in very light nuclei — triaxiality in ^{11}Be

For very light nuclei, there are several advantages [23]) when considering large deformations. Generally, the highest stability is found close to $N = Z$ where proton and neutron shell effects are in phase. Furthermore, in a similar way as for very heavy nuclei, the liquid drop energy is rather soft and large deformations are easily formed. Because of the small number of particles, the shell energies might change a lot with the addition of only one or two particles so that very different shapes might be studied in a limited range of proton and neutron number. One interesting example is ^{16}O which not only shows large shell effects at spherical shape but also a 4p-4h configuration corresponding to a shell energy minimum at $\varepsilon \approx 0.7, \gamma \approx 40°$ and an 8p-8h configuration corresponding to another shell energy minimum at $\varepsilon \approx 1.0, \gamma = 0$ [24]).

Recently, a lot of activity has been centered on the very neutron-rich nuclei of He, Li and Be. A very special feature of these nuclei is the very low neutron binding energy. This seems to lead to a neutronhalo [25]) in some cases and is thus in many ways analogous to the large radius in deuterium due to the low binding energy. Here we will however argue that also deformation might be very important in some of these nuclei [26]). This appears not to be the case for ^{11}Li where for example the magnetic moment [27]) is well understood in the spherical shell model. The main experimental fact [28]) indicating a neutron halo is the large interaction cross section σ_R observed. Then, also in ^{11}Be a similar increase in σ_R has been seen and taken together with the fact that the last neutron has a very low binding energy (~ 500 keV), this could be interpreted as caused by a larger radius of this last neutron. Alternatively, a large deformation, also leading to a larger nuclear radius, might explain this experimental fact.

Some years ago, we pointed out [23]) that the yrast positive parity states in ^{11}B might be interpreted as a rotational band with a moment of inertia corresponding to rigid rotation at $\varepsilon \approx 0.7, \gamma \approx 40°$ at which deformation we also calculated the lowest energy for positive parity (in competition with another minimum being axially symmetric and situated at an even larger deformation). Furthermore, the positive parity ground band in ^{11}Be can then be considered as the isospin, $T = 3/2$, component of this same state. Again, as illustrated in fig. 9, we calculate a similar deformation for the lowest energy positive parity state in ^{11}Be. As discussed below, the $1/2^+$ state might very well be lowest in energy although cranking calculations favour $I = 5/2$.

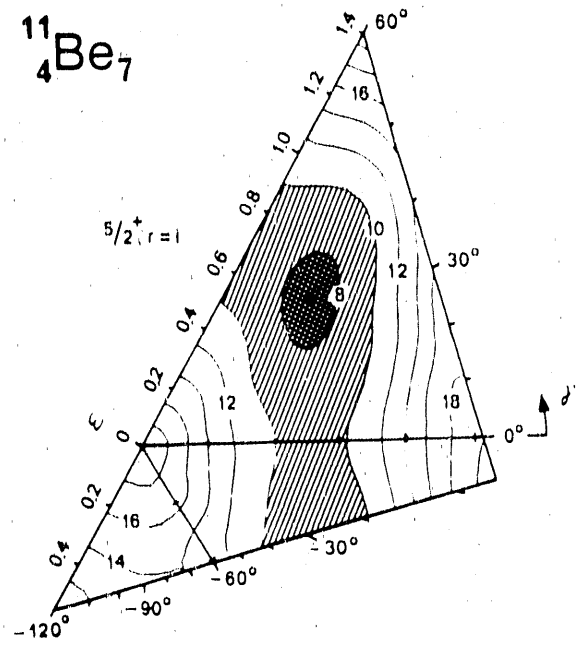

Figure 9: Calculated $5/2^+$ potential-energy surface of ^{11}Be. Note that the nucleus gains more than 10 MeV in energy from deformation. The $5/2^+$ state is lowest in energy in the cranking approximation but see also fig. 11.

Talmi and Unna have argued [29]) that far from stability the $s_{1/2}$ state tends to come down in energy and from systematics for the isotones with neutron number $N = 7$, it should be the ground state (or very close to the ground state) in ^{11}Be, see fig. 10 which is an updated version of the figure originally presented in [29]). A more detailed study of the spectra of the odd nuclei in fig. 10 shows however that within 0-2 MeV above the $1/2^+$ state there is also a $5/2^+$ state (where in ^{11}Be, there is an experimental uncertainty if the spin is 5/2 or 3/2, see fig. 11 below). With previous arguments, this would then suggest that also $d_{5/2}$ is coming down very low which seems rather unlikely. Generally, from a knowledge of the order of the spherical single-particle orbitals, one would expect it to be very difficult to get especially the $s_{1/2}$ state very low in energy and this is also what can be concluded from explicit calculations in the Woods-Saxon model [31]). Thus, it seems that in order to get a spherical $s_{1/2}$ state lowest in ^{11}Be, an unreasonably large residual interaction is needed.

Coming back to the possibility of large deformation, the 4p-4h state in ^{16}O was mentioned above. Indeed, the corresponding 0^+ state is observed at an excitation of 6.05 MeV which is close to the excitation energy of the $1/2^+$ state in ^{15}O (fig. 10). This state might then be a 3p-3h state at large deformation as also supported by explicit cranking calculations. Similarly, we describe the ground state of ^{12}C as strongly deformed which indicates that this is the case also for the $1/2^+$ state in ^{13}C, again supported by our preliminary calculations.

In order to indicate how a positive parity $I = 1/2$ can be described in the deformed case, we have carried out particle-rotor calculations as illustrated in fig. 11. These calculations do indeed give a low-lying $1/2^+$ state which depending on parameters

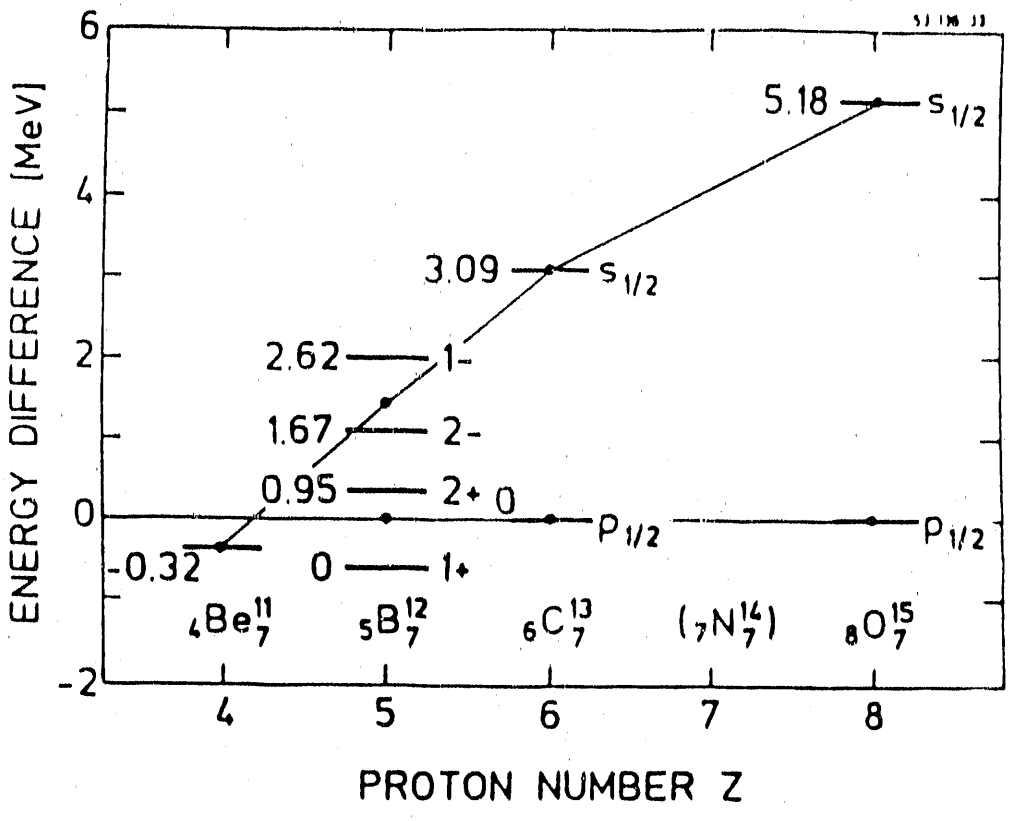

Figure 10: The energy difference between the $1/2^+$ and $1/2^-$ states in the $N = 7$ isotones (centres of gravity of the two doublets were used in ^{12}B). Note the crossing at ^{11}Be. The figure is taken from [30]) and is an updated version of a figure originally presented in ref. [29]).

might be below or slightly above the $5/2^+$ state. Furthermore, this $1/2^+$ state has an approximate amplitude of 75% in the (stretched) $d_{5/2}$ subshell and 25% in $s_{1/2}$. Therefore, we would expect a centrifugal barrier which prevents the last neutron from forming a halo. Thus, the mere fact that the last neutron has a very low binding cannot cause the increased radius. Instead, the large deformation leads to a mean square radius which is approximately 10% larger than for spherical shape in qualitative agreement with experiment.

Several experiments would help to support or reject our interpretation of the structure of the positive parity states in ^{11}Be. It would be important to really pin down the spin of the second positive parity state in ^{11}Be now being given as either $3/2^+$ or $5/2^+$. Second, the magnetic moment is straightforward to calculate in the particle-rotor model so a measurement of this quantity for the $1/2^+$ ground state in ^{11}Be would be of great value. Additionally, in ^{11}N which is the mirror nucleus of ^{11}Be, deformation would lead to a large radius while, even if the proton binding energy is low, the Coulomb barrier would prevent the formation of a proton halo. Other important quantities to measure are higher spin states in either ^{11}Be or in ^{11}B or in their mirror nuclei (the ^{11}C spectrum is very similar to the ^{11}B spectrum), not to forget that the B(E2) strength is a very direct measure of the deformation. This is then one example where it helps a lot to go far from stability to get a general understanding

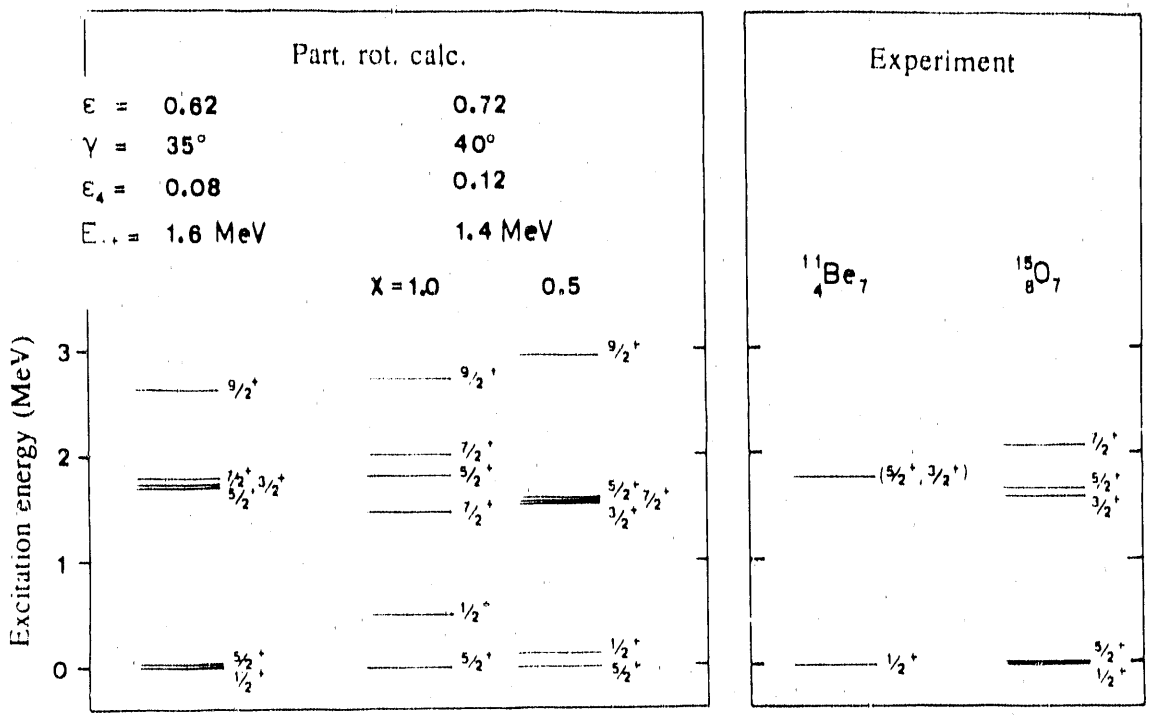

Figure 11: Particle-rotor calculations for the $N = 7$ system at large deformations approximately corresponding to calculated energy minima in ^{11}Be and ^{15}O and observed positive parity spectra in these two nuclei. The spectra have been normalized to the lowest positive parity state. The moment of inertia vary with γ as for irrotational flow and has been normalized to observed spacings in the "rotational bands" of ^{11}B and ^{16}O expressed as the 2^+ energy in the figure. The Coriolis interaction has been attenuated in one case, $\chi = 0.5$. Note that with decreasing γ and decreasing χ, the $1/2^+$ state is lowered relative to $5/2^+$. The resemblance between theory and experiment is a strong support not only of large deformation but also of triaxiality.

of the structure, in this case how the s-d shell orbitals intrude into the p-shell nuclei.

Parts of what I have discussed here have been carried out in collaboration with different colleagues whom I want to thank. On superdeformation in general I have collaborated with Tord Bengtsson and Sven Åberg, on p-shell nuclei with Sven Åberg and Ray Sheline and on particle-rotor calculations with Paul Semmes. Several discussions with Gregers Hansen and Thorleif Ericson on the neutron-rich p-shell nuclei have been very helpful. I am also grateful to the Swedish Natural Science Research Council for economic support.

References

1) P. Fallon, P.J. Twin et al., Copenhagen Workshop, October 1989; T. Byrski et al., Phys. Rev. Lett. **64** (1990) 1650.
2) I. Ragnarsson and R.K. Sheline, Phys. Scripta **29** (1984) 385.

3) W. Nazarewicz, Copenhagen Workshop, Oct. 1989; W. Nazarewicz et al., Phys. Rev. Lett. **64** (1990) 1654.
4) I. Ragnarsson, Copenhagen Workshop, Oct. 1989.
5) J.K. Johansson et al., Phys. Rev. Lett. **63** (1989) 2200.
6) I. Ragnarsson, Proc. Conf. on Nuclear Structure in the Nineties, Oak Ridge, April 1990, to be publ. in Nucl. Phys.
7) P.J. Twin, Proc. Int. Nucl. Phys. Conf., Sao Paulo, Brasil, 1989 (World Scientific, 1990), vol. 2, p. 373.
8) W. Nazarewicz, R. Wyss and A. Johnson, Phys. Lett. **B225** (1989) 208; Nucl. Phys. **A503** (1989) 285.
9) T. Bengtsson, I. Ragnarsson and S. Åberg, Phys. Lett. **B208** (1988) 39; S. Åberg, T. Bengtsson, I. Ragnarsson and P.B. Semmes, Proc. XXVI Int. Winter Meeting on Nuclear Physics, Bormio, Italy, 1988, p. 546.
10) J. Dudek, W. Nazarewicz, Z. Szymański and G.A. Leander, Phys. Rev. Lett. **59** (1987) 1405.
11) I. Ragnarsson, S.G. Nilsson and R.K. Sheline, Phys. Rep. **45** (1978) 1.
12) J. Nyberg, priv. comm.
13) E.F. Moore, R.V.F. Janssens, R.R. Chasman, I. Ahmad, T.L. Khoo, F.L.H. Wolfs, D. Ye, K.B. Beard, U. Garg, M.W. Drigert, Ph. Benet, Z.W. Grabowski and J.A. Cizewski, Phys. Rev. Lett. **63** (1989) 360.
14) M.A. Deleplanque, R. Janssens, M.A. Riley, F.S. Stephens and others, Copenhagen Workshop, October 1989.
15) C.F. Tsang and S.G. Nilsson, Nucl. Phys. **A140** (1970) 275.
16) T. Bengtsson and I. Ragnarsson, Nucl. Phys. **A436** (1985) 14.
17) S. Åberg, Phys. Scripta **25** (1982) 23.
18) R.R. Chasman, Phys. Lett. **B219** (1989) 227.
19) M.A. Riley et al., Nucl. Phys. **A512** (1990) 178.
20) J. Dudek, T. Werner and L.L. Riedinger, Phys. Lett. **B211** (1988) 252.
21) C.G. Andersson, R. Bengtsson, T. Bengtsson, J. Krumlinde, G. Leander, K. Neergård, P. Olanders, J.A. Pinston, I. Ragnarsson, Z. Szymański and S. Åberg, Phys. Scripta **24** (1981) 266.
22) I. Ragnarsson, T. Bengtsson and S. Åberg, Slide report Workshop on Nuclear Structure at High Spins, Bad Honnef, March 1989, p. 97 and to be publ.
23) I. Ragnarsson, S. Åberg, H.-B. Håkansson and R.K. Sheline, Nucl. Phys. **A361** (1981) 1; I. Ragnarsson, T. Bengtsson and S. Åberg, Proc. XIX Int. Winter Meeting on Nuclear Physics, Bormio, Italy, 1981, p. 48.
24) S. Åberg, I. Ragnarsson, T. Bengtsson and R.K. Sheline, Nucl. Phys. **A391** (1982) 327.
25) P.G. Hansen and B. Jonson, Europhys. Lett. **4** (1987) 409.
26) I. Ragnarsson, S. Åberg and R.K. Sheline, to be publ.
27) E. Arnold, J. Bonn, R. Gegenwart, W. Neu, R. Neugart, E.-W. Otten, G. Ulm and K. Wendt, Phys. Lett. **B197** (1987) 311.
28) I. Tanihata, T. Kobayashi, O. Yamakawa, S. Shimoura, K. Ekuni, K. Sugimoto, N. Takahashi, T. Shimoda and H. Sato, Phys. Lett. **B206** (1988) 592.
29) I. Talmi and I. Unna, Phys. Rev. Lett. **4** (1960) 469.
30) P.G. Hansen, Proc. 6th Nordic Meeting on Nuclear Physics, Kopervik, Norway, Aug. 1989, to be publ. in Phys. Scripta.
31) T. Berggren, priv. comm.

Prospects for Nuclear Astrophysics with Intense Radioactive Ion Beams

G. J. Mathews
University of California
Lawrence Livermore National Laboratory
Livermore, CA 94550

Abstract

An overview is made of the current and future nuclear data needs in nuclear astrophysics. Subjects discussed include: 1) Hydrogen burning reactions in various environments; 2) Big-bang nucleosynthesis (particularly with baryon-number inhomogeneities); 3) Heavy-element nucleosynthesis; and 4) Presupernova cores. A wish list is constructed of most desired unknown reaction rates in each of these areas. It is concluded that a facility for producing heavy-ion radioactive nuclear beams may provide a means to determine many of these reaction rates.

1. Introduction

The subject of nuclear data needs in astrophysics has been reviewed a number of times[1-3]) in recent years. Most of what was required five years ago is still needed today. In this talk emphasis will be made upon where there has been progress in the last few years and where significant gaps in available nuclear data still exist which might be filled best with the use of a radioactive ion beam facility.

We discuss four areas of nuclear astrophysics: 1) Hydrogen burning reactions in various environments; 2) Big-bang nucleosynthesis (particularly with baryon-number inhomogeneous models); 3) Heavy-element neutron-capture nucleosynthesis; and 4) Electron-capture rates in presupernova cores.

2. Hydrogen burning

2.1 Main-sequence hydrogen burning

One need not look very far to find an application for radioactive beams. Figure 1 summarizes the well known hydrogen-burning cycles which occur at relatively low temperature ($\sim 1.5 \times 10^7$ K) in a low-mass main sequence star like the Sun, and the current status[4]) of the measured astrophysical S-factor for the $^7Be(p,\gamma)^8B$ reaction. As can be seen, the $^7Be(p,\gamma)^8B$ reaction is a crucial step toward the generation of detectable energetic neutrinos from ^8B decay in the ^{37}Cl solar-neutrino experiment.[5]) Although there have been a number of careful measurements[6-10]) which give the same shape for the S-factor, such measurements have been plagued with the difficulty of accurately determining the thickness of the radioactive ^7Be target. There is a difference of about 30% in the normalization factors for this reaction in Figure 1. Hence, a measurement using a radioactive ^7Be beam would be quite useful even at energies much higher than the stellar Gamow window. In such an experiment there would be no ambiguity in the target thickness or beam intensity so that the proper normalization of this reaction rate could be established.

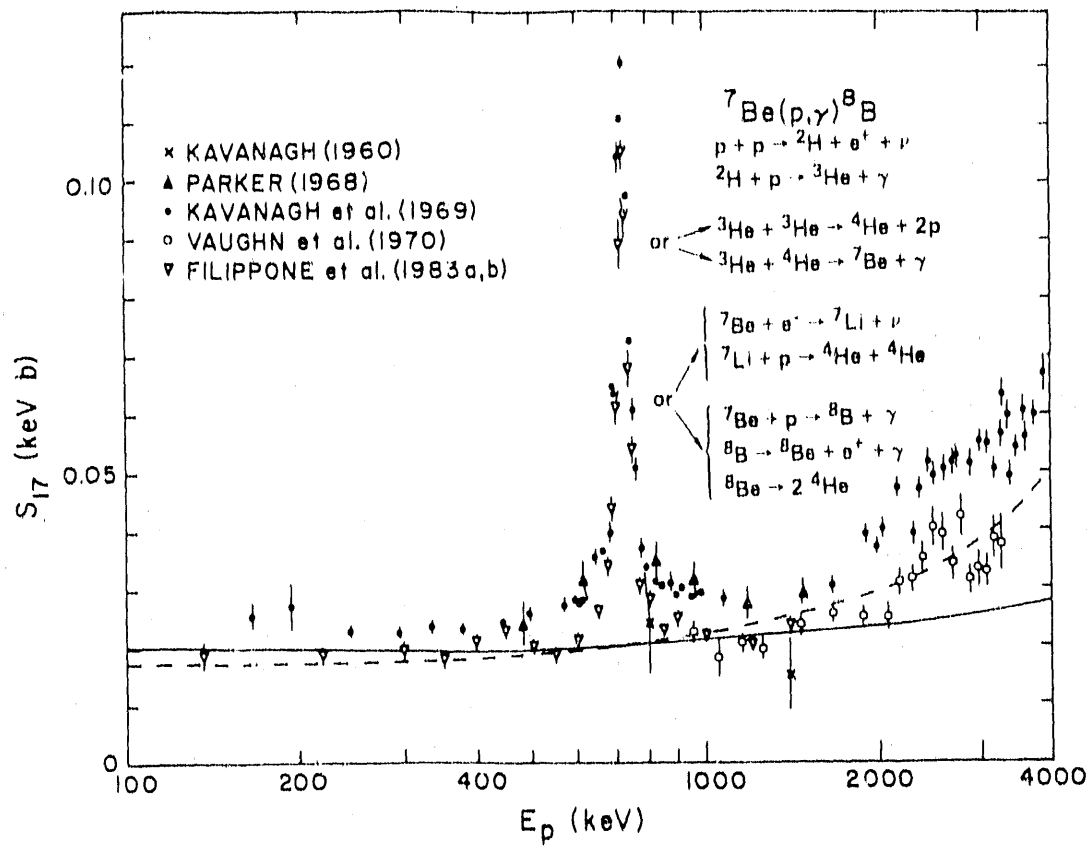

Fig. 1 S-factor for the ^{7}Be(p,γ)^{8}B reaction[4]) and a list of the major chains for thermonuclear burning in the Sun.

2.2 Hot hydrogen burning

As the temperature is increased the main hydrogen-burning reactions shift from the p-p chains to the CNO cycle (Fig. 2). At still higher temperature the CNO cycle is modified when proton captures on ^{13}N become the slowest reaction in the cycle (though still faster than the beta-decay rate of ^{13}N). This is the hot CNO cycle also shown in Fig. 2. Since the energy generation rate is much faster through the hot CNO cycle it is useful to know at precisely what temperatures and densities this transition takes place. Five years ago I would have therefore listed the ^{13}N(p,γ)^{14}O reaction as one of the most important data needs. However, there has been considerable progress in the use of indirect methods to infer this reaction rate. This reaction should be dominated by a single s-wave resonance to the 1$^-$ 2.313 MeV excited state in ^{14}O, analogous to the 424 keV resonance in the ^{12}C(p,γ) reaction and others in this region.[11]) The proton width for the resonant state in ^{14}O has been measured.[12]) This clarified the uncertainty in several thoeretical predictions (e.g. ref. 11). There has also been successful, but much slower, progress[13-15]) in the determination of the gamma-width of this state by indirect means. The three experimental determinations of this width are not entirely consistent (Γ_q/Γ = (3.3 ± 2.1)x10^{-5} (ref. 13);

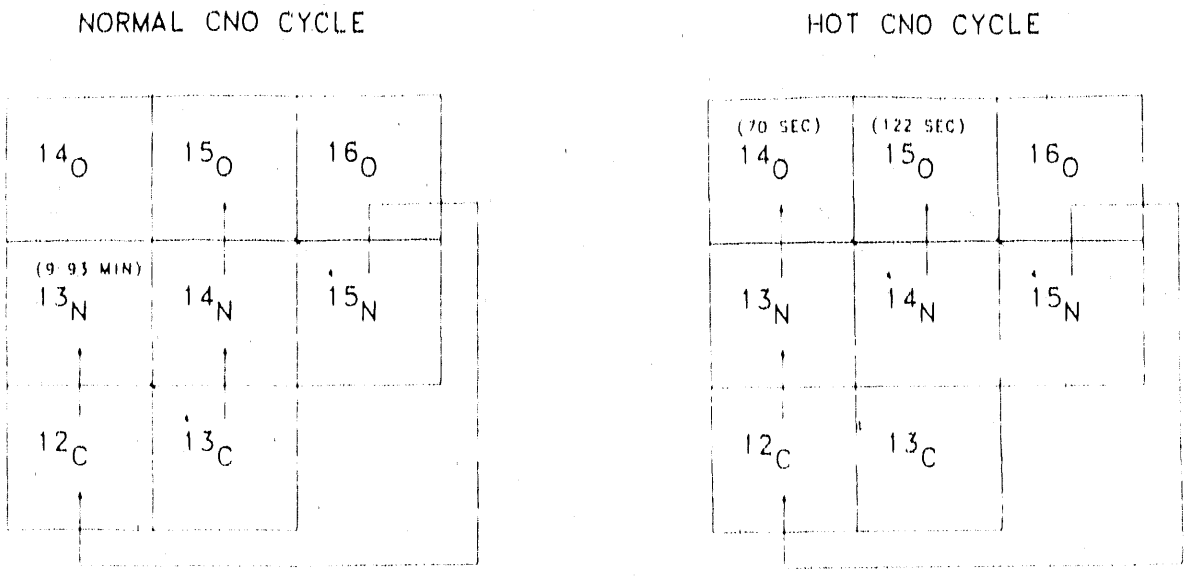

Fig. 2 The normal CNO cycle and the hot CNO cycle.

$= (3.6 \pm 1.7)\times10^{-5}$ (ref. 14); $= (2 \pm 1)\times10^{-4}$ (ref.15). It would therefore be quite useful to have the ability to measure this cross section directly with a radioactive ^{13}N beam.

2.3 rp-Process

At even higher temperatures (~ 5×10^9K) alpha-particle reactions on the waiting point nuclei, ^{14}O and ^{15}O can cause a leak from the hot CNO cycle producing ^{19}Ne. The $^{19}Ne(p,\gamma)^{20}Na$ reaction then leads to a sequence of rapid proton and alpha captures out to the proton drip line. This is called the rp-process,[16] an example of which is shown on Figure 3.

There has been some gradual progress[17-21] in the identification of some of the important resonances for these reactions using the indirect technique. For example, measurements or limits for various resonances in the $^{15}O(\alpha,\gamma)^{19}Ne$ reaction have been determined[17,18] in ^{19}Ne or the mirror nucleus, ^{19}F. Also the level structure relevant to the $^{19}Ne(p,\gamma)^{20}Na$ reaction[19] and the $^{20}Na(p,\gamma)^{21}Mg$ reaction[20,21] have been studied.

It is worth commenting on prospects for future measurements via the indirect method verses the use of a radioactive ion beam facility. Although, such indirect measurements are immediately available with existing accelerators, it has been extremely difficult to determine resonance gamma widths by this technique due to the large backgrounds and low counting rates. In principle, the high beam currents avaliable with a radioactive ion beam facility may overcome this difficulty. Furthermore, there are a number of important rp-process reactions for which there is no simple exchange reaction to form them from stable nuclei for such indirect measurements. These reactions are summarized in Table 1. In this regard, a combination of the two techniques (i.e. indirect measurements involving radioactive ion beams) may be particularly useful in some cases. For example, it is not known whether the rp-process terminates at ^{64}Ge or ^{65}As. This is because it is not known if there are any proton stable states in ^{65}As into which to capture. This could have an

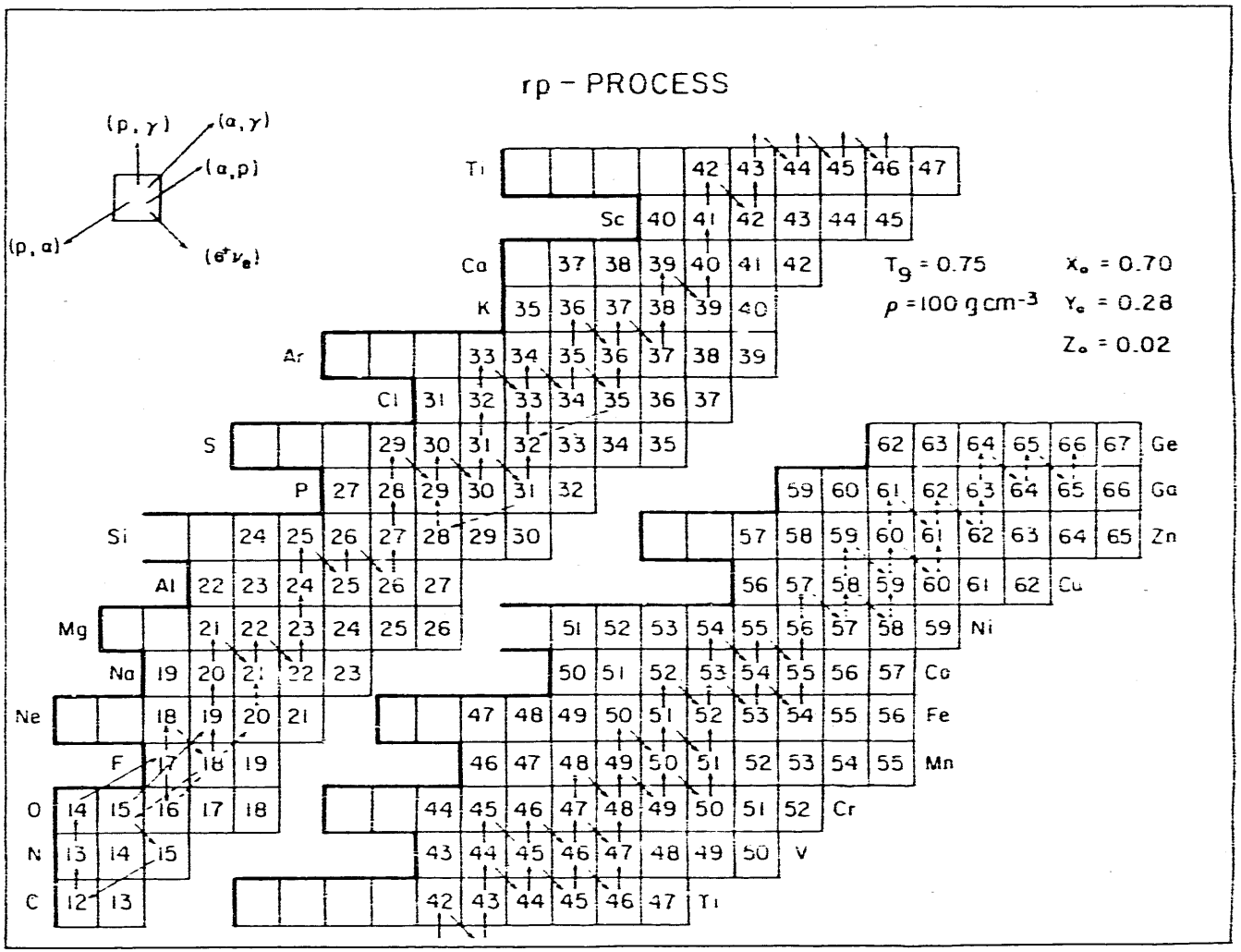

Fig. 3 The rp-process of Wallace and Woosley.[16]

Table 1. Hot hydrogen burning reaction rates which will require radioactive ion beam methods to measure.

^{43}Ti(p,γ), ^{44}Ti(p,γ)
^{44}V(p,γ), ^{45}V(p,γ)
^{45}Cr(p,γ), ^{46}Cr(p,γ)
^{48}Mn(p,γ), ^{49}Mn(p,γ)
^{50}Fe(p,γ)
^{52}Co(p,γ), ^{53}Co(p,γ)
^{54}Ni(p,γ)
^{57}Cu(p,γ)
^{59}Zn(p,γ)
^{61}Ga(p,γ), ^{62}Ga(p,γ), ^{62}Ga(p,γ)
^{64}Ge(p,γ), ^{65}Ge(p,γ)

impact on the energy generation from this process. It might be possible to make ^{65}As by the ^{58}Ni(^{10}C,t)^{65}As or ^{54}Fe(^{14}O,t)^{65}As reactions[22].

3. The Baryon-Number Inhomogeneous Big Bang

There has been considerable recent interest[23-39] in the possibility that during the epoch of nucleosynthesis (~ 100 sec into the big bang) there was an inhomogeneous distribution of nucleons. The interest in this possibility arises for two reasons. For one there are a number of theoretical reasons[25,28] to expect that such inhomogeneities are at least plausible, particularly as a result of a first-order QCD phase transition[31] occuring at an earlier epoch. The other reason for interest has been the recognition[23] that prior to the epoch of nucleosynthesis but after the freezeout of weak-reaction equilibrium (t ~ 1 sec) the diffusion length of the charge-neutral neutrons should be much longer than that of protons in the background plasma of photons and electrons. This could lead to the development of regions of large variations in the n/p ratio which could drastically alter the nucleosynthesis yields[22-39].

In particular, it at first appeared that it might even be possible[23-27] to satisfy all of the light-element abundance constraints in a universe which is closed by baryonic matter at the present time and thus avoid the major motivation for postulated exotic dark-matter such as axions, massive neutrinos, weakly interacting massive particles (WIMPS), etc. However, subsequent work[28-33] seems to indicate that, although the universe could contain a significantly larger fraction of baryons than allowed by the homogeneous big bang there is an over production of helium in models which are presently closed by baryons. Attention more recently[29,34-39] is therefore now directed toward identifying the possible nucleosynthetic signatures of such inhomogeneities which in turn may constrain physics of the QCD phase transition (or other processes) responsible for the generation of inhomogeneities. It is in this context that a number of reaction rates involving nuclei away from stability become important.

Figure 4 shows the reaction network from a recent study[29] of the possible nucleosynthetic signatures of intermediate-mass nuclei from an inhomogeneous big bang. Other recent works have considered possible nucleosynthetic signatures from light elements[35-37] and heavier

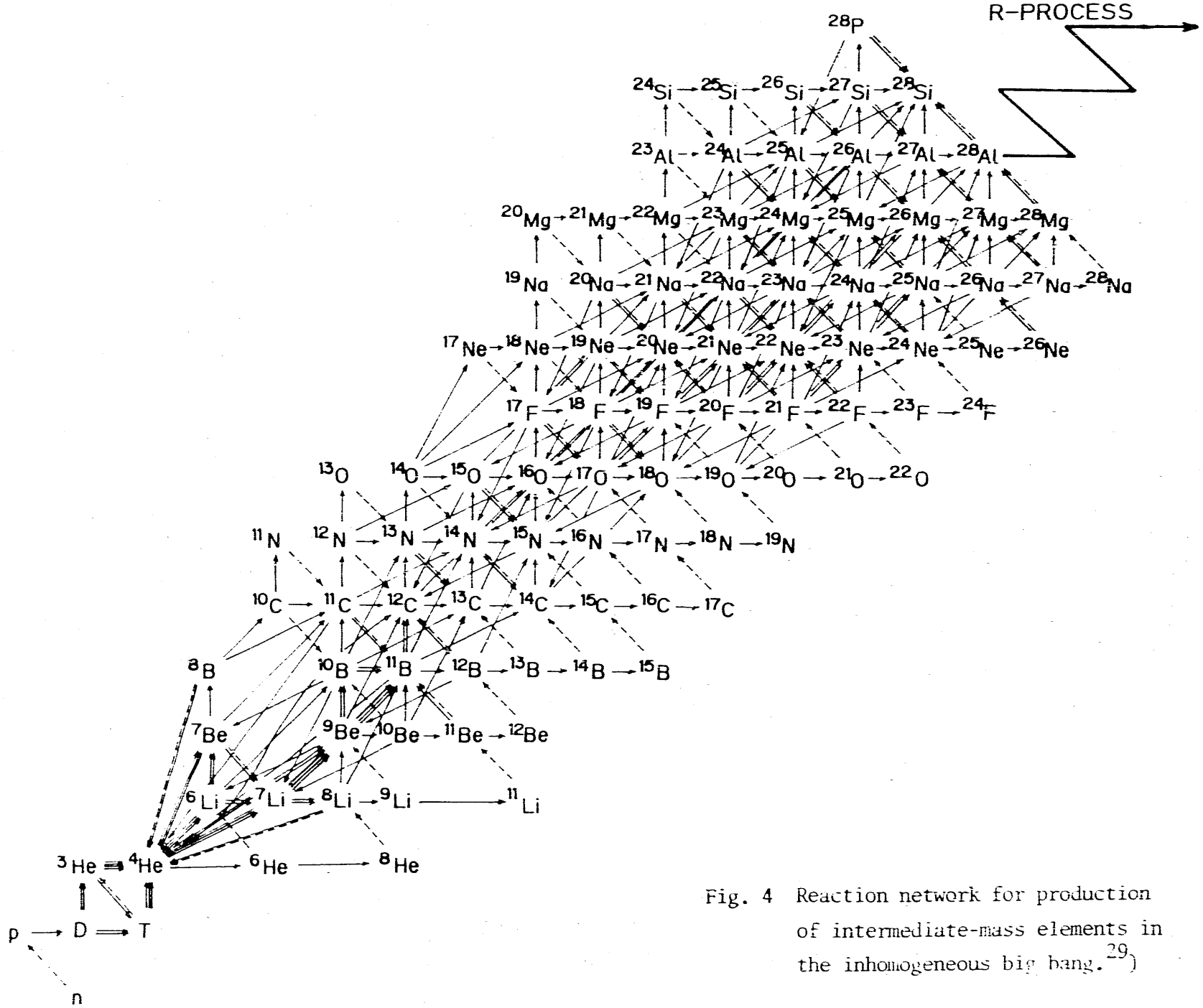

Fig. 4 Reaction network for production of intermediate-mass elements in the inhomogeneous big bang.[29]

elements up to the actinides[39]). A number of important unmeasured reaction rates can be identitified from the major nucleosynthesis flows through this network. In the proton rich regions the nuclear reactions produce a kind of hot hydrogen-burning rp-process as discussed above. For the bridge from light to heavy nuclei in the neutron-rich regions there are a number of reactions involving ^{8}Li. Among intermediate-mass elements there are a number of neutron-capture reactions one or two nuclei away from stability which are important. There are summarized in the wish list given in Table 2. This reaction flow continues on through heavy nuclei. The computed abundances[39]) look at first like an r-process distribution and later as an s-process distribution. The data needs for such processes are discussed below.

Table 2. Inhomogeneous big bang reaction wish list.

^{8}Li(d,n), (α,n), (d,t), (^{3}He,t), (t,n), ...
^{14}C(n,γ), (p,γ), (α,γ)
^{16}N(n,γ)
^{20}F(n,γ), ^{21}F(n,γ)
^{23}Ne(n,γ)
^{24}Na(n,γ)
^{27}Mg(n,γ)
^{28}Al(n,γ)

4. Heavy-Element Nucleosynthesis

The two basic processes for the neutron-capture synthesis of elements heavier than iron are summarized in Figure 5 from ref.'s 40 and 41. In one process the elements are produced by neutron capture on a slow (s-process) time scale (~ 1 capture per 10-1000 yr). This process has most often been associated with helium burning in red-giant stars,[42,43]) although the details are not yet understood and other possibilities have been considered[44-47]). The other process occurs on a rapid (r-process) time scale (~ 1000 captures per sec)[40,42]). This process is probably the least well understood of the nucleosynthesis mechanisms. At least 12 different sites have been proposed over the years[48,68]), but at present it seems most likely that this site is associated with type II supernovae[41]).

4.1 The r-process

The problem of understanding the r-process to some extent has been the problem of quantitatively understanding the solar-system distribution of r-process elements as sketched on Figure 6 from ref. 69. The peaks at mass numbers, A = 130, A = 195, and to some extent A = 80, are identified with the neutron closed shells at N = 80, N = 126, and N = 50, respectively. Technically, there are two different ways in which such peaks could result from an r-process. Originally[43]), it was

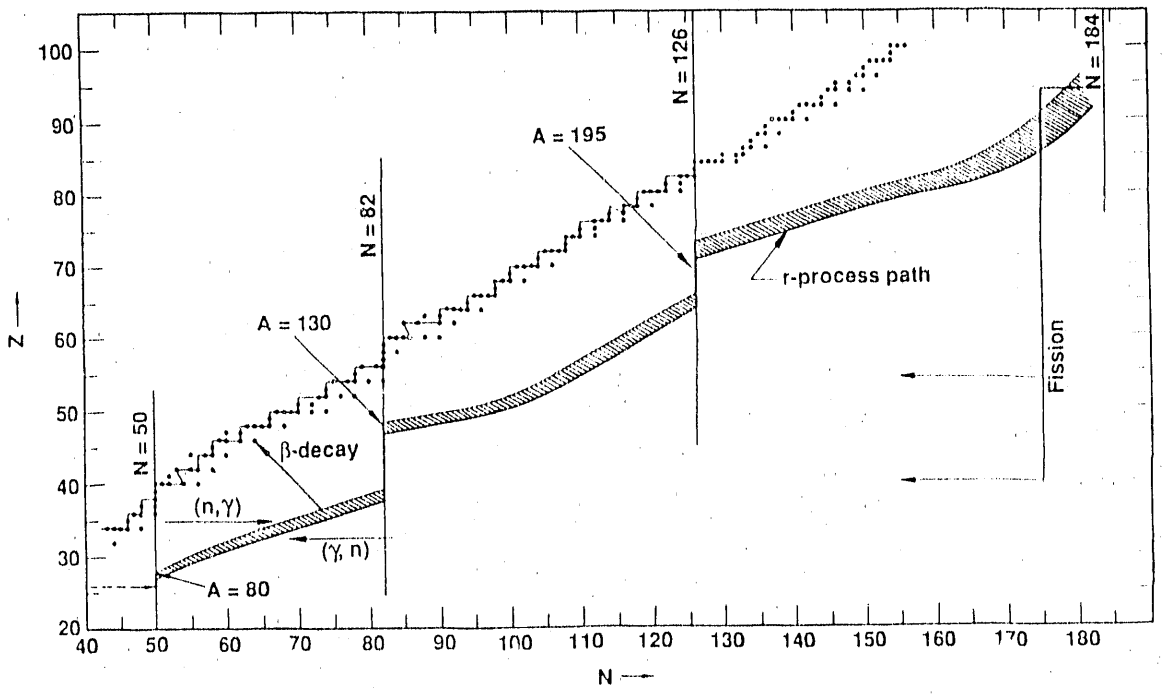

Fig. 5 A schematic view[40,41] of the neutron capture processes responsible for most heavy-element nucleosynthesis. The s-process flows along the beta-stable nuclei. The r-process path is represented by the shaded area away from stability.

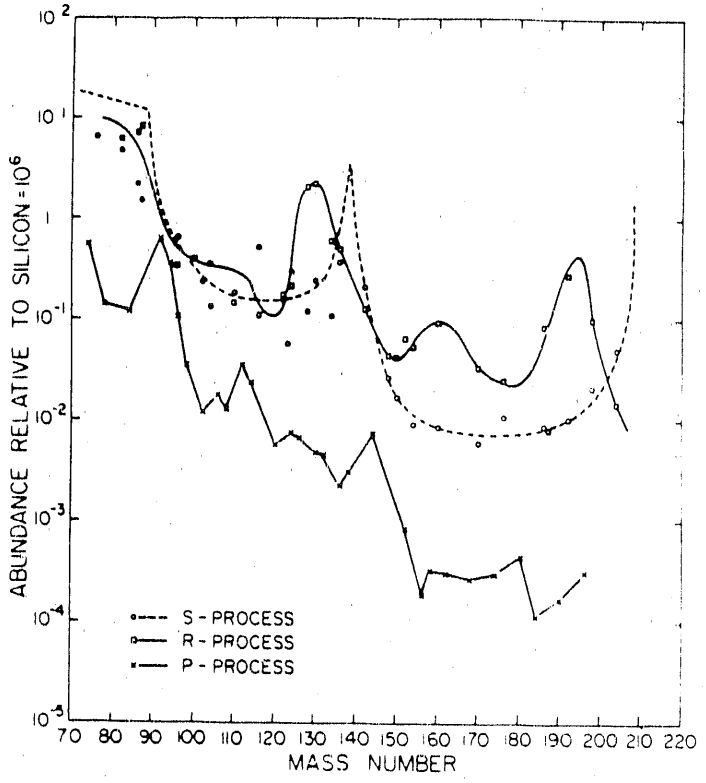

Fig. 6 Decomposition of solar-system abundances into s-process, r-process, and p-process components.[69])

proposed that the r-process occur in an environment in which neutron captures are so rapid that an $(n,\gamma) \leftrightarrow (\gamma,n)$ equilibrium is established. In this case the relative r-process abundances among isotopes of an element are given by a simple nuclear Saha equation. Besides statistical factors, the ratios of abundances of neighboring isotopes are determined by a Boltzmann factor of the neutron separation energy. These abundances peak along the r-process path (see Fig. 5) corresponding to isotopes with a neutron separation energy of ~ 1-2 MeV. The equilibrium waits at the r-process path until an isotope beta decays. Peaks in abundances are then produced near neutron closed shells where the beta-decay rates are slower.

The other scenario[42]) for producting r-process peaks is in what is sometimes called the n-process[70]). In this case the neutron densities and temperatures are too low to sustain (n,γ) equilibrium. Instead, the r-process flow is determined by a sequence of neutron captures and beta decays. Therefore,[41]) the r-process path is determined by the diminished neutron capture cross sections at neutron closed shells and the abundance peaks are determined by the competition between neutron captures and beta decay.

Clearly, it is most important to know beta-decay rates and neutron capture cross sections for nuclei near the r-process path, and particularly near the neutron closed shells. An example of how useful such information can be is given in the recent work of Kratz, et al.[71,72]) Figure 7 shows the r-process flow[72]) through the A = 130 peak. The authors have combined new measurements of the beta-decay rates in this region[73]) and the A = 80 region[74,75]) along with theoretical estimates[76]). By correcting for the contribution from beta-delayed neutron emission it is possible to infer the actual abundances during the r-process. These are given in boxes on Figure 7.

The r-process path from A = 126 to A = 130 involves only one isotope. The authors found that within uncertainty the ratio of abundances for these mass numbers is equal to the ratio of beta-decay half lives which

Table 3. Wish list for r-process nucleosynthesis.

τ_β :	^{129}Ag, ^{128}Pd, ^{127}Rb, ^{79}Cu, ^{78}Ni, ^{77}Co
$n(\beta)$:	^{129}Ag, ^{128}Pd, ^{127}Pd, ^{80}Zn, ^{77,78,79}Cu, ^{76,77,78}Ni, ^{76}Co
(n,γ) :	^{130,131,132}In, ^{131,132,133,134}Sn, ^{80,81,82}Ga, ^{81,82,83}Ge, ^{82,83,84,85}Se
	+ A = 195, N = 126 region
	+ ~ 5000 other unstable nuclei

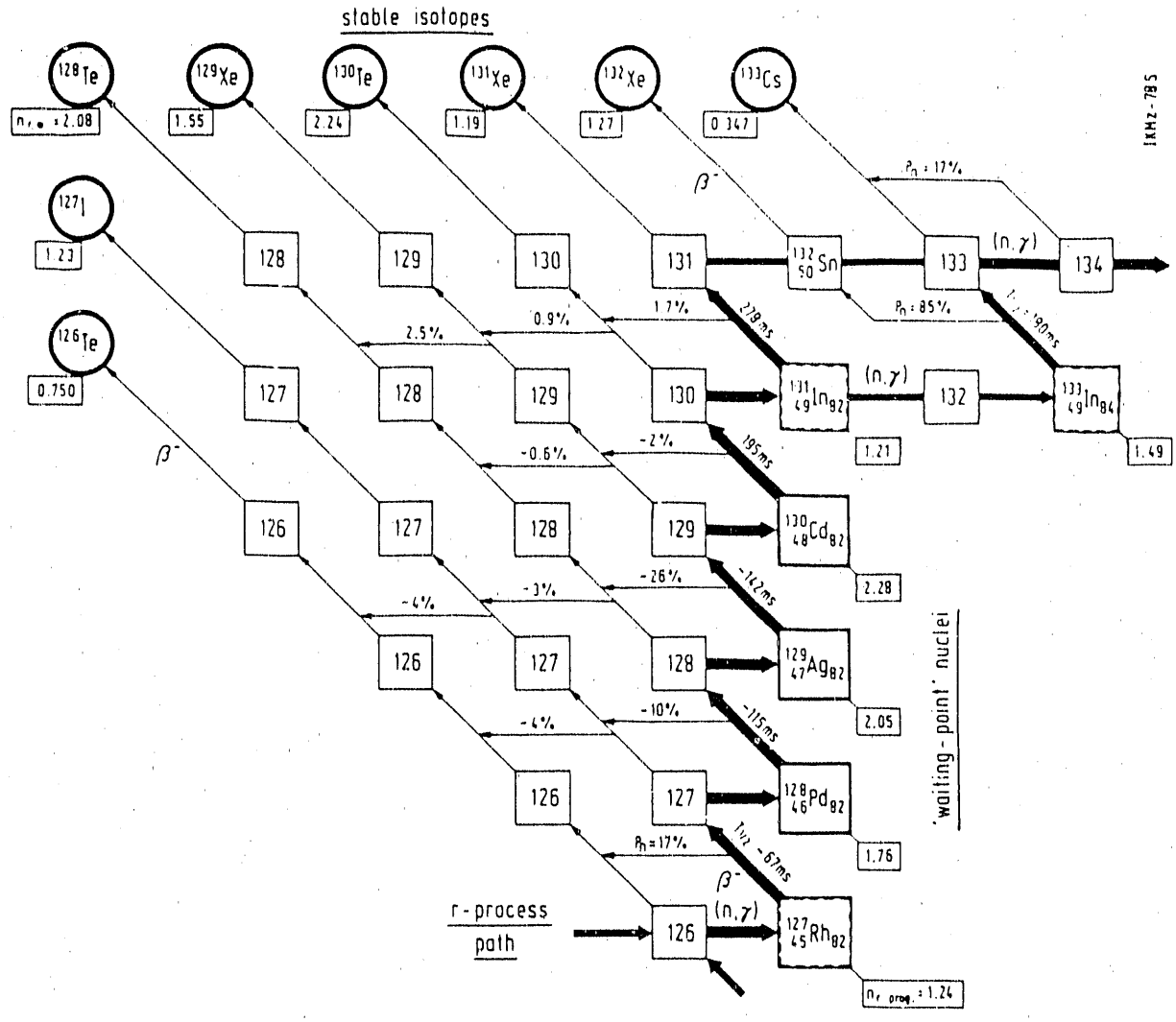

Fig. 7 The r-process flow through the A = 130 waiting point.[71,72]) Beta-decay rates and beta-delayed neutron emission branches that are unknown are indicated by a wavy line.

would imply that beta-flow equilibrium is established in this region. This is important since it indicates that the r-process lasts long enough for the several half lives necessary to achieve such equilibrium. Even more important are the abundances for mass numbers from A = 131 to 133. The relative abundances of these isotopes depend upon binding energies in a classical r-process or neutron capture cross sections in an n-process. The remarkable result[71,72]) is that the abundances seem to nicely agree with those of a classical r-process, while an n-process would predict[41]) an over abundance of A = 132 due to restricted neutron-capture flow through the ^{132}Sn double closed shell. However, this conclusion is shrouded in uncertainty due to the fact that the neutron-capture cross section for ^{132}Sn is not known as well as a number of critical beta decay rates and beta-delayed neutron emission probabilities. Thus, any information relevant to a determination of this cross section, i.e. levels, spins, spectroscopic strengths, would be of

considerable value in determining the environment for the r-process, as would more determinations of beta-decay rates and beta-delayed neutron emission for nuclei near the A = 80, 130, and and 195 neutron closed shells. Table 3 gives my opinion as to a wish list of most crucial nuclear properties for the r-process.

4.2 The s-process

The s-process is most probably associated with red-giant stars[40,42,43]. It may occur in core helium burning[43]) or core carbon burning[44]), but the most popular scenario is due to the thermal-pulse instablilty during the ascent up the asymptotic giant branch for intermediate-mass stars.[45,46]) Also, double helium-star binary coalescence has been recently proposed[47]). The key question surrounding the identification of the s-process environment is the neutron source reaction. Until recently the most popular source reaction was the $^{22}Ne(\alpha,\gamma)^{25}Mg$ reaction. However, this reaction requires a high temperature (~ 2.5×10^8K) which is difficult to achieve[77]), produces a neutron density which is too high[78]) and the predicted enhanced ^{25}Mg abundances from such a neutron source has not been observed[79]). Recently, the $^{13}C(\alpha,\gamma)^{16}O$ reaction seems promising[80]) since it occurs at a lower temperature (T ~ 1.5×10^8 K) and tends toproduce a lower neutron density.

Thus, the identification of the s-process environment can be equated with identifying the temperature and neutron density for the s-process. Fortunately, it is possible[46]) to identify these parameters from the observed solar-system s-process abundances (Fig. 6) and by the measurement of neutron capture cross sections for unstable nuclei near stability. Figures 8 and 9 show two examples of the cross section times abundance (σN) curves. The points are shielded s-only isotopes. The lines are theoretical predictions. The dips and peaks in the curve occur when the s-process capture flow passes through an unstable nucleus with a cross section significantly different from the final stable isotope. The neutron density affects the competition between neutron capture and beta decay at the branch points. A temperature dependence comes in due to thermally enhanced beta decay.

Figures 8 and 9 are from the best fits of temperature and neutron density possible with the data available in 1987[78]) and 1990[81]) respectively. Whereas previously it appeared that the temperatures were most consistent with a ^{22}Ne source, the more recent cross sections seem to indicate a lower temperature, however, there is a controversy surrounding this conclusion[80]). Another important effect during the s-process is the Boltzmann population of excited states

Table 4. Wish list for s-process nucleosynthesis.

(n,γ) :	^{79}Se, ^{85}Kr, ^{95}Zr, ^{107}Pd, ^{141}Ce, ^{151}Sm, ^{169}Er, ^{170}Tm, ^{175}Yb, ^{186}Re, ^{204}Tl, ^{193}Pt
Excited-state (n,γ) :	^{103}Rh, ^{119}Sn, ^{169}Tm, $^{187,189}Os$, ^{193}Pt

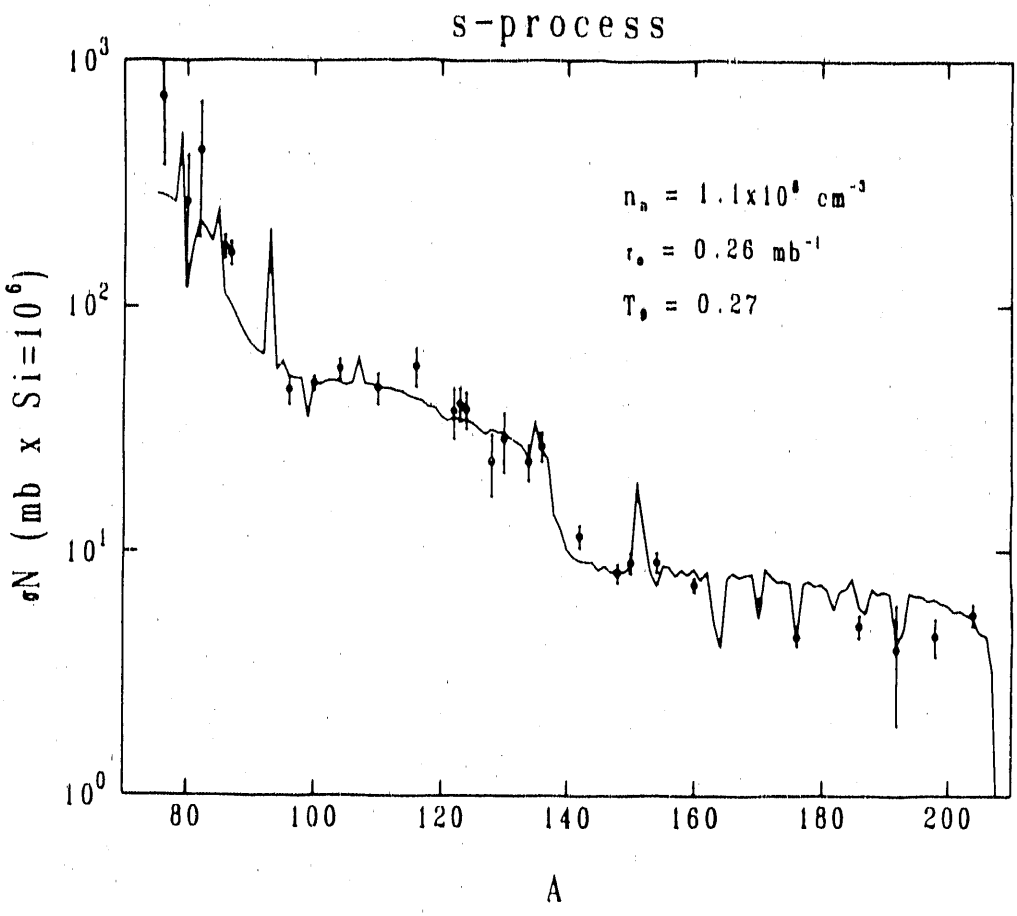

Fig. 8 s-Process σN curve from Howard, et al. (1987).[78])

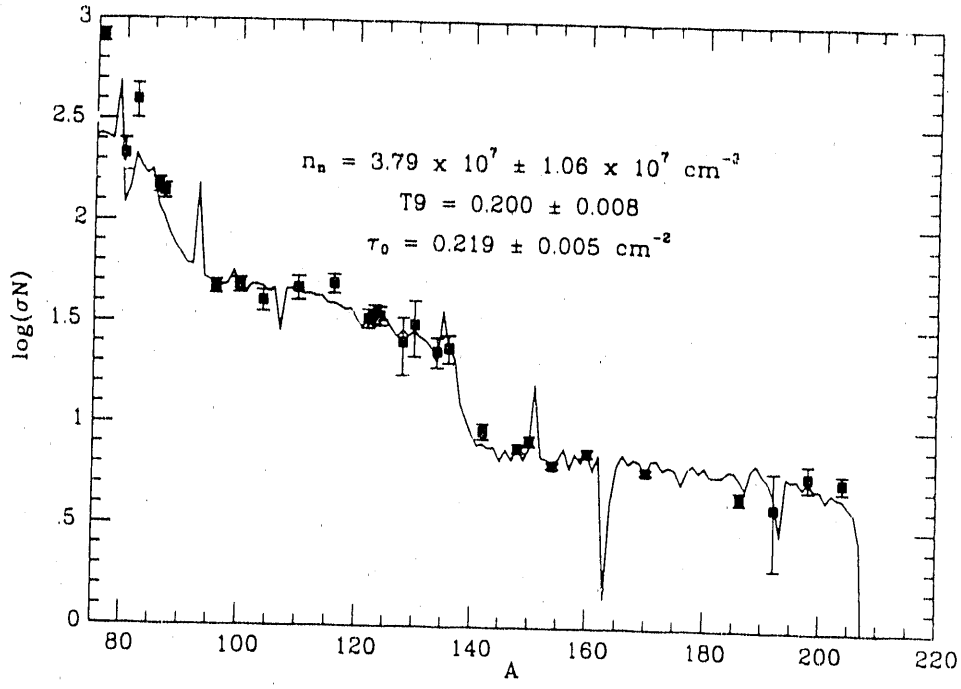

Fig. 9 s-Process σN curve from Bauer, et al. (1990).[81])

which means that neutron capture can occur on thermally excited nuclei. If there is a large difference between the ground-state and excited-state spins there can be a significant effect on the cross section. Some of the largest expected correction factors[82]) for a number of nuclei relevant to the s-process are summarized in Table 4 along with a wish list of other important s-process measurements that come to mind.

4. Presupernova cores

The problem of how type II supernovae explode has been with us for some time[83,84]) and is still not solved. The standard scenario used to be that as the iron core approached the Chandrasakar mass it would collapse to densities in excess of nuclear, then bounce and produce a shock wave heating the outer regions of the core. The problem, however, has been that in numerical simulations the core separates into an inner homologous core which collapses and bounces and an outer core which collapses more slowly. As the shock wave passes through the outer core it is dissapated due to the energy absorbed into the photodissociation of iron. It may be possible to later rejuvinate the shock[85]) by reheating from neutrino emission from the inner regions, but this is still being explored.

Recently,[86]) however it was realized that the core structure may be altered by the electron capture of heavy (A > 60) nuclei with short half lives not previously considered. These nuclei could speed the rate of neutronization of the core and cause the Chandrasakar mass to be reached while the outer core is significantly smaller. This makes it easier for the core-bounce shock to propagate and produce an explosion. However, the electron capture occurs with electrons energetic enough to excite a distribution of Gamow-Teller states. Hence one would like to know Gamow-Teller strength functions for a number of unstable nuclei in the vicinity of A = 60, e.g. ^{60}Co, ^{62}Co, etc. Such strength functions may be measurable with a radioactive ion beam undergoing a (^{3}He,t) reaction.

5. Conclusion

Thus, we have seen that there are a host of different nuclear data needs which if filled could dramatically impact our current level of understanding of a number of phenomena in stellar evolution, stellar nucleosynthesis, and cosmology. The kind of machine we would like to have available for these measurements would probably involve some kind of separator or post accelerator for 2 to 10 MeV/n radioactive ion beams from A = 8 to A = 252. There are a number of direct charged particle reactions on light to intermediate-mass nuclei which should be measured. In addition data relevant to neutron capture cross sections could be obtained by inverse (d,p) reactions with a radioactive heavy-ion beam onto a deuterium target. One might also use other reactions, e.g. (^{3}He,t), (^{3}He,t), etc., to indirectly determine resonance properties for charged-particle reactions. It would also be useful to generate radioactive ion beams with energies up to ~ 100 MeV/n for the determination of Gamow-Teller strength functions.

Work supported under the auspices of the U. S. Department of Energy by the Lawrence Livermore National Laboratory under contract number W-7405-ENG-48.

References

1. G. J. Mathews, et al., in Nuclear Data for Basic and Applied Science", P. G. Young, et al., Eds. (Gordon and Breach; New York) 1985, pp. 835-852.

2. S. E. Woosley in "Proc. Accelerated Radioactive Beams Workshop," 1985, Parksville, Canada Sept. 5-7 (1985) TRIUUMF TRI-85-1, pp.4-28.

3. M. Arnould in "Radioactive Nuclear Beams", W. D. Myers, J. M. Nitschke, and E. B. Norman, Eds. (World Scientific; Singapore) 1988, pp. 209-219.

4. F. C. Barker and R. H. Spear, Astrophys. J. 40, 25 (1986).

5. R. Davis, D. S. Harmer, and K. C. Hoffman, Phys. Rev. Lett. 20 (1968) 1205.

6. R. W. Kavanagh, Nucl. Phys., 15 411 (1960).

7. P. D. Parker, Astrophys. J. Lett., 153, L85 (1968)

8. R. W. Kavanagh, et al., BAPS, 14 (1969) 1209.

9. F. J. Vaughn, et al., Phys. Rev., C2 (1970) 1657.

10. B. W. Filippone, et al., Phys. Rev. Lett., 50 (1983) 412; Phys. Rev. C25 (1983) 2222.

11. G. J. Mathews and F. S. Dietrich, Astrophys. J., 287, (1984) 969.

12. T. E. Chupp, et al., Phys. Rev. C31 (1985) 1023.

13. P. B Fernandez, et al., BAPS, 31 (1989) 1209.

14. T. F. Wang, et al., BAPS, 33 (1989) 1564.

15. P. Auger, et al. in "Heavy Ion Physics and Nuclear Astrophysical Problems", S. Kubono, et al., eds. (World Scientific; Singapore) 1989, pp. 107-113.

16. R. K. Wallace and S. E. Woosley, Astrophys. J. Suppl. 45, 389 (1981).

17. P. D. Parker, in "Cluster '88," K. Ikeda, et al., eds., J. Jap. Phys. Soc. Suppl., 58, 196 (1989)

18. P. V. Magnus, et al., Nucl. Phys., A475, 1 (1987).

19. M. Wiescher, J. Gorres, and F.-K. Thielemann, Astrophys. J. 326, 384 (1988).

20. S. Kubono, et al., Astrophys. J. 344 (1989) 460.

21. S. Kubono, et al. in "Heavy Ion Physics and Nuclear Astrophysical Problems", S. Kubono, et al., eds. (World Scientific; Singapore) 1989, pp. 83-96.

22. E. B. Norman, Priv. Comm.

23. J. H. Applegate, C. J., Hogan, R. J., and Scherrer, R. J., Phys. Rev., D35 (1987) 1151.

24. C. R. Alcock, G. M., Fuller, and G. J., Mathews, Astrophys. J., 320 (1987) 439.

25. G. M. Fuller, C. R., Alcock, and G. J. Mathews, Phys. Rev. D37 (1988) 1380.

26. J. H. Applegate, C. J., Hogan, R. J., and Scherrer, R. J., Astrophys. J., 329 (1988) 572.

27. C. R. Alcock, D. S. Dearborn, G. M. Fuller, G. J. Mathews, and B. S. Meyer, Phys. Rev. Lett. 64 (1990) 2607.

28. G. J. Mathews, B. Meyer, C. R. Alcock, and G. M. Fuller, Ap. J. (1990) in press.

29. T. Kajino, G. J. Mathews, and G. M. Fuller, Ap. J. (1990) in press.

30. H. Kurki-Suonio, Phys. Rev. D37 (1988) 2104.

31. H. Kurki-Suonio, R. A. Matzner, J. M. Centrella, T. Rothman, and J. R. Wilson, Phys. Rev. D38 (1988) 1091.

32. H. Kurki-Suonio and R. A. Matzner, Phys. Rev. D39 (1989) 1046.

33. H. Kurki-Suonio, R. A. Matzner, K. A. Olive, and D. N. Schramm, Ap. J. 353 (1990) 406.

34. R. A. Malaney and W. A. Fowler, Ap. J., 333 (1988) 14.

35. R. N. Boyd and T. Kajino, Ap. J. Lett., 336 (1989) L55.

36. T. Kajino and R. N. Boyd, Ap. J., 359 (1990) 267.

37. Kawano, W. A. Fowler, and R. A. Malaney, Submitted to Ap. J. (1990).

38. M. W. Wiescher, J. Gorres, and F.-K. Thielemann, Ap. J. (1990) in press.

39. J. J. Cowan, F.-K. Thielemann, and M. W. Wiescher, (1990) submitted to Ap. J.

40. P. A. Seeger, W. A. Fowler, and D. D. Clayton, Ap. J. Suppl., 11, (1965) 121.

41. G. J. Mathews and J. J. Cowan, Nature, 345 (1990) 491.

42. G. J. Mathews and R. A. Ward, Rep. Prog. Phys. 48 (1985) 1371.

43. G. R. Burbidge, E. M., Burbidge, W. A., Fowler, and F. Hoyle, Rev. Mod. Phys., 29, (1957) 547.

44. W. D. Arnett and J. W. Truran, Ap. J., 157 (1969) 339.

45. R. K. Ulrich, R. K. 1973, in "Explosive Nucleosynthesis", D. N. Schramm and W. D. Arnett, Ed., (Austin: Univ. of Texas) p. 139.

46. I. Iben and J. W. Truran, Ap. J., 220 (1978) 980.

47. I. Iben, K. Nomoto, A. Tornabe, and A. V. Tutokov, Ap. J., 317 (1987) 717.

48. W. Hillebrandt, K. Takahashi, and T. Kodama, Astron. Astrophys., 52 (1976) 63.

49. S. A. Colgate, Astrophys. J., 163 (1971) 221.

50. J. M. Leblanc and J. R. Wilson, Ap. J., 161 (1970) 541.

51. D. N. Schramm and Z. Barkat, Astrophys. J., 173 (1972) 195.

52. D. L. Meier, R. I. Epstein, W. D. Arnett, and D. N. Schramm, Astrophys. J., 204 (1976) 869.

53. E. Symbalisty, D. N. Schramm, and J. R. Wilson, Astrophys. J. Lett., 291 (1985) L11.

54. R. A. Alpher, H. Bethe, and G. Gamow, Phys. Rev., 73 (1948) 803.

55. J. H. Applegate, C. J. Hogan, and R. J. Scherrer, Ap. J., 329 (1988) 572.

56. J. M. Lattimer and D. N. Schramm, Ap. J. Lett., 192 (1974) L145.

57. J. M. Lattimer and D. N. Schramm, Ap. J., 210 (1976) 549.

58. E. Symbalisty and D. N. Schramm, Astrophys. Lett., 22 (1982) 143.

59. C. R. Evans and G. J. Mathews, in "Origin and Distribution of the Elements", G. J. Mathews, ed. (World Scientific; Singapore) pp. 619-624.

60 F. Hoyle and D. D. Clayton, Ap. J., 191 (1974) 705.

61. W. Hillebrandt and F.-K. Thielemann, Astron. Ap., 58 (1977) 357.

62. J. R. Truran, J. J. Cowan, and A. G. W. Cameron, Ap. J. Lett., 222 (1978) L63.

63. T. Lee, D. N. Schramm, J. P. Wefel, and J. B. Blake, Ap. J., 232 (1979) 854.

64. J. J. Cowan, A. G. W. Cameron, and J. R. Truran, Ap. J., 252 (1982) 348.

65. S. E. Woosley and T. A. Weaver in "Nucleosynthesis and Its Implications for Nuclear and Particle Physics," J. Audouze and N. Mathieu, eds., NATO ASI Ser. C, Vol 163., (D. Reidel, Dordrecht) pp. 145-166 (1986).

66. C. J. Hogan and J. H. Applegate, Nature, 320 (1987) 236.

67. R. I. Epstein, S. A. Colgate, and W. C. Haxton, preprint (1988).

68. S. E. Woosley, D. Hartmann, R. D. Hoffman, and W. C. Haxton, submitted to Astrophys. J. (1989).

69. A. G. W. Cameron, in "Essays in Nuclear Astrophysics," C. A. Barnes, et al., eds. (Cambridge University Press; Cambridge) pp. 23-43 (1982).

70. J. B. Blake and D. N. Schramm, Ap. J., 174 (1973) 207.

71. K.-L. Kratz, F.-K. Thielemann, W. Hillebrandt, P. Moller, V. Harms, A. Wohr, and J. W. Truran, in "Proceedings of the Sixth International Conference on Capture Gamma-Ray Spectroscopy", Leuven (1987).

72. K.-L. Kratz, Rev. Mod. Astron., 1 (1988) 184.

73. K.-L. Kratz, H. Gablmann, W. Hillebrandt, B. Pfeiffer, H. L. Raven, and F.-K. Thielemann, Z. Phys., A325 (1986) 483.

74. R. L. Gill, R. F. Casten, D. D. Warner, A. Plotrowski, Phys. Rev. Lett., 56 (1986) 1874.

75. E. Lund, K. Aleklett, B. Fogelberg, and A. Sangariyavanish, Phys. Scripta, 34 (1986) 614.

76. J. Krumlinde and P. Moller, Nucl. Phys., A476 (1986) 419.

77. G. J. Mathews, R. A., Ward, K. Takahashi, and W. M. Howard, in "Nucleosynthesis and Its Implications on Nuclear and Particle Physics", Audouze and Mathieu, eds., (Nato ASI Series, Vol. 163), (D. Reidel, Dordrecht) pp. 277-284, (1986).

78. W. M. Howard, G. J., Mathews, K. Takahashi, and R. A. Ward, Ap. J., 309 (1986) 633.

79. R. A. Malaney, Ap. J., 321 (1987) 832.

80. F. Kappeler, H. Beer, and K. Wisshak, Rep. Prog. Phys., 52 (1989) 945.

81 R. W. Bauer, et al., (1990) submitted to Phys. Rev. C

82. S. E. Woosley, et al., At. Dat. Nucl. Dat. Tab. 22 (1979) 371

83. G. E. Brown, ed., Phys. Rep., 163 (1988) 1.

84. S. E. Woosley and T. A. Weaver, Ann. Rev. Astron. Ap., 24 (1986) 205.

85. J. R. Wilson, and R. W. Mayle, Phys. Rep., 163 (1988) 63.

86. M. B. Aufderheide, et al., Ap. J. (1990) in press.

APPLICATIONS OF RADIOACTIVE ION BEAMS IN MATERIALS SCIENCE

JERZY A. SAWICKI

Atomic Energy of Canada Limited, Chalk River Nuclear Laboratories, Chalk River, KOJ 1JO Ontario, Canada

Abstract: Intense, pure beams of separated and accelerated radioactive isotopes, such as could be delivered by advanced ISOL facilities, are ideal for materials research and are a subject of increasing interest in the technology. Beams of such short-lived nuclei provide unique opportunities for probing the microstructure of solids, at especially low doping and radiation damage levels. This article outlines the present status and a perspective on experimental techniques based upon the use of radioactive beams in molecular studies and materials engineering. After a brief introduction into the field of ion implantation and surface modification by ion beams, the advantages of radioactive beams and their selected recent applications: with techniques such as surface layer activation, nuclear reaction analysis on radioactive nuclei, channeling of charged particles from radioactive decay, conversion electron spectroscopy, Mössbauer effect on implanted nuclei, on-line nuclear orientation, perturbed angular correlations, on-line NMR and positron emission and annihilation will be discussed.

1. Introduction

Studies on applications of the interaction of energetic ions with materials are conducted in most vigorously expanding fields of research and technology, and will certainly continue to be into the next century. Although the nature and possible application of many processes caused by ion bombardment in solids is still being explored, ion beams are already broadly and beneficially applied to materials modification and surface processing, especially in semiconductor microelectronics, advanced metallurgy and tool-manufacturing industries. Progress in ion beam modification of materials has always been strongly associated with nuclear laboratories, and largely stimulated by development of new experimental facilities.

Radioactive isotopes implanted off-line have been used as probes in solid state studies since the early 1960's. Implantation of isotopes with lifetimes longer than several hours has been performed usually with low energy (<100 keV) mass separators existing in many nuclear laboratories. Availability of a wide variety of exotic beams of short-lived isotopes in the lifetime range from 1 s to 1 h, such as those pioneered by the ISOLDE facility at CERN in the mid-1970's [1-3], resulted in the establishment of novel experimental techniques in nuclear physics and in the determinination of a number of nuclear parameters, especially for nuclei far from stability. The on-line implantation of radioactive

isotopes has also considerably expanded the range of applications of various techniques for materials characterization, and it was instrumental in establishing completely new methods in materials research.

Applications of implanted radioactive isotopes in condensed matter studies perfomed until 1985 were reviewed in connection with the ISOL project at TRIUMF [4,5]. An updated survey presented below merely intends to give a feeling for the dramatic progress made since then in several areas, and -- given the short time and space allowed -- it is subjective and does not pretend to be comprehensive.

2. Ion implantation and beam modification of materials

Ion implantation, regarded initially as an obscure phenomenon obstructing nuclear reaction experiments, has over the past two decades -- thanks to considerable research effort of many nuclear-solid state physicists -- established itself as an innovative approach for changing mechanical and chemical surface properties of materials. Its potential has been realized at first in semiconductors technology [6]) and more recently in non-equilibrium metallurgy [7]). The technique is now applied more and more widely in the manufacture of sophisticated semiconductors, specialized tools and quality components, as well as biocompatible implants; see [8-10]) for recent surveys. In the United States the ion implantation technology is being commercialized by several companies; in particular it is developed and widely used by Spire Corporation Surface Modification Centre, Bedford, Massachusetts [10]).

As a tool for the carefully controlled introduction of impurities in solids, ion implantation has several very attractive features. First, both the lateral location and depth of implants, as well as the ion dose and resultant concentration in the matrix, can be defined with a high degree of precision. Due to the stochastic nature of the elastic collision process, the ions come to rest in a Gaussian distribution with the mean centered about R_p, the projected range, well described by theory of Lindhard, Scharff and Schiott, and with a FWHM = $2.35\Delta R_p$ where ΔR_p is the standard deviation of the mean. The depth of implanted distribution varies as $E^{1/2}$ where E is the incident energy of the implant. At the usual isotope separator energies of 10 - 100 keV, the range R_p in various materials is of the order of 10 - 100 nm, whereas the dose of typically 10^{15} ions/cm^2 corresponds to peak concentrations in the range 0.1 - 1 at%. Secondly, it is an inherently clean, high- or ultra-high vacuum technique, capable of using almost all combinations of ions and targets, and of mixing the elements regardless of the usual solubility limits and alloying rules. Thus, in contrast to conventional thermal alloying or chemical doping techniques, the solid solubility can be exceeded by several orders of magnitude, and thermodynamically metastable systems with normally very low solubility can be formed as well. Thirdly, ion implantation may change the chemical composition and introduce much damage to the target, thereby creating extraordinary new materials or new phases, very often with drastically modified (metastable) properties, as compared to known materials with similar compositions.

An individual implantation event can be divided into three phases:

1. *The collisional phase:* In this phase, lasting roughly 0.1 - 1 ps, energetic heavy ions are slowed down in matter by electronic excitations of the atomic electrons and by elastic collisions with the shielded atomic nuclei. Those elastic collisions produce primary knock-on atoms in the keV energy range. As the energy of the injected ion as well as that of the high energy knock-ons is further dissipated through successive recoils, it results in a collision cascade. The number of displaced atoms due to primary knock-ons and secondary collisions is roughly equal to E/B ~ 10^3 - 10^4, where E is ion energy and B is the displacement energy. The kinetic energies of atoms in the cascade volume far exceed thermal energies and are typical of those achieved at temperatures of 10^4 - 10^6 K. The collisions lead to the creation of a radiation damage cascade at the end of the track, that has a locally high concentration of interstitials, displaced host atoms and vacancies, with a lateral spread of ~3 nm and a depth of ~10 nm along the primary track. At low enough doses, typically below 10^{12} - 10^{13} ions/cm^2, the individual cascades do not overlap and may not interfere with each other. The detailed nature of the collision cascade depends very much on the masses of the projectiles and target constituents. In particular, replacement collisions yielding substitutional implants are favored for equal masses of projectile and target atoms.

2. *The relaxation phase:* The excess energy accumulated in the volume of the radiation damage cascade is relaxed partly in about 0.5 ps by a spontaneous recombination of Frenkel pairs and trapping of lattice defects (vacancies) at the impurity atoms. The final location and the binding of the implant, as well as the final state of the matrix, is to a large extent governed by the mode and rate of these relaxation processes, and therefore it very much depends on the type of the target; different behavior is observed in monoatomic and complex materials or, metals and insulators. When the average energy reaches a magnitude of a few eV per atom, chemical effects start also to play a role in determining final site and bond of the implants.

3. *The cooling phase:* During a further few ps a highly disordered cascade region cools to reach equilibrium with the surroundings. While metals are characterized by a very high cooling (quenching) rate of the order of 10^{14} K/s, in semiconductors, and especially in insulators, the cooling may be substantially slower. The final form of the matrix and the preference for the final lattice position may depend on the chemical nature of the impurity and host atoms, volume of the available sites, heat of alloying, local charge balance, etc. At high implantation doses the non-metals often become amorphous, but one can also form amorphous metal alloys, especially in cases with a particularly large atomic volume and/or electronegativity mismatch between participating elements.

In general, ion bombardment and implantation may result in modification of a number of materials properties: mechanical (hardness, friction, resistance to wear and fatigue, adhesion), chemical (corrosion, oxidation, catalytic activity), electrical (conductivity, semi- and super-conductivity), magnetic (near-surface magnetism) and optical (reflectivity, photosensitivity), etc. For these reasons, the technique has become a powerful tool for materials engineering and is widely applied in the manufacture of sophisticated semiconductor devices and in the refinement of metal surfaces.

Examples of applications in metallurgy are:
N ion implantation in steels, which through formation of nitrides, improves hardness and may increase resistance against wear up to 100-1000 times; this technique is

being used in the refinement of metal cutting tools, space shuttle engine parts, artificial hip joints, etc.
- formation of alloys with unusual properties through ion beam mixing.

Wide applications in semiconductor technology include:
- highly controlled and reproducible doping of P and As ions to form n-type Si, and B ions to form p-type Si,
- high resolution ion beams are used in the manufacture of very large-scale integration (VLSI) devices,
- deeply buried O implants are used in silicon on insulator (SOI), and
- Co implants are used to form deep conducting Co_2Si regions.

In ceramics and insulators implantation technologies are used in:
- improved tungsten carbide tools, photosensitive ceramics, waveguides of implanted silica glass, implanted magnetic bubble garnet memories, and
- implanted polymers, with up to a 10^{14} times increase in conductivity.

The partial listing of successful applications of ion implantation is given in Appendix 1.

Wider application of ion beam technologies in materials processing outside of the semiconductor industry is still hindered rather by economic than by technical factors, and particularly by the poor availability of high current ion sources and accelerators capable of providing very high ion fluences at low enough cost per unit area; see [11]).

Although at present low-energy (10 - 100 keV) ion beams are used commonly, the interest in applications of high-energy ions in the MeV range [12,13]), as well as in the GeV range [14]), is growing rapidly. The penetration of ions having energies of MeV per nucleon is predominantly determined by the electronic stopping power, while the straggling of ions is determined by nuclear stopping. The nature of lattice damage at MeV energies is expected to be similar to that at keV energies, but clear rules can be established only through dedicated systematic research. Because light MeV ions do not deposit much energy in displacement events near the surface, the target sputtering yield is low, ~1 atom per 1 incident ion. In addition, the reflection rates and the probability of channeling is highly diminished at high incident energies. Studies of implanted MeV radioactive isotopes would certainly facilitate a better understanding of the mechanism of various processes that occur at high deposition energies.

High-energy ions are already used in various fabrication processes in silicon semiconductor technology: for instance, in the production of radiation detectors, thick layer devices and bipolar junction transistors. The depth of penetration enables buried oxygen layers to be placed behind device structures, to act as electrically isolating barriers. For high mass binary (e.g., GaAs) or ternary semiconductors, MeV ion implantation may be the only method of doping that avoids chemically less pure film-deposition techniques unsuitable for large-scale integration. One can also improve adhesion of metallic layers on semiconductors by MeV ion bombardment.

In metallurgical applications, the resistance to erosion and wear may be considerably improved by changing oxidation properties or by the creation of thick amorphous alloy

coatings. Similarly, the corrosion properties may be altered by creation of thick alloy coatings or by changing surface oxidation processes.

In insulators, MeV implantation enables electronic, wear or chemical modifications to be made deeply in the material without loss of bulk integrity or other useful properties. In particular, one can induce the conductivity in polymers, reduce the reflectivity of glasses or synthesize unusually hard coatings. MeV ions are also very useful for studying materials used in fission and fusion reactors. A few hours of irradiation can simulate the radiation damage corresponding to many years of reactor operation, at well-controlled and reproducible experimental conditions and without causing hostile reaction by-products.

3. Some Advantages of Radioactive Beams

The advantages of ion implantation as a technique for preparing radioactive sources, for instance for β-spectroscopy, were already realized in the early 1960's [15]. Today, isotope separators on-line (ISOL), which provide intense, clean beams of short-lived isotopes ($T_{1/2}$ > 1 ms), far from the β stability line of most elements (> 70%), represent an extraordinarily valuable tool for ion implantation experiments, and offer dramatic extension of the variety of available local probes over existing off-line techniques ($T_{1/2}$ > 1 h). A wide range of available probe isotopes allows for a choice of the most adequate method for solving a particular problem, thereby permitting a mission- rather than tool-oriented approach. It also allows for a shorter measuring time, sometimes by a factor of 10 - 10^3 times. Also, because the observation is based on the specific radioactive-decay signature of the ions, naturally occuring contaminations from unwanted stable beams, usually do not affect the result of the experiment.

Because the rate of the acquisition of the data, determined by the number of radioactive decays in the specimen per measuring period, is roughly equal to $1/T_{1/2}$, the on-line study can be performed at very low implanted doses, typically three to four orders of magnitude lower than in the case of off-line implantations of long-lived isotopes. This allows for a reduction in doping levels to 10^8 - 10^{10} atoms/cm^2 and for drastic diminishing of radiation damage imparted to the specimen. Such low doping and low radiation damage levels are very useful in studies of semiconductors or bio-materials. Also, by reducing the chance that one implant ion will come to rest in a region of lattice damaged by the stopping of another ion, one can investigate the structure of individual collision cascades, since at implantation fluences below 10^{11}-10^{12} ions/cm^2 the defect environment of the implanted ion is determined by its own slowing-down process.

Furthermore, preparation of ion implanted specimens is highly reproducible and the radioisotope can be well packed under clean surface, whereas initial small activity and minor radioactive contamination of the specimens after the study eases handling and waste disposal problems. Despite the fact that the measurements of ISOL are usually performed in situ on the implanted targets, many valuable data could be obtained as well for the sources transported to other laboratories. In particular, measurements of electrical conductivity and optical absorption can supply valuable data about lattice defects, electron microscopy can characterize structural modifications, measurements of microhardness can give information about mechanical modifications, and the magneto-

optic Kerr-effect can give data about surface magnetism. Therefore, a high-yield ISOL could greatly extend many existing programs.

When radioactive isotopes are implanted, the subsequent radioactive decay may lead to a displacement of the probe if the recoil energy of the decay exceeds the displacement energy. Also, the electronic after-effects of the nuclear decay, may affect the electronic state of the implanted probe, especially in insulators. This suggests the possibility of using subsequent nuclear transformations for some interesting purposes, such as time-delayed chemical or electrical coding. For instance, one can think of the implantation of some electrically neutral impurities into a semiconductor, which only after some time, due to radioactive decay, would accumulate as electrically active species. Or, a long-lived α- or β decaying radioisotope implanted in a memory chip could possibly be used as a random number generator.

In recent years, the off-line separation and implantation of radioactive isotopes has been largely concentrated at European laboratories: for instance, in Aarhus, Bonn, Cracow, Göttingen, Groningen, Konstantz, Leuven, Lyon and Orsay, as well as in Chalk River [16]. The first dedicated on-line facilities have been installed mostly in Europe, in particular in Bonn, Daresbury, Louvain la Neuve and Orsay. A unique on-line separator, with the mass-resolution better than 10 000 and currents up to 20 mA, with FEBiAD and He-jet sources, operates also at TASCC in Chalk River [17]. Characteristically, as seen in Fig. 1, the ISOL is only a small portion of this large accelerator project. Other facilities used at Chalk River for radioactive ion implantation and on-line studies, include the 70 keV isotopes separator and the 2 MeV mass separator.

A major breakthrough in scientific productivity has been accomplished in CERN by setting up the ISOLDE collaboration in the mid-1970' s [1,2]. At the ISOLDE facility, radioactive isotopes are produced as proton-induced spallation or fission products from the targets irradiated by the 600 MeV protons at the CERN synchrocyclotron. The implantation energy is fixed at 60 keV. The on-line mass separator ISOLDE-2 is used intensely for a wide variety of experiments in nuclear, atomic, solid state, surface, and applied physics. A new isotope separator ISOLDE-3, with a mass resolution of 6000 was commissioned in 1989 December. In 1987 the ISOLDE facility ran for a total of 140 shifts of physics, during which 20 experiments took data; almost half of them were in materials research. In 1988, radioactive beams were produced for a record number of 280 shifts [3]. The European example clearly illustrates the urgent need for a dedicated, next-generation facility in North America.

4. Selected research techniques and topics

4.1. Surface layer activation

Probably the most straightforward application of radiotracers at present is surface layer activation (SLA), in which a small amount of radioactive isotope is implanted at a specific depth in the material or part under study, and the loss of radioactivity, is detected later as a function of mechanical wear, chemical erosion, thermal treatment, sputtering, etc. This technique offers considerable advantages over direct activation, in which the radioactivity is produced in the object by nuclear reactions. Direct nuclear reaction activation cannot be used effectively, for instance, in the case of materials composed of elements with low

atomic numbers, such as organics, polymers or light ceramics. The technique of surface activation has many applications in technology and is capable of generating considerable commercial benefits. It has been used for examining automotive components (Karlsruhe [18]) and for testing critical parts during sulphuric acid fabrication (Harwell) [19]). The availability of intense radioactive beams would be very advantageous for further advancement of this valuable technique.

A new version of SLA for tribology studies has been demonstrated at the Michigan State University [20]). In this case ^{7}Be ($T_{1/2}$= 53.3 d), which is produced with a large cross section by fragmentation of a high-energy ^{14}N beam, escapes from the target in a forward direction and stops in the object under examination. ^{7}Be decays by electron capture to ^{7}Li, which emits a 477.6 keV γ–ray. A relatively long half-life and a single, well characterized γ–ray line make ^{7}Be nucleus an excellent candidate for research in tribology of materials such as plastics and ceramics. In recent experiments, an integrated beam current of 4.2×10^{16} ^{14}N ions produced a dose of 3.7×10^{11} ^{7}Be ions.

The implantation of radioactive tracers is applied also in fundamental studies of diffusion, for instance, the self-diffusion of ^{31}Si in silicon, ^{59}Fe in iron and iron alloys or ^{95}Zr in zirconium. The diffusion of the implanted marker is followed as a function of thermal treatment, using step-wise sectioning, chemical stripping or sputtering methods. The study provides data on depth profiles, mechanism of diffusion and diffusion coefficients. Alternatively, by analyzing the conversion electron line shapes, one can determine the depth at which radioactive nuclei are deposited and can establish their diffusion behavior in materials.

Recently, studies of diffusion with radiotracers have started at ISOLDE in CERN, particularly in the diffusion of Se and Te in Cu, Ag and Au matrices. The pressure dependence of Au diffusion in Al has been also measured to clearly demonstrate the vacancy mechanism for the process. The study of technologically very important diffusion of impurities in semiconductors was initiated with Se in Si. Atomic diffusion of Fr in K is being studied to obtain microscopic insight into the atomic motion in alkali metals. A novel technique for using α-spectroscopy from the implanted radionuclei as a depth profiling method in diffusion studies was also tested [3]). The possibility of using radioactive isotopes with much shorter lifetimes, such as can be delivered by an ISOL (<1 s), could considerably extend this field of study. In particular, it would be very interesting to develop a means to investigate the mechanism of radiation-enhanced diffusion, diffusion of virtually insoluble species and fast diffusion processes at high temperatures.

4.2. Nuclear reaction analysis

Ion beam analysis, using a variety of nuclear reactions, as well as Rutherford backscattering and forward recoil scattering, are widely used techniques, invaluable for determination of the content and depth profiling of various isotopes near the surface of materials. By ion beam analysis one examines usually stable isotopes, but it is also possible to analyze radionuclei, especially those with sufficiently long life-times. The application of radioactive beams can be also advantageous in specific cases, for instance when the nuclear reaction has favorable cross-section and sharp resonant characteristics. For quantitative nuclear reaction analysis, the nuclear cross sections for various reactions

have to be known to within about 1%, so that cross sections must often be remeasured to be useful for practical applications.

To demonstrate the application of nuclear reaction analysis in the study of radioactive implants, let us refer to our recent studies of tritium implantation into fusion-related materials [21,22]). The interaction of tritium with materials is extensively studied now in connection with the thermonuclear d-t fusion program. Fast permeation of tritium and its considerable inventory in first walls (graphite) poses a very serious problem in fusion reactor technology. Also, breeding and extraction of tritium requires an extensive knowledge of underglying processes in the blanket (lithium ceramics). As it appears the behavior of tritium in such materials can be conveniently examined using ion implantation and ion beam analysis techniques. To study the behavior of tritium implanted at a depth of <1 μm below the surface, we have developed tritium depth-profiling by detecting α-particles from the d(t,α)n reaction, or by detecting elastically recoiled tritons in forward-scattering geometry [22]). Fig. 3 summarizes our data on retention of tritium in graphite and in γ-$LiAlO_2$ ceramics obtained with the use of d(t,α)n reaction at E_d = 250 keV.

4.4. Channeling of charged particles

Elastic scattering and channeling of light ions are very efficient means of characterizing thin films and interfaces, implanted impurities, and their localization in the matrices, as well as a means of studying of radiation damage in solids[16,23]). It has been shown, for instance, that in many different insoluble host-impurity combinations, the substitutional fraction decreases systematically with the increasing heat of solution ΔH_{sol}, or the decreasing degree of miscibility of host and impurity, respectively. A much steeper dependence for vanadium samples implanted at room temperature than at 78 K, as shown in Fig. 4, has been explained by the fact that at 78 K a rather large fraction of the vacancies are frozen singly or in small clusters, and thus do not participate in vacancy trapping by impurities.

The channeling and blocking of charged particles emitted by radioactive isotopes implanted into single crystals is being used increasingly. The technique is based on the observation of the angular flux distribution of α-, β^--, β^+-particles and conversion electrons emitted in nuclear decays. It allows for localization of ion-implanted impurities at very small concentrations and low implantation fluences, thereby favouring applications in semiconductor studies. In a manner similar to ion channeling, the technique can observe minor lattice site changes caused, for example, by the interaction of impurity atoms with lattice defects in metals and semiconductors. Channeling of conversion electrons or β^--electrons is best suited for the localization of substitutional sites or the determination of small (~0.01 nm) displacements of atoms from regular lattice positions, due to, for instance, vacancy trapping. As with the channeling of positive ions, the channeling of positrons is preferable in the case of interstitially located emitters, especially for the determination of interstitial displacements caused by trapping of self-interstitials, or the formation of large vacancy agglomerates. A direct combination of the channeling measurements with the nuclear hyperfine interaction methods, such as Mössbauer spectroscopy (MS) or time perturbed γ-γ correlation (PAC), often allows a more comprehensive characterization of lattice sites and defects. ISOL represents an extraordinarily valuable tool for such experiments.

Channeling experiments are being performed at ISOLDE by the Konstantz group [24-26]. In particular, the interaction of implanted In impurities with lattice defects in metals (Cu, Ni) and semiconductors (Si) was studied by electron and positron channeling (^{111}In, 2.8 d; ^{112}In, 14 min; ^{112m}In, 20 min; ^{114m}In, 1.2 min), Mössbauer effect (^{119}In, 2.1 min) and perturbed angular correlations (^{111}In). A typical example of conversion electron channeling is shown in Fig. 5. A marked decrease of the peak in the [110] direction observed after annealing at 400 K, followed by a big increase at 675 K, confirms the formation and subsequent dissociation of tetrahedra of vacancies around a part of the indium atoms that have relaxed to interstitial sites in the tetrahedra.

In another study, the channeling and blocking effects of α-particles emitted in the decay of implanted ^{8}Li (0.84 s) as an interstitial probe indicated a different mobility of vacancies in GaAs and GaP below 500 K. A prominent recovery stage was observed in the temperature regime between 200 and 400 K, in which the mobilization of vacancies was detected in GaAs with ^{8}Li probes. Complementary information on the mobility of ^{8}Li could be obtained with a β-NMR technique [3].

4.4. Conversion electron spectroscopy

It was realized long ago that the measurements of conversion electrons from the outermost valence shells of implanted impurity atoms in solids can be directly related to the local density and angular momentum character of the occupied electron states at the probe atom [27]. Although the valence states of atoms can be probed by various electron spectroscopy techniques, such as X-ray (XPS) and ultraviolet photoelectron spectroscopy (UPS), these techniques are not element specific, because the local configuration of the impurity atoms or the various constituents of composite materials cannot be studied separately. In contrast to this, conversion electron spectroscopy is a local method giving information about the electronic structure of the atom labelled with the radionuclide. Using implanted short-lived radioactive isotopes, it is possible to determine the valence electron configuration for as few as 10^{10} - 10^{12} implanted atoms, i.e., with the sensitivity about three orders of magnitude better than the sensitivity of the ESCA technique. Previously, successful measurements have been reported only for very low energy transitions (<2 keV) [28,29]. Such measurements are very useful for the study of atoms and molecules on surfaces, but less suited for bulk studies due to severe energy loss problems at these low energies. Also, the number of useful transitions has been very limited. Especially high sensitivity to the chemical environment has been indicated for M_4 and M_5 conversion electrons of the 2.17 keV transition in ^{99m}Tc (6 h) [28]. The investigation of trace amounts of ^{99}Tc is of particular interest in nuclear medicine.

More conversion electron studies can be performed using beams of isotopes with shorter lifetimes. Many more transitions and elements can be utilized since low energy nuclear transitions are generally highly converted and the nuclear transitions involved do not need to be to the ground state of a stable nucleus.

The development of a novel technique for high-resolution conversion electron spectroscopy for valence electron configurations (CESVEC) for transitions with higher energies has just been reported by the Aarhus-Zurich-ISOLDE collaboration [30]. The measurements were performed for the 23.9 keV M1 transition in ^{119}Sn fed in the decay of

^{119}Sb (38 h), and on the 13.3 keV E2 transition in ^{73}Ge fed in the decay of ^{73}Ga (5 h). The radioactivity obtained from the ISOLDE separator was evaporated into an ion source, ionized, accelerated to 60 keV, mass-separated, and implanted into the substrates (n-type Si and GaAs single crystals or Pd and β-Sn metal foils) under an angle of 5-10 degrees to the surface. The source strength was 10^7 to 10^8 Bq. The average depth of the implanted ions was 5 - 10 nm and the total implanted dose ranged from 10^{11} to 10^{13} ions/cm^2, corresponding to a peak concentration of 10^{17} to 10^{19} atoms/cm^3, which is below the solid solubility for all the impurity systems studied. The obtained radioactive sources were annealed appropriately after implantation to remove the radiation damage. Electron spectra were measured using a high-luminosity β-spectrometer with eV resolution for electron energies up to 100 keV, which had been built in Zurich for a neutrino mass experiment [31]. It is a combined magnetic Tretyakov-type and electrostatic electron retarding spectrometer, in which electrons leaving the source are retarded to 200 eV, magnetically analyzed ($\Delta E/E=0.01$), post-accelerated to 14 keV, and detected by a position sensitive proportional counter.

First applications show a great potential of this new technique in direct observation of a local band structure of the valence states at an impurity atom. For instance, a clear difference between the states of Sn in crystalline and amorphous Si was seen, as expected from theoretical band structure calculations [3].

The spectroscopy of conversion electrons offers many other possibilities in the study of condensed matter. In particular, from the energy losses of conversion and Auger electrons leaving the surface, one can learn about the depth distribution of implanted nuclei and about their mode of diffusion in near surface regions. From the changes in conversion electron yields and decay lifetimes, one can derive the contact electron densities and infer nuclear charge radii. For a recent example of such studies, one can refer to a work [32] in which the nuclear radii changes for isomeric states in ^{197}Au and ^{198}Au have been measured by a combination of Mössbauer spectroscopy in the 77.3 keV state of ^{197}Au, and conversion electron spectroscopy of the 35.8 keV transition in ^{198}Au. For the 77 keV transition in ^{235}U ($T_{1/2}$ = 30 min), the change in the chemical environment from $^{235}UO_2$ to ^{235}U implanted in Ag metal was observed to cause a change in the lifetime of about 10% [28]. Such a big effect is due to high sensitivity of the P and Q electron shells to chemical bonding.

4.5. Mössbauer spectroscopy on implanted isotopes

The application of Mössbauer spectroscopy in the studies of implanted nuclei was initiated in the mid-1960's and has been been extensively covered in numerous surveys; see, e.g. [33-37]. Recoil-free emission and resonant absorption of γ-rays is an especially efficient method for studying ion implantation, radiation damage, and modifications of materials by ion beams. From the quantities measured in Mössbauer spectra, such as the isomer shift, the quadrupole splitting and the magnetic hyperfine splitting, one derives, respectively, the density of electrons, the components of the electric field gradient tensor and the hyperfine magnetic field at the nuclei. From the magnitude of the resonant effect, one determines the mean square vibrational amplitude of the implanted probe nucleus in a host matrix. From the second order Doppler shift, one can also determine the mean square velocity of the nucleus at its residence site and, in some cases, its relaxation and

mode of diffusion can be extracted from the shape of resonant lines. The analysis of the spectra as a function of temperature provides us with information about the chemical state and electronic structure of implanted atoms, their position in the matrix, the configuration of associated lattice defects, characteristics of the phonon spectra and the magnetic properties of the material. Mössbauer spectroscopy applies to both crystalline and non-crystalline (amorphous) solids, and to highly dispersed (such as catalyst particles) materials.

The drawback of Mössbauer spectroscopy is that its application is limited to specific nuclei near the stability line (low isomeric states with excitation energy $E < 200$ keV, life-times ranging from 10^{-6} to 10^{-10} s, and atomic masses $A > 40$). Also, a stable or very long-living counterpart isotope for the absorber is always required. In spite of these limitations, there have been more than 100 resonances used in Mössbauer spectroscopy. Although the possibility for new determinations of nuclear parameters by Mössbauer spectroscopy is already exhausted, a few resonances may still be added to the list and some nuclear parameters may still be refined, based on the advantages of ISOL facilities. However, Mossbauer spectroscopy in ISOL experiments opens a large field of solid state and materials science applications. In addition, because of the decreasing availability of separated enriched isotopes for making Mössbauer sources and absorbers, and the increasing cost of irradiations and subsequent radiochemical processing, the use of on-line techniques promises to be more and more attractive.

The following experimental techniques are now being used in Mossbauer studies of ion implanted specimens:

1. The isotope separator implantation of stable resonant isotopes has been extensively studied in Cracow, using conversion electron Mössbauer spectroscopy (CEMS) [33,34]. Relatively high implanted doses of 10^{13} - 10^{15} ions/cm^2 yielding concentrations of ~10^{-2} - 1 at. % are needed even in most favorable cases of ^{57}Fe and ^{119}Sn. Experiments with ^{151}Eu and ^{197}Au using ~10^{16} - 10^{17} ions/cm^2 have also been reported. CEMS is also very useful in the study of beam-induced modifications in materials containing resonant isotopes. Thanks to its inherent depth selectivity, CEMS makes it possible to determine how a particular property (e.g., valence state, chemical composition or orientation of magnetic moments of Mössbauer atoms) varies with the depth below the surface.

2. Off-line isotope separator implantation of long-lived Mössbauer source nuclei ($T_{1/2}$ >1 d), such as ^{57}Co (270 d), ^{119m}Sn (250 d), ^{119}Sb (1.6 d), ^{125m}Te (58 d), ^{129m}Te (34 d), ^{133}Xe (2.2 d), ^{153}Sm (1.9 d), ^{161}Tb (6.9 d) and ^{169}Er (9.4 d), was studied especially at Groningen, Leuven and Aarhus; see [35,36] for recent surveys. These studies provided a wealth of experimental data and continue to play a leading role in understanding the microscopic nature of the lattice sites occupied by implanted ions, the behavior of lattice defects as a function of temperature, and the local chemistry of the impurity-host system in conditions far from thermal equilibrium. However, it is quite troubleful that the radioactive species used in these studies have to undergo sometimes fairly complex chemical processing before they are inserted in the ion source.

3. In on-line techniques, radioactive isotopes produced by a nuclear reaction in a target are directly transferred into an ion source and subsequently accelerated and mass separated. This technique allows for implantations of short-lived isotopes 100 ms <$T_{1/2}$ <1

Table 1. Successful Ion Implantation applications outside semiconductor technology (from [10]).

Ion species	Material	Problem	Applications	Status
Ti + C	Ferrous Alloys	Wear	Bearings, Gears Valves, Dies	Production
Cr	Ferrous Alloys	Corrosion	Surgical Tools	
Ta + C	Ferrous Alloys	Scuffing Wear	Gears	Pilot Production
P	Stainless Steels	Corrosion	Marine Products Chemical Processing	Research
C, N	Ti Alloys	Wear	Orthopaedic Prostheses	Production
N	Al Alloys	Wear Mold Release	Rubber and Polymer Molds	Pre-Production Evaluation
Mo	Al Alloys	Corrosion	Aerospace, Marine	Research
N	Zirconium Alloys	Hardness Wear Corrosion	Nuclear Reactors Chemical Processing	Production
N	Hard Chrome Plate	Hardness	Valve seats, Godets Travellers	Pilot Production
Y, Ce, Al	Superalloys	Oxidation	Turbine Blades	Research
Ti + C	Superalloys	Wear	Spinnerettes	Pre-Production Evaluation
Cr	Cu Alloys	Corrosion	Battery Technology	Research
B	Be Alloys	Wear	Bearings	Pilot Production
N	WC + Co	Wear	Tool Inserts PC Board Drills	Pilot Production Research
N, Al, Ti, etc.	Ceramics	Oxidation Wear Toughness	Adiabatic Engines Turbine Parts	Research
Ar, N, etc.	Polymers	Conductivity	Microelectronics	Research
Ti, Al, etc.	Polymers	Mechanical Properties	Aerospace Automotive	Research

h, but it also offers intensity advantages for longer-lived isotopes. Several years ago, an on-line Mössbauer spectroscopy set-up was installed at ISOLDE in CERN by an Aarhus team [38]) and later the collaboration has been extended to also involve the Groningen and Leuven groups [37]). Initially, a mass-separated beams of 10^9 $^{119}In^+$ (2.1 min) ions/s, or $^{119}Sn^+$ (38.5 h) were produced by proton-induced fission in a uranium target; other beams produced by spallation reactions on a variety of target materials, placed in surface ionization or plasma dicharge ion sources, have also been used. Table 1 lists beam parameters for the Mössbauer experiments used at present at ISOLDE. Very low doping levels of the order of 10^8 -10^{10} ions/cm^2 can be used, which is essential in investigations of semiconductors. Using this technique, the spectra can be measured in very short periods of time (in some cases about 1 min), which allows one to follow various time-dependent phenomena. Recently, this technique has been used mostly in studies of impurities and defects in metals and semiconductors [38]). In particular, the implantation-produced defects in III-V and II-VI semiconductors, of high technological interest, have been studied. The mechanism of the unusually fast diffusion of Sb donors in n-type Si has also been investigated [3]).

Table 2. ISOLDE beams used for Mössbauer spectroscopy (from [38])

radioact. isotope	Half-life (min)	Mössb. isotope	target mat.	reaction	ion source	intensity (ions/s)
^{119m}Cd	2.7	^{119}Sn	Sn	spallation	plasma	$5x10^7$
^{119}In	2.1	^{119}Sn	UC	fission	W-surf	$1x10^9$
^{119}Xe	5.8	^{119}Sn	La	spallation	plasma	$8x10^8$
^{121}Xe	39	^{121}Sb	"	"	"	$3x10^9$
^{125}Xe	1.0	^{125}Te	"	"	"	$6x10^9$

4. The in-beam recoil-implantation techniques, where excited Mössbauer nuclei are implanted directly into a target, have also been developed. In this case, Mössbauer spectra are measured during the lifetime of excited Mössbauer states (10^{-8} - 10^{-10} s). In particular, the technique of Coulomb recoil implantation Mössbauer effect (CRIME) has been applied in Stanford, Erlangen and Oak Ridge for ^{57}Fe, ^{61}Ni, ^{73}Ge, ^{158}Gd, ^{160}Gd, ^{172}Yb, ^{174}Yb and ^{176}Yb [39]). Recently, Coulomb recoil implantation experiments have been initiated at the heavy-ion accelerator VICKSI in Berlin, using a pulsed 110 MeV beam of ^{40}Ar [40,41]), and at UNILAC in Darmstadt [42]).

Two examples of the results from the author's recent studies are presented in Fig. 7 and Fig. 8. Fig. 7 shows the systematics of Mössbauer isomer shifts obtained for low-energy ^{57}Fe and ^{57}Co implants in a variety of elemental targets. The systematics indicates large variation of the electron density at ^{57}Fe nuclei along the periodic table, with characteristic dependences in the regions of 3d, 4d and 5d transition elements [43]). In Fig. 8, one observes how the population of different valent states of Fe ions implanted in ZrO_2 matrix varies as a function of the concentration of implanted iron [44]).

4.6. On-line nuclear orientation

Measurements of the anisotropy of the angular distributions of α, β and γ from oriented nuclei have supplied rich data on the multipolarities of transitions, spins and nuclear moments of isotopes with long or medium lifetimes [45]. Although, at present, nuclear orientation is primarily used to measure nuclear moments, it also yields data on the hyperfine magnetic fields and electric field gradients in solids, Knight shifts, vacancy trapping and recombination, as well as on the spin-lattice relaxation processes in metals, semiconductors and insulators at temperatures of a few millikelvins. The capabilities of nuclear orientation have considerably expanded by combining nuclear orientation (NO) with nuclear magnetic resonance (NMR) and by introducing the method of 'level-mixing'. Ion implantation permits the introduction of nuclear probes into systems that have not yet become accessible, as well as for measurements of hyperfine fields in cases of very small solubility (e.g., Bi, In or Ag in Fe). As the result, the magnitudes of the hyperfine magnetic fields in iron are already well established for the majority of implanted elements [35,46], as shown in Fig. 9. In addition, it has been shown that in certain systems (for instance, In<u>Fe</u> and Ag<u>Fe</u>) almost completely substitutional implantations are possible at low temperature, and below a certain dose limit. It is believed that the high substitutional fraction is the result of the immobility of vacancies at low temperatures, since the formation of impurity-vacancy complexes is possible only during the collision cascade, and is therefore highly suppressed.

At present, on-line nuclear orientation (OLNO), suitable for studies of isotopes with life-times down to 1 s, is a vigorously developing technique [47-49]. It involves large, complex facilities and the considerable effort of multinational research teams, on a scale typical rather of 'big science' for elementary particle physics than for hyperfime interactions. The first generation of NO facilities with isotope production, mass separation, and cold implantation all on-line was put into operation in the early 1980's and includes the LISOL-KOOL facility at the cyclotron in Louvain-la-Neuve, Belgium, and the DOLIS-COLD set-up on the 20 MeV tandem accelerator at Daresbury, UK. A new, major low-temperature nuclear orientation facility was commissioned in 1988 at ISOLDE-3, and it is used intensely by the NICOLE collaboration (Bonn-CERN-Daresbury-Delft-Gent-Louvain-Lyon-Manchester-Munich-Orsay-Oxford-Paris-Strasbourg-Surrey). The UNISOR/NOF facility at Oak Ridge and the JINR/SPIN-2 facility at Dubna have also begun operation. Several more laboratories are also interested in setting up OLNO. Various on-line NO facilities and the obtained results were recently reviewed by Herzog [48], Stone [49] and Wouters et al. [50].

Typically, as depicted in Fig. 10, the focused beam of separated radionuclei, accelerated through about 100 keV, is implanted into a polarized ferromagnetic foil, cooled to the temperature below 20 mK by a high-performance ^{3}He-^{4}He dilution refrigerator. The lowest on-line base temperatures are close to 7 mK. As with other hyperfine interaction techniques, on-line nuclear orientation yields information with small-activity production, and at very small doping levels. Though technically fairly complex, the method is generally applicable to a very large class of nuclei having sufficiently large magnetic or electric quadrupole moments. Investigations have already been made on elements ranging from fluorine (Z=19) to francium (Z=87). The technique allows for studies of nuclei far from stability line; for instance, the lightest cesium isotope on which

measurements have been made, ^{118}Cs, is 15 mass numbers from the stability line. The recent introduction of α– and β–particle detection to an on-line facility by the Leuven group has significantly broadened the scope of studies of short-lived nuclei by NO [51]. It is expected that this important extension of the technique will be rapidly adapted to the other on-line set-ups.

The nuclear lifetime is limited only by the spin-lattice relaxation time T_1, which for most impurities in iron lattices is of the order of 10 - 100 s at 10 mK. The shortest half-life yet studied is ^{191m}Au (0.9 s). Recently, the Daresbury group made the first direct on-line measurement of the relaxation time. The experiment involved pulsing an implanted ^{121m}Cs (121 s) beam for 4 s into an iron foil kept at ~ mK [53]. The beam was then interrupted and the implanted nuclei observed, as they relaxed towards the foil temperature over a period of two half lives. This cycle was repeated 50 times to give the data in Fig. 11. Shortening of the relaxation time is possible by appropriate doping of crystals, introducing lattice defects or magnon cooling in ferromagnetic materials. Extensive solid studies are still required to find the limits of the method.

4.7. Time-resolved perturbed angular correlations (PAC)

Similarly to other hyperfine interaction techniques, PAC also measures the interaction of the nucleus in an excited state with the hyperfine magnetic field and the electric field gradient, from which both nuclear moments and the local structure of solids near the probe atoms can be determined. Unlike the Mössbauer effect, nuclear orientation or channeling techniques, the applications of PAC are not limited to solids, but can be studied also for liquids, and even at high temperatures. Suitable are γ-γ and β–γ cascades with the intermediate state spin I = 1 or I > 1 and a lifetime in the range of 1 - 1000 ns. The most-often used isotopes (cascades) are ^{111}In (2.8 d) or ^{111m}Cd (48.6 min) -> ^{111}Cd (171 - 245 keV, 84 ns, I = 5/2) and ^{181}Hf (42.4 d) -> ^{181}Ta (133 - 482 keV, 10.8 ns, I=5/2). The list of other parent isotopes suitable for PAC spectroscopy includes, as well, ^{99}Mo (2.75 d), ^{99}Rh (15 d), ^{100}Pd (3.6 d), ^{116m}Sb (60.4 min), ^{117}Cd (2.4 h), ^{118m}Sb (5 h), ^{140}La (40.3 h), ^{155}Tb (5.3 d), ^{172}Lu (6.7 d), ^{187}W (23.9 h), ^{199m}Hg (42.6 min), ^{204m}Pb (67 min). The application of an ISOL should considerably enlarge the available selection of short-lived PAC isotopes.

PAC spectroscopy is especially suitable for measuring principal components of the electric field gradient tensor. Such data are very useful in studies of radiation damage in materials and for the characterization of the annealing processes. For instance, the PAC method is particularly useful for identification of impurity-defect configurations; combined with the change of the relative populations in the annealing stages, it provides information on the nature of the defect (vacancy or interstitial), released or mobile at the particular annealing temperature. Various applications of PAC in solid-state studies have been surveyed thoroughly in ref. [54], and a progress report on recent applications of PAC in chemistry, materials science, and biophysical chemistry has been given in ref. [55]. Closely related to this subject is a survey of hyperfine interaction studies with perturbed angular distributions (PAD) on pulsed heavy ion beams, ref. [56].

Applications of PAC spectroscopy are being explored at ISOLDE by the Konstanz-Erlangen group, especially for study of microscopic, structural and electronic properties of

semiconductors. Several donor-acceptor complexes in semiconductors have been already characterized [3]. It was shown that the electronic structure can be different for probe atom (^{111}Cd) depending on its decay modes (resp. from ^{111m}Cd or ^{111}In). PAC is also being used in CERN to characterize surface sites of metals (Aarhus-Berlin-Konstantz) [3,57,58]. For instance, the localization of isolated ^{111}In (and ^{111m}Cd) atoms on the close-packed Pd(111) surface was thoroughly investigated. Five different states have been characterized that were occupied successively through diffusion processes with the final incorporation into the top surface layer. In the case of the Mo(110) surface, the Cd atoms, after diffusion from terrace to ledge to kink sites, leave the surface. In an example shown in Fig. 12, isolated ^{111}In probes were used to characterize Cu (100) and (110) surfaces. From the analysis of the Fourier transform of the PAC spectra measured with varying geometrical arrangements, it was found that the electric field gradient at In probes on the (100) surface is perfectly axial and that its z-component is perpendicular to the surface, whereas on the (110) surface the electric field gradient is non-axial [57,58].

Another new application of PAC was demonstrated for studying the near-surface magnetism in solids [59]. In this case, 50 keV ^{111}In ions were implanted into single iron crystals at fluences between 10^{12} and 10^{13} ions/cm^2, and the modifications in the domain structures near the surface of the crystals were examined as a function of the ion fluence, crystal orientation and applied magnetic field. A parallel study on the same specimens was performed using Mössbauer spectroscopy. It has been shown that the magnetization of the near-surface closure domains lags considerably behind the magnetization of the bulk, and that it depends on the crystal orientation, shape (demagnetization factor) and the degree of the radiation damage.

4.8. On-line NMR techniques

The application of implanted radionuclei as NMR probes in condensed matter represents a broad range of research possibilities. In this case, both solids and liquids can be studied. The experiments have so far been carried out in-beam with the β-emitters and isomeric γ-emitters having lifetimes in the range of 10^{-5} - 10^3 s (see survey [60]). Using ONNMR, one not only can measure nuclear moments, but also determine hyperfine magnetic fields, electric field gradients and relaxation times. Many probes have already been used in these studies, e.g., ^{8}Li, ^{11}B, ^{12}C, ^{17}F, ^{25}Al, ^{31}S, and there are many other possible candidates. An ISOL may help to extend the range of nuclei investigated by this technique, especially in the region of highly deformed nuclei with large spins.

4.9. Positron emission and annihilation

A separate huge field of applications, especially in medicine, is associated with the positron emission tomography (PET), which provides a noninvasive method for the determination of blood flow and metabolism, for diagnosis and for basic research of various diseases. It is advantageous to use very short half-life positron emitters for PET studies, because sufficient doses of radioactivity can be administered to permit high statistical quality of the reconstructed image, while minimizing the radiation dose to the patient. Short-lived positron emitters can be used, such as ^{10}C (19.3 s), ^{11}C (20.4 m), ^{13}N (10 m), ^{14}O (70.6 s), ^{15}O (2.0 m), ^{18}F(109 m), ^{23}Mg (11.3 s), ^{30}P (2.5 m), ^{39}Ca (0.9 s), or long-lived parent isotopes suitable as generators for short -lived positron emiters, such

as ^{52}Fe (8.3 h), ^{62}Zn (9.1 h), ^{68}Ge (275 d), ^{82}Sr (25 d), ^{118}Te (6 d), ^{122}Xe (20 1 h), ^{128}Ba (2.4 d) [61,62], and many others.

On-line implanted β^+ emitters, especially those having short life-times and low end-point energy, can be very useful in positron annihilation studies. From the measurements of the angular correlation of the annihilation γ-rays, the Doppler broadening and positronium life-time, one extracts data about the electronic structure of the target. In particular, one can follow the formation of the vacancy-like defects and binding of vacancies and impurities. The application of high-fluence ion implantation in such studies and in the manufacture of positron sources with high specific activity is of great interest.

5. Concluding remarks

Off-line isotope separators and the few existing ISOL devices have already provided a wealth of scientific data and sufficient technical know-how, as well as establishing the sophisticated experimental techniques, necessary for successful development and use of a dedicated, next-generation facility. A high-intensity beam of radioactive ions would offer new perspectives in solid state studies and in emerging new materials technologies. Therefore, its implementation should be strongly supported not only by nuclear physicists and astrophysicists, but also by the condensed matter and materials science communities. Certainly, any dedicated facility should be multidirectional, with the strong involvement of solid-state physics, chemistry, advanced materials engineering and industrial communities. However, the involvement of those communities in the project must be regarded by the nuclear teams as symbiotic rather than parasitic.

Although ion implantation and ion beam materials processing using ISOL at keV energies will certainly continue to be an increasingly important tool in research and high technology, the optional high-energy 1-2 MeV post-accelerator and a high-current co-implanter is worth considering. Relative costs and capabilities of these units must be assessed if they are to meet the needs of emerging programs in view of recent trends in materials processing, the physics and technology of semiconductor devices, micrometallurgy, manufacture of improved parts and tools, modifications of ceramics and polymeric materials, and the simulation of materials behavior in nuclear-power reactors and in outer space.

Because, the next ISOL facility could only be hosted by the most advanced nuclear laboratory, it should offer external users the best support available (technology, supplementary analytical tools, consulting, scientific interaction, logistics, etc.). However, since many specialized research techniques required for proper and efficient use of the ISOL facility must be developed ahead of time, and/or mature considerably earlier in external laboratories, collaboration in the preparation of the research programs and facilities would certainly be extremely useful for national, academic and industrial organizations. Therefore, concerted effort in establishing a strong materials study and processing center around any proposed ISOL is necessary, and should start as soon as possible. Early formation of the users group, similar to those associated with synchrotron radiation sources and neutron scattering facilities, would be highly desirable.

Last but not least, there exists a non-negligible syndrome of homesickness! Namely, nuclear scientists working in applied materials research usually would like to come back, at least from time to time, to their native places. Such strange, nostalgic, but stubborn characters would strongly support an ISOL project. So, so long, see you soon working together !!!

References

1) P.G. Hansen, Ann. Rev. Nucl. Sci. 29 (1979) 69
2) H.L. Ravn, Phys. Rep. **54** (1979) 201; also H.L. Ravn and B.W. Allardyce, in: Nuclei far from stability, Vol. 8, ed. D.A. Bromley (Plenum, New York) in print
3) Progress Reports of the European Organization for Nuclear Research (CERN), 1987 and 1988
4) J.A. Sawicki, in Proc. of the accelerated radioactive beams workshop, 1985, eds. L. Buchmann and J.M. D'Auria (TRI-85-1) p. 307
5) J.A. Sawicki, in The TRIUMF-ISOL facility, A proposal for an intense radioactive beams facility, TRIUMF (1985) p. 45
6) J.W. Meyer, L. Ericksson and J.A Davies, Ion implantation in semiconductors, (Academic Press, New York) 1970
7) G.S. Was, Progr. Surf. Sci. **32** (1989) 211
8) S.T. Picraux, Physics Today **37** (1984) 38; Ann. Rev. Mater. Sci. **14** (1984) 335
9) S.T. Picraux and P.S. Peercy, Scientific American **252** (1985) 102
10) P. Sioshansi, Materials Engineering, February 1987
11) T. Taylor, in Materials modifications by high-fluence ion beams, eds. R. Kelly and M.F da Silva (NATO ASI Series E: Applied Sciences - Vol. 155), p. 295
12) D.C. Ingram, Nucl. Instr. Meth. **B12** (1985) 161.
13) F.W. Saris, Vacuum **39** (1989) 173; J.G. Bannenberg and F.W. Saris, Nucl. Instr. Meth. **B37/38** (1989) 398
14) M. Toulemonde, E. Balanzat, S. Bouffard and J.C. Jousset, Nucl. Instr. Meth. **B39** (1989) 1
15) I. Bergström, F. Brown, J.A. Davies, J.S. Geiger, R.L. Graham and R. Kelly, Nucl. Instr. Meth. **21** (1963) 249
16) J.A. Davies, Physica Scripta **28** (1983) 294
17) J.C. Hardy, H. Schmeing and E. Hagberg, in Proc. of the accelerated radioactive beams workshop, 1985, eds. L. Buchmann and J.M. D'Auria (TRI-85-1) p. 143
18) G. Essig and P. Fehsenfeld, in Nuclear physics methods in materials research, eds. K. Bethe et al., (Vieweg, 1980) p. 70
19) T.W. Conlon, Contemp. Phys. **26** (1985) 521
20) M.L. Mallort, R.M. Ronningen, W.C. McHarris, B. Sherrill and Y.X. Dardenne, Nucl. Instr. Meth. **B40/41** (1989) 579
21) J.A. Sawicki, Fusion Tech. **14** (1988) 884
22) J.A. Sawicki, J. Roth and L.M. Howe, J. Nucl. Mat. **162-164** (1989) 1019
23) A. Turos, A. Azzam, M.K. Kloska and O. Meyer, Nucl. Instr. Meth. **B19/20** (1987) 123
24) G. Lindner, H. Hofsäss, S. Winter, B. Besold, E. Recknagel, G. Weyer and J.W. Petersen, Phys. Rev. Letters **57** (1986) 2283
25) G. Lindner, S. Winter, H. Hofsäss, S. Jahn, S. Blässer, E. Recknagel and G. Weyer Phys. Rev. Letters **63** (1989) 179
26) S. Winter, S. Blässer, H. Hofsäss, S. Jahn, G. Lindner, U. Wahl and E. Recknagel, Nucl. Instr. Meth. **B48** (1990) 211
27) T.A. Carlson, P. Erman and K. Fransen, Nucl. Phys. **A111** (1968) 371
28) O. Dragoun, M. Fiser, V. Brabec, A. Kovalik, A. Kuklik and P. Mikusik, Phys. Lett. **99A** (1983) 187
29) V.N. Gerasimov, A.G. Zelenkov, V.M. Kulakov and A.A. Soldatov, Sov. Phys. JETP **62** (1985) 307
30) J.W. Petersen, G. Weyer, E. Holzschuh, W. Kündig, and ISOLDE Collaboration,

Phys. Lett. A **146** (1990) 226
31) M. Fritschi, E. Holzschuh, W. Kündig, J.W. Petersen, R.E. Pixley and H. Stüssi, Phys. Lett. B **173** (1986) 485
32) K. Schreckenbach, J.A. Sawicki, P. Maier-Komor, G.M. Kalvius and F.E. Wagner, Hyp. Int. **28** (1986) 701
33) J.A. Sawicki, Mat. Sci. Eng. **69** (1985) 501
34) J.A. Sawicki, in Industrial applications of the Mössbauer effect, eds. G.J. Long and J.G. Stevens, (Plenum, New York, 1986), p. 83
35) H. de Waard and L. Niesen, in Mössbauer spectroscopy applied to inorganic chemistry, ed. G.J. Long, Vol. 2 (Plenum, New York, 1987), p. 1
36) H. de Waard, Hyp. Int. **40** (1988) 31
37) G. Weyer, Hyp. Int. **29** (1986) 249
38) G. Weyer, Nucl. Instr. Meth. **186** (1981) 201
39) P.B. Russell, G.L. Latshaw, S.S. Hanna and G. Kaindl, Nucl. Phys. **A210** (1973) 133
40) Y. Yoshida, M. Menningen, R. Sielemann, G. Vogl, G. Weyer and K. Schröder, Phys. Rev. Lett. **61** (1988) 195
41) M. Menningen, R. Sielemann, G. Vogl and Y. Yoshida, Hyp. Int. **47-48** (1989) 573.
42) P. Schwalbach, S. Laubach, M. Hartrick, U. Imkeller, E. Kankeleit, M. Memingen and R. Sielemann, Hyp. Int. **47-48** (1989) 570
43) J.A. Sawicki and B.D. Sawicka, Nucl. Instr. Meth. **B46** (1990) 38
44) J.A. Sawicki, G. Marest and B. Cox, in Proc. of the NATO School on structure-property relationship in surface-modified ceramics, eds. C.J. McHargue, R. Kossowsky and W.O. Hofer, Vol. 170, 1989, p. 209
45) W.D. Brewer, Rep. Progr. Phys. **53** (1990) 483
46) H. Akai, M. Akai, S. Blugel, R. Zeller, and P. Dederichs, J. Magn. Mag. Mat. **45** (1984) 291
47) N.J. Stone and J. Rikovska, eds. Proc. 1st Int. Conf. on on-line nuclear orientation Hyp. Int. **43** (1988)
48) P. Herzog, in Low-temperature nuclear orientation, eds. N.J. Stone and H. Postma (North Holland, 1986) Ch. 15, p. 731
49) N.J. Stone, Hyp. Int. **34** (1987) 91; **49** (1989) 103
50) J. Wouters, N. Severijns, J. Vanhaverbeke, W. Vanderpoorten and L. Vanneste, Hyp. Int. **43** (1988) 395
51) E. van Walle, D. Vandeplassche, J. Wouters, N. Severijns and L. Vanneste, Hyp. Int. **34** (1987) 105
52) D. Vandeplassche, E. van Walle, J. Wouters, N. Severijns and L. Vanneste, Hyp. Int. **22** (1985) 483
53) T.L. Shaw, V.R. Green, C.J. Ashworth, J. Rikovska, N.J. Stone, P.M. Walker and I.S. Grant, Hyp. Int. **34** (1987) 821.
54) J. Christiansen, ed. Hyperfine interactions of radioactive nuclei, in Topics in Current Physics, Vol. 31, (Springer, 1983)
55) A. Lerf and T. Butz, Angew. Chem. Int. Ed. Engl. **26** (1987) 110
56) H.-E. Mahnke, Hyp. Int. **49** (1989) 77
57) T. Klas, J. Voigt, W. Keppner, R. Wesche and G. Schatz, Phys. Rev. Lett. **57** (1986) 1068
58) G. Schatz, T. Klas, R. Platzer, J. Voigt, and R. Wesche, Hyp. Int. **34** (1987) 555
59) H. de Waard, J.A. Sawicki, B.D. Sawicka, F. Pleiter and K. Frantz, J. Mag. Mag. Mat. 49 (1985) 50

60) H. Ackerman, P. Heitjans and H.J. Stöckmann, in Hyperfine Interactions of radioactive nuclei, Topics in Current Physics, Vol. 31, (Springer, 1983) ed. J. Christiansen, p. 291
61) R. Votaw and R.J. Nickles, Nucl. Instr. Meth. **B40/41** (1989) 1093
62) Y. Yano, Nucl. Instr. Meth. **B40/41** (1989) 1105

Figure Notations

Fig. 1. General outline of the tandem accelerator superconducting cyclotron (TASCC) facility at Chalk River.

Fig. 2. The ISOLDE 2 facility at CERN: (1) 600 MeV proton beam from the synchrocyclotron, (2) target and ion source, (3) acceleration chamber, (4) magnet, (5) switch yard, (6) beam lines and experimental setups, (7) central room, (8) low-activity experiments.

Fig. 3. Nuclear reaction d(t,α)n depth-profiling analysis of tritium. Top: amount of tritium trapped in the near-surface region of graphite as a function of temperature for a sample implanted with 40 keV HT^+ ions to a fluence of 5×10^{15} ions/cm^2. Bottom: similar data for tritium-breeding γ-$LiAlO_2$ ceramics (from [22]).

Fig. 4. Substitutional fraction of various impurities in vanadium vs. heat of solution, derived from channeling experiments (from [23]).

Fig. 5. Channeling peaks of conversion electrons emitted by ^{114m}In atoms implanted in Ni single crystals for two different crystal orientations, measured after room temperature implantation and after annealing at 400 K and 675 K (from [3]).

Fig. 6. Conversion electron end-point spectra of the 23875 eV M1 transition of ^{119}Sn showing the different valence band structure for crystalline and amorphous forms (from [3,30]). The bars indicate the inferred band energies and relative integrated intensities from a least square fit analysis. The energy corresponding to the Fermi level of the electronic system is indicated by an arrow.

Fig. 7. Isomer shifts and corresponding contact electron densities $\psi^2(0)$ measured for ^{57}Fe and ^{57}Co ions implanted in various matrices (from [43]). Open circles represent cases where the impurity was introduced by diffusion from the surface.

Fig. 8. Evolution of various valent states of Fe implanted in ZrO_2 as a function of implanted dose (from [44]).

Fig. 9. Magnetic hyperfine fields of isolated impurities in iron (from [35]). Note the difference in scale for lanthanides.

Fig. 10. The lower section of the LISOL-KOOL cryostat showing the side access tube. The sample holder is at (1), (2) is the mixing chamber of the dilution refrigerator, (3) the 0.6 K shield, (4) the 4 K shield and (5) the 4 K baffle motion feedthrough, (6) the 77 K shield, (7) the 0.5 T polarizing magnet, (8) the bellows in the side access tube, (9) the 77 K diaphragm with linear and rotary motion feedthroughs (10) and (11), (12) is the beamline sealing plunger with motion feedthrough, and (14) a buffer chamber where scattering processes can be carried out prior to implantation (from [52]).

Fig. 11. Relaxation of ^{121m}Cs implanted into iron at T = 8 mK. The full and light dotted lines correspond to $T_1 = 3 + 1$ s (from [53]).

Fig. 12. PAC spectra with Fourier transforms for isolated ^{111}In probe atoms at Cu (100) and Cu (110) surface (from [58]).

3736 B

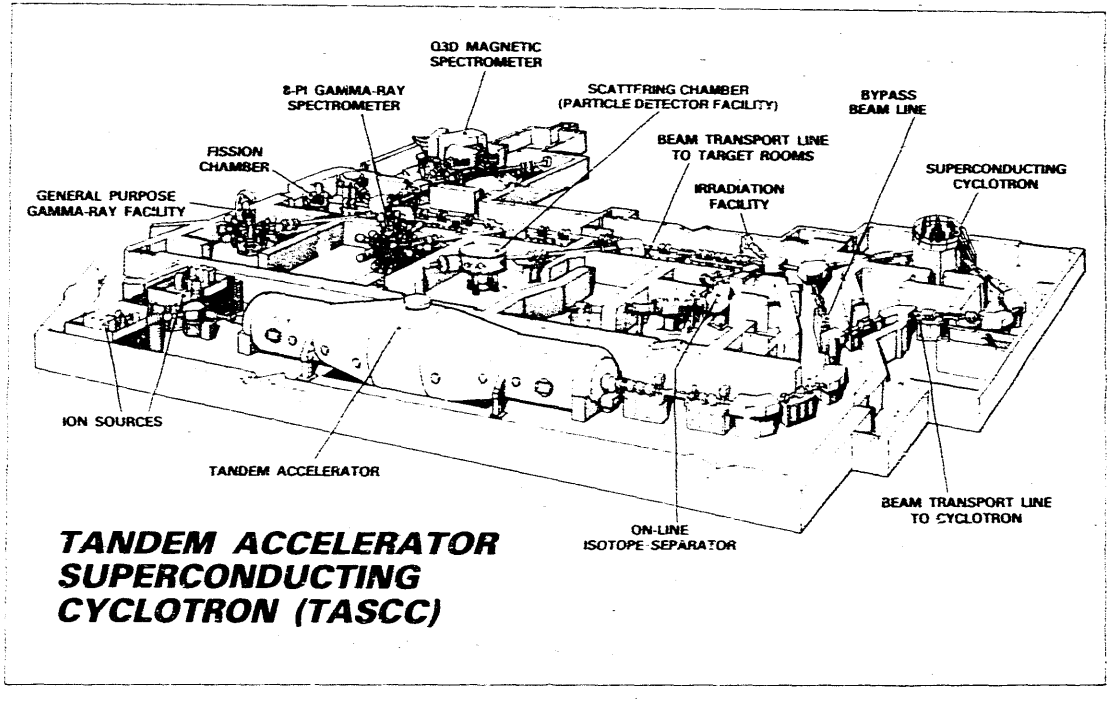

FIGURE 1

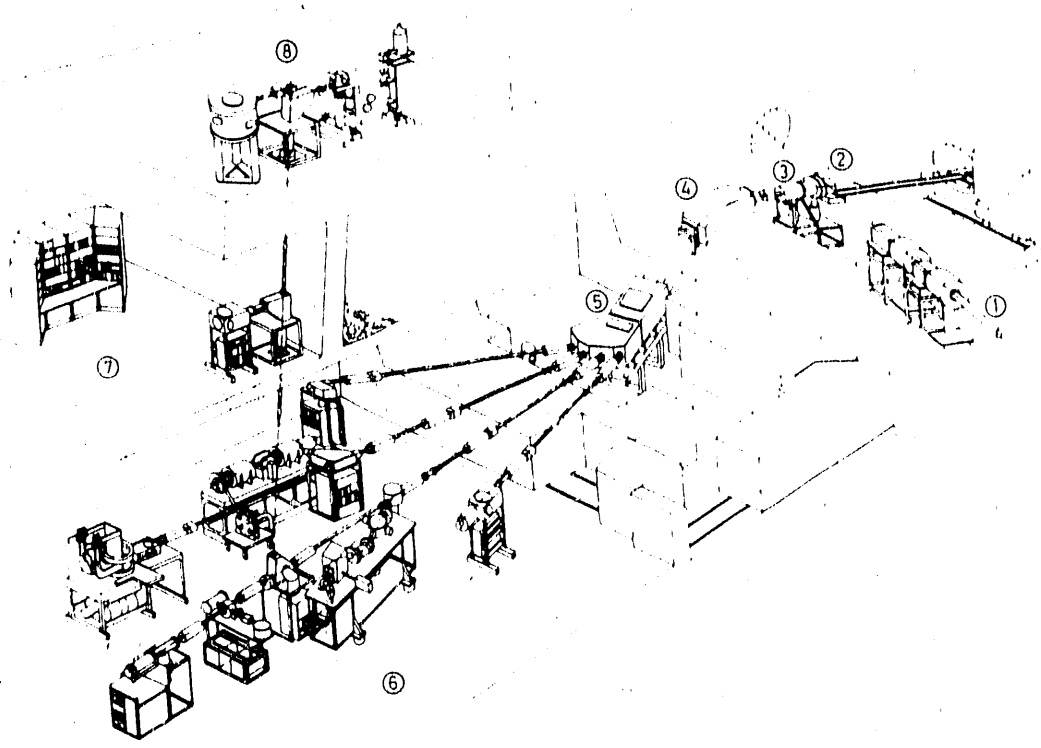

FIGURE 2

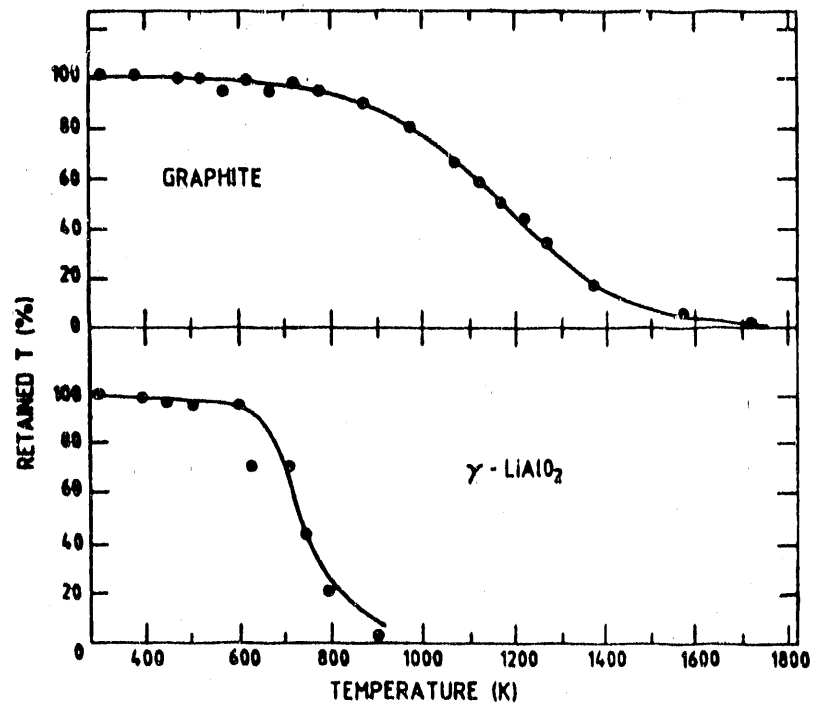

FIGURE 3

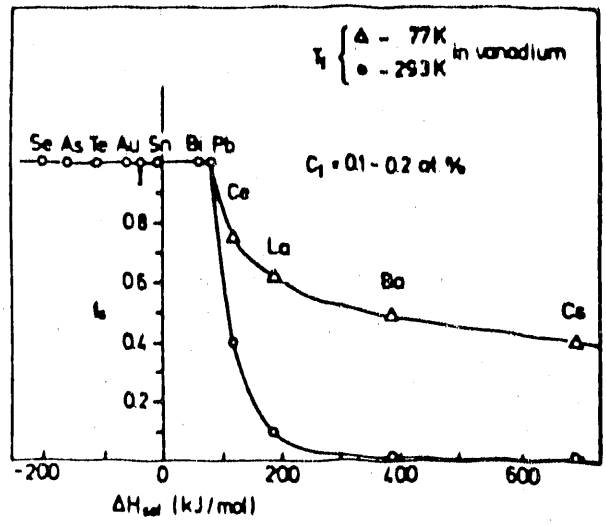

FIGURE 4

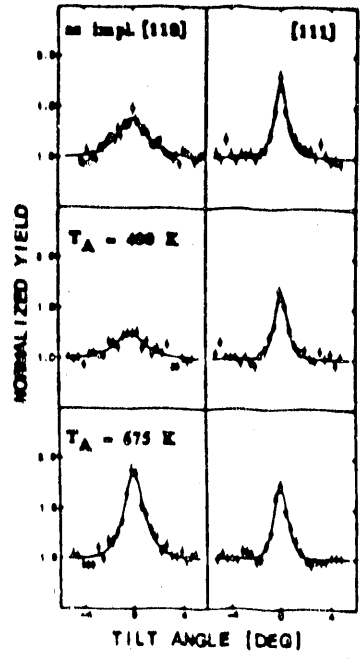

FIGURE 5

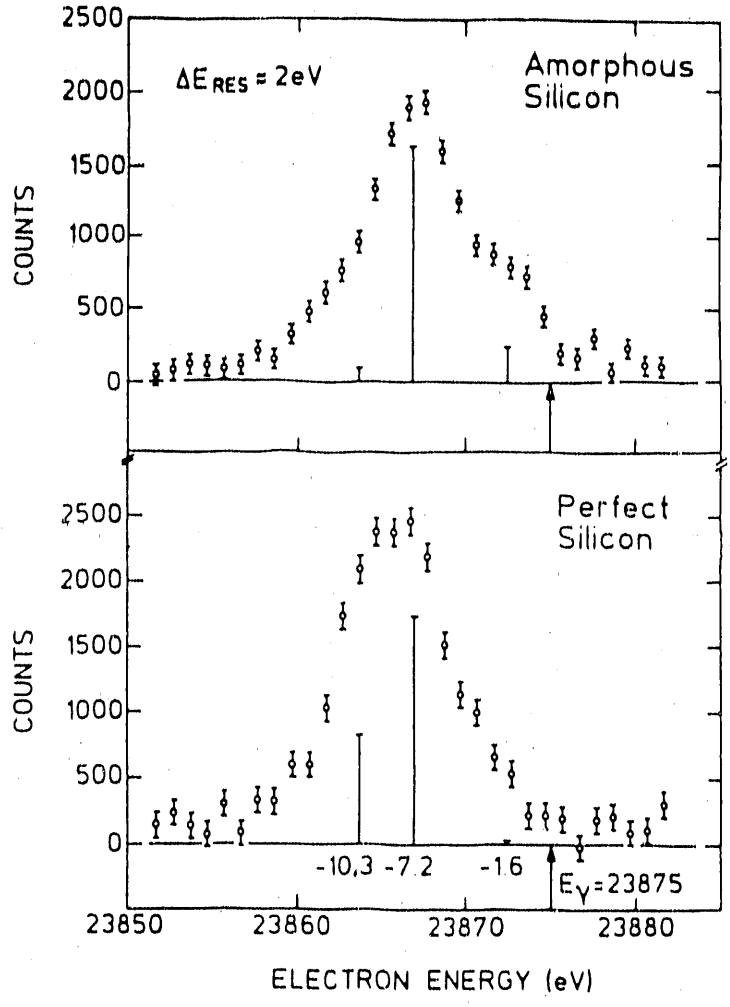

FIGURE 6

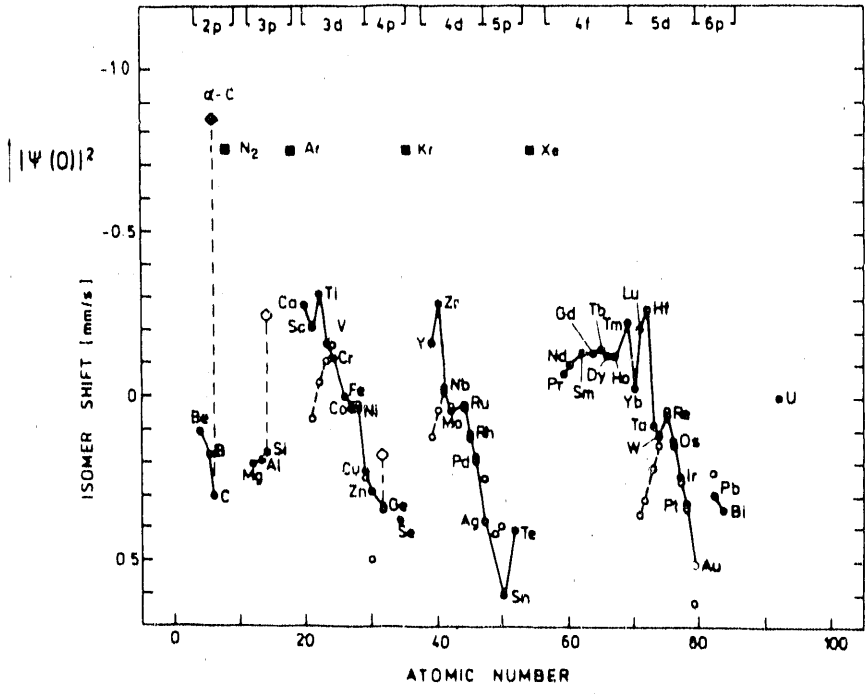

FIGURE 7

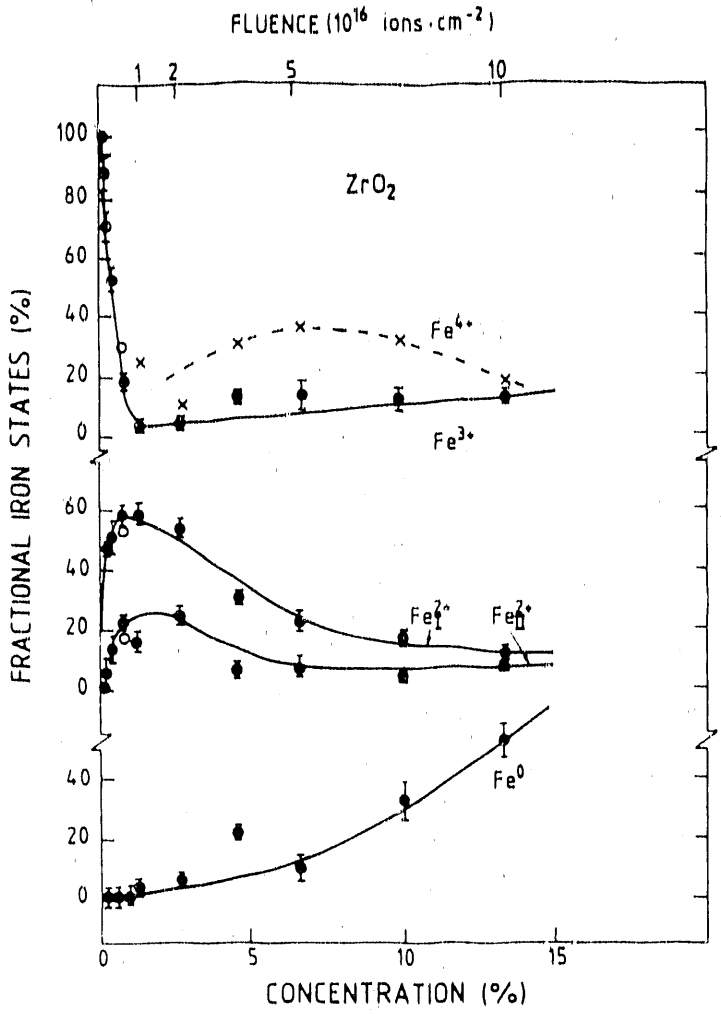

FIGURE 8

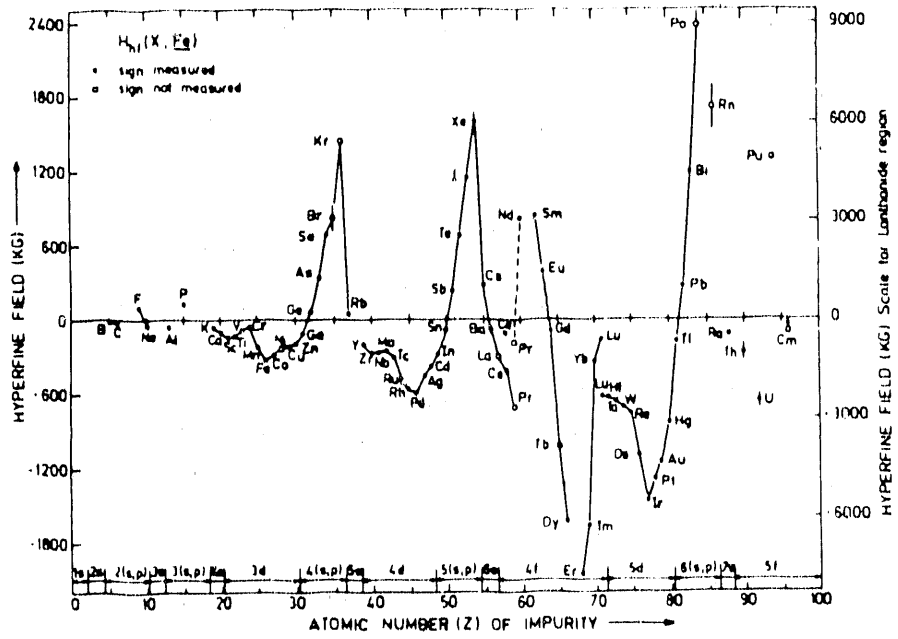

FIGURE 9

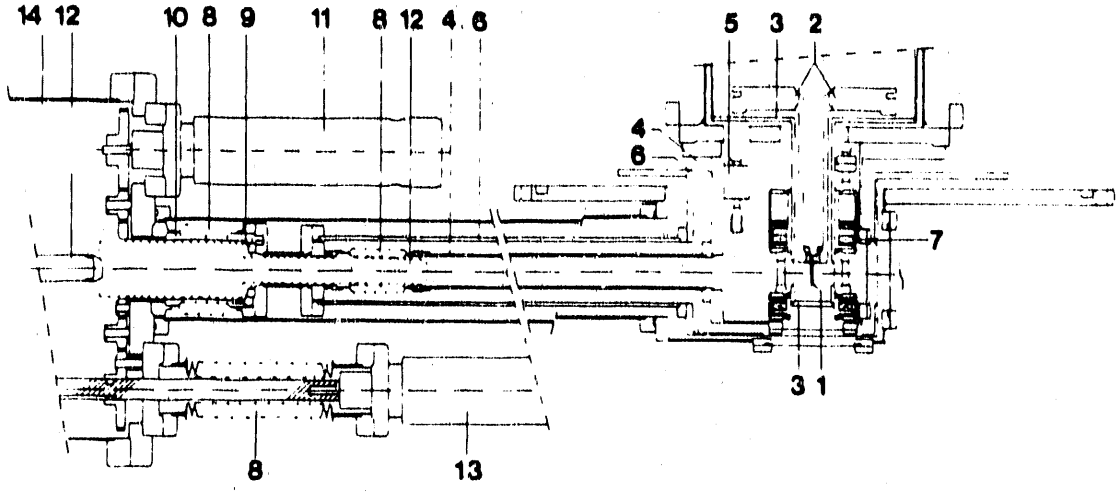

FIGURE 10

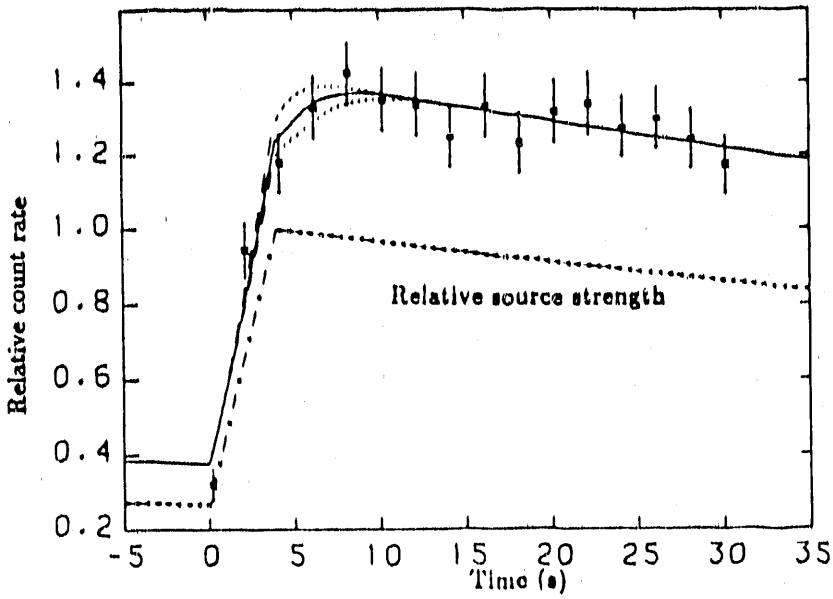

FIGURE 11

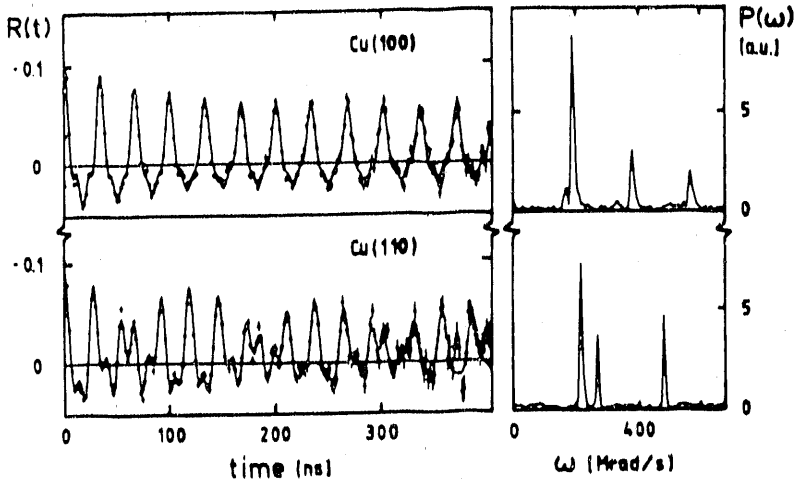

FIGURE 12

PRODUCTION OF HIGH INTENSITY RADIOACTIVE BEAMS

J.M. NITSCHKE

Lawrence Berkeley Laboratory
Nuclear Science Division
University of California, CA 94720

Invited paper presented at the Workshop on the
Science of Intense Radioactive Ion Beams
Los Alamos, NM
April 10–12, 1990

Abstract

The production of radioactive nuclear beams world-wide is reviewed. The projectile fragmentation and the ISOL approaches are discussed in detail, and the luminosity parameter is used throughout to compare different production methods. In the ISOL approach a thin and a thick target option are distinguished. The role of storage rings in radioactive beam research is evaluated. It is concluded that radioactive beams produced by the projectile fragmentation and the ISOL methods have complementary characteristics and can serve to answer different scientific questions. The decision which kind of facility to build has to depend on the significance and breadth of these questions. Finally a facility for producing high intensity radioactive beams near the Coulomb barrier is proposed, with an expected luminosity of $\sim 10^{39}$ cm^{-2} s^{-1}, which would yield radioactive beams in excess of 10^{11} s^{-1}.

1. Introduction

One of the central thrusts of nuclear science is the understanding of the properties of nuclear matter. Thanks to modern accelerator technology we are able to make almost all stable nuclei react with each other, giving rise to a plethora of phenomena involving electroweak and strong interactions, and creating new nuclei at the limits of stability. After more than three decades of heavy ion experiments, however, the limitations of our tools have become apparent. To explore the equation of state of nuclear matter and to search for phase transitions higher energies are necessary, and proposals are underway to address these topics. On the other hand, many open questions remain with regard to nuclear matter at moderate excitation energies; some of the most fascinating ones involving nuclei with extreme N/Z ratios. Many of these nuclei can not be synthesized with stable beams and targets and it was therefore proposed during the NSAC long range planning process last year [Nit89] to build a National High Intensity Radioactive Beam (RNB) Facility. There are several methods available to produce such beams and the purpose of this contribution to the workshop is to compare these approaches and to develop a working concept that may serve as a basis for further discussions. Table 1 gives an overview of several RNB facilities that are presently operating or in an advanced

Table 1. Radioactive beam facilities.

Project (Location)	Production Method, Instrument	Mass/Energy Range	Status
BEVALAC (LBL, Berkeley)	Fragmentation, Separator	(A < 100) 30–500 MeV/u	Operating
SIS 13/ESR (Germany)	Fragmentation, Achromat, Storage Ring	A < 238 5–500 MeV/u	1990/91
Hadron Project (INS, Tokyo)	Fragmentation, 1 GeV p + ISOL + Postacceleration	A < 238 1–1000 MeV/u	Proposed
Meson Facility (Moscow)	Spallation, ISOL + Postacceleration	$A \leq 150$ $E \leq 600\ Q^2/A$	Proposed
TISOL/TRIUMF (Vancouver)	500 MeV p + ISOL + RFQ + LINAC	A < 60 ≤ 1 MeV/u	Operating/ Proposed
GANIL (Caen)	Fragmentation, Achromat, v-Filter	$A \leq 100$ (?) $E \leq 50$ MeV/u	Operating
CYCLONE I/? (Louvain)	30 MeV p + ISOL + Cyclotron	$A \leq 40$ (?) $E \leq 110\ Q^2/u$	Operating
ISOLDE (CERN)	Spallation, 600 MeV p + ISOL + Postacceleration	$A \leq 27$ $E \leq 1.4$ MeV/u	Proposed
TOFI LANL (Los Alamos)	Fragmentation, Bρ/ToF	$A \leq 60$ (?) $E \approx 4$ MeV/u	Operating
RPMS/A1200 (MSU)	Fragmentation, Achromat	A < 100 (?) $E = 1200\ Q^2/A$	Operating/ Planned
RIPS (RIKEN, Japan)	Fragmentation, Achromat	$A \leq 100$ (?) $E = 1300\ Q^2/A$	Proposed
RMS (NSRL, Rochester	Transf. Reactions, Recoil Separator	$A \leq 50$ (18 MV)	Operating
Daresbury (England)	CN Reactions, Recoil Separator	$A \leq 238$ (22 MV)	Operating
SC Solenoid (U. of Michigan, U. of Note Dame)	Transf. Reactions, SC Solenoid	$A \leq 40$ $E \leq 5$ MeV/u	Operating
QSBTS (LLNL, Livermore)	Transf. Reactions, Quadrupoles	$A \leq 20$ (12 MV)	Operating

proposal stage. (There is in addition a facility in Osaka that produces RNBs via transfer reactions.) Details and references on most of these facilities can be found in Ref. [Con89]. Included in Table 1 are some facilities that do not use RNBs to induce secondary reactions but are geared towards the study of the nuclear properties of the RNBs themselves. Figure 1 gives a schematic representation of the two principal RNB production methods: the ISOL approach and projectile fragmentation. In the following chapters we intend to compare the different production methods and comment on the quality of RNBs that they produce. The main characteristics we will try to evaluate are: 1. Intensity, 2. Energy, and 3. Beam quality (i.e., energy/momentum spread, transverse emittances, and beam purity). Information on recent developments in the emerging field of RNB research can be found in Ref. [Con89]. This was also the source of much of the data used in this contribution.

2. Production Methods

2.1 PROJECTILE FRAGMENTATION

Projectile Fragmentation (PF) becomes a significant reaction mechanism at heavy ion beam energies of ~50 MeV/u to several GeV/u. It is characterized by a peripheral interaction of the projectile with the target nucleus that leaves the projectile with much of its initial momentum and only a small angular spread. Details of this mechanism are discussed in a separate contribution to this workshop [She90]. Inherent in this reaction mechanism is that it produces a wide variety of nuclei with a large spread in A, Z and N/Z ratios, and it is in almost all cases necessary to employ a beam purification step before the RNBs can be used for secondary reactions or be studied themselves. Due to overlapping charge-to-mass ratios a purely magnetic separation is insufficient and a profiled energy degrader has to be introduced between the separator magnets, which leads to the concept of a "momentum loss achromat" [Sch87]. Even then, the beam purity may not be sufficient to study isotopes with extreme N/Z ratios that are produced with orders of magnitude lower cross sections than nuclei near β-stability. The LISE group at GANIL, for example, is therefore planning to add a Wien-type velocity filter after their achromatic spectrometer [Mue89] to suppress unwanted particles that overload the detection system and limit the primary beam intensity. The advantages of projectile fragmentation for the production of RNBs are: short separation times (~μs), no chemical selectivity, simple production targets (no large amounts of radioactivity), high product collection efficiency (≥50%) and reliable operation. (Some of these advantages are lost when the RNBs are decelerated in a storage ring.) The disadvantages are: low primary beam intensity compared to p, d and ^{3}He beams, target thickness limited by acceptable momentum spread $\Delta p/p$, high energies (300–1000 MeV/u) necessary to obtain fully stripped ions (q = Z) in the projectile fragment separator, poor emittance (depending on production mechanism), moderate beam purity, large momentum/energy spread, and deceleration/cooling difficult without intensity loss.

To compare different RNB production methods the concept of "luminosity" L in units of $cm^{-2}\ s^{-1}$ will be used, which is the product of beam intensity times effective target thickness. This eliminates the cross section dependence of the yield, which is justified in particular for the comparison between the PF and the spallation and fragmentation

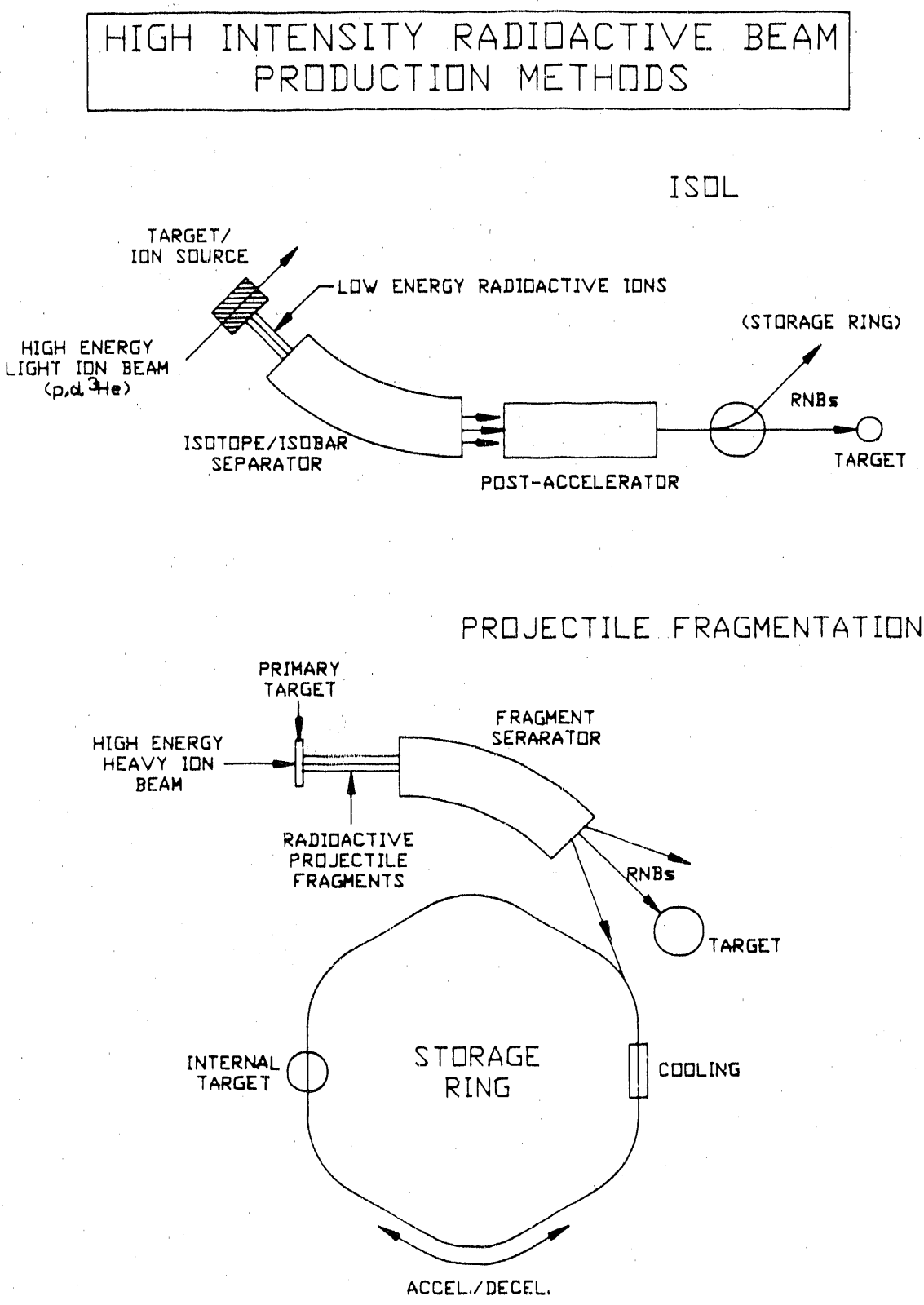

Figure 1. Schematic representation of two approaches to the production of high intensity radioactive beams: the ISOL method (top) and the projectile fragmentation method (bottom). (For details see text.)

reactions used in the on-line isotope separator (ISOL) techniques, which will be discussed later, since one is the kinematic inverse of the other and the cross sections are, therefore, in most cases similar. Actual yields Y can be obtained from $Y = \sigma L$ (s^{-1}) where σ is the cross section in cm^2. It should be emphasized that luminosity is only one of several important criterial for evaluating RNB facilities; others being: energy, beam purity, time structure, transverse emittances, and (A,Z) ranges. In Table 2 the production luminosity L_p is calculated for different PF facilities and operating parameter ranges; it reaches a maximum of 3×10^{-35} $cm^{-2}s^{-1}$ for the fragment separator at GSI (GSI/FRS). A special case is the U. of Michigan-U. of Notre Dame facility (UM-UND) that produces RNBs via transfer reactions, where the luminosity is limited due to delicate thin targets and consequently low primary beam intensity. This is, however, often compensated by relatively large resonant cross sections. The last row in Table 2 shows the principal parameters of a potential future PF facility discussed in these proceedings [She90] where the luminosity is increased by one order of magnitude over GSI/FSR by increasing the primary beam intensity correspondingly.

2.2. STORAGE RINGS

Thus far the only way to decrease the energy of secondary beams has been to interpose degraders in the beam path. These not only degrade the energy but unfortunately also the beam emittance. A more elegant (and costly) way is being realized at GSI where the PF separator FRS is coupled to an experimental storage ring ESR. The full momentum bite of $\Delta p/p = 2\%$ of the FRS can be injected into the ESR.

Table 2. Examples of radioactive beam production by projectile fragmentation and transfer reactions. Ranges of primary beam energy E_p, intensity I_p, and target thickness t are given and the RNB production luminosity L_p is calculated.

Facility	E_p(MeV/u)	$I_p(s^{-1})$	Target	t(g/cm^2)	$L_p(cm^{-2}s^{-1})$
Be'alac	200–1000	10^9–10^{10}	^{9}Be	2–5	10^{32}–3×10^{33}
GSI/FRS	100–1000	10^7–5×10^{11}	^{12}C	0.1–10	5×10^{28}–3×10^{35}
MSU/A1200	45–100	3×10^{11}	^{6}Li	0.5–1.5	$(2–5)\times10^{34}$
GANIL/LISE	30–95	10^{10}–2×10^{12}	^{58}Ni/^{181}Ta	0.2–0.4	8×10^{30}–10^{34}
UM-UND	2–3	~6×10^{10}	TiH_2	~10^{-3}	~3×10^{28}
Future Facility[a)]	300–1000	6×10^{12}	^{9}Be	4–18	$(2–7)\times10^{36}$

a) Under discussion.

One of the main objectives of the ESR is to cool the "hot" RNB beams stochastically and via momentum exchange with a "cold" electron beam, and to decelerate them to lower energies. While this will produce beams with excellent longitudinal and transverse emittances, the time scale for cooling and deceleration is on the order of 0.1 to a few seconds and hence nuclei with short half-lives will be lost. Furthermore, it is estimated that phase space density considerations will limit the beam intensity from the FRS that can be cooled stochastically to 10^7 s^{-1}. If deceleration to Coulomb barrier energies is desired the e$^-$–cooling may limit the beam intensity to 10^6 s^{-1} [Mun90]. For internal target experiments these beam intensities are boosted by a factor ~2×10^8 due to the circulating beam and multi-turn injection, which yields effective beam currents of up to 2×10^{15} s^{-1}. For uncooled beams intensities up to 2×10^{16} s^{-1} are expected [Mun89]. With an internal target density of ~2×10^{14} cm^{-2} a maximum target luminosity L_T of 4×10^{30} cm^{-2}s^{-1} can be achieved. The luminosity gain G for an experiment using the internal target in the ESR (~2×10^{14} cm^{-2}) versus a single pass experiment with an external target is about $G \approx 7 \times 10^{-2}$ A/ρ where A is the external target mass number and ρ its density in g/cm^2. For a thin 10 mg/cm^2 carbon target this works out to G ≈ 80, which is significant considering in addition the good emittance properties of the internal beam. It is obvious that for thicker external targets the advantages of the storage ring will diminish. Table 3 taken from Ref. [Muh89] gives a summary of expected efficiencies for primary and secondary reactions at the GSI facility.

2.3 ISOL METHOD

The on-line isotope separator ISOL method takes a complementary approach to the production of RNBs: a high energy beam of light particles (p, d, or ^{3}He) impinges on a heavy target and produces radioactive nuclides via spallation, fission, or target fragmentation. If the target is thin the recoiling nuclei emerge from the target and can be collected on aerosol particles suspended in a He gas atmosphere, and transported to a

Table 3. Efficiencies for primary and secondary reactions at GSI.

Fragment production	Target (carbon)	0.1 – 10	g cm^{-2}
	SIS Beam	$10^7 - 5 \times 10^{11}$	s^{-1}
	Luminosity	$5 \times 10^{28} - 2 \times 10^{35}$	s^{-1} cm^{-2}
Single pass experiments with secondary beams	Target (lead)	100	mg cm^{-2}
	Secondary Beam	$50 - 10^8$	s^{-1}
	Luminosity (100mg/cm^2)	$10^{21} - 10^{29}$	s^{-1} cm^{-2}
Stored beam experiments in ESR (100 bunches circulating)	Gas Target	2×10^{14}	cm^{-2}
	Effective Beam	$10^{10} - 2 \times 10^{16}$	s^{-1}
	Luminosity	$2 \times 10^{24} - 4 \times 10^{30}$	s^{-1} cm^{-2}

collection device or introduced into an ion source as shown in Fig. 2. The ion source serves as the first stage of an acceleration process that is common to all ISOL/RNB methods since the recoil velocities in the light ion reactions are too low to be of any practical use for inducing secondary reactions. The acceleration process will be discussed below. The basic idea behind the thin target approach is that the reduced target thickness is compensated by a very intense primary beam: up to 1 mA of 800 MeV protons from LAMPF, for example [Tal90].

In the thick target ISOL approach the primary beam intensities are about an order of magnitude lower and the targets are ~10 times thicker. The recoils stop in the hot target, diffuse to the surface from which they desorp, and enter an ion source for acceleration. Table 4 shows several operating or proposed RNB facilities and their operating parameters. Special mention should be made of the RNB facility at Louvain where intense beams of ^{13}N are being produced with a low energy proton beam (30 MeV) of up to 0.5 mA current on a 1 g/cm^2 ^{13}C target. A similar facility EB-88 is being proposed for the 88-Inch Cyclotron at LBL.

Comparing the thin to the thick target approach several advantages for thin targets are noted: intense primary beam, simple target design, rare target materials can be used, no target diffusion/ desorption problems, and no chemical selectivity (except for gases). Some of the disadvantages of the thin target approach are: thin targets, the effective target thickness is further reduced for spallation products, no chemical selectivity which may cause reduced beam purity and ion source contamination, volatile species can not be transported, efficient He-jet/ion source coupling is difficult, and the high ion source gas load will affect the efficiency, in particular for charge states $q > 1$.

Advantages of the thick target methods are: thick targets, moderately intense primary beams, high beam purity (element dependent), and experience in target/ion source

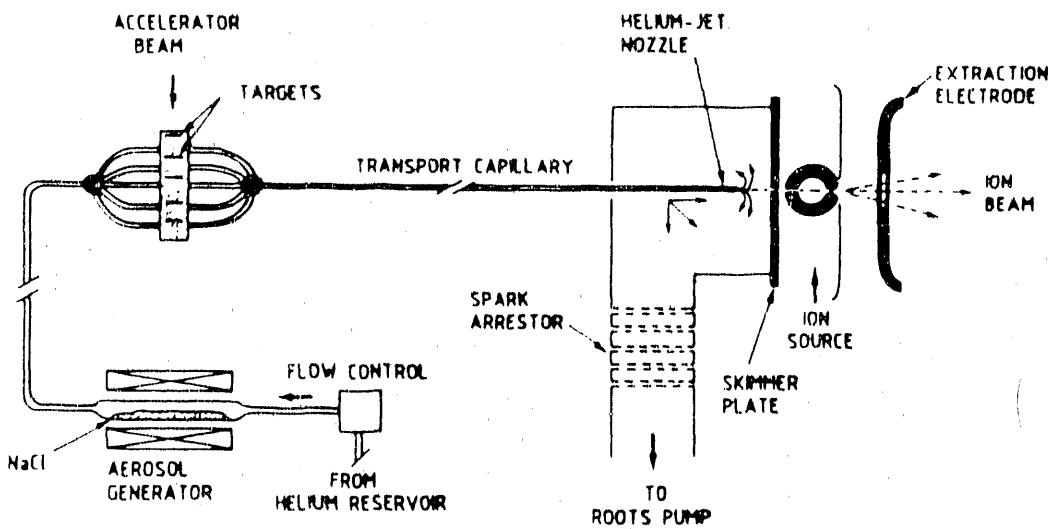

Figure 2. Schematic representation of the thin target version of the ISOL method for RNB production. Only the first three stages involving the target, the He-jet and the ion source are shown. The isotope/isobar separation, acceleration and storage ring would be similar to the scheme shown in Fig. 3.

Table 4. Examples of radioactive beam production via the ISOL method, using spallation, target fragmentation and fission reactions. Ranges of primary beam energy E_p intensity I_p and target thickness t are given, and the production luminosity L_p is calculated.

Facility	Beam	E_p(MeV)	$I_p(s^{-1})$	Target	t(g/cm^2)	$L_p(cm^{-2}\,s^{-1})$
Louvain	p	30	3×10^{15}	^{13}C	1	$\leq10^{38}$
TISOL	p	500	$(1–2)\times10^{12}$	a)	1–15	$3\times10^{33}–2\times10^{35}$
(Proposed)	p	500	3×10^{13}			$\sim3\times10^{36}$
ISOLDE	p, ^{3}He	600/910	2×10^{13}	b)	3–170	$\leq10^{37}$
(Proposed)	p, ^{3}He	600/910	3×10^{13}	c)		$(1–7)\times10^{37}$
JHP (Proposed)	p	1000	$\sim6\times10^{13}$	b)	50–300	$\sim2\times10^{37}–10^{38}$
Moscow (Proposed)	p		$\sim10^{15}$	b)	10–100	$(1–3)\times10^{38}$
EB-88, LBL (proposed)	p	30	3×10^{15}	b)	1	$\leq10^{38}$
Future Facility[d] (Thin Target)	p	800	6×10^{15}	Th	$\sim5\times10^{-2}$	$8\times10^{35}–2\times10^{36}$
Future Facility[d] (Thick Target)	p, d, ^{3}He	500–1000	1×10^{15}	b)	50–300	$10^{38}–10^{39}$

a) Targets of ^{48}Ti, ^{93}Nb, ^{90}Zr, ZrC, SiC, and UO$_2$/C heave been used; b) A variety of targets can be used; c) Production of light RNBs; d) under discussion.

designs. Some of the disadvantages are: yield strongly dependent on target/radioactive-product chemistry, and large amounts of unwanted radioactivity and high radiation fields are generated.

As was done for the PF method in Table 2, the production luminosities L_p for the different ISOL based RNB facilities were calculated and are shown in the last column of Table 4. The high luminosities of $\sim 10^{38}$ $cm^{-1}s^{-1}$ for the low-primary-beam-energy facilities (Louvain, EB-88 LBL) should be particularly noted, since it results in the production of intense RNBs near β-stability. In a suggested facility that will be discussed in greater detail below, using the thick target approach, a production luminosity of 10^{39} $cm^{-2}s^{-1}$ can be obtained (last row in Table 4).

The luminosity in the thin target approach is $\sim 10^3$ smaller than in the thick target case. Assuming that ion source and post-acceleration efficiencies would be the same this would result in similarly reduced final beam intensities. Table 5 gives a summary of the qualitative comparison between the two ISOL methods and the PF method.

3. Comparison Between Projectile Fragmentation and ISOL Method

A comparison between the PF and ISOL methods is difficult since the two are essentially complementary. For the purpose of this discussion we will assume that the parameters for the two hypothetical facilities shown in the last rows of Tables 2 and 4 are realistic. We will further assume that the PF luminosity is reduced to the range of $(1–4) \times 10^{36}$ $cm^{-2}s^{-1}$ due to transmission losses through the separator and that the ISOL luminosity is reduced by $(.5–5) \times 10^{-2}$ due to losses in the ion source, the isotope/isobar separator, stripping and acceleration, giving an effective luminosity range of 5×10^{35} – 5×10^{37} $cm^{-2}s^{-1}$. This brings the two luminosities much closer together and the expected beam intensities could be similar within an order of magnitude. However, the beam characteristics would be very different! The projectile fragment beam would be in the energy range of 300–1000 MeV/u with a relatively large momentum spread and transverse emittance, depending on the production mechanism, while the post-accelerated ISOL beam would have an energy of ~10 MeV/u with the beam quality of a modern normal or superconducting LINAC, for example. The physics that can be addressed by the two devices is very different and the decision which kind of facility to build has to depend on the significance and breadth of the scientific questions that can be answered.

It was pointed out earlier that if the PF beam is to be decelerated to the Coulomb barrier the maximum beam intensity, in the ESR for example, is limited to $\sim 10^6$ s^{-1}. At a PF luminosity of 4×10^{36} this corresponds to a production cross section of ~0.3 μb. At this cross PF section the ISOL facility would deliver similar beams of 1×10^5 – 1×10^7 s^{-1}. At cross sections larger than ~0.3 μb the ISOL facility would, however, produce larger beams than the storage ring since it does not have any saturation characteristics. For cross sections of, say, 10 mb near β-stability this can amount to a factor 5×10^3 to 5×10^5 higher intensity in the ISOL case over the storage ring operated as a "cooler"/decelerator. Even taking the increased luminosity of internal target experiments in the storage ring into account there is still a significant advantage of the ISOL approach for beams near the Coulomb barrier. The highest luminosity is, however, obtained when the ISOL approach is combined with a storage ring. This will be discussed in the next chapter. In Table 6 a comparison between a future PF and an ISOL based high intensity RNB facility is attempted.

Table 5. Comparison of different high intensity RNB production methods

Production Method	Advantages	Disadvantages
Projectile Fragmentation	• Short separation times (~μs)[a)] • No chemical selectivity • Simple production target (no large amounts of radioactivity) • High product collection efficiency (≥50%) • Reliable operation	• Low primary beam intensity compared to p, d, ^{3}He • Target thickness limited due to momentum spread $\Delta p/p$ • Poor emittance (depending on production mechanism) • Moderate beam purity • Large momentum/energy spread • Deceleration/cooling difficult without intensity loss[b)] • Tertiary reactions
ISOL (thick target)	• Thick targets • Intense primary beams • High beam purity (element dependent) • Excellent beam quality (emittance) • Low energy spread • Experience in target/ion source design	• Yield strongly dependent on target/product chemistry • Large amounts of unwanted radioactivity, high radiation fields, robots • Delay due to diffusion/desorption (element dependent) • Post-acceleration necessary
ISOL (thin) He-jet (target)	• Intense primary beam (~1 mA) • Simple target design • No target diffusion/desorption problems • Ion source is in a low radiation field • Rare target materials can be used • Excellent beam quality • Low energy spread • Not chemically selective	• Thin targets, effective target thickness is further reduced for spallation products • Not chemically selective, reduced beam purity, ion source contamination • Delay due to sweep-out and transport • High ion source gas load, low yield for charge states $q > 1$ (ECR) • Volatile species cannot be transported • Efficient He-jet/ion source coupling is difficult • Post-acceleration necessary

a) No advantage when storage ring is used; b) ions can not be shared except in a ring.

Table 6. Performance comparison between a future PF and an ISOL based RNB facility.

	PF	PF + Ring (100 turns)	ISOL (thick target)	ISOL + Ring (3000 turns)
Energy range (MeV/u)	300–1000	10–500	0.001–10	~1–10
Momentum width (%)	1–5	~0.001[a)]	~0.1	~0.001[a)]
Emittance (πmm•mrad)	~20	0.1[a)]	0.2–1	0.01(?)[a)]
Production Luminosity L_p ($cm^{-2}s^{-1}$)	$(2–7)\times10^{36}$	—	$10^{38}–10^{39}$	—
Target Luminosity L_t ($cm^{-2}s^{-1}$)	$3\times10^{30} – 10^{31}$[b)]	$\leq4\times10^{30}$[c)e)] $\leq4\times10^{28}$[a)e)] $\leq4\times10^{29}$[e)f)]	$2\times10^{28}–2\times10^{30}$[d)]	$\sim10^{31}–10^{32}$[c)e)] $\sim10^{30}–10^{31}$[a)e)]

a) e^--cooled.

b) production cross section: $\sigma_p = 10$ mb, transmission: 50%, target: Pb 100 mg/cm^2.

c) uncooled.

d) production cross section: $\sigma_p = 10$ mb, acceleration efficiency $(.5–5)\times10^{-2}$, target: Pb 1 mg/cm^2.

e) internal target: 2×10^{14} cm^{-2}.

f) stochastically cooled.

4. A High Intensity Low Energy RNB Facility

Thoughts similar to those presented in the previous chapters have led to the development of a "working concept" for a high intensity low energy RNB facility based on the thick target approach. It should, however, be pointed out that the ideas discussed in this chapter are preliminary and represent the personal opinions of the author at this time (April 1990).

For a future facility the thick target ISOL approach was chosen because, as was shown above, it will produce the highest intensities and the best beam qualities of low energy (0.1–10 MeV/u) RNBs of the methods investigated. The effective luminosity of the proposed facility, i.e., the luminosity after taking losses due to ionization, etc., into account, is expected to be in the range of 5×10^{35} to 5×10^{37} cm^{-2} s^{-1} (2×10^{38} for light ions). This means, in practical terms, that an exotic nucleus that is produced by the interaction of the primary proton beam and the target with, for example, a cross section of 1 mb will be available as a radioactive beam with intensities between 5×10^{8} and 5×10^{10} s^{-1} (depending on A and Z) and energies up to 10 MeV/u. (For energies of ~100 keV the intensities may be 10 times higher).

The concept of the facility is shown schematically in Fig. 3. A light particle beam of 500–1000 MeV energy and 100–300 μA intensity traverses a 100–300 g/cm^2 thick target where it looses ~200 MeV of energy and generates ~40 kW of power. The radioactive species emanate from the hot target and undergo a chemical/physical separation step that removes unwanted activities. This is followed by an ion source that produces radioactive ions with charge-to-mass ratios $Q/A \gtrsim 0.01$. The ions are accelerated to an energy of ~100 keV and undergo a coarse separation in an isotope separator. Satellite beams will be available for low-energy RNB research similar to ISOLDE at CERN. The low energy RNB beam is then subjected to further analysis to remove unwanted isobaric nuclei and is injected into a low-β, low Q/A preaccelerator. At an intermediate energy of 1–1.5 MeV/u the RNB ions are stripped and subsequently post-accelerated to the final energy of maximally ~10 MeV/u. They can now be used in "conventional" single pass experiments or injected into a storage ring. The main purpose of the storage ring is to make optimal use of the RNB ions by employing multi-turn injection, cooling and "stacking" of the beam, and having the RNB ions traverse an internal target. The heating of the beam by the internal target and the small energy loss is continuously compensated by electron cooling. If an accumulation factor of ~10^3 can be achieved (ESR:10^2, IUCF Cooler: 6×10^3) a significant gain in luminosity for an internal target experiment over an external single-pass target can be expected (c.f. Table 6). The storage ring scheme will, however, only work *efficiently* if a difficult condition can be achieved: the injecting accelerator and the ion source have to be *pulsed* and the radioactive ions should be *stored* between beam pulses. Pulsed operation would also greatly reduce the cost of the accelerator due to lower power requirements. The storage ring could then also function as *stretcher* providing external beams with large duty factors.

There are many questions regarding the operation of the storage ring that remain to be answered, but it should be emphasized that the viability of the presented concept does not depend on the storage ring option.

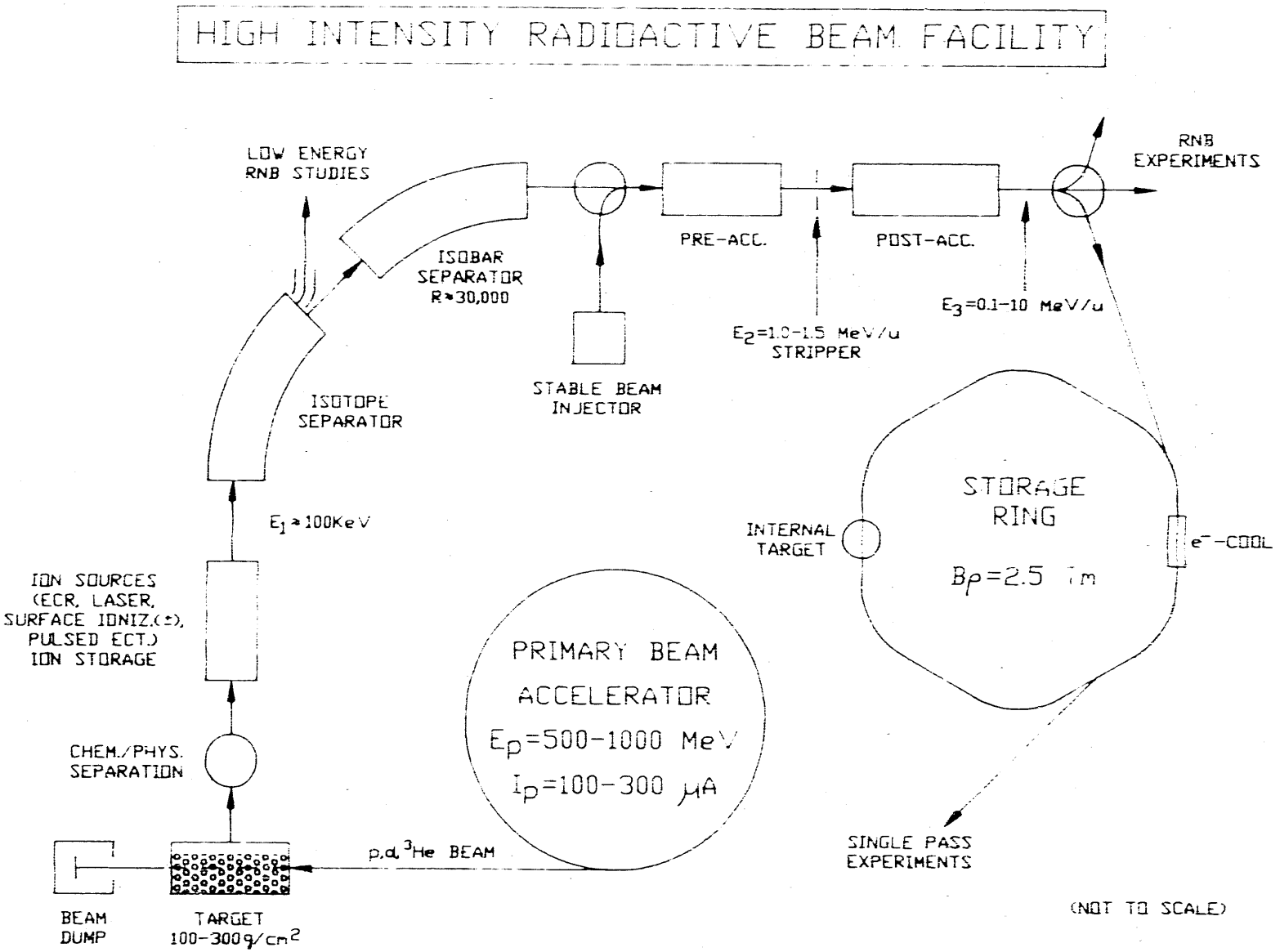

Figure 3. Schematic representation of a proposed high intensity RNB facility based on the thick target version of the ISOL approach. (For details see text.)

Table 7. Technical research and development topics related to a High Intensity RNB Facility.

A. General

- Development of efficient detectors for experiments with low beam intensities
- Exploration of the role of storage rings in RNB research, internal targets, etc.

B. Projectile Fragmentation Method

- Design of a High Energy (300–1000 MeV/u) High Intensity ($\sim 6\times10^{12}$ s^{-1}) Heavy Heavy Ion Accelerator (~10×SIS18)
- Improvement of secondary beam purification techniques
- Efficient deceleration/cooling techniques

C. ISOL Method (Thick Target)

- Cost effective primary beam production (500–1000 MeV, p, d, ^{3}He; 100–300 μA)
- High beam power targets (≤50 kW)
- Element specific target matrices
- Physical/chemical purification schemes
- Ion source research: high efficiency for low to moderate charge states ($1^+ - 3^+$), high temperature operation, chemical selectivity, laser, pulsed operation, storage capability (traps)
- Charge state boosters: EBIS/ECR, stripping
- Radiation hardened target/ion source components, robotics
- Low-β, low Q/A preaccelerator
- Post-acceleration

D. ISOL Method (Thin Target)

- High intensity (~1 mA) beam studies of thin (multiple) targets, target life time
- Spallation yields
- Physical/chemical purification
- Efficient He-jet/ion source coupling
- High pressure ion source operation (charge states $1^+ - 3^+$)
- Post-acceleration

5. Conclusions

There has been a widespread interest in the nuclear physics community regarding questions that can be addressed with radioactive beams. While several years ago the concept of accelerating radioactive ions was rejected as a "crazy" idea, it has now become possible to produce radioactive beams of sufficient intensity for a wide range of experiments, as discussed at this and several previous workshops, and at the first international conference on this topic [Con89]. The feasibility of such a project has increased dramatically in recent years due to many technological advances: high intensity proton and heavy ion accelerators, superconducting linacs, RFQs, storage rings, electron and stochastic cooling, ECR sources, multi-photon ionization, magnetic separators . . . to mention only a few. There remain, however, several R&D topics specific to a future high intensity RNB facility that need to be addressed. For brevity a list of R&D topics that does, however, not make any claim to completeness is presented in Table 7. The breadth of the necessary research is such that it will require the collaboration of many Laboratories and Universities, and the entire endeavor will benefit greatly from international cooperation.

References

[Con89] Proceedings of the First International Conference on Radioactive Nuclear Beams, October 16–18, 1989, Berkeley, California, eds. W.D. Myers, J.M. Nitschke, E.B. Norman (World Scientific, Singapore, 1990).

[Mun89] Reference [Con89], p. 91.

[Mue89] Reference [Con89], p. 132.

[Mun90] G. Munzenberg, 1990.

[Nit89] M. Nitschke, "Workshop on Future Perspectives for Nuclei Far from Stability for the Long Range Plan for Nuclear Science," Argonne National Laboratory, April 9–10, 1989, unpublished; and "Town Meeting on Low Energy Nuclear Physics," Argonne National Laboratory, April 17–18, 1989, unpublished.

[Rav87] H.L. Ravn and B.W. Allardyce, "On-Line Mass Separators" in "Treatise on Heavy-Ion Science," ed. D.A. Bromley (Plenum Press, New York, 1989), Vol. 8, p. 363.

[Sch87] K.H. Schmidt, E. Hanelt, H Geissel, G. Münzenberg and J.P. Dufur, Nucl. Instr. and Meth. **A260**, 287 (1987).

[She90] B. M. Sherrill, D. J. Morissey, and J. A. Winger.

[Tal90] W.L. Talbert and D.J. Vieira, private communication, and these proceedings.

CLOSING COMMENTS ON THE WORKSHOP ON SHORT-LIVED NUCLEAR BEAMS

GERALD T. GARVEY
Los Alamos National Laboratory
Los Alamos, New Mexico 87545

It was a great pleasure to have heard so many interesting and forward-looking talks at the plenary sessions and vigorous discussion within the working groups. One feels being in on the emergence of a new field, which is very exciting. As time is quite short my remarks will be by way of observations and comments rather than an attempt to summarize this stimulating and diversified conference.

First, there is clearly an ever increasing interest in this area of research. For example, note the recently expressed interest of Brookhaven National Laboratory (BNL) and the Rutherford Laboratory in using their proton beams to provide a basis for a radioactive beam facility. There is also, I can assure you, great interest at Los Alamos in studying how effectively LAMPF can provide an outstanding facility for this community. As you know, we have an 800-MeV, 1000-μA proton beam that might provide the very best source of short-lived nuclei in the world.

There seemed to be some initial feelings of competition between those advocating production of exotic beams by fragmentation and those who want to achieve it via spallation. I see no need for this apparent contest. The production of beams via fragmentation creates useful yields in the regime above 100 MeV/amu. To get high-quality beam at lower energy via this process requires collecting these fragments in a storage ring, cooling them, and then collecting and deaccelerating them, but that takes time and so the technique will not likely be profitable with nuclei whose lifetime is less than, say, a second. It also seems unlikely that it would be profitable to accelerate radioactive beams generated via spallation from thermal energies to much above 10 MeV/amu. Thus, it appears that there is a natural separation in the field between high-energy beams from fragmentation and low-energy beams produced by acceleration following production via spallation. The physics in the two regimes is quite different as the lower energy focuses on issues of nuclear structure while the higher energies deal with nuclear properties such as the equation-of-state.

If you would allow me a moment to reminisce, I can tell you how I first got into the interesting business of exotic nuclei. At Lawrence Berkeley Laboratory (LBL) in the summer of 1965 there was great excitement as ^{8}He had been discovered by Poskanzer [1]) and collaborators and its mass had been measured [2]) by Joe Cerny's group at the Lawrence Berkeley Laboratory (LBL) 88-inch cyclotron. The question of the moment was whether or not ^{10}He was stable. In dealing with that question, the idea of employing mass-difference equations [3]) was developed. It is, of course, evident that large binding for ^{8}He makes it easier for ^{10}He to decay into ^{8}He + $2n$. By way of a further remark, a few years later I realized that insofar as ^{10}He is

a doubly magic nucleus its mass could be directly predicted using the Cohen and Kurath [4]) matrix elements ($T = 1$, $1p$ shell).

$$\mathrm{BE}(^{10}\mathrm{He}) - \mathrm{BE}(^{4}\mathrm{He}) = 4\epsilon_{3/2} + 2\epsilon_{1/2} + \left(\frac{3^2}{2}\right)^{J=0} + 5\left(\frac{3^2}{2}\right)^{J=2} + \left(\frac{1^2}{2}\right)^{J=0} + 3\left(\frac{1}{2},\frac{3}{2}\right)^{J=1} + 5\left(\frac{1}{2},\frac{3}{2}\right)^{J=2} = -2.29\ \mathrm{MeV}$$

using their (6-16)2BME matrix elements. In the above expression, ϵj indicates the single particle energies while the other terms are the $(2J + 1)$ weighed values of the two-body $T = 1$ interaction energies. The fact that this procedure predicts ^{10}He to be unbound against decay in ^{4}He + $6n$ was a further clear indication of its instability against strong decays. Of course, ^{10}He has not been found to be stable. However, ^{11}Li has been discovered and is a very interesting case.

^{11}Li drew much attention at this conference. The talk by Ingemar Ragnarsson [5]) was very informative in this regard. It is very interesting to understand the wave function of ^{11}Li in shell model terms. Of course, the radial wave function of the last two neutrons will be unusual because of their very small separation energy S_{2n} (^{11}Li) ~0.2 MeV, whatever their shell model configuration. The question is, "What is the orbital of the last two neutrons in $^{11}_{3}\mathrm{Li}_8$?" Are all the nucleons in the $1p$ shell, or does the system take advantage of the possibility that both the last two neutrons and third proton can gain energy by taking on the prolate deformed orbits ($K = 1/2$) as shown in Fig. 1? A similar argument could be made for $^{11}_{4}\mathrm{Be}_7$, which has a $J^\pi = (1/2)^+$ ground state! In the discussion following Ragnarsson's talk:, John Schiffer pointed out in experiments done at Argonne many years ago on the $^{10}\mathrm{Be}(d,p)^{11}\mathrm{Be}$ reaction the spectroscopic factor for the ^{11}B ground state was found to be $S = 0.73 \pm 0.06$ [6]). Such a large value would not be compatible with a deformed $K = 1/2^+$ Nilsson orbit, as one expects a value of $S \simeq 0.3$ for large deformation [7]). However, John has more faith than I do in our

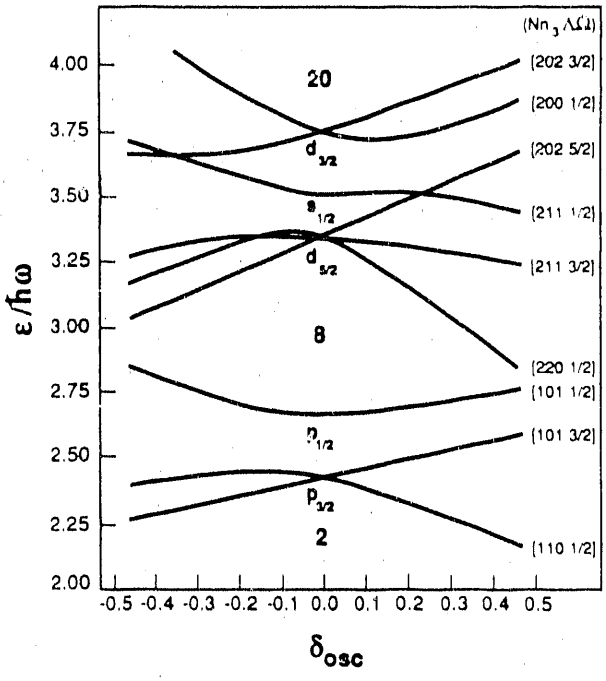

Fig. 1. Figure showing the energies of single-particle orbits as a function of deformation parameters for the anisotropic oscillator. The orbits are labeled by the asymptotic quantum numbers $[Nn_3\Lambda\Omega]$ for large prolate deformation.

ability to extract absolute spectroscopic factors from these reactions. In a very deformed case the orbit could be appreciably larger than one generated in a spherical potential and might lead one to considerably overestimate the spectroscopic factor from the measured yield. Be that as it may, it remains a challenge to determine the nature of exotic light nuclei that may be undergoing deformation in those cases where both the last *protons* and *neutrons* have the possibility to lower their energy by assuming deformed orbits.

Another remark that caught my attention was Frank Stephen's observation that because the Coulomb interaction tends to induce fission the formation of high-spin systems that are richer in neutrons might let experimenters reach even larger angular momenta. At present, high-spin studies are of necessity carried out on the proton-rich side of the valley of stability. A rule-of-thumb appears to be that for each additional neutron added to the nucleus about one unit of angular momentum can be picked up without danger of fission. This gain in angular momentum before fission may be all that is needed to make ultra-deformed states (ratio of major to minor axis of 3/1) observable. This shape should come down to the yrast line at sufficiently high spin both because its moment of inertia is larger and certain single particle states will benefit from the large Coriolis interaction. The production of neutron-rich beams of medium-A nuclei to use as projectiles in formation of high-spin levels should let one gain the order of five units in $N - Z$ and hence in angular momentum of the decaying systems. The unambiguous discovery of physical states with a (3/1) deformation would be most exciting.

One cannot fail to be impressed with the power of the nuclear models developed by Bohr-Mottelson, Nilsson, and further elaborated by Strutinsky. They have provided uncanny direction in understanding the behavior of nuclei at high spin. These models work so well that there really needs to be some careful study to determine how well these models of nuclear spectra should work. Only with a sharper understanding of the limits of this family of models can one effectively pursue this subject at greater depth. The experimental apparatus has become so powerful that researchers can comb through data and reject "uninteresting" decays to get at the specific type of system that one wants to examine. While very beautiful, and at some level very satisfying, what are we learning that would alter our view of the nature of nuclear excitations? With respect to the yrast line, the lowest lying ultra-deformed states will very likely have very small matrix elements coupling them to the neighboring levels. This is because it will have an intrinsic state made up of several high angular momentum single particle states. A glance at a Nilsson diagram for this large deformation and high rotation shows many crossings of single particle states. Each of these crossings requires a two-body interaction to rescatter the particles; hence the mixing matrix elements are small and the ultra-deformed states near the yrast line will appear to be very pure. One needs carefully formulated questions to investigate this matter at a depth that will reveal new information about nuclear behavior.

Attention should also be paid to investigating appropriate detector schemes for exotic beam research. The low intensities necessarily associated with exotic beams

will require and allow detection systems of much greater acceptance than are now employed. There may be some very interesting and profitable trade-offs to be made between efficient detection systems and heroic efforts to increase the beam intensity. Once the beam drops below 10^5 s^{-1}, it should be easy to observe and analyze each incident particle.

This has been an excellent and pleasurable workshop, and one readily sees the community of nuclear structure physicists rallying around a new and exciting possibility to expand our understanding of the atomic nucleus in its more exotic, quantum states. Your idea to organize a steering committee that is not site nor technology specific is an excellent idea at this time. I don't think there is a single idea or system yet so compelling that the entire nuclear physics community will rally behind it. However, I believe that by working hard on the scientific opportunities provided by exotic beams and the means of producing them, you will develop an irresistible plan. It is exciting seeing this process in motion!

References

1) A. M. Poskanzer, R. A. Esterlund, and R. McPherson, Phys. Rev. Lett. **15** (1965) 1030.

2) J. Cerny, S. W. Cosper, G. W. Butler, R. H. Pehl, E. S. Goulding, D. A. Landis, and C. Detraz, Phys. Rev. Lett. **16** (1966) 469.

3) G. T. Garvey and I. Kelson, Phys. Rev. Lett. **16** (1966) 197.

4) S. Cohen and D. Kurath, Nucl. Phys. **73** (1965) 1.

5) Ingemar Ragnarsson (this conference).

6) F. Ajzenberg-Selove and C. L. Busch, Nucl. Phys. **A336** (1980) 1.

7) A. Bohr and B. Mottelson, *Nuclear Structure*, Vol. II (W. A. Benjamin, Inc., Reading, Massachusetts, 1975), p. 290.

Outlook

By the end of this workshop a strong concensus had developed within the entire group that a proposal for an intense radioactive ion beam facility was appropriate and should be prepared at the earliest possible time. It was decided that a steering committee should be appointed to head-up the preparation of this proposal and that this initiative should be a joint US and Canadian undertaking. A selection committee made up of the working group chairman and myself was given the charge of appointing this steering committee and within a month the following people had been selected:

Rick Casten (Brookhaven), 1st year chairman

Cary Davids (Argonne)

John D'Auria (Simon Fraser)

Jerry Garrett (Oak Ridge)

Mike Nitschke (Berkeley)

Brad Sherrill (Michigan State)

Dave Vieira (Los Alamos)

Michael Wiescher (Notre Dame)

Ed Zganjar (Louisiana State)

Since that time, the steering committee has been active in setting up a users group for this new initiative. Work has already started by several working groups to further refine the scientific case and to develop the set of key experiments to be carried out at this new facility. A technical sub-committee has started work on a baseline facility design and to define key areas where technical R&D are needed. Several meetings are planned in the coming months to expedite this work and a follow-up workshop is tentatively scheduled for Oct. 22-23, 1991 in East Lansing preceeding the Fall meeting of the American Physical Society/Division of Nuclear Physics.

The momentum is building on this exciting initiative. Your active participation has been, and continues to be, the driving force.

David J. Vieira

Los Alamos Workshop on the Science of Intense Radioactive Ion Beams

April 10-12, 1990

J. Robert Oppenheimer Study Center

Agenda

Tuesday - April 10, 1990

8:00 - 8:30 a.m.	Registration
8:30 - 8:45 a.m.	Welcome/Organization
	Roger Perkins, Deputy Associate Director of Research
	Overview Talks
8:45 - 9:30 a.m.	Talk 1 - Reaction Physics J. Schiffer (ANL)
9:30 - 10:15 a.m.	Talk 2 - Nuclei Far from Stability/Nuclear Structure.
	I. Ragnarsson (LUND)
10:15 - 10:45 a.m.	Coffee Break
10:45 - 11:30 a.m.	Talk 3 - Nuclear Astrophysics. G. Mathews (LLNL)
11:30 - 12:15 p.m.	Talk 4 - Materials Science.
	G. Sawicki (Chalk River)
12:15 - 1:45 p.m.	Lunch at Otowi Cafeteria
1:45 - 2:30 p.m.	Talk 5 - Facilities. M. Nitschke (LBL)
2:30 - 3:00 p.m.	Organization of Working Groups
3:00 - 3:30 p.m.	Coffee Break
3:30 - 5:15 p.m.	Working Group Sessions
5:15 - 7:15 p.m.	Director's Reception/
	Light Supper - Sponsored by EG& G Ortec
7:15 - 9:30 p.m.	Working Group Sessions
	Transportation back to Hilltop Hotel
	and Los Alamos Inn

Wednesday - April 11, 1990

Working Group Parallel Sessions

8:30 - 10:00 a.m.	Working Group Sessions
10:00 - 10:30 a.m.	Coffee Break
10:30 - 12:00 p.m.	Working Group Sessions
12:00 - 1:30 p.m.	Lunch at Otowi Cafeteria
1:30 - 3:00 p.m.	Working Group Sessions
3:00 - 3:30 p.m.	Coffee Break
3:30 - 5:30 p.m.	Working Group Sessions
5:30 - 6:30 p.m.	Mixer (Sponsored by LeCroy Corporation)
6:30 - 8:00 p.m.	Banquet at Otowi
	Transportation back to Hilltop Hotel and Los Alamos Inn

Thursday - April 12, 1990

Results of Working Group Deliberations

8:30 - 8:55 a.m.	Report of Working Group 1	R. Stokstad (LBL)
8:55 - 9:20 a.m.	Report of Working Group 2	R. Casten (BNL)/ J. Garrett (ORNL)
9:20 - 9:35 a.m.	Report of Working Group 2A	W. Bauer (MSU)
9:35 - 10:00 a.m.	Report of Working Group 3	M. Howard (LLNL)
10:00 - 10:30 a.m.	Coffee Break	
10:30 - 11:00 a.m.	Report of Working Group 4	S. Hanna (Stanford)
11:00 - 11:30 a.m.	Report of Working Group 5	J. D'Auria (SFU/TRIUMF)
11:30 - 11:45 a.m.	Concluding Remarks	G. Garvey (LAMPF)
11:45 - 12:00 p.m.	Closing Organizational Topics	
	Transportation back to Hilltop Hotel and Los Alamos Inn	

NOTE: Rooms will be available at the Study Center Thursday afternoon, April 12, 1990 for further discussions if needed.

A LAMPF tour may be arranged either during or after the Workshop for those interested in seeing the experimental facilities.

Agenda for Working Group 1 on Reaction Physics

Bob Stokstad, Chairman
Dan Strottman and Ray Nix, Coordinators

To stimulate new ideas on the indicated topics, brief introductory comments will be made by the discussion leaders and additional persons listed for the working sessions.

Tuesday, April 10

2:45--3:00 p.m.	Organizational Meeting Bob Stokstad, Chairman
3:30--5:15 p.m.	Multidimensional Reaction Dynamics/Subbarrier Fusion Ray Nix, Discussion Leader Hee Kim Bob Stokstad
7:15--9:30 p.m.	Charge Exchange Reactions/Transfer Reactions/Fission Dan Strottman, Discussion Leader Dennis Moltz Jerry Wilhelmy

Wednesday, April 11

8:30--10:00 a.m.	Isomers/Scattering/Optical Potentials Fred Becchetti, Discussion Leader Dave Madland
10:30--12:00 a.m.	Halos: Physics of Loosely Bound Nuclei Wolfgang Bauer, Discussion Leader Anna Hayes Dave Vieira
1:30--3:00 p.m.	Reverse Kinematics Ed Siciliano, Discussion Leader Dave Madland Additional Topics and/or Carryover from Previous Sessions Begin Report Preparation
3:30--5:30 p.m.	Report Preparation

Agenda for Working Group 2
on
Nuclei Far from Stability -- Nuclear Structure

Rick Casten and Jerry Garrett, Chairmen
Peter Möller, Coordinator

To stimulate new ideas a d thinking about the indicated topics, brief overviews and discussions will be informally directed by the following discussion leaders.

Tuesday, April 10

2:45--3:00 p.m.	Organizational Meeting Rick Casten and Jerry Garrett, Chairmen
3:30--5:15 p.m.	Overviews & Initial Discussions Fission, Transuranics, Superheavies -- Peter Möller ß-Decay -- Cary Davids Masses & Stability -- Peter Haustein High-Spin Studies with RIBs -- Jerry Garrett
7:15--9:30 p.m.	Overviews & Initial Discussions (cont.) Nuclear Shapes, Collectivity, Phase Transitions Magicity, Valence p-n Interactions -- Fred Wohn & Rick Casten Neutron Halos, Properties of Drip-line Nuclei, Neutron-Like Matter, Nuclei Under Extreme Isospin "Stress", other Exotica -- form a topical subgroup/select a discussion leader(s)

Wednesday, April 11

8:30--10:00 a.m.	Detailed Discussions & New Ideas Superheavies, ... -- Peter Möller ß-Decay -- Cary Davids Masses & Stability -- Peter Haustein High-Spin Studies with RIBs -- Jerry Garrett
10:30--12:00 p.m.	Detailed Discussions & New Ideas (cont.) Nuclear Shapes, ... -- Fred Wohn & Rick Casten Neutron Halos, ... -- subgroup discussion leader(s)
1:30--3:00 p.m.	Additional Discussions -- Report Preparation Split-up in Subgroups
3:30--5:30 p.m.	Report Preparation -- Discuss Consensus Ideas Entire Working Group

Agenda for Working Group 3
on
Nuclear Astrophysics

W. Michael Howard, Chairman
Paul Koehler, Coordinator

Tuesday, April 10

2:30--3:00 p.m.	Introduction -- Howard
3:30--5:15 p.m.	Review of Work in Progress and Plans for the Near Future
	TRIUMF -- Buchman INS -- Kubono Louvain -- Leleux LLNL/OSU -- Mathews Others

Wednesday, April 11

8:00--10:00 a.m.	Discussion of Theory and Data Needs
10:00--12:00 p.m.	Experimental Approaches -- Comparison to Other Techniques
1:30--5:30 p.m.	Redrafting of Position Paper/Discussion of General Questions
	Identify highlight(s) Projects for the near term Quests for the long term Identification of facility requirements

Agenda for Working Group 4
on
Materials Science/Atomic Physics/Isotope Production

R. D. Taylor, Coordinator
S. S. Hanna, Chairman
Physics Department, Varian Bldg.
Stanford University
Stanford, CA 94305-4060
(415) 723-4612 -- FAX (415) 725-6544
E-MAIL: SS.HAN@STANFORD

Agenda Topics:

Materials Science/Condensed Matter Physics
Diffussion-migration, latice defects, materials modification

Hyperfine Interaction/Spin Alignment
Mossbauer spectroscopy, nuclear orientation, NMR, perturbed angular correlation, conversion electron spectroscopy, laser spectroscopy

Polarized Nuclear Beams
Methods, nuclear moments, relaxation times

Radioisotopes Production/Uses
Medical isotopes, short lifetimes, high specific activity sources for Mossbauer spectroscopy

Radiation Damage/Reactor Data

Atomic Physics
Electronic levels of charged atoms

Commercial Applications
Host modifications, tracer implementation, surface and sub-surface analysis

Agenda for Working Group 5
on
Facilities

J. M. D'Auria, Chairman
T. S. Bhatia, Coordinator

Tuesday -- April 10

1:45--2:30 p.m. Invited Talk -- M. Nitschke
Overview of the Present Plans for Radioactive Beam Facilities in the World

3:30--5:15 p.m. Working Session 1
Topic: Projected Specifications of ISOL/Accel Approach (and Related Methods) /Vices/Virtues

Possible Speakers

M. Fujioka (Japan) -- The Proposed RB Facility at the JHP

T. G. Walker (RAL) -- The Proposed RB Facility at Rutherford

M. Loiselet (Louvain-au-Neuve) -- Results and Prospects for RIB at Louvain-au-Neuve

D. J. Clark (LBL) – An Optimal Energy for a Proton Production Source

W. Talbert/J. D'Auria -- Expected Yields from a Thin and Thick Target System

7:15--9:30 p.m. Working Session 2
Topic: Projected Specifications of the Projectile Fragmentation/Recoil Transfer System

Possible Speakers

B. Sherrill (Michigan State) -- Overview of Projectile Fragmentation and Recoil Separators

J. Winger (NSCL) -- Projected Yields from Projectile Fragmentation

(F. Becchetti -- Use of Solenoids and Transfer Reactions)

Kruno Subotic (Yugoslavia) -- Decelerating Projectile Fragmentation in a Cyclotron

Wednesday -- April 11

8:30--10:00 a.m. — Working Session 3
Topic: Problems with Each Approach

Possible Speakers

D. J. Clark (LBL) -- Advantages of a Cyclotron as the Secondary Accelerator

G. McMichael (Chalk River) -- Energy Variability in a 1.0 MeV/u LINAC and Prospects at Higher Energies

Y. Arai (Japan) -- Low Energy RFQ LINAC at the JHP

H. Wollnik -- Possibilities of Isobaric Separation in an ISOL/Accelerator System

10:30--12:00 p.m. — Working Session 4
Topic: Pilot Development Studies (Planned or Needed)

Possible Speakers

W. Talbot (LAMPF) -- A Pilot Thin Target System at LAMPF

R. Stokstad (LBL) -- Studies Related to a High Intensity, 30 MeV p Cyclotron System at LBL

T. Ward (BNL) -- Development of Special Handling Systems for very Radioactively Hot Targets"

J. D'Auria -- Thick Target and ECR ISOL Studies at TRIUMF

H. Penttila (Finland) -- IGISOL for Radioactive Beams

(G. McMichael -- Studies of 4-Rod versus 4-Vane RFQ)

12:00--1:30 p.m. — Lunch

1:30--3:00 p.m. — Working Session 5
Topic: Preparation of Final Report

3:30--5:30 p.m. — Working Session 6
Topic: Matching of User Specifications with Facility Capabilities
Discussion of Questionnaire

Appendix C

Attendee List

Edward D. Arthur
Los Alamos National Laboratory
P. O. Box. 1663, MS B210
Los Alamos, NM 87545
Telephone: (505) 665-1708
Telefax:
E-Mail:

Richard E. Azuma
Caltech
Kellogg Laboratory
Pasadena, CA 91125
Telephone: (818) 356-4587
E-MAIL: REA@CALTECH

Wolfgang W. Bauer
Michigan State University
East Lansing, MI 48824
Telephone: (517) 353-5965
Telefax:
E-MAIL: BAUER@MSUNSCL

Fred Becchetti
University of Michigan
Randall Laboratory
Department of Physics
Ann Arbor, MI 48109
Telephone: (313) 764-1598
Telefax:
E-MAIL: BECCHETTI@UMIPHYS

Tarlochan S. Bhatia
Los Alamos National Laboratory
P. O. Box 1663, MS H817
Los Alamos National Laboratory
Telephone: (505) 667-3203
Telefax: (505) 665-0919
E-MAIL: BHATIA@LAMPF

J. David Bowman
Los Alamos National Laboratory
P. O. Box 1663, MS H846
Los Alamos, NM 87545
Telephone: (505) 667-4363
Telefax: (505) 665-1712
E-MAIL: BOWMAN@LAMPF

James N. Bradbury
Los Alamos National Laboratory
P. O. Box 1663, MS H844
Los Alamos, NM 87545
Telephone: (505) 667-5051
Telefax: (505) 665-1712
E-MAIL: GARDUNO@LAMPF

Daeg Scott Brenner
Clark University
Chemistry Department
950 Main Street
Worcester, MA 01610
Telephone: (508) 793-7114
Telefax: (508) 793-7780
E-MAIL: DBRENNER@CLARKU

Lothar Buchmann
TRIUMF
4004 Wesbrook Mall
Vancouver, BC
CANADA V6T 2A3
Telephone: (604) 222-1047
Telefax: (604) 222-1074
E-MAIL: LOTHAR@TRIUMFCL

Gilbert W. Butler
Los Alamos National Laboratory
P. O. Box 1663, MS J514
Los Alamos, NM 87545
Telephone: (505) 667-6005
Telefax:
E-MAIL:

Richard F. Casten
Brookhaven National Laboratory
Physics Deparment
Upton, NY 11973
Telephone: (516) 282-3979
Telefax: (516) 282-3000
E-MAIL: RICK@BNLUX0.BNL.GOV

David J. Clark
Lawrence Berkeley Laboratory
Building 88
Berkeley, CA 94720
Telephone: (415) 486-5088
Telefax: (415) 486-7983
E-MAIL: DJCLARK@LBL

John Eric Crawford
Foster Radiation Laboratory
McGill University
3610 University St.
Montreal, Quebec
CANADA H3A 2B2
Telephone: (514) 398-7029
Telefax: (514) 398-7022
E-MAIL: PY10@MUSICA.MCGILL.CA

John D. Auria
Simon Fraser University
Barnaby, British Columbia
CANADA V5A 1S6
Telephone: (604) 291-4607
Telefax: (604) 291-3765
E-MAIL: DAUR@SFU

Cary N. Davids
Argonne National Laboratory
PHY203, 9700 S. Cass Avenue
Argonne, IL 60439
Telephone: (708) 972-4062
Telefax: (708) 972-3903
E-MAIL: DAVIDS@ANLPHY

Thierry Delbar
University of Louvain
Chemin du Cyclotron, 2
B-1348 Louvain-La-Neuve
BELGIUM
Telephone: 32-10-473202
Telefax: 32-10-452183
E-MAIL:

Peggy L. Dyer
Los Alamos National Laboratory
P. O. Box 1663, MS D449
Telephone: (505) 667-3987
Telefax: (505) 665-3644
E-MAIL:

Bruce Robert Erdal
Los Alamos National Laboratory
P. O. Box 1663, MS J519
Los Alamos, NM 87545
Telephone: (505) 667-5338
Telefax: (505) 667-2964
E-MAIL:

Alexander J. Gancarz
Los Alamos National Laboratory
P. O. Box 1663, MS J515
Los Alamos, NM 87545
Telephone: (505) 667-4457
Telefax: (505) 665-4355
E-MAIL:

Robert W. Garnett
Los Alamos National Laboratory
P. O. Box 1663, MS H817
Los Alamos, NM 87545
Telephone: (505) 667-0919
Telefax: (505) 665-2835
E-MAIL:

Jerry D. Garrett
Oak Ridge National Laboratory
Mailstop 6371
Oak Ridge, TN 67831
Telephone: (615) 576-5489
Telefax: (615) 574-1268
E-MAIL: GARRETT@ORPH01

Gerald T. Garvey
Los Alamos National Laboratory
P. O. Box 1663, MS H836
Los Alamos, NM 87545
Telephone: (505) 667-2000
Telefax: (505) 665-1712
E-MAIL: JUDYVAL@LAMPF

Kenneth Gregorich
Lawrence Berkeley Laboratory
1 Cyclotron Road
MS 7DA-3307
Berkeley, CA 94720
Telephone: (415) 486-5088
Telefax: (415) 486-7983
E-MAIL: KEGREGORICH@LBL

Frank W. Guy
Los Alamos National Laboratory
P. O. Box 1663, MS H817
Los Alamos, NM 87545
Telephone: (505) 667-9137
Telefax: (505) 667-0919
E-MAIL:

Erik G. Hagberg
Atomic Energy of Canada Ltd.
Chalk River Nuclear Laboratories
Ontario, CANADA K0J 1J0
Telephone: (613) 584-3311 Ext. 4111
Telefax: (613) 584-4024
E-MAIL: 02373@AECLCR

Kevin Insik Hahn
Yale University
WNSL, P. O. Box 6666
272 Whitney Avenue
New Haven, CT 06511
Telephone: (203) 432-5827
Telefax: (203) 432-3522
E-MAIL: HAHN@YALVMS

William Dennis Hamilton
Oak Ridge National Laboratory
P. O. Box 2008
Building 6008, MS 6374
Oak Ridge, TN 37831
Telephone: (615) 576-8763
Telefax: (615) 574-1268
E-MAIL:

Stanley S. Hanna
Stanford University
Physics Department
Varian Building
Stanford, CA 94305-4060
Telephone: (415) 723-4612
Telefax: (415) 725-6544
E-MAIL: SS.HAN@STANFORD

Samuel Harar
GANIL BP 5027
14021 Caen Cedex
FRANCE
Telephone: 31-45-4598
Telefax: 31-45-4647

Peter Eugene Haustein
Lawrence Berkeley Laboratory
Building 88
1 Cyclotron Road
Berkeley, CA 94720
Telephone: (415) 486-5088
Telefax: (415) 486-7983
E-MAIL: PEHAUSTEIN@LBL

Anna Catherine Hayes
Los Alamos National Laboratory
P. O. Box 1663, MS B283
Los Alamos, NM 87545
Telephone: (505) 667-3887
Telefax:
E-MAIL: HAYES@LAMPF

W. Michael Howard
Lawrence Livermore National Lab
Mailstop L-197
Livermore, CA 94550
Telephone:
Telefax:
E-MAIL:

Hsiao-Hua Hsu
Los Alamos National Laboratory
P. O. Box 1663, MS D410
Los Alamos, NM 87545
Telephone: (505) 667-2480
Telefax:
E-MAIL:

H. J. Kim
Oak Ridge National Laboratory
P. O. Box X, Building 6003
Oak Ridge, TN 37831
Telephone: (615) 574-4708
Telefax:
E-MAIL: KIM@OR01

Paul E. Koehler
Los Alamos National Laboratory
P. O. Box 1663, MS H803
Los Alamos, NM 87545
Telephone: (505) 667-7237
Telefax: (505) 665-4121
E-MAIL: KOEHLER@LAMPF

Dennis Gene Kovar
Argonne National Laboratory
Physics Division, Bldg. 20
Argonne, IL 60439
Telephone: (301) 353-4703
Telefax: (301) 353-5079
E-MAIL: KOVAR@ANLPHY

Gary F. Krebs
Lawrence Berkeley Laboratory
Building 88
Berkeley, CA 94720
Telephone: (415) 486-5575
Telefax: (415) 486-5788
E-MAIL: KREBS@LBL.GOV

Shigeru Kubono
Institute for Nuclear Study
University of Tokyo
3-2-1 Midori-cho
Tanashi, Tokyo
188 JAPAN
Telephone: 0424-61-4131 Ext. 404
Telefax: 0424-68-5844
E-MAIL: KUBONO@JPNUTINS

George P. Lawrence
Los Alamos National Laboratory
P. O. Box 1663, MS H817
Los Alamos, NM 87545
Telephone: (505) 667-9349
Telefax: (505) 667-0919
E-MAIL:

Pierre J. Leleux
University of Louvain
Chemin du Cyclotron, 2
B-1348 Louvain-La-Neuve
BELGIUM
Telephone: 32-10-473273
Telefax: 32-10-452183
E-MAIL:

V. Gordon Lind
Physics Department
Utah State University
Logan, UT 84322-4415
Telephone: (801) 750-2851
Telefax:
E-MAIL: UF7061@USU

Marc Loiselet
Centre de Recherches du Cyclotron
2 ch du Cyclotron
Louvain-La-Neuve
BELGIUM
Telephone: 32-10-47-3273
Telefax: 32-10-45-2183
E-MAIL: LOIS@CYC.UCL.AC.BE

David G. Madland
Los Alamos National Laboratory
P. O. Box 1663, MS B243
Los Alamos, NM 87545
Telephone: (505) 667-6007
Telefax: (505) 667-9671
E-MAIL: MADLAND@LAMPF

Carl J. Maggiore
Los Alamos National Laboratory
P. O. Box 1663, MS K765
Los Alamos, NM 87545
Telephone: (505) 667-6133
Telefax: (505) 665-2992
E-MAIL: 104141@CCVAX

Grant J. Mathews
Lawrence Livermore National Lab.
L-405
Livermore, CA 94550
Telephone: (415) 422-4265
Telefax:
E-MAIL:

John B. McClelland
Los Alamos National Laboratory
P. O. Box 1663, MS H841
Los Alamos, NM 87545
Telephone: (505) 667-7291
Telefax: (505) 665-1712
E-MAIL: JOHN@LAMPF

Gerry E. McMichael
Atomic Energy of Canada Ltd.
Chalk River, Ontario
CANADA, K0J 1J0
Telephone: (613) 584-3311
Telefax: (613) 584-4024
E-MAIL: 01042@AECLCR

David F. Measday
University of British Columbia
Physics Department
Vancouver, BC
CANADA V6T 2A6
Telephone: (604) 228-5098
Telefax: (604) 228-5324
E-MAIL: MEASDAY@TRIUMFCL

Peter Möller
Los Alamos National Laboratory
P. O. Box 1663, MS B243
Los Alamos, NM 87545
Telephone: (505) 665-2210
Telefax:
E-MAIL: MÖLLER@LAMPF

Dennis M. Moltz
Lawrence Berkeley Laboratory
Building 6000
1 Cyclotron Road
Berkeley, CA 94720
Telephone: (415) 486-5088
Telefax:
E-MAIL: DMMOLTZ@LBL

Joel M. Moss
Los Alamos National Laboratory
P. O. Box 1663, MS D434
Los Alamos, NM 87545
Telephone: (505) 667-4117
Telefax:
E-MAIL:

William D. Myers
Lawrence Berkeley Laboratory
1 Cyclotron Road
Berkeley, CA 94720
Telephone: (415) 486-5626
Telefax:
E-MAIL: MYERS@LBL

Subrata Nath
Los Alamos National Laboratory
P. O. Box 1663, MS H817
Los Alamos, NM 87545
Telephone: (505) 665-1953
Telefax: (505) 667-0919
E-MAIL:

George H. Neuschafer
Los Alamos National Laboratory
P. O. Box 1663, MS H817
Los Alamos, NM 87545
Telephone: (505) 667-1958
Telefax:
E-MAIL:

J. Michael Nitschke
Lawrence Berkeley Laboratory
1 Cyclotron Road
Berkeley, CA 94720
Telephone: (415) 486-6471
Telefax: (415) 486-4808
E-MAIL: OASIS@LBL

J. Rayford Nix
Los Alamos National Laboratory
P. O. Box 1663, MS B243
Los Alamos, NM 87545
Telephone: (505) 667-5325
Telefax: (505) 667-9671
E-MAIL: MER@LANL.GOV

Harold A. O'Brien
Los Alamos National Laboratory
P. O. Box 1663, MS D449
Los Alamos, NM 87545
Telephone: (505) 665-4179
Telefax: (505) 665-3644
E-MAIL:

David K. Olsen
Oak Ridge National Laboratory
Building 6000
Oak Ridge, TN 37831
Telephone: (615) 574-67122
Telefax: (615) 574-1268
E-MAIL: OLSEN@ORPH01

Heikki Tapana Penttila
Department of Physics
University of Jväskylä
Seminarrinyatu 15
SF-40100 Jyväskylä
FINLAND
Telephone: 358-41-602371
Telefax: 358-41-602351
E-MAIL: PENTTILA@FINJYU

Dennis R. Phillips
Los Alamos National Laboratory
P. O. Box 1663, MS J514
Los Alamos, NM 87545
Telephone: (505) 667-5425
Telefax: (505) 665-3403
E-MAIL:

Ingemar Ragnarsson
Department of Mathematical Physics
Box 118
S-221 00 Lund
SWEDEN
Telephone:
Telefax:
E-MAIL:

Paul L. Reeder
Battelle Pacific Northwest Lab
P. O. Box 999
Mailstop P8-08
Richland, WA 99352
Telephone: (509) 376-0948
Telefax: (509) 376-2329
E-MAIL:

Robert G. H. Robertson
Los Alamos National Laboratory
P. O. Box 1663, MS D449
Los Alamos, NM 87545
Telephone: (505) 667-1346
Telefax: (505) 665-3644
E-MAIL: RGHR%WEAKS@LANL.GOV

Neil Rowley
Science & Engineering Research Council
Daresbury Laboratory
Warrington WA4 4AD
UNITED KINGDOM
Telephone: 925-603472
Telefax: 925-603173
E-MAIL: NR@UK.AC.DARESBURY.NNGA

Leonid Sagalovski
Argonne National Laboratory
Building 207
Argonne, IL 60439
Telephone: (708) 972-4305
Telefax: (708) 972-4007
E-MAIL:

Jack Sample
EBCO Industries
7851 Alderbridge Way
Richmond, BC
CANADA V6X 2A4
Telephone: (604) 278-5578
Telefax: (604) 278-7230
E-MAIL:

Jerzy A. Sawicki
Chalk River Nuclear Labs
Chalk River, Ontario
CANADA K0J 1J0
Telephone: (613) 584-3453
Telefax: (613) 584-4523
E-MAIL: 02583@AECLCR

John P. Schiffer
Argonne National Laboratory
Argonne, IL 60439
Telephone: (708) 972-4066
Telefax: (708) 972-3903
E-MAIL: SCHIFFER@ANLPHY

Friedhelm Schreiber
Los Alamos National Laboratory
P. O. Box 1663, MS H824
Los Alamos, NM 87545
Telephone: (505) 667-4372
Telefax:
E-MAIL: SCREIBER@LAMPF

Hardy Lothat Seifert
Los Alamos National Laboratory
P. O. Box 1663, MS H824
Los Alamos, NM 87545
Telephone: (505) 667-5557
Telefax: (505) 665-1712
E-MAIL: SEIFERT@LAMPF

Bradley M. Sherrill
Michigan State University
Cyclotron Laboratory
East Lansing, MI 48824-5375
Telephone: (517) 353-5375
Telefax: (517) 353-5967
E-MAIL: SHERRILL@MSUNSCL

Tsutomu Shinozuka
Cyclotron & Radioisotope Center
Tohoku University
Aramakz-Aoba Aobaku
Sendar, 980 JAPAN
Telephone: 022-263-5350
Telefax: 022-263-5358
E-MAIL:

Edward R. Siciliano
Los Alamos National Laboratory
P. O. Box 1663, MS B243
Los Alamos, NM 87545
Telephone: (505) 667-5445
Telefax: (505) 667-9671
E-MAIL: ERS@LAMPF

Arnold John Sierk
Los Alamos National Laboratory
P. O. Box 1663, MS B279
Los Alamos, NM 87545
Telephone: (505) 667-6784
Telefax:
E-MAIL: AJS@T2AJS.LANL.GOV

Walter F. Sommer
Los Alamos National Laboratory
P. O. Box 1663, MS H838
Los Alamos, NM 87545
Telephone: (505) 667-1269
Telefax: (505) 665-1712
E-MAIL:

Gene D. Sprouse
Stony Brook
Physics Department, SUNY
Stony Brook, NY 11794-3800
Telephone: (516) 632-8118
Telefax: (516) 632-8176
E-MAIL: SPROUSE@SUNYSBNP

Frank S. Stephens
Lawrence Berkeley Laboratory
1 Cyclotron Road, 70 A-3307
Berkeley, CA 94720
Telephone: (415) 486-5724
Telefax: (415) 486-5401
E-MAIL: FSS@LBL

Robert G. Stokstad
Lawrence Berkeley Laboratory
1 Cyclotron Road, Bldg. 88
Berkeley, CA 94720
Telephone: (415) 486-5088
Telefax: (415) 486-7983
E-MAIL: STOKSTAD@LBL

James Stovall
Los Alamos National Laboratory
P. O. Box 1663, MS H817
Los Alamos, NM 87545
Telephone: (505) 667-5521
Telefax:
E-MAIL:

Daniel Strottman
Los Alamos National Laboratory
P. O. Box 1663, MS B243
Los Alamos, NM 87545
Telephone: (505) 667-5608
Telefax:
E-MAIL: STROTTMA@LAMPF

Krunoslav Subotic
Boris Kidrich Institute
POB 522, 11001 Beograd
YUGOSLAVIA
Telephone: 38-11-453681
Telefax: 38-11-4440195
E-MAIL: GYUBGSS21

Willard Talbert
Los Alamos National Laboratory
P. O. Box 1663, MS D466
Los Alamos, NM 87545
Telephone: (202) 586-2245
Telefax: (202) 586-6789
E-MAIL:

Thurman Talley
Los Alamos National Laboratory
P. O. Box 1663, MS B243
Los Alamos, NM 87545
Telephone: (505) 665-1322
Telefax:
E-MAIL:

R. Dean Taylor
Los Alamos National Laboratory
P. O. Box 163, MS K764
Los Alamos, NM 87545
Telephone: (505) 667-4729
Telefax: (505) 665-2992
E-MAIL: RDT@LANL

Henry A. Thiessen
Los Alamos National Laboratory
P. O. Box 1663, MS H847
Los Alamos, NM 87545
Telephone: (505) 667-8991
Telefax: (505) 665-1712
E-MAIL: HAT@LAMPF

Kimberly W. Thomas
Los Alamos National Laboratory
P. O. Box 1663, MS J514
Los Alamos, NM 87545
Telephone: (505) 6670-4379
Telefax:
E-MAIL:

Kenneth S. Toth
Oak Ridge National Laboratory
P. O. Box 2008, MS 6371
Oak Ridge, TN 37831-6371
Telephone: (615) 574-4732
Telefax: (615) 574-1268
E-MAIL: TOTH@CESARVAX

Xiao-Lin Tu
Los Alamos National Laboratory
P. O. Box 1663, MS H824
Los Alamos, NM 87545
Telephone: (505) 667-7235
Telefax:
E-MAIL: TU@LAMPF

John L. Ullman
Los Alamos National Laboratory
P. O. Box 1663, MS H803
Los Alamos, NM 87545
Telephone: (505) 667-2517
Telefax:
E-MAIL: ULLMAN@LAMPF

David J. Vieira
Los Alamos National Laboratory
P. O. Box 1663, MS H824
Los Alamos, NM 87545
Telephone: (505) 667-7231
Telefax: (505) 665-1712

Antonio Villari
IFUSP
CP 20516
01498 Sao Paulo, SP
BRAZIL
Telephone: (11) 211-2742
Telefax: (11) 814-0503
E-MAIL: VILLARI%47551.HEPNET@LBL

Robert George Voss
Science & Engineering
Research Council
Polaris House, North Star
Swindon, SN2 1ET
ENGLAND
Telephone:
Telefax:
E-MAIL:

Thomas Gordon Walker
Rutherford Appleton Laboratory
Chilton, Didcot
Oxon OX11 OQX
ENGLAND
Telephone: (0235) 445211
Telefax: (0235) 445147
E-MAIL: TGW@UKAC.RL.IB

William B. Walters
University of Maryland
Department of Chemistry
College Park, MD 20742
Telephone: (301) 454-1724
Telefax: (301) 454-0556
E-MAIL: WALTERS@UMCINCOM

Thomas E. Ward
Brookhaven National Laboratory
Building 902C
Upton, NY 11973
Telephone: (516) 282-7842
Telefax: (516) 282-7650
E-MAIL: WARD@BNL

Michael Wiescher
University of Notre Dame
Department of Physics
Notre Dame, IN 46556
Telephone: (219) 239-6788
Telefax:
E-MAIL: IMYBA3@IRISHMVS

Bryan Hobson Wildenthal
University of New Mexico
201 Ortega Hall
Albuquerque, NM 87131
Telephone: (505) 277-3046
Telefax: (505) 277-0351
E-MAIL: WILDENBH@UNMB

Jerry B. Wilhelmy
Los Alamos National Laboratory
P. O. Box 1663, MS J514
Los Alamos, NM 87545
Telephone: (505) 665-3188
Telefax: (505) 665-3403
E-MAIL: WILHELMY@LAMPF

Mahlon T. Wilson
Los Alamos National Laboratory
P. O. Box 1663, MS K762
Los Alamos, NM 87545
Telephone: (505) 667-4555
Telefax: (505) 667-2662
E-MAIL:

Jeff Allen Winger
Michigan State University
NSCL/MSU
East Lansing, MI 48824
Telephone: (517) 355-0276
Telefax: (517) 353-5967
E-MAIL: WINGER@MSUNSCL

Fred K. Wohn
Iowa State University
Physics Department
Ames, IA 50011
Telephone: (515) 294-3545
Telefax: (515) 294-3226
E-MAIL: WOHN@ALISUVAX

Hermann Wollnik
University Giessen
2 Physik Institut
H. Buffring 16
6300 Giessen
WEST GERMANY
Telephone: 49-641-7022770
Telefax: 49-641-74390
E-MAIL: WOLLNIK@DGIPIG5

Jan M. Wouters
Los Alamos National Laboratory
P. O. Box 1663, MS H824
Los Alamos, NM 87545
Telephone: (505) 667-7233
Telefax:
E-MAIL: WOUTERS@LAMPF

Xiao-Gang Zhou
Los Alamos National Laboratory
P. O. Box 1663, MS H824
Los Alamos, NM 87545
Telephone: (505) 667-7235
Telefax:
E-MAIL: ZHOU@LAMPF

Zong-Yuan Zhou
Los Alamos National Laboratory
P. O. Box 1663, MS H824
Los Alamos, NM 87545
Telephone: (505) 667-5557
Telefax:
E-MAIL: ZZHOU@LAMPF

END

DATE FILMED

11 / 07 / 90